Lithogeochemical Discrimination and Classification of Archean Shales in Volcanic Assemblages of the Western Abitibi Greenstone Belt

Rhian Dentelbeck

Thesis submitted to the University of Ottawa
in partial Fulfillment of the requirements for the
Masters of Earth Sciences

Department of Earth and Environmental Sciences
Faculty of Science
University of Ottawa

© Rhian Dentelbeck, Ottawa, Canada, 2026

Acknowledgements

I would like to express my gratitude to all the individuals who supported me throughout this process. First and foremost, I would like to thank Mark Hannington for his patience, dedication, and considerable effort he devoted to mentoring me and helping shape this thesis.

I am also grateful to my research group, including Alan Baxter, Marc Fassbender, Chris Galley, Thomas Mcloughlin-Coleman, Carlos Braga, and Erin Bethell for their support, insight, and encouragement.

I would like to acknowledge my family and friends whose unwavering support carried me through all stages of this pursuit. To my parents, thank you for supporting me in my academic endeavours from the very beginning. To my sister, thank you for your support and for being yourself, even while managing your own academic challenges. To my friends, thank you for being a constant source of humour and grounding presence throughout this process.

Abstract

The Abitibi Greenstone Belt (AGB) hosts world-class base and precious metal deposits and continues to be a primary exploration focus. However, increasing depletion of near-surface deposits requires improved geological models to identify future targets at greater depth. Carbonaceous argillites or black shales are present in most ore-hosting volcanic units throughout the AGB, and they are common hosts for synvolcanic base metal deposits and for orogenic gold. Most of the black shale occurrences are in small volcanosedimentary basins that belong to regionally extensive volcanic complexes. Because they have a strong electromagnetic response many of these rocks are targeted for drilling during exploration. This has resulted in a vast, yet widely underappreciated archive of core and data on shales that may hold valuable information to identify potentially ore-hosting sequences at depth.

The study examines the geochemistry of the shales in different settings using machine learning approaches to develop new classification strategies. The study uses a comprehensive lithogeochemical database of over 500 black shale samples from the western AGB to test: i) whether they can be reliably classified according to their sediment source (e.g., felsic versus mafic provenance), and ii) whether machine learning techniques can improve the identification of these underlying geochemical patterns. Multielement correlations characteristic of different source rocks and depositional processes were identified by Principal Component Analysis (PCA) and classified by Random Forest (RF) a machine learning algorithm. PCA differentiates between shales derived from mafic and felsic volcanic source rocks, shale that has been hydrothermally altered (or derived from altered volcanic rocks at their source), and shale that may have been hydrothermally altered after deposition. The results show that the geochemistry of shales can be treated much like that of their source volcanic rocks and a strong relationship exists between major geologic features and different types of shales. In particular, black shales that were deposited in restricted volcanic basins can be distinguished from black shales that are more closely associated with regionally extensive turbidite sequences. This outcome can also improve our understanding of mineral potential, distinguishing between shale lithotypes in settings that commonly host base metal deposits and shale lithotypes in other settings that may host later gold deposits. We identify "orogenic gold-type shales" as mainly felsic-type, derived from eroded

arc-like assemblages along major crustal-scale faults where orogenic gold deposits are found. We also identify "VMS-type shales" as mainly mafic-type, deposited in rift basins where base metal deposits formed.

Résumé

La ceinture de roches vertes de l'Abitibi (AGB) abrite des gisements de métaux de base et précieux de classe mondiale et continue d'être une zone d'exploration prioritaire. Cependant, l'épuisement des gisements ès de la surface force l'amélioration des modèles géologiques afin d'identifier de nouvelles cibles à plus grandes profondeurs. Des argilites carbonées ou des schistes noirs sont présents dans la plupart des unités volcaniques contenant des minerais à travers l'AGB, et sont souvent associés à des gisements de métaux de base synvolcaniques et à de l'or orogénique. En raison de leur forte réponse électromagnétique, bon nombre de ces roches sont ciblées pour le forage lors de l'exploration. Il en résulte une vaste archive, pourtant largement sous-estimée, de carottes et de données sur les mudstones carbonés, qui pourrai contenir des informations précieuses pour localiser des types de gisements connexes en profondeur. La plupart des occurrences de schistes noirs se trouvent dans de petits bassins volcano-sédimentaires appartenant à des complexes volcaniques régionaux étendus. Ces complexes abritent des gisements de métaux communs et, s’étant minéralisé plus tardivement, de l'or orogénique.

Cette étude examine la géochimie de ces schistes dans divers contextes en employant l'apprentissage automatique (*machine learning*) pour développer de nouvelles stratégies de classification. Une base de données lithogéochimique exhaustive, comprenant plus de 500 échantillons de schistes noirs de l'ouest de l'AGB, a été utilisée pour tester : i) la fiabilité de leur classification selon la source sédimentaire (ex. provenance felsique vs mafique), et ii) la capacité des techniques d'apprentissage automatique à améliorer l'identification de ces signatures géochimiques sous-jacentes. Les corrélations multi-élémentaires caractéristiques des différentes roches sources et des processus de dépôt ont été identifiées par analyse en composantes principales (ACP) et classées par forêts d’arbres décisionnels (*Random Forest*).

L'ACP permet de distinguer les schistes dérivés de sources volcaniques mafiques ou felsiques, ceux ayant subi une altération hydrothermale (ou dérivés de sources déjà altérées), et ceux potentiellement altérés après leur dépôt. Les résultats démontrent que la géochimie des schistes peut être traitée de manière analogue à celle de leurs roches volcaniques sources et qu'un lien étroit existe entre les traits géologiques majeurs et les types de schistes. Plus précisément, les schistes noirs déposés dans des bassins volcaniques restreints se distinguent de ceux associés à des séquences de turbidites régionales. Ces résultats permettent d'affiner l'évaluation du potentiel minéral en différenciant les lithotypes de schistes typiques des contextes de métaux usuels de ceux associés aux systèmes aurifères plus tardifs. Nous identifions ainsi les « schistes de type orogénique » comme étant principalement de nature felsique, dérivés de l'érosion d'assemblages d'arcs le long de failles crustales majeures. À l'inverse, les « schistes de type SMV » sont principalement de nature mafique, déposés dans des bassins de rift propices à la formation de gisements de métaux usuels.

Table of Contents

Acknowledgements..…….. ii
Abstract..……. iii
Résumé…..…….. iv
Table of Contents..…….. v
1.0 – Introduction..……. 1
Previous Work..…… 1
Thesis Objectives and Questions……..…… 3
2.0 – Geology of Shales in the Western Abitibi Greenstone Belt ……... 5
2.1 Regional Geology ……..... 5
2.2 Local Geology – Lithostratigraphic Assemblages …….……. 6
2.3 Characteristics of Graphitic Argillite and Shale Units ……..... 10
2.4 Distribution of Shale Units ……..…… 12
3.0 – Methods ……..… 31
3.1 Sample Archive ……..…….. 31
3.2 Lithogeochemical Data ……..…….. 33
3.3 Multivariate Statistical Techniques ……..... 35
3.3.1 Principal Components Analysis (PCA) ……..... 36
3.3.2 Empirical Bayesian Kriging (EBK) ……..… 38
3.3.3 Random Forest (RF) ……..… 38
4.0 – Classification of Shale Lithotypes ……... 54
4.1 Geochemistry of Shales……..……... 54
4.2 Geochemistry of WAGB Shales……..…….. 55
4.2.1 Source Rock Classification Using Immobile Element Ratios ……..…. 58
4.2.2 Major Elements ……..... 59
4.2.3 Other Trace Elements……..…... 60
4.3 Pearson's Correlation……..…….. 61
4.4 Immobile Element Ratios and REE of Shale Lithotypes……..... 70
4.5 Source Rock Contributions…….. 72
4.6 Spatial Distribution of Shale Lithotypes……..……. 73

4.7 Effects of Hydrothermal Alteration……. 74
4.8 Shales in Different Assemblages……. 76
4.9 Shales Associated with Different Mineral Deposit Types……..... 77
5.0 – Principal Component Analysis……. 140
5.1 Principal Components and Element Groups……...……. 141
5.2 Spatial Distribution of PC Scores……..... 142
5.2.1 Kriged Values of PC1……... 143
5.2.2 Kriged Values of PC2……... 144
5.2.3 Kriged Values of PC3……... 146
5.2.4 Kriged Values of PC4……..... 146
5.3 Relationship to Volcanic and Tectonic Settings ……..... 147
6.0 – Random Forest Classification ……. 160
6.1 Random Forest Classification of Shale Lithotypes…….. 160
6.2 Random Forest Classification of Associated Mineral Deposit Types…….. 161
6.3 Random Forest Classification of Lithostratigraphic Assemblages…….. 163
6.4 Conclusions ……..... 163
7.0 – Conclusions……..... 178
7.1 Comparison to Global Standards (PAAS)……..... 179
7.2 Missing Kidd Creek Data……..... 180
References…… 188
Appendix…….. 203

Chapter 1 – Introduction

The Abitibi Greenstone Belt (AGB) is host to world-class gold and base metal deposits (Hannington et al., 2012; Monecke et al., 2017). However, increasing depletion of near-surface deposits requires improved geological models to identify future exploration targets. Carbonaceous argillites, or black shales, are common ore-hosting units in the AGB and their distinct electromagnetic properties have resulted in many of these rocks being targeted during drilling campaigns. A vast, yet widely underappreciated archive, holds valuable information to locate deeper mineral deposits associated with these rocks.

The black shales are mainly synvolcanic and formed in volcanosedimentary basins spatially correlated with magmatic complexes (Potter et al., 1980; Hannington et al., 2012). However, the black shales are typically unclassifiable by simple observation. We have identified geochemically distinct groups of shales in the Western Abitibi Greenstone Belt (WAGB) related to source rock composition (felsic, mafic) weathering and transport, and post-depositional processes. Element groupings, ratios, and alteration indices have been used to characterize sediment sources and post-depositional processes, and a machine learning approach has been used to develop a trace-element classifier of the different shale types.

Two machine learning techniques − Principal Component Analysis (PCA) and Random Forest (RF) Clustering. The Random Forest model can predict source rock provenance with an accuracy of 91%. This outcome is valuable for exploration in identifying volcanic and tectonic settings where different mineral deposit types may be expected.

Previous Work

Some of the earliest works on shales include those by Vine & Tourtelot (1970) who classified the geologic setting of black shale ranging in age from Precambrian to Eocene using their geochemical composition. Tourtelot (1979) summarized emerging work on the interpretation of black shale sequences, including their geologic settings, depositional environment, presence in the geologic record, and diagenesis. One year later, Potter et al. (1980) published: *Sedimentology*

of Shale; study guide and reference source, the first book-length guide summarizing information and ideas about shales. Improved analytical techniques for determining the chemical composition of these heterogeneous rocks has led to an increasing number of publications on black shale.

Bhatia & Crook (1986) examined the trace element characteristics of graywackes of eastern Australia to identify the optimum element ratios to discriminate the tectonic settings of sedimentary basins. At about the same time, Feng and Kerrich (1990) used major and trace elements to define two distinct geochemical populations of clastic sediments in the AGB. They identified the depositional setting of the Archean sandstone and shale samples as proximal to or within an active oceanic rift and sequences formed in an island arc-like setting. Davies and Whitehead (1993) also devised a method to determine the original chemical composition of the clay component of pelitic rocks. Nesbitt et al. (1996) developed a model to calculate the modal compositions of siliciclastic sediments using bulk geochemical compositions.

Shales in the AGB is commonly a host rock for diverse mineral deposits in different settings, including orogenic gold, komatiite-hosted Ni-Cu-(PGE) and VMS (Hannington et al., 1999; Hannington et al., 2012; Pilote et al., 2019). These include important mine sites and mineral deposits including the massive Kidd Creek VMS deposit ~20 km north of Timmins, smaller VMS deposits (e.g., Potter mine), Ni-Cu-(PGE) deposits (e.g., Langmuir, Redstone) and numerous orogenic gold deposits along the Porcupine-Destor fault zone and the Larder Lake-Cadillac fault zone including but not limited to the Hollinger-McIntyre, Dome, Pamour, and Holloway mines (Monecke et al., 2017). Many of the orogenic gold deposits in the western Abitibi, especially in the Porcupine and Timiskaming assemblages, are hosted by sulphide-bearing carbonaceous shale horizons in structurally complex settings where carbonaceous units have localized strain and hydrothermal alteration. Pyrite nodules that are common hosts for Au in the sediments may have originated from diagenetic processes and were overprinted by these events (Pilote et al., 2019).

Because the sediments are mostly volcanic-derived, their compositions are thought to reflect a combination of the host volcanic rocks and the sediment provenance. Argillite units may represent material from a local or a broad catchment and the distance to a source may be

reflected in the maturity of the sediment. Major, minor, and trace elements of volcanic rocks have been used over the past 40 years to classify them according to their diverse magmatic history and geodynamic settings (e.g., Lesher et al., 1986; Kerrich and Wyman., 1997; Piercey, 2011; Greber and Dauphas., 2019; Fassbender et al., 2023; 2024). This study suggests that similar treatment of volcanic-derived sediments may provide similar insight into the origins of the black shales, taking advantage of new large-scale databases that have been lacking in previous literature.

Thesis Objectives and Questions

This study uses geochemical data from shales collected during the Regional Lithogeochemical Study of the Kidd-Munro MEGATEM Survey (Hannington et al., 2012). Whole-rock geochemical analysis was performed on 564 shale samples from 84 townships, determining the concentration of 68 elements to build a lithogeochemical database. The objective of this new study was to test a geochemical classification scheme for shales from the AGB as a tool for mineral exploration. Using the black shale database, we have attempted to identify different compositions related to different source rock domains. We proposed that black shales can be classified into groups that reflect different sedimentation history and magmatic evolution of the host volcanic complexes (e.g., felsic versus mafic volcanic episodes), and that machine learning techniques can reveal these underlying geochemical patterns, including possible relationships to different types of mineralization.

This approach addresses 3 main questions:

(i) given the high degree of alteration, weathering, and transport is it possible to effectively distinguish different shale lithotypes?
(ii) what combinations of trace elements are the most important for determining the provenance of the shales?
(iii) can the geochemistry of shale be used to distinguish potential host rocks for different types of mineralization?

Chapter 2 describes the geology of shale units in the western Abitibi Greenstone Belt (WAGB) and their defining characteristics. Chapter 3 details the methodology, including bivariate and

spatial analysis. Chapter 4 outlines the different approaches to classification of shale compositions using Pearson's correlation of the elements. Chapter 5 describes PCA and its application to the black shale database. Chapter 6 introduces a new Random Forest classification scheme that can be used to identify shale lithotypes in other datasets to make predictions.

Chapter 2 – Geology of Shales in the Western Abitibi Greenstone Belt

2.1 Regional Geology

The AGB is a subprovince of the Superior Province, which is the largest Archean craton in the world, spanning Quebec, Ontario, and parts of Manitoba. The east-west trending terranes comprise a series of granite-greenstone belts and metasedimentary belts hundreds of kilometers across and up to 1,000 km in width (Figure 2.1: Percival, 2007). The Superior Province contains continental fragments of Mesoarchean age and Neoarchean oceanic plates aggregated between 2720 and 2680 Ma (Percival, 2007). Volcanic units are subvertical and form large east-west trending folds. The linear nature of the assemblages is partially due to a north-south compression during the Kenoran orogeny after 2700 Ma. The Superior Province contains nearly 80% of the worlds known Archean Cu-Zn deposits. Gold endowment related to the two major fault zones of the AGB exceeds ~ 200 M oz making the belt one of the economically most important terranes in the world (Monecke, 2017).

The AGB sits within the southern part of the Superior and straddles the border between Ontario and Quebec, extending 500 km from east to west and 350 km from north to south. It is bordered to the north by the Opatica subprovince, to the west by the Kapuskasing tectonic zone, to the east by the Grenville Province, and to the south and south-east by sedimentary rocks of the Pontiac subprovince (Mercier-Langevin et al., 2023) (Figure 2.1). One model of crustal growth involved accretion of oceanic terranes onto the Opatica subprovince to the north and a complex history of oceanic arc formation, evolution, collision and fragmentation (Mueller et al., 1996; Percival, 2007; Mueller et al., 2009; Monecke et al., 2017).

The western AGB contains some of the world's largest Cu-Zn, significant amounts of Ni-Cu-PGE mineralization, and many orogenic gold deposits. All three are commonly hosted by or spatially associated with sulphide-bearing carbonaceous shale or occur in volcanic rocks containing carbonaceous units. (Mercier-Langevin et al., 2023). VMS deposits formed during episodes of extension in arc and backarc-like settings between 2747 to 2700 Ma. The region contains a total of ~775 million tonnes of polymetallic massive sulphides. Carbonaceous shales

are common as interflow sediments in the volcanic basins that host the deposits (Hannington et al., 1999). In komatiite-hosted Ni-Cu-PGE deposits, these rocks similarly occur within the volcanic subbasins that host the komatiite flows and are a source of sulfur (in diagenetic sulphides) for the formation of Ni deposits (Lesher et al., 2002).

The gold deposits are predominantly contained within late orogenic quartz-carbonate veins and replacement-style deposits. More than 40 gold mines have been developed in the WAGB. Gold endowment along the Destor-Porcupine and Larder Lake-Cadillac fault zones exceeds 6200 tonnes (Monecke et al., 2017). In orogenic gold deposits, graphitic argillites are commonly host to gold-bearing quartz-carbonate veins, because they localize deformation and the graphitic component may be a chemical reductant for gold deposition (Goldfarb and Pitcairn, 2023).

2.2 Local Geology – Lithostratigraphic Assemblages

The stratigraphy of the AGB comprises six major volcanic-dominated assemblages (2795 - 2695 Ma) and two uncomfortably overlying metasedimentary packages (Porcupine and Timiskaming). Assemblages are divided on the basis of lithology, geochemistry, and structural style. Mafic rocks compose about 89% of the volcanics in the western Abitibi, with felsic and ultramafic composing the remaining 11% (Hannington and Barrie, 1999). From oldest to youngest the volcanic assemblages are the Pacaud, Deloro, Stoughton-Roquemaure, Kidd-Munro, Tisdale and Blake River assemblages (Figure 2.2). They are separated by “sedimentary interface zones” which include banded iron formations (BIFs), breccias, sandstone, epiclastic units and graphitic argillite (Thurston et al., 2008; Monecke et al., 2017). More localized synvolcanic sedimentary deposits (i.e., thin interflow units) occur throughout the volcanic assemblages. The following is summarized from Monecke et al. (2017).

The Deloro assemblage contains intermediate (to felsic) metavolcanic rocks/intrusions including massive, pillowed, variolitic, amygdaloidal flows and tuff. In the northern section of the study area in Crawford and Lucas townships, the Deloro assemblage comprises intermediate metavolcanic rocks, some ultramafic intrusive rocks, including peridotite and pyroxenite, and graphitic argillite units.

The next youngest assemblage, Stoughton-Roquemaure, crops out primarily in the northern part of the AGB and consists mainly of basalts, komatiites, and felsic volcanic rocks. The townships that border the North Branch Porcupine – Destor Deformation Zone (PDFZ), including Calvert and Teefy, contain thick massive and pillowed flows that continue for 10s of kilometers with minor clastic metasedimentary rocks. Further east in Knox and Kerrs townships, the Stoughton Roquemaure assemblage contains pillowed and massive basalts within minor felsic volcanic units and ultramafic sills (Figure 2.3). Argillite units are particularly common in Lucas, Aubin, Nesbitt, Ottaway, Lennox, Reaume, Warden, and Lamplugh townships. Here, many lithologic units classified as Archean chemical metasedimentary rocks are also mapped and exposed at the surface (Figure 2.10).

The Kidd-Munro assemblage is a 200 km long, east-west trending belt extending from the Kapuskasing structural zone to the Grenville province. The assemblage is comprised mainly of mafic, ultramafic and felsic metavolcanic rocks including basaltic komatiites, pyroxenite, Fe- and Mg-rich tholeiite, high alumina basalt, mafic-ultramafic intrusions and high silica rhyolite. The Kidd Creek VMS deposit is contained within the western section of the Kidd-Munro assemblage comprising bimodal volcanic successions, with subequal amounts of mafic volcanics and rhyolite (Hannington et al., 1999; Monecke et al., 2017). Farther east, Clergue and Walker townships include mafic pillowed and variolitic flows with lesser felsic to intermediate massive flows, tuff, lapilli tuff, and ultramafic intrusions. In Munro township the sulphide lenses of the Potter deposit are hosted in a succession of basaltic volcaniclastic rocks with well-exposed komatiite flows (Monecke et al., 2017). Mafic intrusions/komatiites in this township include spinifex- textured flows. Argillite units typically span two or three townships following the east-west trend from MacDiarmid, Tully, Dundonald, and Munro townships.

Rocks of the Tisdale assemblage crop out from the Kapuskasing structural zone in the west to the Larder Lake area in the east. They are the main host rocks of the quartz-carbonate orogenic gold deposits in the WAGB (Monecke et al., 2017). Macklem, Bond, and Currie townships that border the PDFZ to the south are dominated by mafic massive and pillowed flows of the Tisdale assemblage. Argillite units are found in the Lower Tisdale assemblage in Whitney and Hoyle

townships, and in the upper Tisdale within Reaume, Duff, and Mann townships. However, large parts of the Tisdale assemblage are without any argillite units.

The Blake River assemblage is bounded by the PDFZ in the north and the LLCFZ in the south. The lower Blake River unit is primarily composed of mafic to intermediate metavolcanic rocks (andesite and basalt) ~ 6 km thick. Felsic intrusions are located throughout the assemblage, including in Clifford and Ben Nevis townships. Argillite units are in the Lower Blake River in Jamieson, Godfrey, and Jessop townships, and in the Upper Blake River in Maisonville, Bernhardt, and townships closer to the PDFZ including Michaud, Garrison, Harker, and Holloway.

Deposition of volcanic rocks of the AGB was followed by the Porcupine and Timiskaming sediments derived from a shallow marine or subaerial hinterland and deposited into aerially extensive successor basins (Monecke et al., 2017). Closure of the basins accompanied widespread and extensive deformation and burial metamorphism to greenschist facies until 2650 Ma.

The Porcupine and Timiskaming assemblages disconformably to paraconformably overlie the older volcanic assemblages and were deposited by submarine turbidity currents. Different outcrops of the Porcupine assemblage represent distinct basins that formed progressively southwards across the AGB (Monecke et al., 2017; Frieman et al., 2017). The largest of the Porcupine successor basins is confined between the PDFZ and the Pipestone Fault and ranges in age from 2690 to 2685 Ma. It is comprised of clastic rocks including greywacke, arenite, conglomerate and shale. Shale units found in the Porcupine assemblage are located in Thornloe, Ogden, Hoyle, German, and Evelyn townships.

The Timiskaming assemblage comprises the youngest supracrustal rocks in the southern AGB and is contained in a narrow zone along the major E-trending fault zones. Sedimentary deposition in the Timiskaming likely occurred in a post-collisional extensional setting within strike-slip basins, comprising alluvial-fluvial sediments like conglomerates, sandstones, and turbidites (Mueller et al., 1996; Monecke et al., 2017; Freiman et al., 2017). Argillite units within

the Timiskaming are found in Whitney and Tisdale townships. However, few samples of shale from the Timiskaming assemblage are included in the WAGB archive.

Mueller and Donaldson (1992) defined a series of sedimentary cycles that broadly correspond to the volcanic episodes of the AGB. These rocks are generally interstratified with or overlie volcanic assemblages. Four main sedimentary cycles span ~ 50 million years:

(i) cycle 1, 2730 – 2720 Ma (Deloro and Stoughton - Roquemaure)
(ii) cycle 2, 2715 – 2705 Ma (Kidd-Munro, Tisdale)
(iii) cycle 3, 2700 – 2687 Ma (Blake River, and the Porcupine assemblage, 2700 – 2685 Ma)
(iv) cycle 4, 2685 – 2675 Ma (Timiskaming)

Cycle 1 was interpreted by Mueller and Donaldson (1992) as deposited in incipient intra-arc basins dominated by volcaniclastic debris associated with the Deloro (2734 – 2724 Ma) and Stoughton-Roquemaure (2723 – 2720 Ma) volcanic episodes. These basins, mainly in the northeast of the AGB, include banded iron-formations and resedimented conglomerate.

Cycle 2 was interpreted as unroofing of arc volcanoes into deep basins adjacent to the arcs during the Kidd-Munro (2720 – 2711 Ma) and Tisdale (2711 – 2704 Ma) episodes. These basins include conglomerate-sandstone, sandstone-argillite, deposited in submarine-fan environments, a shallow-marine setting, or a terrestrial succession (Figure 2.4; Mueller and Donaldson, 1992).

Cycles 3 has been interpreted as deep marine basins connecting arc terranes (Mueller and Donaldson, 1992). Cycle 3 is associated with the Blake River Group volcanic rocks and the upper Tisdale group, and may also include lowermost turbidites of the Porcupine assemblage. Cycle 4 belongs to the Timiskaming assemblage (Mueller and Donaldson, 1992).

Shale occurrences in the volcanic assemblages of the AGB were deposited in time periods lasting no more than 5 to 10 m.y. indicating rapid and localized deposition (Monecke et al., 2017). Because the subbasins were isolated from terrigenous sediment input, they have typical deep-marine sedimentation patterns. Lateral and vertical facies variations may be due to the progradation of a volcaniclastic apron into a widening basin (e.g., Busby and Pérez, 2012), but

the majority of the extensive carbonaceous units are fine-grained and broadly uniform in composition.

2.3 Characteristics of the Graphitic Argillite and Shale Units

Shales are ubiquitous in greenstone belts and often mark productive ore horizons for several mineral deposit types. However, their classification is incomplete, and many different names are used interchangeably. **Shale** is the general term for variably laminated, fine-grained clastic sediments mostly composed of clay minerals and with more than 50% grains smaller than 0.062 mm in diameter (Potter et al., 2012). **Black shale** contains significant amounts of organic matter leading to its darker colour. **Mudstone** is a fine-grained rock, consisting of a subequal mixture of clay and silt-sized particles. This term has been used very broadly, is misleading and is discarded in favour of black shale and graphitic argillite. **Argillite** is defined as a shale with a high degree of induration that has undergone some degree of metamorphism but commonly lacks visible cleavage (Weaver, 1980). **Carbonaceous argillite** or **carbonaceous shale** are also commonly used when graphite cannot be positively identified. The terms commonly used in this study include both graphitic argillite and carbonaceous shale because some samples (e.g., Dundonald township) are indeed barely metamorphosed, whereas others show strong metamorphic fabric. Table 2.1 lists other common descriptors found in core logs and the corresponding interpretation in this study.

The black shales and graphitic argillite units in this study are mainly composed of volcaniclastic material (e.g., ash) and sediment derived from erosion of local volcanic rocks. The bulk compositions reflect the composition of the volcanic source rocks (mafic, intermediate, felsic) as well as any hydrothermal alteration of those rocks prior to or during erosion. Because the sediments are so fine grained and typically black in colour, they are unclassifiable by simple observation, despite highly variable compositions. Therefore, geochemical analysis is an invaluable tool for characterizing the sediments. Colour is often directly correlated to carbon content. All graphitic units in the WAGB are black, and Fe has likely been converted to pyrite (FeS_2), chlorite, and iron carbonates during diagenesis and/or metamorphism.

Black shales contain high amounts of non-carbonate carbonaceous matter and graphite as well as authigenic iron sulphides and fine-grained detrital particles that accumulated over time under anoxic bottom water conditions in a marine sedimentary basin (Tourtelot, 1970, 1979; Large et al., 2011; Hiebert et al., 2018). The carbonaceous component of shale is considered to be synsedimentary organic matter from chemoautotropic bacteria (e.g., sulfur-reducing bacteria and methanogens). The graphite in metamorphosed shales is generally considered to be from decomposition of the organic precursors (Rickard et al., 2017; Liu et al., 2021). Archean shales predate complex life and therefore organic matter is not associated with body fossils. The quantity of organic matter in the shale is thought to be directly related to the biological productivity of the depositional environment. Anoxic marine basins with high sedimentation rates favour the preservation of the organic matter (Potter et al. 1980). Diagenetic structures are formed during or very soon after sediment deposition. Pyrite and marcasite nodules are common and indicate local chemical precipitation around organic and other nuclei without disrupting the surrounding mud matrix (Potter et al., 1980). In some cases, the sulphides were deposited as massive layers, such as in Dundonald and Hoyle townships.

Core logs indicate a range of sample types, including sulphide-poor and sulphide-rich graphitic argillite, as well as argillite with secondary carbonate or quartz (Table 2.2). The average thickness of the graphitic layers is 24 cm, with a range from 0.06 to 4 m. However, multiple layers can have combined stratigraphic thicknesses of up to 6 m in a single intersection. The intervening layers are mostly interbedded siltstone and finer-grained, dark grey to black argillite with massive texture and occasional pyrite streaks or grains. In addition to nodules, pyrite occurs as euhedral cubic shapes, or “pinstripes” along cleavage planes. Some diagenetic nodules display continuous radial growth. Other pyrite growth manifests as infilling of pore space and overgrowths on earlier nodules. Many have diverse mineral inclusions of other sulphide minerals, particularly of the base metals (Figure 2.9). Some may be clastic sulphides. Euhedral pyrite commonly encloses silicate mineral grains, and the pyrite grains themselves may be strongly modified by deformation (Jonasson, 1999). Pyrite may constitute up to nearly one-third of the total sample mass; these samples were avoided (Hannington et al., 2012) ; however, pyrite abundance in the samples is strongly correlated with trace element geochemistry such as As, Ni, Pb, Cu, Co and Au (Chapman et al., 2008; Hannington et al., 2012; Gregory et al., 2015).

Tuffaceous units, pillowed mafic volcanics and massive mafic volcanics are the most common host rocks. Common structures of the interbedded sediments include lamination, coarse- and fine-grained interbeds, and parallel stratification between shale units and greywacke, suggesting episodic suspension and deposition. The fine laminae are produced by clay-rich particles that formed by flocculation and aggregation, followed by settling onto the seafloor (Potter et al., 1980; Feng & Kerrich, 1990; McLennan, 1993). Bottom currents were generally insufficient to cause erosion or create lenticular beds, but intercalation of mud and coarser material may be caused by turbidity currents (Figure 2.7). Some samples display quartz veins between sediment laminations (Figure 2.5 and Figure 2.6).

The original mineralogy of shales typically includes framework silicates, aluminous clay minerals, carbonates, oxides and hydroxides, sulfur minerals, and organic materials (Weaver, 1989). Smectite may have originated from a volcanic, especially mafic, parent material, whereas kaolinite may have originated from a felsic source rock. These phases are now dominantly chlorite and muscovite. The secondary minerals commonly include chlorite, silica, sericite, albite, and carbonates. These minerals may have been derived from an altered source rock or they may be products of weathering during transport or hydrothermal alteration after deposition. Shales respond to the hydrothermal alteration in much the same way as the host volcanic rocks because the sediments are compositionally and mineralogically similar to the original volcanic rocks. In some samples, the shales contain trace minerals, including sulphides, reflecting nearby VMS mineralization. In others, the carbonaceous shale units can show alteration patterns typically associated with orogenic gold mineralization that was superimposed on the argillites (Rottier et al., 2025).

2.4 Distribution of Shale Units

The fine-grained graphitic units in this study are part of the volcanic assemblages. They are mainly deep-water facies, occurring locally with fine-grained turbidites and BIFs. The samples were collected from 75 townships spanning roughly 170 x 110 km in the western part of the southern AGB on the Ontario side of the Quebec-Ontario border. The different lithologies in the study area are (Hannington et al., 2012): felsic to intermediate intrusive suites (40% by area),

mafic metavolcanic rocks (29%), intermediate metavolcanic rocks (12%), Porcupine assemblage clastic metasedimentary rocks (8%), felsic metavolcanic rocks (2%), mafic intrusive rocks (3%), alkalic intrusive suites (2%), ultramafic intrusive suites (1%), chemical and fine-grained metasedimentary rocks (including argillite and banded iron formation (1%), Timiskaming-type clastic metasedimentary rocks (1%), and porphyritic intrusions (<1%). Graphitic argillites represent less than 1% of the lithologies in the study area; however, they are important marker units and hosts for metals. Carbonaceous argillites are present in most ore-hosting volcanic units, including in VMS and orogenic gold settings, but they are underrepresented in lithogeochemical databases such as Ontario's PETROCH database (Haus and Pauk, 2010). Although, their spatial distribution is well established from geophysical measurements, sampling has been limited.

Mueller and Donaldson (1992) considered the sediments to be dominantly volcaniclastic in origin, resulting from 1) subaerial and subaqueous eruptions and erosion of arc complexes, 2) hyaloclastite deposits from back-arc spreading centers, and 3) minor subaqueous gravity-flow deposits from the remnant arcs (Figure 2.4). The rift basins experienced a rapid influx of volcaniclastic material during early rifting and increased fine-grained input with increasing basin maturity (Ingersoll, 1988). This material is interstratified with ultramafic-mafic to felsic volcanic successions (Mueller and Donaldson, 1992). The fine-grained sedimentary units were deposited during breaks in submarine volcanism.

On the Abitibi lithology map (Figures 2.10 – 2.12), shales are thin, laterally extensive (1 to 10 km strike length) depositional units frequently located at the boundary between volcanic episodes (Thurston et al., 2008). The distance from source to deposition of the sediments is highly variable. Most samples collected in the western Abitibi were volcanic-derived shales that formed proximal to the volcanic centers and were deposited in adjacent sub-basins. Because of the high graphite content, and in some cases abundant sulphide, the argillite units are electromagnetically conductive and can be traced in airborne resistivity maps. Grains of conductive minerals such as graphite and pyrite are the main source of conductivity. Clay minerals also create an effective pathway for the flow of ions and increasing conductivity (Waxman and Smits, 1968). These anomalies are routinely drilled in mineral exploration. We have compiled regional electromagnetic anomaly data to present a more complete picture of the

graphitic argillite distribution beyond the sampling (Figure 2.14). Although the units are of variable thickness (< 1 m to more than 100 m), they are mostly overturned and therefore appear as linear features at surface. The major conductive units extend to at least 200 m depth, which is the limit of detection of the airborne surveys.

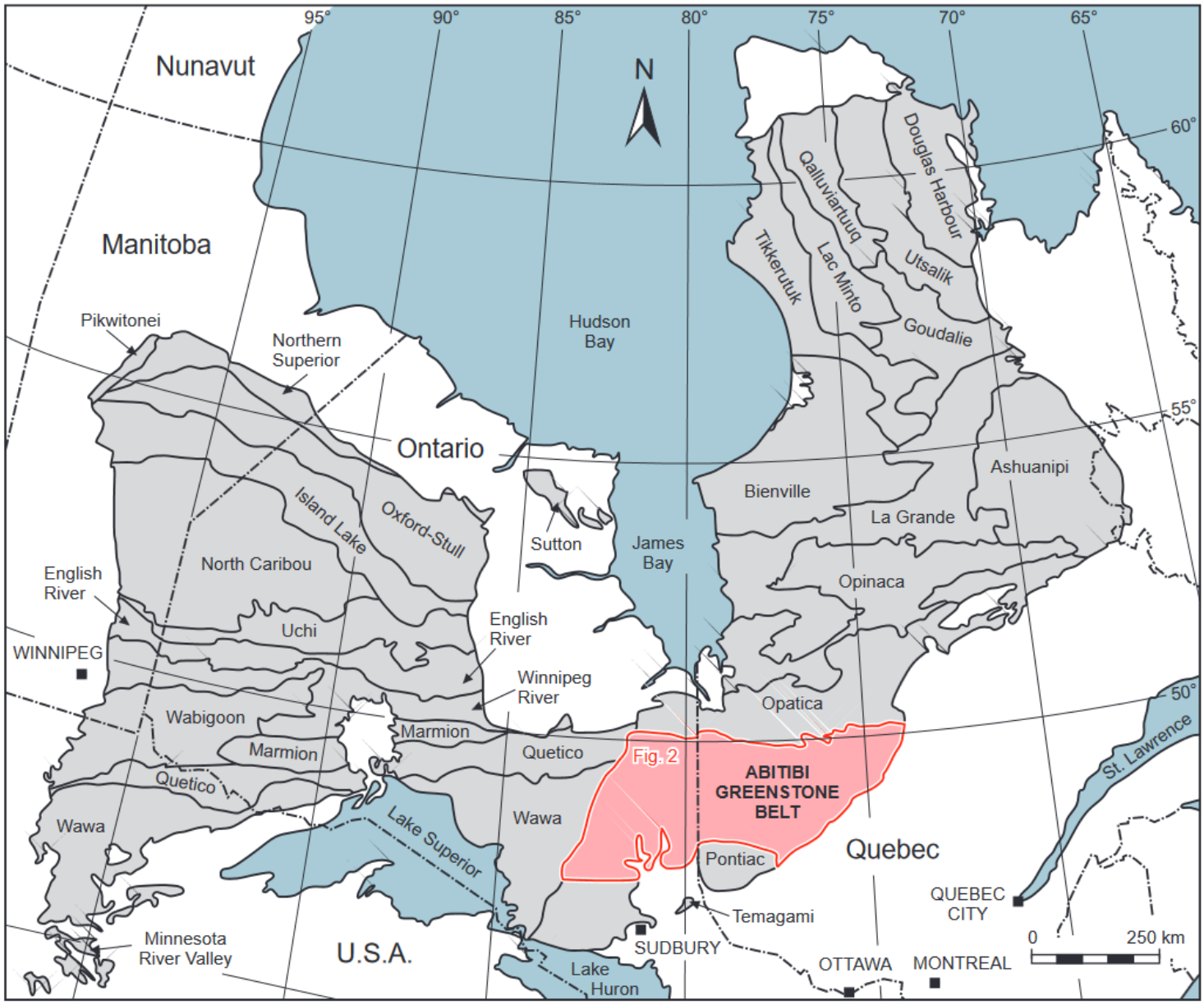


Figure 2.1 Location of the Abitibi Greenstone Belt within the Superior province (Monecke et al., 2017). The AGB is bordered to the north by the Opatica subprovince, to the west by the Kapuskasing tectonic zone, to the east by the Grenville Province, and to the south and south-east by sedimentary rocks of the Pontiac subprovince (Mercier-Langevin et al., 2023).

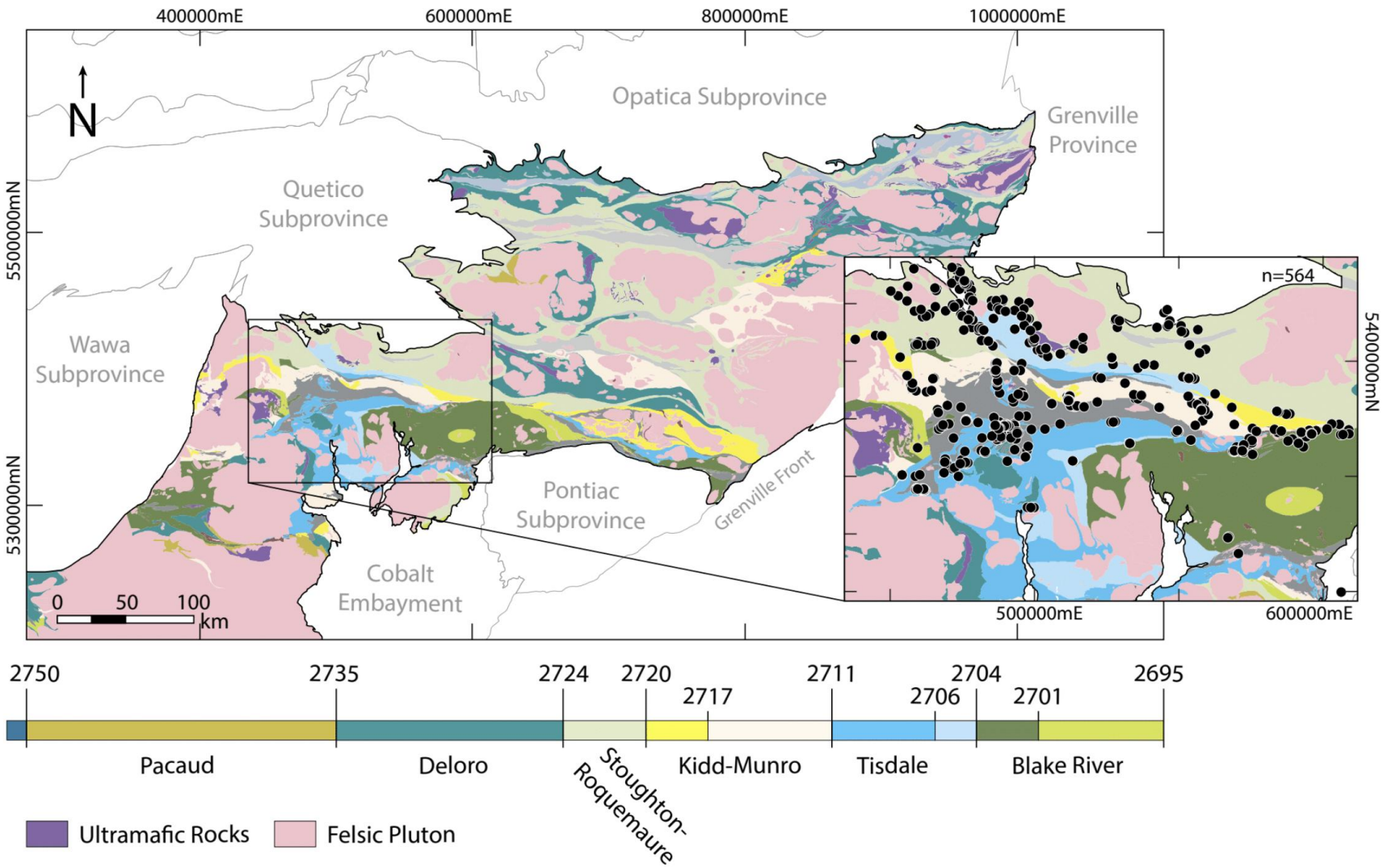


Figure 2.2. Regional map of sample locations and assemblages of the Western Abitibi from Jørgensen and Gibson (2024). Assemblage compilation of the Abitibi subprovince, Superior Province, Canada. Metal Earth Project, Mineral Exploration Research Centre (MERC).

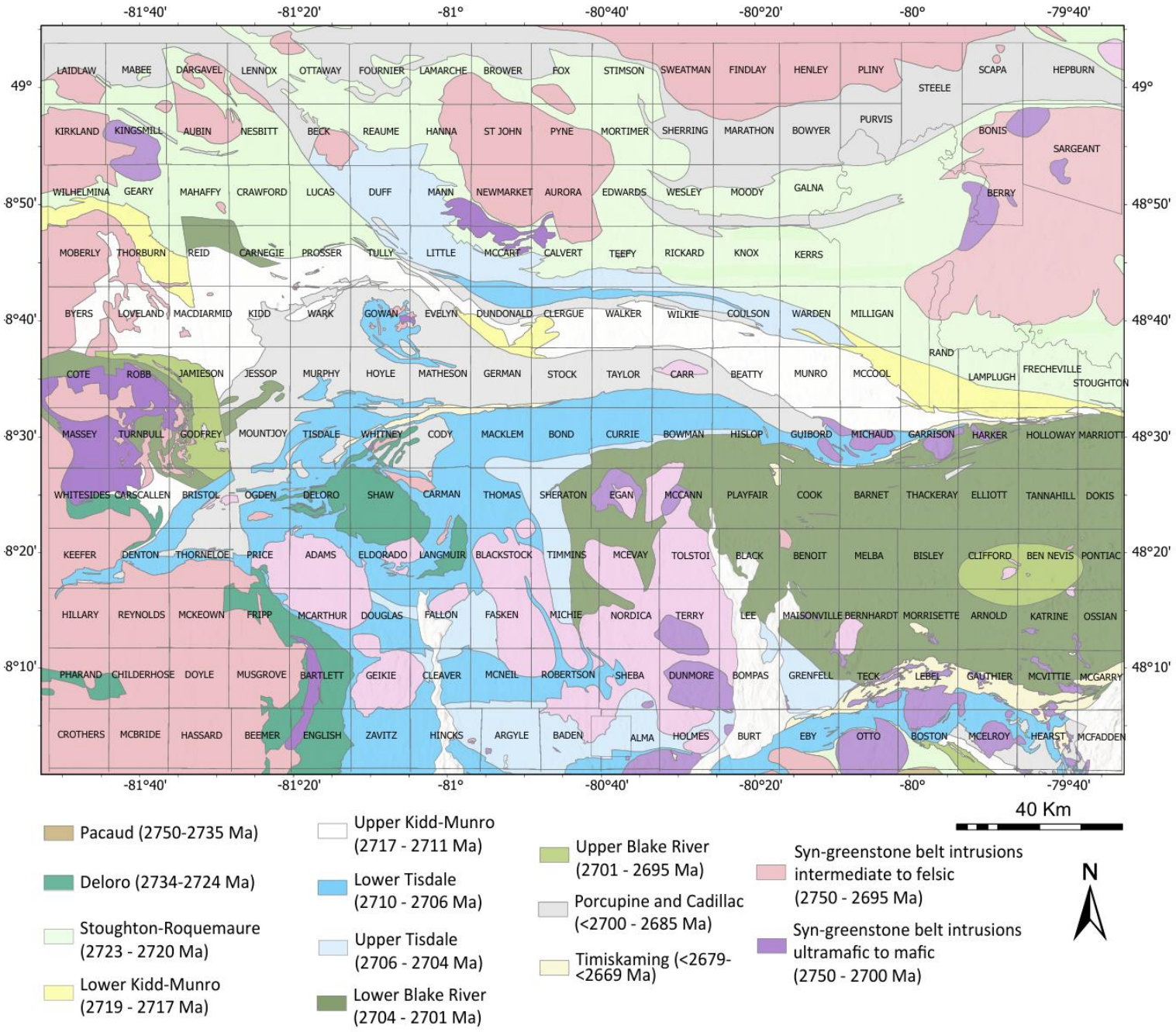


Figure 2.3. Assemblage map of the Western Abitibi Greenstone Belt with geographic township grid. Geological base shows 6 major volcanic-dominated lithostratigraphic assemblages in the area and 2 unconformably overlying metasedimentary packages (Porcupine and Timiskaming assemblages) defined by age, contact relationships, rock types and chemical affinities from Ayer et al. (2005a). Units shown in pink and purple are later-stage intrusions.

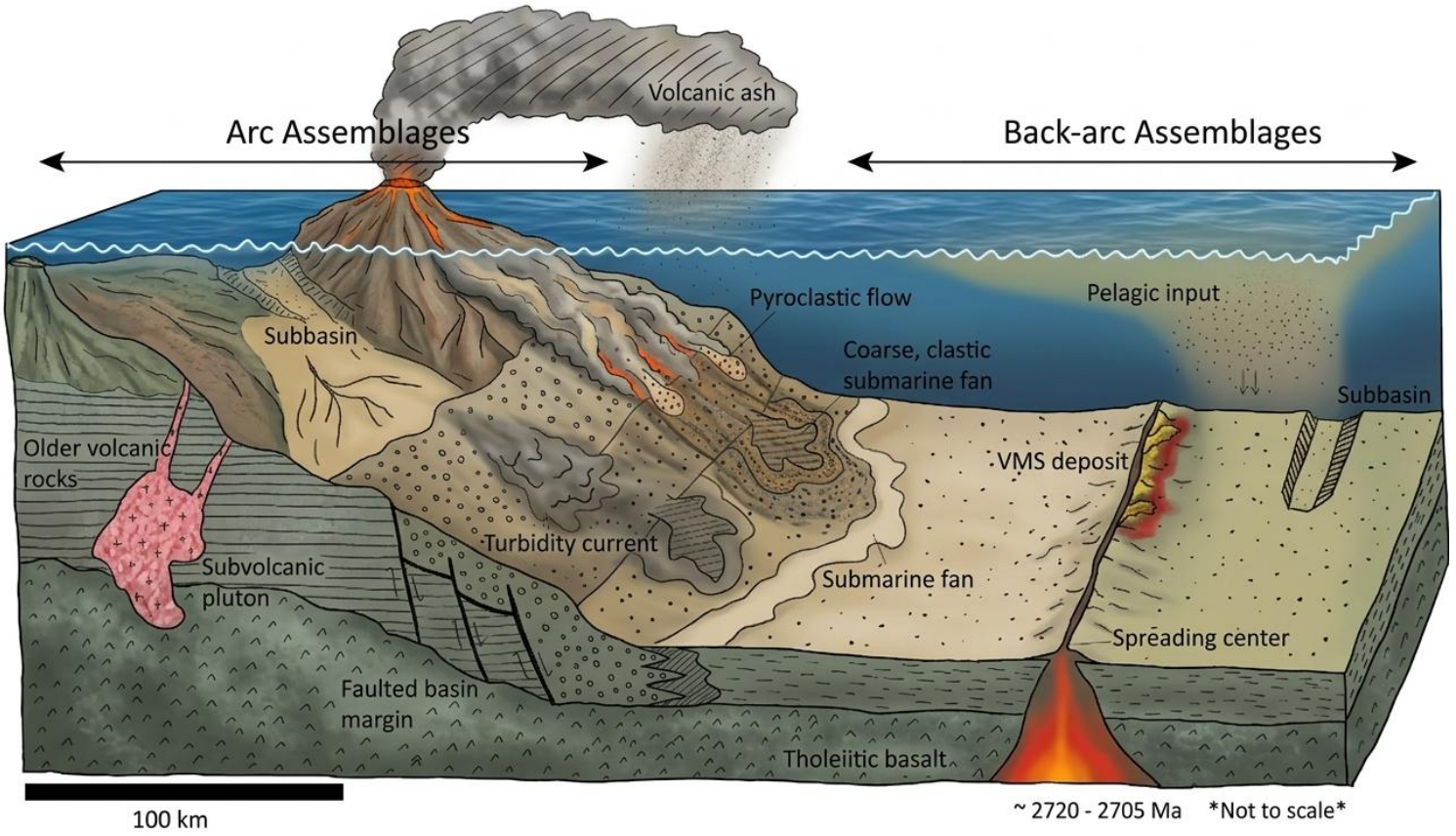


Figure 2.4. Schematic illustration of different sources and processes of sedimentation in back-arc basins and arc assemblages. Sediment is transported from the magmatic arc by volcanic eruptions and gravity-driven processes including debris flow, and turbidity currents. In back-arc basins, MOR-type volcanism is a source of mafic volcaniclastic material that is deposited in associated rifts. In deep-water facies continuous pelagic sedimentation also contributes to the fine-grained sediments. High and low PC1 values are explained in Chapter 5. Basin schematic adopted from Mueller et al., (1994), Chown et al., (1992), Mueller & Donaldson (1992), Kehew (2023). Note that this diagram was colourized with the assistance of AI.

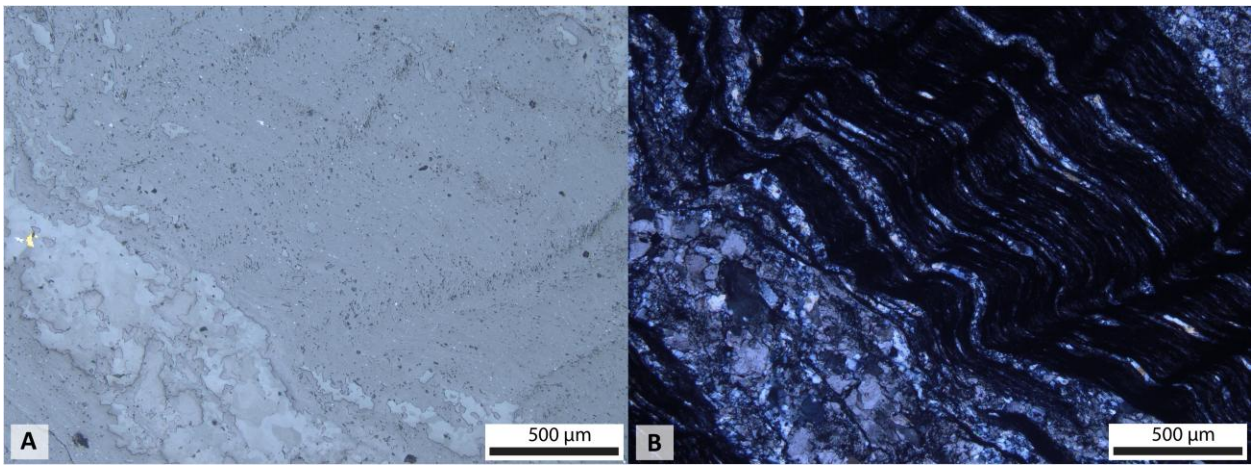


Figure 2.5. Sample #7449 from Thornloe township in the Porcupine assemblage shown in (A) reflected light and (B) transmitted light. The sample consists of graphitic argillite with contorted white bands (quartz) and disseminated pyrite euhedra. This sample illustrates the carbonaceous laminae that are deformed by the main cleavage.

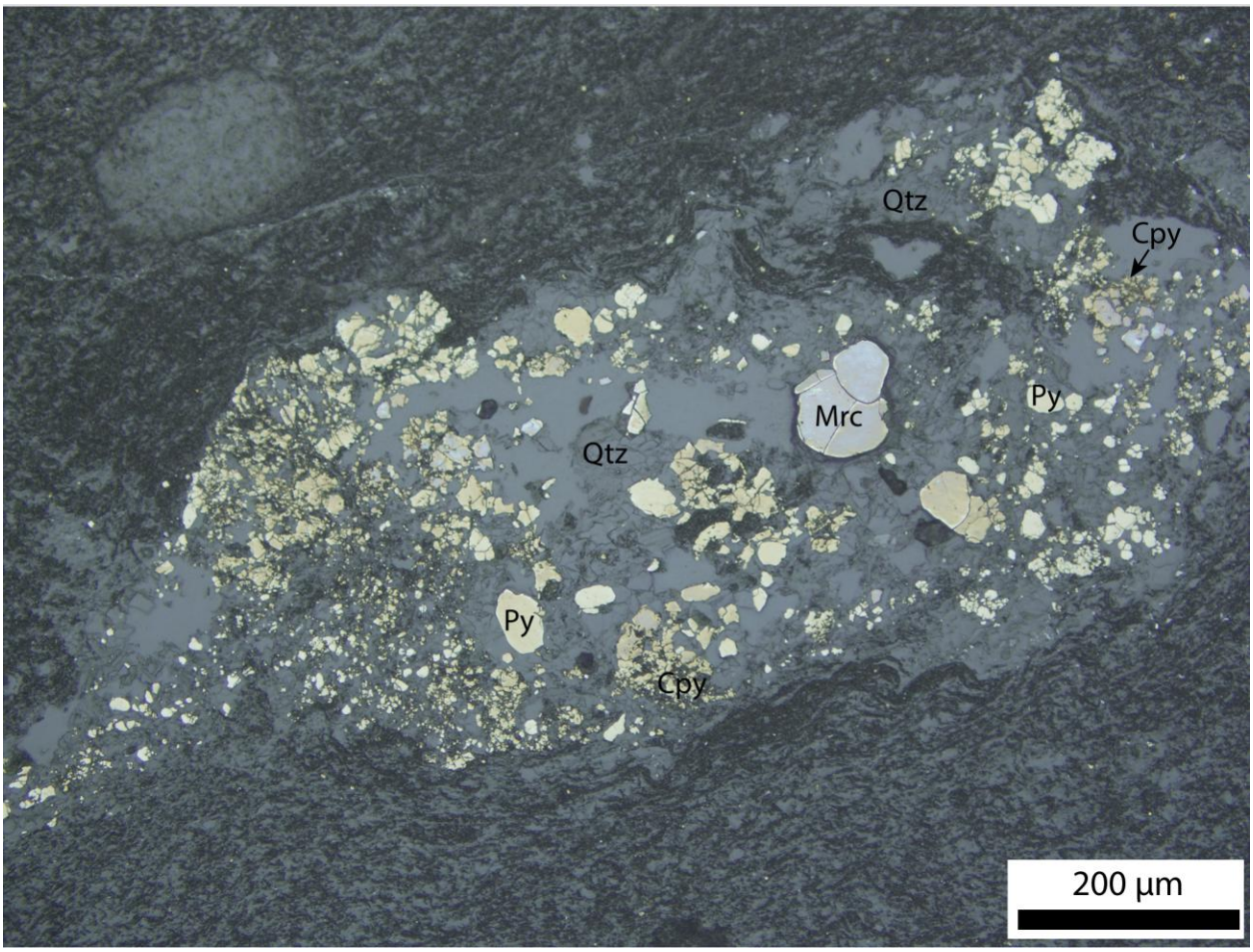


Figure 2.6. Sample #7440 from Hoyle township under 10x magnification and reflected light, containing minor pyrite in a deformed quartz-carbonate vein. Note deformation of the black carbonaceous material around the quartz-carbonate clot. Qtz = quartz, Mrc = marcasite, Cpy = chalcopyrite, Py = pyrite.

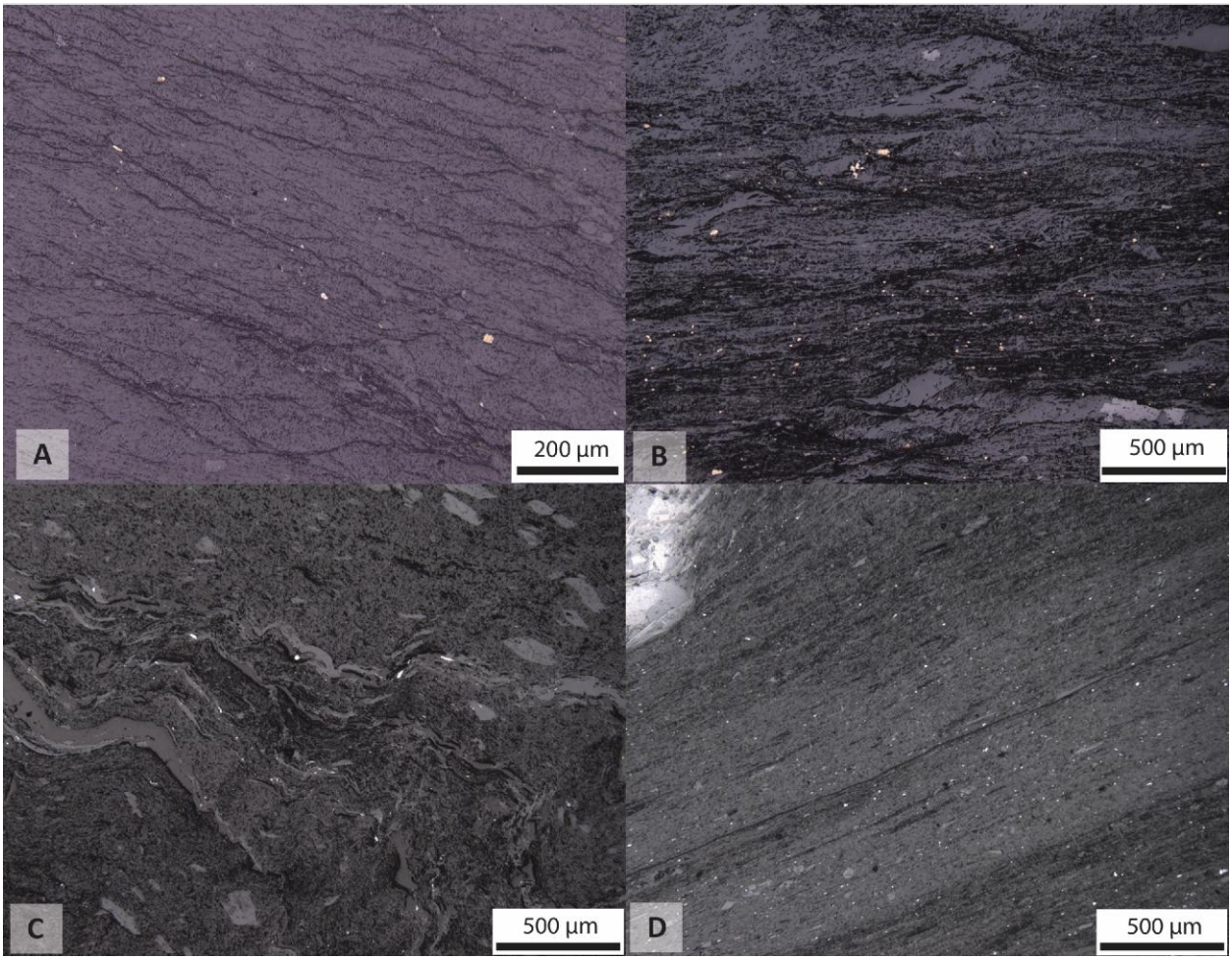


Figure 2.7. A) Sample #4379 from Warden township in the Stoughton-Roquemaure assemblage, showing deformation fabric in homogeneous carbonaceous argillite matrix (reflected light). B) Sample #4413 from Hoyle township in the Tisdale assemblage, showing lenticular deformation domains in homogeneous carbonaceous argillite matrix (reflected light). C) Sample #4151 from Mahaffy township in the Blake River assemblage, showing deformation of carbonaceous laminae. D) Sample #4320 from Hoyle township in the Tisdale assemblage showing streaky carbonaceous material and disseminated pyrite.

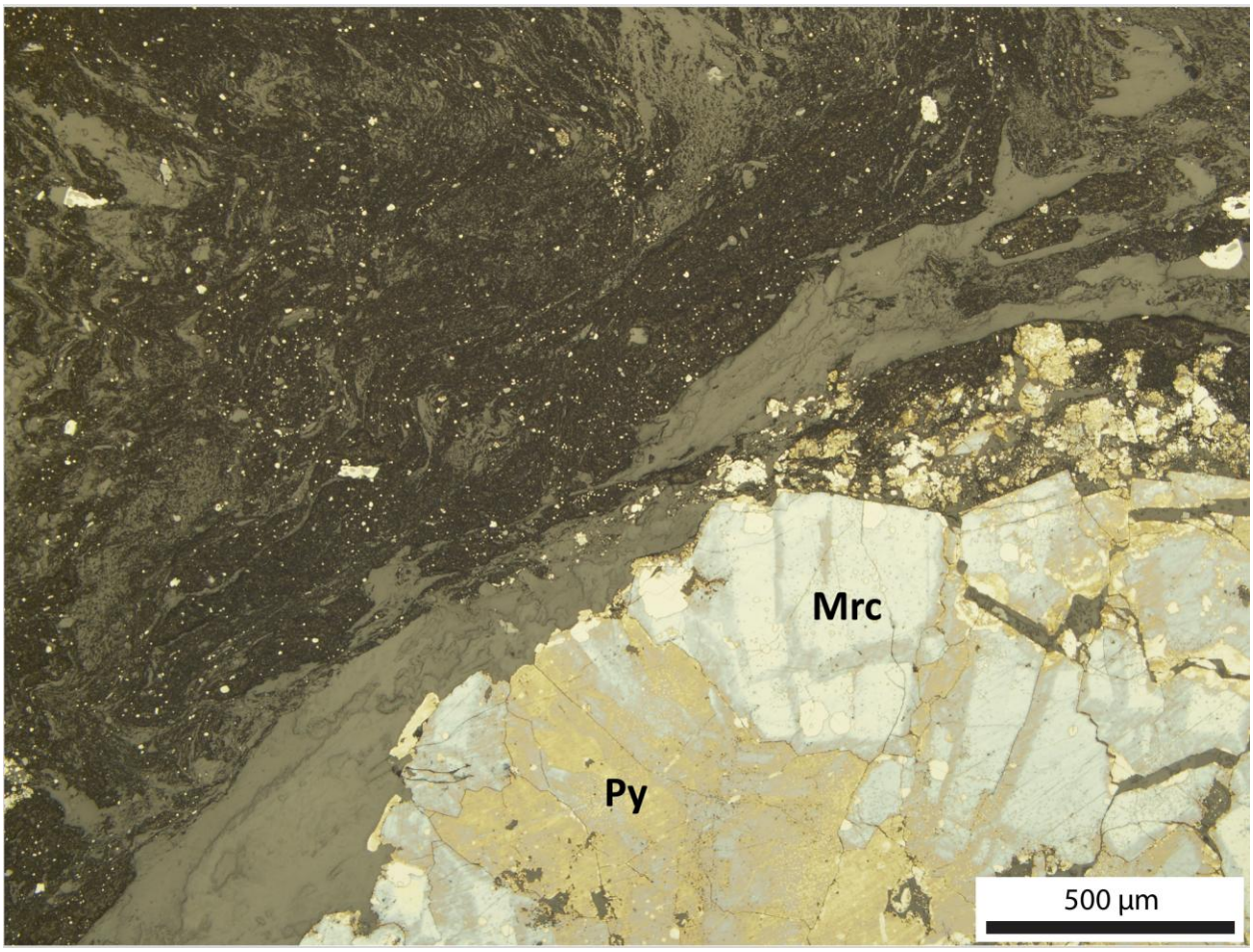


Figure 2.8. Sample #4142 from MacDiarmid township in the Upper Blake River assemblage. Large pyrite-marcasite nodules of this type are common in core and thin section samples and are interpreted to be mostly syn-diagenetic in origin. Darker black material is shale with deformed/wavy carbonaceous and silica laminations and fine-grained disseminated pyrite (reflected light). Mrc = marcasite, Py = pyrite.

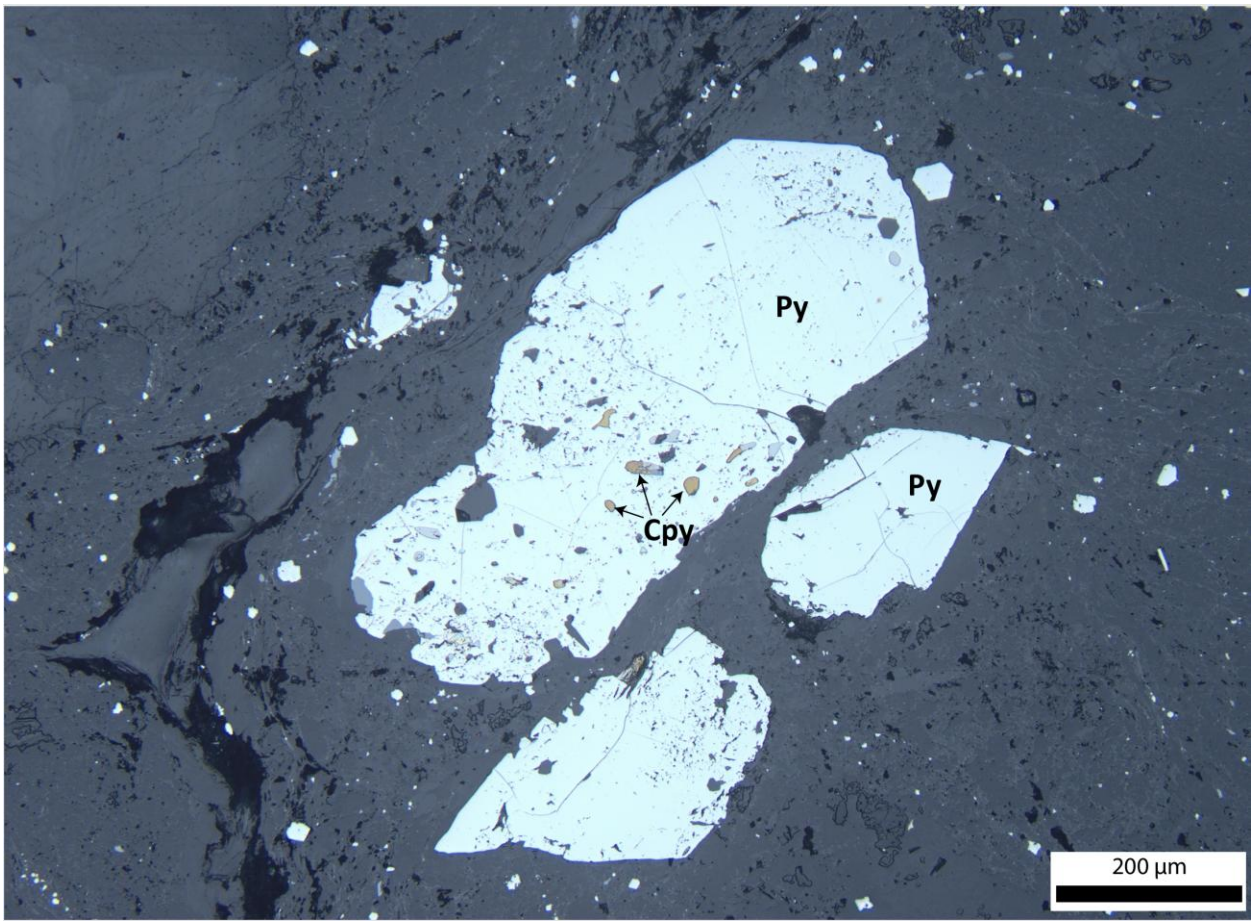


Figure 2.9. Sample #4441 from Whitney/Pamour township in the Tisdale assemblage. The black graphitic argillite contains a 1 cm pyrite euhedra thought to have formed by syn- to late-deformation growth. The largest pyrite grain contains small inclusions of chalcopyrite (reflected light). Cpy = chalcopyrite, Py = pyrite.

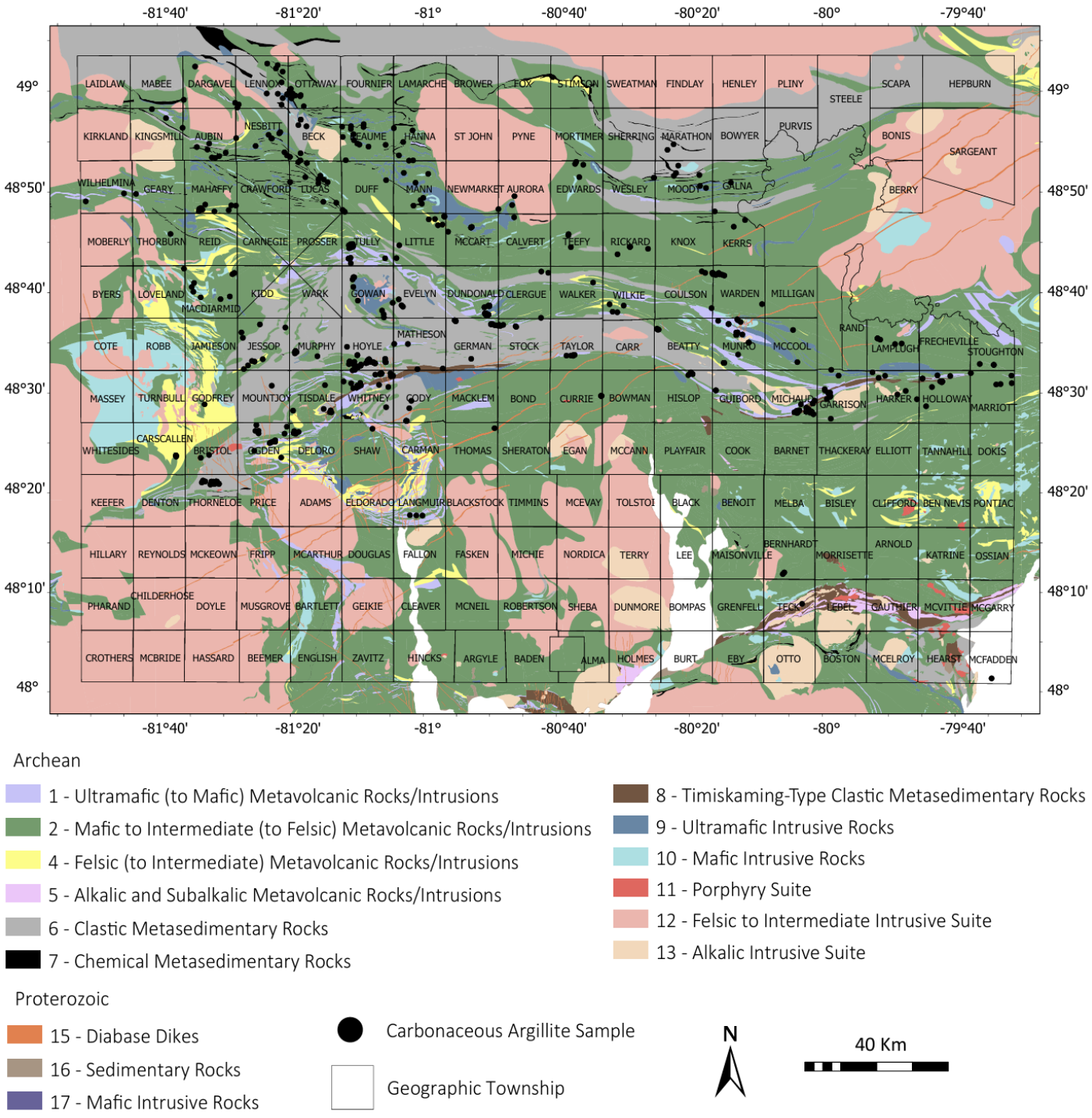


Figure 2.10. Location of 564 samples from the study area in the Western Abitibi Greenstone Belt (from Hannington et al., 2012). Lithology map from Jørgensen and Gibson (2024). A large proportion of the sampled argillite units are in the north of the map area, reflecting the extent of exploration drilling in all the volcanic and sedimentary units north of the DPFZ.

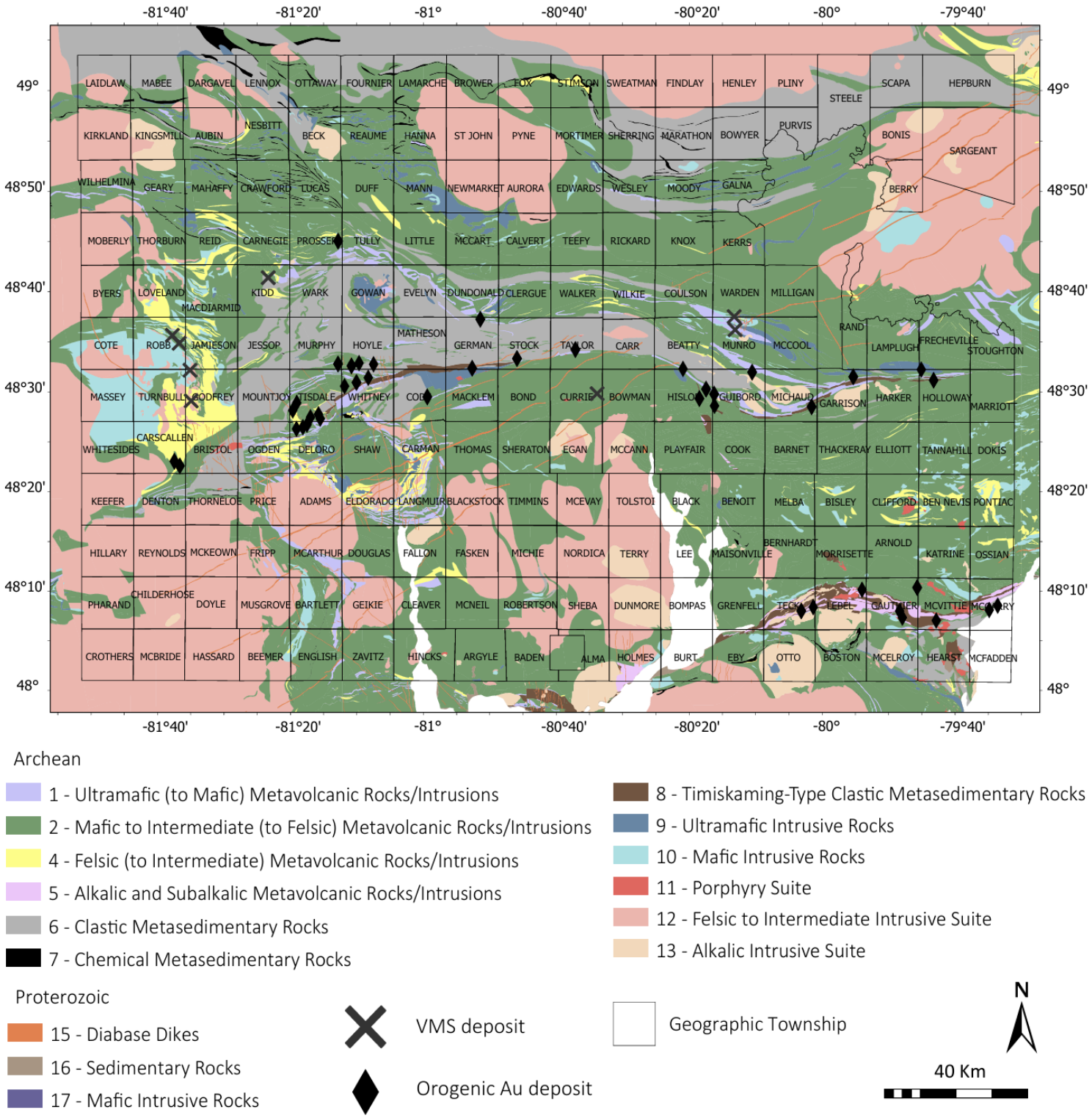


Figure 2.11. Locations of major mineral deposits in the study area. Black diamond and "X" symbols are known orogenic gold and VMS deposits, respectively. Lithology map from Jørgensen and Gibson (2024).

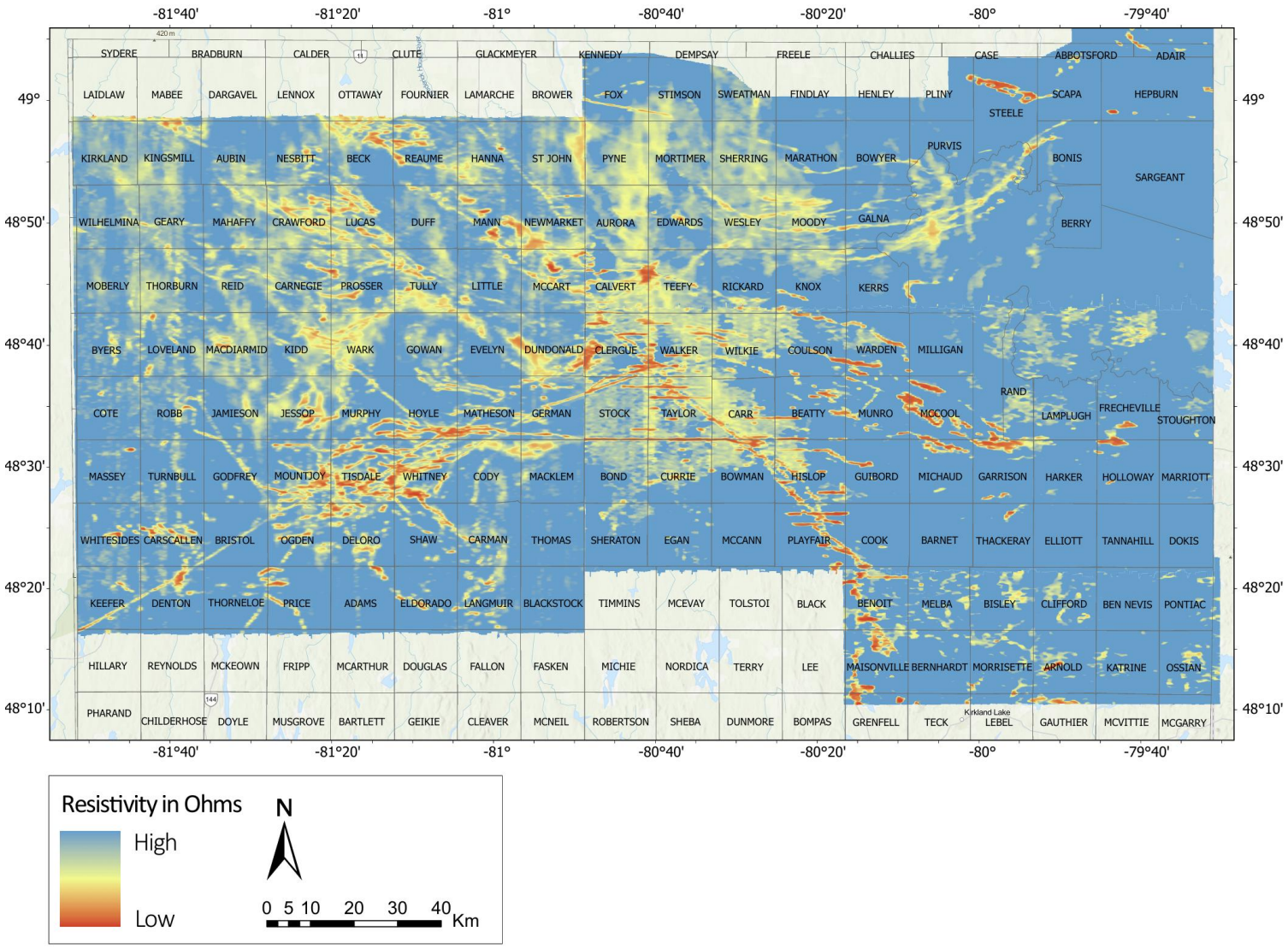


Figure 2.12. Distribution of electromagnetic anomalies (resistivity) determined from multiple Ontario Geological Survey geophysical data sets (GDS). The resistivity lows show the distribution of all positive electromagnetic conductors which may include iron formations, sulphide-bearing lithologies, and clay-rich alteration. Data sources: GDS1001 - Ontario Airborne Geophysical Surveys, Magnetic and Electromagnetic Data, Grid and Profile Data, ASCII and Geosoft Formats, Black River-Matheson Area (2003), GDS1004 - Ontario Airborne Geophysical Surveys, Magnetic and Electromagnetic Data, Timmins Area (2003); GDS1006 - Ontario Airborne Geophysical Surveys, Magnetic and Electromagnetic Data, Grid and Profile Data, Blake River Syncline Area (2003) ; GDS1007 - Ontario Airborne Geophysical Surveys, Magnetic and Electromagnetic Data, Detour-Burntbush-Abitibi West

Area (2003) ; GDS1041A, GDS1041B - Ontario Airborne Geophysical Surveys, Magnetic and Electromagnetic Data, Grid and Vector Data, Timmins Area MEGATEM (2003) ;GDS1042 - Ontario Airborne Geophysical Surveys, Magnetic and Electromagnetic Data, Kamiskotia Area MEGATEM II Survey (2003) ; GDS1044 - Ontario Airborne Geophysical Surveys, Magnetic and Electromagnetic Data, Grid and Vector Data, Kidd-Munro, Blake River Area MEGATEM II Survey (2003).

Table 2.1. Examples of sample descriptions from the Western AGB black shale drill-hole database (MRD Report 291). Note that not all descriptors from drill-hole logs were appropriate.

Common Drill-log Terminology	Description (This study)	Grain Size / Context
Pelite	Fine-grained, clay-rich rock	Very fine (clay - sized)
Mudstone	Fine-grained, consisting of a subequal mixture of clay and silt-sized particles	Fine (clay – sized)
Siltstone	Fine-grained, sedimentary rock comprised of consolidated silt particles	Fine (silt - sized)
Argillite - "Graphitic argillite", "Carbonaceous argillite"	Shale with high degree of induration that has undergone some degree of metamorphism but commonly lacks visible cleavage	Fine
Slate	Low-grade metamorphic derivative of shale or mudstone	Fine (metamorphosed)
Metapelite	Metamorphosed fine-grained, clay-rich rock	Fine (metamorphosed)
Greywacke	Dark, coarse-grained sandstone with a high clay content	Coarse (sand - sized)
Interflow sediments	Layers of sedimentary rock interbedded within sequences of volcanic rocks	N/A

Table 2.2 Common field description / core log entries used to describe the shale samples.

	Core log entry	Interpretation
Samples with no veining or sulphides	Black, fine-grained shale	Fine-grained texture indicates that grains are too small to see without a microscope. Black colour indicates high organic matter content
	Dark grey to black, graphitic, fine-grained shale	Graphitic texture indicates metamorphosed organic matter and colour variation reflects changes in organic matter content
	Sedimentary fine-grained, graphitic-argillaceous shale	Clay-rich matrix with disseminated graphite typical of low-energy depositional environment
	Shale part of gradational greywacke turbidite sequence (dark grey to black)	Colour gradation reflects a changing depositional environment and organic matter input
Samples with veining and minor sulphides	Black, fine-grained, shale with coarse pyrite and minor quartz-carbonate veins	Coarse pyrite suggests diagenetic growth and veining represents later fluid flow
	Black, fine-grained, graphitic, laminated shale with 1% nodular pyrite and 1-2% quartz-carbonate veins	Lamination indicates low-energy depositional conditions with pyrite nodules formed during early – late diagenesis and veins represent later fluid flow
	Dark grey-black, fine-grained shale with strong banded graphite, up to 7% pyrite, and < 5% quartz-carbonate veins	Banded graphite indicates metamorphism and high pyrite content suggest a euxinic depositional environment
	Black, very fine-grained shale with 3-5% pyrite nodules/blebs and quartz-carbonate stringers	Pyrite nodules and blebs represent early – late diagenesis and stringers represent later fluid flow

Samples with structural fabric and sulphides	Black, fine-grained, laminated shale with <1% nodular pyrite, <1% quartz-carbonate veins and pressure shadows around pyrite nodules	Pressure shadows microstructures indicate deformation around more rigid pyrite nodules formed during peak to post-peak metamorphism

Chapter 3 – Methods

In 2002 the Geological Survey of Canada conducted a time-domain-electromagnetic survey and magnetic (MEGATEM) survey in the Timmins-Kirkland Lake area which covered approximately 40,000 line-kilometers and was supported by Industry Canada's FedNor 'Discover Abitibi' program, the Ontario Geological Survey, and Falconbridge Limited (now Glencore). This initiative identified large numbers of electromagnetic conductors that were targeted for drilling during exploration. The dominant sedimentary rocks in the region are wacke, sandstone/arenite, chert, iron formation and tuffaceous sediment (Hannington et al., 2012). The rock units sampled in this study were argillite, graphitic argillite, shale, pelite, metapelite or siltstone, as identified in drill logs, with an emphasis on fine-grained carbonaceous sediments.

3.1 Sample Archive

Many of the discovered electromagnetic conductors were identified as sulphide-bearing carbonaceous interflow sediments. The black shales occur in linear belts defining synvolcanic sedimentary horizons within regionally extensive mafic, ultramafic, and felsic volcanic successions of the AGB (Hannington et al., 2012). This study examines the different types of sediments in the belt and the spatial variations in the geochemistry. The sampled drill holes were selected using the following criteria:

i. containing intersections that correspond to well-identified electromagnetic conductors in the region;
ii. containing significant thicknesses of sulphide-bearing and/or carbonaceous argillite (typically >1 m);
iii. representing a wide range of lithostratigraphic associations across the region.

Drill cores were collected from the Ministry of Northern Development and Mines as well as from 19 private companies operating in the area. Drill holes were selected to provide diversity in sample locations both proximal to (e.g., within 100 m) and distal from (e.g., more than 1 km) known mineral deposits. In most drill cores multiple distinct layers of carbonaceous argillite

were present and the most representative material was sampled from the thickest intersection of argillite.

The original sampled area included 76 townships covering more than 15,000 km^2. Between February and June 2011, two geologists accessed core yards where the samples were stored. Sampled holes were widely spaced, commonly 15 km apart, aimed at identifying geochemically anomalous sub-basins but not variations between drill holes. Samples from 4 townships surrounding the giant Kidd Creek mine in Kidd Township, were not included in this study (Figure 2.3 – 2.4). These include proprietary company data that were not part of the Discover Abitibi project. A public-domain subset of data from these townships (Chapman et al., 2010) is discussed at the end of the thesis.

The shale samples were grouped according to bulk composition and their relationship to the different assemblages of the AGB. Drill holes that were originally targeted for discovery of VMS or later orogenic gold mineralization were also identified. Drill hole samples obtained during the exploration for specific types of deposits are considered to be spatially and/or genetically associated with the deposits independent of intersecting mineralization. Drill holes that targeted orogenic gold mineralization are generally close to the Porcupine-Destor fault zone (PDFZ). Drill holes that targeted VMS mineralization are generally within the more widely distributed volcanic assemblages north of the fault. The shales are often the host rocks of orogenic gold and VMS.

Preliminary classification of the samples was based on drill-hole logs and map locations. Assemblages were identified by map location. The typical sample consisted of 25 to 30 cm of core from the thickest argillite intervals: sampled at the centers of intervals. Information on the drill hole, location, depth, sample type, and bounding lithologies are from Hannington et al. (2012), summarized in Appendix 3. Most samples (90%) were collected at a depth shallower than 500 m with 75% of all samples recovered around 200 m (Figure 3.1) which is close to the limit of detection for an airborne EM survey tool (Hannington et al., 2012). Some centrally located townships contain no samples. This may be due to lack of drilling, or lack of usable samples.

3.2 Lithogeochemical Data

Whole-rock geochemical analysis was performed on 564 samples of shale from over 500 drill holes spanning the study area (Table 3.1 and Table 3.2). Whole-rock samples were analyzed by inductively coupled plasma optical emission spectrometry (ICP-OES), inductively coupled plasma mass spectrometry (ICP-MS), and instrumental neutron activation analysis (INAA) to develop a complete geochemical picture of the black shale. The sample handling, preparation, and methods used are described in Appendix A1 from Hannington et al. (2012). The lithogeochemical database is contained in MRD Report-291.

These data were used to classify the shale samples based on major and trace element compositions (Appendix A5). The first step involved an inspection of the geochemical data for evidence of post-depositional alteration of the sediments, including weathering. Numerous studies have established that certain major and trace element ratios are especially useful for this purpose even in cases of extensive weathering, alteration, and mineral sorting (Weaver, 1980; Bhatia & Crook, 1986; Winchester & Floyd, 1977; Large et al., 2001). The ratio of Ti to Zr was used to discriminate between shales derived from different source rocks. Although the concentrations of Ti and Zr may be affected by sediment sorting and recycling, the ratios are largely preserved because they are present mainly in heavy and resistant minerals with similar hydraulic properties (e.g., zircon, titanite). As a first characterization of the sediments, we use the Ti/Zr ratio to identify three main lithotypes of shales, namely felsic-, intermediate-, and mafic-type. Sediments may be enriched in Zr due to preferential sorting and recycling of zircon and depleted in Ti due to preferential loss of ilmenite compared to zircon during weathering. These processes can be visualized in ternary plots such as those developed by Bhatia & Crook (1986).

The Th – Sc – Zr/10 ternary diagram was originally used by Bhatia & Crook (1986) for classifying greywackes. Samples with low abundances of Th and Zr and higher Sc reflect a more mafic source whereas elevated concentrations of Th and Zr reflect a more felsic source. Bhatia and Crook (1986) suggested the trace element ratios could also be used for tectonic discrimination when applied to Phanerozoic greywackes in eastern Australia, distinguishing between oceanic island arc, continental arc, active continental margin, and passive margin

settings. However, the tectonic discrimination diagrams have not been extended to the interpretation of Archean tectonic regimes.

Immobile trace element ratio plots of Th/Sc vs. Zr/Sc are used for characterizing fine-grained sedimentary rocks in terms of sediment provenance and igneous fractionation trends preserved in argillite (Taylor & McLennan, 1985). High Zr/Sc ratios indicate sedimentary sorting, recycling and zircon enrichment while low ratios suggest mafic input and minimal sediment reworking. REE are also useful for tracking sediment source. In deep-sea settings, a strong correlation between P_2O_5% and REE indicates the presence of heavy-mineral phosphates enriched in REEs and resistant to weathering (Tanaka et al., 2025). The relative abundances of REE-bearing phosphate minerals, monazite and xenotime in the source region of the sediments are preserved through sediment recycling and metamorphism allowing us to interpret the source rock composition.

Another important aspect is the degree of weathering and alteration of the sediment components and its impact on geochemical classification. The Na_2O/Al_2O_3 vs. K_2O/Al_2O_3 biplot developed by Davies & Whitehead (1994), is used to quantify the relative abundance of albite, K-feldspar, illite and muscovite resulting from hydrothermal alteration and diagenetic processes. The Al_2O_3-(CaO+Na_2O)-K_2O (A-CN-K) ternary diagram, introduced by Nesbitt & Young (1984), is also widely used to evaluate chemical weathering processes and sedimentary sorting and recycling (Nesbitt et al., 1996; Veizer & Mackenzie, 2005). It captures feldspar alteration trends and helps distinguish between primary mineral input and secondary weathering effects and mineral sorting in sedimentary basins (e.g., McLennan et al., 2003).

A number of alteration boxplots also have been developed for igneous rocks that can be used to characterize sedimentary rocks. The alteration box plot developed by Large et al. (2001), combines two alteration indices, the Ishikawa Alteration Index (AI) and the Chlorite-Carbonate-Pyrite Index (CCPI), to characterize different alteration trends. The Ishikawa Alteration Index [AI = 100 (K_2O + MgO) / (K_2O + MgO + Na_2O + CaO)] was defined by Ishikawa et al. (1976) to quantify the intensity of sericite and chlorite alteration that occurs in volcanic rocks near Kuroko-type base metal deposits. It records the addition of muscovite and chlorite and the

destruction of plagioclase. The Chlorite-Carbonate-Pyrite Index [CCPI = 100 (MgO + FeO) / (MgO + FeO + Na_2O + K_2O)] measures the intensity of chlorite and carbonate alteration. The plot effectively separates the field of hydrothermal alteration from the field of diagenetic alteration (Figure 4.28). Although the Alteration Box Plot was originally intended for igneous rocks, we show that it can also be applied to sediments that are derived from igneous rocks. A high proportion of shales plot within the least altered box at the centre of the diagram and are shifted towards slightly high AI (Figure 4.28). The samples that plot within the least altered box have compositions that are close to those of unaltered igneous rocks. Samples that plot outside of the least altered box have compositions that trend towards end-member mineral compositions, including i) epidote and carbonate, ii) dolomite and ankerite, iii) chlorite and pyrite, iv) albite, and v) K-feldspar and sericite.

3.3 Multivariate Statistical Techniques

Multivariate statistical analysis was undertaken to determine how the geochemistry of the shales varies between:

(i) sediments derived from different source rocks (including sources that may have been hydrothermally altered), and
(ii) sediments in areas that host synvolcanic base metal mineralization versus later orogenic gold.

Multielement correlations were first examined using Pearson's Correlation Coefficients (Appendix A2); then PCA and Random Forest classification. The main outcomes of PCA were interpreted in terms of primary volcanic rock geochemistry, processes of sediment transport and deposition, and hydrothermal alteration and mineralization. We used Random Forest (RF) to develop two classification schemes for black shales based on source rock (i.e., provenance) and the association with different deposit types (i.e., VMS and orogenic gold). The RF model for provenance was trained on a subset of shales identified as mafic, felsic or intermediate in composition according to immobile element ratios (Ti/Zr) of the volcanic rock precursor. An important outcome of the Random Forest classification was to validate the host rock classification scheme using a larger range of immobile trace elements.

3.3.1 Principal Components Analysis (PCA)

The workflow of PCA is shown in Figure 3.2. Principal Component Analysis (PCA) reduces the dataset into a limited number of combined components that account for the largest amount of variance. Each principal component (PC) represents a fraction of the total variance of the dataset and is affected by all the variables. The first PC describes the largest variance in the data. No elements were removed from the dataset for PCA.

The first step in PCA is ensuring that the data are standardized − i.e., all the data have the same unit, and, in this case, all elemental concentrations are in parts per million (ppm). Secondly, centered-log ratio (CLR) transformations are applied to overcome the constant sum problem. Closure effects are a result of covariations between elements in a closed system (i.e., increasing the concentration of one element causing a decrease in the concentration of another: Aitchison, 1982). This is a problem mostly for the major elements. The CLR transformation involves two steps: 1) calculating the geometric mean of each value, and 2) the natural logarithm of the ratio of each value to the geometric mean. The fully log-transformed data used in this study are included in Appendix A4.

A covariance matrix of the CLR values is then calculated. The covariance matrix is a representation of the variance between each variable and all other variables in a dataset (Shlens, 2014). In PCA, the eigenvectors of the covariance matrix define the principal components. Eigenvectors indicate the direction of variance in multivariate space along which variance is maximized. When projected onto a scatterplot they correspond to the axes of maximal spread. Each principal component is a normalized linear combination of variables that capture a portion of the total variance. In biplots of the principal components, the coordinate system of the PCA is oriented to maximize the variance represented (Figure 3.3). The principal components themselves are vectors, meaning they have a magnitude and direction. The direction is determined by the eigenvectors and the magnitude of the principal component is defined by its eigenvalue (Figure 3.4).

In high-dimensional datasets, such as geochemical data, components accounting for the lowest amount of the total variance are often discarded to reduce dimensionality (Anderson, 2003). This can be illustrated in a Scree plot, which shows the distribution of the eigenvalues among the principal components (see Chapter 5). In a Scree plot, eigenvalues typically decrease exponentially with the number of components, forming a curve with a distinct “elbow”; beyond this point all additional PCs contribute little variance and are considered insignificant (Jackson, 1993).

The contribution of individual elements to the variance represented by each component is described as "loading". The loadings are the correlations or weights that connect the original variables to the principal components (Figure 3.5). The loadings are calculated by multiplying the eigenvectors from the covariance matrix by the square root of their corresponding eigenvalues (Jackson, 1991). Positive loadings mean that the element and PC are positively correlated, and negative loadings indicate that a variable and a PC are negatively correlated. Scores of each datapoint projected onto the principal components can be visualized in a PCA biplot with the loadings shown as vectors/arrows. The PCA scores for each sample in this study are listed in Appendix A6.

Evaluation Steps:

(i) Scree plots indicate the proportion of variance associated with each principal component.
(ii) Biplots of PCs combine the scores and loadings of different principal components into a single plot in which longer vectors indicate strong influence of a variable and the angle between vectors indicates positive or negative correlations.
(iii) Maps of PC loadings for PC1 through PC4 help to visualize how the different geochemical components of the sediment vary geographically

In this study, PCA was performed in ioGAS, which uses classical PCA. The results are presented in Appendix A6 – A8.

3.3.2 Empirical Bayesian Kriging (EBK)

Kriging was used to analyze spatial relationships between shales of different composition in the study area. Kriging is a moving-average estimation technique that uses spatial correlation to estimate values at unmeasured points and calculates the uncertainty associated with the interpolated values (Oliver & Webster, 1990). The uncertainty is captured as a raster of the average standard error values (Appendix A9). It predicts values at unsampled locations using a weighted average of neighbouring samples (Franceschi et al., 2024). Ordinary Kriging is an appropriate method when the sample data have a normal or close to normal statistical distribution. Because the distribution of principal components in this study is not normal (Figure 3.6), we employed Empirical Bayesian Kriging (EBK: Gelman, 2004). EBK uses a semi-variogram to make the predictions. A semi-variogram is a geostatistical tool that records the degree of spatial correlation of random components (Figure 3.7). The semivariogram measures the half mean-squared difference between the values of each pair of points in the dataset as a function of the distance between them, known as lag distance (Pyrcz & Deutsch, 2006; Bivand et al., 2008). The semi-variogram assumes spatial autocorrelation − i.e., that samples closer together are more alike than those further away – and takes into account that this similarity diminishes with increasing distance between the samples. EBK uses multiple semivariogram functions to identify a potential correlation structure in the whole dataset (Oliver & Webster, 1990).

Figure 3.6 shows the distribution of eigenvalues for each principal component. The non-normal distribution of PC2 and PC3 means that Empirical Bayesian Kriging (EBK) is particularly important for these components. Data that are normally distributed (e.g., PC1 and PC4) will yield a similar output to Ordinary Kriging and the transformation step built into EBK becomes redundant without negatively impacting the results (Gribov and Krivoruchko, 2020).

3.3.3 Random Forest

Random Forest (RF) is a supervised machine learning algorithm that sorts samples using decision trees into pre-determined classes identified with a training data set (Breiman, 1984,

2001, 2002; Cutler et al., 2007; McClarren, 2021; Fassbender et al., 2023). Decision trees are a flowchart of questions (i.e., the nodes) that filter samples into clusters based on attributes such as geochemical data (Figure 3.8). The code and example decision tree are provided in Appendix A10, A11 and A12. The final sorting is an average of the results of all the trees in the forest. The following description is derived from Fassbender et al. (2023), which outlines the approach used in our research group.

We used RF to sort samples into known classes (e.g., mafic-type, intermediate-type, and felsic-type) using hierarchical clustering and a "training" data set. The training is an iterative process by which random forest learns what values are meaningful to achieve the best classification outcome which become a model that can be used as a classification scheme. Following the method of Gholamy et al. (2018), the data were divided into a training set (80% of the data) and a test data set (20% of the data) that was not used to train the model (Appendix A10).

To assess the accuracy and validate the RF models a procedure called "Bootstrapping" is used. Multiple decision trees (usually a thousand or more) are created by randomly selecting elements (i.e., the nodes) from a training data set. Each decision tree is then evaluated or "trained" with randomly chosen samples (equal to the total number of samples in the data base). Importantly, during this process samples can be picked multiple times, which leaves behind a pool of samples that were not picked and therefore not involved in some decision trees (so-called "out of bag" OOB samples), typically about one-third of all samples. OOB samples were not included in the training of specific decision trees and can therefore be used to independently validate the classification performance of the RF model. Validation is done by comparing the predicted classifications of the OOB samples with their true, known classes providing an unbiased estimate of the model's accuracy (Fassbender et al., 2023). Validating the classification involves separating the data into training and test datasets. At every node the "impurity" of the separation can be measured in terms of the probability of a parameter falsely classifying a sample. This is determined using the "Gini Index". Gini indexes were calculated to evaluate the performance of each node, ordered from the highest to their lowest predictive power.

The OOB Score = Number of correct OOB Predictions / Total Number of OOB Predictions.

An OOB score close to 1 indicates good performance.

Unequal sample sizes within the target clusters may create an imbalance that can negatively affect the performance of the RF model. Imbalance means that the classification categories/classes are not equally represented, and the predictive accuracy may significantly decrease as a result. To prevent this, the Synthetic Minority Oversampling Technique (SMOTE) creates new synthetic samples for the minority class until each class contains an equal number of samples (Chawla et al., 2002). SMOTE creates new samples by slightly altering the geochemical composition of original samples until each class in the training set contains the same number of samples as the largest class (Fassbender et al., 2023).

Each node of the decision tree splits the samples into groups based on a single parameter or criterion. An example query at one node could be: “Is the concentration of Sc in the sample greater than or equal to 22 ppm? If true, the sample is felsic in composition, if false the sample is mafic” (Figure 3.6). The cut-off that successfully separates all samples into predetermined mafic and felsic groups is identified through an iterative process testing several Sc concentrations until the best separation occurs, referred to as “pure” separation. At every node the “impurity” can be measured using the Gini index (Breiman, 2001; Breiman et al., 1984). The impurity for each node is referred to as the "mean decrease Gini" and corresponds to the probability of misclassification. Nodes with a low Gini index have a high probability of correctly classifying a sample (Breiman, 2001). The Gini importance score represents the frequency of a certain feature being selected during a split and the overall importance of the feature for the binary classification task (Disha and Waheed, 2022). It identifies the most important variables (elements) in determining whether a sample is classified correctly (see Chapter 5).

RF is a popular classification method because randomizing precautions built into the model (e.g., Bootstrapping) reduce sensitivity to minor changes in the data that could greatly impact the classification. Random forest also shows how many times samples are improperly classified and which variables (e.g., elements) are the most important for making accurate predictions (Sprague and Vermaire, 2018). The RF models for shale lithotype and for shales targeted for different mineral deposit types were trained separately on subsets of shales previously identified as

belonging to a particular lithotype (i.e., by Ti/Zr ratio) or associated mineral deposit types (i.e., targeted in exploration for VMS or orogenic gold mineralization. We also tested a RF model based on lithostratigraphic assemblage to determine if it is possible to identify shales from different volcanic episodes in the AGB. Building and testing the RF models was done in Jupyter Notebook using the Python programming language developed by Fassbender et al. (2023) and the online platform: Scikit Learn (Scikit-Learn Developers, Tree-based models, n.d.; Scikit-Learn Developers, Random Forest Classifier, n.d.) (Appendix A10).

In this study, the number of trees (also known as "estimators") was set to 500 to optimize the model and reduce variance. The greater the number of estimators, the better the performance of the model because it leads to more stable predictions. However, there is a limit to how many trees will improve the model. Overfitting occurs when the model shows good training accuracy but low testing accuracy and is one of the largest issues in developing a decision tree model (Verdhan, 2020). We used the entire database of 564 samples with each sample classified according to provenance (Zr/Ti), targeted ore type (VMS or orogenic gold) and assemblage type (Appendix A3). The training set (80% of the data) consists of the analyzed elements and the predetermined target classes for each sample. The accuracy of a RF model can be visualized by using the Receiver Operating Characteristic (ROC) which plots the true positive rate of classification vs false positive rate. The true positive rate measures how many shales the model correctly classified out of all shales, and the false positive rate is a measure of how many shales were misclassified. The area under the curve (AUC) represents the ability of the model to distinguish between classes across all possible thresholds. The AUC can range from 0 (worst result) to 1 (perfect result).

The following summarizes the steps in developing a Random Forest classifier:

(i) define the target classes (e.g., sediments derived from felsic, mafic, or intermediate source rocks)

(i) split the data into a training set (80%) and a test set (20%)

(ii) balance the training data using SMOTE

(iii) train the random forest classifier model using the bootstrapping procedure to build the decision trees

(iv) validate the model using a subset of samples remaining from the bootstrapping procedure (i.e., “out of bag” samples)

(v) generate a prediction based on test data

(vi) evaluate the model performance using

a. Mean Decrease in Gini (i.e., the probability of a sample being correctly classified) and the Importance Score / Feature Importance (i.e., a derivative of MDG indicating how important a variable is for model performance)
b. A comparison of the actual values vs predicted values (i.e., a Confusion Matrix)
c. Area Under the Curve (ROC-AUC; i.e., ability of the classifier to distinguish between multiple different classes)

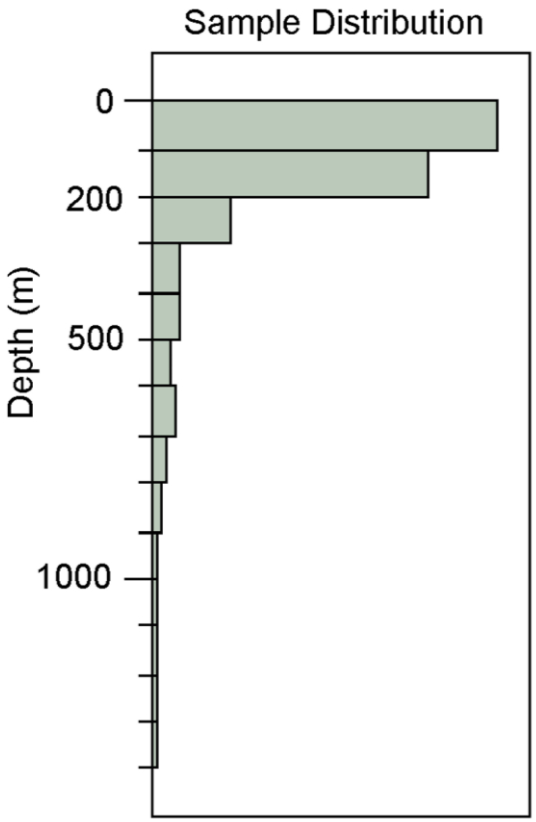


Figure 3.1. Drill-hole depth distribution of samples collected in the Regional Lithogeochemical Study of the Kidd-Munro MEGATEM Survey (Hannington et al., 2012). The average depth (~200 m) is close to the limit of detection of major conductors in MEGATEM surveys (Hannington et al., 2012).

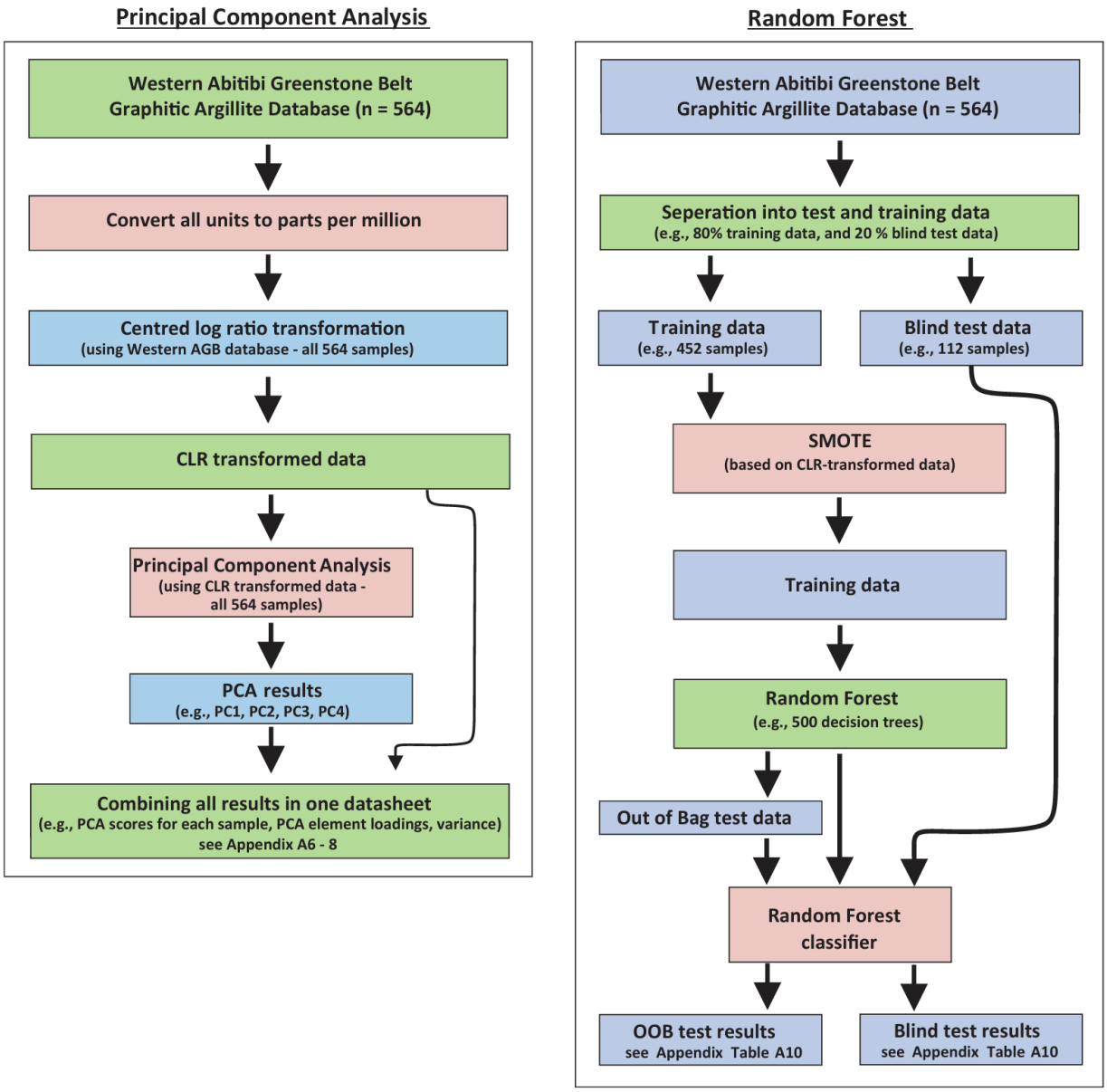


Figure 3.2. Workflow of PCA analysis and Random Forest Classification adapted from Fassbender et al. (2023).

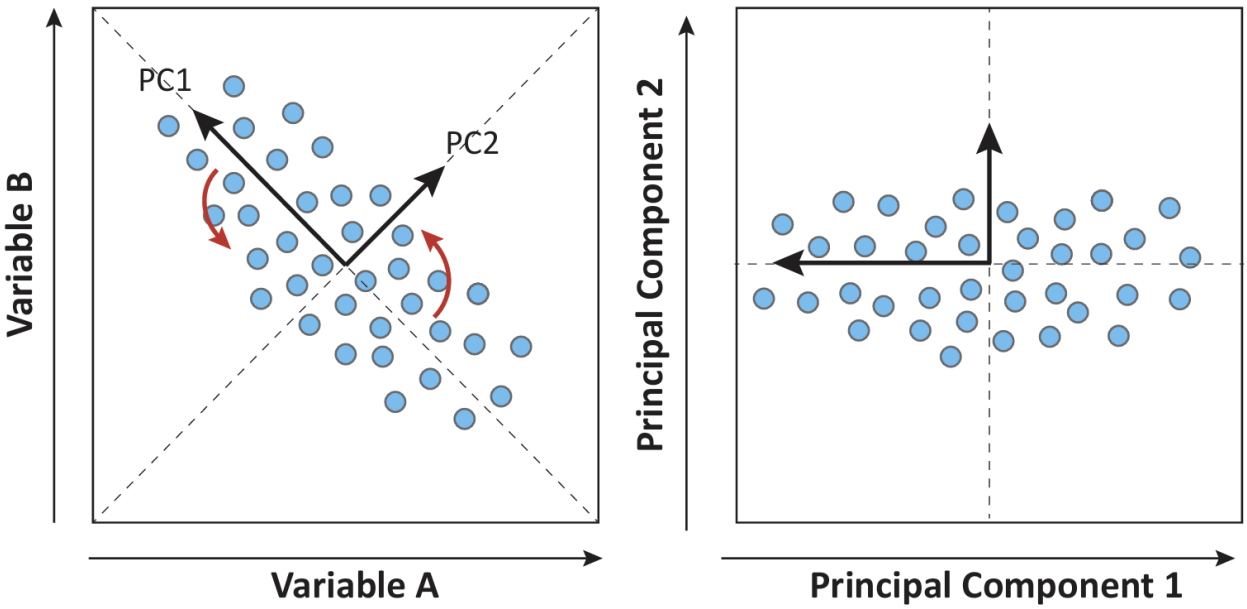


Figure 3.3. Schematic illustration of principal components analysis. The principal components are normalized linear combinations of variables that capture maximum variance in the data set. The first principal component explains the greatest variance. The coordinate system of the PCA is oriented to maximize the variance represented in biplots of the principal components. This transformation can be visualized as a rotation of the coordinate system with directions of greatest variability based on the covariance matrix. Partially developed from Prabhakaran, S. n.d., Principal Component Anlaysis – How PCA algorithms work, the concept, math and implementation, Machine Learning Plus.

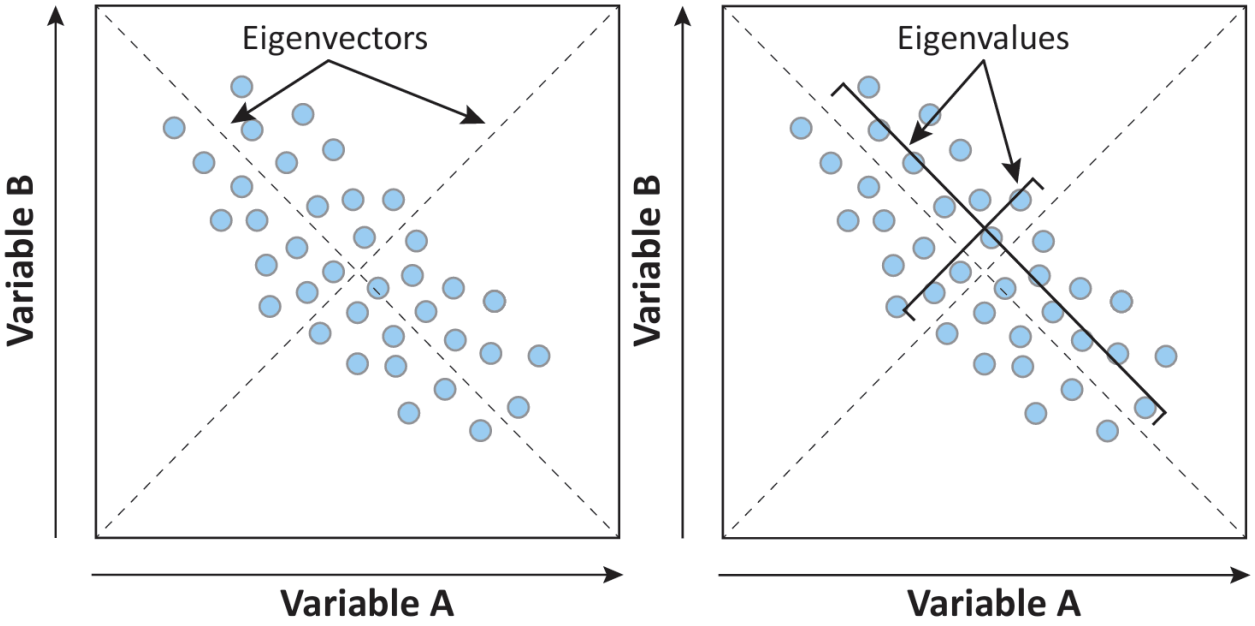


Figure 3.4. Schematic illustration of eigenvectors and eigenvalues. In PCA, the eigenvectors of the covariance matrix define the principal components. Eigenvectors are represented by the direction and eigenvalues are the magnitude of the variance represented by the sample points.

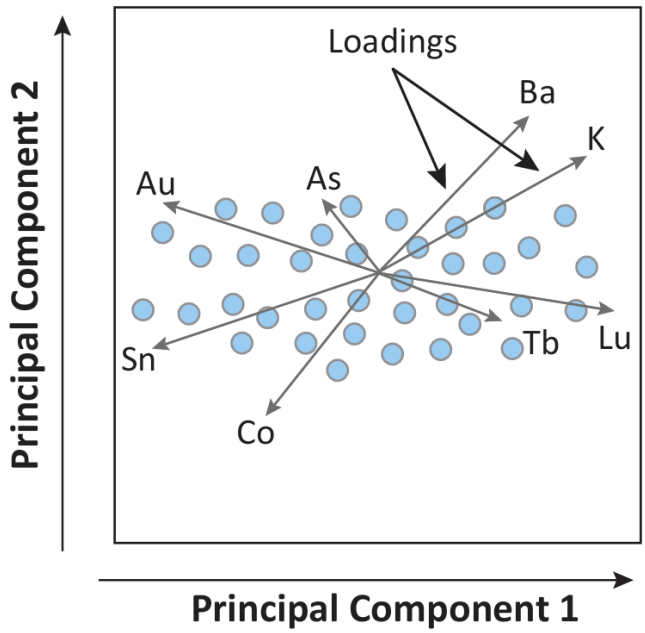


Figure 3.5. Schematic illustration of the loadings of different elements on principal components 1 and 2. The loadings are the contribution of individual elements to the variance represented by the principal component. They are calculated by multiplying the eigenvectors of the covariance matrix by the square root of their corresponding eigenvalues (Jackson, 1991).

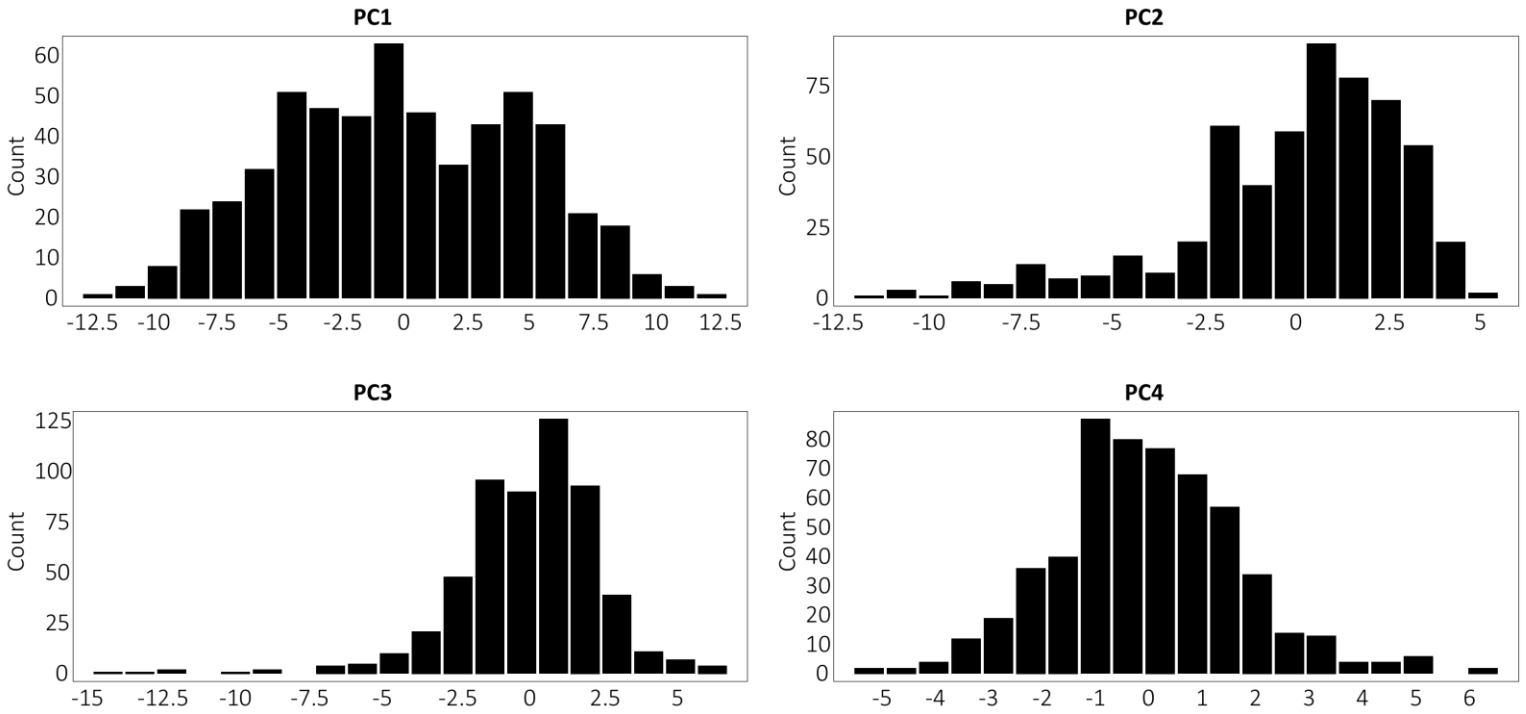


Figure 3.6. Histograms of the eigenvalues for Principal Component 1 through 4. PC1 and PC4 have broadly normal distributions, whereas PC2 and PC3, are skewed. The non-normal distribution means that Empirical Bayesian Kriging (EBK) is particularly important for these components (see text for discussion).

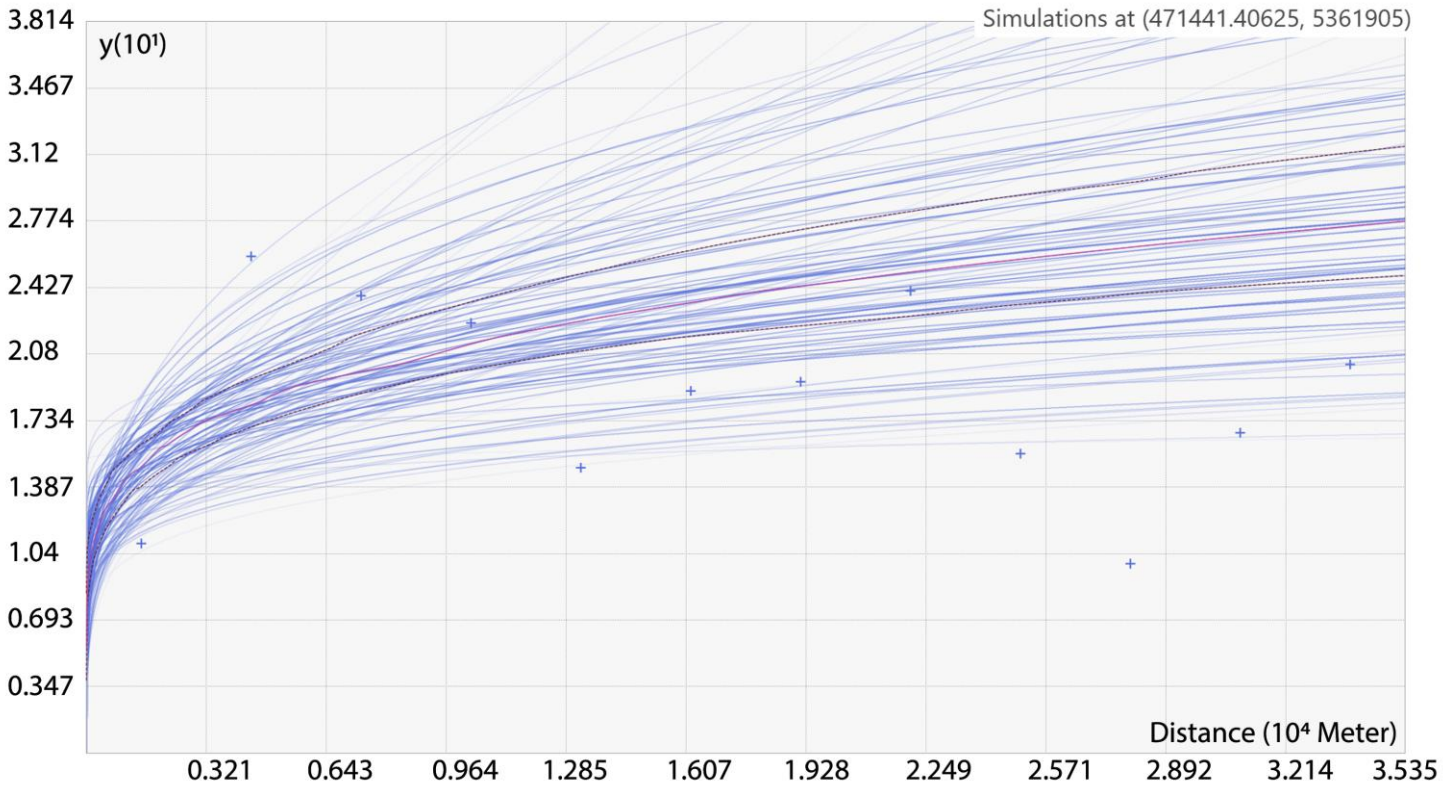


Figure 3.7. Empirical Bayesian Kriging (EBK) semivariogram simulation in ArcGIS Pro, at location (471441.41, 5361905) centered on a cluster of samples in Ogden township. At this location EBK generated multiple local semivariograms to model spatial correlation in PC1. Each blue curve represents one simulation, illustrating how spatial correlation changes with distance. The x-axis represents lag distance (see text) in tens of thousands of meters, and the y-axis shows unitless semivariance, reflecting variance in PC1 scores between sample pairs. The darker the blue regions indicate areas where more simulated semivariograms overlap. The tight clustering of curves at shorter lag distances suggests similarity among nearby samples. As lag distances increase, the spread of the curves reflects uncertainty in spatial structure across local subsets. The semivariograms capture the degree of spatial autocorrelation – assuming that samples closer together are more alike than those farther apart – and describe how this similarity diminishes with distance (Oliver and Webster, 1990).

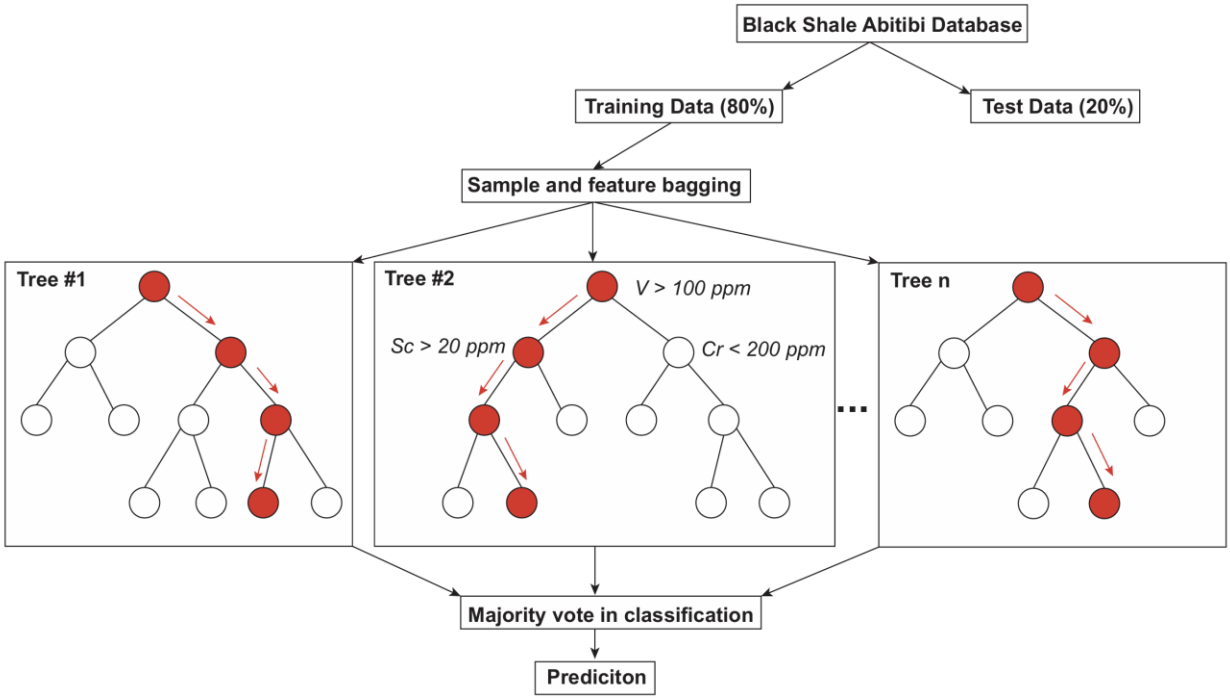


Figure 3.8. Visualization of Random Forest Classifier model used to make predictions about the Abitibi black shale database. This is explained in-depth in Chapter 5.

Table 3.1. Summary statistics for the bulk geochemistry of major elements in graphitic argillite of the Western AGB (from Hannington et al., 2012).

Major Oxide (wt %)	Mean	Median	1st Quartile	3rd Quartile
SiO_2	57.07	59.43	52.89	63.95
Al_2O_3	13.24	13.94	10.02	16.69
Fe_2O_3	8.19	6.52	4.73	9.62
MnO	0.076	0.050	0.025	0.077
MgO	2.46	1.65	1.02	2.95
CaO	2.66	1.49	0.72	2.91
Na_2O	2.17	1.93	0.85	3.03
K_2O	2.17	2.33	0.98	3.08
TiO_2	0.505	0.478	0.344	0.665
P_2O_5	0.11	0.11	0.08	0.14
LOI	10.30	7.61	4.94	12.56
CO_2	2.11	1.00	0.13	2.56

Table 3.2. Summary statistics for the bulk geochemistry of trace elements in graphitic argillite in the Western AGB (from Hannington et al., 2012).

Element (ppm)	Mean	Median	1st Quartile	3rd Quartile
Au (ppb)	101	12	1	32
Ag	0.9	0.6	0.3	0.9
As	131	61	19	177
Ba	437	446	201	608
Be	1	1	1	2
Bi	2.4	1.0	0.5	2.1
Br	1.7	0.3	0.3	2.1
Cd	2.6	0.7	0.3	2.9
Co	47.2	33.2	24.6	53.9
Cr	139.5	73.9	40.8	155.0
Cs	2.4	1.8	0.6	3.1
Cu	383	109	59	249
Ga	19	19	14	23
Ge	1.8	1.6	1.2	2.0
Hf	3.1	3.1	2.4	3.6
Hg (ppb)	212	31	5	196
In	0.08	0.05	0.05	0.05
Mo	6	4	2	7
Nb	5.8	5.5	4.1	6.8
Ni	157	108	75	155
Pb	54	13	5	33
Rb	61	64	26	90
Sb	4.7	1.9	0.6	5.2
Sc	16.71	15.70	12.10	20.40
Se	2.5	0.3	0.3	2.3
Sn	4	2	1	5
Sr	131	100	53	183
Ta	0.46	0.44	0.33	0.53

Th	4.63	4.29	2.79	6.13
Tl	0.83	0.56	0.24	1.05
U	1.37	1.19	0.79	1.69
V	100	88	61	137
W	2	1	1	3
Y	17	15	12	19
Zn	1059	323	98	1335
Zr	118	120	92	138
La	20.54	20.30	12.68	26.53
Ce	44.23	44.00	28.55	56.50
Pr	5.26	5.22	3.42	6.61
Nd	20.46	20.50	13.38	25.50
Sm	4.01	3.95	2.84	4.76
Eu	1.129	1.080	0.823	1.310
Gd	3.39	3.24	2.48	3.85
Tb	0.54	0.49	0.40	0.59
Dy	3.09	2.82	2.24	3.34
Ho	0.62	0.55	0.44	0.67
Er	1.83	1.59	1.30	1.99
Tm	0.274	0.234	0.194	0.297
Yb	1.88	1.63	1.34	2.04
Lu	0.321	0.275	0.231	0.360

Chapter 4 – Classification of Shale Lithotypes

Classification of shale lithotypes in the field or in drill core is difficult because of their uniformly dark, fine-grained nature. Classifying them based on geochemistry is also complicated by a range of sedimentary processes (e.g., sorting, mixing, recycling, chemical weathering, diagenesis) that can obscure the provenance. A comprehensive classification of shale lithotypes offers insight into sediment sources, transport, and the scale of the depositional sub-basins. Identifying whether shales originated from a mafic or felsic source terrane, for example, can be important for reconstructing synvolcanic sedimentary sequences within greenstone belts, which may in turn be important for resource exploration. Alteration of the parent rock can serve as a vector for different mineral deposit types that may be hosted by or associated with the sediments. Different shale lithotypes also can indicate different depositional environments that may be more or less favourable for mineralization.

4.1 Geochemistry of Shales

The distinction between shale lithotypes is a direct reflection of their parent rock composition. However, the type of material deposited is also a function of distance from its source and process of transport (e.g., by sorting of heavy minerals: Weaver, 1990). Turbidity currents, pyroclastic flows, submarine fans, gravity settling, and input from chemical sedimentation (BIFs) can all contribute to the sediment load (Mueller & Donaldson, 1992). Sorting, dilution, recycling, and redox reactions may all impact the geochemical composition of the sediment, and different elements can respond in different ways. For example, Na and Ca are often more mobile and more reactive than K which is retained longer in weathered rocks (e.g. Nesbitt et al., 1996). Sediment that has been transported farther can experience weathering and destruction of anorthite and albite, with K preferentially enriched in the secondary clay minerals such as illite (Nesbitt et al., 1996). Alkali earth elements such as Rb, Cs, and Ba can be variably leached or retained in the sediments (e.g., incorporated in the structure of or adsorbed on clays). To illustrate these processes, Nesbitt & Young (1996) developed the chemical index of alteration (CIA) to quantify the degree of weathering using molecular proportions of Al_2O_3, CaO, Na_2O, and K_2O.

In contrast, chemically resistant minerals, including zircon and REE-bearing heavy minerals, may be enriched by sedimentary processes such as heavy-mineral sorting. However, the immobile element ratios are commonly preserved and therefore are a useful proxy for the original bulk rock composition and sediment source. Immobile element ratios provide a valuable means of classifying the source rock composition, despite sediment sorting and recycling, because the immobile elements are present mainly in heavy minerals with similar hydraulic properties. This is especially apparent among the high field strength elements (HFSE). The average concentrations of REEs are also a commonly used reference (e.g., in post-Archean Average Australian Shale or PAAS). The abundances of certain trace elements in the primitive mantle, average continental crust, and average post-Archean shale are shown in Table 4.1.

The heavy trace minerals with high HFSE concentrations, namely zirconium (Zr), hafnium (Hf), niobium (Nb), and tantalum (Ta) correlate with mainly felsic minerals in the rock. HFSEs are generally immobile in most geologic settings; however, they can be enriched in shales through sedimentary processes, such as sorting, that concentrate resistant heavy minerals such as zircon (Taylor & McLennan, 1985; Bhatia & Crook, 1986; Totten & Hanan, 2007). In contrast, shale that formed in a low-energy environment undergo minimal additional sorting and enrichment once they have been deposited.

Environmental conditions during deposition such as redox, the basin setting, and organic matter content also influence the behaviour of trace elements in shale (Potter et al., 1980; Feng & Kerrich, 1990; Veizer & Mackenzie, 2005). For example, black shales can be highly enriched in redox-sensitive metals (e.g., V, Ag, Mo, Ni, Cu, and U) that are precipitated or adsorbed onto other minerals under anoxic conditions (Pašava et al., 2023). Post-depositional processes such as diagenesis and hydrothermal alteration also can modify the chemical composition of the shale (Large et al., 2011; Busby & Pérez, 2012).

4.2 Geochemistry of WAGB Shales

Sedimentary rocks in Archean greenstone belts are dominantly: 1) volcaniclastic and chemical sediments interbedded with volcanic rocks in the lower volcanic portion of greenstone belts, and

2) thick clastic sedimentary deposits above the volcanic sequences (e.g., Porcupine – Timiskaming sedimentary basin) (Thurston, 2015). The main volcanic episodes in the Abitibi are capped by thin sedimentary interface zones of graphitic argillites that are directly related to volcanism rather than marine sedimentation (Thurston et al., 2008). These beds were deposited in deep-water settings during a hiatus in volcanism (Monecke et al., 2017). In most drill holes, horizons of carbonaceous argillite are intercalated with volcanic and other sedimentary rocks.

The geochemistry of black shale from the AGB differs from that of younger successions. The Archean crust was less evolved which is reflected in the juvenile volcanic provenance of the sediments (Taylor & McLennan, 1985; Monecke et al., 2017). The host volcanic assemblages are dominated by mafic and ultramafic rock, and there was limited crustal differentiation. As a result, the shales have anomalously high mafic-element concentrations, including Ni and Cr associated with the ultramafic units. Feng and Kerrich (1990) analysed sandstone and shale samples from the southern volcanic zone of the Abitibi and defined two populations: mafic element (MEP) and low mafic element (LMEP) populations. MEP were defined as having concentrations of MgO > 5%, Cr > 400ppm, and Ni > 200 ppm. MEP samples have a narrow range of SiO_2 contents and lower Al_2O_3, K_2O, and Na_2O, but higher Fe_2O_3, and MnO contents. MEP were thought to have formed in basins proximal to or within volcanic rifts, and LMEP formed in island arc-like settings.

Redox-sensitive trace elements including V, Mo, and U have variable enrichment based on the depositional conditions and all have lower concentrations in Archean sediment compared to present global averages (Granitto et al., 2017). Conversely, low oxygen levels during the Archean led to low primary productivity meaning less organic-rich depositional matter (Condie, 2001; Hiebert et al., 2018). Redox-sensitive trace elements are typically concentrated in sediments with higher organic carbon content. Increased concentrations of sulphide in the water column may also reflect localized hydrothermal venting in-restricted Archean basins.

The average concentrations of the major and trace elements in the WAGB shales are listed in Appendix A5. The samples are grouped according to an initial classification based on Ti/Zr ratio and also classified according to possible associated mineralization (i.e., drill holes originally

targeted for discovery of VMS or later orogenic gold) and volcanic assemblage (i.e., based on map location). Tables 4.2 – 4.4 summarize the major oxide concentrations for each shale lithotype.

Figure 4.1 shows the three populations of volcanic rocks from the Abitibi Greenstone Belt from Fassbender et al. (2023, 2024), identified as felsic, intermediate, and mafic based on the Ti/Zr ratio. The data of Fassbender et al. (2023, 2024) included nearly 6000 samples of mafic and felsic volcanic rocks from the Abitibi. The felsic rocks have Ti/Zr values less than 25, intermediate rocks between 25 and 80, mafic rocks between 80 and 125, and ultramafic rocks greater than 125. These cut-offs were chosen based on natural breaks in the populations of data on the histogram and correspond closely to Ti/Zr values for rhyolite, dacite, and basalt (Fassbender et al., 2023, 2024). The Ti/Zr ratios of the shale samples in this study show a similar multimodal distribution (Figure 4.2). The 30th, 60th, and 90th percentiles were chosen to subdivide the populations into felsic, intermediate and mafic volcanic source rocks similar to the ratios for Phanerozoic volcanic rocks (e.g., Winchester and Floyd, 1977: see Figure 4.12). The lower 30^{th} percentile of Ti/Zr values were chosen to represent shales with a felsic composition, the 30^{th} to 60^{th} percentile represent shales with an intermediate composition, and the 90^{th} percentile represent shales with a mafic composition, with breaks at Ti/Zr < 25 and 45 reflecting the felsic, intermediate and mafic endmembers. The shale data are strongly skewed to the left with a long right-tail. Choosing 45 as the boundary between intermediate- and mafic-type shales is a conservative threshold that ensures that mafic-type samples are represented by dominantly mafic geochemical signatures. The lower Ti/Zr ratio of the shales compared to the volcanic source rocks may mean that zircon has been concentrated in the sediments by sorting and recycling. Lower Ti values in the shales might indicate ilmenite and rutile is less durable than zircon during sediment transport. Another possible reason for the difference between the shales and igneous rocks is that some shale samples were derived from multiple sources with a range of Ti/Zr values.

4.2.1 Source Rock Classification Using Immobile Element Ratios

Immobile element ratios of western Abitibi black shales can be used to discriminate between potential source rocks with mafic to felsic affinities despite the extensive weathering, alteration, and mineral sorting. Heavy minerals are sensitive indicators of provenance and are virtually unaffected by weathering. They have specific and restricted parageneses that track igneous fractionation in the source rocks of the sediments (Morton and Hallsworth, 1999; Morton, 1985). They have very similar hydraulic properties and densities (ilmenite 3.8 - 4.2 g/cm^3, zircon 4.7 g/cm^3, and rutile 3.8 – 4.2 g/cm^3: Valiev et al., 2022) and so are not sorted from each other during transport and deposition, although ilmenite tends to weather at the margins of grains. As a result, the immobile element ratios of the igneous source rock are largely preserved during transport and deposition of the derived sediment.

The average concentration of Zr in AGB rhyolite is ~ 226 ppm (Fassbender et al., 2023), whereas the average concentration in the WAGB shales is ~118 ppm (this study). In the sediments, these concentrations may be increased by sorting or alternatively diluted by quartz. Minerals like ilmenite, rutile, tourmaline, monazite, xenotime, and zircon are among the most persistent and stable minerals (Morton, 1985). Because they have high chemical and mechanical stability, they also tend to become concentrated during sediment recycling.

The compatible-incompatible element ratios of the shales are particularly sensitive indicators of igneous fractionation of their source rocks. Ti is compatible and generally enriched in mafic components of the rock, whereas Zr is incompatible and enriched in felsic components. A low Ti/Zr ratio of the sediments corresponds to more felsic source rocks and a higher ratio corresponds to more mafic source rocks. The average concentration of TiO_2 across all samples in this study is 0.5% wt and the average concentration of Zr is 118 ppm, close to the concentrations in the igneous sources (Hallberg, 1984; Barrett et al., 1993).

4.2.2 Major Elements

SiO_2 is consistently the most abundant oxide component of the shales (~ 57 wt %), followed by Al_2O_3 (13 wt %) and Fe_2O_3 (8.2 wt %). The least abundant oxides include TiO_2 (0.51 wt %), MnO (0.076 wt %), and P_2O_5 (0.11 wt %). Mafic-type shales contain slightly lower Na_2O and K_2O concentrations and higher MgO and TiO_2 concentrations than felsic- to intermediate- type shales (Figure 4.3).

Samples from drill holes that were targeted for VMS are dominantly mafic-type shales (Tables 4.4, 4.6 and 4.10, Figure 4.5). Samples from drill holes that were targeted for orogenic gold include more felsic-type shales and have higher average concentrations of SiO_2, Al_2O_3, Na_2O, K_2O, TiO_2, and P_2O_5 (Table 4.5). They are also enriched in Al_2O_3 and K_2O consistent with potassic and aluminous alteration. Conversely, CaO and Fe_2O_3 are more abundant in mafic-type shales that were targeted for VMS mineralization.

The average CO_2 concentration across all samples is 2.11 wt%. Felsic-type samples have around 1.65 wt% CO_2, intermediate-type samples have about 2.15 wt % CO_2, and mafic-type samples have 5.05 wt% CO_2. Mafic-type samples have a higher C in CO_2 value than intermediate or felsic-type samples and the lowest mean concentration of non-carbonate carbon in all shale lithotypes (Figure 4.4). Samples associated with orogenic gold contain on average 1.90 wt% CO_2, and samples associated with base metal contain 2.34 wt % CO_2. Samples associated with base metal mineralization have the highest non-carbonate carbon concentration (Figure 4.6).

Samples from all six volcanic assemblages have similar trends in major element concentrations, but there are some variations (Figure 4.7). Samples from the Deloro assemblage and Kidd-Munro have elevated Fe_2O_3, CaO, and MgO values. The Deloro assemblage comprises mostly intermediate to felsic metavolcanic rocks and intrusions with some ultramafic components. The Kidd-Munro assemblage comprises mainly mafic, ultramafic and felsic metavolcanics, which is reflected in low mean SiO_2 and Al_2O_3 concentrations in the interbedded shales. Shales from the Kidd-Munro assemblage contain some of the highest CaO, MgO, and Fe_2O_3 values, consistent with the dominantly mafic composition of the host volcanic rocks. Shales from the Stoughton –

Roquemaure assemblage have a mixed mafic and felsic volcanic signature which is reflected in the lowest average MgO, CaO and MnO concentrations in the associated shales. Shales of the Tisdale group are dominantly mafic to ultramafic which is consistent with the relatively high average concentrations of Na_2O, TiO_2, and P_2O_5 in the associated shales. Shales from the Porcupine assemblage have the highest mean Al_2O_3, Na_2O, and TiO_2 values, consistent with the associated clastic metasedimentary rocks and concentration of heavy minerals via sedimentary processes.

Shale samples from Kidd-Munro and Stoughton-Roquemaure have some of the highest average concentrations of non-carbonate carbon (Figure 4.8). This carbon fraction reflects organic matter that was subsequently metamorphosed to graphite. The deposition of organic matter was contemporaneous with VMS mineralization in mafic-dominated regions. The Porcupine assemblage has the lowest average concentrations of non-carbonate carbon.

A comparison of average volcanic rock compositions for Archean-age rocks in the AGB and south-east Superior Craton is provided in Table 4.7.

4.2.3 Other Trace Elements

The average trace element concentrations for shale samples are summarized in Appendix A5 and Table 3.4. Overall, felsic-, intermediate-, and mafic-type shales display similar trace element patterns. The base metals, Zn and Cu, and the trace elements Ba, Sr, and V are abundant among all shale lithotypes. Felsic-type shales have the highest average concentrations of Cu (~ 494 ppm) and Zn (~ 1290 ppm). Intermediate-type shales have the highest average concentrations of Ba (~ 495 ppm) and Sr (~ 1290 ppm), and mafic-type shales are enriched in As (~ 146 ppm), Ni (~ 234 ppm), V (~ 217 ppm), and Cr (~ 449 ppm). Sc, V, and Cr increase systematically from felsic- to intermediate- to mafic-type shales (Figure 4.9). In contrast, Rb, Cs, Ba, Hf, Nb, Th, U, and Th are significantly lower in mafic-type shales, and felsic and intermediate-type samples have higher concentrations of Th, U, and Hf, and Zr. The average concentrations of thorium (Th) and uranium (U) in the shales are 4.6 ppm and 16.7 ppm, respectively. The average concentrations of redox-sensitive elements from this study, the Global Geochemical Database for

Critical Metals in Black Shales (CMIBS) and post-Archean Australian shales are summarized in Table 4.8.

Shales from drill holes that were originally targeted for mineralization are enriched in Zn (~ 794 – 1290 ppm), Cu (~ 259 – 494 ppm), and Ba (~ 296 – 496 ppm). Light REEs are slightly more abundant than heavy REE (Figure 4.10). Shales associated with orogenic gold mineralization are enriched in Ba (~ 533 ppm), Sr (147 ppm), and V (~ 117 ppm), consistent with carbonate and muscovite alteration typical of orogenic gold systems. In contrast, shales associated with base metal mineralization contain elevated levels of Cu (~ 612 ppm), Ni (~ 189 ppm), and Zn (~ 1260 ppm), possibly reflecting the influence of VMS-related hydrothermal fluids. Shales associated with VMS-style mineralization also have a broader range of certain elements, such as V, Cr, Hf, and Nb.

Trace element enrichments, such as Cr, Ni, Co, As, Zn and V (Figure 4.11) reflect the dominantly mafic composition of many assemblages. Shales from the Stoughton Roquemaure assemblage contain slightly higher Pb, As and REE than shales from Deloro. Shales from Kidd-Munro are enriched in Cu and Ni relative to shales from other assemblages. Shales from the Tisdale assemblage are slightly enriched in Cs, Rb, and Th. Zinc stands out for its consistently high abundance in shales from all assemblages, ranging from ~559 ppm in Porcupine to ~1515 ppm (or 0.15 wt %) in Stoughton-Roquemaure, suggesting widespread hydrothermal influence and base metal enrichment. By contrast, trace elements such as Au are relatively low (~ 0.2 ppb).

4.3 Pearson's Correlations

Multielement correlations identified using Pearson's Correlation Matrix highlight relationships among the different lithotypes of shale, shales in different lithostratigraphic assemblages, and shales associated with different mineralization. The multielement correlations reflect a combination of source rocks (i.e, sediment provenance), alteration during transport, deposition, and diagenesis, and mineralizing processes. Pearson's correlation coefficient (r) is a measure of the linear covariation of two variables, with r values from -1 to +1 (Kirch, 2008). The correlation matrix is a symmetrical table of the correlation coefficients of each variable in a set with every

other variable (Sokal & Rohlf, 1995). In this study, a correlation matrix was created no distinction made between shale lithotype, associated mineralization or assemblage. By not removing any samples it reduces any bias that these groupings may create. The critical correlation threshold for 564 samples (Pearson's r value) is 0.073 at a 90% confidence interval (Sokal & Rohlf, 1995). The element correlations were interpreted in terms of the mineralogy of the shales empirically sorted according to different element groupings:

- Major oxides (SiO_2, Al_2O_3, Fe_2O_3, MnO, MgO, CaO, Na_2O, K_2O, TiO_2, P_2O_5)
- Muscovite (Rb, Sr, Cs, Ba)
- Carbonate (CO_2, CaO, Sr)
- Mafic elements (Sc, V, Cr)
- Felsic elements/HSFE (Zr, Hf, Nb, Ta, Ga)
- Other incompatible elements (Th, U)
- Rare earth elements (Y, La, Ce, Pr, Nd, Sm, Eu, Gd, Tb, Dy, Ho, Er, Tm, Yb, Lu)
- Carbon and diagenetic sulphide (LOI, C, CO_2, S, Total S)
- Mafic-associated sulphides (Co, Ni, Se, Mo, Ge, As)
- Polymetallic sulphides (Cu, Pb, Zn, Cd, Hg, Sn, Tl)
- Orogenic gold-related elements (Sb, Ag, Au, W, Bi, B)

Many positive correlations between elements can be explained by similar geochemical properties (e.g., similar ionic potential of K^+ and Rb^+) and host minerals. However, there may be multiple ways to explain the correlation between elements (e.g., crystal lattice substitution, similar adsorption onto clay minerals, byproducts of other processes). In addition, some specific element associations serve as pathfinders for different styles of mineralization (e.g., B plus As, Sb, W, CO_2 as a pathfinder for orogenic Au; Cd, Ag, Sn as a pathfinder suite for VMS) (Hannington et al., 2012).

Muscovite component

The major oxides, K_2O and Al_2O_3 are correlated with the muscovite content of the samples. Trace elements, such as Rb, Sr, Cs, Ba, and to a lesser extent LREE and Ga, strongly partition into the

white micas and clay minerals, as well as K-feldspar, and substitute for Na and K in the crystal lattice. Additionally, these elements may be adsorbed onto carbonaceous matter.

Carbonate component

CO_2 has a strong correlation with CaO suggesting that the dominant carbonate mineral is calcite. There is a moderate correlation between CaO and Sr. Sr also has a moderate correlation with MgO and so at least some of the Sr is in dolomite ($CaMg(CO_3)_2$). In an anoxic ocean basin Mn^{2+} will be the dominant ionic species and is commonly incorporated in carbonate. This is supported by the strong correlation between MnO and CO_2 in the correlation matrix.

High Field-Strength Elements (HFSE)

Zirconium is commonly associated with hafnium in the mineral zircon ($ZrSiO_4$) while niobium and tantalum are also present as trace elements in ilmenite and titanite (Morton & Hallsworth, 1994; Jones et al., 2017). During weathering and synvolcanic hydrothermal alteration, HFSEs in shales can be mobilized with the breakdown of accessory minerals and the formation of new minerals (Jiang et al., 2005). However, the bulk concentrations mainly reflect a strong detrital enrichment of the refractory heavy minerals, although the absolute concentrations of the elements also can be diluted by quartz.

Tourmaline, apatite, monazite and xenotime are also concentrated by sorting in high-energy depositional environments, but the trace elements themselves are not fractionated. The HFSE and REE are strongly correlated with muscovite and negatively correlated with Fe_2O_3, CaO, and volatiles like sulfur, CO_2 and carbon. The latter reflects dilution of the felsic minerals by Fe-sulphide, carbonate and other non-silicates of the shales, especially under anoxic, low-energy, aqueous environments that had a high organic matter content.

Gallium is strongly correlated with Al_2O_3 and TiO_2 suggesting that it may substitute for aluminum in clay minerals and for Ti in titanium-oxide minerals. Ga also has a strong correlation

with uranium and REE that are present in the REE-bearing phosphate minerals monazite and xenotime.

Mafic-element component

The mafic minerals of the shales contain scandium (Sc), vanadium (V), and chromium (Cr). Vanadium and scandium have a strong positive correlation with the major oxides Al_2O_3, MgO, P_2O_5, and TiO_2. Chromium has a strong correlation with Ni, Co, and MgO, and a negative correlation with the HFSE and the LREE.

Vanadium is incorporated into clays as V^{3+} during diagenesis as well as in iron-bearing minerals. Vanadium as V^{5+} occurs in aluminosilicate minerals such as vanadium-bearing mica (Kelley et al., 2017; Wang, 2024). V is strongly correlated with Al_2O_3, Fe_2O_3, MgO, Sc, Cr and therefore is most likely substituting in heavy minerals like magnetite and ilmenite, or in mafic phyllosilicates such as biotite and chlorite.

Scandium and chromium show a strong positive correlation with Ni, Mg, Fe, Ti, Co and V, reflecting their shared origin from mafic and ultramafic source rocks. Scandium (Sc^{3+}) is sourced exclusively from mafic igneous rocks and is typically concentrated in titanium-rich minerals, including ilmenite, and is also found in mafic minerals such as pyroxenes and amphiboles (Cotton, 2011). Chromium may be present in Cr-rich white mica, known as fuschite, formed by hydrothermal alteration of the ultramafic rocks.

Uranium and Thorium component

The highest concentrations of U in black shales are found in zircon ($ZrSiO_4$) and, to a lesser extent, titanite ($CaTiSiO_5$), consistent with the positive correlation of U with Zr and a weaker correlation with Ti. Both Th and U are commonly hosted in monazite [(Ce, La, Nd, Th)(PO_4, SiO_4)] and show a strong correlation with other elements present in monazite, particularly the LREE. Monazite behaves as a detrital heavy mineral, and its enrichment in shales may be due to

sedimentary sorting. This behaviour is supported by strong correlations with HFSE including Hf, Nb, and Ta.

Uranium is more soluble in its oxidized hexavalent state (U^{6+}) but in reduced basins of the Archean greenstone belts it was likely in its reduced tetravalent state (U^{4+}), leading to its precipitation as uraninite. U is positively correlated with Al_2O_3, Be, Ga, Hf, Zr, and LREE. The reduced form, U^{4+}, is highly reactive and can also be incorporated into the crystal structure of accessory minerals like zircon ($ZrSiO_4$). However, its high charge precludes substitution into major rock-forming minerals. Thorium, by contrast, is mostly insoluble in natural waters but readily adsorbed onto the surfaces of clay minerals like kaolinite ($Al_2Si_2O_5(OH)_4$) and smectite. Thorium is concentrated in the phosphate mineral monazite [(Ce, La, Nd, Th)(PO_4, SiO_4)] but may also occur in apatite ($Ca_5(PO_4)_3$), titanite ($CaTiSiO_5$), allanite [$(Ca,Sr)_2(Al,Fe,Mn,Mg)_3Si_3O_{12}[OH]$], and zircon ($ZrSiO_4$). Thorium shows strong correlations with Zr, the LREE, and HFSE such as Hf, Nb, and Ta. Thorium is positively correlated with Al_2O_3 and K_2O, as well as trace elements associated with muscovite including Rb, Sr, Cs, and Ba.

Rare earth element component

REE are primarily hosted in the phosphate minerals monazite and xenotime, as well as zircon. As a result, sedimentary sorting processes tend to concentrate the REE. REE can also substitute for calcium in phosphate minerals such as apatite (Totten & Hanan, 2007; Morton & Hallsworth, 1994).

Under specific hydrothermal conditions including low pH, high water/rock ratios, and the presence of complexing ions such as carbonate (CO_3^{2-}), fluoride (F^-) and chlorite (Cl^-), REEs can be mobilized and transported in hydrothermal fluids (Fulignati et al., 1999). However, they are mostly resistant to dissolution. Cerium (Ce) and europium (Eu) are particularly noteworthy due to their unique geochemical behaviours. Ce is positively correlated with Al_2O_3, K_2O, Hf, Nb, Th, and REE. Eu is positively correlated with LOI, Hg, Th, and REE. Cerium has a negative correlation with Fe_2O_3 and MnO and shows no negative Ce anomaly, consistent with anoxic

Archean bottom waters and Ce being present in its reduced state (Cao et al., 2022). Ce has a positive correlation with Ga and Al_2O_3 indicating that it may have been derived from a more felsic source rock and/or incorporated in clay minerals. Sample #4253 from Gowan township in the Tisdale assemblage has one of the highest Ce/Ce* values within the black shale dataset, indicating a strongly reducing environment (Maynard, 2013). Samples #4400 from Guibord township, sample #4386 from Warden township, and sample #4095 from Munro township also have high Ce/Ce* values.

Europium is positively correlated with HFSE, U, Th, and other REE and is found in the detrital heavy minerals monazite and xenotime but is also present in the REE-carbonate mineral bastnäesite. Because Eu^{2+} is mobilized under reduced conditions and at high temperatures, positive Eu anomalies can occur in hydrothermal precipitates, including chemical sediments (e.g., Liu et al., 2017). Samples #8514 and #8518 from Dundonald township, and sample #8595 from Munro township have the highest Eu/Eu* for all three shale lithotypes (felsic-, intermediate-, and mafic-type). This is a strong positive indicator of proximity to a hydrothermal source for the Eu^{2+} (see below).

Carbon and diagenetic sulphide component

The total carbon content in the shale samples is strongly correlated with LOI, Mo, Co, Se, Eu, and S reflecting the influence of redox-sensitive and sulphide-associated trace elements. The LOI represents H_2O, CO_2, and SO_2 lost during pyrolysis. The total carbon highlights a correlation with mafic-element components in the host basins. In other samples, the negative correlation between total carbon and muscovite/HFSE suggests limited deposition or low preservation of organic matter associated with felsic detrital input. The strong correlation between total sulfur and carbon indicates biological processes active in the sediments.

The carbon and sulphide contents of the shale are positively correlated with elements present in organic matter, such as Co, As, Se, Mo, Sb, and Hg which bind strongly with the organic material (Gregory et al., 2019). The metals associated with sedimentary organic matter originate from the diagenetic transformation of organic compounds (porphyrins and chlorophyll) that

sequester heavy metals (Tissot & Welte, 1984). Specifically, the S-Co, S-Se, and S-Mo correlations reflect the typical diagenetic enrichment of these elements in organic-rich shales, whereas the S-Au, S-Sb, and S-Hg correlations suggest a hydrothermal contribution to the shales. The correlation between sulphur and trace elements is controlled by pyrite, which is the dominant form of sulphur in the sediment. This pyrite is disseminated throughout the shale samples as: 1) diagenetic sulphide nodules, 2) sulphide laminae, 3) euhedral metamorphic sulphide (cubic), and 4) "pinstripe" sulphide on cleavage planes. Trace elements are typically enriched in pyrite either by direct substitution (e.g., Ni^{2+}) or as metal sulphide inclusions (e.g., ZnS).

The strong correlation between Ni and V is explained by shared redox sensitivity, similar biological interactions, and similar volcanic provenance. Trace amounts of Ni and V are essential nutrients that are incorporated into organic carbon. In modern anoxic marine basins dissolved V is reduced to V^{4+} and V^{3+}, that is eventually incorporated into sedimentary organic matter (e.g., Kelley et al., 2017; Wang, 2024). However, there is a negative correlation between V and non-carbonate carbon in our samples suggesting that V was not significantly incorporated into organic matter upon burial. In the most carbon-rich samples, V is more strongly correlated with Al_2O_3, Fe_2O_3, MgO, Ga, Sc, Cr than non-carbonate carbon and may be substituting in heavy minerals like magnetite, ilmenite, and biotite. Nickel is particularly enriched in black shales wherever ultramafic rocks, including komatiite lava flows, are present. Submarine volcanic eruptions rich in komatiitic lavas provided abundant Ni to the Archean seawater, and the metabolisms of primitive chemoautotropic bacteria may have relied on Ni as a catalyst and an enzyme cofactor (Glass and Dupont, 2017). The accumulation of organic matter may also create a reducing environment that facilitates uranium precipitation (Spirakis, 1996). The absorption of U by organic matter is also supported by the moderate correlation between U and non-carbonate carbon in our samples.

Mafic-associated sulphide component

The primary igneous source rocks of the shales are mafic volcanic rocks, which are geochemically distinct in terms of trace elements. The mafic-associated sulphide minerals of the

shales contain As, Co, Ni, Se, Mo, and Ge. Co and Ni show a strong correlation with mafic-associated elements such as Fe_2O_3, MgO, Se, Sc and Cr. They have a negative correlation with SiO_2, Al_2O_3, Sr, Ga, and Ba. Although sourced from the mafic rocks, because of their redox sensitivity, Co, Ni, Se and Mo are typically found in the diagenetic sulphides and carbonaceous matter in the sediments. Arsenic is highly soluble and has a positive correlation with Fe_2O_3, MnO, CaO, Co, Se, S, Au, Sb, Ni, C, Hg, wherever sulphides are present. Germanium is also commonly enriched with As.

Elements in the mafic-associated sulphides of the shales are positively correlated with total carbon as most of the small sedimentary basins hosting abundant organic matter are part of mafic and ultramafic volcanic successions. Total carbon has a negative correlation with muscovite abundance and certain HFSE more typical of felsic volcanic rocks.

Polymetallic sulphide component

Cu, Pb, Zn, Cd, Hg, Sn and Te are among the polymetallic sulphide elements in some of the shales. These elements may be found in argillite-hosted diagenetic sulphide nodules as well as authigenic pyrite. The trace metal enrichments are generally considered to be associated with low-temperature submarine hydrothermal venting related to volcanism in the host basins. The trace metals are contained in pyrite, pyrrhotite, marcasite, and trace amounts of sphalerite, galena and chalcopyrite, but they are typically too fine-grained to be observed in drill core. The trace element enrichments reflect the bulk composition of the underlying volcanic rocks (Hannington, 2014).

Cu has a clear correlation with S, LOI, C, In, Co, Mo, Ag and Bi, whereas Zn and Pb are correlated with Cd, Ag, and Se. Mercury has a good correlation with redox-sensitive elements of the mafic-associated sulphides and some of the elements associated with polymetallic sulphides including Sn, Tl, As, Co, Ni, Se, and Eu. Mercury may also be transferred to sediments via adsorption onto suspended particles, binding with organic matter or precipitation with reduced sulphides (Zhu et al., 2021).

Orogenic gold-related elements

Abitibi shales show enrichment in trace elements associated with orogenic gold mineralization, including correlations of Au, Sb, Ag, W, Bi, and B. These geochemical signatures are due to hydrothermal overprinting events, during regional metamorphism and deformation. Orogenic gold fluids have interacted widely with different rock types in the greenstone belt, including interflow sedimentary units. Most of the gold is hosted in late-stage, orogenic quartz-carbonate veins along major fault zones (Dubé & Mercier-Langevin, 2020). However, gold is also present in late-stage hydrothermal pyrite in the sedimentary wall rocks where carbonaceous material may have acted as a reductant for the gold-bearing fluids (Hannington et al., 2012)

Au is positively correlated with As, W, and CO_2 suggesting a hydrothermal signature. Sb is positively correlated with LOI, As, Br, and S indicating a connection with elements that behave partly as volatiles. Mo, Bi, and W are enriched in vein minerals in some specific deposits (e.g., in Kirkland Lake). However, Mo, Bi, Au, As, and Sb are also commonly enriched in diagenetic pyrite in the black shales (e.g., Pašava et al., 2023). In one model, the gold-associated elements are released from organic matter and incorporated into pyrite nodules. During subsequent metamorphism these elements are mobilized into fluids by the transition from pyrite to pyrrhotite (Goldfarb and Pitcairn, 2023). Additionally, gold can precipitate with graphite derived from the hydrocarbon-rich fluids. Redox-sensitive elements (e.g., Ni, Co, Se, Mo, As, Eu/Eu*) that were originally incorporated into sedimentary deposits may also be released to hydrothermal fluids during metamorphism.

CO_2 is positively correlated with MnO, CaO, LOI, Au and As, reflecting carbonate alteration typical of orogenic gold systems. Most of the shale samples contain some carbonate, which is either syngenetic or metamorphic in origin. The alteration associated with orogenic gold systems is dominated by quartz, carbonate, and muscovite, with enrichments in Rb, Cs, and CaO. MgO and Sr are also correlated, suggesting that at least some of the carbonate species present is dolomite [$CaMg(CO_3)_2$].

4.4 Immobile Element Ratios and REE of Shale Lithotypes

Figures 4.12 and 4.13 show the shale compositions on commonly used discrimination diagrams for igneous rocks. Figure 4.12 is plot of Nb/Y versus Zr/TiO_2, commonly referred to as the Winchester & Floyd discrimination diagram. These immobile element ratios are typically used to classify fresh volcanic rocks and are often interpreted in terms of tectonic settings. Although the discriminations are based on modern volcanic rock compositions and do not reflect Archean tectonics or magmatic systems, the distribution of shale samples shows a remarkably close parallel to primary igneous rock compositions in the Phanerozoic. Figure 4.13 was adopted from Bhatia and Crook (1986), which uses trace element ratios to characterize contemporary tectonic regimes of greywackes. Due to the relative immobility of Ti, Zr, La, and Sc used in the classification, the ratios of these elements in the derived sediments show the mafic-type WAGB shales are most similar to the compositions of volcanic rocks in oceanic settings, with intermediate- and felsic-type shales having compositions more similar to volcanic rocks from arc-like settings (e.g., active and passive margins).

Figure 4.14 shows the distribution of shale samples in comparison to igneous fractionation trends of parental tholeiitic volcanic rocks. The composition of the shale lithotypes range from basaltic to dacitic in composition. Shale samples that plot above the tholeiitic fractionation curve have experienced mass loss due to weathering or alteration and samples that plot below the curve have experienced mass gain such as addition of quartz. Figure 4.15 is a binary plot of Zr/Sc versus Th/Sc, illustrating the source rock control and effects of sediment sorting and recycling. Mafic-type samples plot on the bottom left of the diagram corresponding to a low Th/Sc and Zr/Sc (i.e., high Sc content). Intermediate-type samples plot in the center of the diagram and felsic-type samples plot in the top right with higher concentrations of Th and Zr. An increasing Zr/Sc ratio can also indicate abundant sediment recycling as zircon is concentrated in the heavy mineral fraction of extensively reworked sediments. The trends reflect zircon addition and Th enrichment (e.g., as monazite). The bulk of the shales plot to at higher Th/Sc than the endmember basalt, andesite, dacite, and rhyolite averages for the AGB (i.e, above the average Archean basalt-andesite-dacite-rhyolite values) suggesting addition of monazite. This is seen in the ternary Th-Zr-Sc plot in Figure 4.16. The three shale lithotypes are clearly distinguished on the ternary

diagram. Mafic compositions plot closer to Sc; increasingly felsic shales are characterized by higher Zr, although greater concentrations of Zr may also reflect sediment recycling and sorting. Higher Th may indicate greater stability of Th-bearing minerals compared to Sc-bearing minerals during sediment recycling. The association with different assemblages and mineral deposit types is discussed below.

Figure 4.17 shows that most of the REE in the shales are hosted in phosphate minerals such as monazite [(Ce, La, Nd)PO_4] and xenotime [(Y, Yb, Gd)PO_4]. Representative compositions for these REE-bearing phosphates are shown as dashed lines, calculated using idealized stoichiometric values for $CePO_4$ and $YbPO_4$ relative to P_2O_5. 5% of the total phosphorous is hosted in monazite or xenotime, with the remaining 95% hosted in apatite. Samples that plot on or near the lines are consistent with the P_2O_5 – REE relationship controlled by monazite and xenotime. Monazite preferentially incorporates the light REEs and xenotime preferentially incorporates the heavy REEs in their crystal structures. Samples that fall off the lines indicate that REE are present in other minerals. In other samples, P_2O_5 is primarily hosted in minerals that do not have high REE concentrations such as apatite [$Ca_5(PO_4)$]. Samples that have a higher REE concentration and plot above the monazite line may contain bastnäesite [$(La,Ce,Y)CO_3F$)], allanite [$(Ce,Ca,Y)_2(Al,Fe)_3(SiO_4)_3(OH)$] or zircon which are common accessory minerals that accommodate REEs in their crystal structure. Felsic-type shales likely contain a greater amount of the accessory minerals bastnäesite, allanite, and zircon. Mafic-type shales have low REE concentrations and moderate P_2O_5 values suggesting their REE budget is controlled almost entirely by apatite. Intermediate-type shales have REE concentrations that fall between apatite and monazite and xenotime. Felsic-type shales show the greatest variance with many plotting on or above the monazite line. Many samples contain a mixture of both LREE- and HREE-hosting minerals.

Felsic-type shales exhibit HREE enrichment due to sedimentary sorting and recycling that concentrates resistant HREE-bearing heavy minerals (Figure 4.18). Intermediate-type shales are relatively depleted in HREE compared to the felsic-type, reflecting a mix of felsic and mafic sources. They have a composition similar to their parent volcanic rock (except for the Eu

anomaly). Mafic-type shales exhibit LREE depletion relative to PAAS reflecting their geochemical similarity to their primitive volcanic precursor (e.g., basalt).

Figure 4.19 compares the average REE concentrations for the three shales lithotypes normalized to PAAS. The mafic-type shales show a characteristic LREE depletion. This profile reflects primitive volcanic provenance in contrast to LREE enrichment typical of more evolved continental crust. Figure 4.20 shows the REE profiles of possible source rocks of WAGB shales, also normalized to PAAS. All primary rock types plot higher than the values for the WAGB shales. All groups show a similar trend which is an increasing slope that gradually plateaus. For most samples, the LREE depletion and HREE enrichment is consistent with a dominantly mafic source rock composition, typical of the less evolved Archean crust.

Each shale lithotype exhibits a strong positive Eu anomaly. A positive Eu anomaly suggests Eu is preferentially incorporated into plagioclase in the volcanic source rocks. However, Eu^{2+} is mobilized under reduced conditions and at high temperatures, so positive Eu anomalies can also occur in hydrothermal precipitates, including chemical sediments (e.g., Liu et al., 2017). This is a strong positive indicator of proximity to a hydrothermal source for the Eu^{2+}. Dark black, sulphide-rich shales have the greatest Eu anomaly because they likely formed in small, reduced basins with sufficient metal input. Eu is correlated with elements commonly carried in hydrothermal fluids including As, Co, Mo, Se, and Hg.

4.5 Source Rock Contributions

Shale lithotypes may be a mixture of different mafic and felsic sources. In this case, the Ti/Zr ratio does not perfectly match a single source rock composition. To unravel the source rock compositions, we require a 3-way mixing model with multiple precursors (felsic, intermediate, mafic), or a 2-way mixing model in which all the intermediate compositions are, in fact, mixtures of mafic and felsic endmembers. The latter makes the most sense for the southern Abitibi, where the volcanic centers are dominantly bimodal mafic and felsic successions. However, intermediate volcanic rock compositions may also be partly due to hydrothermal alteration (e.g., Barrett et al., 1993; Gibson et al., 1997).

To quantify the contributions of mafic and felsic sources in a binary mixing model a trend line was fitted through the cloud of data points (Figure 4.14), and two representative points on this line were chosen as endmembers: one reflecting a more mafic composition (high Ti, moderate to low Zr) and the other a more felsic composition (low Ti, moderate Zr). From the concentration of Ti or Zr, the fraction of each endmember contributing to the bulk composition of the shale sample is then expressed as:

$$C_{mixed,\ Ti} = f \times C_{mafic,\ Ti} + (1 - f) \times C_{felsic,\ Ti}$$

$$f = C_{mixed} - C_{felsic} / C_{mafic} - C_{felsic}$$

- $C_{mixed,\ Ti}$ is the concentration of Ti in the shale sample
- $C_{mafic,\ Ti}$ is the concentration of Ti in the mafic endmember
- $C_{felsic,\ Ti}$ is the concentration of Ti in the felsic endmember
- And f is the fraction of mafic contribution (ranging 0 - 1)

For example, using the endmember concentrations of Ti, sample #4400 yielded a mafic fraction of 0.74, indicating a source that is 74% mafic and 26% felsic. These proportions can then be used to calculate the predicted concentrations of any element in sample #4400. In this case, the actual Zr concentration (116 ppm) is higher than the predicted value (95 ppm). This suggests Zr enrichment relative to its source rock, likely due to zircon being concentrated via sedimentary sorting.

4.6 Spatial Distribution of Shale Lithotypes

Figures 4.21 and 4.22 show the spatial distribution of the different shale lithotypes overlain on a map of the volcanic assemblages and the township grid, respectively. A high proportion of intermediate-type shales occur in the Porcupine assemblage close to the DPFZ. A higher proportion of mafic-type and felsic-type endmembers occur in Kidd-Munro and Stoughton-Roquemaure north above the Pipestone fault. Figure 4.23 shows a stacked bar chart representing the number of shale samples in each assemblage categorized by lithotype. Kidd-Munro and Tisdale have distinctly bimodal volcanics with more felsic than intermediate samples. Blake

River has roughly equal numbers of felsic and intermediate samples. The Porcupine assemblage has more intermediate-type samples. Mafic-type samples are the minority across all assemblages. Figure 4.24 shows the distribution of shale lithotypes overlain on mapped lithologic units, as opposed to assemblages. A total of 226 drill holes are located in mafic to intermediate metavolcanic rocks / intrusions, 121 in clastic metasedimentary rocks, 58 in intermediate to felsic metavolcanic rocks/intrusions, 55 in ultramafic to mafic metavolcanic rocks/intrusions, and 26 in Timiskaming-type clastic metasedimentary rocks. The remaining 78 samples are located in other units or were not described in the logs. There is a clear distinction in the shale lithotypes between the oceanic rift-like terrane north of the Pipestone Fault and the arc-like volcanosedimentary terrane of the Porcupine assemblage and proximal to the DPFZ.

4.7 Effects of Hydrothermal Alteration

Hydrothermal alteration makes it extremely difficult to determine the original chemical composition of shale samples, however, molar ratio plots provide insights into mineralogical changes accompanying alteration. Davies and Whitehead (1994) proposed that greywacke-argillite sequences can be characterized by considering the molar ratios of major oxides (SiO_2, Al_2O_3, K_2O, Na_2O) and the associated minerals (quartz, plagioclase, K-felsdpar and the clay minerals). Much of the scatter in major element plots is related to SiO_2, but plotting molar K_2O/Al_2O_3 versus Na_2O/Al_2O_3 permits the interpretation of the bulk compositions in terms of major mineral proportions. This is similar to the approach of Pearce-element ratio diagrams. The proportions of secondary minerals such as sericite in altered samples can be determined readily from the molar ratio plots. Figure 4.25 shows the Na_2O/Al_2O_3 vs K_2O/Al_2O_3 plot of Davies and Whitehead (1994) and the regression lines for each shale lithotype.

Major cation ratios of the AGB shales show a general negative trend in Na_2O/Al_2O_3 versus K_2O/Al_2O_3 indicating sodium depletion from the destruction of albite. Samples that cluster in the upper left corner indicate Na-enrichment and K-depletion (e.g., albite alteration) and the bottom right corner indicate Na-depletion and K-enrichment (e.g., sericitic alteration). The alteration lines (i.e., the regression lines) intersect the x-axis at 0.32 (felsic-type samples), 0.29 (intermediate), and 0.21 (mafic). The range of K_2O/Al_2O_3 values corresponds to that of illite,

roughly 0.20 – 0.33, suggesting the clay component was illite in all samples (Davies and Whitehead, 1994). The alteration patterns of the sediments are remarkably consistent with those of the host volcanic rocks, suggesting that most of the major and trace element characteristics of the sediments can be interpreted in terms of well-established primary and secondary geochemical trends in igneous rocks. Figure 4.26 shows the alteration trends for the different shale lithotypes, together with the carbonate content of the samples, indicating almost no correlation with carbonate alteration.

Figure 4.27 is a ternary A-CN-K plots of the western Abitibi shales derived from the molar proportions of Al_2O_3 (A-apex), CaO + Na_2O (CN-apex), and K_2O (K apex) following the approach of Nesbitt and Young (1982) which shows distinct compositional and weathering trends. The corresponding molar ratios of the cations in plagioclase (albite endmember) and K-feldspar plot at 50% Al_2O_3 on the left and right boundaries. Biotite plots close to K-feldspar near 60% Al_2O_3, and illite and muscovite plot between 70 – 80% Al_2O_3. Chlorite plots at the A apex (100% Al_2O_3). Nesbitt et al. (1996) defined the Chemical Index of Alteration (CIA), which describes the destruction of plagioclase and K-feldspar. Samples that plot lower on this scale have experienced less chemical weathering and are more compositionally similar to their source rock. Fresh basalts have CIA values between 30 and 45. The values for average shales range from 70 to 75 (Nesbitt and Young, 1982). In the A-CN-K ternary diagram, most of the western Abitibi shales plot along the A-CN line and progressively shift towards illite-muscovite composition with increasing alteration. Felsic-type shales show higher proportions of K-rich clay minerals. The association with different assemblages and mineral deposit types is discussed below.

Another commonly used alteration plot for volcanic rocks is the alteration box plot developed from Large et al. (2001) in Figure 4.28. Shales with mafic-type compositions show the highest degree of alteration according to the CCPI indicating increased chlorite-carbonate alteration. Felsic and intermediate-type shales have a similar distribution with felsic samples plotting at slightly lower degrees of alteration. Shales with intermediate and felsic compositions trend toward sericite +/- chlorite alteration. Shales with intermediate-type compositions plot mostly within the least altered box, whereas nearly all mafic-type samples plot outside the box. Nearly

all samples plot above the alteration line separating diagenetic from hydrothermal alteration. The association with different assemblages and mineral deposit types is discussed below.

4.8 Shales in Different Assemblages

Shales assigned to different volcanic episodes of the AGB (i.e., lithostratigraphic assemblages) broadly reflect the compositions of the dominant volcanic rock types in each episode (Table 4.9). The different volcanic events produce compositionally heterogeneous shale because they contain varying proportions of the volcanic rocks. Each assemblage comprises a mixture of mafic and felsic rock types and this variability is reflected in the shale lithotypes.

Th-Zr/10-Sc ternary diagrams for shales from each volcanic assemblage are shown in Figure 4.29. Shales from all assemblages show distinct populations but some degree of overlap between the shale lithotypes. Shales belonging to Deloro and Stoughton-Roquemaure show minimal Th enrichment. Samples identified as belonging to Kidd-Munro, Tisdale, and Blake River are relatively enriched in Th. Elevated Th in younger assemblages may reflect more sediment reworking but also more evolved arc-like volcanic suites (e.g., Monecke et al., 2017). The older Deloro and Stoughton-Roquemaure assemblages either experienced less sedimentary sorting resulting in minimal Th enrichment or reflect the more juvenile oceanic rift-like volcanic rocks.

In the Tisdale and Blake River assemblages there is a wider range of felsic-type samples, with both Zr addition and greater Th enrichment. Shales belonging to the Porcupine assemblage display less compositional variability because the detrital material has experienced longer transportation and sediment homogenization prior to deposition. Notably, shales from the Porcupine assemblage are geochemically distinct from the shales in the volcanic assemblages. This suggests that the Porcupine assemblage received sediment from a different source (e.g., continental or arc sources). The geochemical behaviour of Th-Zr-Sc are summarized in Table 4.10.

Figure 4.30 shows the position of the shales in A-CN-K plots for each assemblage. Shales from the mafic-dominated Kidd-Munro and Deloro assemblages cluster toward the CaO-Na_2O (CN)

apex, consistent with their mafic sources. Figure 4.31 shows the position of the shales from each assemblage in the "alteration box plot". Again, shale samples from Kidd Munro exhibit compositions reflecting their mafic provenance, including basalts and komatiites that are affected by chlorite, carbonate and pyrite alteration. These samples yield some of the highest CCPI values in the alteration boxplots. Shale samples from the Blake River and Tisdale assemblages are derived from both basalts and intermediate to felsic volcanics with chlorite and muscovite alteration. In contrast, shales from the Porcupine assemblage are dominated by metasedimentary rocks with lower CCPI values but moderate-to-high AI values. Shales from the Deloro and Stoughton-Roquemaure assemblages are more dispersed. In the Deloro Assemblage, shale samples trend towards dolomite and ankerite endmembers (upper-center) which could indicate CO_2-rich alteration, although carbonate is not explicitly calculated in the CCPI. Samples from Stoughton-Roquemaure also trend towards the chlorite and pyrite endmembers (upper-right). A high proportion of shale samples from the Kidd-Munro assemblage plot outside the least-altered compositions. Blake River samples suggest some degree of sericitization, and chlorite-pyrite alteration. Tisdale samples display a wide range in Ishikawa Alteration Index (AI) values. Porcupine samples form a smaller cluster within the least-altered part of the box plot.

4.9 Shales Associated with Different Mineral Deposit Types

Figure 4.16 shows the compositions of shales that were originally targeted for different mineral deposit types during drilling. Samples from drill holes originally targeted for orogenic gold plot mostly in the field of intermediate-type shales in the Th-Zr/10-Sc ternary diagram, whereas the shales from volcanic assemblages that contain VMS are mainly felsic- and mafic-type. Figure 4.27 shows that samples associated with orogenic gold mineralization cluster more densely at high CIA values than samples associated with base metals mineralization.

A cluster of shale samples at the bottom left of the Davies and Whitehead (1994) plot in Figure 4.25 corresponds to removal of both Na_2O and K_2O (e.g., replacement by carbonate). Roughly 30 samples were identified as having these low molar ratios, and 26 are associated with base metal mineralization. Samples associated with orogenic gold mineralization cluster within the least-altered part of the Alteration Box Plot and in the upper right corner towards chlorite and pyrite

(Figure 4.28) (see for comparison: Dubé and Mercier-Langevin, 2020; Goldfarb and Pitcairn, 2022). Samples associated with base metal mineralization show greater sericite – chlorite – pyrite alteration and calcite, epidote, ankerite, dolomite alteration, reflecting Na-depletion and carbonate alteration.

Figure 4.32 shows the distribution of shales from drill holes that were targeted for discovery of VMS or later orogenic gold mineralization overlain on a lithology map. Shales associated with VMS deposits commonly reflect geochemical input from synvolcanic hydrothermal fluids and tend to be enriched in base metals like Zn, Cu, and Pb and redox-sensitive trace elements (Hannington et al., 2012). For example, in Munro township, the small Potter and Potterdoal massive sulphide lenses occur within a succession of basaltic volcaniclastic rocks and intercalated carbonaceous shale that are enriched in base metals (Monecke et al., 2017). Zinc concentrations in shale samples from Munro township range from 95 to 6350 ppm with an average of 1326 ppm that exceeds the WAGB average of 1058 ppm. The average copper concentration in shales from Munro township is 1424 ppm nearly four times the WAGB average of 382 ppm.

Shale samples close to the structural breaks that host orogenic gold mineralization in some cases contain abundant graphite that may have acted acts as a chemical trap creating a reducing environment that promotes the precipitation of gold (Dubé et al., 2020). For example, the Hoyle Pond gold mine located in the Tisdale assemblage is hosted in heavily deformed mafic-ultramafic volcanic rocks and shales with intense graphite alteration (Dubé & Mercier-Langevin, 2020). Geochemical signatures characteristic of orogenic gold mineralization in these samples include strong muscovite-sericite alteration (enrichment in K, Rb, Sr, Cs, Ba) and carbonate alteration. The summary of geochemical groupings of WAGB black shales based on Pearson's correlation matrix is shown in Table 4.11.

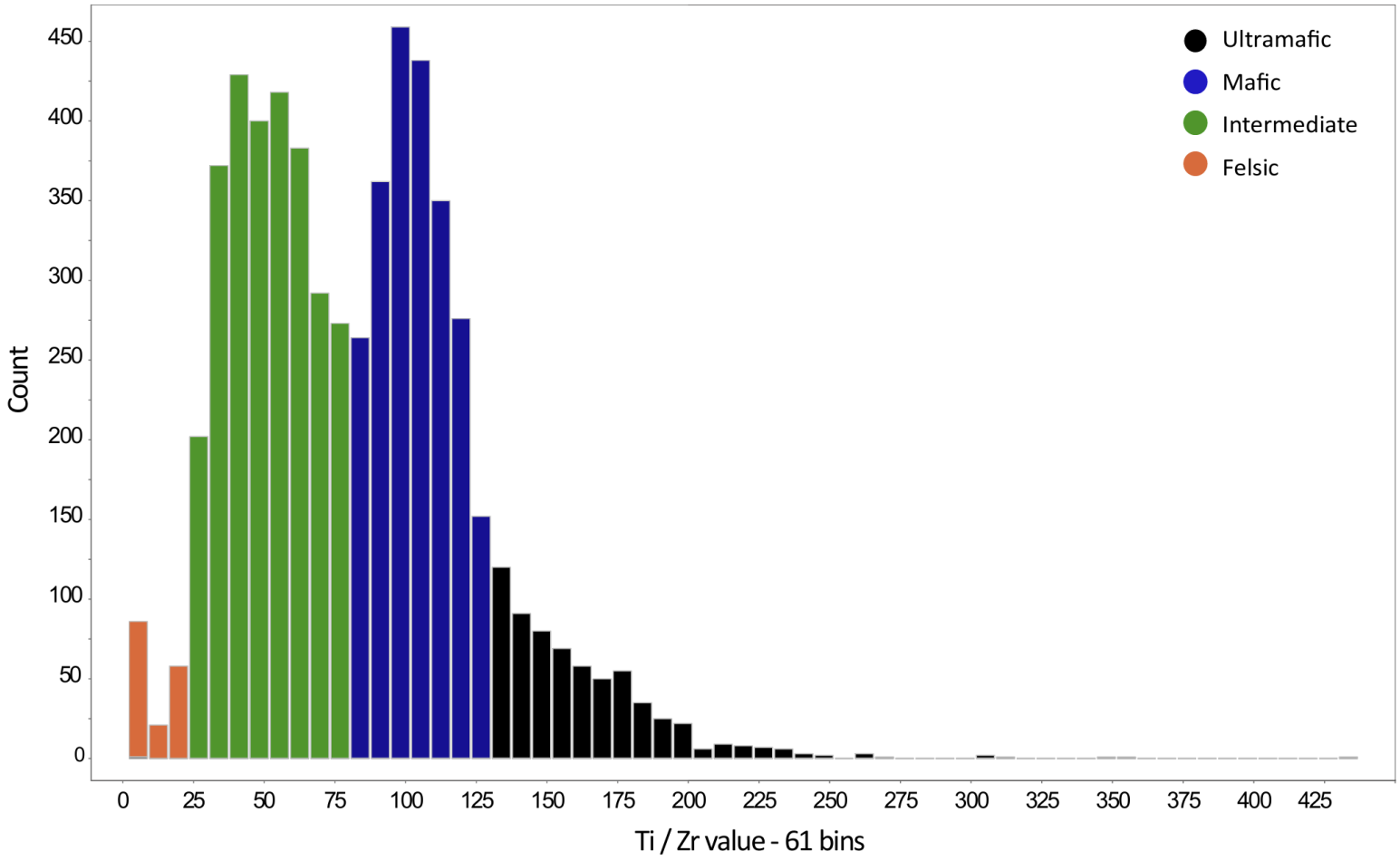


Figure 4.1. Histogram of Ti/Zr (in ppm) for volcanic rocks of the Abitibi Greenstone Belt (data from Fassbender et al., 2023, 2024) showing the multimodal distribution of possible volcanic source rocks of regional clastic sediments (N = 5892). Ti/Zr ratios have the following ranges: felsic (< 25), intermediate (15 - 80), mafic (80 – 125), and ultramafic (> 125).

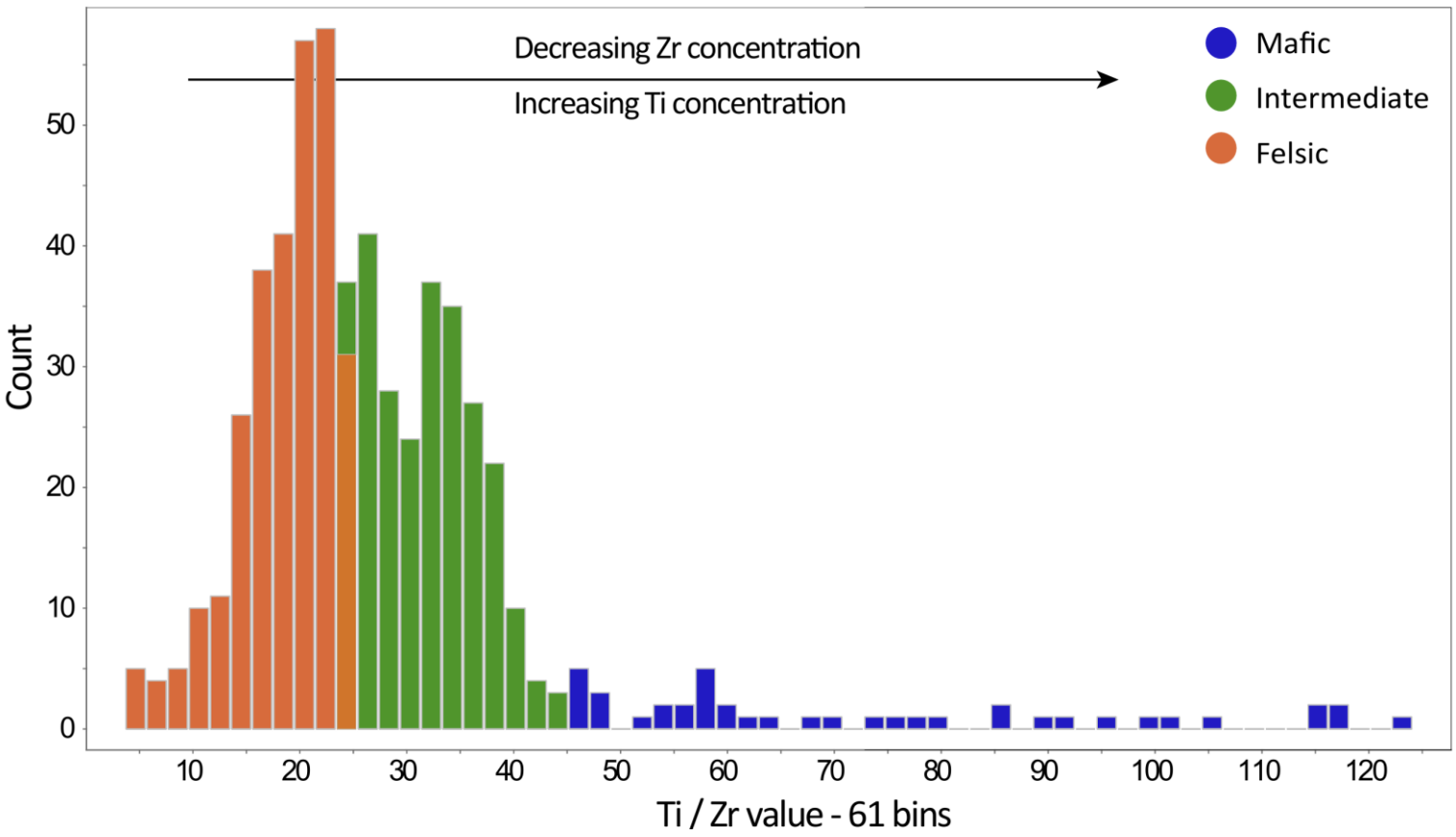


Figure 4.2. Histogram of Ti/Zr (in ppm) of western Abitibi shales showing three populations classified as felsic-type (Ti/Zr<25), intermediate (Ti/Zr=25-45) and mafic-type (Ti/Zr>45) (N = 564). A multimodal distribution is indicated, similar to the volcanic source rocks but at lower Ti/Zr values (Figure 4.1). The sediments generally have lower Ti/Zr than the parental volcanic rocks because of weathering and the effects sorting and recycling. The high proportion of felsic compositions among the shale samples reflects sediment sorting and concentration of zircon. We chose the boundaries between the shale lithotypes to be the 60th and 90th percentiles which subdivide the population into roughly equal numbers similar to the distribution of the volcanic source rocks. The 60th percentile encompasses samples with Ti/Zr value below 25 and is assigned to felsic-type shales. The 90th percentile encompasses samples with Ti/Zr>45 and is assigned to mafic-type shales. These subdivisions correspond closely to the Ti/Zr ratios for Phanerozoic volcanic rocks defined by Winchester and Floyd (1977), see Figure 4.12.

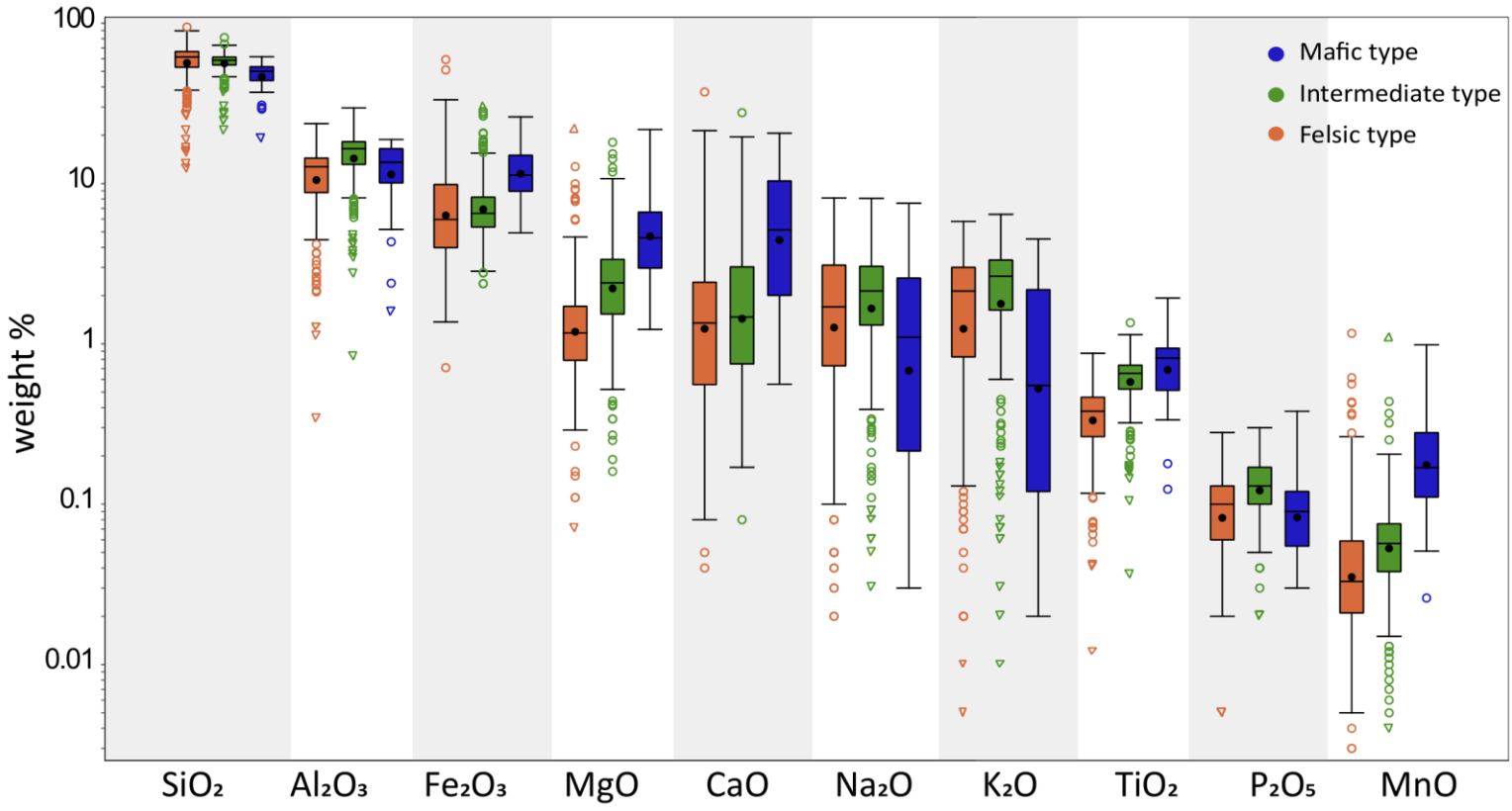


Figure 4.3. Box and whisker plot of the concentrations of major oxides in weight percent in the three shale lithotypes. Oxides are arranged from highest to lowest average concentration.

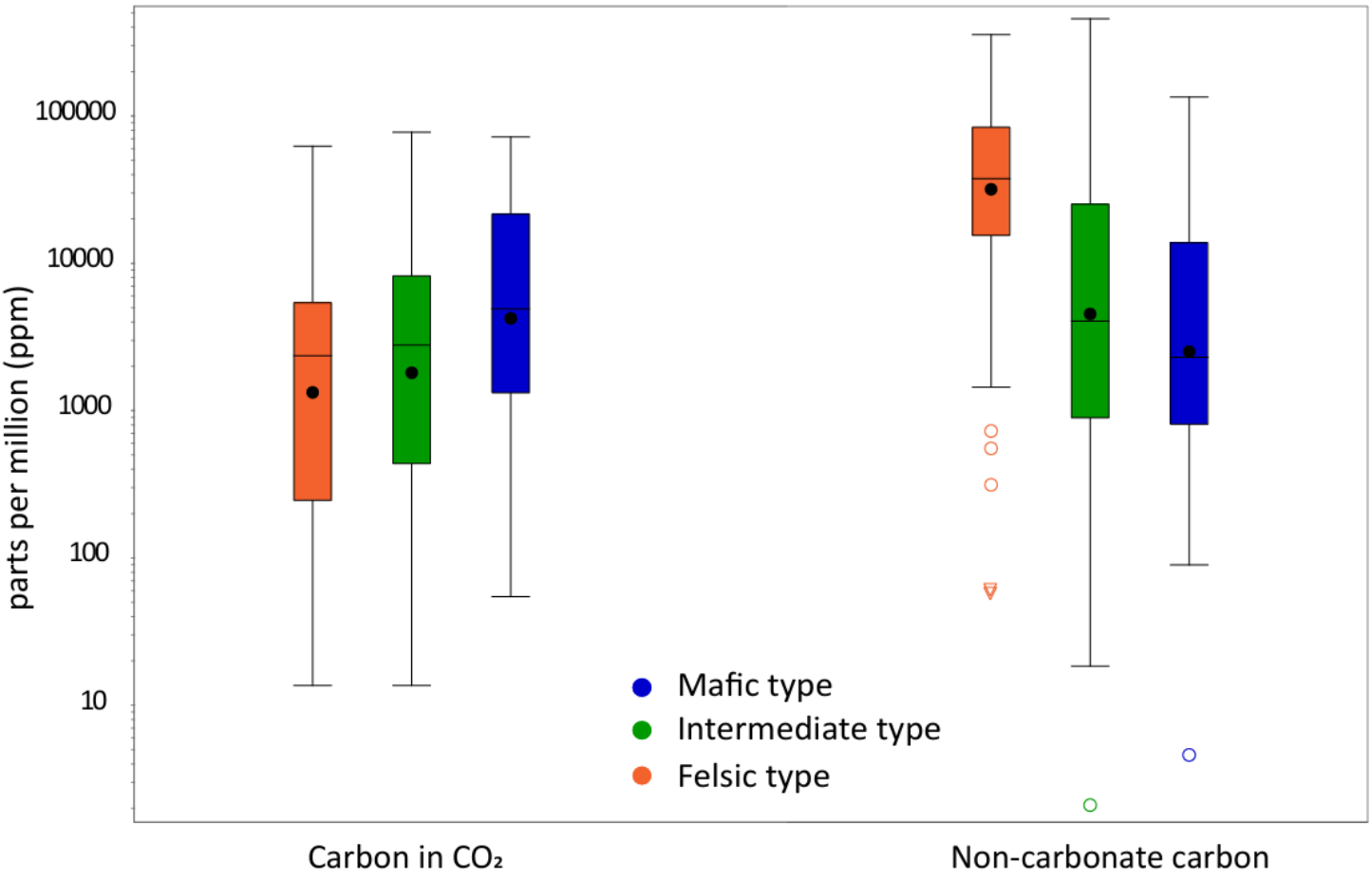


Figure 4.4. Box and whisker plot showing the concentration in ppm of carbon contained in CO_2 and non-carbonate carbon which is considered to be the organic carbon content for each shale lithotype. Mafic-type shales may have a greater capacity for sequestering CO_2 in carbonate minerals, owing to the high concentrations of reactive Fe and Mg.

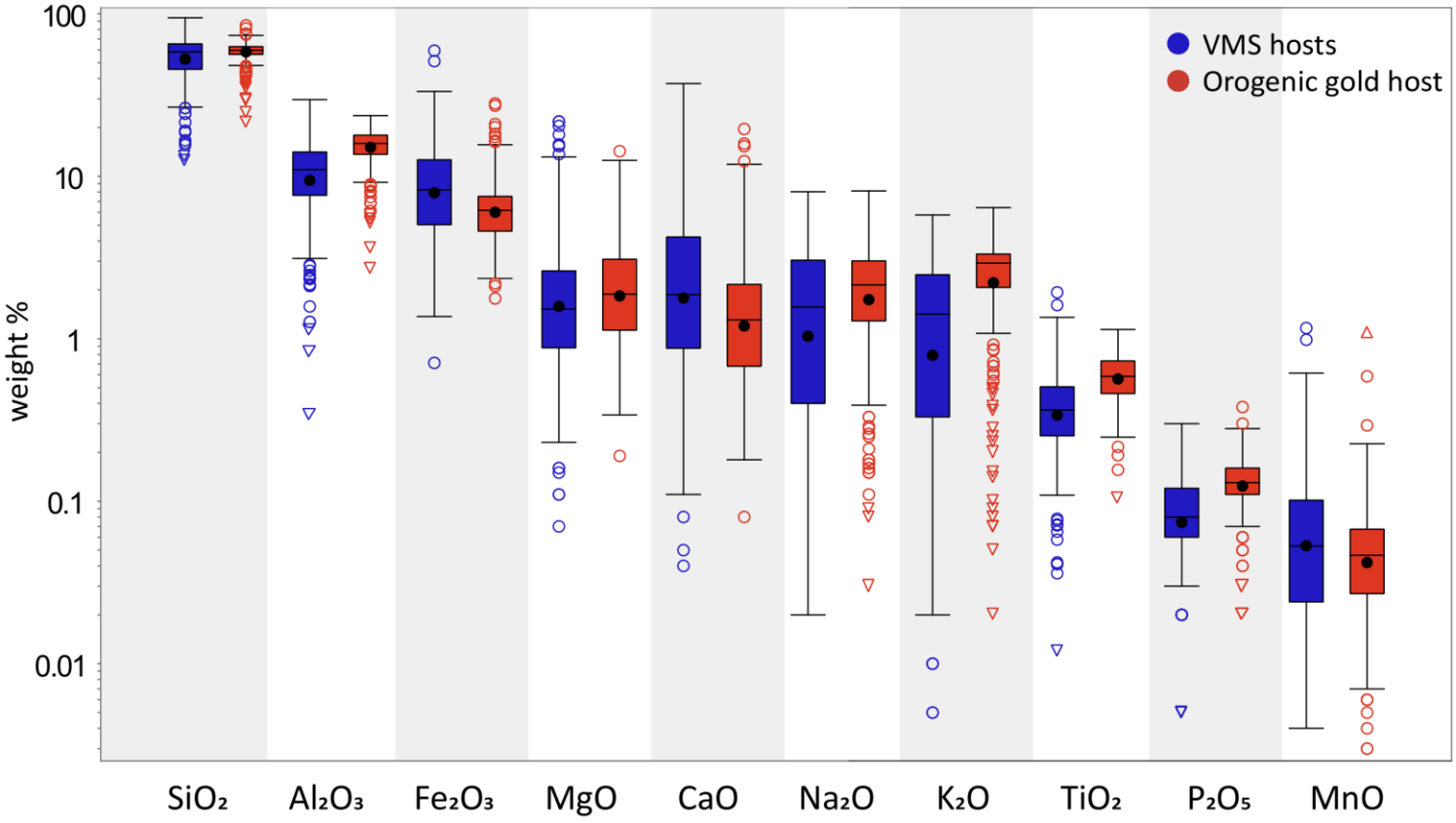


Figure 4.5. Box and whisker plot of the concentrations of major oxides in weight percent in shales from drill holes that were originally targeted for discovery of VMS or later orogenic gold mineralization.

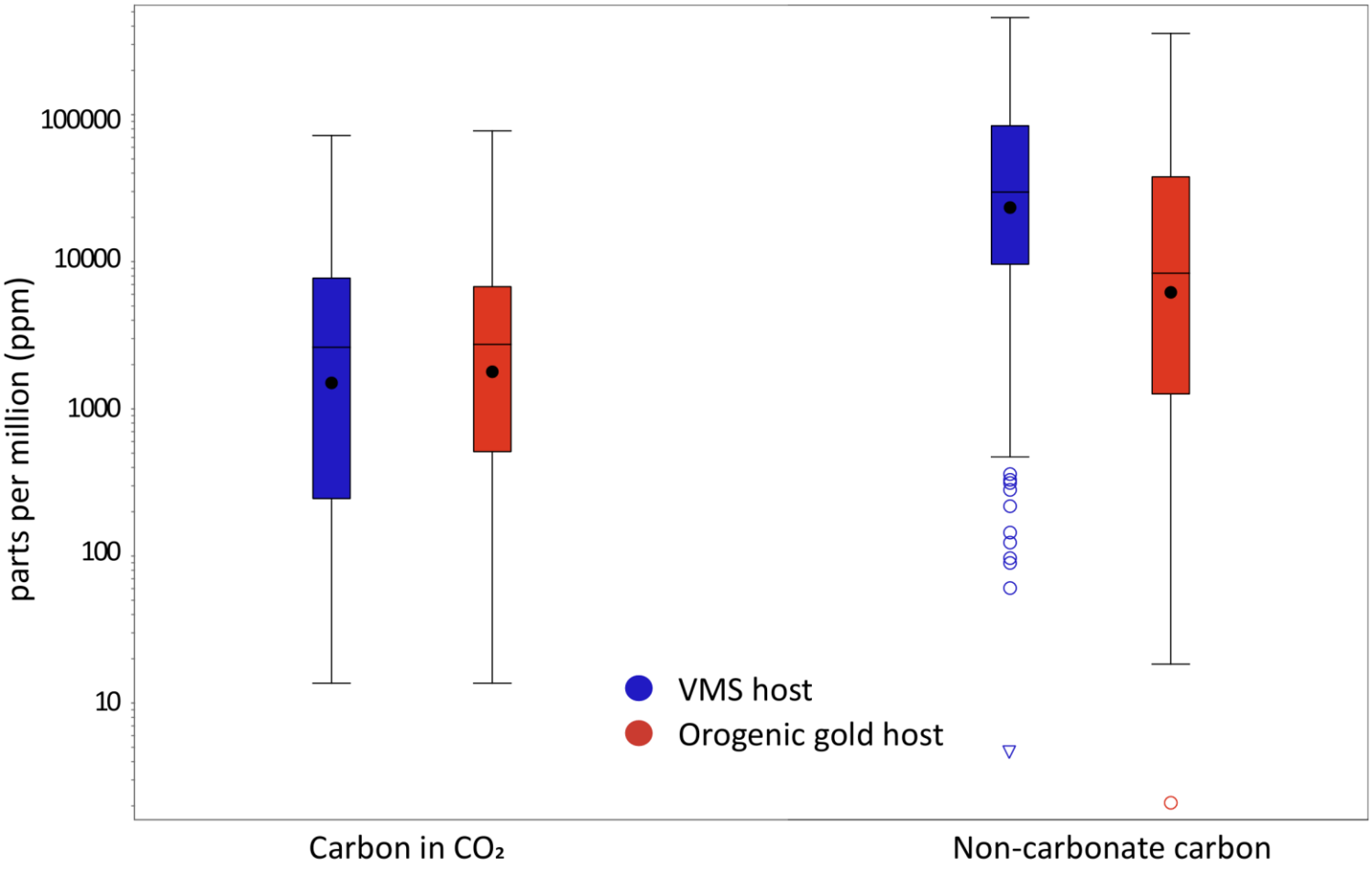


Figure 4.6. Box and whisker plot showing the concentrations in ppm of carbon contained in CO_2 and non-carbonate carbon in shales from drill holes that were originally targeted for discovery of VMS or later orogenic gold mineralization. Shales associated with base metal mineralization have some of the highest non-carbonate carbon concentrations.

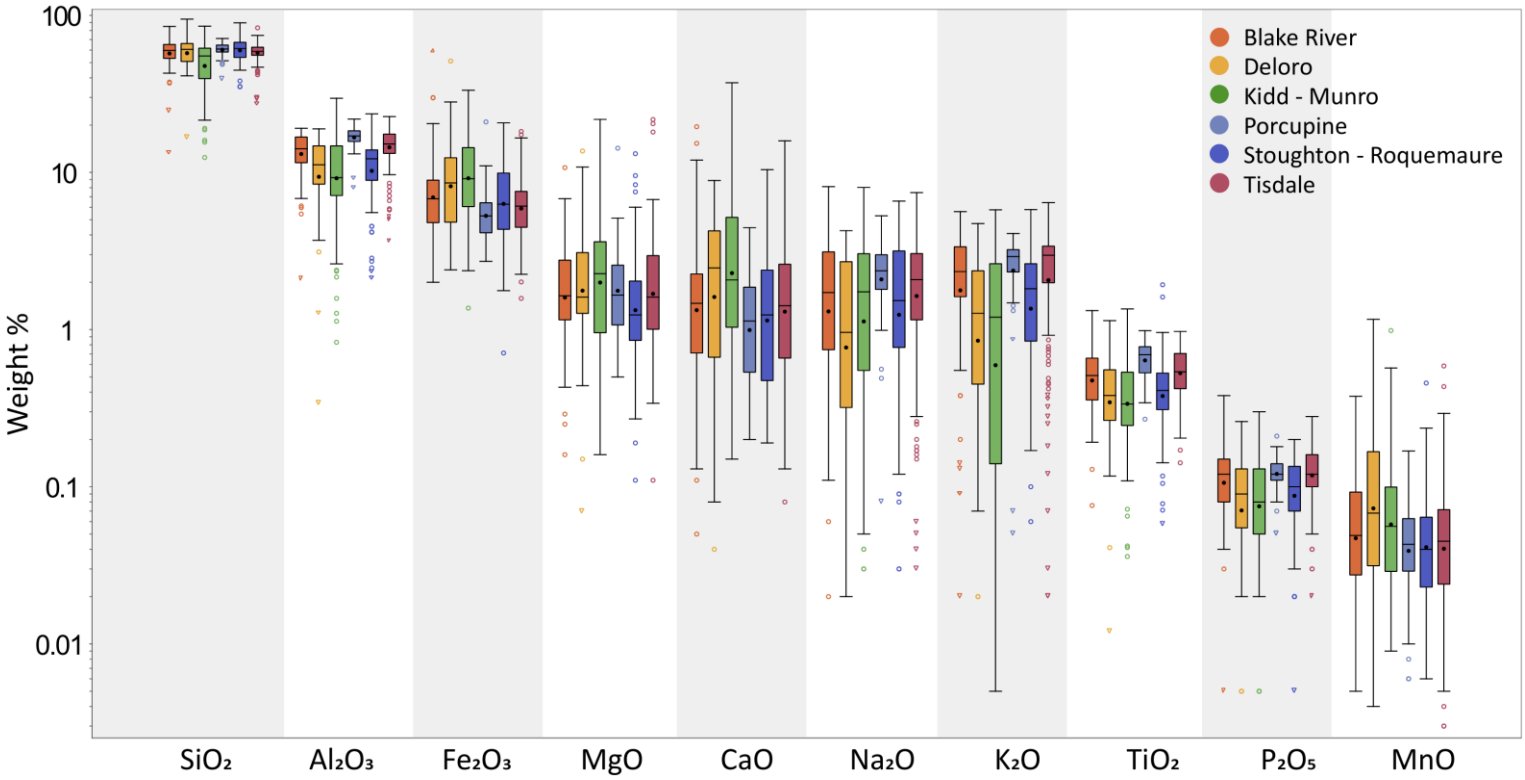


Figure 4.7. Box and whisker plot of the concentrations of major oxides in weight percent in shales from different volcanic assemblages of the AGB.

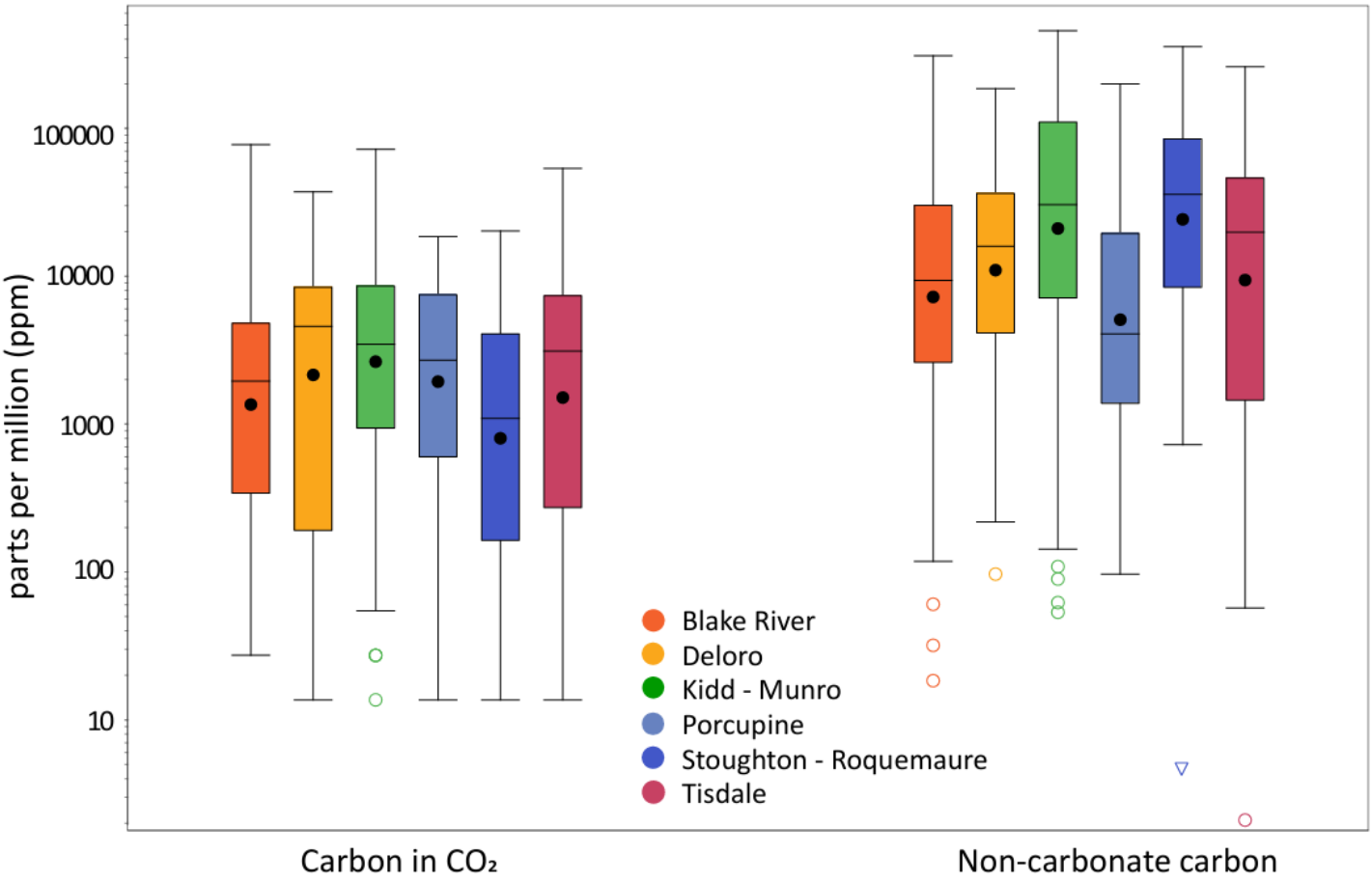


Figure 4.8. Box and whisker plot showing the concentration in ppm of carbon contained in CO_2 and non-carbonate carbon in shales from different volcanic assemblages of the AGB.

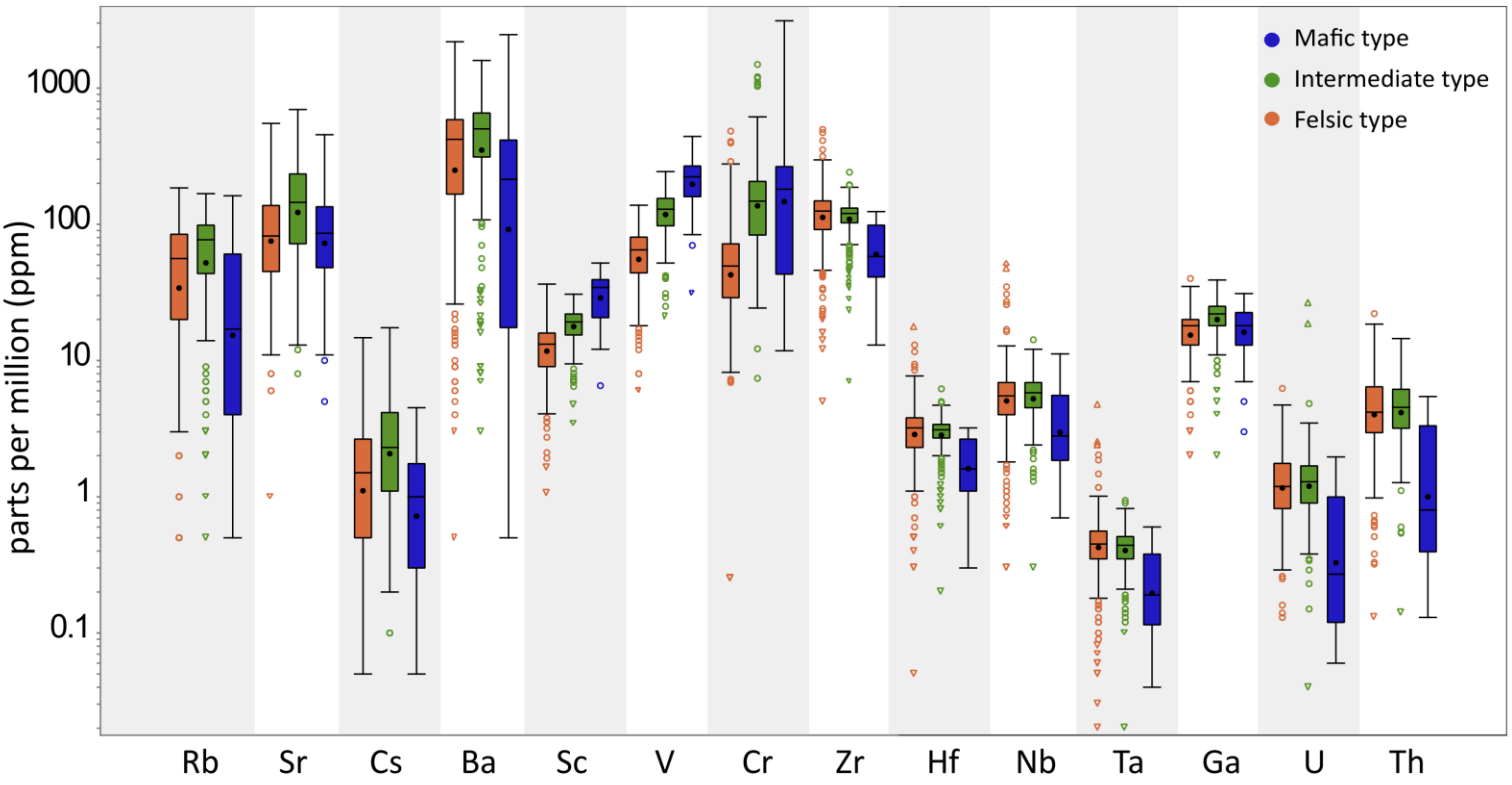


Figure 4.9. Box and whisker plot of the concentrations of trace elements in parts per million in the three shale lithotypes. Trace elements shown here include those associated with the muscovite group (Rb, Sr, Cs, Ba), mafic element group (Sc, V, Cr), the felsic element / HFSE group (Zr, Hf, Nb, Ta, Ga), plus uranium and thorium.

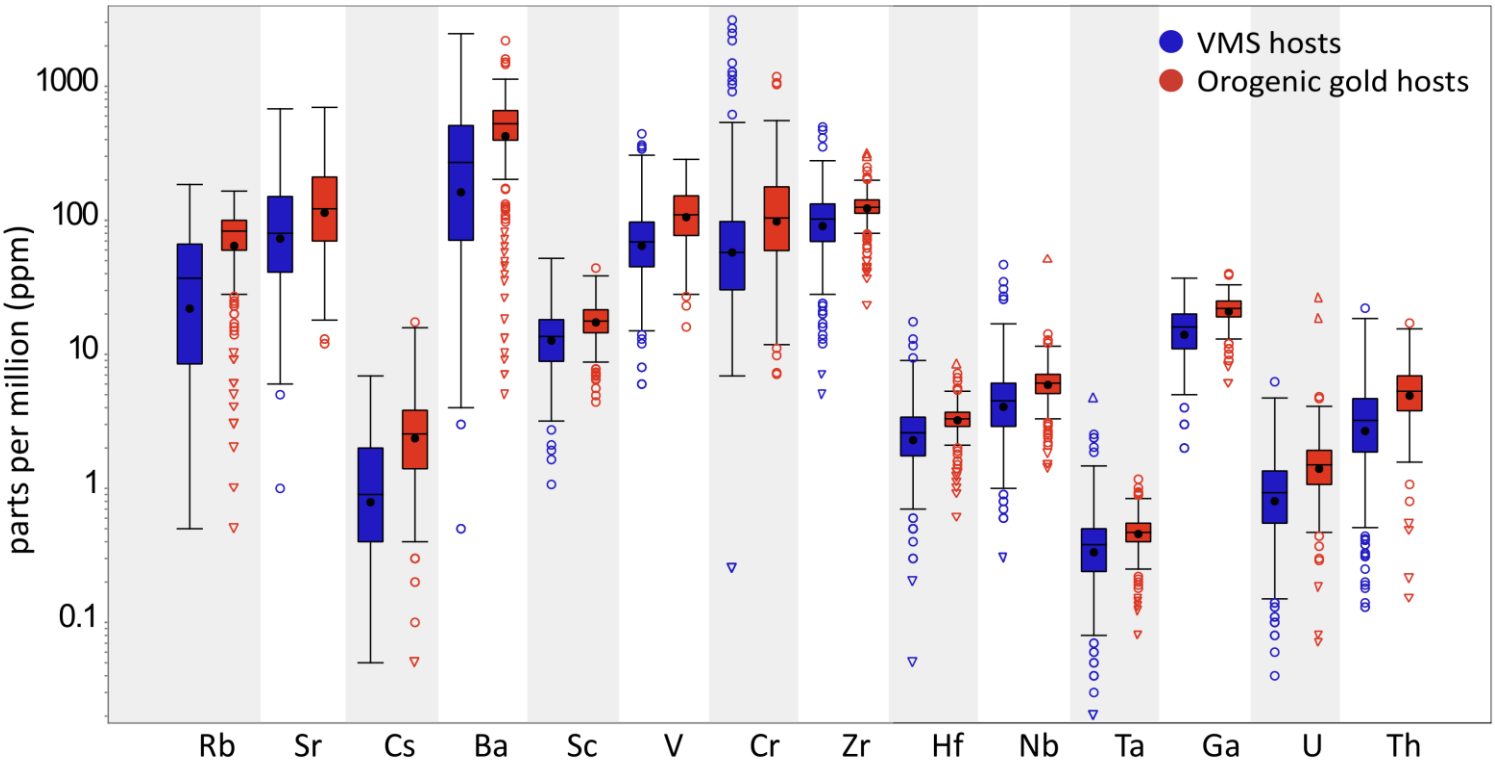


Figure 4.10. Box and whisker plot of the concentration of trace elements in parts per million in shales from drill holes that were originally targeted for discovery of VMS or later orogenic gold mineralization. Trace elements shown here include those associated with the muscovite group (Rb, Sr, Cs, Ba), mafic element group (Sc, V, Cr), the felsic element / HFSE group (Zr, Hf, Nb, Ta, Ga), plus uranium and thorium.

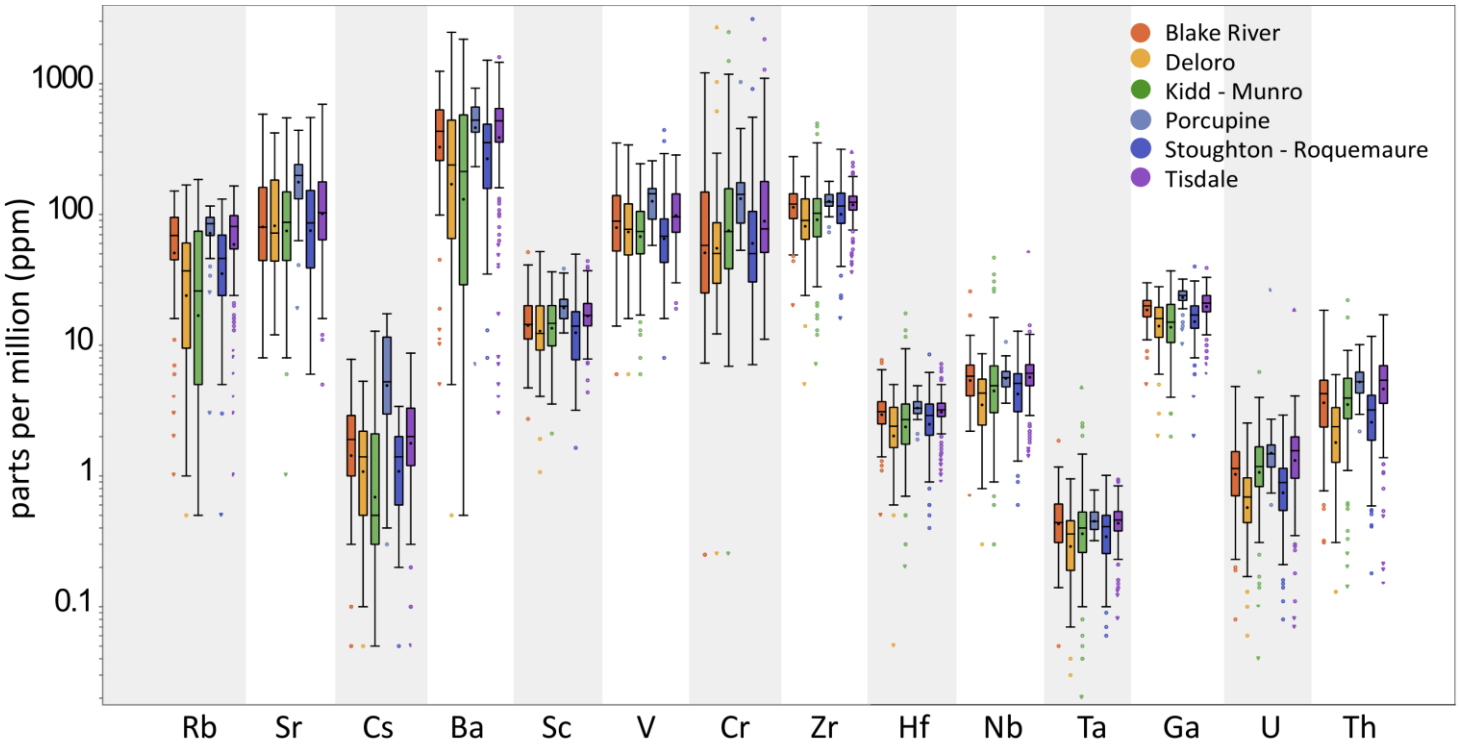


Figure 4.11. Box and whisker plot of the concentrations of trace elements in parts per million in shales from different volcanic assemblages of the AGB. Trace elements shown here include those associated with the muscovite group (Rb, Sr, Cs, Ba), mafic element group (Sc, V, Cr), the felsic element / HFSE group (Zr, Hf, Nb, Ta, Ga), plus uranium and thorium.

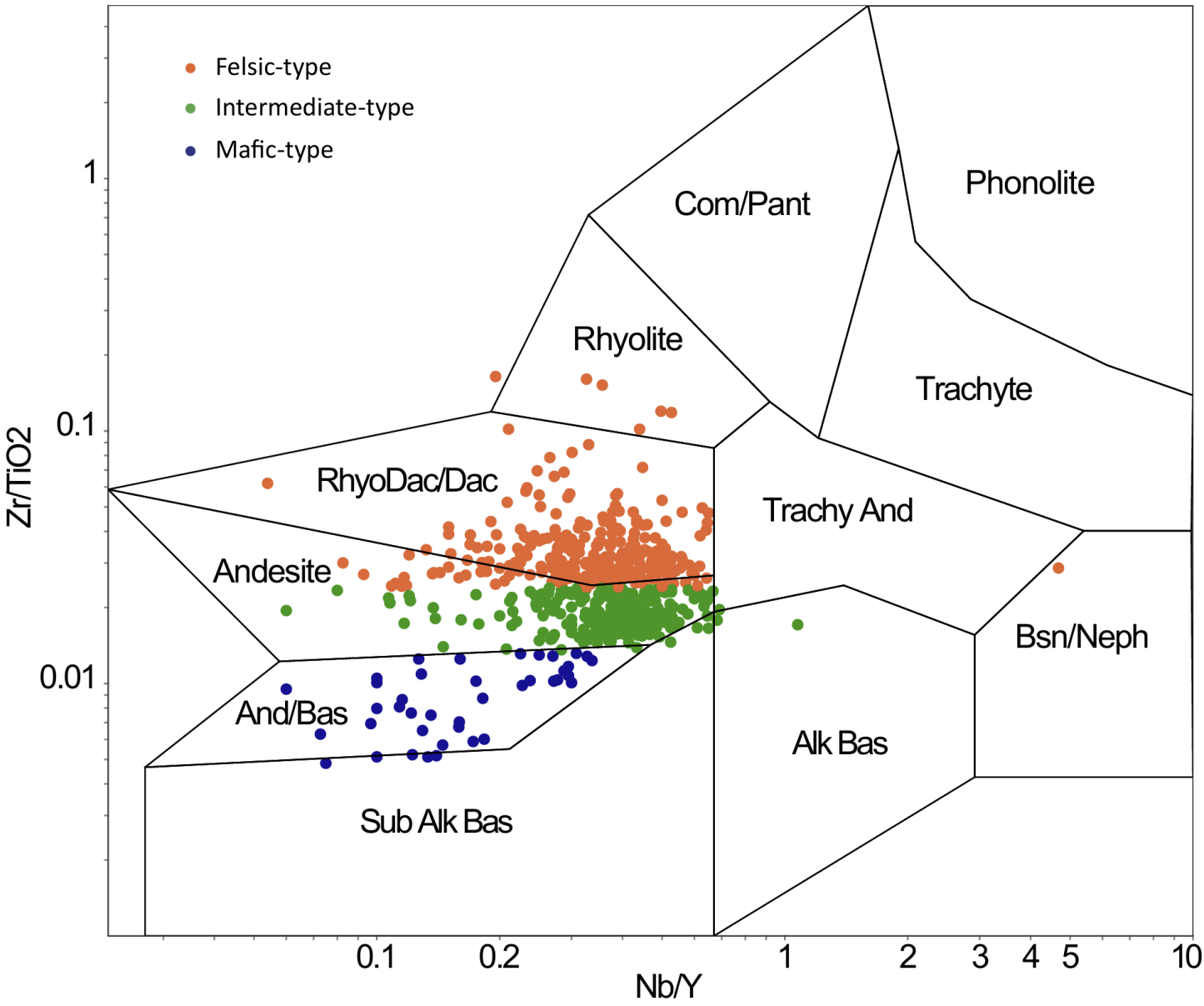


Figure 4.12. Nb/Y versus Zr/TiO₂ of WAGB shale lithotypes (this study) on the plot of Winchester and Floyd (1977). The rhyodacite-andesite boundary corresponds approximately to the Ti/Zr cut-off of 25 in Figure 4.2. The andesite-basalt boundary corresponds approximately to the Ti/Zr cut-off of 45. Mafic-type shale samples cluster within the andesite/basalt field; intermediate-type shale samples fall within the andesite field, and felsic-type samples cluster in the rhyodacite/dacite field.

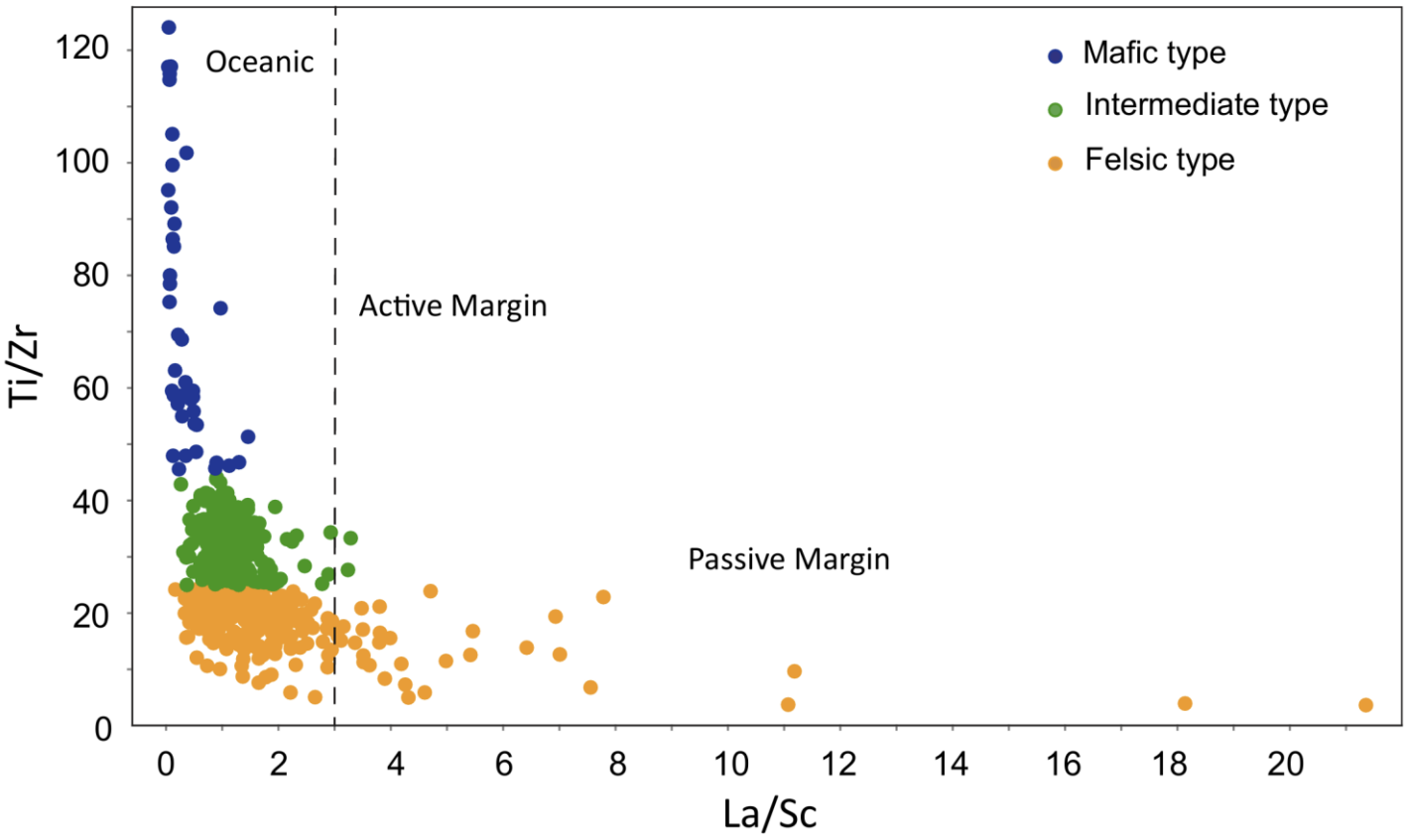


Figure 4.13. La/Sc versus Ti/Zr plot of WAGB shale lithotypes (this study) on the plot of Bhatia and Crook (1986). The tectonic discriminations are based on greywackes of Paleozoic turbidite sequences of eastern Australia. Sediments from oceanic island arc settings are characterized by a Ti/Zr ratio greater than 40 and La/Sc ratios less than one. Sediments from active continental margin settings have higher La/Sc ratios. Passive margin greywackes have larger variation in the La/Sc ratio and a Ti/Zr ratio less than 10. While the recent tectonic settings cannot be compared to the those in the Archean AGB, the sediment compositions of the WAGB are most similar to those of an active continental margin or oceanic island arc settings with primitive geochemistry, and mafic provenance.

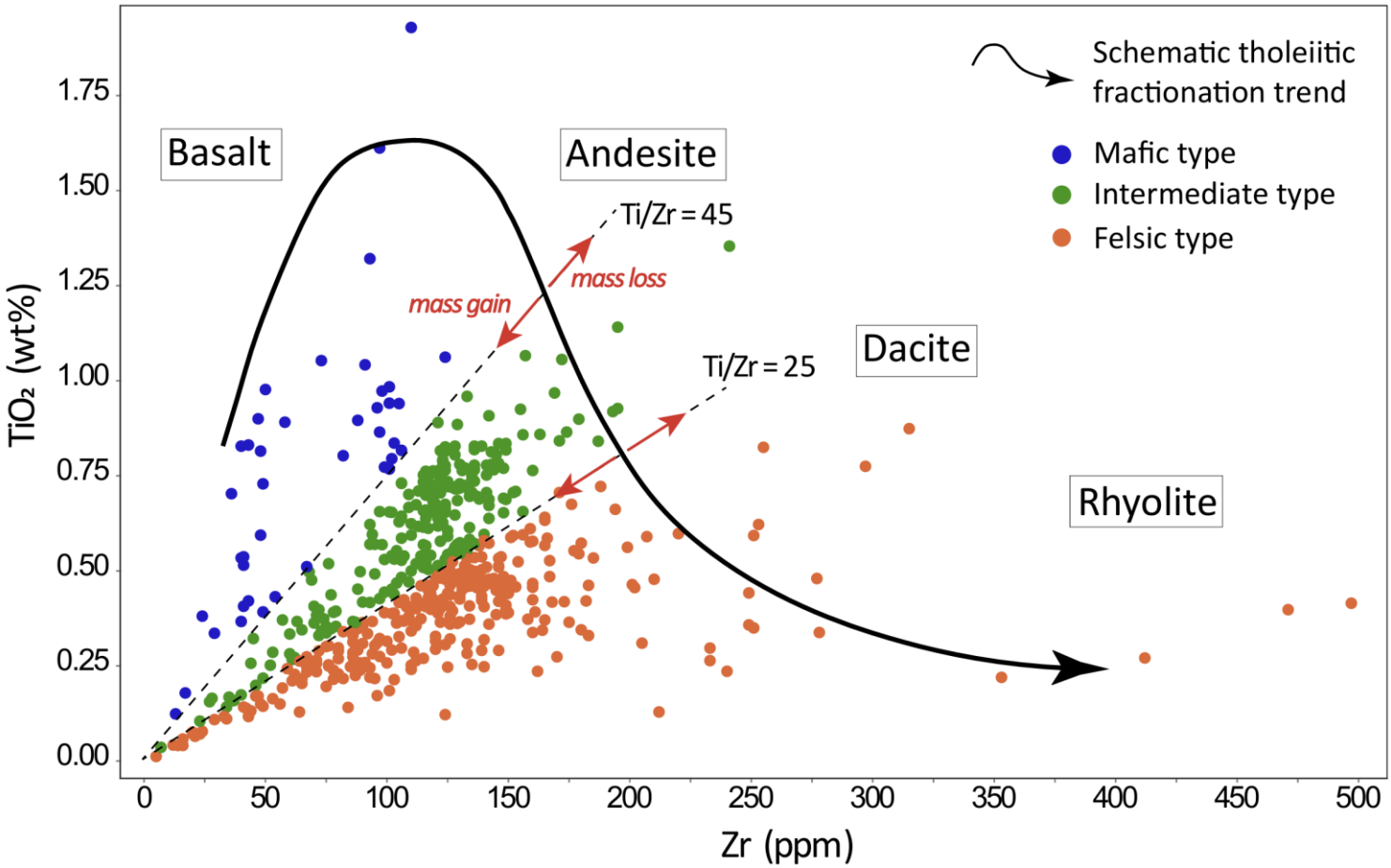


Figure 4.14. Plot of TiO_2 (wt.%) versus Zr (ppm) of WAGB shale lithotypes (this study) on the fractionation trend for tholeiite from Barrett and MacLean (1993). Shale lithotypes are colour-coded by source rock composition. Boundaries between colours correspond to the Ti/Zr values chosen in Figure 4.2. The solid line is the fractionation curve for mafic tholeiites from unaltered basalt to andesite, dacite and rhyolite compositions. The array of Ti/Zr values reflects a combination of source rock and sedimentary processes. Shale samples that plot above the curve reflect mass loss relative to an unaltered source rock (e.g., due to alteration or weathering); samples that plot below the curve reflect a mass gain (e.g., by addition of quartz). The Ti/Zr values are calculated from ppm.

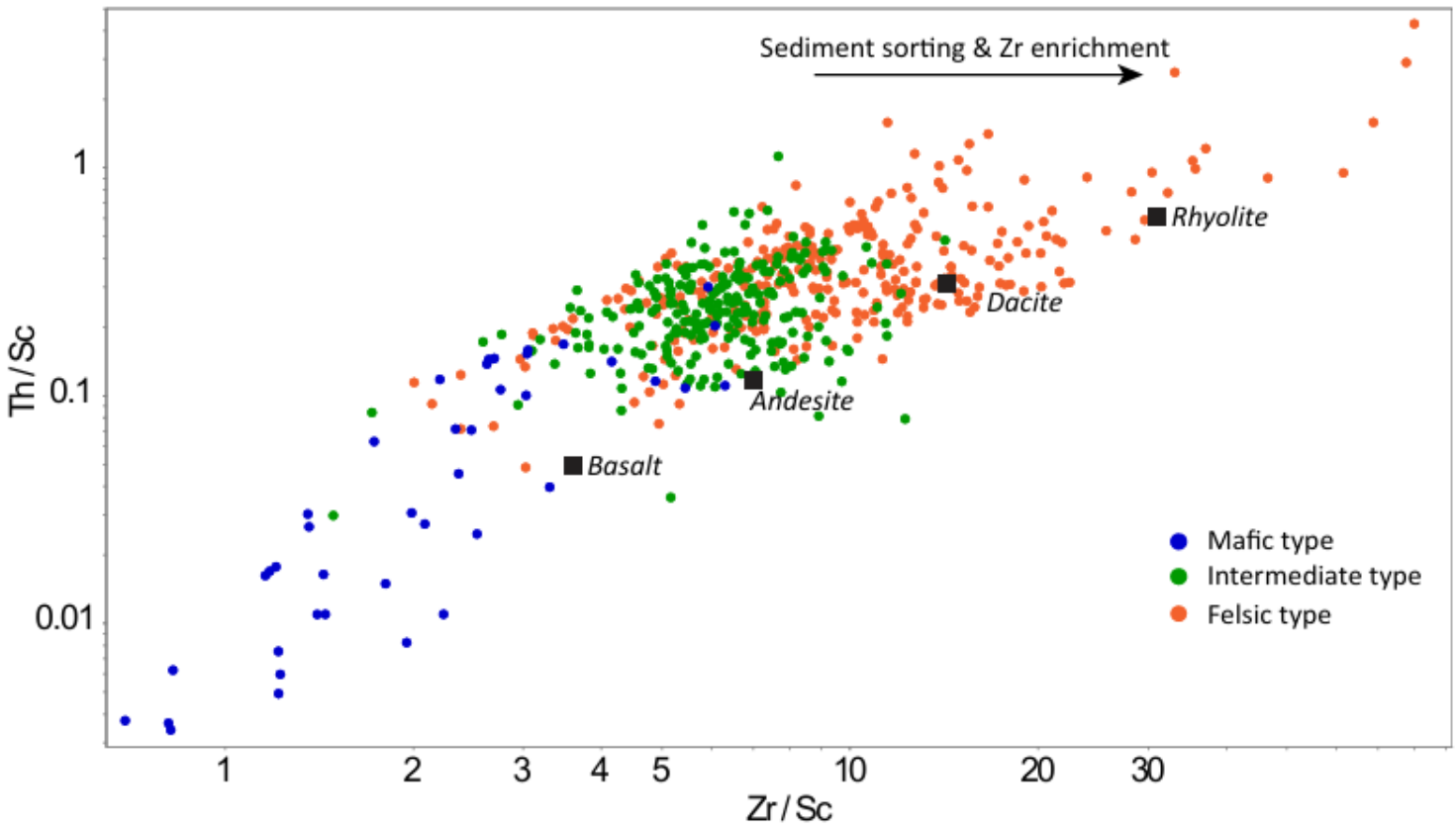
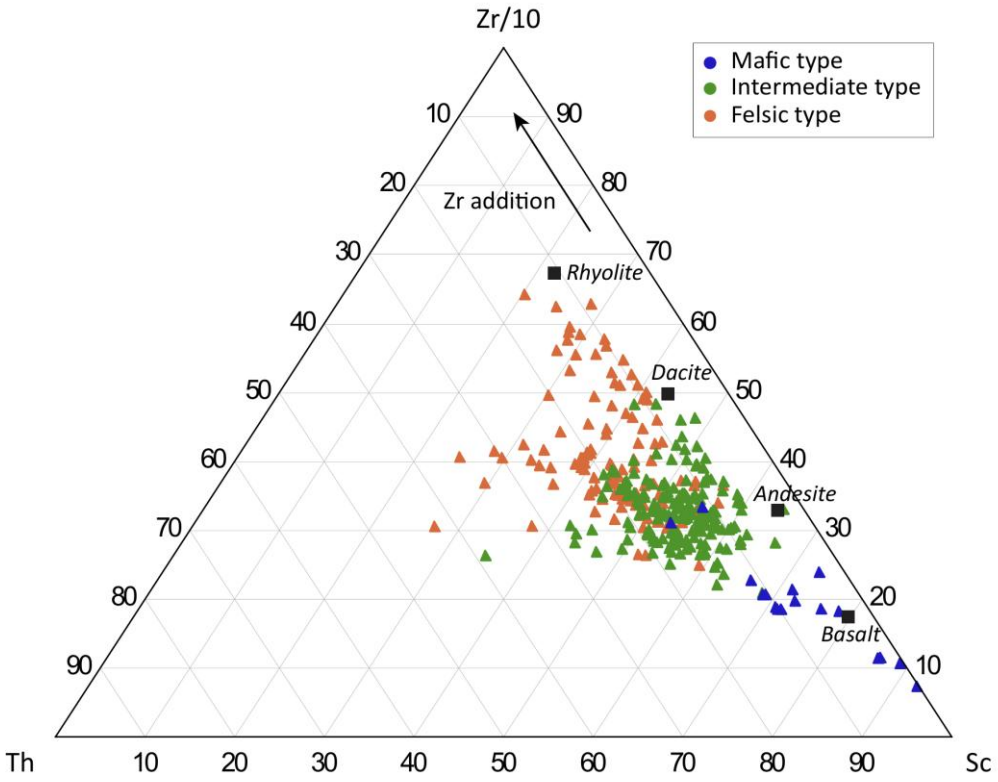
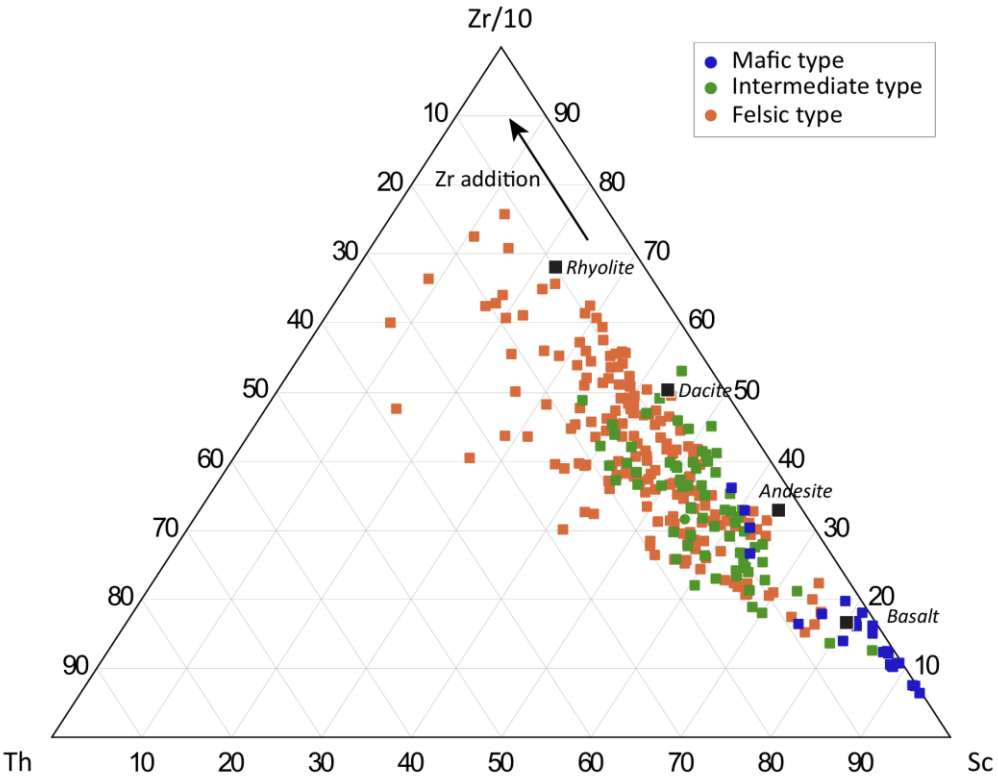


Figure 4.15. Plot of Th/Sc versus Zr/Sc of western Abitibi shale samples, modified from McLennan et al. (1993). Shale lithotypes are colour-coded by source rock as defined in Figure 4.2. Typical igneous rock compositions are indicated by the black boxes, corresponding to average Archean rhyolite values from Pearson and Gaboury (2008) and average basalt, andesite, and dacite values from Mole et al. (2021). The bulk of the shales plot at higher Th/Sc than the endmember basalt, andesite, dacite, and rhyolite averages for the AGB, which could be due to sediment recycling (McLennan, 2018). In this plot, there is significant overlap in the compositions of the intermediate- and felsic-type shales. Both trace element ratios increase with igneous differentiation, and both Zr/Sc and Th/Sc increase independently due to sediment recycling and concentration of more refractory Zr and Th relative to Sc. Concentrations used in ratios are ppm.


Zr/10
Mafic type
Intermediate type
Felsic type
Zr addition
Rhyolite
Dacite
Andesite
Basalt
Th
Sc
10
20
30
40
50
60
70
80
90

A)


Zr/10
Mafic type
Intermediate type
Felsic type
Zr addition
Rhyolite
Dacite
Andesite
Basalt
Th
Sc
10
20
30
40
50
60
70
80
90

B)

Figure 4.16. Th-Zr/10-Sc ternary diagram after Bhatia and Crook (1986) of western Abitibi shale samples classified according to Ti/Zr (felsic-type, intermediate-type, and mafic-type) Plot A is for shales from drill holes that were originally targeted for discovery orogenic gold mineralization (triangles). Plot B is for shales from drill holes that were originally targeted for discovery of VMS (squares). Volcanic rock compositions are shown by black boxes. The composition of average Archean rhyolite is from Gaboury and Pearson (2008), and the average compositions of Archean andesite, basalt, and dacite are from Mole et al. (2021). In both plots, felsic-type samples reflect strong sorting and sediment recycling (i.e., Th and Zr addition). The shale compositions are shifted to higher Th and Zr from those of the end-member volcanic source rocks as seen in Figure 4.15 due to sediment recycling. See text for discussion.

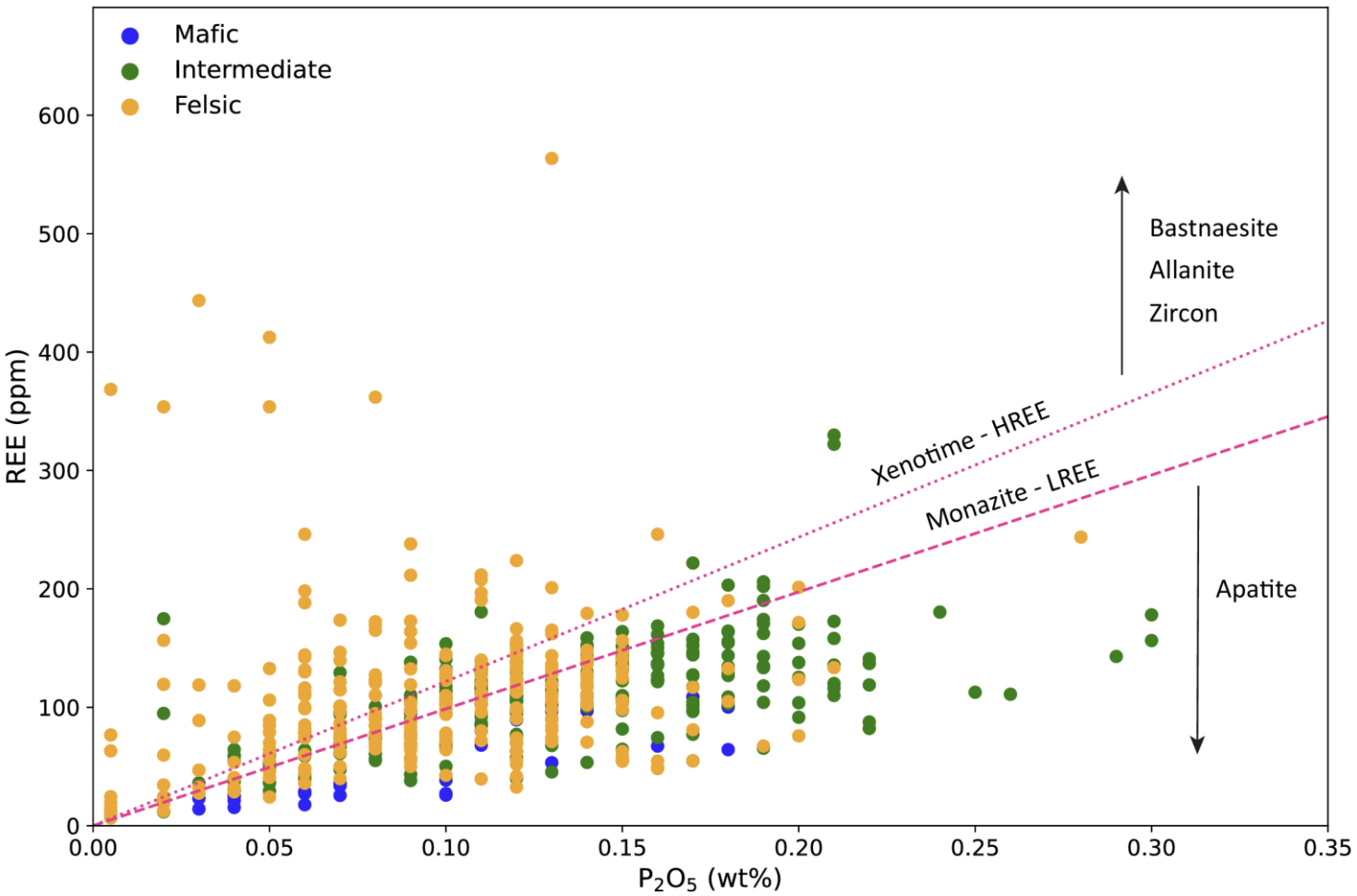
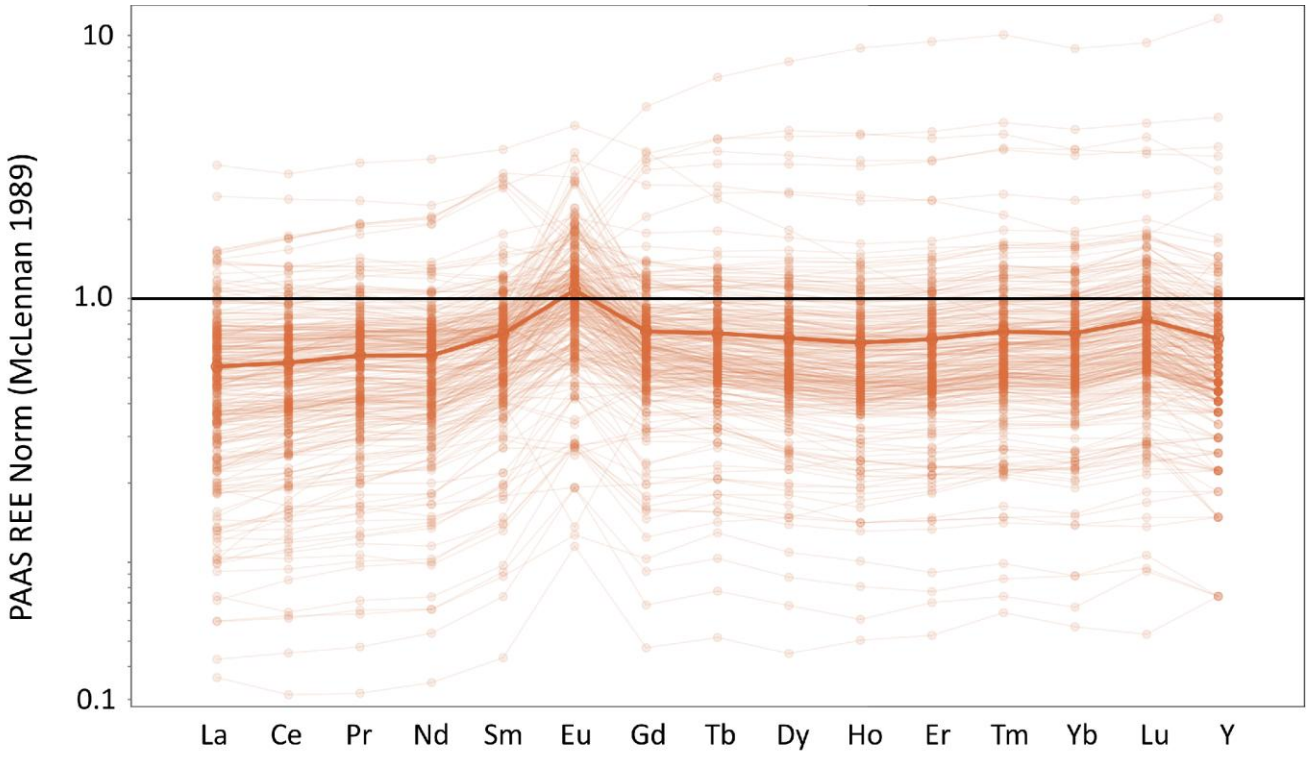
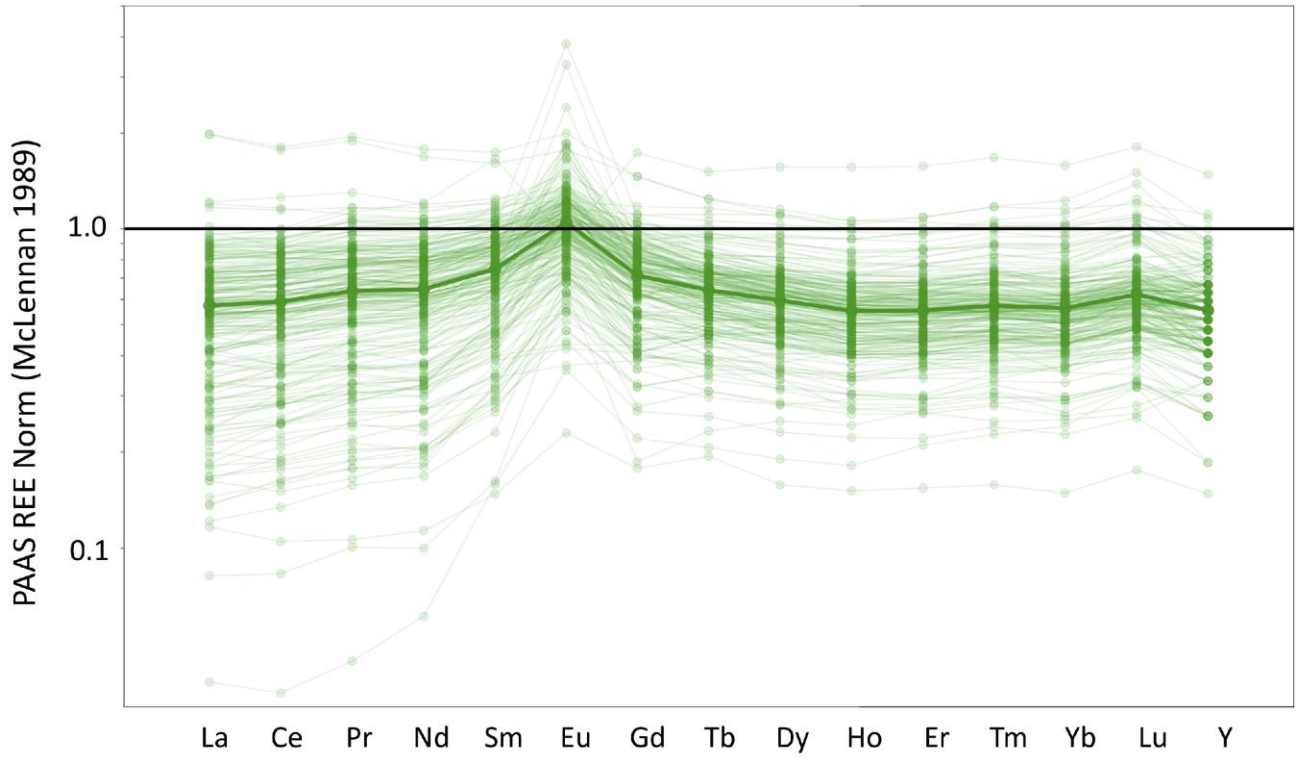


Figure 4.17. Rare earth element (REE) concentrations versus P_2O_5 (wt%) of western Abitibi shale samples classified according to Ti/Zr (felsic-type, intermediate-type, and mafic-type). The positive correlation between REE and P_2O_5 strongly suggests that phosphate minerals are major REE hosts in felsic and intermediate lithotypes. The dashed lines represent the REE contribution to the bulk rock corresponding to a 5% contribution of phosphorous from monazite (LREE – selective) or xenotime (HREE – selective), calculated according to the composition of endmember $CePO_4$ and $YbPO_4$. The arrows indicate the possible influence of other REE-bearing minerals. Most samples cluster near the monazite line, suggesting it is the dominant REE-bearing phase. However, it is likely that other minerals with lower REE contents, such as apatite, are also present. Note that bastnaesite and zircon do not contain any P_2O_5.


PAAS REE Norm (McLennan 1989)
10
1.0
0.1
La
Ce
Pr
Nd
Sm
Eu
Gd
Tb
Dy
Ho
Er
Tm
Yb
Lu
Y


PAAS REE Norm (McLennan 1989)
1.0
0.1
La
Ce
Pr
Nd
Sm
Eu
Gd
Tb
Dy
Ho
Er
Tm
Yb
Lu
Y

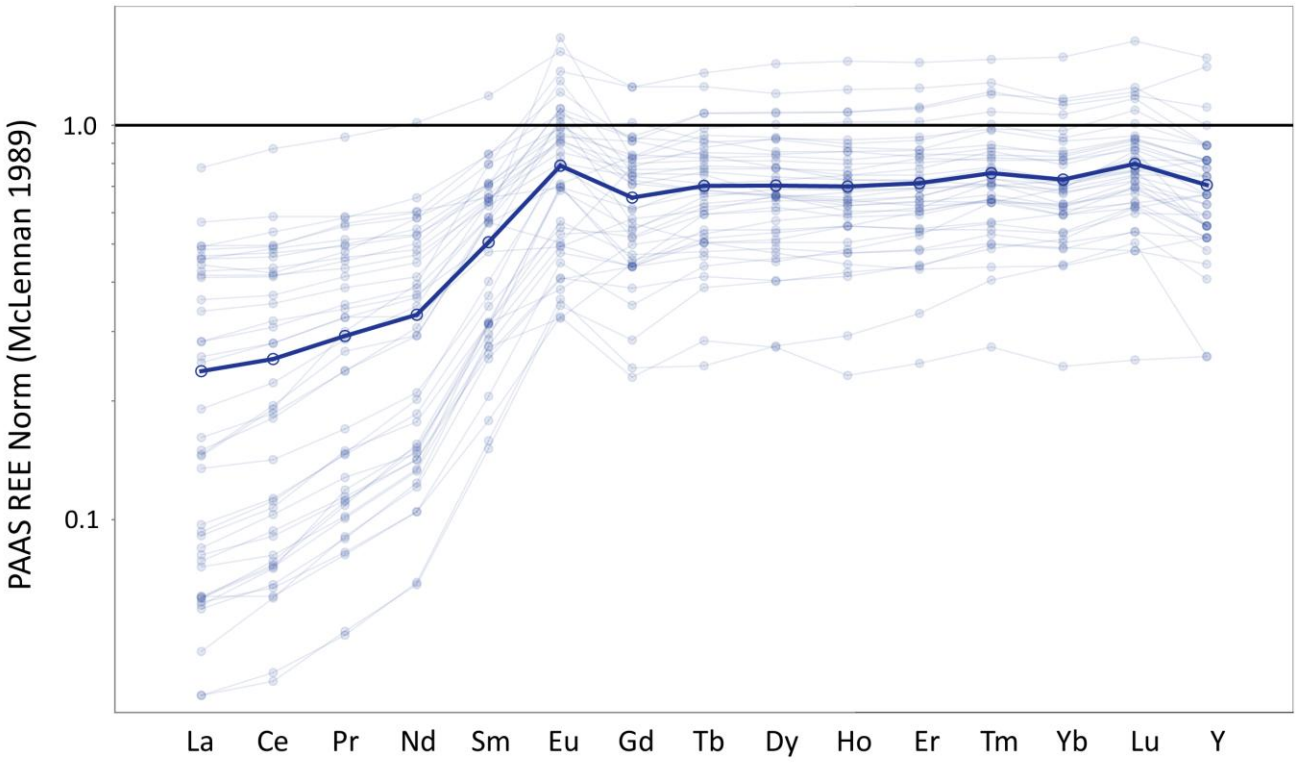


Figure 4.18. REE concentrations of felsic-, intermediate-, and mafic-type black shale samples of the WAGB normalized to Post-Archean Australian Shale (PAAS; values from Taylor & McLennan, 1985). See text for discussion.

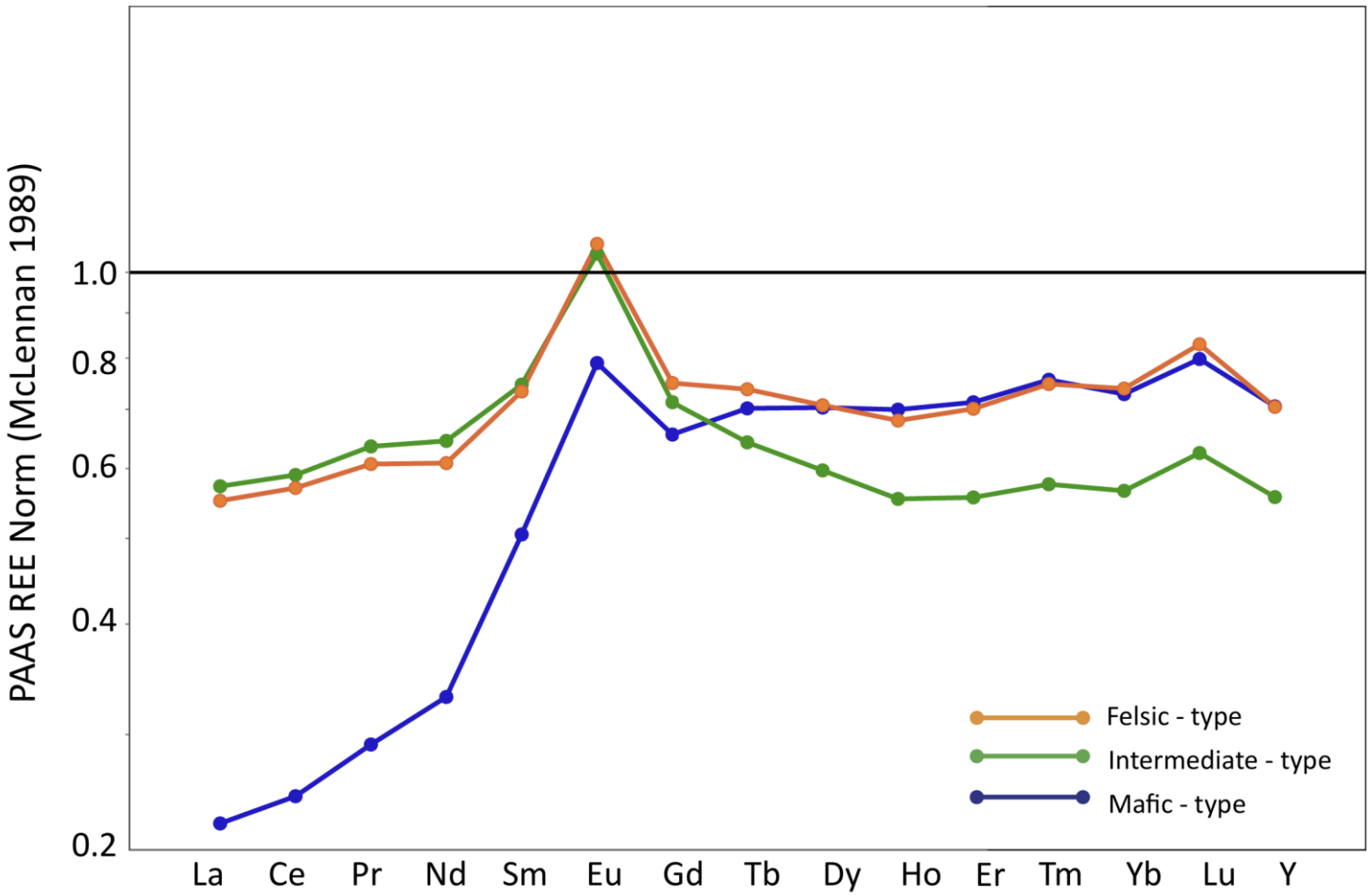


Figure 4.19. Average REE concentrations in WAGB black shale samples normalized to Post-Archean Australian Shale (PAAS; values from Taylor & McLennan, 1985) grouped by shale lithotype. Mafic-type samples show a depletion of the LREE. See text for discussion.

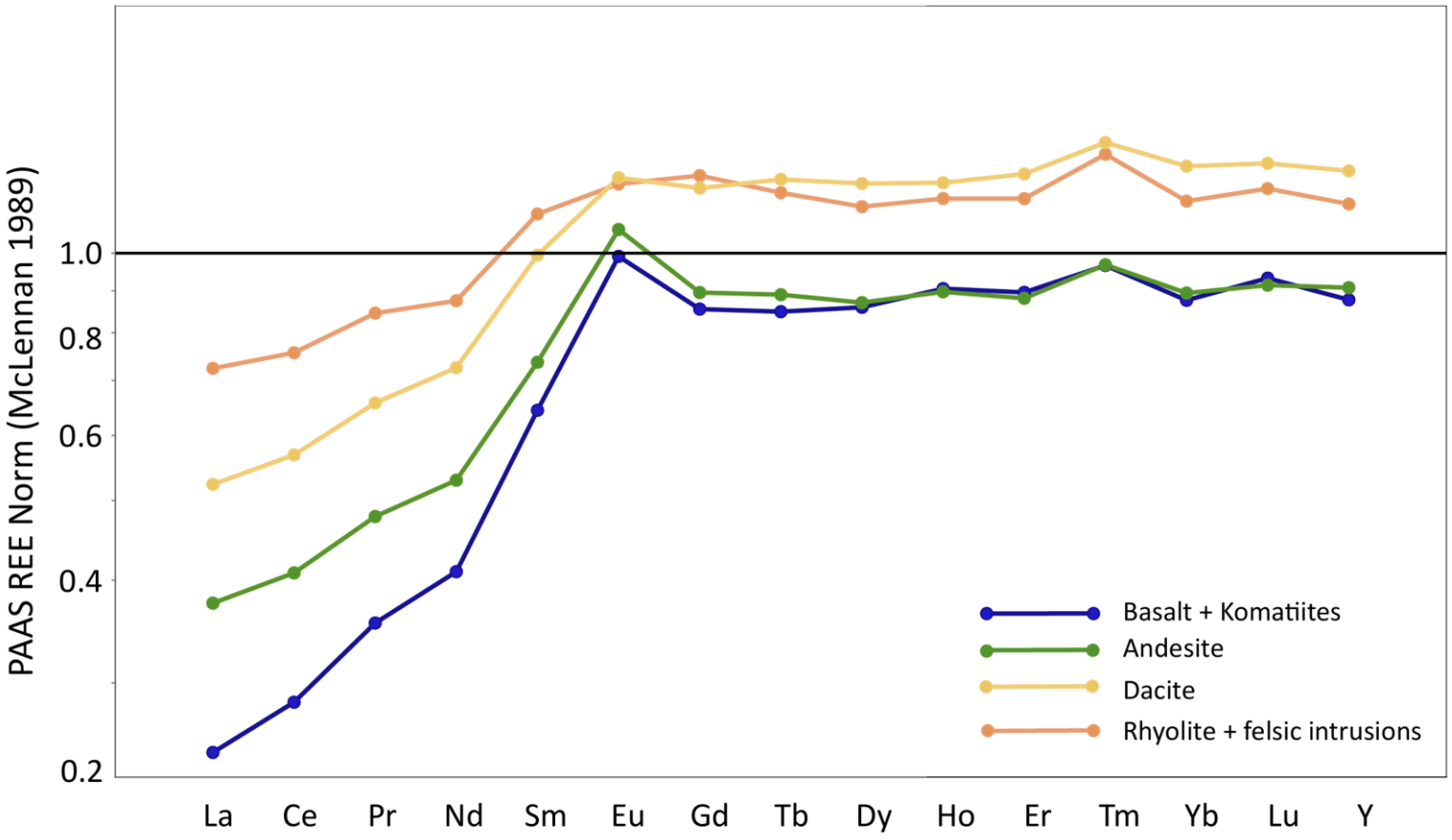


Figure 4.20. REE profiles of possible sources rocks of WAGB shales, normalized to Post-Archean Australian Shale (PAAS; values from Taylor & McLennan, 1985). Data for the volcanic rocks are from Gaboury and Pearson (2008) and Mole et al. (2021).

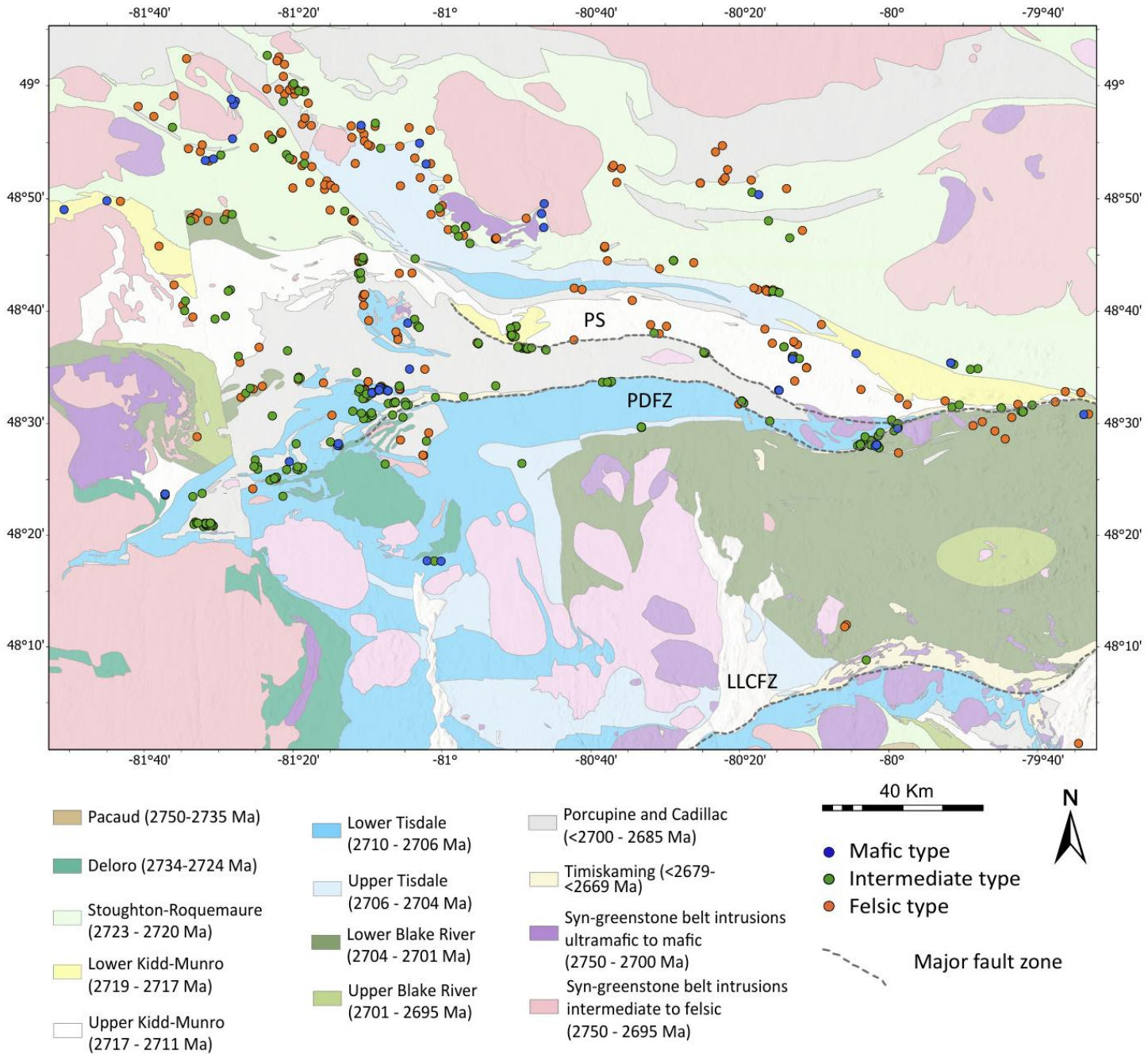


Figure 4.21. Map distribution of shale lithotypes in the western AGB. Shale lithotypes are colour-coded by source rock composition as defined in Figure 4.2. Samples are overlain on the volcanic assemblages of the AGB from Thurston et al. (2008). Major faults are represented by dashed lines: the Destor Porcupine Fault Zone (DPFZ), Pipestone Fault (PS), and the Cadillac Larder Lake Fault Zone (LLCFZ). A high proportion of the intermediate-type shales occur in the Porcupine assemblage close to the PDFZ. A high proportion of the mafic-type and felsic-type shales occur in Kidd-Munro and Stoughton-Roquemaure assemblages north of the Pipestone Fault. Note that all samples are hosted in volcanic rocks, including in the sediment-dominated Porcupine Assemblage.

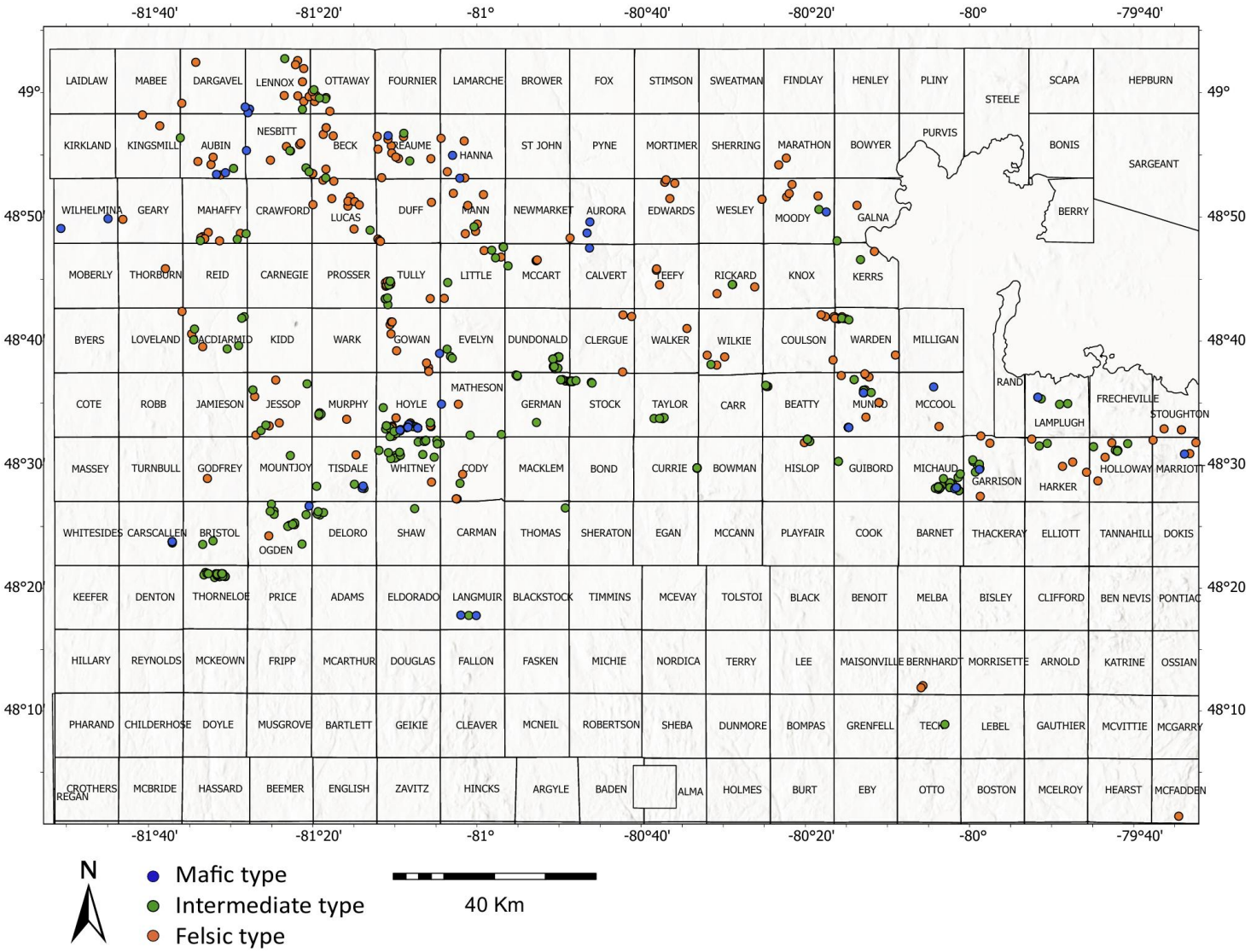


Figure 4.22. Map distribution of shale lithotypes in the western AGB overlain on the township grid for reference. Note that samples from 4 townships surrounding the Kidd Creek Mine (Kidd, Wark, Carnegie, and Prosser) were omitted from the analyzed data set.

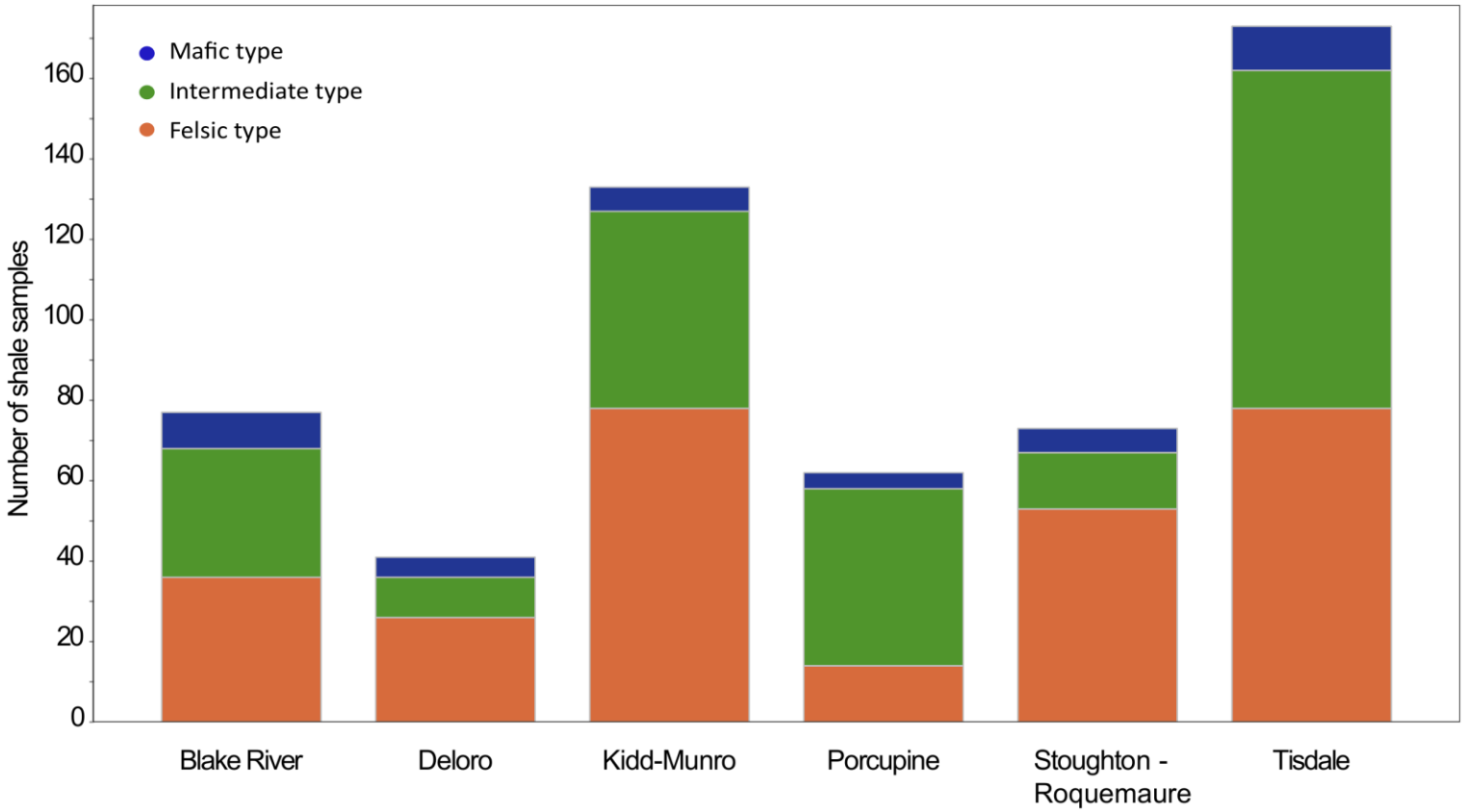


Figure 4.23. Distribution of shale lithotypes in the volcanic assemblages of the WAGB. Stacked segments show the contribution of individual lithotypes to the total number of shale samples from each assemblage.

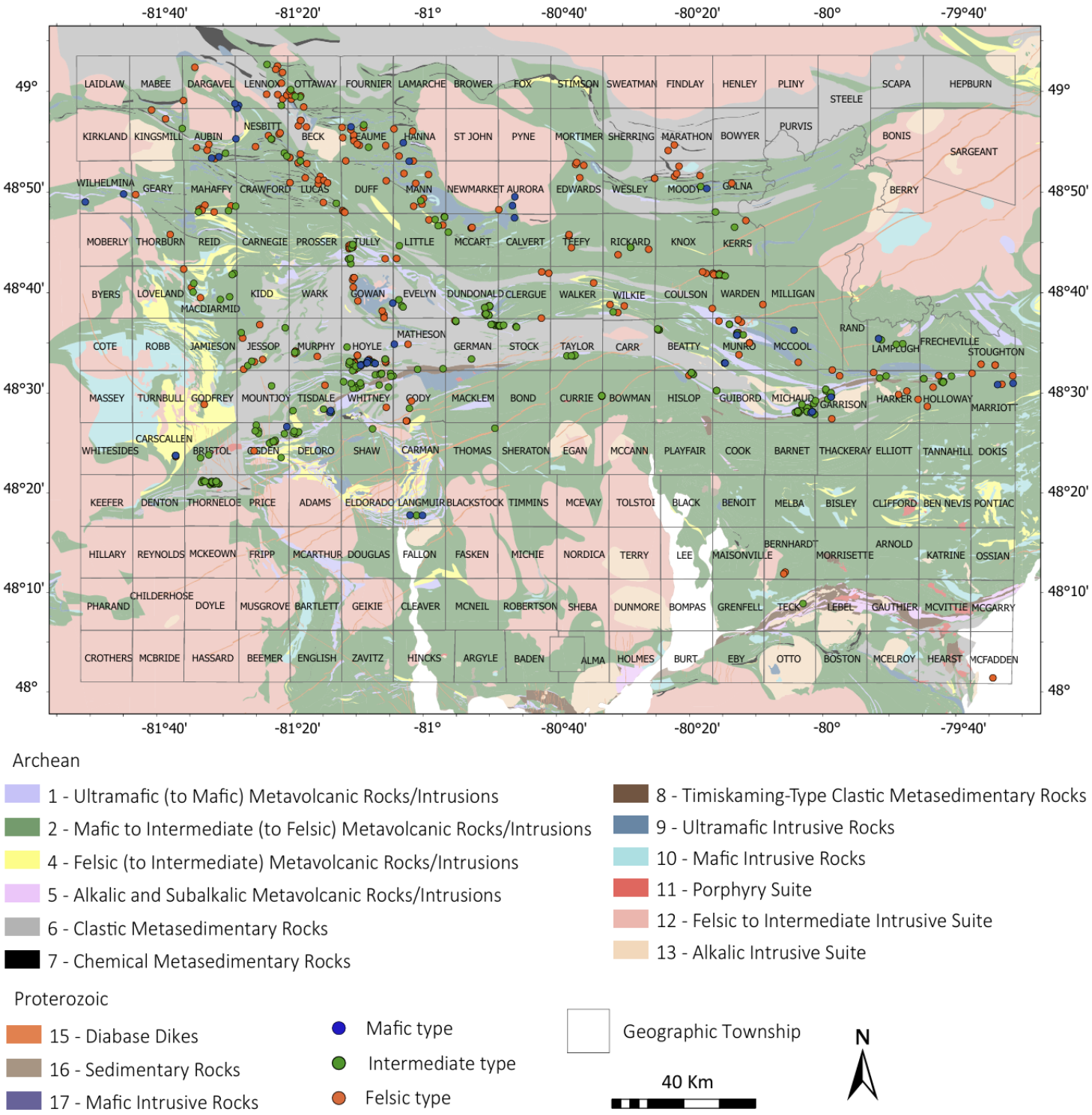


Figure 4.24. Map distribution of shale lithotypes in the western AGB overlain on the lithologies from Jørgensen & Gibson (2024). Note that all samples are hosted in volcanic rocks, including in the sediment-dominated Porcupine Assemblage.

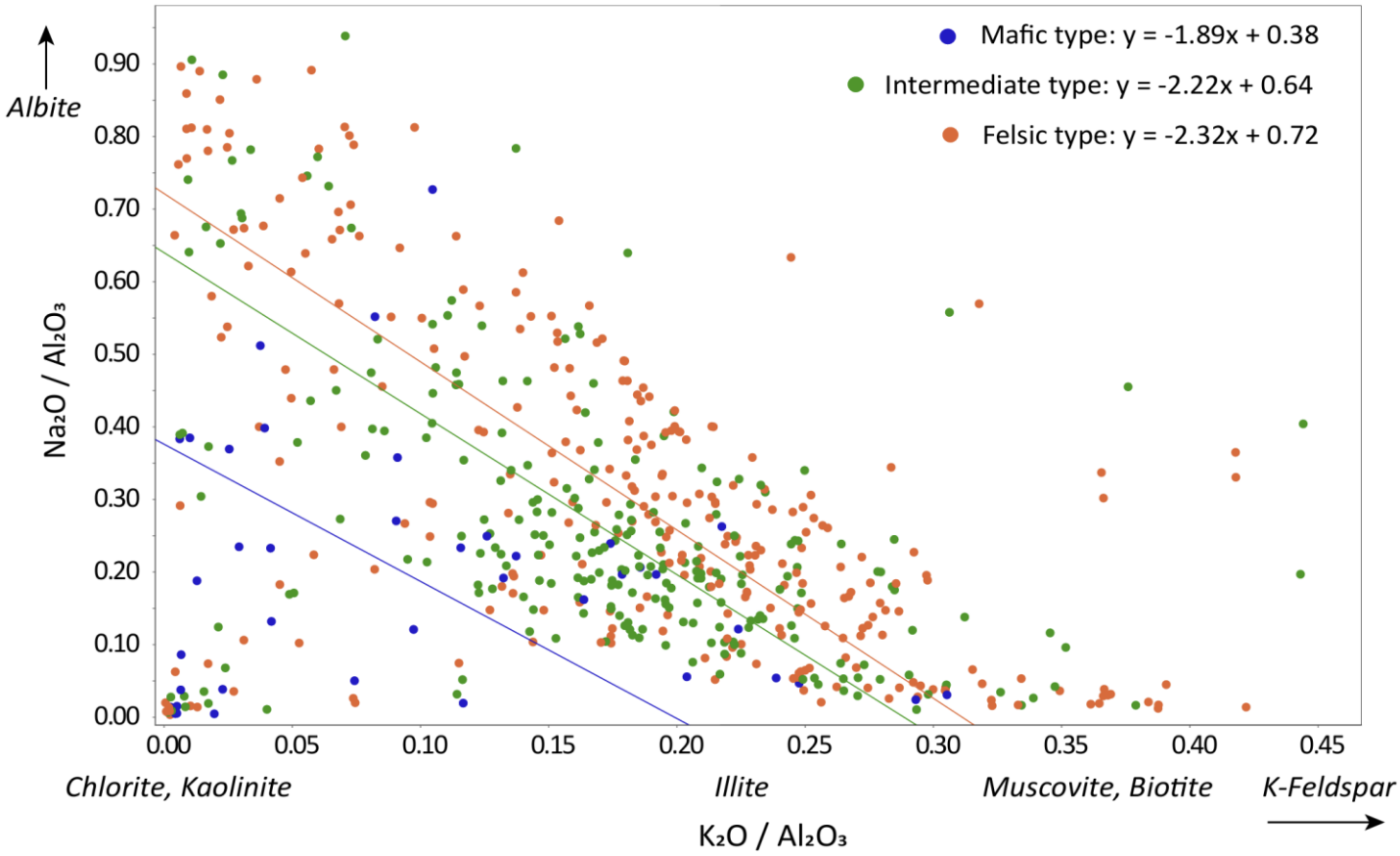
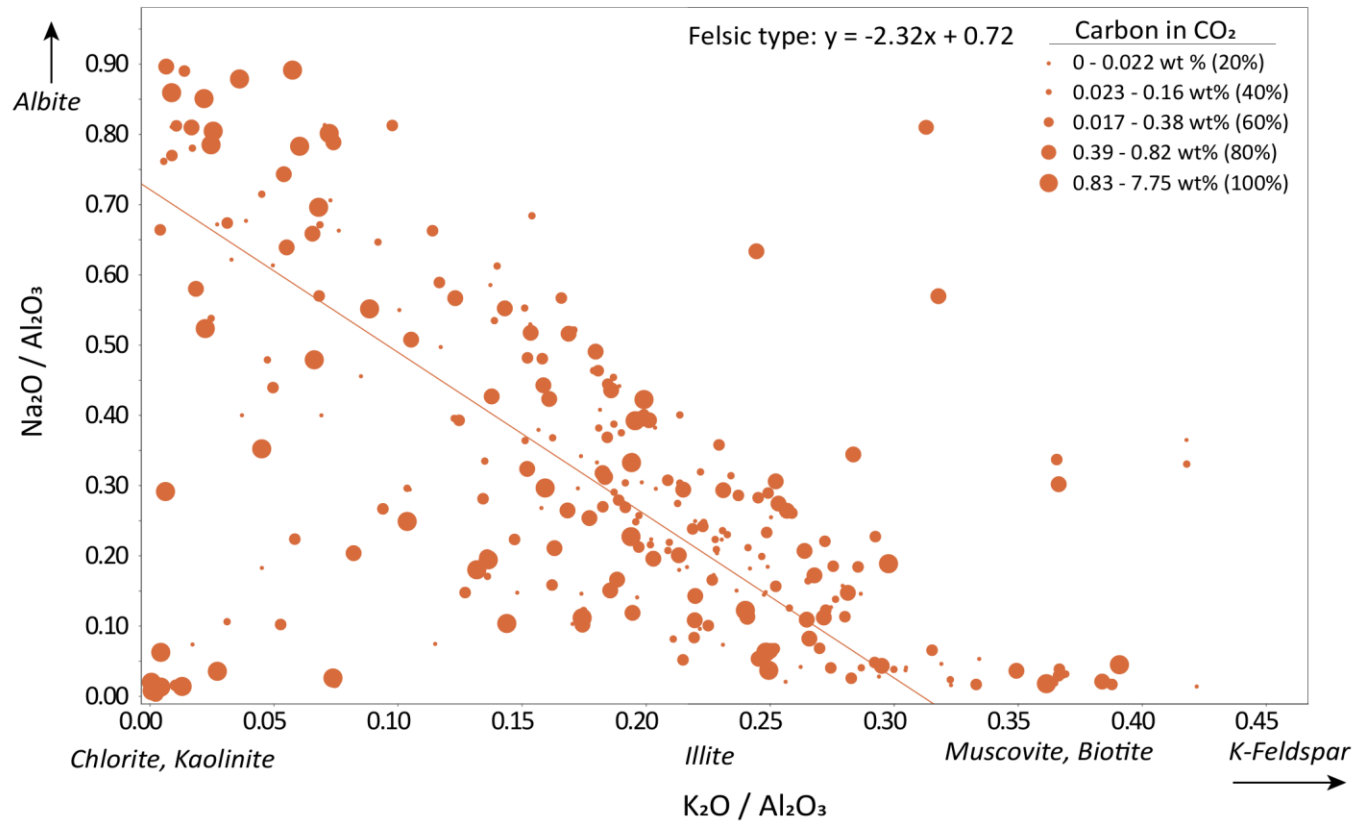
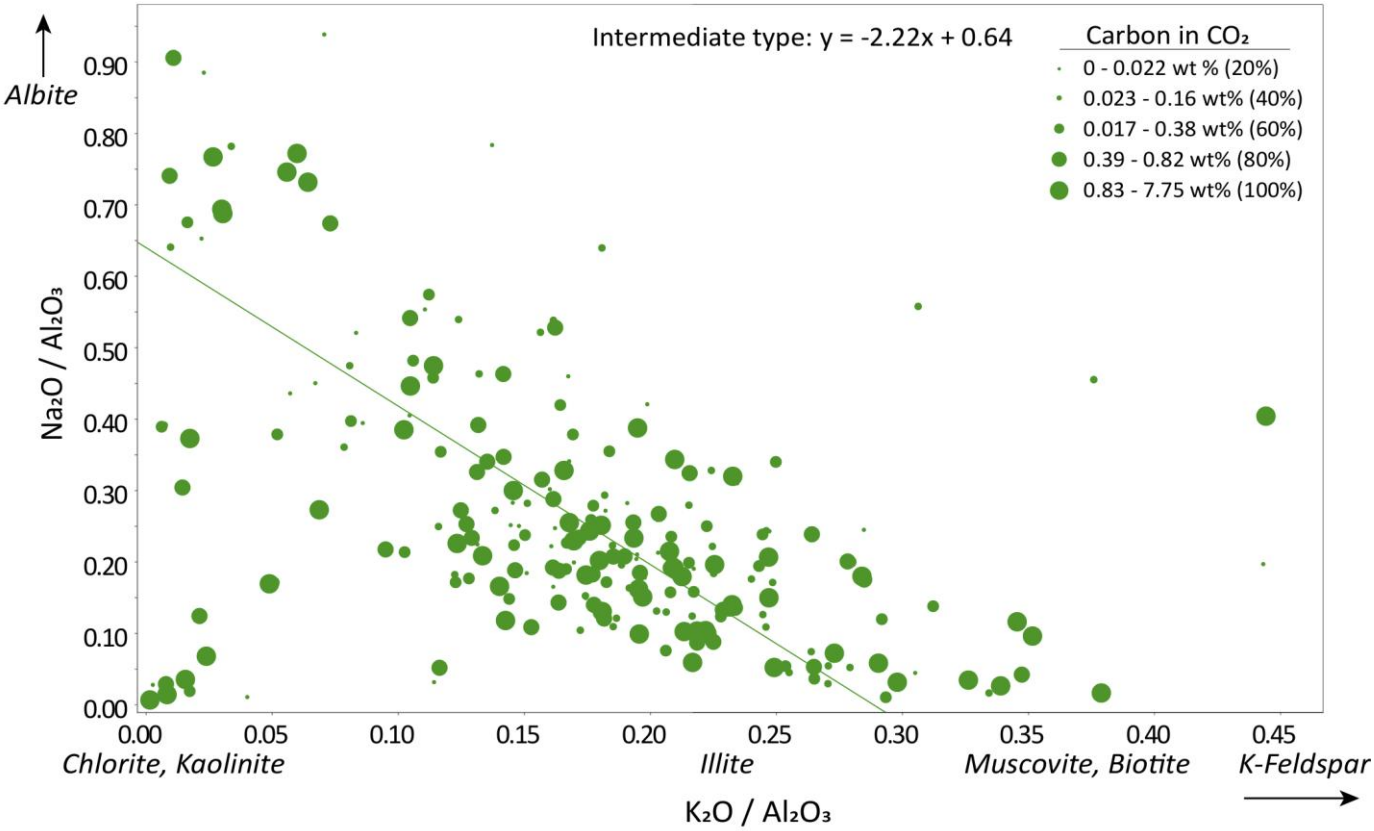


Figure 4.25 shows the Na_2O/Al_2O_3 vs K_2O/Al_2O_3 plot of Davies and Whitehead (1994) and the regression lines for each shale lithotype. Molar K_2O/Al_2O_3 versus Na_2O/Al_2O_3 ratios permit the interpretation of the bulk compositions in terms of major mineral proportions. A general negative trend in Na_2O/Al_2O_3 versus K_2O/Al_2O_3 indicates sodium depletion from the destruction of albite. Samples that cluster in the upper left corner indicate Na-enrichment and K-depletion (e.g., albite alteration) and the bottom right corner indicate Na-depletion and K-enrichment (e.g., sericitic alteration). A cluster of shale samples at the bottom left corresponds to removal of both Na_2O and K_2O (e.g., replacement by Mg-Fe carbonate or chlorite). Roughly 30 samples were identified as having these low molar ratios, and 26 are associated with base metal mineralization.


Felsic type: y = -2.32x + 0.72
Carbon in CO₂
0 - 0.022 wt % (20%)
0.023 - 0.16 wt% (40%)
0.017 - 0.38 wt% (60%)
0.39 - 0.82 wt% (80%)
0.83 - 7.75 wt% (100%)
Albite
Na₂O / Al₂O₃
0.00
0.10
0.20
0.30
0.40
0.50
0.60
0.70
0.80
0.90
0.00
0.05
0.10
0.15
0.20
0.25
0.30
0.35
0.40
0.45
Chlorite, Kaolinite
Illite
Muscovite, Biotite
K-Feldspar
K₂O / Al₂O₃


Intermediate type: y = -2.22x + 0.64
Carbon in CO₂
0 - 0.022 wt % (20%)
0.023 - 0.16 wt% (40%)
0.017 - 0.38 wt% (60%)
0.39 - 0.82 wt% (80%)
0.83 - 7.75 wt% (100%)
Albite
Na₂O / Al₂O₃
0.00
0.10
0.20
0.30
0.40
0.50
0.60
0.70
0.80
0.90
0.00
0.05
0.10
0.15
0.20
0.25
0.30
0.35
0.40
0.45
Chlorite, Kaolinite
Illite
Muscovite, Biotite
K-Feldspar
K₂O / Al₂O₃

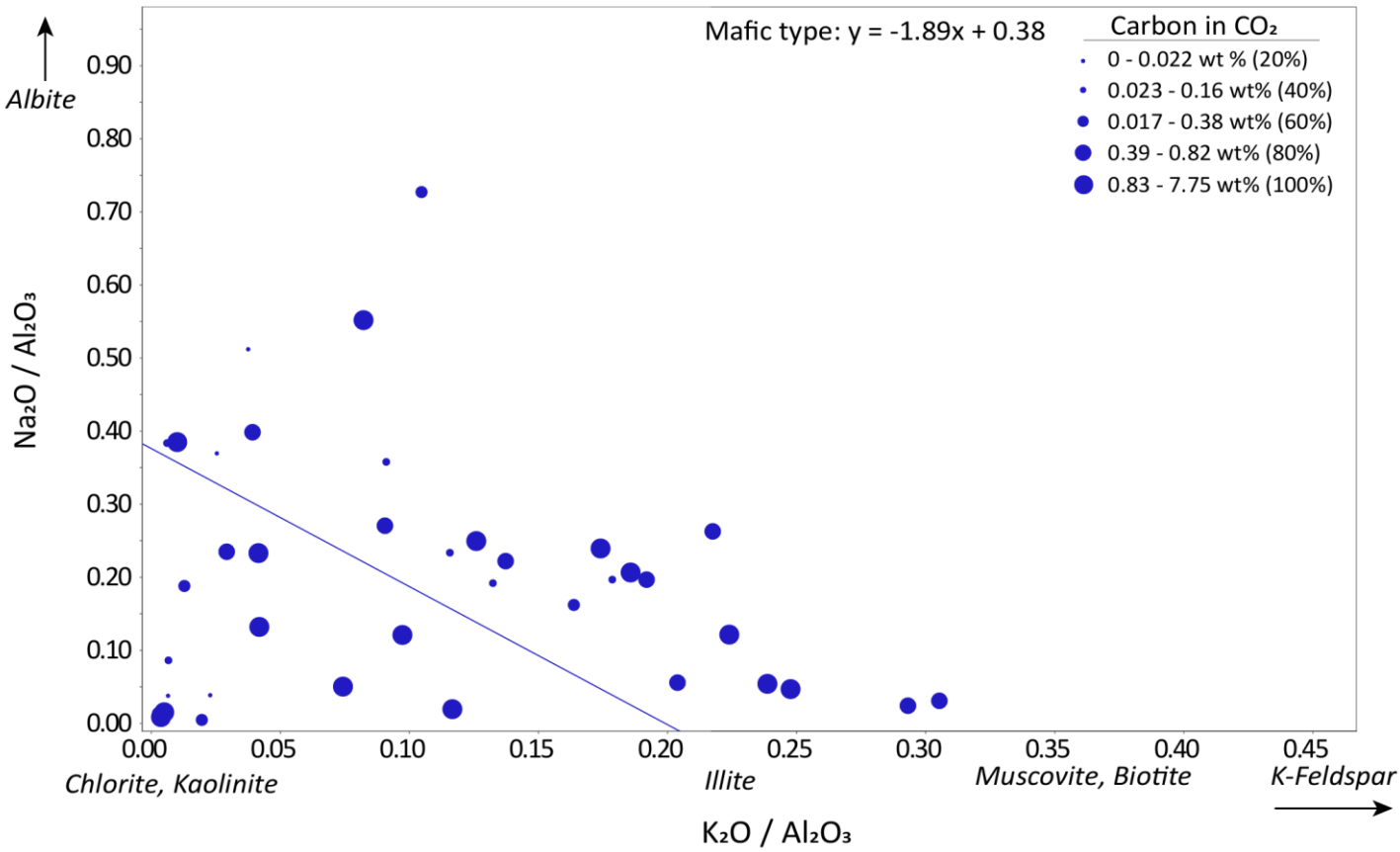
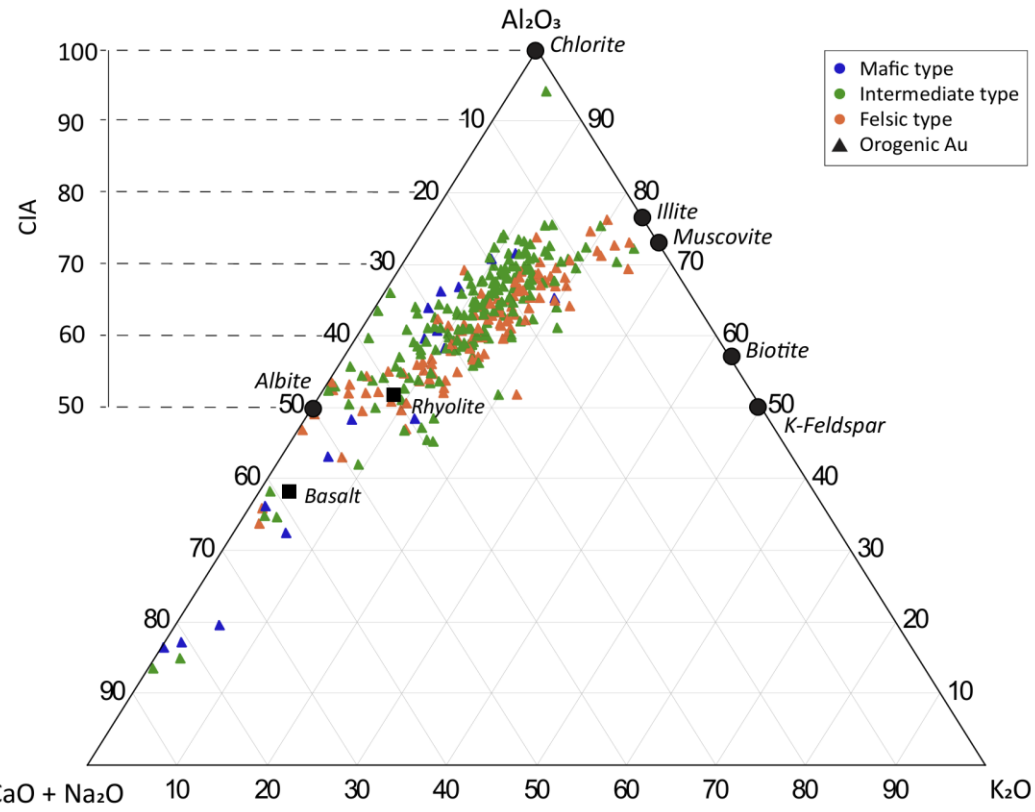
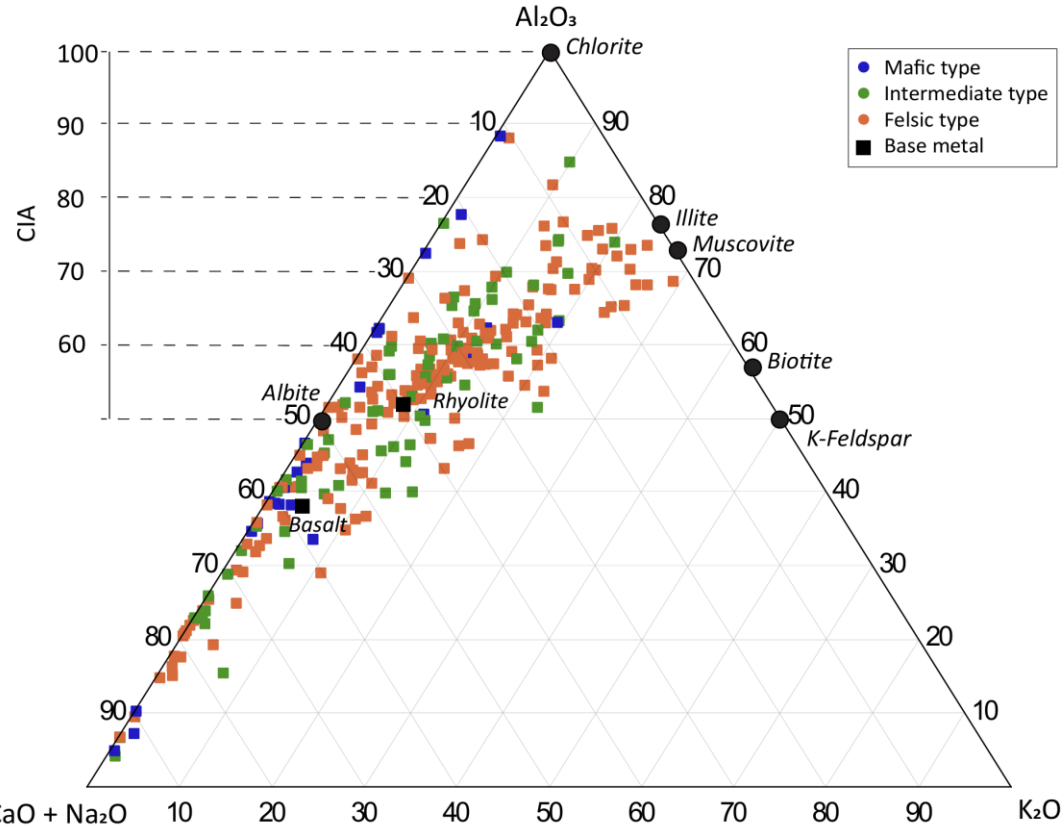


Figure 4.26. Subsets of Figure 4.25 showing the lack of correlation between alteration of the shale lithotypes and total carbon in CO_2. Larger symbols indicate a higher proportion of carbonate.

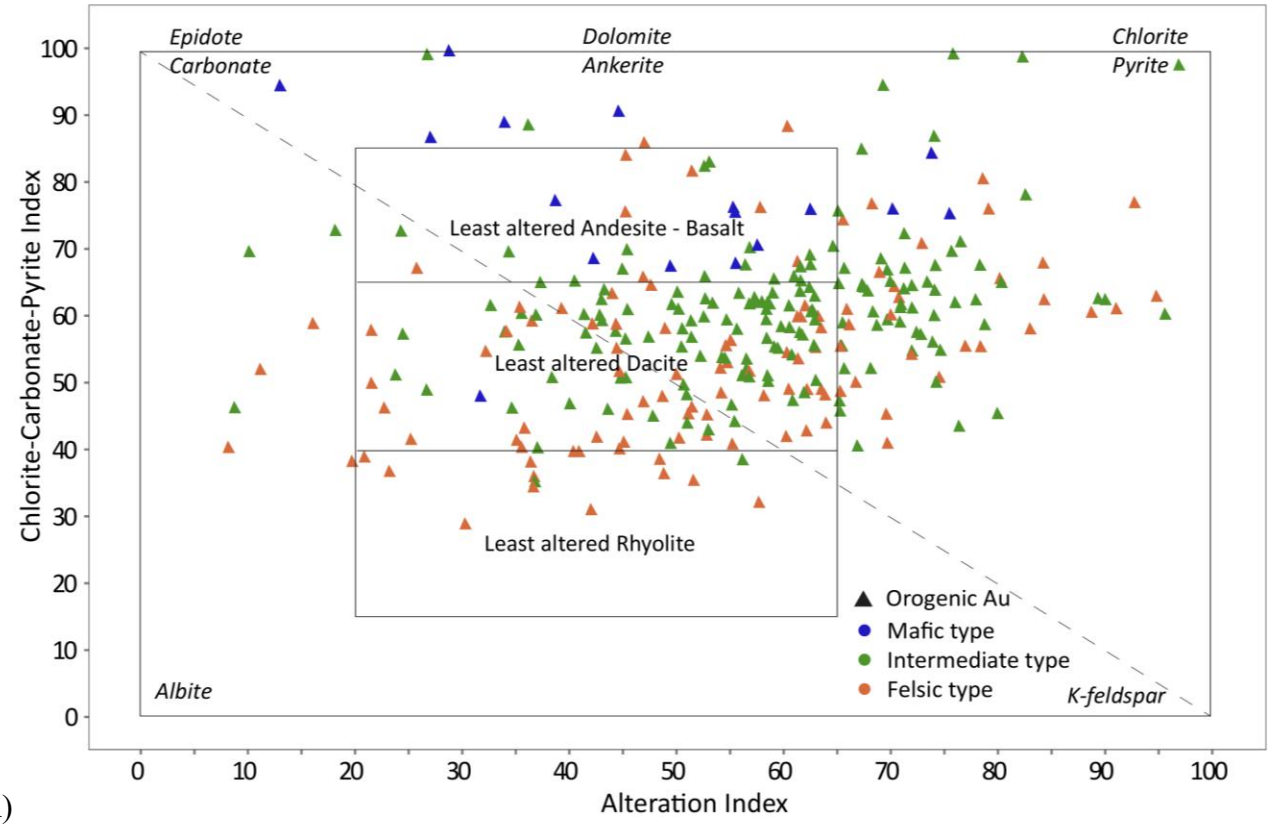

Al₂O₃
Chlorite
Mafic type
Intermediate type
Felsic type
Orogenic Au
CIA
Illite
Muscovite
Biotite
Albite
Rhyolite
K-Feldspar
Basalt
CaO + Na₂O
K₂O

A)

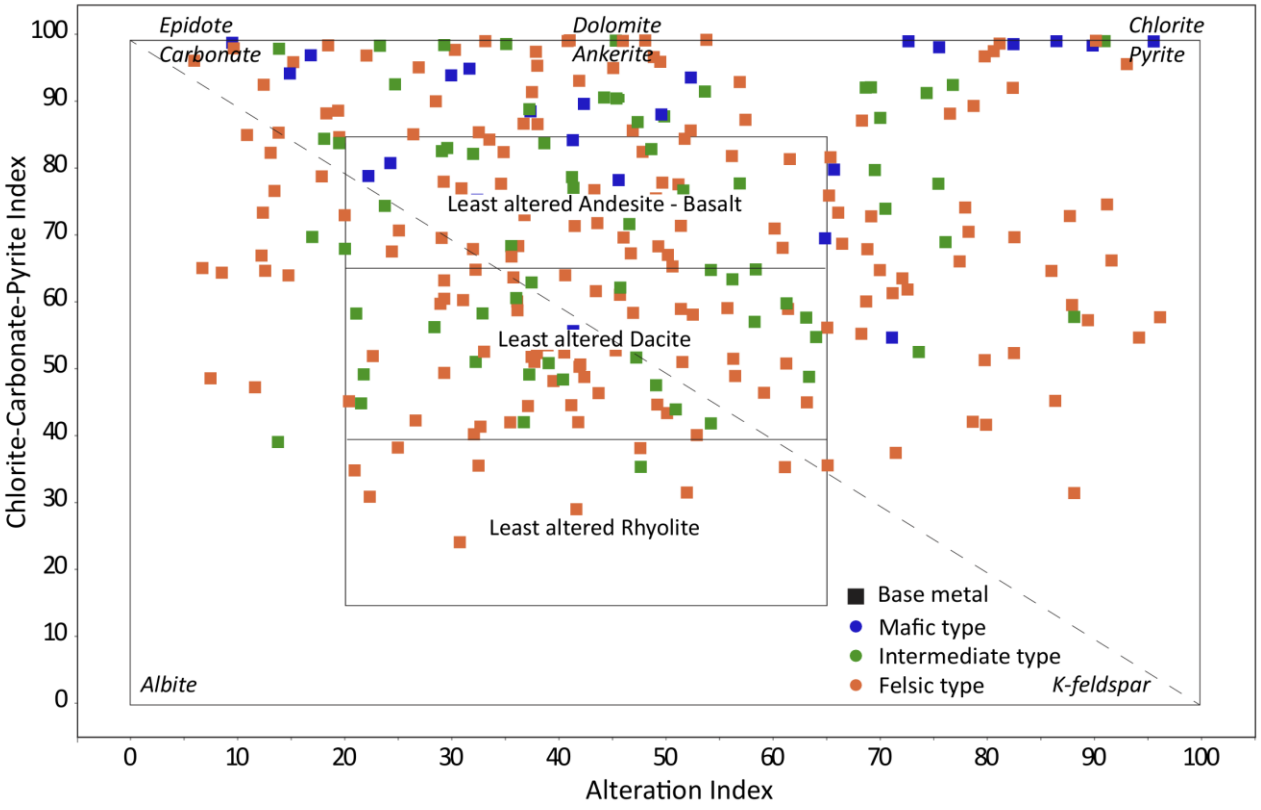

Al₂O₃
Chlorite
Mafic type
Intermediate type
Felsic type
Base metal
CIA
Illite
Muscovite
Biotite
Albite
Rhyolite
K-Feldspar
Basalt
CaO + Na₂O
K₂O

B)

Figure 4.27. A-CN-K diagram after Nesbitt and Young (1982) of western Abitibi shale samples classified according to Ti/Zr (felsic-type, intermediate-type, and mafic-type). Plot A is for shales from drill holes that were originally targeted for discovery orogenic gold mineralization (triangles). Plot B is for shales from drill holes that were originally targeted for discovery of VMS (squares). Volcanic rock compositions are shown by black boxes. The composition of average Archean rhyolite values from Gaboury and Pearson (2008), and fresh basalt from (Nesbitt and Young, 1984; McLennan, 1993; McLennan et al., 1993; Fedo et al., 1995, Babechuk and Fedo, 2023). The Chemical Index of Alteration (CIA) is derived from the molar proportions of Al_2O_3 (A-apex), $CaO + Na_2O$ (CN-apex), and K_2O (K apex) and shows the degree of chemical weathering in terms of the destruction of plagioclase and K-feldspar. Samples that plot lower on this scale have experienced less chemical weathering and are more compositionally similar to their source rock. Most of the western Abitibi shales plot along the A-CN line and progressively shift towards illite-muscovite composition with increasing alteration. Most samples from drill holes originally targeted for VMS plot at intermediate to low CIA values. Most samples from drill holes originally targeted for orogenic Au mineralization plot at intermediate to high CIA values typical of sedimentary basins (e.g., Porcupine).

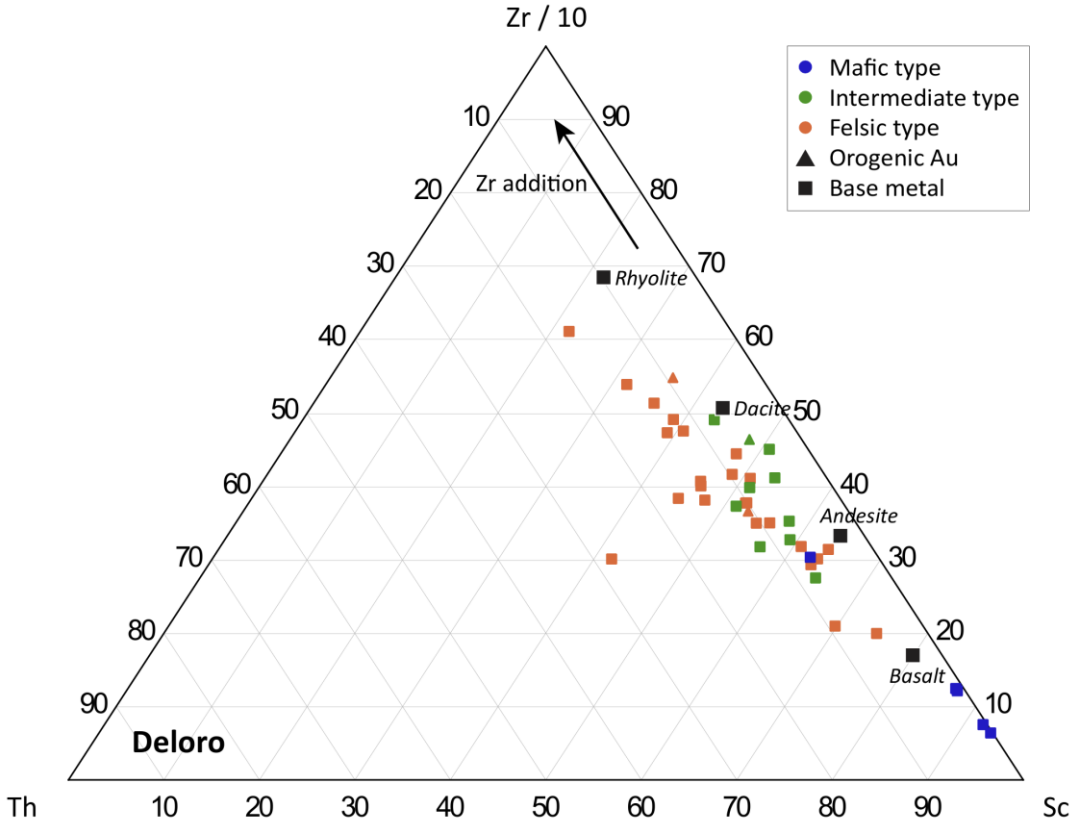

Epidote
Carbonate
Dolomite
Ankerite
Chlorite
Pyrite
Least altered Andesite - Basalt
Least altered Dacite
Least altered Rhyolite
Orogenic Au
Mafic type
Intermediate type
Felsic type
Albite
K-feldspar
Chlorite-Carbonate-Pyrite Index
Alteration Index
0
10
20
30
40
50
60
70
80
90
100

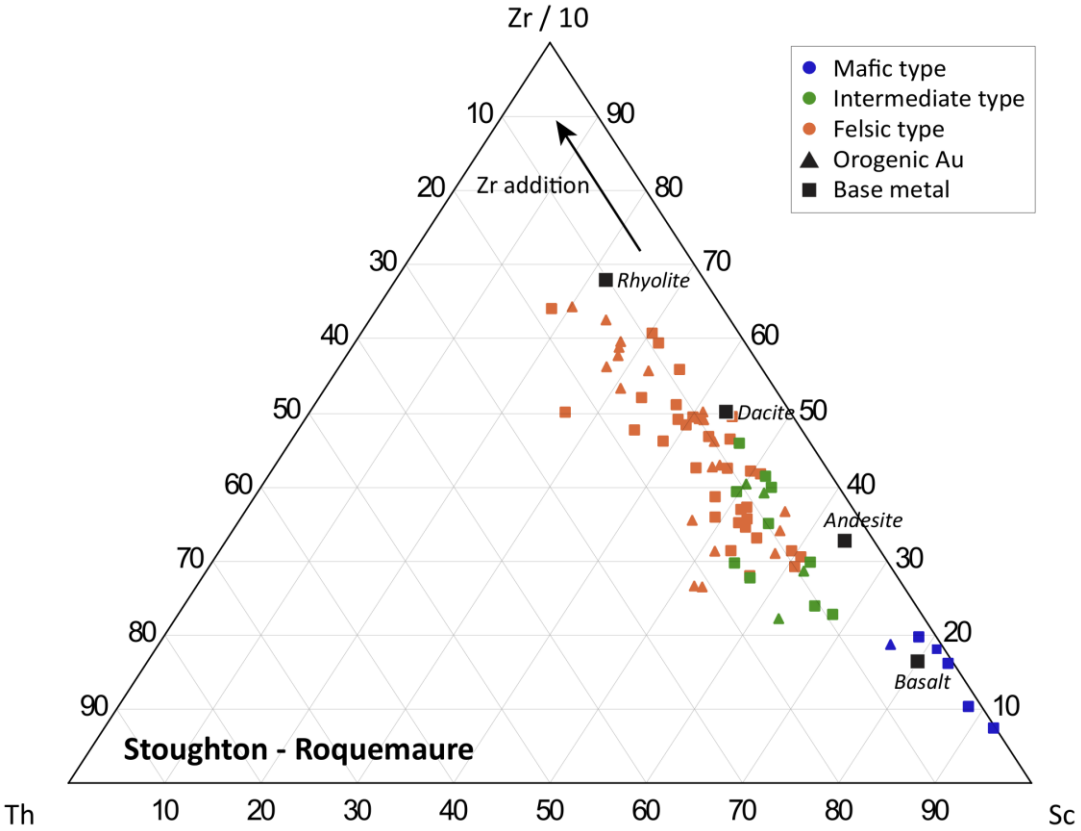
A)

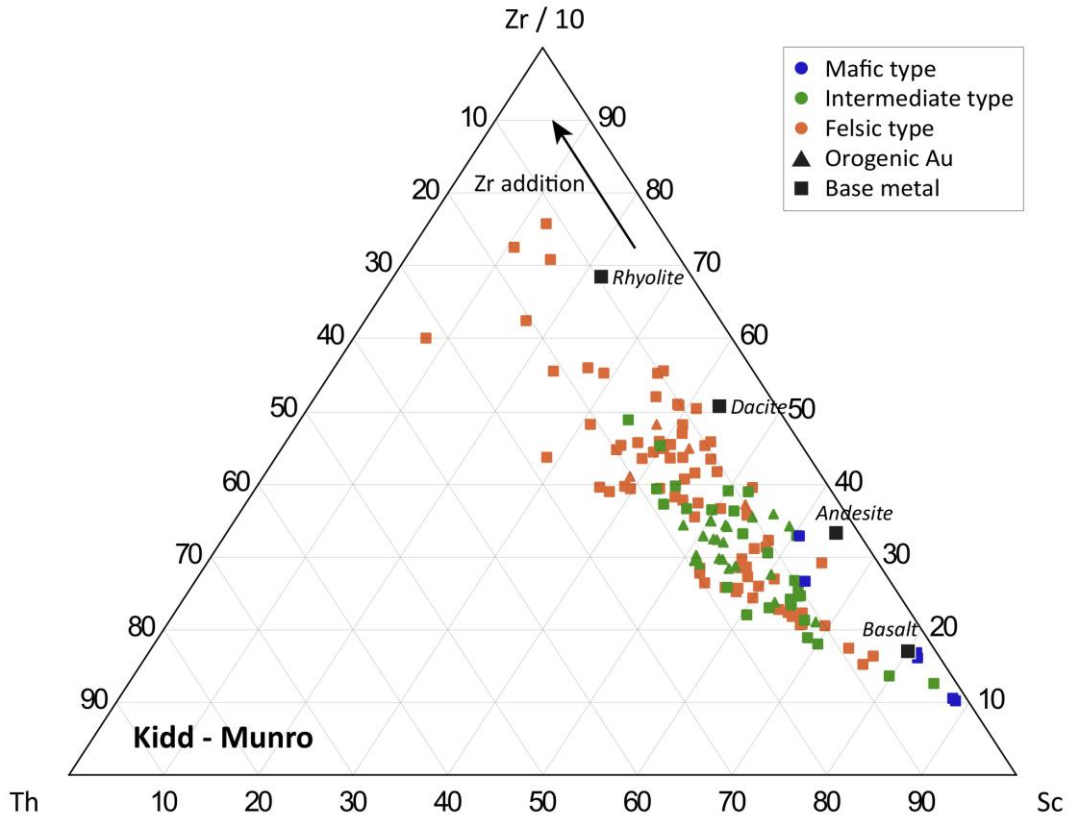

Epidote
Carbonate
Dolomite
Ankerite
Chlorite
Pyrite
Least altered Andesite - Basalt
Least altered Dacite
Least altered Rhyolite
Base metal
Mafic type
Intermediate type
Felsic type
Albite
K-feldspar
Chlorite-Carbonate-Pyrite Index
Alteration Index
0
10
20
30
40
50
60
70
80
90
100

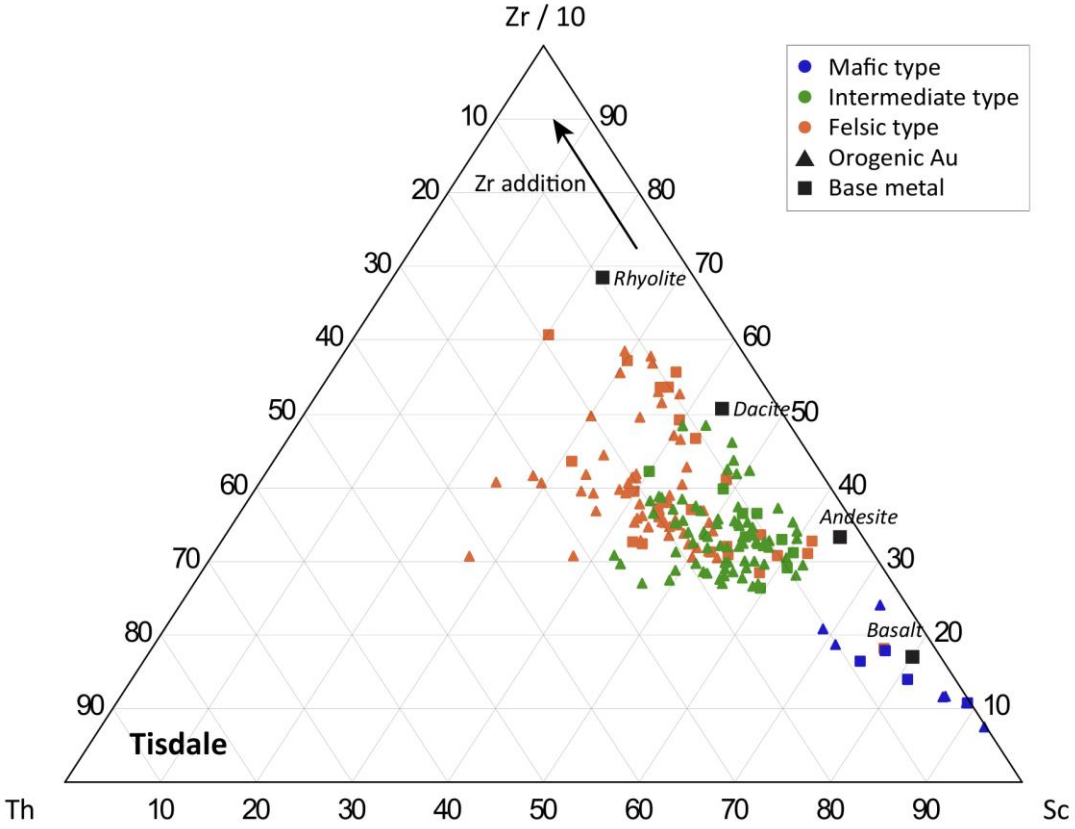
B)

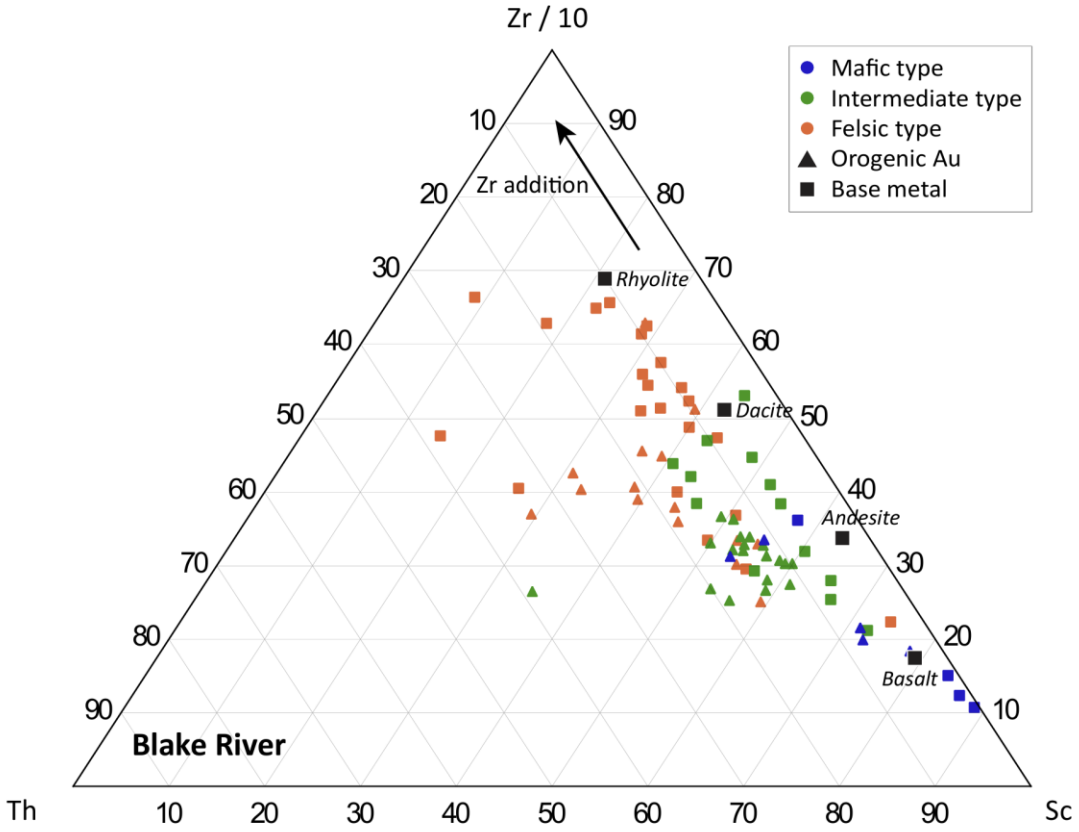
Figure 4.28. Alteration box plot after Large et al. (2001) showing the compositions of western Abitibi shale samples classified according to Ti/Zr. Plot A is for shales from drill holes that were originally targeted for discovery orogenic gold mineralization (triangles). Plot B is for shales from drill holes that were originally targeted for discovery of VMS (squares). The Ishikawa Alteration Index [AI = 100 (K_2O + MgO) / (K_2O + MgO + Na_2O + CaO)] was defined by Ishikawa et al. (1976) to quantify the intensity of sericite and chlorite alteration that occurs in volcanic rocks near Kuroko-type base metal deposits. It records the addition of muscovite and chlorite and the destruction of plagioclase. The Chlorite-Carbonate-Pyrite Index [CCPI = 100 (MgO + FeO) / (MgO + FeO + Na_2O + K_2O)] measures the intensity of chlorite and carbonate alteration. The mineral end members (albite, K-feldspar, chlorite, pyrite, dolomite, ankerite, and epidote) plot along the boundaries of the box. Least altered volcanics plot toward the center of the diagram and hydrothermally altered volcanics plot at varying positions according to the alteration minerals present. The dashed diagonal line joining epidote to K-feldspar effectively separates the field of hydrothermal alteration (upper right) from the field of diagenetic alteration (lower left) in the diagram. A high proportion of the shales plot outside the least altered box for volcanic rocks, with mafic-derived shales showing compositions consistent with significant chlorite and carbonate alteration and felsic- to intermediate-derived shales showing significant muscovite and chlorite alteration.


Zr / 10
Mafic type
Intermediate type
Felsic type
Orogenic Au
Base metal
Zr addition
Rhyolite
Dacite
Andesite
Basalt
Deloro
Th
Sc


Zr / 10
Mafic type
Intermediate type
Felsic type
Orogenic Au
Base metal
Zr addition
Rhyolite
Dacite
Andesite
Basalt
Stoughton - Roquemaure
Th
Sc


Zr / 10
Mafic type
Intermediate type
Felsic type
Orogenic Au
Base metal
Zr addition
Rhyolite
Dacite
Andesite
Basalt
Kidd - Munro
Th
Sc


Zr / 10
Mafic type
Intermediate type
Felsic type
Orogenic Au
Base metal
Zr addition
Rhyolite
Dacite
Andesite
Basalt
Tisdale
Th
Sc


Zr / 10
Mafic type
Intermediate type
Felsic type
Orogenic Au
Base metal
Zr addition
Rhyolite
Dacite
Andesite
Basalt
Blake River
Th
Sc

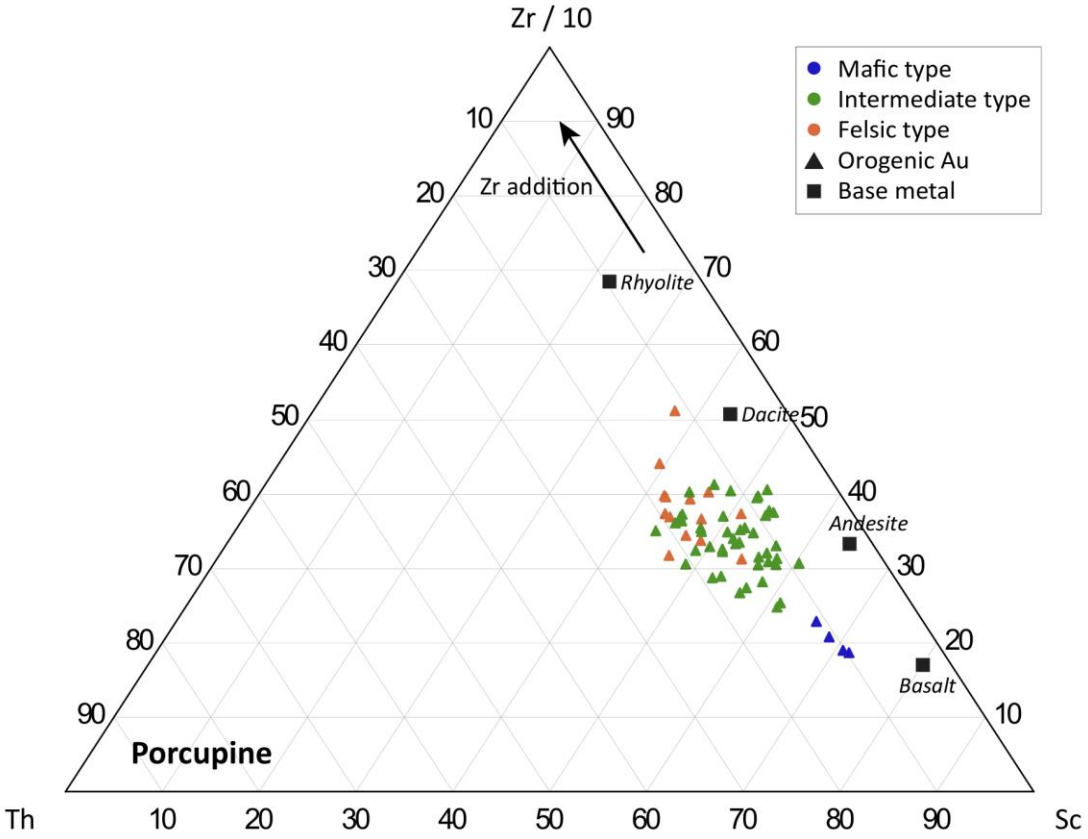
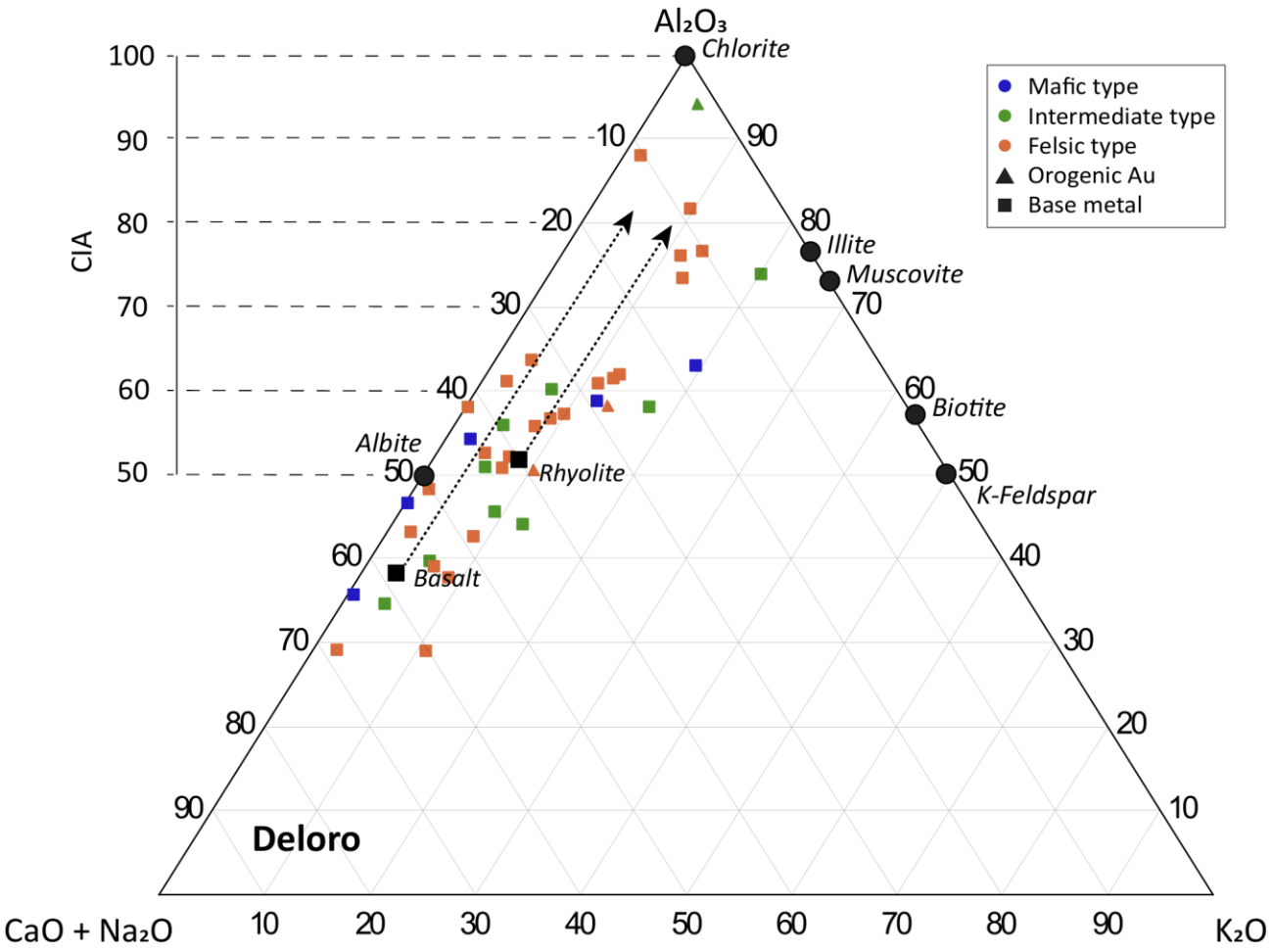
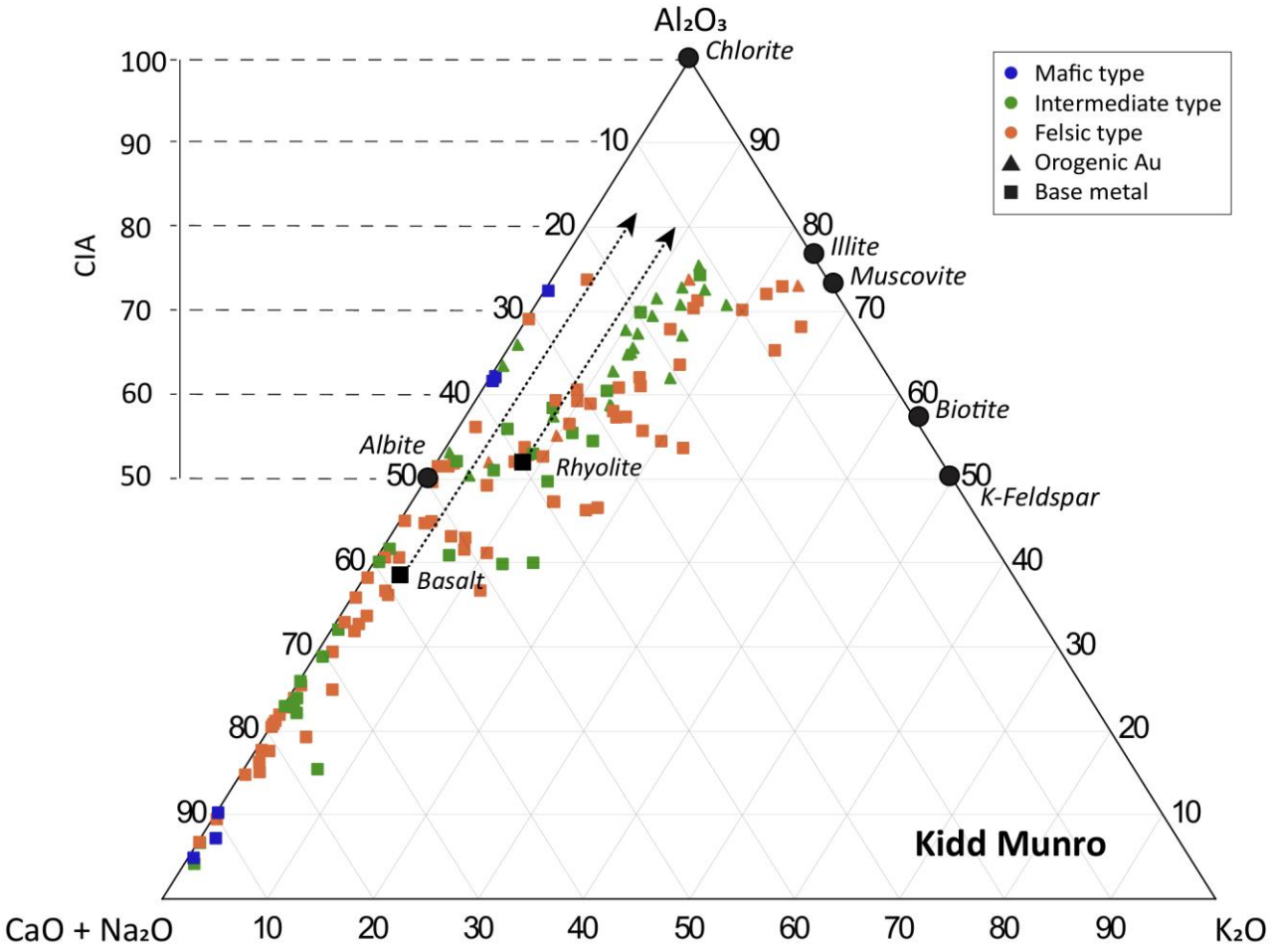
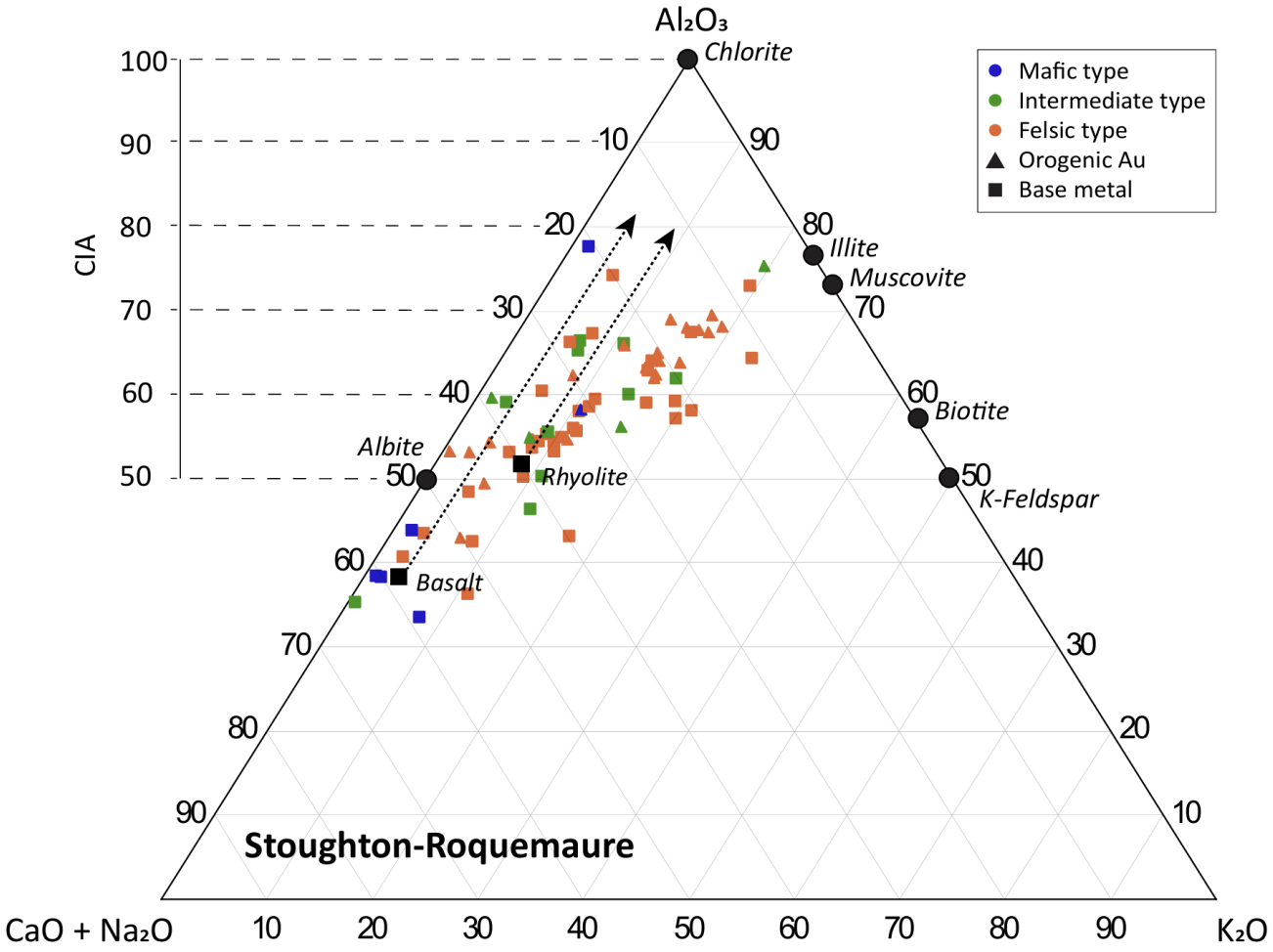
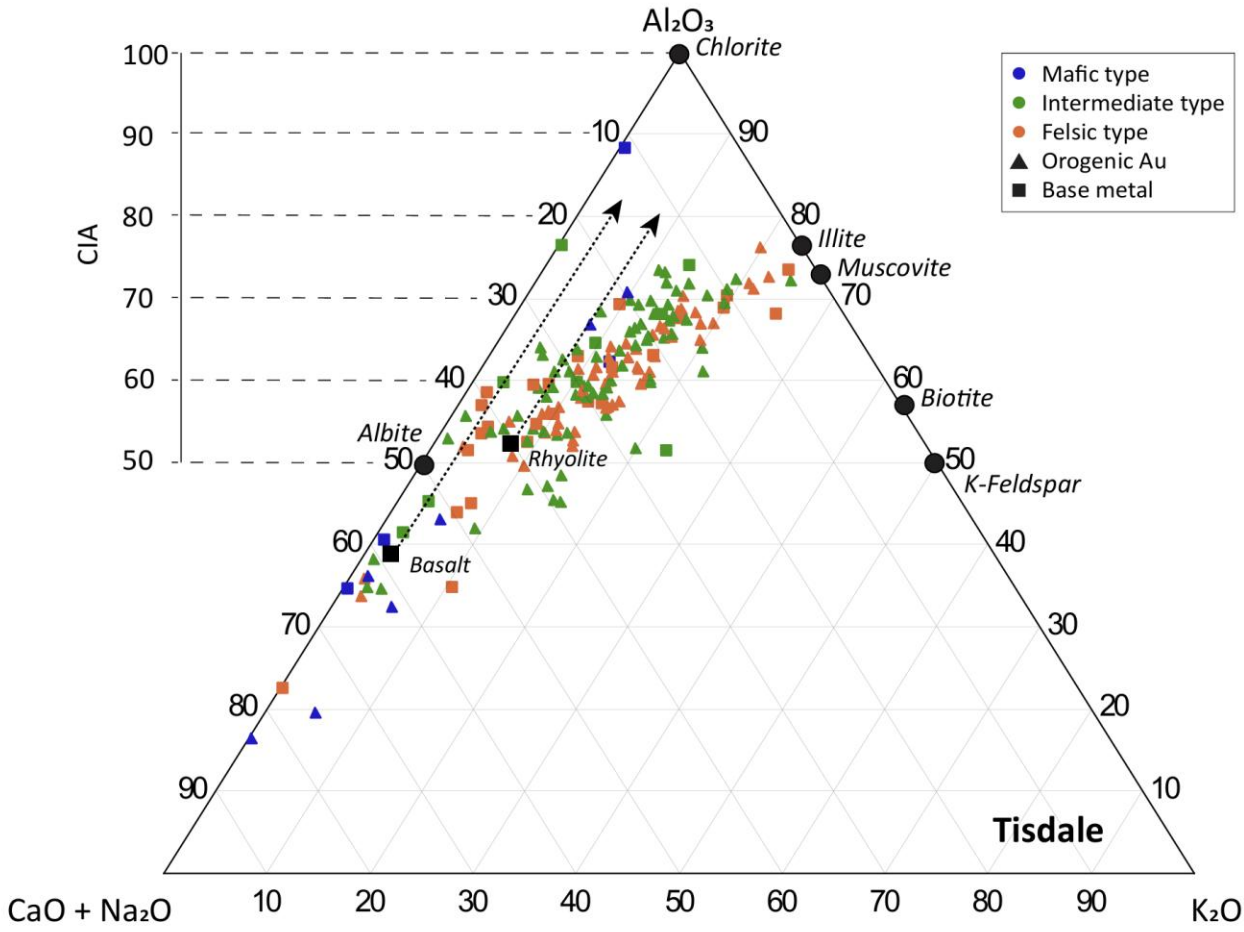

Zr / 10
Mafic type
Intermediate type
Felsic type
Orogenic Au
Base metal
Zr addition
Rhyolite
Dacite
Andesite
Basalt
Porcupine
Th
Sc

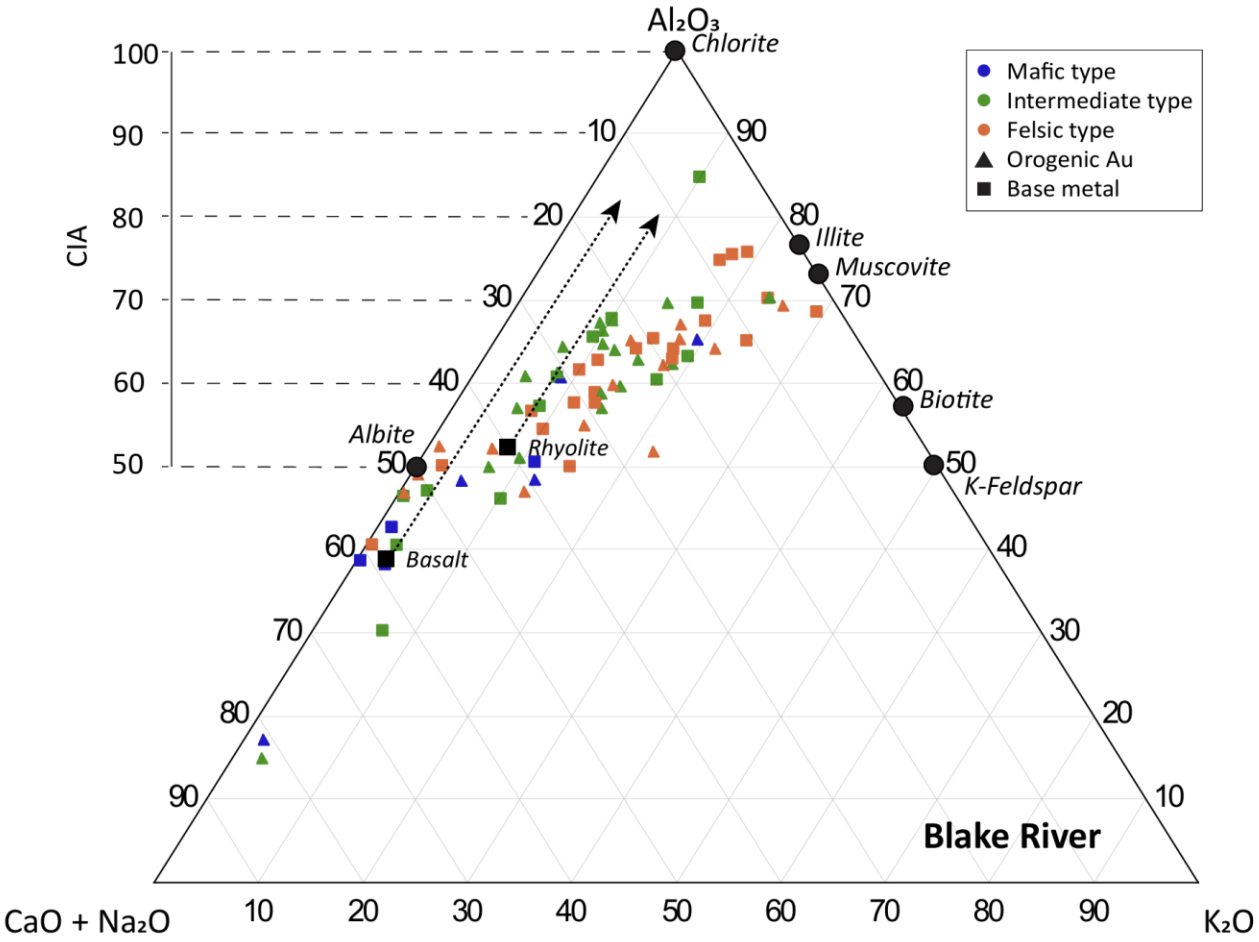
Figure 4.29. Th-Zr/10-Sc ternary diagrams after Bhatia and Crook (1986) of western Abitibi shale samples in different volcanic assemblages. See Figure 4.16 for explanation. Shales have slightly different compositions in each assemblage reflecting different volcanic source rocks and varying degrees of sediment sorting and recycling (see the text for discussion).


Al₂O₃
Chlorite
Illite
Muscovite
Biotite
K-Feldspar
Albite
Rhyolite
Basalt
Deloro
CIA
CaO + Na₂O
K₂O
Mafic type
Intermediate type
Felsic type
Orogenic Au
Base metal


Al₂O₃
Chlorite
Illite
Muscovite
Biotite
K-Feldspar
Albite
Rhyolite
Basalt
CIA
CaO + Na₂O
K₂O
Mafic type
Intermediate type
Felsic type
Orogenic Au
Base metal
Kidd Munro


Al₂O₃
Chlorite
Illite
Muscovite
Biotite
K-Feldspar
Albite
Rhyolite
Basalt
CIA
CaO + Na₂O
K₂O
Stoughton-Roquemaure
Mafic type
Intermediate type
Felsic type
Orogenic Au
Base metal


Al₂O₃
Chlorite
Illite
Muscovite
Biotite
K-Feldspar
Albite
Rhyolite
Basalt
CIA
CaO + Na₂O
K₂O
Tisdale
Mafic type
Intermediate type
Felsic type
Orogenic Au
Base metal


Al₂O₃
Chlorite
CIA
CaO + Na₂O
K₂O
Albite
Rhyolite
Basalt
Illite
Muscovite
Biotite
K-Feldspar
Mafic type
Intermediate type
Felsic type
Orogenic Au
Base metal
Blake River

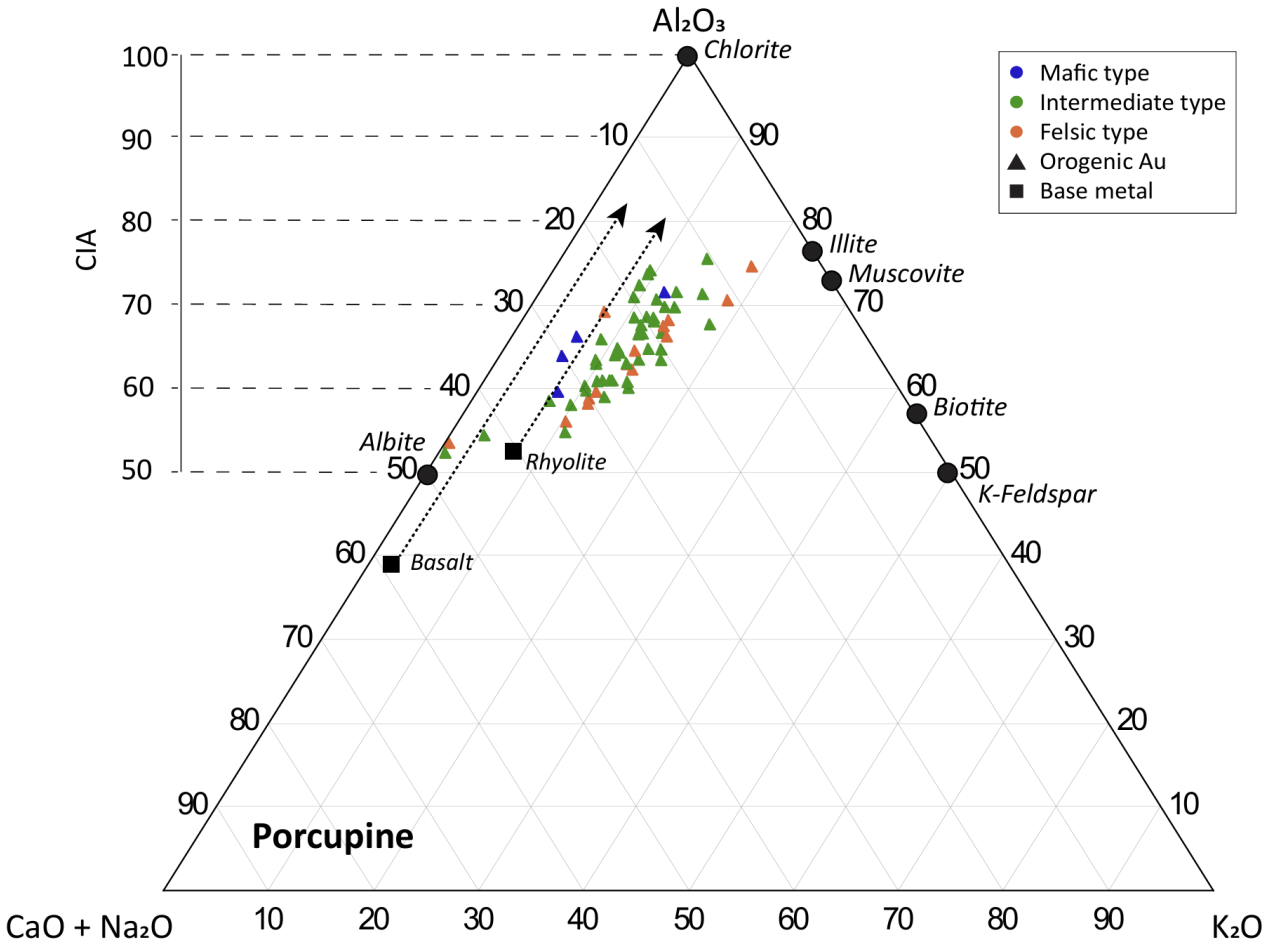
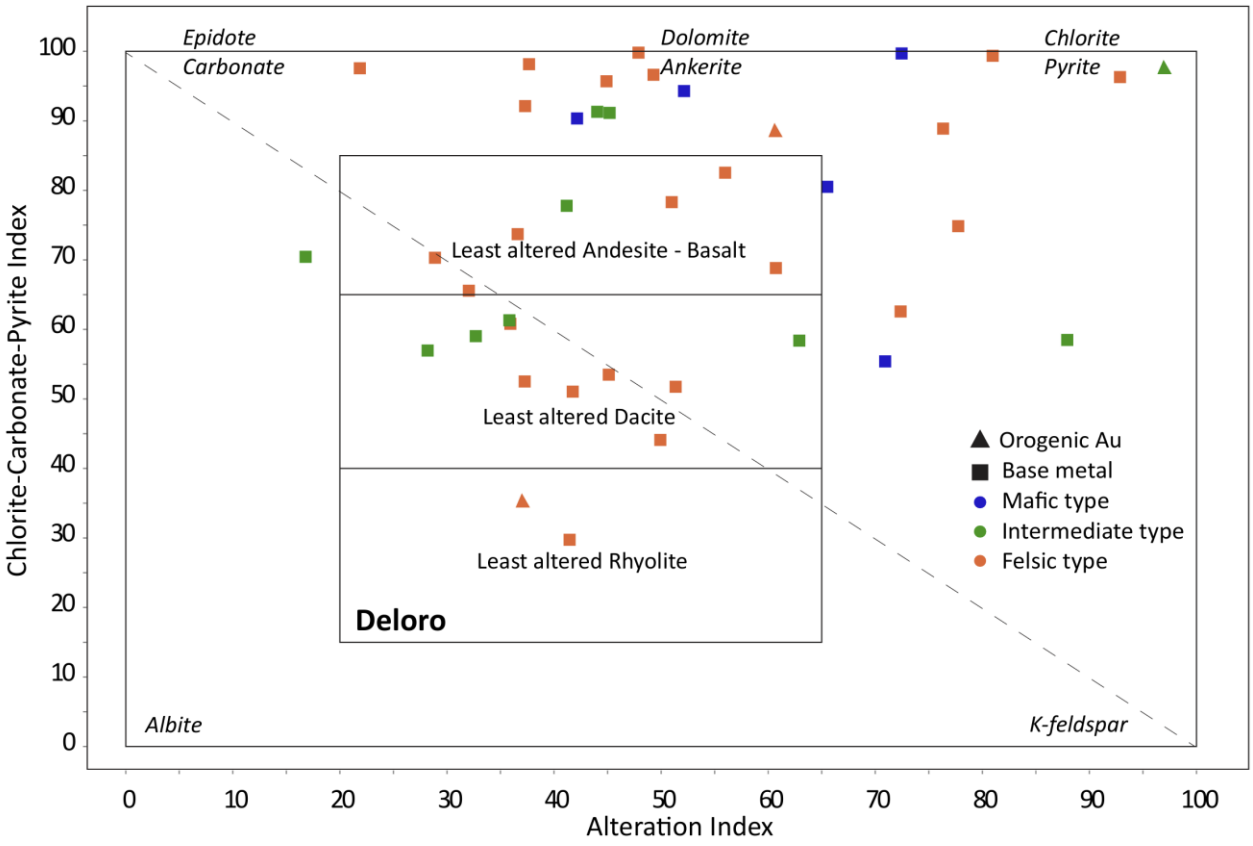
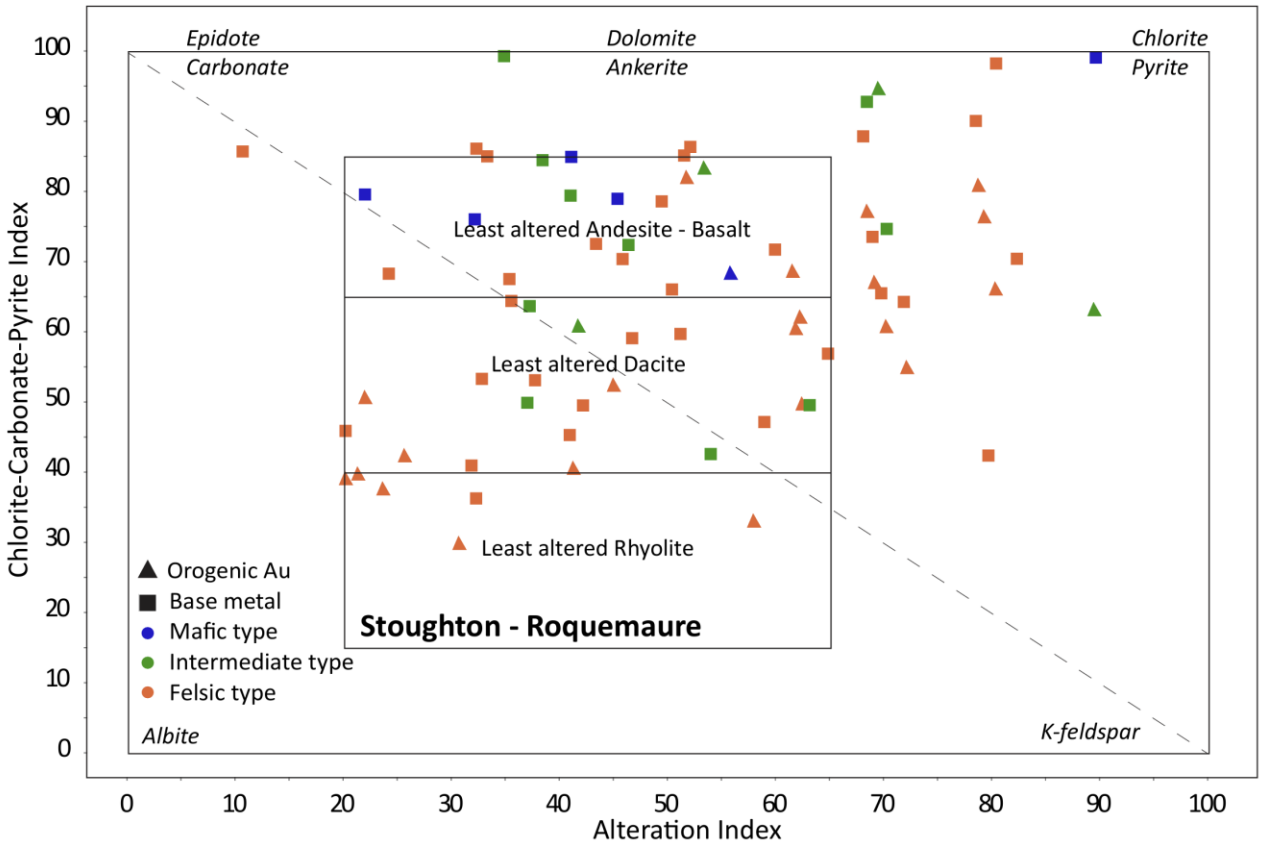
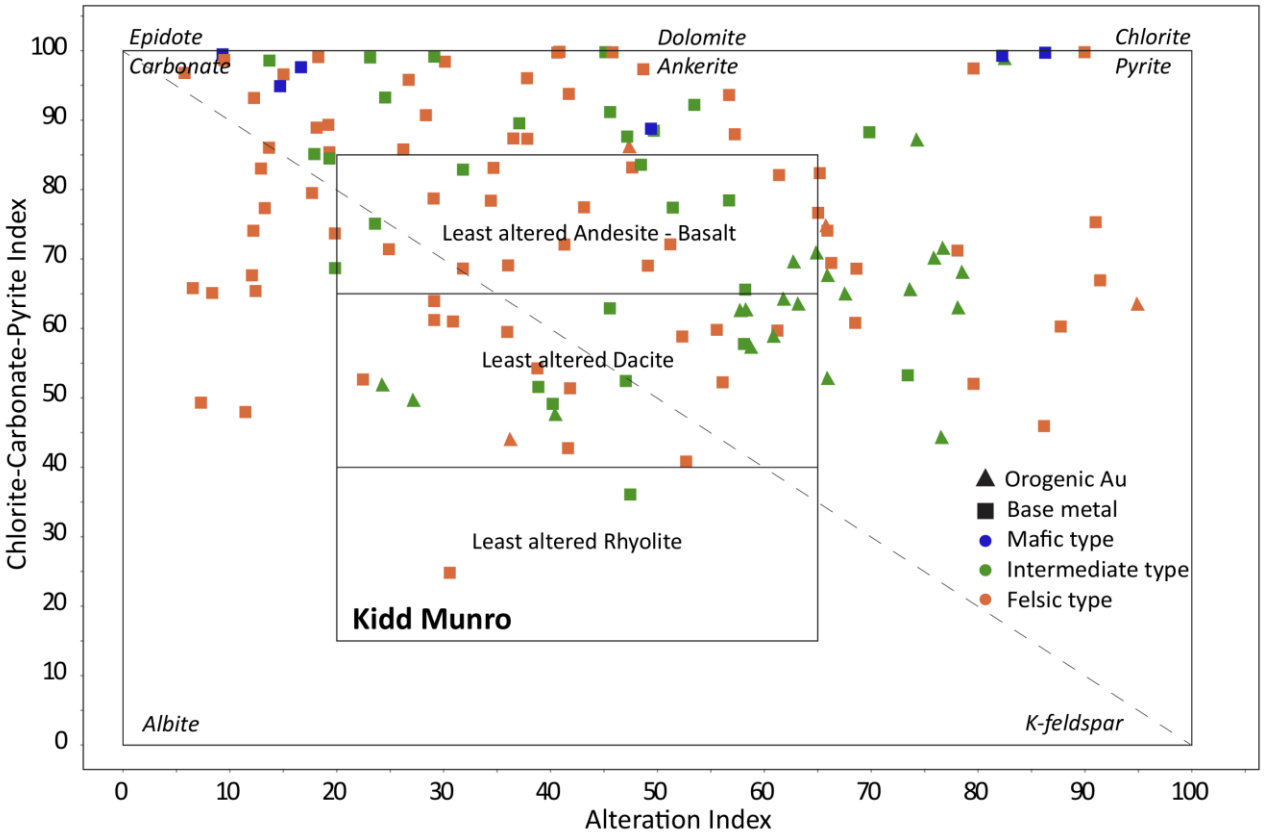
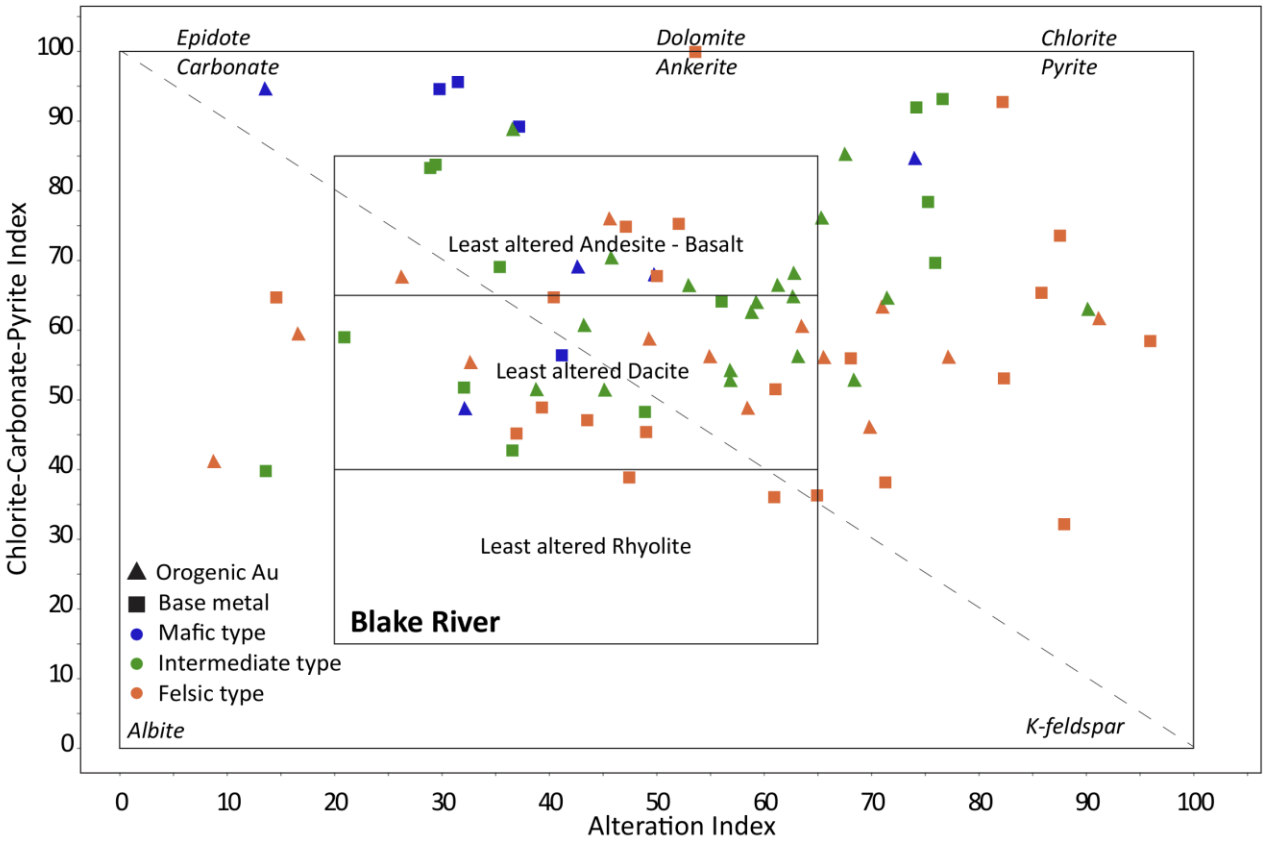


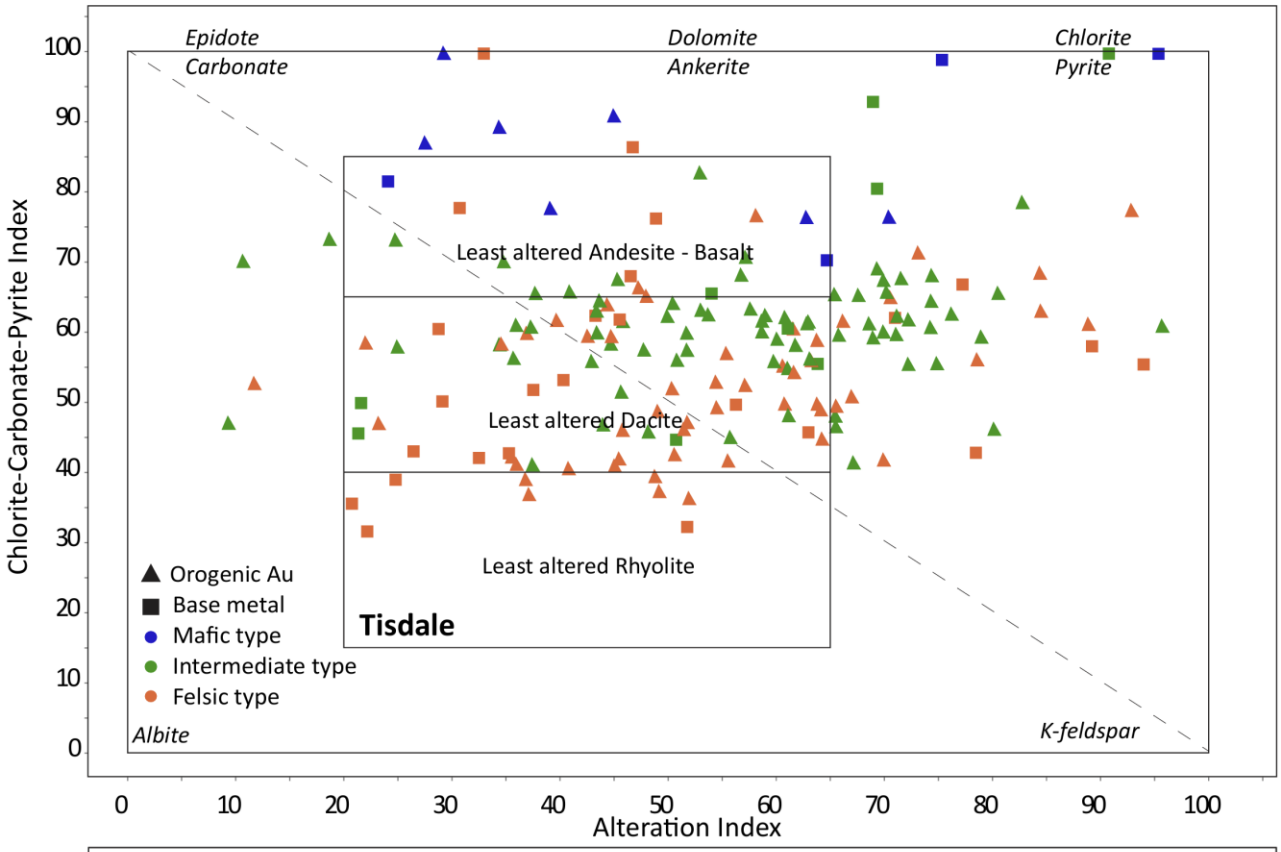
Figure 4.30. A-CN-K diagrams after Nesbitt and Young (1982) of western Abitibi shale samples classified according to Ti/Zr (felsic-type, intermediate-type, and mafic-type) classified by assemblage. Triangles are shales from drill holes that were originally targeted for discovery orogenic gold mineralization. Squares are shales from drill holes that were originally targeted for discovery of VMS. Volcanic rock compositions are shown by black boxes. The composition of average Archean rhyolite values from Gaboury and Pearson (2008), and fresh basalt from (Nesbitt and Young, 1984; McLennan, 1993; McLennan et al., 1993; Fedo et al., 1995, Babechuk and Fedo, 2023). Shale samples from Deloro and Stoughton-Roquemaure have intermediate CIA values. Shales samples from the Kidd Munro assemblage are dominantly mafic in composition, derived at least in part from tholeiitic basalts, and komatiites. Shale samples from the Blake River and Tisdale assemblages are more bimodal in character, derived from tholeiitic basalts and felsic volcanics with moderate to high CIA values. Shales from the Porcupine assemblage are more mature and weathered contributing to their higher CIA value.


Epidote
Carbonate
Dolomite
Ankerite
Chlorite
Pyrite
Least altered Andesite - Basalt
Least altered Dacite
Least altered Rhyolite
Deloro
Orogenic Au
Base metal
Mafic type
Intermediate type
Felsic type
Albite
K-feldspar
Chlorite-Carbonate-Pyrite Index
Alteration Index
0
10
20
30
40
50
60
70
80
90
100


Epidote
Carbonate
Dolomite
Ankerite
Chlorite
Pyrite
Least altered Andesite - Basalt
Least altered Dacite
Least altered Rhyolite
Stoughton - Roquemaure
Orogenic Au
Base metal
Mafic type
Intermediate type
Felsic type
Albite
K-feldspar
Chlorite-Carbonate-Pyrite Index
Alteration Index
0
10
20
30
40
50
60
70
80
90
100


Epidote
Carbonate
Dolomite
Ankerite
Chlorite
Pyrite
Least altered Andesite - Basalt
Least altered Dacite
Least altered Rhyolite
Kidd Munro
Orogenic Au
Base metal
Mafic type
Intermediate type
Felsic type
Albite
K-feldspar
Chlorite-Carbonate-Pyrite Index
Alteration Index


Epidote
Carbonate
Dolomite
Ankerite
Chlorite
Pyrite
Least altered Andesite - Basalt
Least altered Dacite
Least altered Rhyolite
Blake River
Orogenic Au
Base metal
Mafic type
Intermediate type
Felsic type
Albite
K-feldspar
Chlorite-Carbonate-Pyrite Index
Alteration Index


Epidote
Carbonate
Dolomite
Ankerite
Chlorite
Pyrite
Least altered Andesite - Basalt
Least altered Dacite
Least altered Rhyolite
Tisdale
Orogenic Au
Base metal
Mafic type
Intermediate type
Felsic type
Albite
K-feldspar
Chlorite-Carbonate-Pyrite Index
Alteration Index
0
10
20
30
40
50
60
70
80
90
100

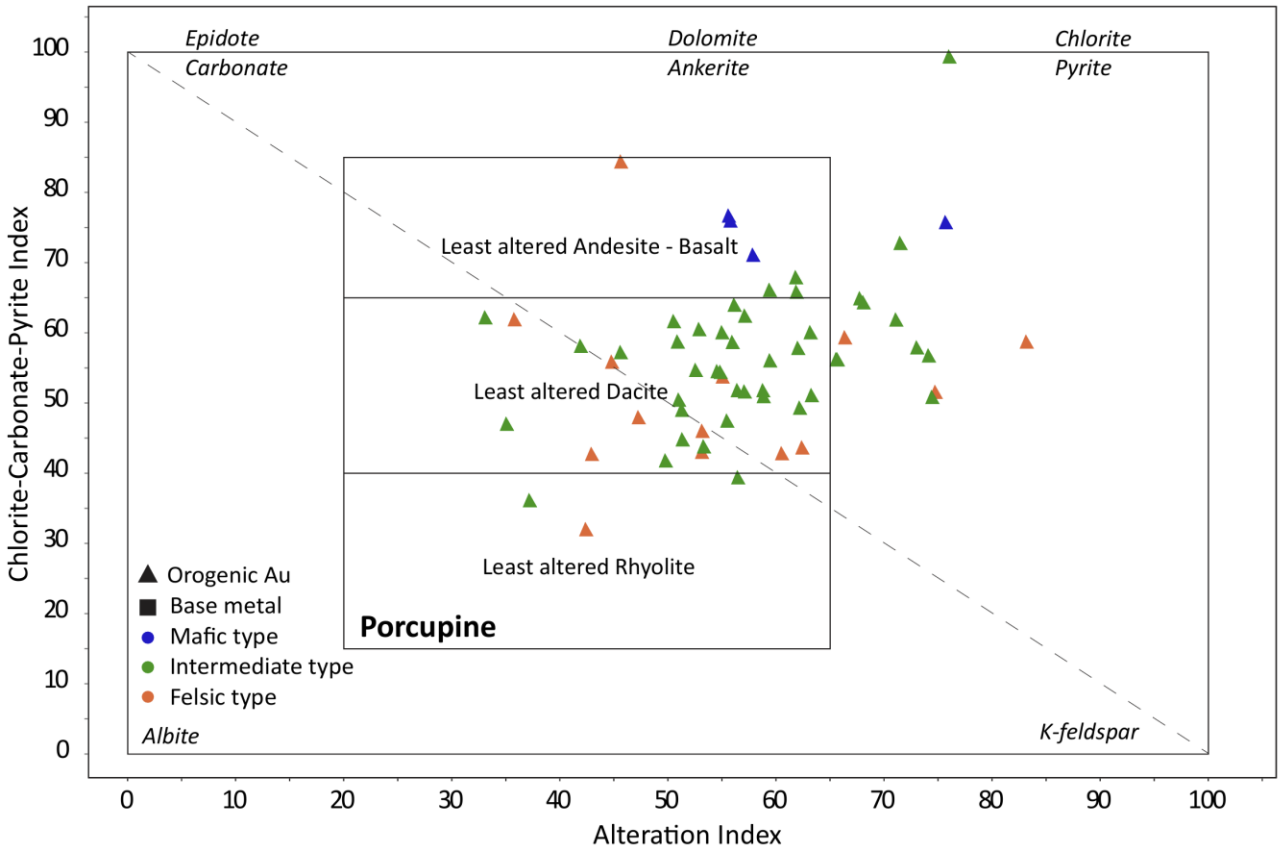

Epidote
Carbonate
Dolomite
Ankerite
Chlorite
Pyrite
Least altered Andesite - Basalt
Least altered Dacite
Least altered Rhyolite
Porcupine
Orogenic Au
Base metal
Mafic type
Intermediate type
Felsic type
Albite
K-feldspar
Chlorite-Carbonate-Pyrite Index
Alteration Index
0
10
20
30
40
50
60
70
80
90
100

Figure 4.31. Alteration box plot after Large et al. (2001) showing the compositions of western Abitibi shale samples classified according to Ti/Zr. Triangles are shales from drill holes that were originally targeted for discovery orogenic gold mineralization. Squares are shales from drill holes that were originally targeted for discovery of VMS. See Figure 4.28 for explanation. Shales from the Deloro assemblage trend toward the upper part of the diagram. Samples from Stoughton-Roquemaure have a wide range of CCPI values trending towards the upper right corner of the diagram. Shales from the Kidd-Munro assemblage reflect a mafic to ultramafic provenance with chlorite, pyrite, and intense carbonate alteration with high CCPI values. Shales from the Blake River assemblage trend towards chlorite and pyrite, typical of a VMS-proximal environment. Shales from the Tisdale assemblage display a broad range of AI values, many remain within the last-altered box. Shales from the Porcupine form a smaller cluster within the least altered part of the box plot.

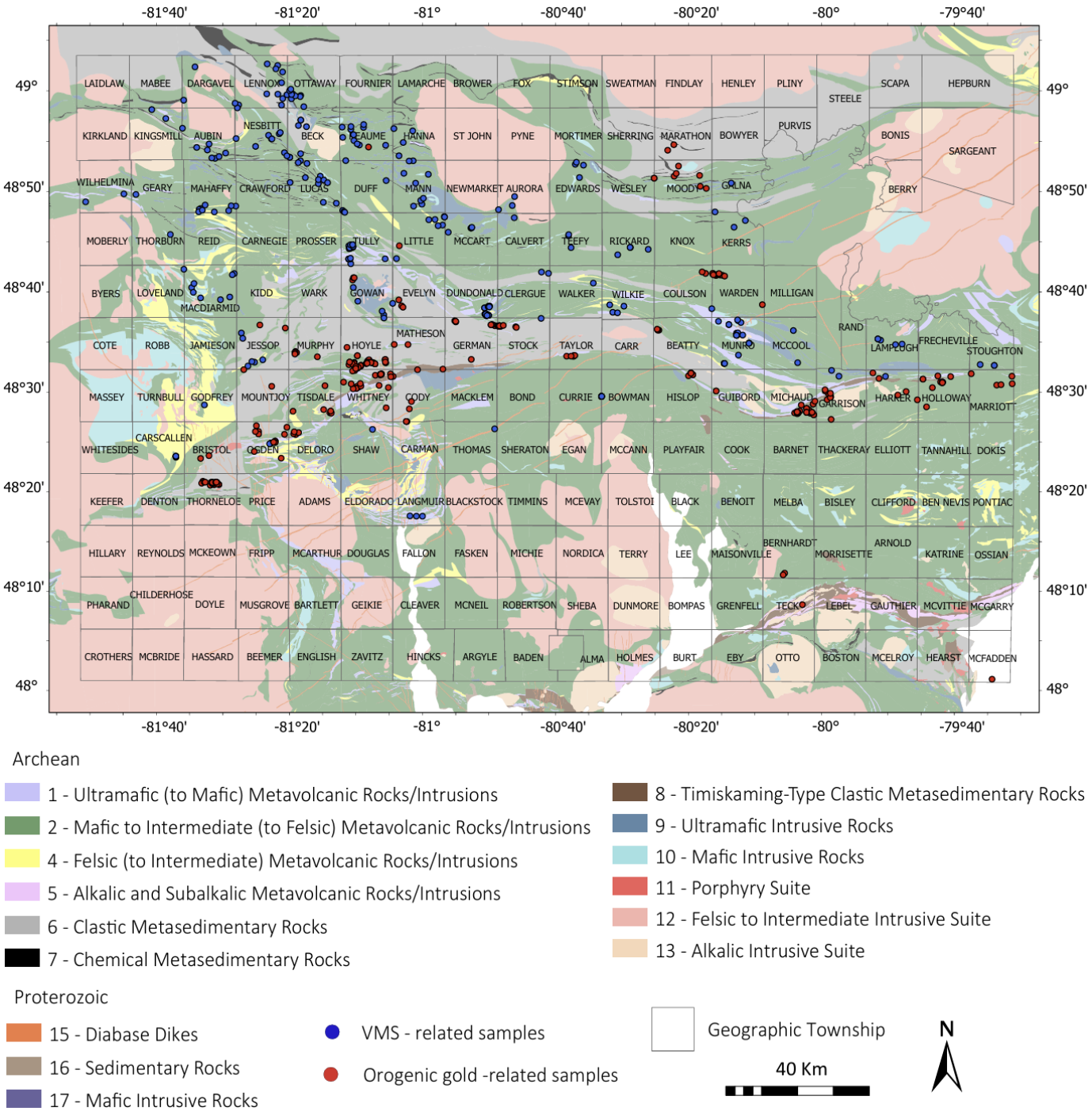


Figure 4.32. Map distribution of shale samples in the Western AGB from drill holes that were originally targeted for discovery of VMS or later orogenic gold mineralization. A high proportion of the shales from drill holes targeted for orogenic gold were intermediate-type shales in the Porcupine Assemblage along the DPFZ. A high proportion of the shales from drill holes targeted for VMS were either felsic-type or mafic-type and occur in the north of the study area. Lithology map from Jørgensen and Gibson (2024).

Table 4.1. Trace elements concentrations in the primitive mantle, continental crust and post-Archean shales.

Element (ppm)	Primitive Mantle (McDonough and Sun, 1995)	Avg. Continental Crust (Rudncick and Gao, 2003)	Avg. Shale (PAAS) (Taylor & McLennan, 1985)
Cs	0.021	4.9	5.0
Au (ppb)	1.0	1.5	3.0
Rb	0.6	84.0	140
Ba	6.6	628	580
Th	0.078	10.5	11.0
U	0.020	2.7	3.2
La	0.648	31.0	40.0
Zr	10.6	193	200
Zn	55	67	80

Table 4.2. Summary statistics of major oxide concentrations for felsic-type shales including the mean, median, 25th, 75th, and 90th percentile.

Felsic Type - Element (wt%)	Mean	Median	25 percentile	75 percentile	90 percentile
SiO_2	58.6	61.6	53.1	66.5	70.9
Al_2O_3	11.6	12.7	8.79	14.4	15.8
Fe_2O_3	7.95	5.97	3.98	9.85	14.9
MgO	1.64	1.17	0.79	1.71	2.83
CaO	2.34	1.35	0.56	2.42	5.06
Na_2O	2.12	1.70	0.73	3.10	4.71
K_2O	2.03	2.14	0.83	3.00	3.52
TiO_2	0.37	0.38	0.26	0.46	0.54
P_2O_5	0.10	0.10	0.06	0.13	0.15
MnO	0.06	0.03	0.02	0.06	0.10
LOI	12.1	9.47	6.28	14.9	24.9
Total S	3.88	2.94	1.36	5.14	7.57
CO_2	1.66	0.87	0.09	1.98	3.74

Table 4.3. Summary statistics of major oxide concentrations for intermediate-type shales including the mean, median, 25th, 75th, and 90th percentile.

Intermediate type - Element (wt%)	Mean	Median	25 percentile	75 percentile	90 percentile
SiO_2	56.9	58.7	54.9	61.5	64.6
Al_2O_3	15.3	16.5	13.2	18.2	19.6
Fe_2O_3	7.77	6.51	5.36	8.22	13.9
MgO	2.84	2.40	1.54	3.37	4.45
CaO	2.37	1.47	0.75	3.02	5.02
Na_2O	2.33	2.14	1.31	3.05	4.26
K_2O	2.49	2.64	1.63	3.34	4.00
TiO_2	0.62	0.65	0.52	0.74	0.83
P_2O_5	0.13	0.13	0.10	0.17	0.20
MnO	0.07	0.06	0.04	0.08	0.12
LOI	8.27	6.06	4.25	9.02	17.5
Total S	2.01	0.67	0.13	2.95	6.04
CO_2	2.16	1.02	0.16	2.98	5.00

Table 4.4. Summary statistics of major oxide concentrations for mafic-type shales including the mean, median, 25th, 75th, and 90th percentile.

Mafic type – Element (wt%)	Mean	Median	25 percentile	75 percentile	90 percentile
SiO_2	47.4	50.1	43.8	53.5	57.3
Al_2O_3	12.6	13.6	10.1	16.5	17.7
Fe_2O_3	12.4	11.3	8.98	15.0	19.2
MgO	6.04	4.59	2.97	6.63	13.6
CaO	6.60	5.14	2.01	10.4	15.8
Na_2O	1.52	1.10	0.22	2.58	3.36
K_2O	1.25	0.55	0.12	2.18	3.11
TiO_2	0.77	0.82	0.51	0.94	1.06
P_2O_5	0.10	0.09	0.06	0.12	0.17
MnO	0.23	0.17	0.11	0.28	0.54
LOI	9.24	7.33	4.69	14.0	16.7
Total S	2.03	0.90	0.18	2.57	6.06
CO_2	5.05	1.79	0.49	7.92	16.8

Table 4.5. Summary statistics of major oxide concentrations for shales from drill holes originally targeted for orogenic gold mineralization including the mean, median, 25th, 75th, and 90th percentile.

Orogenic Au - Element (wt%)	Mean	Median	25 percentile	75 percentile	90 percentile
SiO_2	58.8	59.6	56.3	62.8	66.3
Al_2O_3	15.5	15.9	13.6	17.9	19.3
Fe_2O_3	6.63	6.17	4.60	7.52	9.88
MgO	2.31	1.88	1.13	3.08	4.02
CaO	1.88	1.31	0.68	2.16	3.54
Na_2O	2.36	2.15	1.29	3.01	4.42
K_2O	2.69	2.93	2.07	3.32	4.00
TiO_2	0.597	0.587	0.460	0.730	0.827
P_2O_5	0.13	0.13	0.11	0.16	0.19
MnO	0.059	0.047	0.027	0.066	0.102
LOI	8.10	6.67	4.37	9.85	14.6
Total S	1.99	1.18	0.17	2.95	5.45
CO_2	1.90	1.01	0.19	2.48	4.41

Table 4.6. Summary statistics of major oxide concentrations for shales from drill holes originally targeted for VMS including the mean, median, 25th, 75th, and 90th percentile.

Base Metal - Element (wt%)	Mean	Median	25 percentile	75 percentile	90 percentile
SiO_2	55.2	58.4	45.5	65.3	70.9
Al_2O_3	10.7	11.0	7.63	14.1	16.0
Fe_2O_3	9.90	8.25	5.04	12.6	18.1
MgO	2.63	1.52	0.87	2.62	5.91
CaO	3.52	1.87	0.88	4.23	9.01
Na_2O	1.96	1.57	0.40	3.05	4.26
K_2O	1.59	1.42	0.33	2.48	3.32
TiO_2	0.404	0.364	0.253	0.506	0.672
P_2O_5	0.09	0.08	0.06	0.12	0.15
MnO	0.098	0.053	0.024	0.102	0.205
LOI	12.6	9.33	5.87	16.9	27.7
Total S	4.01	3.00	0.99	5.78	8.97
CO_2	2.35	0.96	0.09	2.84	7.37

Table 4.7. Average volcanic rock compositions from Archean-age rocks in the Abitibi Greenstone Belt and south-east Superior Craton based on data from Gaboury and Pearson, 2008, Mole et al., 2021, Fassbender et al. 2023, 2024, and data from the Western Abitibi Greenstone Belt (Hannington et al., 2012).

Database	Rocktype / classification	SiO_2 (%)	Al_2O_3 (%)	MnO (%)	Fe_2O_3 (%)	MgO (%)	CaO (%)	Na_2O (%)	K_2O (%)	TiO_2 (%)	P_2O_5 (%)	Sc (ppm)	Th (ppm)	Zr (ppm)	Ti (ppm)	Ti/Zr
Gaboury and Pearson, 2008	Rhyolite	71.7	12.6	0.1	4.1	1.4	2.4	3.1	1.8	0.4	0.1	7.30	3.8	229	2290	10.0
Mole et al., 2021	Rhyolite	72.8	13.2	0.1	4.6	1.6	2.3	3.1	1.8	0.4	0.1	10.0	4.2	229	2370	10.4
Fassbender et al., 2023	Felsic	72.7	12.4	-	-	-	-	-	2.0	0.4	-	-	4.3	226	2280	10.1
Western Abitibi Greenstone Belt	Felsic	58.6	11.6	0.1	8.0	1.6	2.3	2.1	2.0	0.4	0.1	13.1	4.9	128	2230	17.4
Mole et al., 2021	Dacite	66.5	14.8	0.1	6.5	2.4	3.8	3.6	1.4	0.7	0.2	15.0	2.9	179	3970	22.2
Western Abitibi Greenstone Belt	Intermediate	57.0	15.3	0.1	7.8	2.8	2.4	2.3	2.5	0.6	0.1	18.5	4.8	115	3720	32.4
Mole et al., 2021	Andesite	58.8	15.9	0.2	9.1	4.3	6.4	3.4	0.9	0.9	0.2	24.3	1.8	125	5620	45.0
Mole et al., 2021	Basalt	53.4	15.2	0.2	12	5.8	8.4	2.9	0.5	1.1	0.2	38.6	1.0	89.4	6800	76.0
Fassbender et al., 2024	Mafic	51.5	14.9	-	-	-	-	2.9	0.6	1.1	-	-	1.0	91.6	6660	72.7
Western Abitibi Greenstone Belt	Mafic	47.3	12.6	0.2	12	6.0	6.6	1.5	1.3	0.8	0.1	31.7	1.9	67.9	4640	68.3

The data were divided into rock types based on the chosen classification scheme in each paper and this study.

Table 4.8. Average concentrations of selected redox-sensitive elements in WAGB shales (this study, N = 564) and global shale composites from the literature.

	Average Conc. in Abitibi Archean samples (this study)	Average conc. from CMIBS database (Archean & Neoarchean)	Average conc. from CMIBS database (Phanerozoic)	Average PAAS (Taylor and McLennan, 1985)	Explanation
Ni	158 ppm	140 ppm	133 ppm	55.0 ppm	More juvenile mafic source rocks in the AGB
Cr	140 ppm	135 ppm	125 ppm	110 ppm	More juvenile mafic and ultramafic sources in the AGB
V	100 ppm	182 ppm	302 ppm	150 ppm	More reduced conditions in the AGB
Mo	5.80 ppm	132 ppm	68.0 ppm	1.00 ppm	More reduced conditions in the AGB
U	1.37 ppm	N/A	N/A	3.10 ppm	N/A
TOC	4.63 wt %	5.32 wt %	N/A	N/A	N/A

Data are from the Discover Abitibi database, and the Global Geochemical Database for Critical Metals in Black Shales (CMIBS, Granitto et al., 2017). Note that the entire WAGB database is also contained in CMIBS.

Table 4.9. Lithostratigraphic assemblages of the Western AGB their associated ages, the compositions of the dominant rock type, shale lithotypes, and any associated mineralization (summarized from Thurston et al., 2008; Monecke et al., 2017)

Assemblage	Dominant rock type	Dominant Shale Lithotype	Associated Mineralization
Deloro (2734 – 2724 Ma)	Intermediate to felsic metavolcanics and intrusions (tholeiitic and felsic calc-alkaline volcanics)	Mixed felsic and intermediate-type samples with minor mafic-type	VMS deposits associated with major volcanic hiatuses
Stoughton-Roquemaure (2723 – 2720 Ma)	Mafic (basalt, komatiites) and local felsic volcanics, tholeiitic to calc-alkaline	Mixed, majority felsic-type	VMS deposits associated with mafic-type samples
Kidd-Munro (2719 – 2711 Ma)	Mafic-dominated; komatiites and minor felsic volcanics, tholeiitic to calc-alkaline	Mixed with some important ultramafic and felsic-type outliers	VMS deposits associated with bimodal mafic- and felsic- samples
Tisdale (2710 – 2704 Ma)	Mafic-dominated (komatiites) and minor intermediate-felsic volcanics, tholeiitic to calc-alkaline	Mixed intermediate to felsic with minor mafic-type.	Orogenic gold mineralization associated with intermediate- and felsic- type shales.
Blake River (2704 – 2695 Ma)	Mafic to intermediate volcanics and volcaniclastics, tholeiitic to calc-alkaline	Mixed mafic-, intermediate- and felsic-type	VMS deposits predominantly associated with felsic-type shales
Porcupine (2700 – 2685 Ma)	Metasedimentary rocks. Local basal felsic pyroclastic rocks overlain by turbiditic sediments.	Mixed felsic and intermediate-type with minor mafic-type	All samples associated with orogenic gold occurring along major structures (DPFZ and CLLFZ)

Shales identified as belonging to different volcanic episodes (i.e., assemblages) broadly reflect the compositions of the dominant volcanic rock types in each episode. The different volcanic events produce compositionally heterogeneous shale because they contain varying proportions of the volcanic rocks.

Table 4.10. Geochemical behaviour of elements in the Th-Zr-Sc discrimination diagram of Bhatia and Crook (1986)

Variable	Interpretation	Behaviour
Th (ppm)	Indicates felsic provenance, enriched in heavy minerals	Incompatible element preferentially incorporated into accessory minerals (e.g., zircon, monazite, xenotime) during magmatic differentiation. Felsic-type samples tend to show elevated Th values.
Zr/10 (ppm scaled)	Indicates felsic provenance zircon abundance, reflects sediment sorting and recycling and felsic input	Incompatible element preferentially incorporated into zircon. Felsic and intermediate-type samples have moderate to high Zr/10 values due to igneous fractionation and sorting.
Sc (ppm)	Indicates mafic provenance; enriched in pyroxenes and amphiboles	Compatible element that preferentially partition into mafic minerals (e.g., pyroxene, amphibole) during crystallization of less evolved (primitive) magma. Mafic-type samples cluster near the Sc corner of the diagram, with low Th and Zr/10 values.

Table 4.11. Summary of geochemical groupings of WAGB black shale database based on Pearsons's correlation matrix with examples from the field.

Example group	Elements	Example of an occurrence from the field	Host rock / inclusions / details / context	Associated mineralization
Muscovite	K_2O, Rb, Sr, Cs, Ba	Sample #4130, Garrison township, Lower Blake River	Dacite hanging wall & footwall; clastic metasediments south of DPFZ	Orogenic Au
Carbonate	CO_2, CO, Sr	Sample #4355, Holloway township, Blake River	Interbedded greywacke – argillite with patchy silica and albite	Orogenic Au
Mafic elements	Sc, V, Cr	Sample #4030, Wilhelmina township, Upper Blake River	Mafic volcanic schist hanging wall and footwall.	Base metals
Felsic element / HFSE	Zr, Hf, Nb, Ta, Ga	Sample #4095, Munro township, Kidd-Munro	Interbedded black chert and felsic sediments, graphitic, slightly conductive, containing pyrite and pyrrhotite	Base metals
Uranium & Thorium	U, Th	Sample # 8590, Beatty township, Porcupine	Dark grey sediments in sandstone sequence	Orogenic Au
Rare Earth Elements	Y, La - Lu	Sample #4049, Mahaffy township, Upper Blake River	Felsic sediments; high REE concentration	Base metals

Carbon & diagenetic sulphide	LOI, C, CO_2, S, Total S	Sample #8511, Dundonald township, Lower Kidd-Munro	Laminated black shale with pyrite nodules; ultramafic hanging wall and footwall.	Base metals
Mafic-associated sulphide	Co, Ni, Se, Mo, Ge, As	Sample #4149, MacDiarmid township, Upper Blake River	Pyrite nodules, mafic volcanic host rocks	Base metals
Polymetallic sulphide	Cu, Pb, Zn, Cd, Hg, Sn, Tl	Sample #8508, Whitney township, Lower Tisdale	Pyrrhotite laminations and nodules, quartz – carbonate veins	Orogenic Au
Orogenic gold	Rb, Sr Cs, Ba	Sample #8586, Beatty township, Lower Kidd-Munro	Quartz veins, with Fe-carbonate staining, porphyry dyke hanging wall and sericite alteration in the footwall.	Orogenic Au

Chapter 5 – Principal Components Analysis

The preceding chapters have shown that the geological history of the AGB and processes related to crustal growth and mineralization are recorded in the interflow sediments of the volcanic assemblages. The shale units harbour information about the source of the sediments as well as their interaction with hydrothermal fluids during burial diagenesis and subsequent deformation that are relevant to ore formation. Importantly, the provenance of the shales is reflected in their geochemistry, even in parts of the greenstone belt where distal source rocks may have been removed. Evidence of the provenance in combination with alteration indicators can be used to guide exploration into potentially prospective subbasins of large volcanic complexes. Graphitic argillite, in particular, is directly related to volcanism and therefore represents an important "sample" of the volcanic complex (Feng & Kerrich, 1990; Mueller et al., 1994; Piercey, 2009; Hannington et al., 2012; Haugaard et al., 2023). In particular, trace element behaviour reflects igneous fractionation processes in the volcanic source rocks of the shales and can be used to discriminate between mafic-derived and felsic-derived sediment.

In the previous chapter, we identified different geochemical signatures of the shales that can be related to their origin and mineral potential. In this chapter, we use Principal Components Analysis (PCA) to quantify many of the relationships already inferred from inspection of the data in Chapter 4. PCA serves as a more robust clustering metric and is amenable to machine learning to address the following questions:

(i) Are the sediments derived from a proximal or distal source?
(ii) What elements are the most important for determining the provenance of the samples?
(iii) Given the high degree of alteration, weathering, and transport, is it possible to effectively constrain the provenance of the shales?

The principal components (PCs) themselves are linear combinations of random variables that describe the maximum variance in the data set. The first principal component captures the greatest amount of variance in the correlation matrix. Each subsequent principal component captures a decreasing portion of the remaining variance as summarized in a scree plot (Figure 5.1). The direction and magnitude of the PC are defined by an eigenvector and its eigenvalue (see Chapter

3). In the analysis presented in this study PC1 through PC4 collectively explain the majority of the variance. Loadings are the numerical weighting of the original variables (e.g., elemental concentrations) on each principal component. The loadings are distinct from the abundance of those elements and instead are a measure of the amount of variance represented by that element. Each sample receives a score corresponding to its projection onto the principal component in PC space, which can be visualized in a biplot of the PCs.

5.1 Principal Components and Element Groups

In the analysis, PC1 is defined by positive loadings of Sm, Hf, Al, Nd, Zr, Nb, and Gd consistent with the heavy mineral component. PC2 is defined by positive loadings of Rb, K, Ba, Tl, and Cs representing a strong muscovite component and incompatible element enrichment in mostly felsic volcanic-derived sediments and especially muscovite-bearing hydrothermal alteration. PC3 is defined by positive loadings of V, Cr, Sc, Mn, and Ti representing a mafic component that includes most of the highly compatible elements in mafic source rocks. PC3 also has high loadings of Ni, C in CO_2, Mg, Co and Ge, which are commonly enriched in the carbonaceous or sulfidic component of the shales. PC4 is defined by positive loadings of C in CO_2, B, W, K, Rb, Mn, Ca, and REEs related to the graphitic and sulfidic components of the sediment and with hydrothermal alteration associated with some types of mineralization. PC4 has a significant accessory mineral component including V-bearing muscovite, B-bearing tourmaline, LREE-bearing monazite and Y-bearing xenotime.

The biplots in Figures 5.2 - 5.6 illustrate the principal component scores for each sample, with the distribution of loadings of each element shown as arrows. The scores for each sample are given in Appendix A6. Figure 5.2 displays the relationship between PC1 (REE-bearing heavy mineral component) and PC2 (muscovite component), which together account for the greatest proportion of variance in the black shale samples. The element groupings discussed in Chapter 4 are represented by dashed circles. The mafic sulphide grouping is characterized by negative scores on both PC1 and PC2. The orogenic gold grouping has negative PC1 scores but clusters near 0.0 for PC2. The REE, muscovite, and felsic element groupings all exhibit positive PC1 scores but are differentiated by their PC2 values. The muscovite grouping has the highest PC2 scores, the REE

grouping has negative PC2 scores, and the felsic element grouping has intermediate scores. Additionally, mafic-type shales are generally associated with negative PC2 scores.

The relationship between PC1 (REE-bearing heavy minerals) and PC3 (mafic volcanic-derived components) is shown in Figure 5.3, revealing a distinct separation of the lithological types along the PC3 axis from felsic (lowest scores) to mafic (highest scores). The muscovite grouping plots near the PC3 origin with positive PC1 values, and the felsic element and REE groupings occupy the lower-right quadrant with positive PC1 and negative PC3 values. The polymetallic sulphide grouping is located in the lower left corner with negative values across both components. The classification of shale lithotypes is further supporting by Figure 5.4 (PC2 versus PC3), where the mafic grouping has positive PC3 and negative PC2 values. Notably, this biplot distinguishes between LREE and HREE, with the latter clustering in the lower left quadrant. This clustering arises because HREE are primarily hosted in xenotime whereas LREE are hosted in a range of other minerals including monazite, bastnäesite, allanite, and zircon. The inverse separation of HREE and the mafic element grouping (V, Sc, Cr) in Figure 5.4 reflects either alteration or sediment sorting, as both groups otherwise signify mafic provenance.

PC4, which represents the carbonate and accessory mineral component of the shales is shown in Figures 5.5 and 5.6. The groupings unique to PC4 include the carbonate grouping (CO_2, CO, Sr), and the carbon and diagenetic sulphide grouping (LOI, C, CO_2, S, Total S). Samples with high HREE have slightly positive PC4 scores, while those with LREE enrichment have negative PC4 scores. In PC3 versus PC4, the mafic grouping is defined by positive PC3 and negative PC4 scores.

5.2 Spatial Distribution of PC Scores

The kriged maps of the PC scores are shown in Figure 5.7 – 5.10. They were generated in ArcGIS, running the Empirical Bayesian Kriging (EBK) tool to generate a continuous surface raster. Each raster represents a spatial gradient with values on a range from blue (negative) to red (positive) corresponding to the PCA scores of the samples. The rasters were clipped to the extent of the sample distribution, removing regions with no data and the four townships surrounding the Kidd

Creek VMS deposit where the data are not in the public domain (crossed out). The four maps produced here account for approximately 61% of the total variance in the dataset, ranking in importance from the REE-bearing heavy mineral component (PC1), the muscovite component (PC2), the mafic-volcanic derived component (PC3), and the carbonaceous and accessory mineral component (PC4). The spatial distribution of the PC scores obtained by kriging show where each component exerts the greatest influence on the shale geochemistry.

5.2.1 Kriged Values of PC1

The highest loadings on PC1 are associated with sediments of the Porcupine basin. Less mature sediments occur in the Kidd-Munro and Stoughton-Roquemaure assemblages in the north of the study area (Figure 5.7). The high loadings on PC1, which accounts for approximately 33% of the total variance in the dataset, are consistent with the behaviour of the heavy minerals (Totten and Hanan, 2007). This includes REE-bearing phosphate minerals such as monazite and xenotime, and in the Porcupine assemblage there may be additional contributions from detrital zircon, tourmaline, rutile, and apatite. However, core logging has not identified significant observable differences between the samples.

Shale samples from the southern part of the study area (e.g., Garrison township in the east to Godfrey township in the west) are anomalous in PC1, with large positive loadings reflecting the maturity of the sediments in the Porcupine basin. Shale samples from the northern part of the study area (e.g., Munro township to Kidd Creek) have low to negative loadings on PC1. In contrast, sample # 7492 from Mountjoy township in the Porcupine assemblage has an anomalously high PC1 value. It consists of interbedded greywacke and its high PC1 score suggests a more mature sediment typical of the Porcupine basin. Sample # 4095 from Munro township consists of interbedded argillite and siltstone with interbedded chert and felsic sediments, graphitic material, and the presence of pyrite and pyrrhotite. Despite having a mafic footwall and hanging wall, the sample is classified as felsic type with a high PC1 score suggesting a local felsic source unrelated to the more regional mafic host rocks. Elements with negative loadings on PC1 include C and S, highlighting depositional environments typical of reduced volcanic basins. These settings are often associated with much finer-grained sediments deposited in small volcanic sub-basins possibly with

strong hydrothermal input (e.g., Table 5.2). Townships with shales having some of the largest negative scores on PC1 include those north of the Pipestone fault, such as Beck, Duff, Warden, and Munro. The shales from Munro township have the strongest hydrothermal signatures in the study (e.g., at the small Potter VMS deposit). Sample # 4117B from Beck township is composed of graphitic, cherty argillite with mafic volcanics forming both the hanging wall and footwall. It has a low PC1 score suggesting that some heavy minerals were concentrated but that the sediment experienced limited weathering and transport.

The low PC1 scores for shales in these townships reflect a limited contribution from REE-bearing heavy minerals, suggesting minimal sediment sorting and recycling. Sample # 4086 from Munro township is also classified as felsic-type and includes graphitic argillite with up to 30% nodular pyrite. It is bounded by mafic and ultramafic volcanics in the hanging wall and graphitic breccia and siliceous sediments in the footwall. Its low PC1 score, combined with the mafic host rock lithology indicates a sediment with a geochemical composition more closely related to its immediate host volcanic rocks. However, local variability in the PC1 scores is evident at the township scale. In Munro township, for example, sample # 4096 and # 8601 are separated by only ~ 2 km yet have very different PC1 scores highlighting the complexity of the depositional environment and possibly differences in sediment transport, sorting, and provenance. The example from the Potter mine (#4096) may represent a localized felsic volcanic source within a small volcanic-subbasin ideal for VMS formation. These samples also show elevated values of non-carbonate carbon and features of alteration consistent with VMS-style mineralization.

5.2.2 Kriged Values of PC2

PC2 corresponds to the muscovite component identified in Chapter 4. It accounts for 14% of the total variance in the dataset including Rb, K, Ba, and Cs in muscovite, uranium and thorium in monazite and, to a lesser extent, the light rare earth elements (LREEs). This includes material likely derived from felsic volcanic rocks and associated hydrothermal alteration, either VMS or gold-related. The highest loadings are closely associated with sediments of the Porcupine basin in the south of the study area (e.g., proximal to the DPFZ: Figure 5.8) and in felsic-dominated

volcanic settings (e.g., Kamiskotia, Kidd Creek, Lucas township and Marathon township: Figure 5.8).

Shales from sub-basins of the Kidd-Munro and Stoughton-Roquemaure assemblages in the north of the study area (e.g., Aurora, Dundonald and Munro townships) have negative loadings on PC2 indicative of mafic sources. Other townships dominated by mafic and ultramafic volcanic rocks contain shales with low PC2 scores, such as sample # 4032 from Aubin township and sample # 4069 from Nesbitt township. Samples with some of the highest PC2 scores are classified as felsic-type and include shales from Mann, Lucas, Kingsmill, Currie, Hoyle, and Whitney townships. The shales from Mann, Lucas, Mahaffy, and Kingsmill townships are dominated by mafic to intermediate lithologies, but many of the samples are associated with chemical metasedimentary rocks. In Hoyle township the shales are interbedded with greywacke, which may account for the felsic signature. In Currie township (sample # 4194, 4197, 4196, 4195), nearly all samples have positive PC2 scores and negative PC1 scores reflecting a greater influence of the muscovite component within these shales.

Many of the samples in the younger felsic-dominated volcanic assemblages of the Porcupine assemblage have high PC2 scores. They are predominantly felsic-type, contain disseminated and nodular pyrite, are associated with quartz-carbonate pyrite veins, and may contain calcite alteration. The hanging wall and footwall are highly variable and include volcanic rocks such as rhyolite, dacite, lapilli tuff, and basalt suggesting their deposition during felsic volcanic activity. This includes samples # 4192 from Currie township that consists of very-fine grained black graphitic argillite with chalcopyrite replacing pyrite nodules. It has a feldspar-porphyry in the footwall and a moderately high PC2 score suggesting it was derived from felsic volcanic rocks and is potentially associated with gold-related hydrothermal alteration. Graphitic argillite samples # 4392 and # 4319 from Hoyle township have a similarly high PC2 score and contain pyrite streaks and minor quartz-carbonate-pyrite veins. They are bounded by greywacke and argillite in the hanging wall and altered mafic volcanics in the footwall. The abundant pyrite and carbonate indicate hydrothermal alteration typical of the nearby orogenic gold deposits.

Despite being hosted in mafic-volcanic rocks, shales proximal to the major orogenic gold systems almost all have high PC2 scores, such as sample # 4358 from Holloway township and sample #7434 from Hislop township.

5.2.3 Kriged Values of PC3

PC3 corresponds to the mafic element component identified in Chapter 4. It accounts for approximately 10% of the total variance in the dataset, with significant loadings of V, Cr, Sc, Mn, and Ti. The positive loadings of these elements reflect sediments sourced from mafic and ultramafic rocks such as the abundant komatiites in the Kidd-Munro and Stoughton-Roquemaure assemblages. High loadings of Ni and As are similarly related to proximal mafic-ultramafic sources and high carbon content (now graphite). The highest loadings are found in parts of the study area known to be well endowed in mafic-ultramafic volcanics (e.g., Aubin, Nesbitt, Crawford, Mann, Aurora, Munro townships: Figure 5.9). Sample # 4063 from Reaume township and # 4013 from Hanna township are mafic-type argillite with high Ni, Cr, and Sc contents and a high PC3 score. Sample # 4013 has peridotite in the footwall. Samples with high PC3 scores also include # 4169 and # 4170 from Aurora township, both classified as mafic-type shales in the Stoughton-Roquemaure Assemblage. Sample # 4069 from Nesbitt township, and # 4170 from Aurora have a mafic volcanic hanging wall and mafic to ultramafic footwall.

Samples with negative loadings on PC3 (mostly felsic-type shales) occur in the Kamiskotia area (e.g., Godfrey and Jamieson townships) but also in the eastern part of the Kidd-Munro Assemblage in the Coulson and Walker township areas. Samples with low PC3 scores show little to no enrichment of mafic elements. Sample # 4049 from Mahaffy township, is classified as felsic-type shale and has a strongly negative PC3 score. This suggests local provenance from a felsic source.

5.2.4 Kriged Values of PC4

PC4 corresponds to the elements closely associated with regional carbonate alteration and orogenic gold mineralization identified in Chapter 4. It accounts for 5 % of the total variance in the dataset characterized by significant positive loadings of C in CO_2, B, W, LREE and Y suggesting

the influence of minerals such as hydrothermal carbonate, tourmaline, scheelite or wolframite, and LREE-bearing monazite and Y-bearing xenotime. These minerals and their associated elements reflect hydrothermal overprinting related to orogenic gold systems (Figure 5.10). Moderate loadings of K, Rb, Mn, Ba, and Cs on the same samples suggest the presence of muscovite alteration, which is also typical of gold-bearing systems. However, PC4 shows the least discrimination between shale lithotypes in biplots of the principal components, consistent with the relatively few examples of this alteration style in the data set. Elements with negative loadings on PC4 include Th, U, Ni, and Cr, typical of mafic to ultramafic input.

Samples with high PC4 scores include those from Mahaffy, Lennox, Aurora, and Hoyle townships (Figure 5.10). Sample # 4366 from Hoyle township is an example, classified as mafic-type, is hosted by pillowed mafic volcanics in both the hanging wall and footwall and contains chlorite fracture-fill with moderately high C in CO_2 as well as non-carbonate carbon. Samples with the lowest PC4 scores are from Dundonald and Langmuir townships, which are associated with anomalous nickel mineralization and non-carbonate carbon. Langmuir contains a suite of ultramafic to mafic metavolcanics cut by diabase dykes and hosts komatiite-nickel deposits. Dundonald contains komatiite-hosted nickel occurrences with anomalously high concentrations of Cu, Ni, Co, Se and Mo. Sample # 8543 from Dundonald township, classified as intermediate-type, contains pyrite nodules and a high concentration of non-carbonate carbon (e.g., organic carbon).

5.3 Relationship to Volcanic and Tectonic Settings

The map distribution of the PC scores confirms the presence of distinct shale compositions in different parts of the study area, indicating different sources (proximal versus distal, mafic versus felsic) and depositional or alteration histories (more or less sorted or recycled, barren or overprinted by hydrothermal fluids). These variations show a clear spatial relationship to different volcanic rock assemblages and proximity to the major crustal-scale breaks (DPFZ). The implication is that the shale geochemistry can be used to map depositional environments and sub-basins at a regional scale. In particular, the kriged maps clearly identify different sub-basins across the map area, including the Porcupine basin in the south, and the Kidd-Munro and Stoughton-Roquemaure rift basins in the north.

The maps for PC1 and PC3 show two distinct corridors: one corresponding to the Porcupine assemblage and another of mafic-ultramafic rocks of the Stoughton-Roquemaure and Kidd-Munro rift assemblages. These trends are regionally consistent and show clear geochemical differences between the shale units. The map for PC3 (Figure 5.9) shows a corridor of felsic volcanic rocks from Kamiskotia through Kidd Creek to Munro township. This has possible implications for exploration given the importance for VMS of felsic volcanic centers in otherwise mafic-dominated sub-basins.

As noted above, the highest PC1 scores are mostly distributed along the PDFZ and in the Porcupine Assemblage between the DPFZ and Pipestone Fault. These are distally derived turbidites with a high degree of sorting and Si-enrichment. Heavy detrital minerals as well as quartz are particularly concentrated in sediments along the break and most of the sampled shales in these assemblages are of intermediate-type (i.e., high maturity, mixed mafic and felsic sources). Low PC1 scores north of the Pipestone Fault are mainly related to mafic-type shales more closely associated with base metal mineralization. High PC2 scores for samples from the Porcupine basin are more closely associated with orogenic Au mineralization. These shales are enriched in B-bearing tourmaline, LREE-bearing monazite and xenotime, and C in CO_2 indicated by high scores for PC4. Muscovite alteration north of the Pipestone Fault may be related to hydrothermally altered felsic volcanic rocks in those areas.

A schematic illustration of the possible sources of sediments in volcanic-dominated systems was shown in Figure 2.4, with distal and proximal sources corresponding to high versus low PC1 values. In this interpretation, low PC1 sediments are thought to be typical of immature back-arc basin settings, whereas high PC1 values may be related to arc-like settings where major crustal-scale faults (e.g., DPFZ) also may have developed.

The effect of the missing data in the 4 townships surrounding Kidd Creek is discussed in the next Chapter.

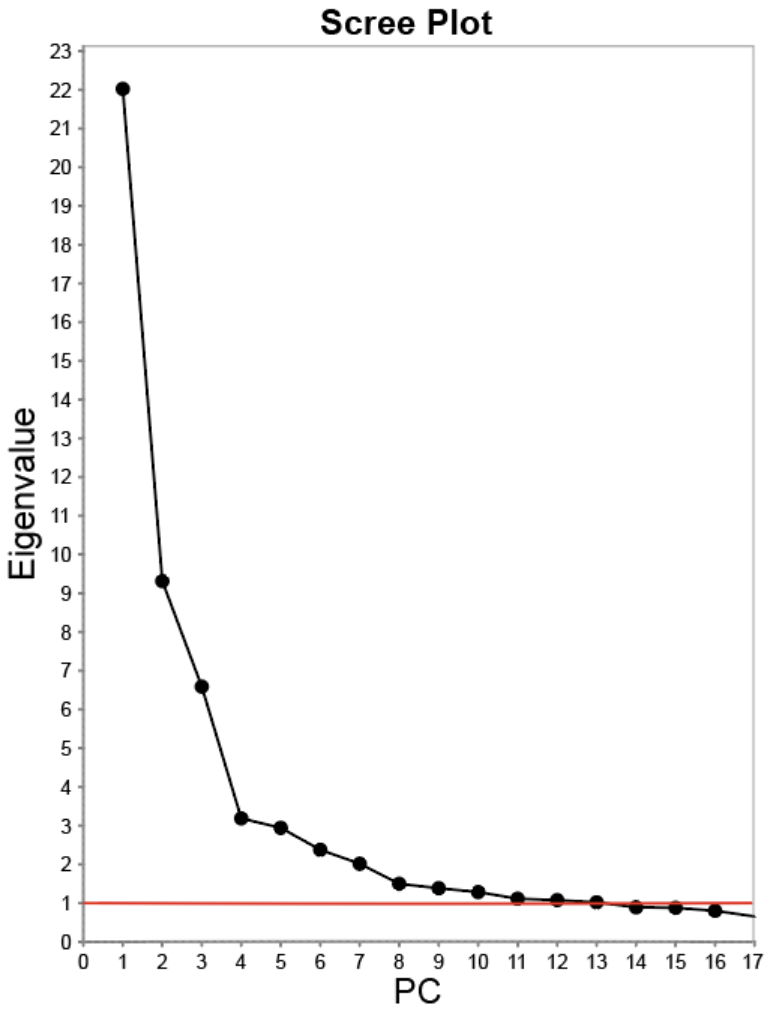


Figure 5.1. Scree plot showing the distribution of eigenvalues according to the principal component analysis of the WAGB black shales. No elements were removed form the data resulting in the large numbers of principal components. Principal component 1 explains 33% of the variance and is mainly heavy mineral detrital components concentrated in the sediments. Principal component 2 explains 14% of the variance and is mainly related to hydrothermal alteration of the original volcanic rocks from which the shales were derived (or alteration after deposition) with a strong loading of the muscovite component. Principal component 3 and 4 explain 10% and 5% of the variance, respectively, and are related to the mafic-element components and carbonate components of the shale samples.

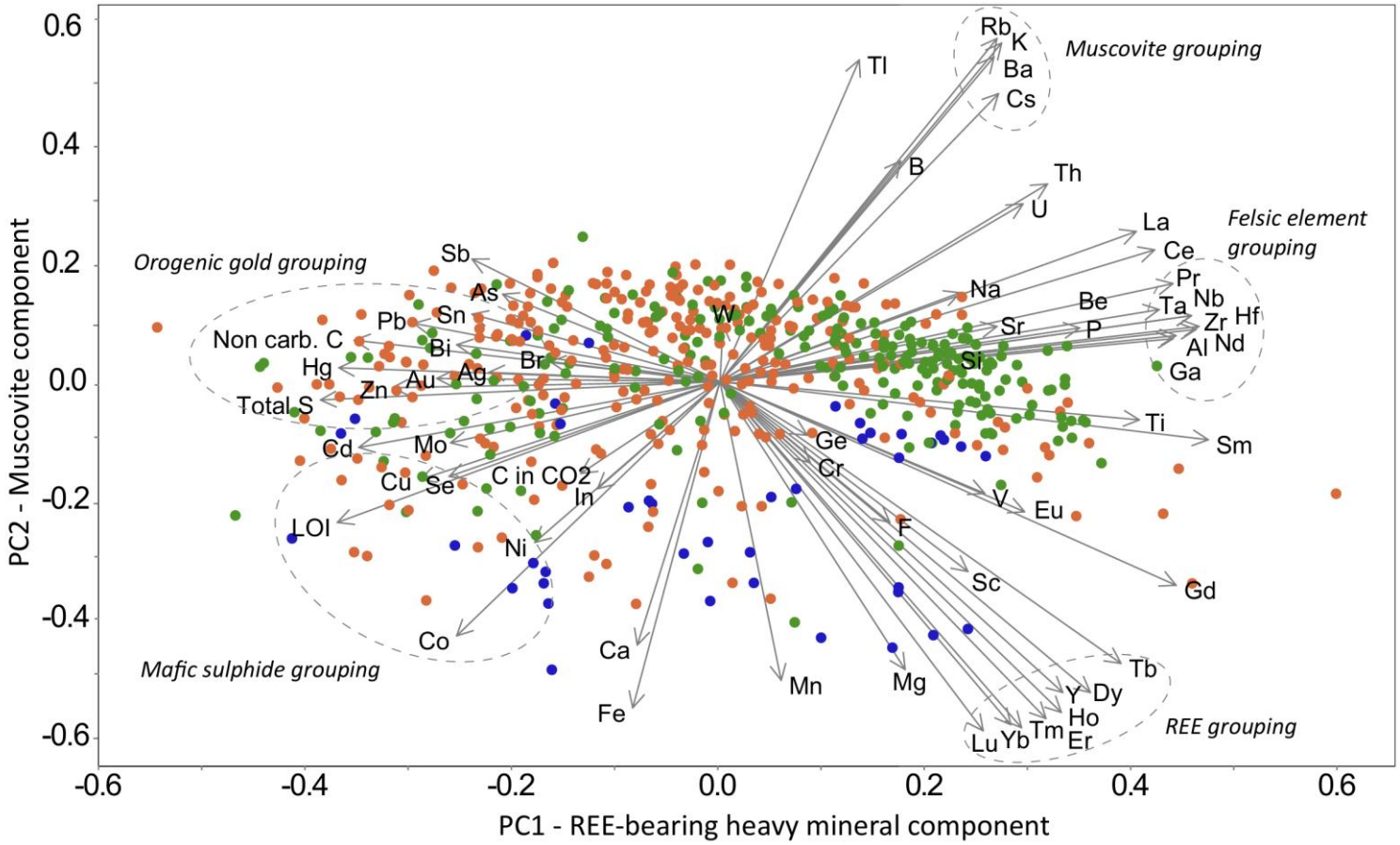


Figure 5.2. Principal component analysis (PCA) biplot of all WAGB black shale samples projected onto PC1 and PC2. The plotted points are scores for individual samples, and the relative loadings of each element are shown as arrows. The contribution of different elements to the principal components is indicated by the length of the arrows. PC1 on the x-axis accounts for 33% of the total variance and PC2 on the y-axis accounts for 14 % of the total variance. Samples are colour-coded according to their source rock composition: mafic-type (blue), felsic-type (orange), and intermediate-type (green). The dashed circles enclose the groupings of elements discussed in Chapter 4. The groupings unique to PC1 include the REE grouping, and for PC2 the muscovite grouping (K_2O, Rb, Sr, Cs, Ba).

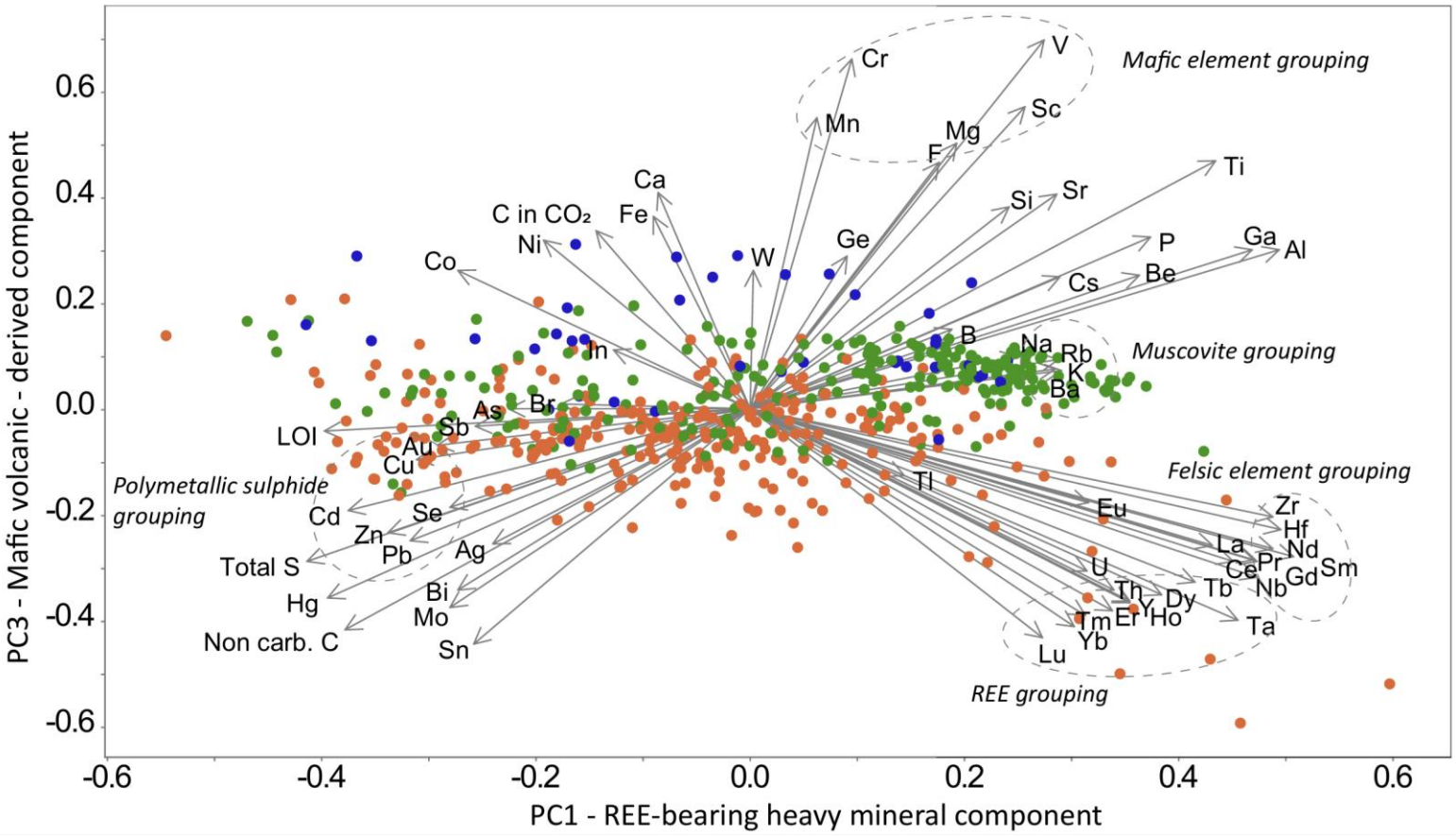


Figure 5.3. Principal component analysis (PCA) biplot of all WAGB black shale samples projected onto PC1 and PC3. The plotted points are scores for individual samples, and the relative loadings of each element are shown as arrows. The contribution of different elements to the principal components is indicated by the length of the arrows. PC1 on the x-axis accounts for 33% of the total variance and PC3 on the y-axis accounts for 10 % of the total variance. Samples are colour-coded according to their source rock composition: mafic-type (blue), felsic-type (orange), and intermediate-type (green). The dashed circles represent the groupings of elements identified in Chapter 4. The groupings unique to PC3 include the mafic element grouping (Sc, V, Cr).

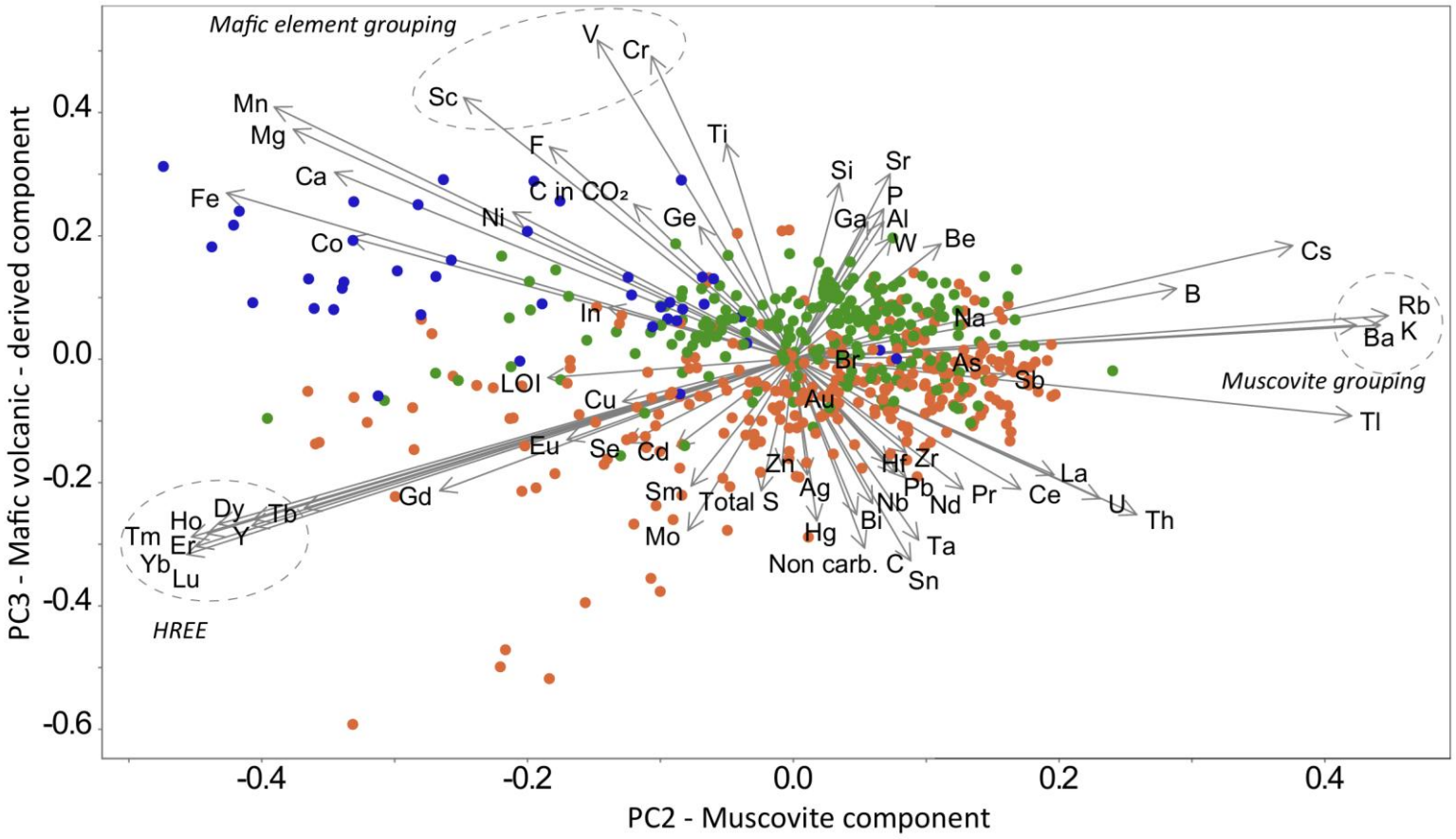


Figure 5.4. Principal component analysis (PCA) biplot of all WAGB black shale samples projected onto PC2 and PC3. The plotted points are scores for individual samples, and the relative loadings of each element are shown as arrows. The contribution of different elements to the principal components is indicated by the length of the arrows. PC2 on the x-axis accounts for 14 % of the total variance and PC3 on the y-axis accounts for 10 % of the total variance. Samples are colour-coded according to their source rock composition: mafic-type (blue), felsic-type (orange), and intermediate-type (green). The dashed circles represent the groupings of elements discussed in Chapter 4. The groupings unique to PC2, and PC3 are the muscovite grouping (K_2O, Rb, Sr, Cs, Ba) and the mafic element grouping (Sc, V, Cr), respectively.

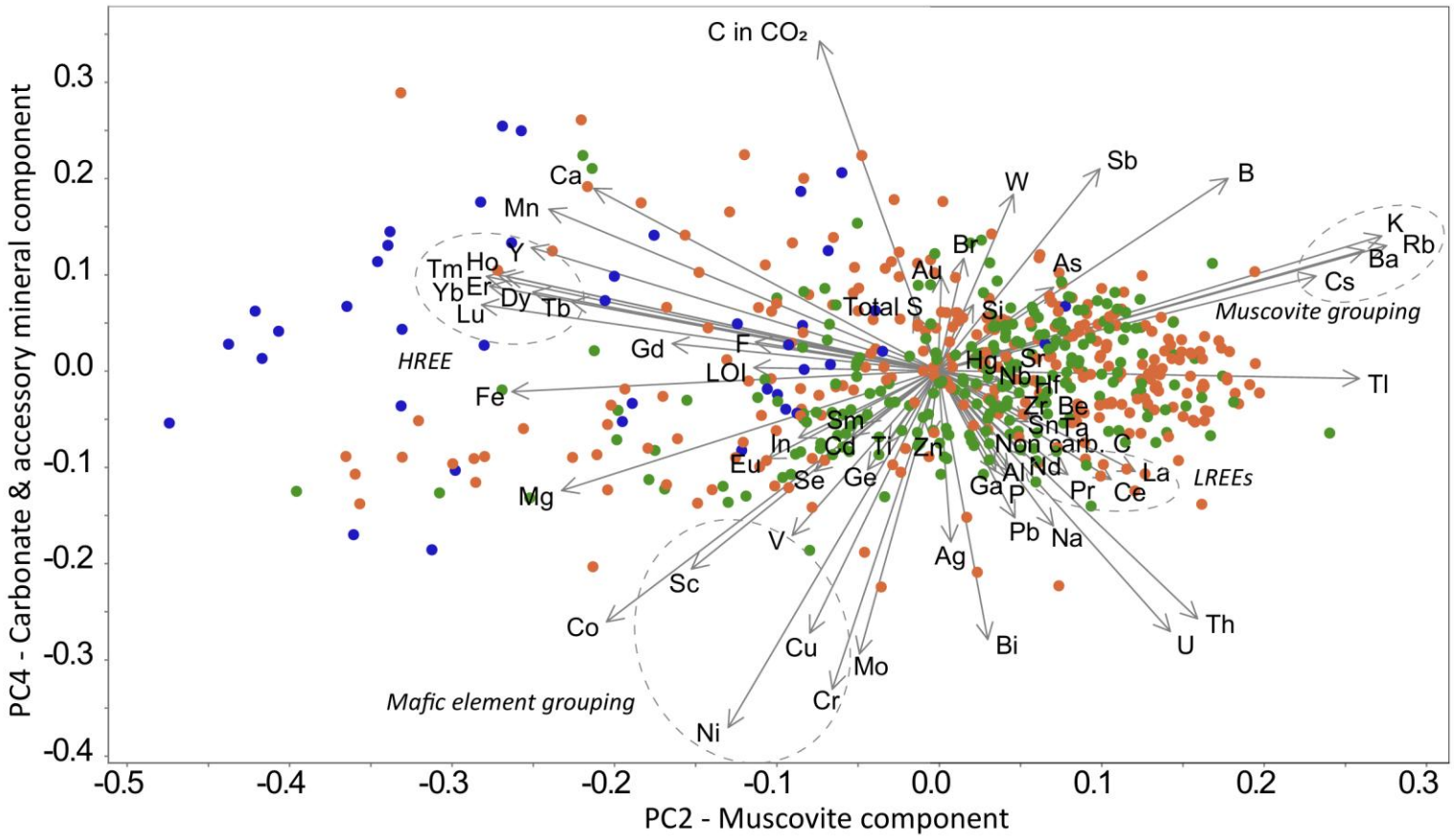


Figure 5.5. Principal component analysis (PCA) biplot of all 564 WAGB black shale samples projected onto PC2 and PC4. The plotted points are scores for individual samples, and the relative loadings of each element are shown as arrows. The contribution of different element to PC2 and PC4 is indicated by the length of the arrows. PC2 on the x-axis accounts for 14 % of the total variance and PC4 on the y-axis accounts for 5 % of the total variance. Samples are colour-coded according to their source rock composition: mafic-type (blue), felsic-type (orange), and intermediate-type (green). The dashed circles represent the groupings of elements identified in Chapter 4. The groupings unique to PC4 include the carbonate grouping (CO_2, CO, Sr), and the carbon and diagenetic sulphide grouping (LOI, C, CO_2, S, Total S).

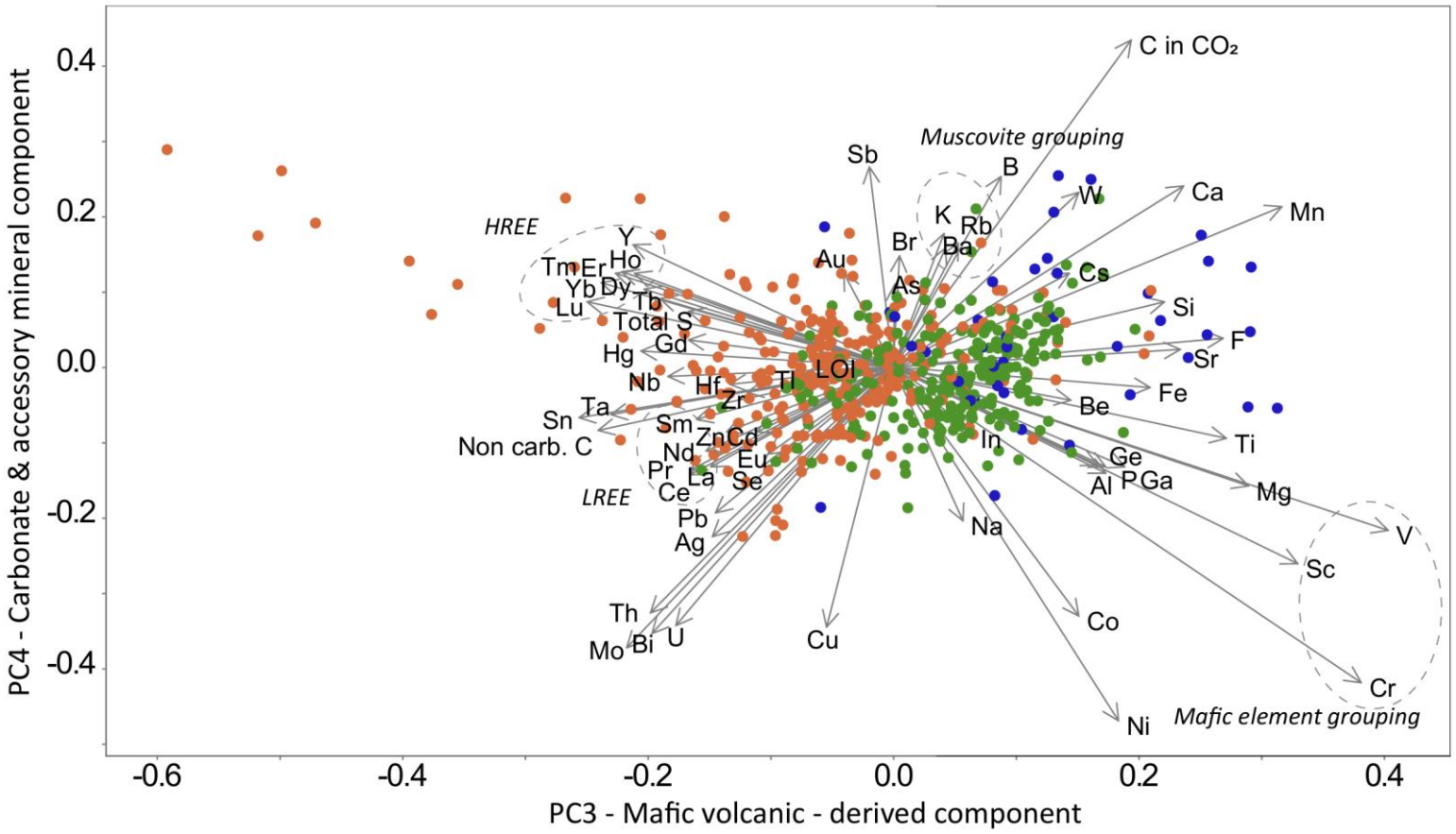


Figure 5.6. Principal component analysis (PCA) biplot of all WAGB black shale samples projected onto PC3 and PC4. The plotted points are scores for individual samples, and the relative loadings of each element are shown as arrows. The contribution of different elements on the principal components is indicated by the length of the arrows. PC3 on the x-axis accounts for 10 % of the total variance and PC4 on the y-axis accounts for 5 % of the total variance. Samples are colour-coded according to their source rock composition: mafic-type (blue), felsic-type (orange), and intermediate-type (green). The dashed circles represent the groupings of elements identified in Chapter 4.

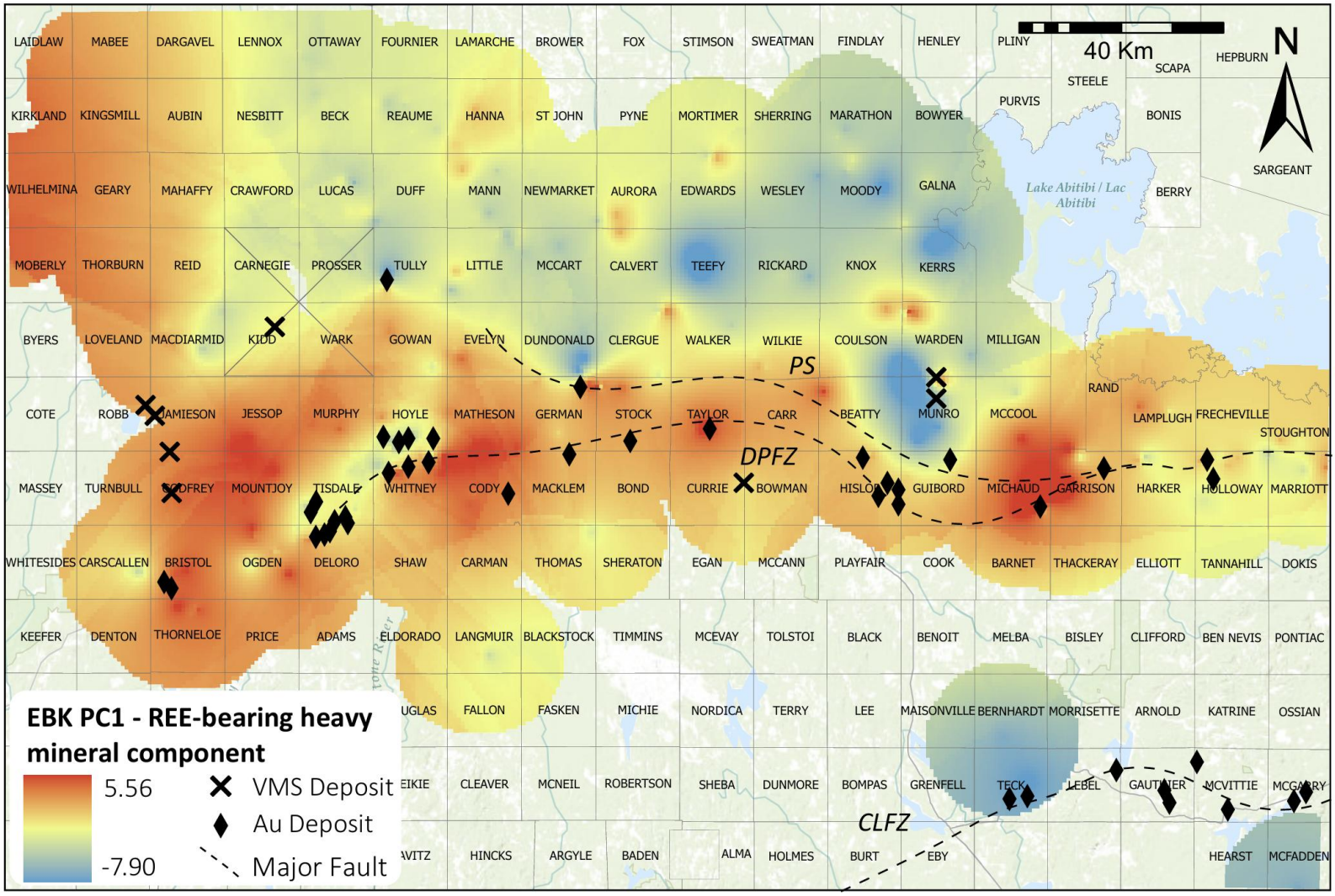


Figure 5.7. Empirical Bayesian Kriging of PC1 scores (detrital heavy mineral component) of 564 graphitic argillite samples from the western AGB. The X's and diamonds represent the locations of known VMS and gold deposits, respectively. No samples from Carnegie, Prosser, Kidd, and Wark townships were used in this study. High PC1 scores are predominantly located, along the DPFZ and Pipestone Fault, associated with the turbidite sequences of the Porcupine assemblage. This map shows a clear corridor of low PC1 scores mainly in the north of the study area in the Kidd-Munro, Tisdale, and Stoughton-Roquemaure assemblages and from Kidd Creek to Munro Township.

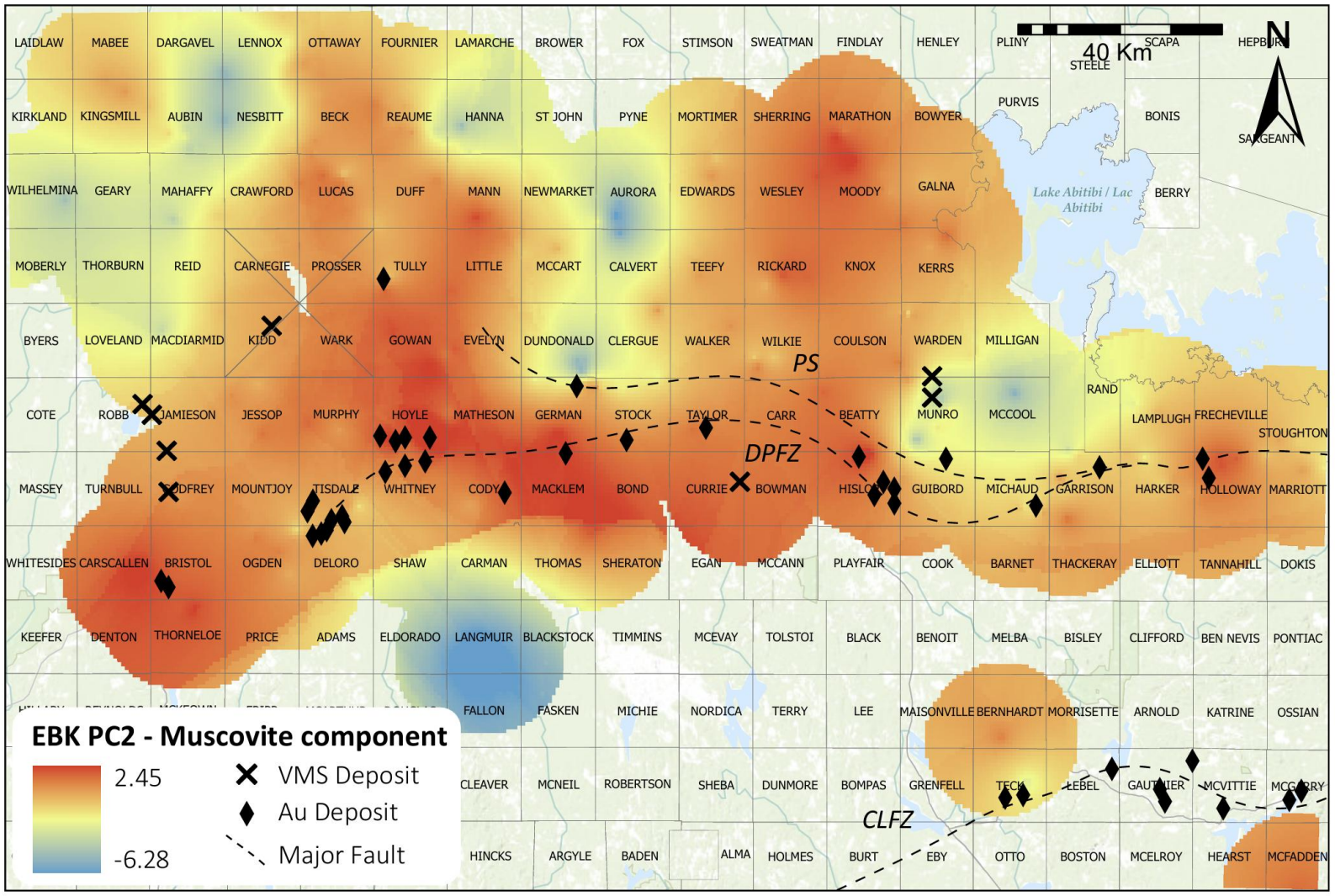


Figure 5.8. Empirical Bayesian Kriging interpolation of PC2 scores (muscovite component) of 564 graphitic argillite samples from the western AGB. The X's and diamonds represent the locations of known VMS and gold deposits, respectively. No samples from Carnegie, Prosser, Kidd, and Wark townships were used in this study. High PC2 scores occur broadly along the DPFZ, and in the bimodal volcanic successions in the north of the study area.

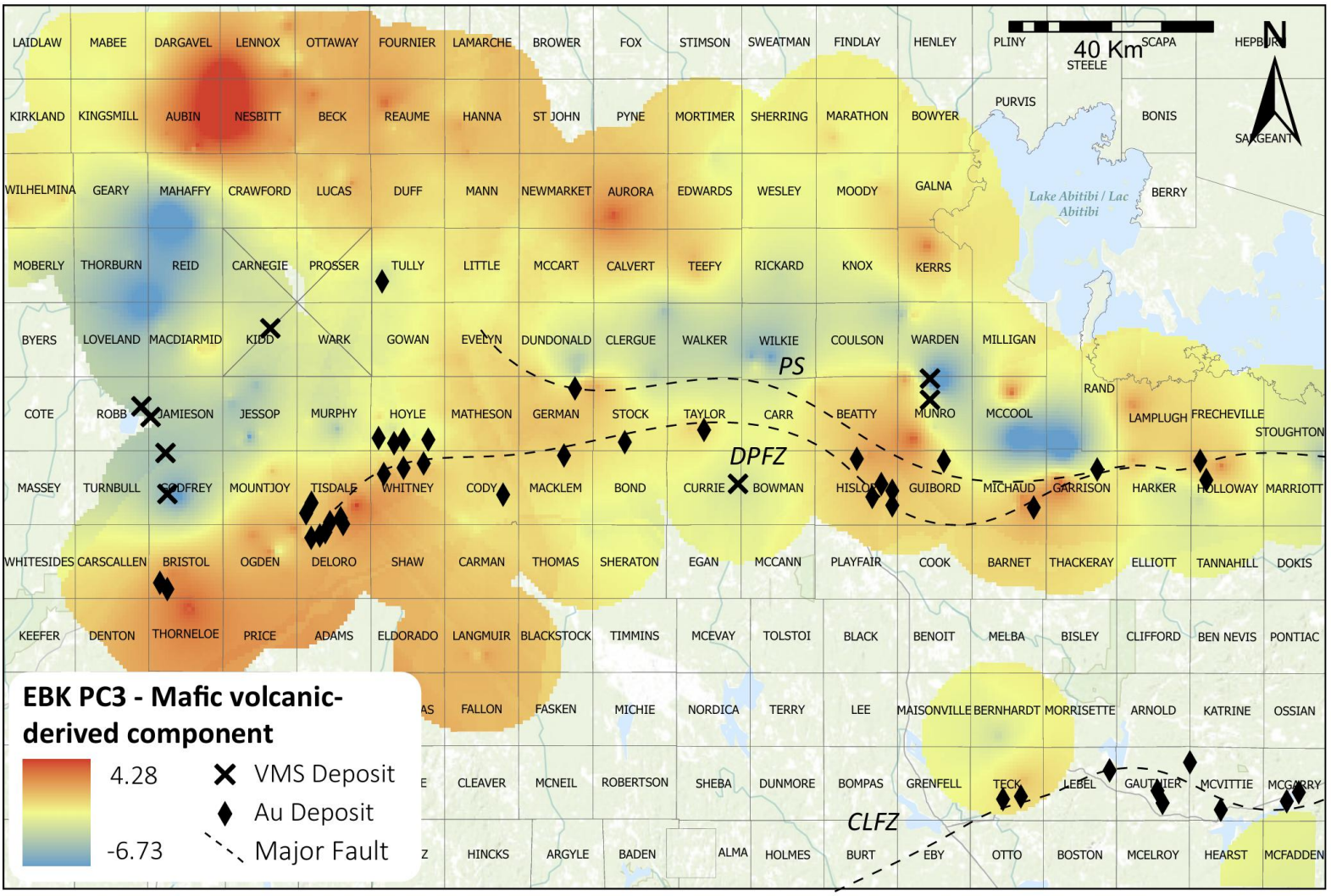


Figure 5.9. Empirical Bayesian Kriging interpolation of PC3 scores (mafic and ultramafic component) of 564 graphitic argillite samples from the western AGB. The X's and diamonds represent the locations of known VMS and gold deposits, respectively. No samples from Carnegie, Prosser, Kidd, and Wark townships were used in this study. High PC3 scores occur within the Blake River, Tisdale, Kidd-Munro, Stoughton-Roquemaure assemblages north of the DPFZ and Pipestone Fault. This map shows a clear corridor with negative loadings on PC3 (mostly felsic-type shales) from Kamiskotia through Kidd Creek to Munro township.

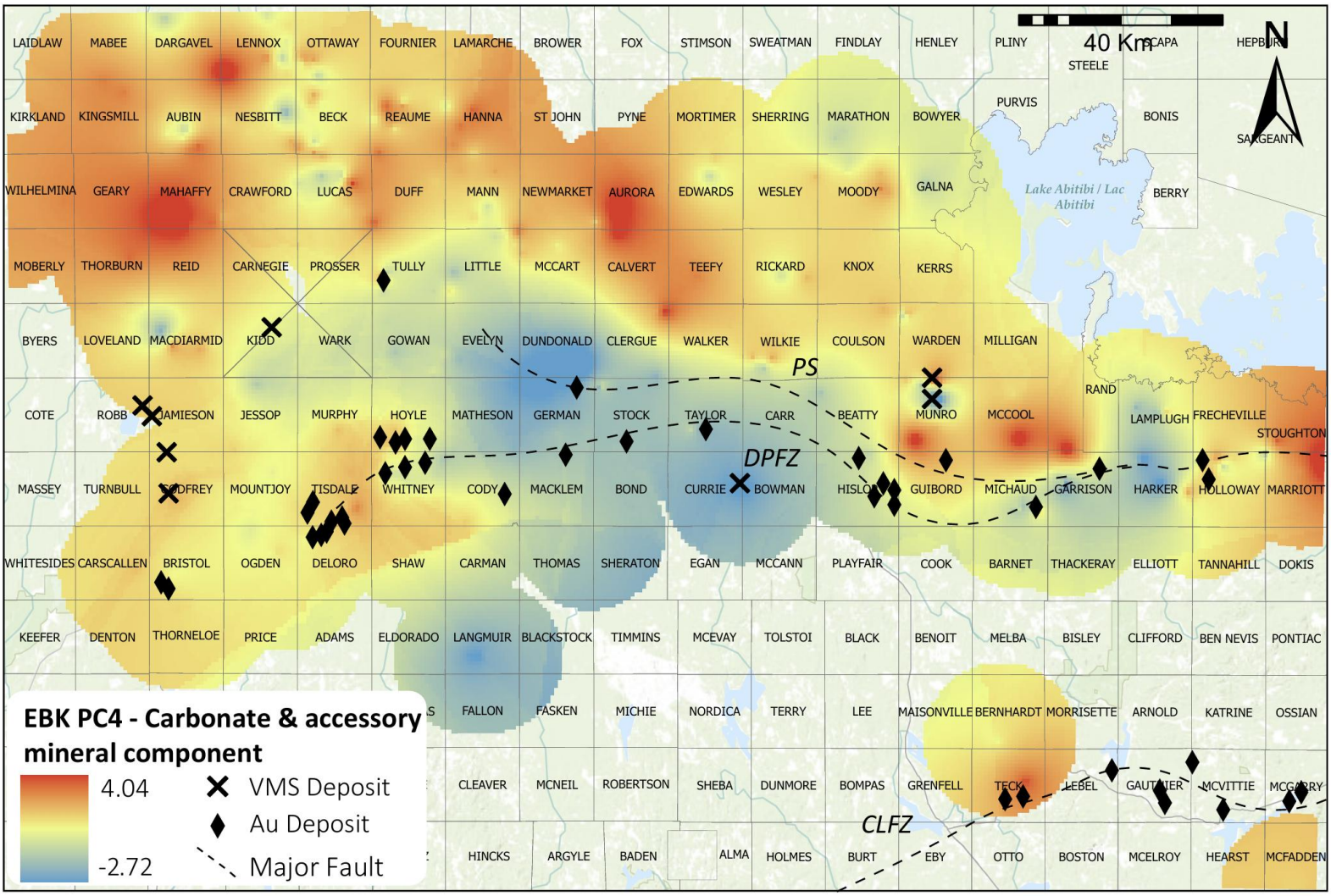


Figure 5.10. Empirical Bayesian Kriging interpolation of PC4 scores (accessory minerals including V-bearing muscovite, B-bearing tourmaline, monazite and xenotime) plus carbonate in 564 graphitic argillite samples from the western AGB. The X's and diamonds represent the locations of known VMS and gold deposits, respectively. No samples from Carnegie, Prosser, Kidd, and Wark townships were used in this study. High PC4 scores indicate the presence of carbonate and low PC4 scores suggest non-carbonate / graphitic carbon present. Lower PC4 scores are focused in locations with a significant (reduced) carbonaceous component such as Dundonald and parts of Munro townships.

Table 5.1. Eigenvalues, variance, and cumulative variance for the first four principal components of the PCA for 564 WAGB black shale samples.

	Eigenvalues	Variance (%)	Cumulative variance (%)
PC1	21.75	32.95	32.95
PC2	8.92	13.52	46.46
PC3	6.44	9.76	56.23
PC4	3.20	4.85	61.98

PC1 captures the most variance in the data followed by PC2, and so on. Values beyond PC4 are in Appendix A8.

Table 5.2. Summary table for the first four principal components of the PCA on 564 WAGB black shale samples.

	Shorthand name	Positive element loading	Negative element loading
PC1	REE-bearing heavy mineral component	Al, Hf, Zr, Nd, Gd	S, C, Hg, LOI, Cd, Zn
PC2	Muscovite component	Rb, K, Tl, Ba, Cs, B	Fe, Mn, HREE
PC3	Mafic volcanic-derived component	Cr, V, Sc, Mn, F, Ti	Lu, Yb, Tm, Er, Y, Ho
PC4	Carbonate and accessory mineral component	CO_2, B, W, K, Rb, Mn	Ni, U, Th, Cr, Mo

Shorthand names associated with each principal component and the first six elements with high positive and negative loadings out of 68 total elements.

Chapter 6 – Random Forest Classification

6.1 Random Forest Classification of Shale Lithotypes

Creating a classification scheme is a machine-learning task that sorts samples into predefined classes identified using a training dataset. This training is an iterative process by which a machine learning classifier, such as Random Forest, learns what geochemical variables are meaningful to achieve the best classification outcome and builds a model that can be used as a classification scheme (Fassbender, 2023). The classifier developed by Fassbender et al. (2023) was developed in Jupyter Notebook using the Python programming language. The workflow follows three distinct stages including labeling, training, and validation. We first sorted samples into known classes (e.g., mafic-type, intermediate-type, and felsic-type) using the Ti/Zr immobile element ratio. The RF model for shale lithotype was then trained on this subset of shales previously identified as belonging to a particular lithotype. The RF algorithm used additional elements to identify the geochemical signatures that best distinguish each lithotype. The resulting RF classifier is illustrated in Figure 6.1 by a single decision tree from the 500-tree forest. All 68 elements were included in this study to leverage the RF algorithm's ability to handle large feature sets. See Methods section (3.3.3) for a more detailed explanation.

The RF classifier was trained using all the available elements, however, following this initial step, only the elements with the greatest influence on the classification ability of the model were used. The classifier identified 8 elements in addition to Ti and Zr to best differentiate shale lithotypes. The relative importance of these variables was determined by the MDG shown in Figure 6.2 (see below). Elements typically associated with mafic minerals are the most important. The concentration of these elements in ppm is shown in Figure 6.3.

The accuracy of the classifier is described by a confusion matrix that compares the true positive versus false positive classifications (i.e., the number of samples that were correctly classified versus the number of samples misclassified) (Figure 6.4). It compares the output of the RF classification with the classes identified in the original training set and identifies which classes the model is performing well on and which classes it is struggling to identify. The accuracy of the

model is given by the true positive + true negatives divided by the total number of predictions (Singh et al., 2021).

The RF model for classifying shale lithotype achieved an overall accuracy of 91% with an OOB score of 0.92. All lithotypes had an ROC-AUC score greater than 0.95 (Figure 6.5). Out of a total of 68 elements considered in this study, the RF classifier for shale lithotype relies primarily on the 10 elements − V, Sc, Ti, Zr, Cr, Mn, Hf, Mg, La, and Si, corresponding to the 8 elements noted above plus Ti and Zr − as the most important based on the mean decrease in Gini. Although V has the highest mean decrease in Gini, the model is built on all the elements. One of the drawbacks of this method is that the 10 elements used in the classifier include two elements that were also used to create the training dataset. This may lead to an overestimated accuracy and overfitting. We can test and quantify this bias by comparing the training accuracy to the OOB accuracy and/or evaluating the classifier on an independent dataset.

6.2 Random Forest Classification of Associated Mineral Deposit Types

In this part of the study, the terminal nodes on the decision trees of the Random Forest classifier in Figure 6.1 were replaced with shale types from drill holes that were targeted in exploration for orogenic gold mineralization and VMS (Figure 6.6). Unlike the shale lithotype classifier, the RF classifier for shales associated with each mineralization style did not rely on elements (e.g., Ti/Zr) to define the initial training groups. We first sorted samples into these two categories based on the original target for discovery. The RF model was trained on this subset and then used elements to identify geochemical signatures that best distinguish between shales associated with each deposit type. Figure 6.6 represents one decision tree from the 500-tree forest in the RF classification scheme. Branching occurs at concentration thresholds and node impurity progressively decreases moving down the tree. Each node includes the node #, the splitting conditions for the elemental concentration and the Gini impurity which corresponds to colour intensity. The “samples” entry indicates the percentage of the total dataset within that node. The value field represents the class probability distribution (e.g., mafic, intermediate, felsic) and the class label is the predicted majority vote based on these probabilities. In applications with only two outcomes possible (e.g., classification by deposit association: either orogenic gold or base metal), the classification will be

forced. However, even in cases such as this, e.g., where some samples are not associated with any mineralization, the outcome is remarkably good for the known samples based on their characterization from the drill logs.

The MDG was used to evaluate which elements most significantly influenced the model's classification ability (Figure 6.7). For example, out of a total of 68 elements, the RF classifier identified Rb, Al, Ga, Ti, P, Cs, Th, Sc, V, and B as the ten most important elements for this distinguishing between shales associated with different mineralization types. The average concentrations of the top 10 elements listed in Figure 6.8 are all consistently higher in samples from drill holes that were targeted for orogenic Au mineralization than those targeted for base metal mineralization.

Rb and Al may be direct indicators of alteration associated with orogenic gold systems, and they are also enriched in sediments like those of the Porcupine Assemblage, which hosts many of the Abitibi orogenic gold deposits. Gallium often substitutes for Al in the crystal lattice of many Al-rich minerals such as muscovite, and likely accounts for the importance of this element in the RF classification, despite its low concentration in the shales. Cs and B also reflect the phyllosilicate alteration and abundant tourmaline in gold-quartz vein systems. The importance of the mafic elements (Ti, V, Sc) may reflect the higher proportion of Fe-rich mafic volcanic rocks associated with some gold mineralization along the DPFZ, whereas felsic volcanic rocks may be more associated with VMS mineralization. Titanium is mostly in ilmenite and rutile; phosphorous is hosted in monazite and xenotime which may also be associated with orogenic gold mineralization. The unexpected lack of importance of non-carbonate carbon and sulfur appears to reflect that graphitic carbon can be equally abundant in shales associated with Au mineralization and shales associated with volcanic-hosted base metals.

The RF model for associated mineralization styles achieved an overall accuracy of 79% with an OOB score of 0.80. However, it was stronger at classifying shales associated with VMS-style mineralization compared to those associated with orogenic gold deposits (Figure 6.9). Notably, 19 samples were incorrectly assigned to the base metal category despite being more closely associated with orogenic gold mineralization. The lower performance of the model relative to the RF model

for classifying shale lithotypes likely relates to the forced classification of all samples as either VMS-related or gold-related, when in fact many examples are not related to any known mineralization at all. Nevertheless, the model has a high ROC-AUC score of 0.86 indicating a strong predictive power between the two classes (Figure 6.10).

6.3 Random Forest Classification of Lithostratigraphic Assemblages

In this experiment, terminal nodes correspond to one of the six lithostratigraphic assemblages in the region. The RF model was trained on a subset and then used additional elements to identify geochemical signatures that best distinguish between shales associated with each lithostratigraphic assemblage. The MDG was used to evaluate which elements most significantly influenced the model's classification ability (Figure 6.11). Out of a total of 68 elements, the RF classifier identified Cs, Mg, U, Co, Mn, Au, Th, non-carbonate C, Sr, and Al as the most important elements for differentiating between shales from different assemblages.

The confusion matrix indicates that a greater number of shales were correctly classified in the Tisdale, Blake River and Kidd-Munro assemblages compared to other assemblages (Figure 6.12). The multiclass ROC-AUC score for the assemblage classification is 0.86 and the OOB score is 0.85 (Figure 6.13). However, the model's accuracy was only 61%. The poor performance is most likely due to errors in the identification of the host assemblages or lack of discrimination between the assemblages. In particular, the classification of the training set was based only on map location relative to the assemblage boundaries assigned by Ayer et al. (2002). It is likely that some samples were incorrectly assigned and therefore limited information can be extracted from this model. A better result may be possible using the new lithological map of the region to classify the samples, rather than the assemblage map.

6.4 Conclusions

The RF model for classification of the shale lithotypes proved to be the most reliable machine learning algorithm. It achieved an accuracy of 91% with an OOB score of 0.92. The RF model for associated mineral deposit types was able to distinguish shales associated with orogenic gold

versus base metal mineralization, as originally defined in exploration targeting of the drill holes with the true positive rate significantly higher than the false positive rate, indicated by a ROC value of 0.86. The RF classifier achieved an accuracy of 79% and an OOB score of 0.80. The RF model for classifying shales according to their host assemblage was the least reliable, suggesting there is no strong distinction between shales among the different volcanic assemblages. The RF model has a low accuracy of 61%, indicating that many samples were classified into the incorrect assemblage. Shales in the Porcupine sedimentary assemblage are distinct, but this mainly reflects sedimentary processes and not the source rocks.

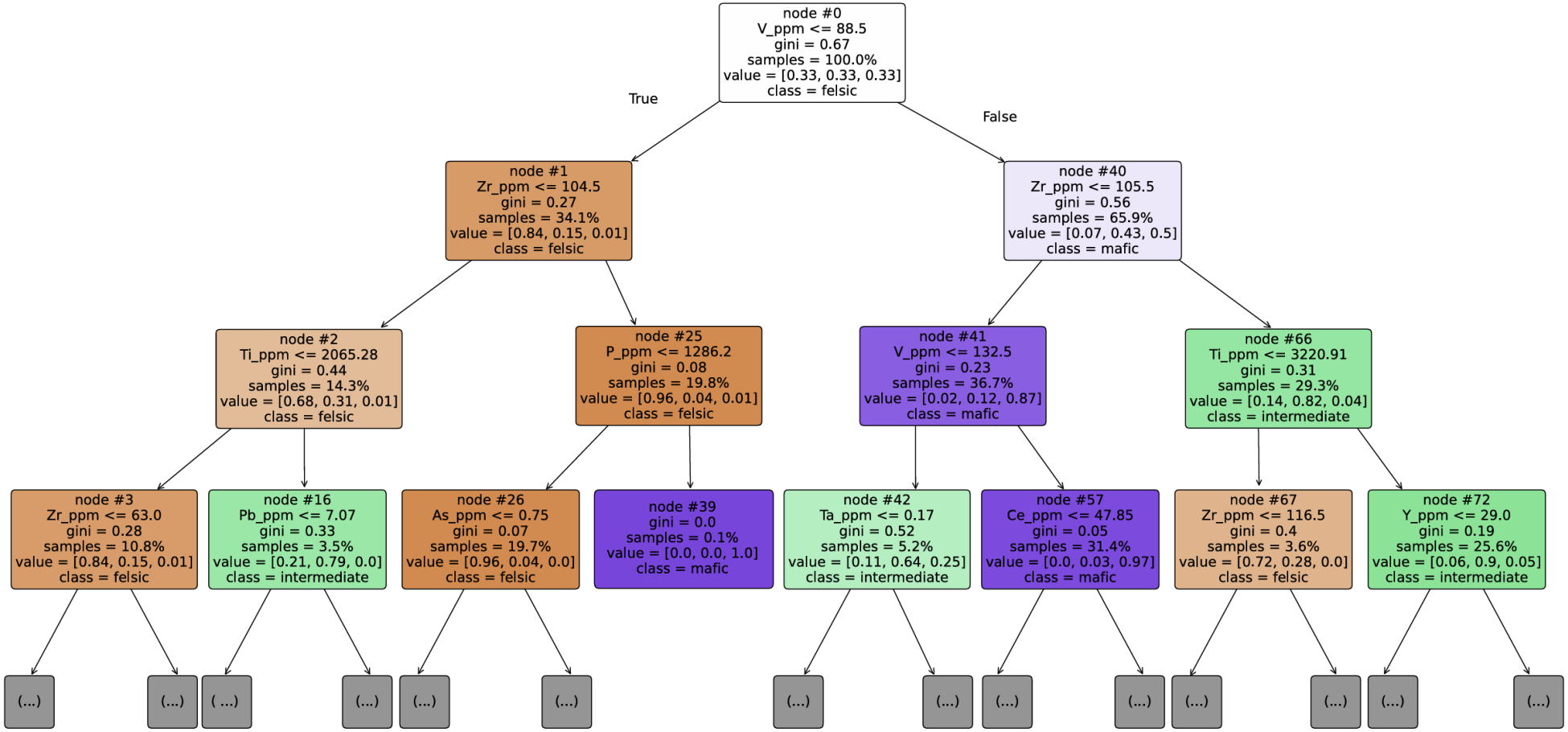


Figure 6.1. Schematic illustration of a decision tree from the 500-tree Random Forest classifier used to identify the source rock composition of shales. This tree contains 143 nodes, however, for illustration purposes it has been trimmed to the first four levels. The first node in this model has an impurity of 0.67 indicating poor separation of samples. Branching occurs at concentration thresholds and node impurity progressively decreases. Each node includes the node #, the splitting conditions for the elemental concentration and the Gini impurity. The "samples" entry indicates the percentage of the total dataset within that node. The value field represents the class probability distribution (e.g., mafic, intermediate, felsic) and the class label is the predicted majority vote based on these probabilities.

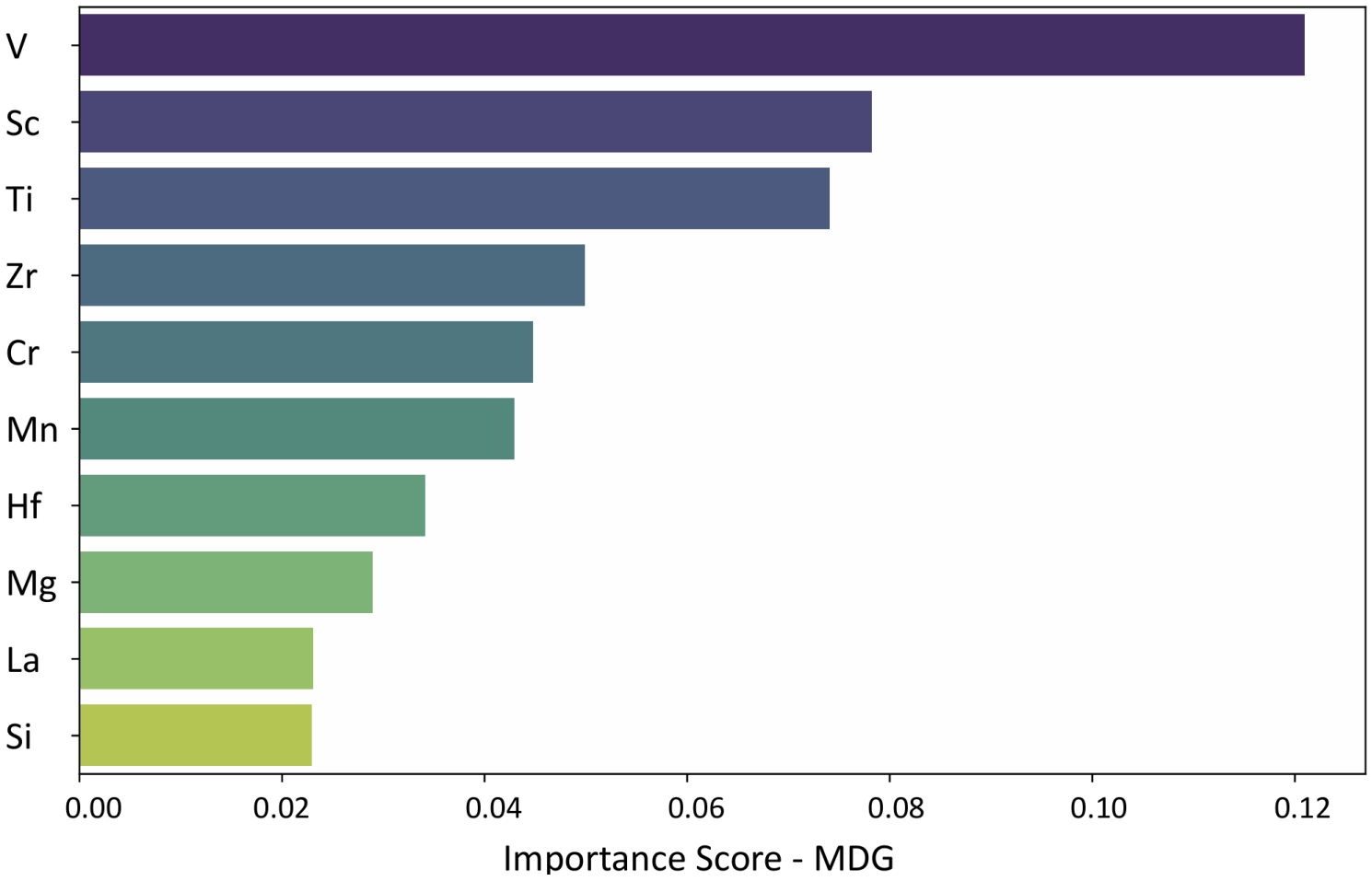


Figure 6.2. Mean Decrease Gini (MDG) scores for the top 10 predictors in the classification of WAGB black shale by lithotype. MDG measures the decrease in node impurity, averaged over all the trees in the RF model. Elements with the largest MDG values contribute most to sample separation and have the greatest predictive power.

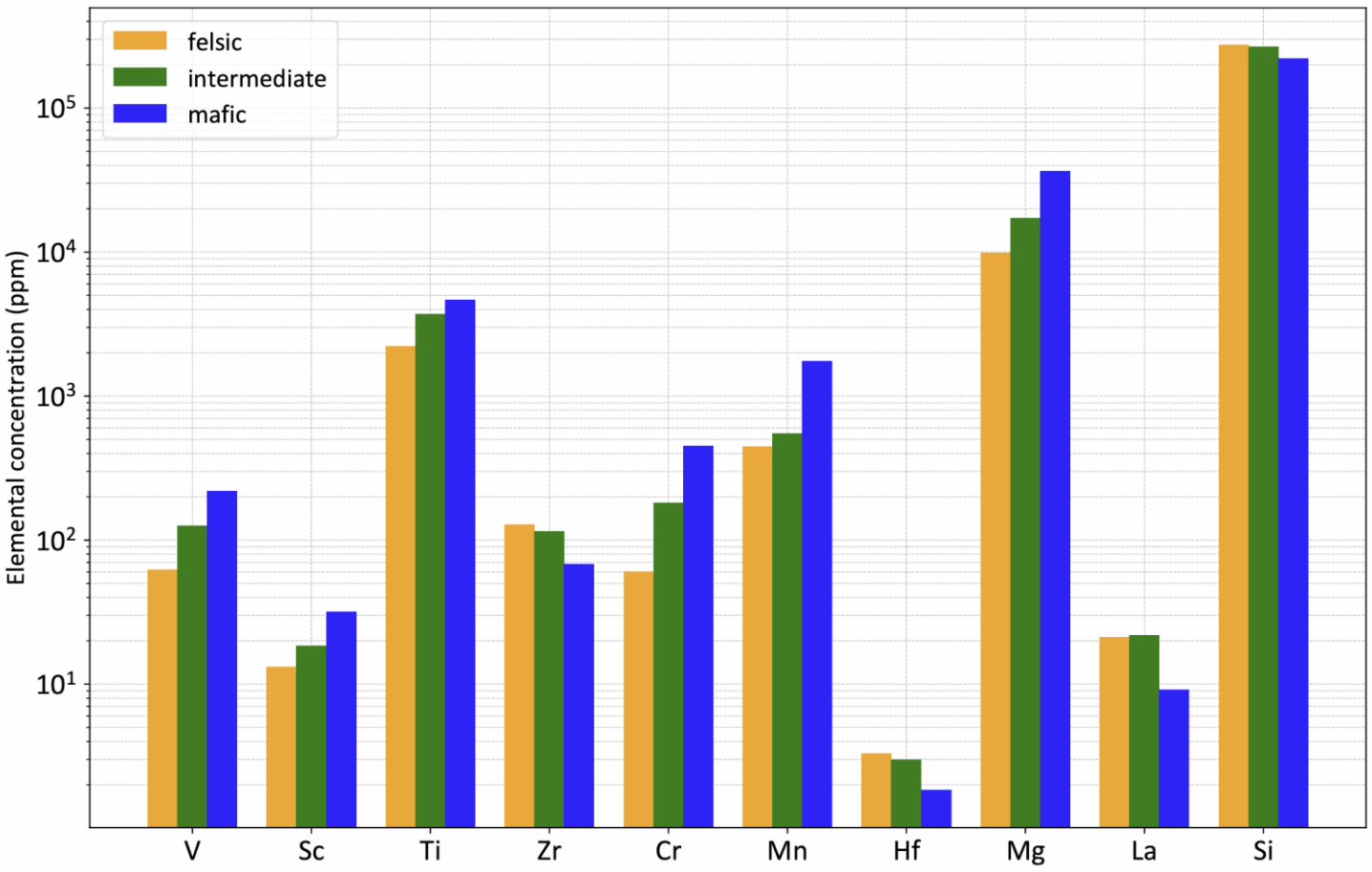


Figure 6.3. Concentrations of the 10 most important elements for RF classification of shale samples by lithotype. The elements are ordered from left to right by Importance Score indicated in Figure 6.2.

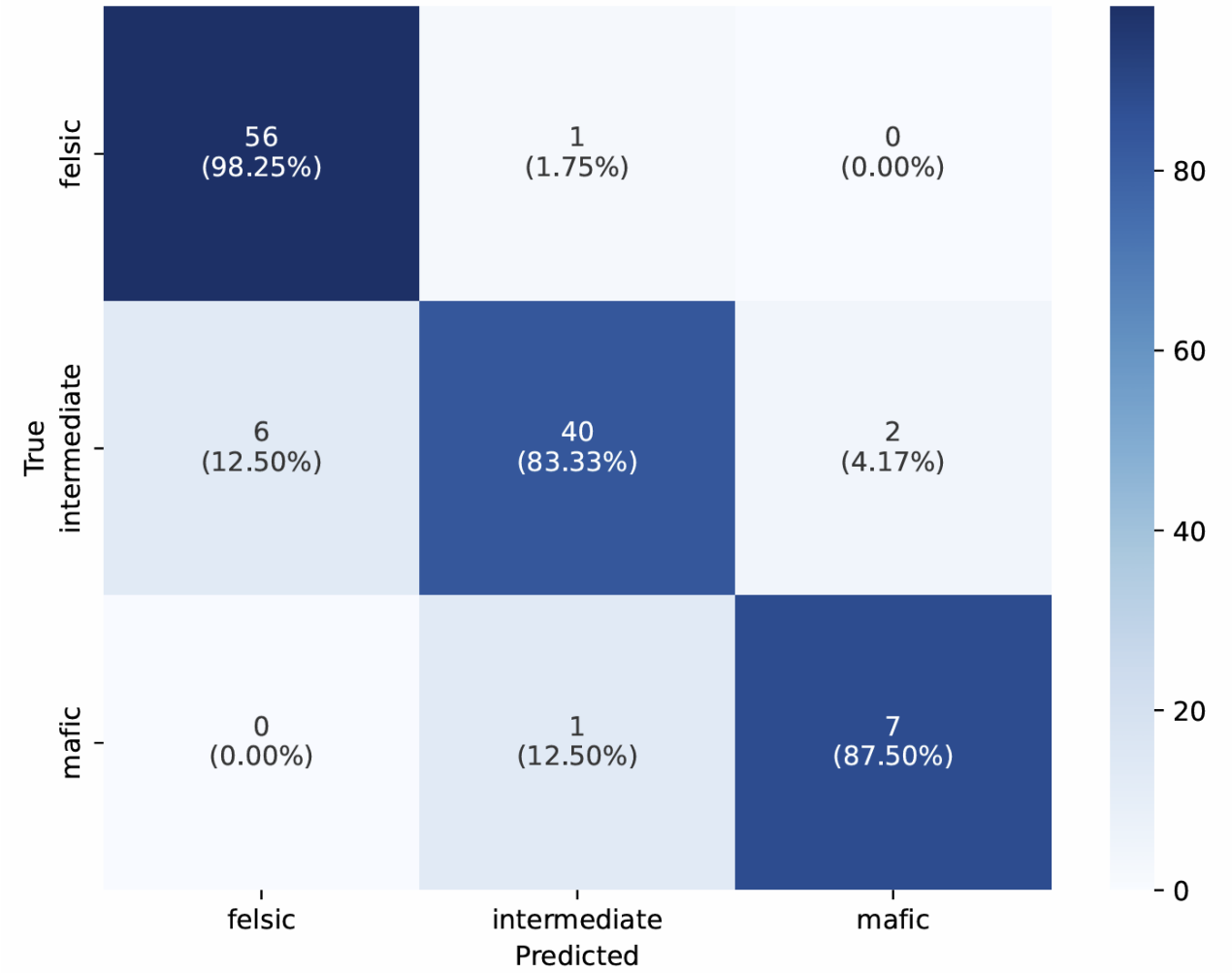


Figure 6.4. « Confusion Matrix » showing the proportion of correct classifications of shale lithotype in the test dataset. The model achieved an overall accuracy of 91%, with the majority of samples correctly assigned to felsic, intermediate, and mafic source rock categories. The accuracy of the model is calculated as the sum of true positive + true negative values (56 + 40 + 7) divided by the total number of predictions (57 + 48 + 8).

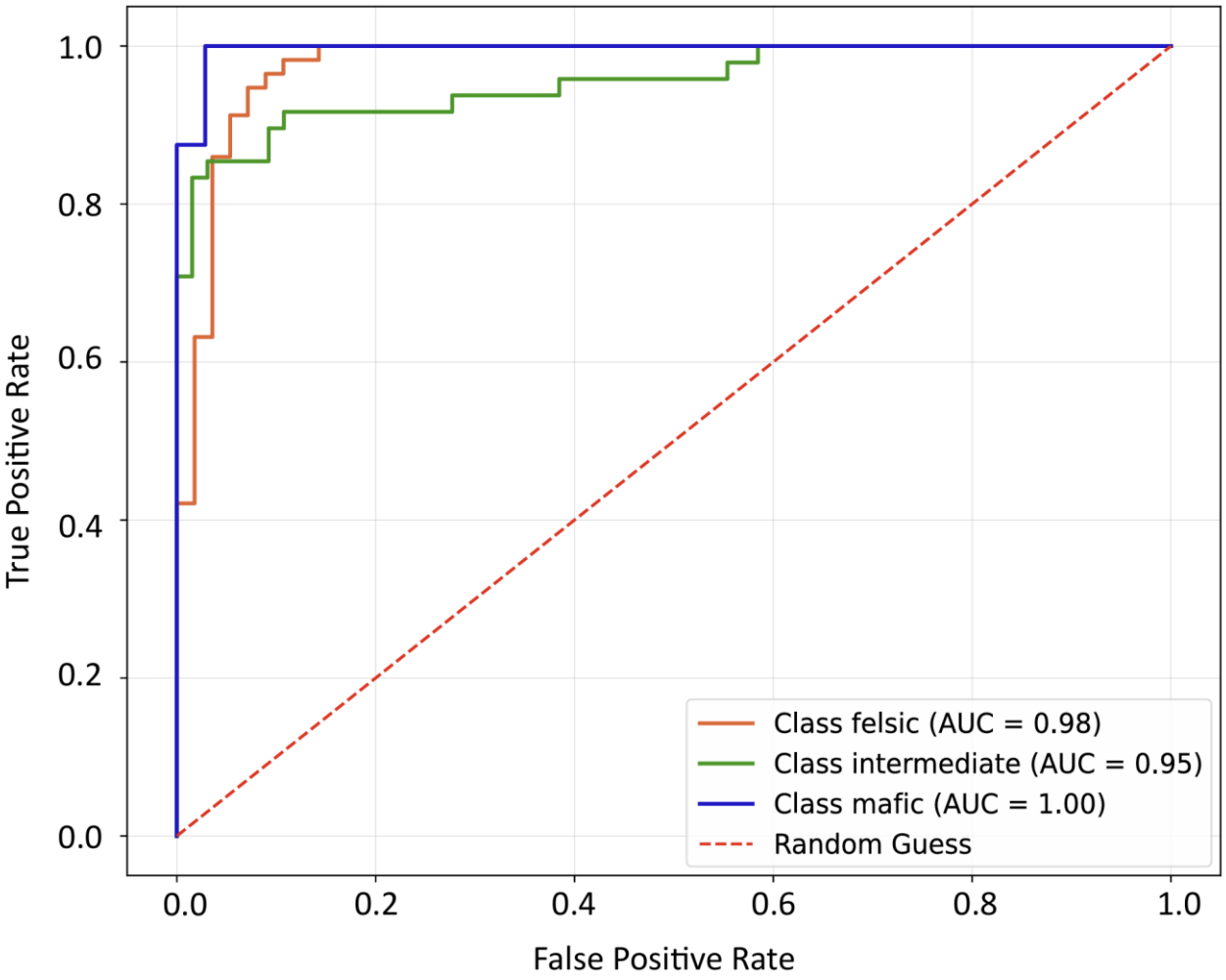


Figure 6.5. Receiver Operating Characteristic (ROC) curves and associated Area Under the Curve (AUC) values for shale lithotype classification. The plot depicts the true positive rate versus the false positive rate. The AUC quantifies the model's ability to differentiate between lithological classes. AUC values ≥ 0.95 for all classes indicate excellent class separation.

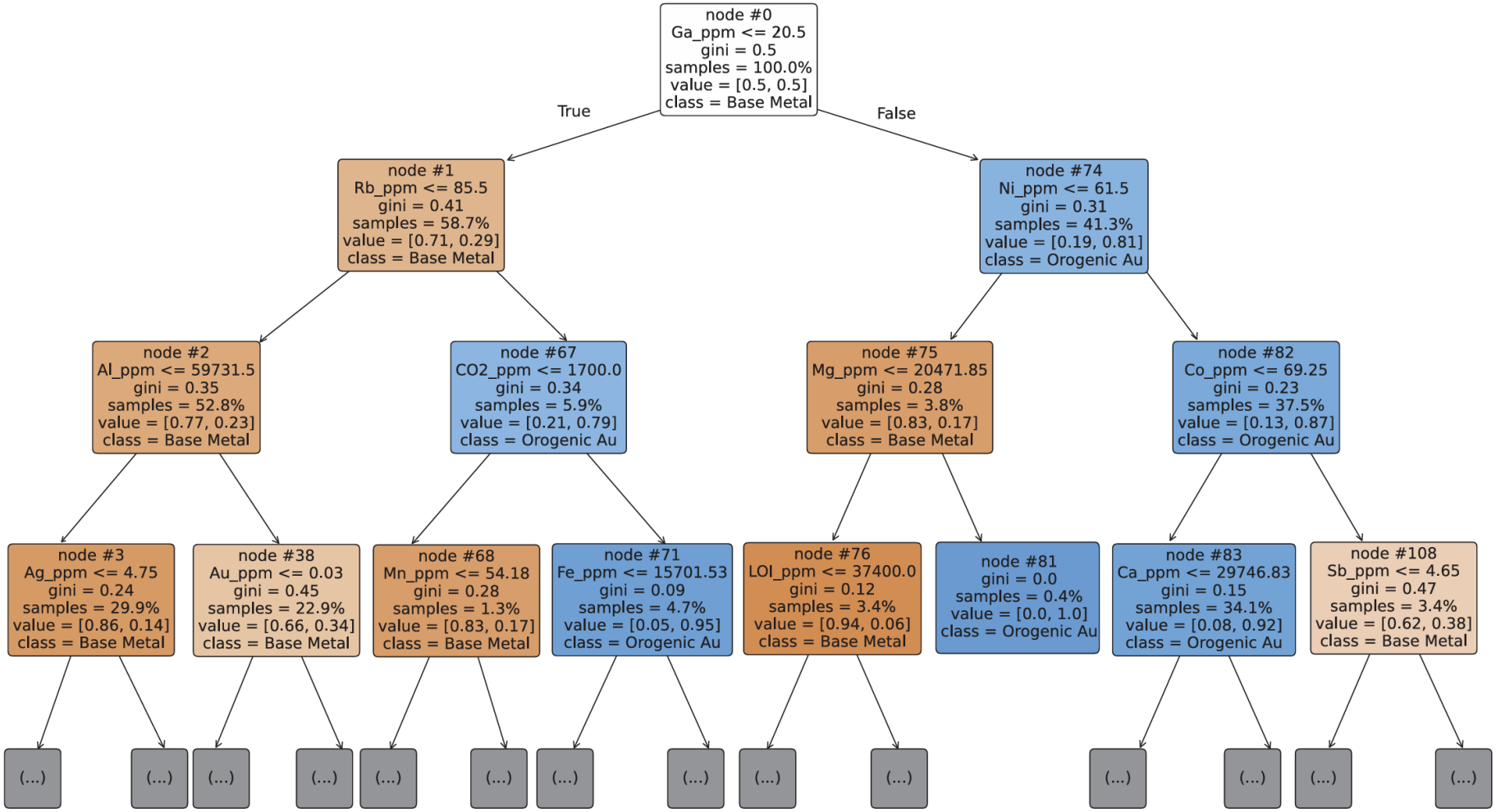


Figure 6.6. Schematic illustration of a decision tree from the 500-tree mineral Random Forest classifier used to identify shales associated with different mineralization styles. This tree contains 105 nodes, however, for illustration purposes it has been trimmed to the first four levels. The root node has an impurity of 0.5 indicating an equal split of variables into two classes. Branching occurs at concentration thresholds and node impurity progressively decreases. Each node includes the node #, splitting conditions for the elemental concentration and the Gini impurity. The "samples" entry indicates the percentage of the total dataset within that node. The value field represents the class probability distribution (e.g., orogenic gold, base metal) and the class label is the predicted majority vote based on these probabilities.

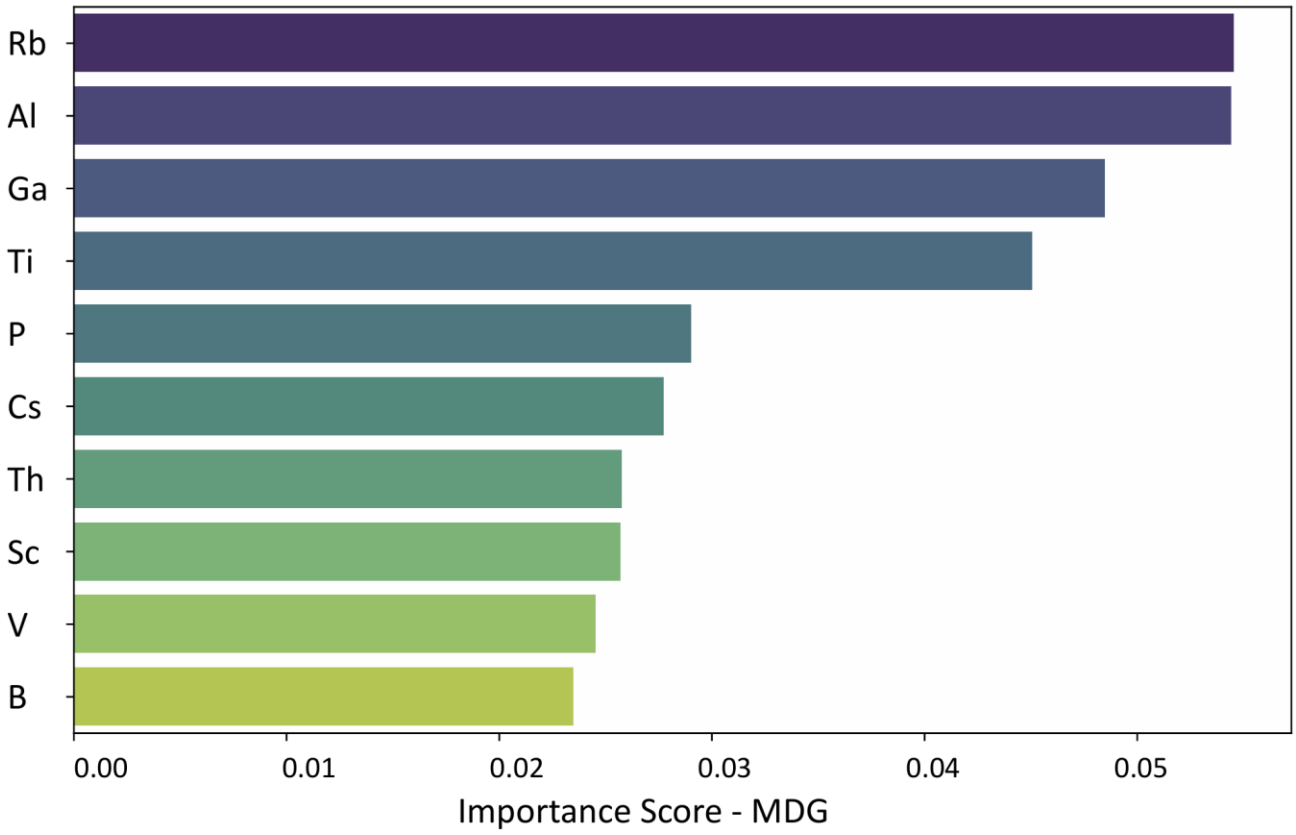


Figure 6.7. Mean Decrease Gini (MDG) scores for the top 10 predictors in the classification of WAGB black shale by associated mineralization. MDG measures the decrease in node impurity, averaged over all the trees in the RF model. Elements with the largest MDG values contribute most to sample separation and have the greatest predictive power.

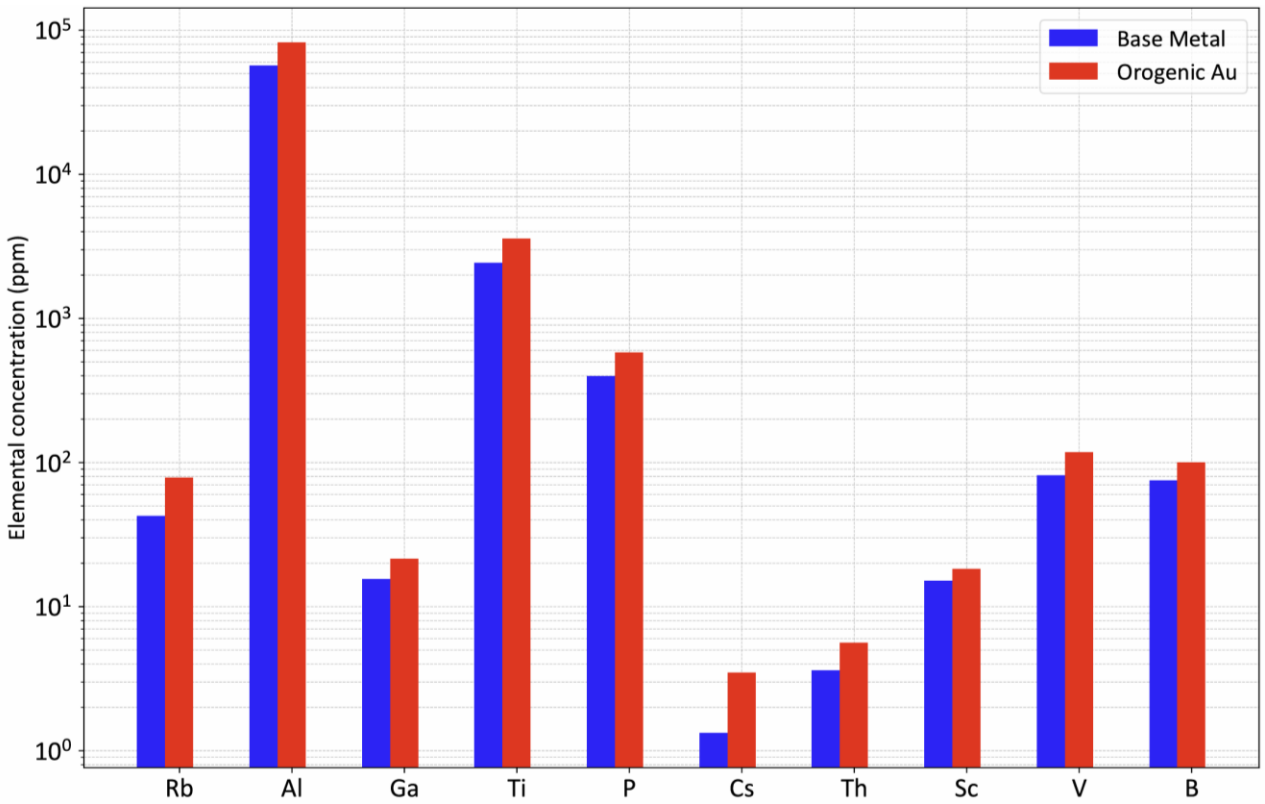


Figure 6.8. Concentrations of the 10 most important elements for RF classification of shale samples by associated mineralization. The elements are ordered from left to right by Importance Score indicated in Figure 6.7.

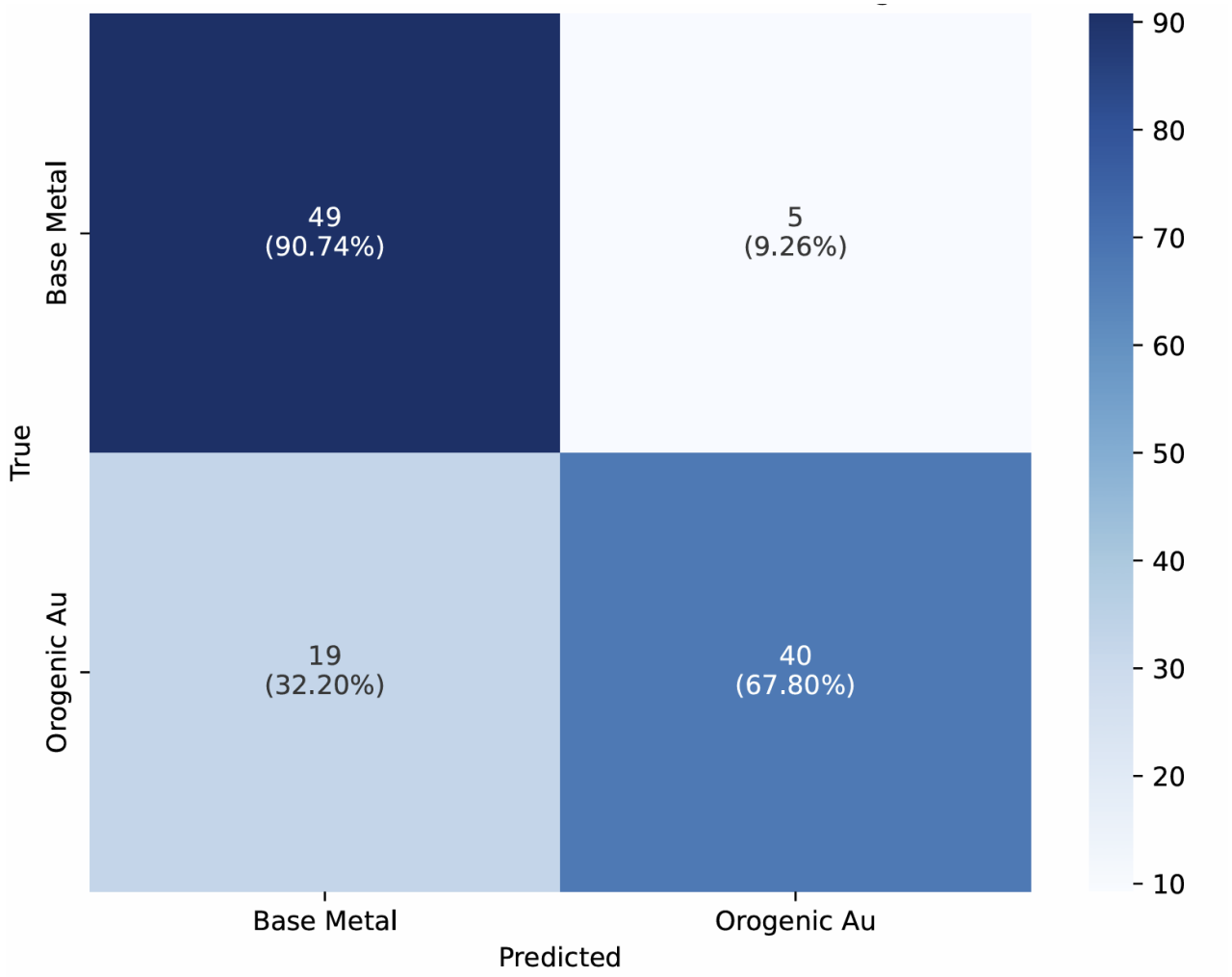


Figure 6.9. « Confusion Matrix » showing the proportion of correct classifications of shales associated with different mineralization in the test dataset. The model achieved an overall accuracy of 79%, with most samples correctly assigned to orogenic gold or base metal mineralization categories. The accuracy of the model is calculated as the sum of true positive + true negative values (49 + 40) divided by the total number of predictions (54 + 59).

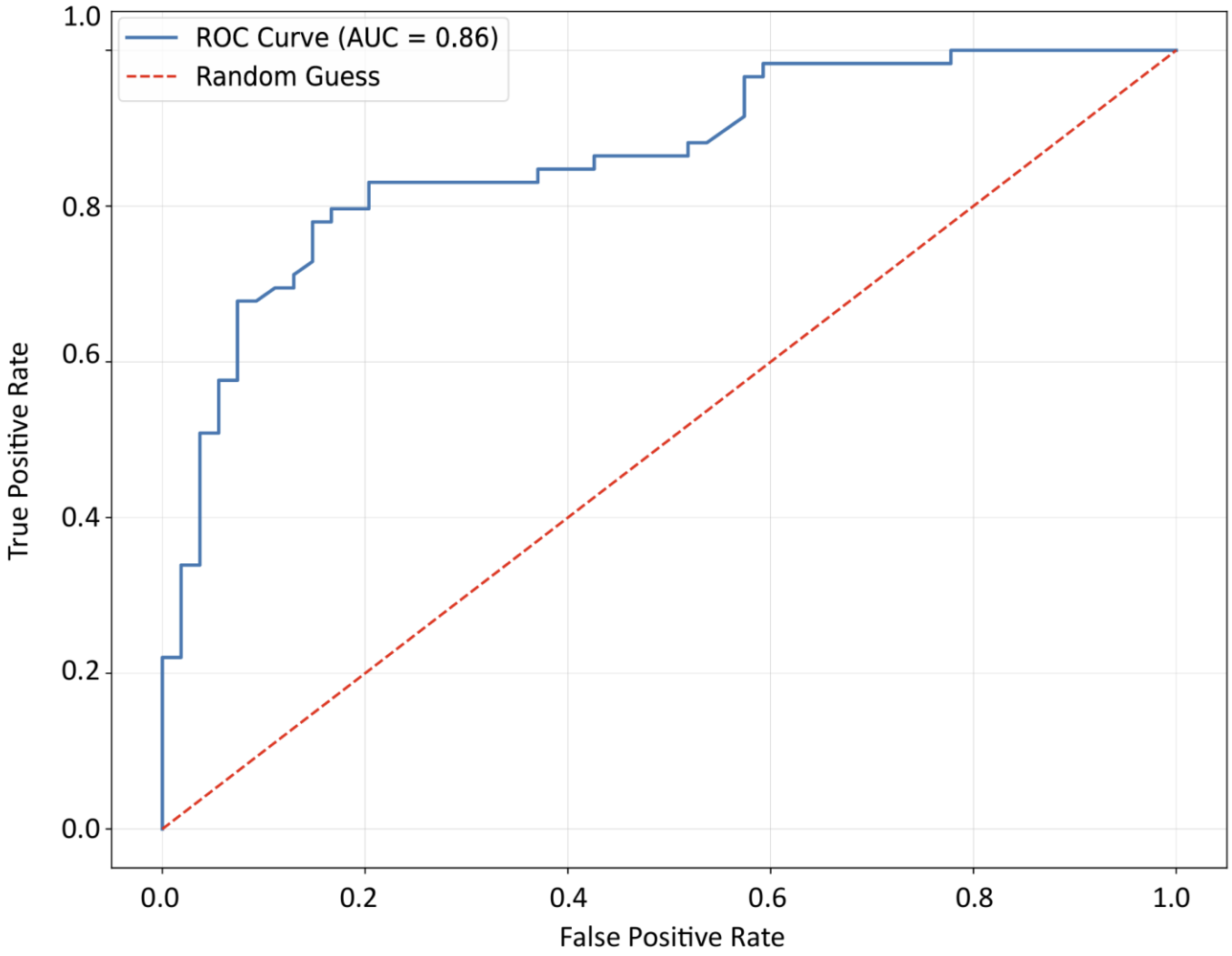


Figure 6.10. Receiver Operating Characteristic (ROC) curves and associated Area Under the Curve (AUC) values for shales classified by associated mineralization. The plot depicts the true positive rate as a function of the false positive rate. AUC quantifies the model's ability to differentiate between shales associated with orogenic gold and VMS-style mineralization. AUC values ≥ 0.86 for all classes indicates excellent class separation. Only two classes were used in this classification (orogenic Au, base metal) creating a binary ROC curve.

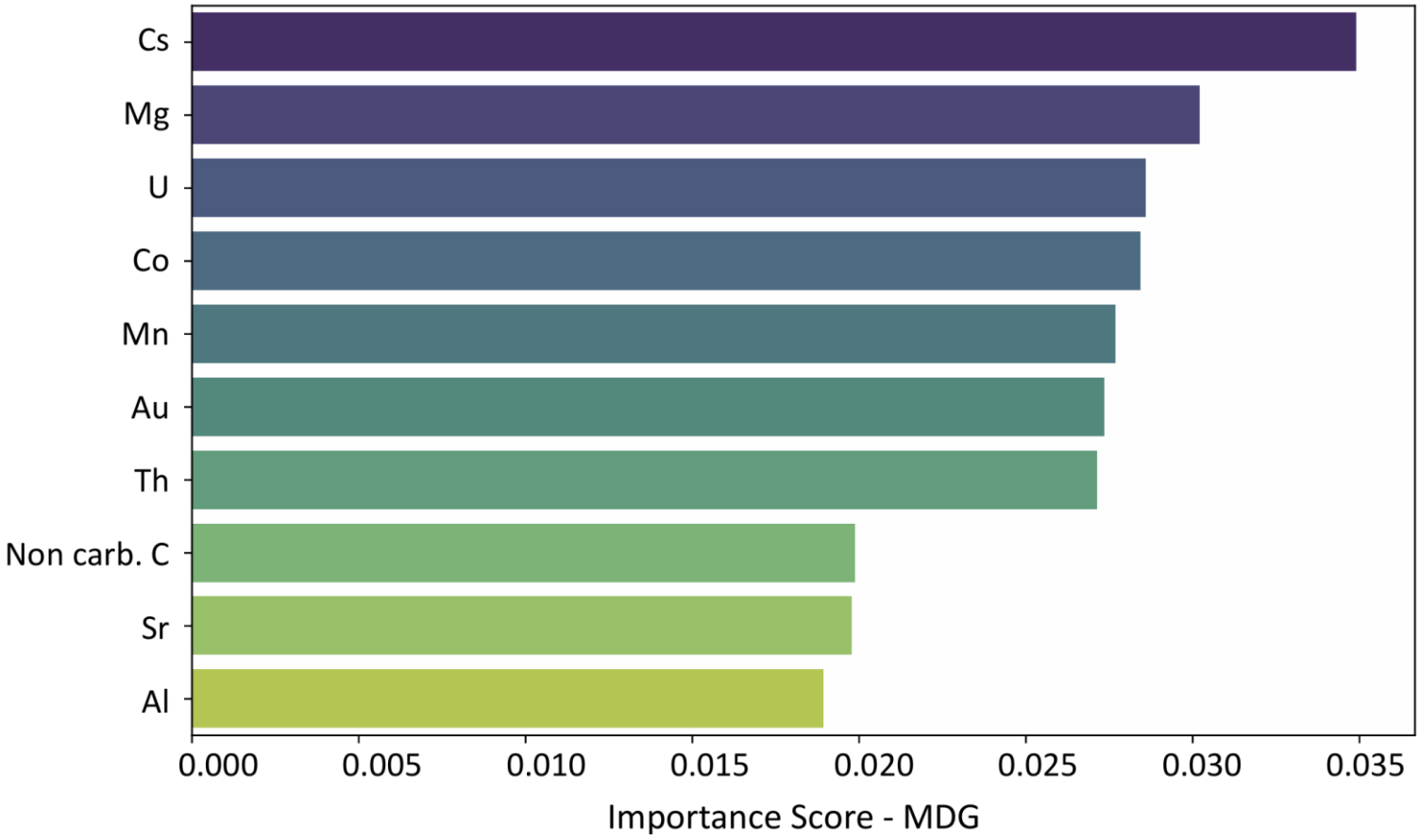


Figure 6.11. Mean Decrease Gini (MDG) scores for the top 10 predictors in the classification of WAGB black shale by associated mineralization. MDG measures the decrease in node impurity, averaged over all the trees in the RF model. Elements with the largest MDG values contribute most to sample separation and have the greatest predictive power.

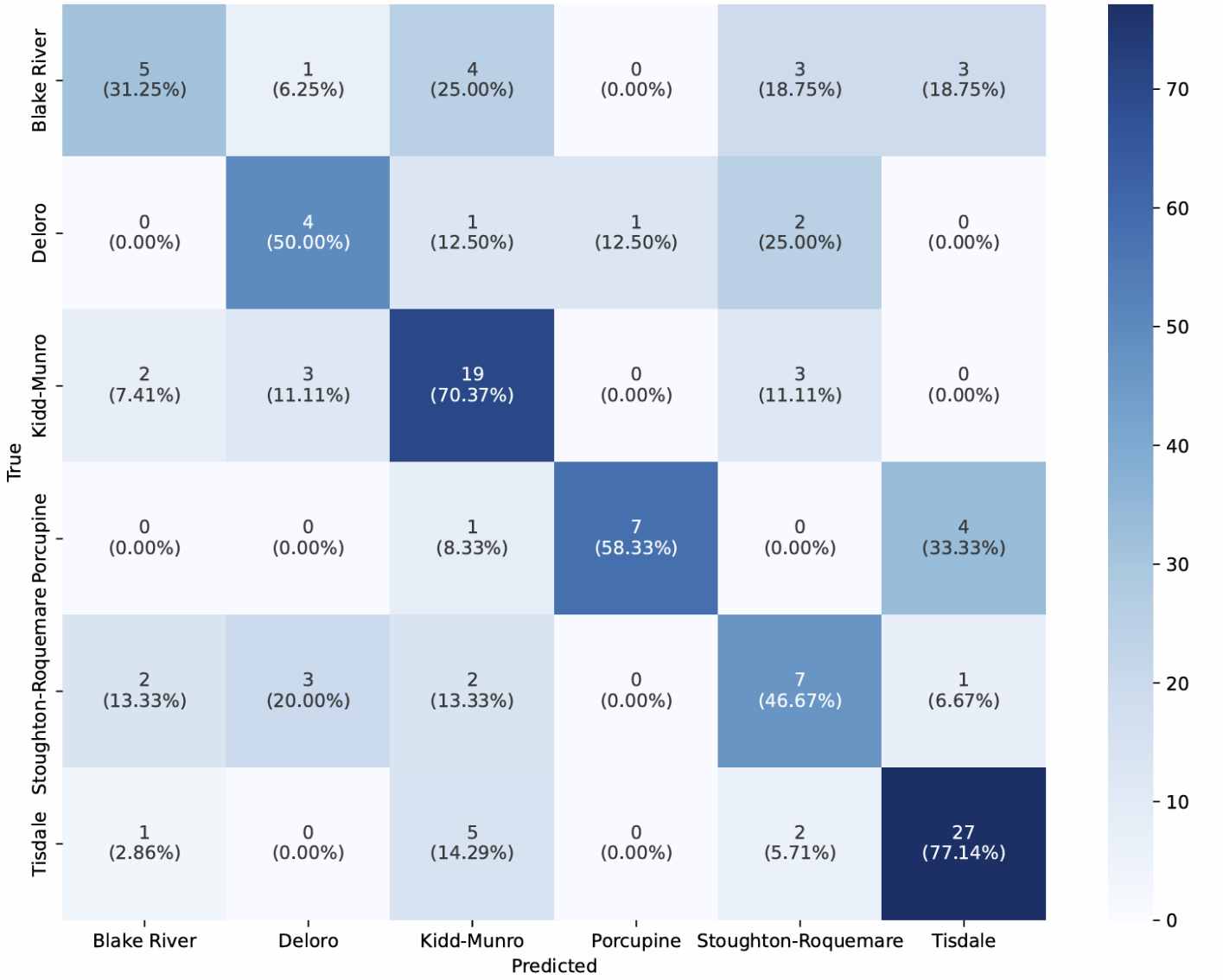


Figure 6.12. « Confusion Matrix » showing the proportion of correct classifications of shale associated with lithostratigraphic assemblages. The model achieved a low accuracy of 61%, with the samples assigned to one of the six assemblages. The accuracy of the model is calculated as the sum of true positive + true negative values (5 + 4 + 19 + 7 +7 + 27) divided by the total number of predictions (16 + 8 + 27 + 12 + 15+ 35). A large proportion of samples were misclassified into the wrong assemblage; however, a greater proportion of shales were successfully classified in the Tisdale and Kidd-Munro assemblages.

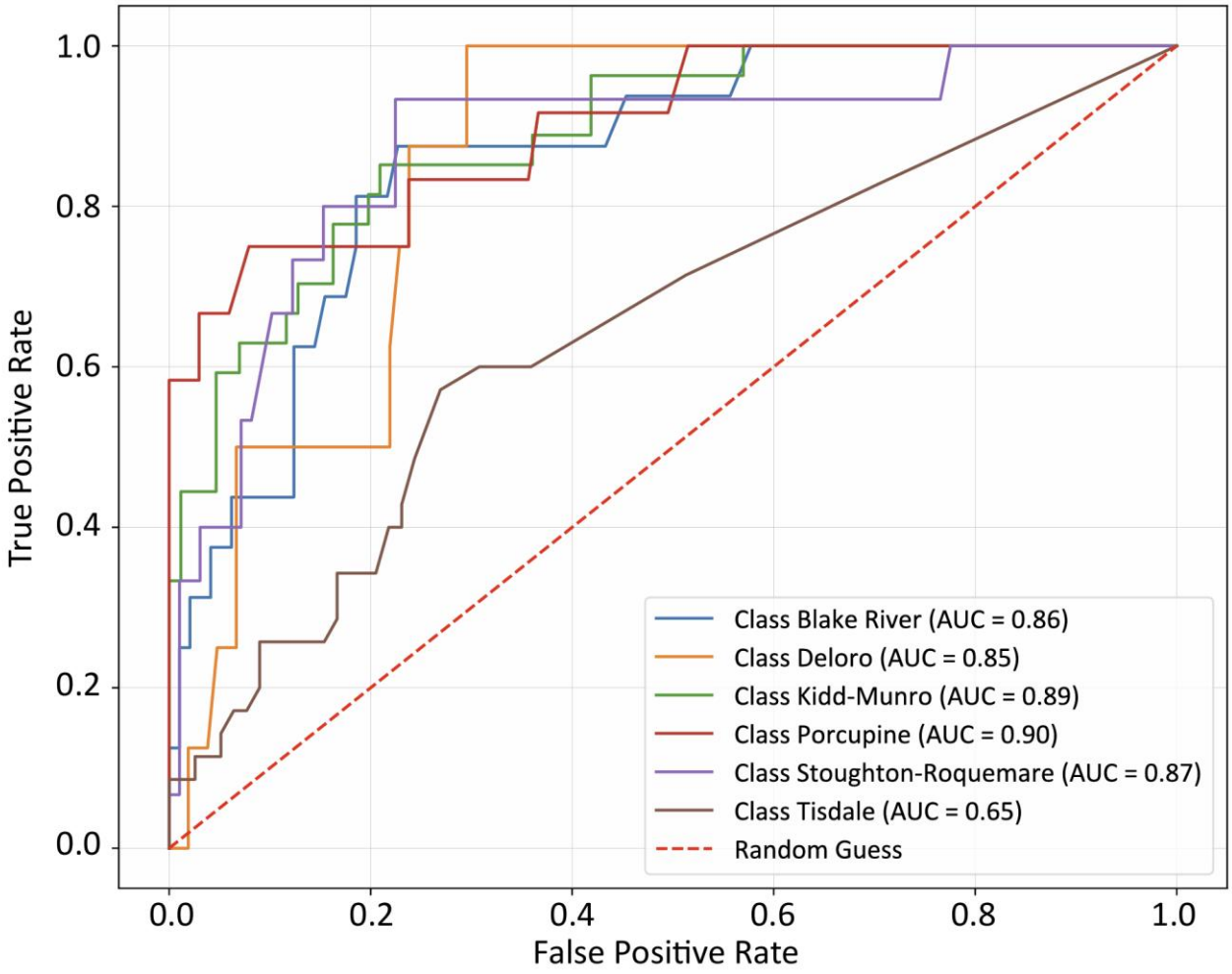


Figure 6.13. Receiver Operating Characteristic (ROC) curves and associated Area Under the Curve (AUC) values for shales classified by lithostratigraphic assemblage. The plot depicts the true positive rate as a function of the false positive rate. AUC quantifies the model's ability to differentiate between volcanic assemblages. AUC values ≥ 0.79 for all classes indicates satisfactory class separation.

Chapter 7 – Conclusions

This study used a combination of statistical analysis and machine learning to reveal previously unrecognized structure in the geochemical data of Abitibi shales. The results showed clear differences in the provenance, alteration, and possible relationship to mineralization of graphitic argillites in the Western Abitibi Greenstone Belt. Classifying shales based on the immobile element ratios, we successfully distinguished between mafic-, intermediate-, and felsic-type source rock compositions revealing differences in sediment transport, chemical weathering and alteration. Mafic-type shales are characterized by lower degrees of alteration and weathering on A-CN-K diagrams supporting the idea that they originate from a more proximal source (e.g., smaller volcanic sub-basins) and have undergone less transport and sediment sorting compared to felsic and intermediate-type shales (e.g., in larger turbidite-filled basins). This is a powerful tool for classification of samples that are indistinguishable in drill core.

Graphitic argillites were sampled throughout the Western AGB in bimodal mafic- and felsic-dominated volcanic successions of the Deloro, Stoughton-Roquemaure, Kidd-Munro, and Blake River assemblages as well as from regional turbidites in the Porcupine assemblage. Whole-rock geochemistry was found to be a robust discriminator between sediments derived from the proximal volcanic successions and those intercalated with more distal turbidite sequences. Key geochemical markers include REE enrichment and depletion due to sorting and recycling during transport, K metasomatism related to hydrothermal alteration of the (dominantly felsic and intermediate) source rocks, and enrichment in compatible elements (e.g., V, Cr, Sc) in mafic source rocks. Trace elements such as Sm, Zr, Al, Nd, Gd, Ce, Ti and La associated with REE-bearing heavy minerals like monazite, xenotime, and zircon collectively account for approximately 33% of the total variance in the dataset. Pearson correlation analysis and PCA identified the main mineralogical controls on the geochemistry of the sediments. Within this structurally complex and intensely altered region we successfully distinguished between shales from volcanic succession that were targeted for VMS and shales that were targeted for orogenic Au mineralization. Black shale enriched Rb, Sr, Cs, and Ba correlate with known orogenic gold deposits, while polymetallic sulphide components and mafic-associated elements, including Ni and Co, are enriched in shales associated with VMS and komatiite-hosted mineralization.

Spatial analysis, including Empirical Bayesian Kriging of the dataset, revealed strong correlations between geochemical characteristics of the shales and regional geological setting, including rift-related volcanic basins of the Kidd-Munro Assemblage arc-like terranes of the Blake River and later Porcupine assemblages. Clear divisions are seen separating the shale lithotypes in the northern and southern parts of the WAGB. Notably, samples with high PC1 scores (REE-bearing heavy mineral component) exhibit a strong spatial association with the Destor-Porcupine Fault Zone (DPFZ), aligning with the distribution of Porcupine metasediments along the main break and between the DPFZ and the Pipestone Fault. Shales with high PC3 scores (mafic volcanic-derived component) are considered to represent locally derived shales within reduced rift basins.

Random Forest classification, based on the Ti/Zr ratio as a proxy for shale lithotype, achieved a 91% classification accuracy. Future applications of the RF model should focus on the previously untested data sets in the region, including SIGEOM whole-rock compilations from the Eastern Abitibi. The RF model should also be applicable to classification of large data sets, such as the USGS Global Geochemical Database for Critical Metals in Black Shales (CMIBS; Granitto et al., 2017), which includes nearly 90,000 samples from all seven continents.

7.1 Comparison to Global Standards (PAAS)

Taylor & McLennan (1985) compiled an average of 23 post-Archean Australian shale (PAAS) samples that provides a widely used geochemical reference for average shale composition and for normalizing similar lithologies. Figure 7.1 presents a box and whisker plot comparing the weight percent concentration of major oxides in shales of the Western Abitibi Greenstone Belt to PAAS. The differences in abundance of major oxides (in weight percentage) reflect the more mafic and ultramafic input from the less evolved Archean crust in the Abitibi. This is indicated by preferential removal of more mobile elements like Na and Ca while concentrating residual, immobile elements like Al and Ti (Nesbitt and Young, 1982; Morton and Hallsworth, 1999). Elevated concentrations of Al_2O_3, K_2O and TiO_2 in post-Archean shales also suggest the presence of clay minerals and rutile. Most trace elements exhibit slightly higher concentrations in PAAS relative to AGB samples, although Sr and Eu are notably enriched in Abitibi shales possibly

reflecting their proximal volcanic derivation and lower degree of weathering (Figure 7.2). The WAGB shales are depleted in LREE compared to PAAS and show a positive Eu anomaly (see Chapter 4). This is interpreted to reflect the more mafic composition of the Archean shales. The positive Eu anomaly in some shales may also be related to alteration by reduced hydrothermal fluids. Positive Eu anomalies can occur in hydrothermal precipitates, including chemical sediments (e.g., Liu et al., 2017). This is a strong positive indicator of proximity to a hydrothermal source for the Eu^{2+}.

7.2 Missing Kidd Creek Data

The effect of the missing data in the 4 townships surrounding Kidd Creek is shown in Figure 7.3. Limited public domain data on shales from Carnegie, Prosser, and Kidd townships from Chapman et al. (2010) were added to the Kriged data set for PC1. The data were taken through the same steps outlined in Chapter 3 including PCA and Empirical Bayesian Kriging. The additional data demonstrate that the initial Kriging accurately interpolated the shale geochemistry in the area with no samples, and the same PCs account for the majority of the variance in both data sets (Table 7.1). However, a large number of the 184 samples in the Chapman et al. (2010) collection were intensely mineralized, and the alteration of the shales is indicated by the scatter of the samples in the Th-Zr/10-Sc ternary diagram and Th/Sc versus Zr/Sc plot (Figures 7.4 and 7.5).

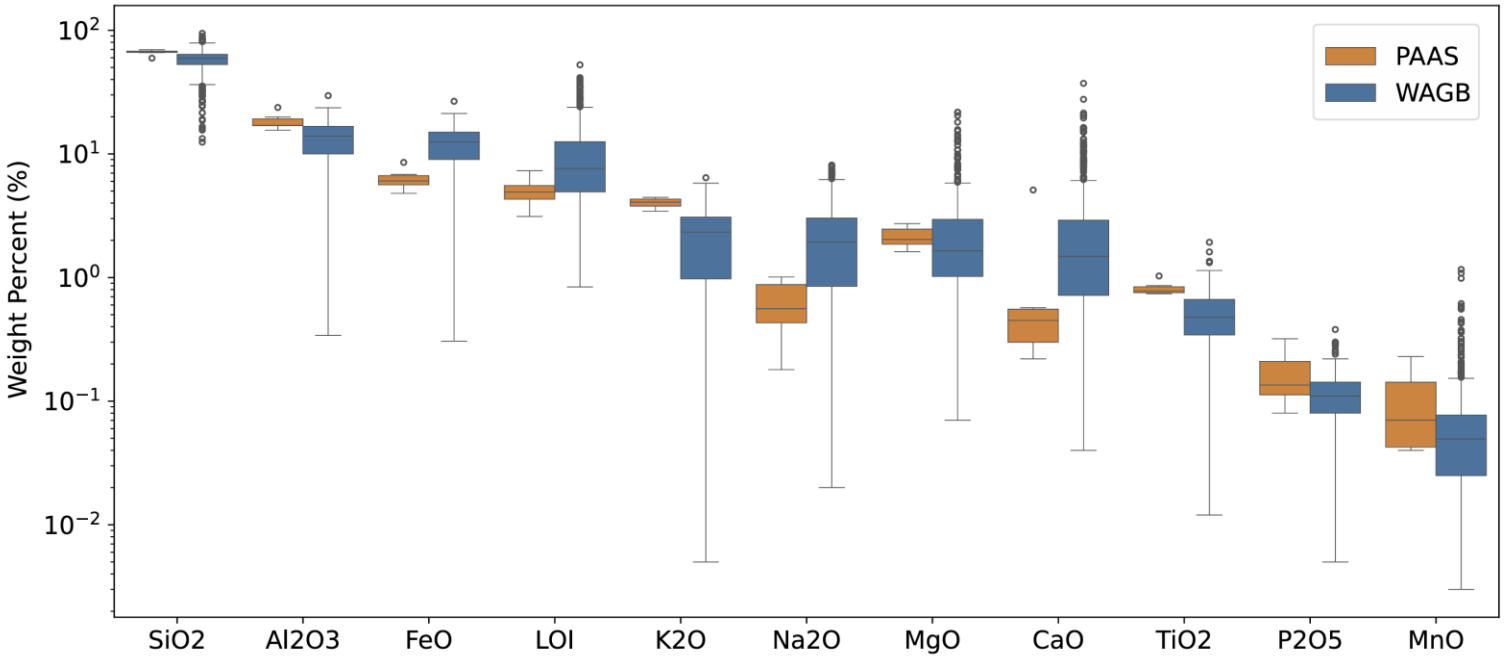


Figure 7.1. Box and whisker plots showing the weight percent concentration of major oxides in shales of the Western Abitibi Greenstone Belt (WAGB) compared to the Post-Archean Australian Shale (PAAS) average from Taylor & McLennan (1985). Whiskers extend to minimum and maximum values with outliers marked as individual points. WAGB samples exhibit a broader compositional spread for several major oxides. Notably, PAAS values for SiO_2, Al_2O_3, K_2O, TiO_2 are consistently higher than those in Abitibi shales, while FeO, Na_2O, and CaO concentrations are lower. These differences may reflect a greater mafic influence in the Abitibi source rocks on the composition of shales.

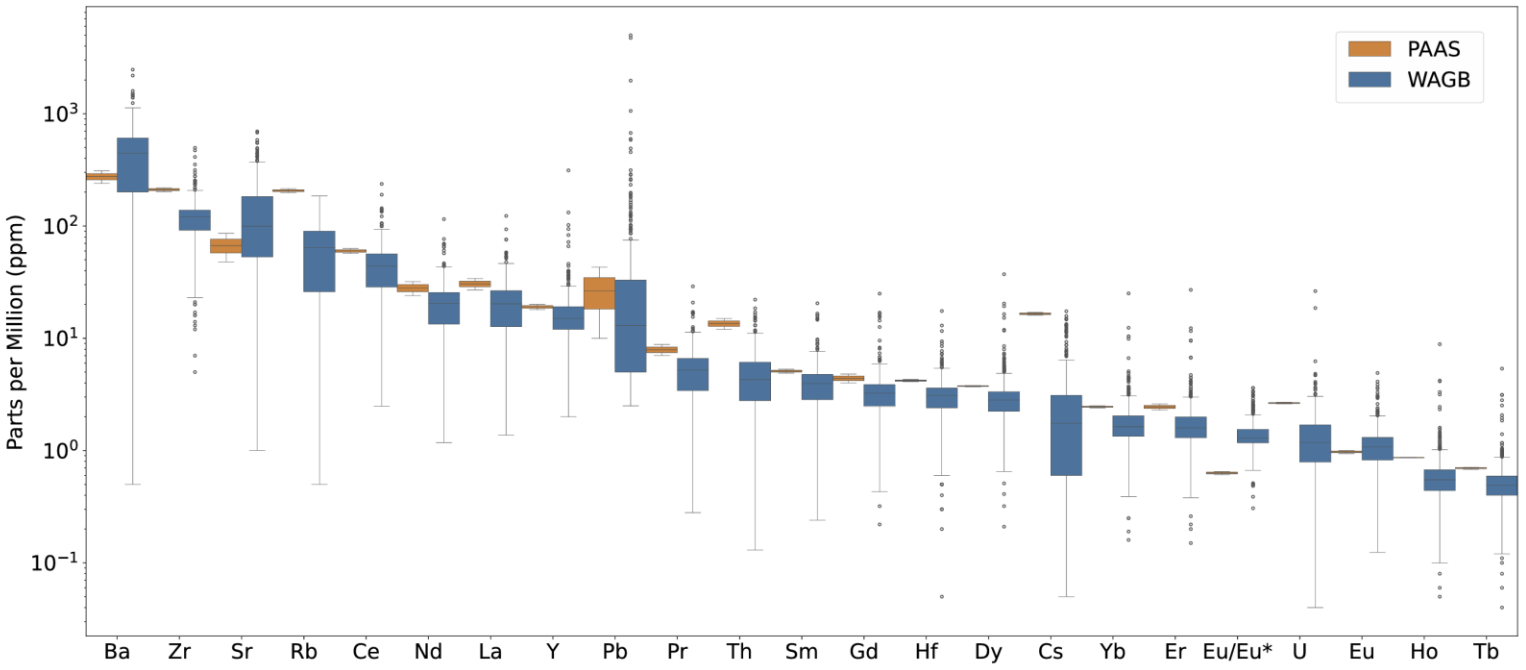
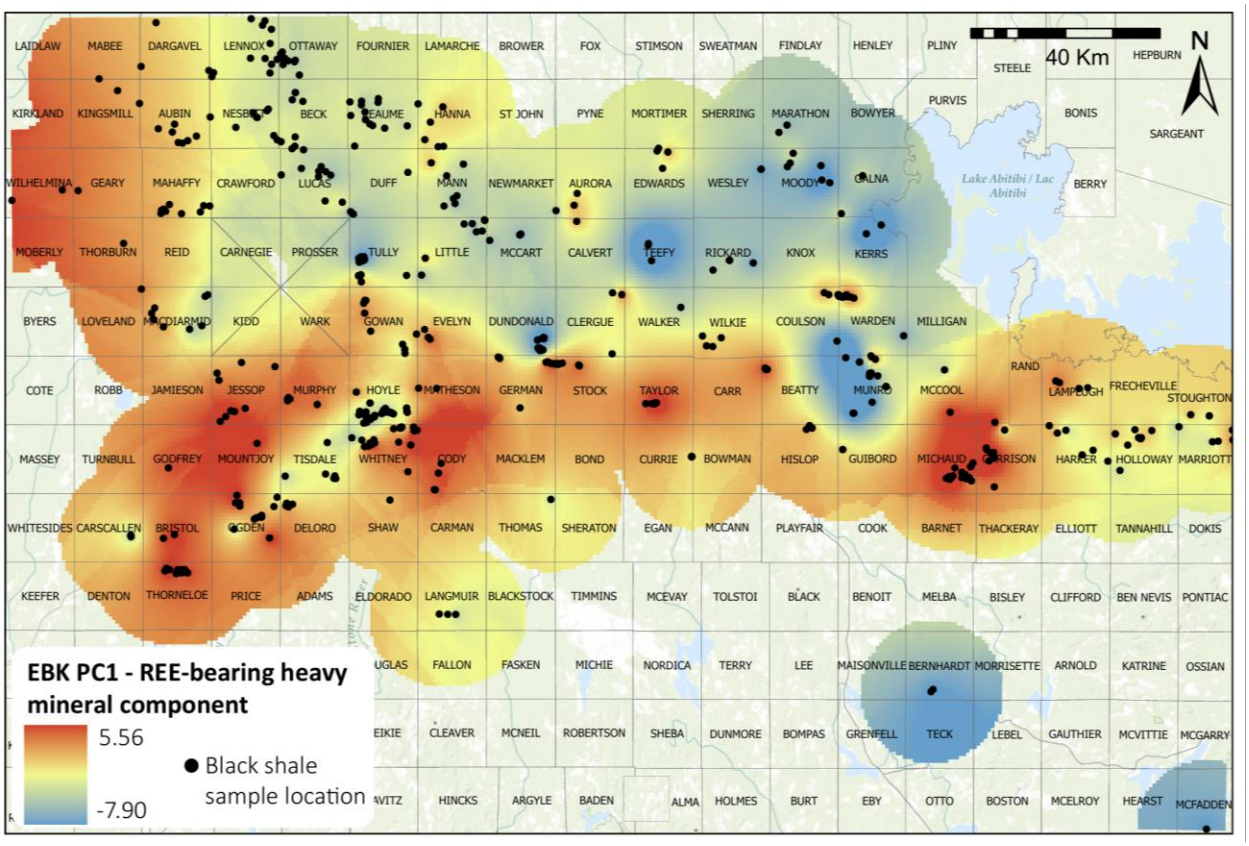


Figure 7.2. Box and whisker plot showing trace elements concentrations (ppm) in shale samples from the Western Abitibi Greenstone Belt (WAGB) compared to the Post-Archean Australian Shale (PAAS) average from Taylor & McLennan (1985). Whiskers extend to minimum and maximum values with outliers marked as individual points. Most trace elements exhibit slightly higher concentrations in PAAS relative to Abitibi samples.

A)


EBK PC1 - REE-bearing heavy mineral component
5.56
-7.90
Black shale sample location
40 Km
N
LAIDLAW
MABEE
DARGAVEL
LENNOX
OTTAWAY
FOURNIER
LAMARCHE
BROWER
FOX
STIMSON
SWEATMAN
FINDLAY
HENLEY
PLINY
STEELE
HEPBURN
SARGEANT
KIRKLAND
KINGSMILL
AUBIN
NESBIT
BECK
BEAUME
HANNA
ST JOHN
PYNE
MORTIMER
SHERRING
MARATHON
BOWYER
PURVIS
BONIS
WILHELMINA
GEARY
MAHAFFY
CRAWFORD
LUCAS
DUFF
MANN
NEWMARKET
AURORA
EDWARDS
WESLEY
MOODY
CALNA
Lake Abitibi / Lac Abitibi
BERRY
MOBERLY
THORBURN
REID
CARNEGIE
PROSSER
TULLY
LITTLE
MCCART
CALVERT
TEEFY
RICKARD
KNOX
KERRS
BYERS
LOVELAND
MACDIARMID
KIDD
WARK
GOWAN
EVELYN
DUNDONALD
CLERGUE
WALKER
WILKIE
COULSON
WARDEN
MILLIGAN
RAND
COTE
ROBB
JAMIESON
JESSOP
MURPHY
HOYLE
MATHESON
GERMAN
STOCK
TAYLOR
CARR
BEATTY
MUNRO
MCCOOL
LAMPLUGH
FRECHEVILLE
STOUGHTON
MASSEY
TURNBULL
GODFREY
MOUNTJOY
TISDALE
WHITNEY
CODY
MACKLEM
BOND
CURRIE
BOWMAN
HISLOP
GUIBORD
MICHAUD
HARKER
HOLLOWAY
MARRIOTT
WHITESIDES
CARSCALLEN
BRISTOL
OGDEN
DELORO
SHAW
CARMAN
THOMAS
SHERATON
EGAN
MCCANN
PLAYFAIR
COOK
BARNET
THACKERAY
ELLIOTT
TANNAHILL
DOKIS
KEEFER
DENTON
THORNELOE
PRICE
ADAMS
ELDORADO
LANGMUIR
BLACKSTOCK
TIMMINS
MCEVAY
TOLSTOI
BLACK
BENOIT
MELBA
BISLEY
CLIFFORD
BEN NEVIS
PONTIAC
UGLAS
FALLON
FASKEN
MICHIE
NORDICA
TERRY
LEE
MAISONVILLE
BERNHARDT
MORRISETTE
ARNOLD
KATRINE
OSSIAN
EIKIE
CLEAVER
MCNEIL
ROBERTSON
SHEBA
DUNMORE
BOMPAS
GRENFELL
TECK
LEBEL
GAUTHIER
MCVITTIE
MCGARRY
AVITZ
HINCKS
ARGYLE
BADEN
ALMA
HOLMES
BURT
EBY
OTTO
BOSTON
MCELROY
HEARST
MCFADDEN

B)

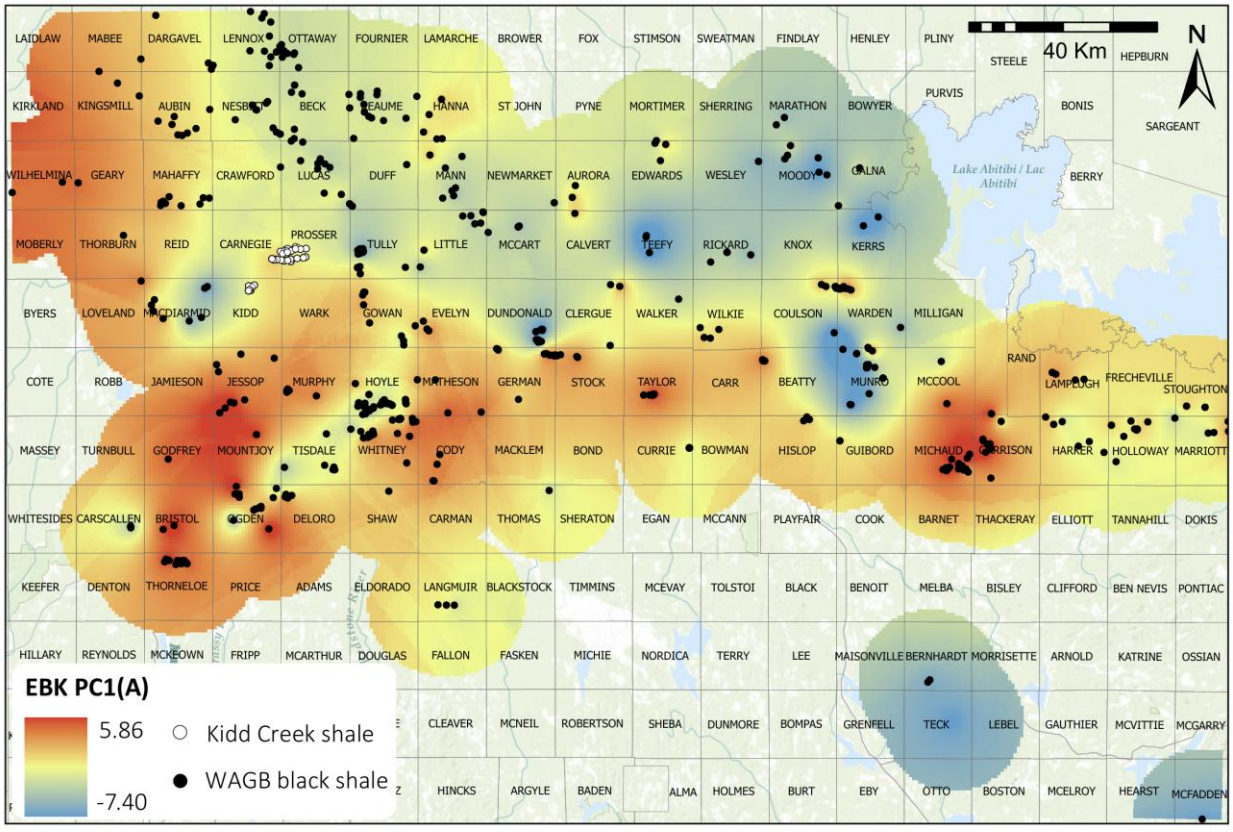

EBK PC1(A)
5.86
-7.40
Kidd Creek shale
WAGB black shale
40 Km
N
LAIDLAW
MABEE
DARGAVEL
LENNOX
OTTAWAY
FOURNIER
LAMARCHE
BROWER
FOX
STIMSON
SWEATMAN
FINDLAY
HENLEY
PLINY
STEELE
HEPBURN
SARGEANT
KIRKLAND
KINGSMILL
AUBIN
NESBIT
BECK
BEAUME
HANNA
ST JOHN
PYNE
MORTIMER
SHERRING
MARATHON
BOWYER
PURVIS
BONIS
WILHELMINA
GEARY
MAHAFFY
CRAWFORD
LUCAS
DUFF
MANN
NEWMARKET
AURORA
EDWARDS
WESLEY
MOODY
CALNA
Lake Abitibi / Lac Abitibi
BERRY
MOBERLY
THORBURN
REID
CARNEGIE
PROSSER
TULLY
LITTLE
MCCART
CALVERT
TEEFY
RICKARD
KNOX
KERRS
BYERS
LOVELAND
MACDIARMID
KIDD
WARK
GOWAN
EVELYN
DUNDONALD
CLERGUE
WALKER
WILKIE
COULSON
WARDEN
MILLIGAN
RAND
COTE
ROBB
JAMIESON
JESSOP
MURPHY
HOYLE
MATHESON
GERMAN
STOCK
TAYLOR
CARR
BEATTY
MUNRO
MCCOOL
LAMPLUGH
FRECHEVILLE
STOUGHTON
MASSEY
TURNBULL
GODFREY
MOUNTJOY
TISDALE
WHITNEY
CODY
MACKLEM
BOND
CURRIE
BOWMAN
HISLOP
GUIBORD
MICHAUD
HARKER
HOLLOWAY
MARRIOTT
WHITESIDES
CARSCALLEN
BRISTOL
OGDEN
DELORO
SHAW
CARMAN
THOMAS
SHERATON
EGAN
MCCANN
PLAYFAIR
COOK
BARNET
THACKERAY
ELLIOTT
TANNAHILL
DOKIS
KEEFER
DENTON
THORNELOE
PRICE
ADAMS
ELDORADO
LANGMUIR
BLACKSTOCK
TIMMINS
MCEVAY
TOLSTOI
BLACK
BENOIT
MELBA
BISLEY
CLIFFORD
BEN NEVIS
PONTIAC
HILLARY
REYNOLDS
MCKEOWN
FRIPP
MCARTHUR
DOUGLAS
FALLON
FASKEN
MICHIE
NORDICA
TERRY
LEE
MAISONVILLE
BERNHARDT
MORRISETTE
ARNOLD
KATRINE
OSSIAN
CLEAVER
MCNEIL
ROBERTSON
SHEBA
DUNMORE
BOMPAS
GRENFELL
TECK
LEBEL
GAUTHIER
MCVITTIE
MCGARRY
HINCKS
ARGYLE
BADEN
ALMA
HOLMES
BURT
EBY
OTTO
BOSTON
MCELROY
HEARST
MCFADDEN

Figure 7.3. A) Empirical Bayesian Kriging of PC1 scores (detrital heavy mineral component) of 564 graphitic argillite samples from the western AGB (See Figure 5.7 for explanation). Black dots represent sample locations. No samples from Carnegie, Prosser, Kidd, and Wark townships were used for this model. B) Kriged data for PC1 including limited public domain data on shales from Carnegie, Prosser, and Kidd townships from Chapman et al. (2010). The Kidd Creek data were added to the WAGB data set and taken through the same steps outlined in Chapter 3 including PCA and Empirical Bayesian Kriging. The comparison shows the initial Kriging attempt in A) accurately predicted the shale geochemistry in the townships with no data. One of the challenges of incorporating new data was that multiple graphitic argillite units were sampled from the same drill hole. To overcome this, only the average values were used from each new drill hole added to the global data set.

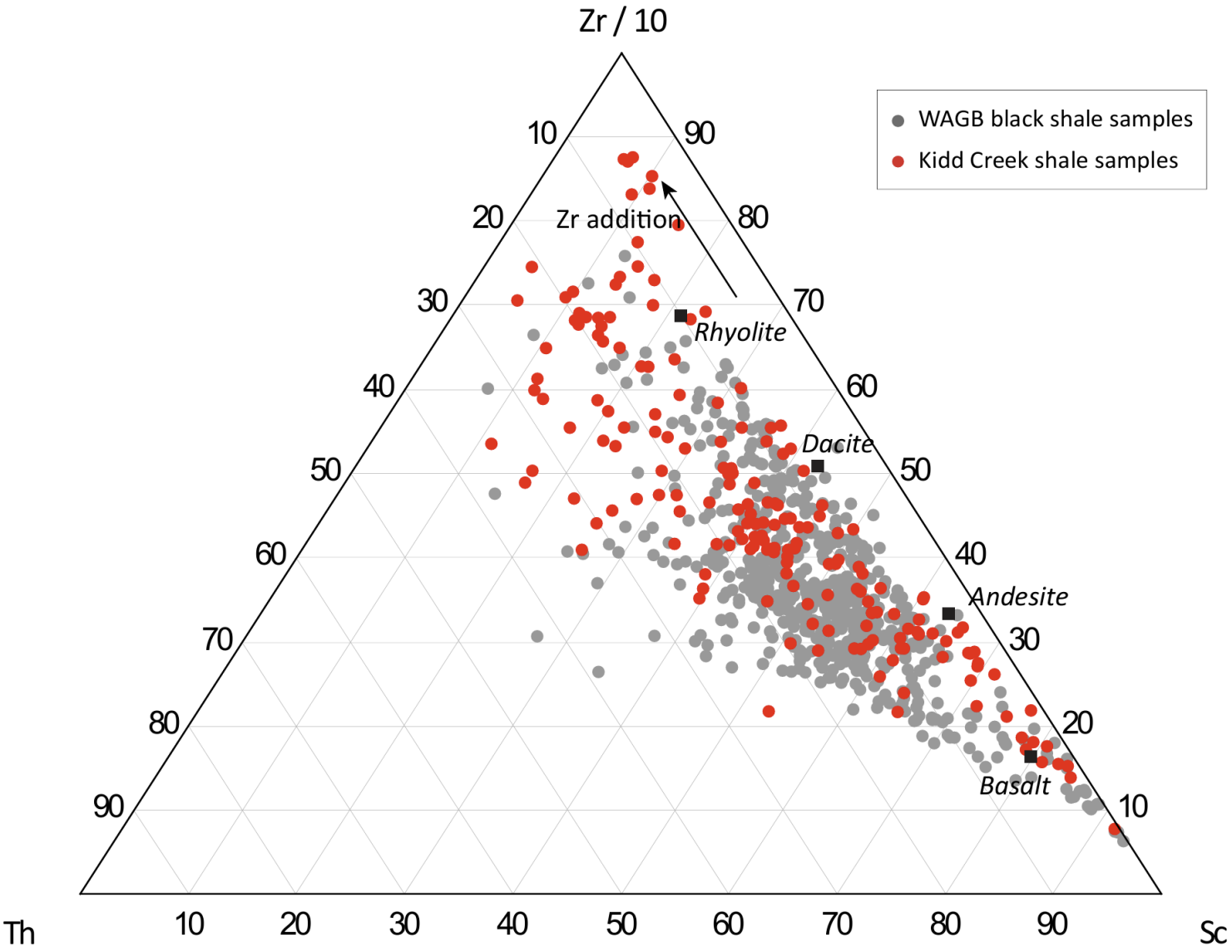


Figure 7.4. Th-Zr/10-Sc ternary diagram after Bhatia and Crook (1986) of western Abitibi shale samples near the Kidd Creek VMS deposit (N = 185) from Chapman et al. (2010). The Kidd Creek shale samples show a broad range of compositions with distinct Zr enrichment compared to the WAGB black shale samples. The scatter in the Kidd Creek data is an indication of intense alteration and therefore a potential indicator of nearby mineralization.

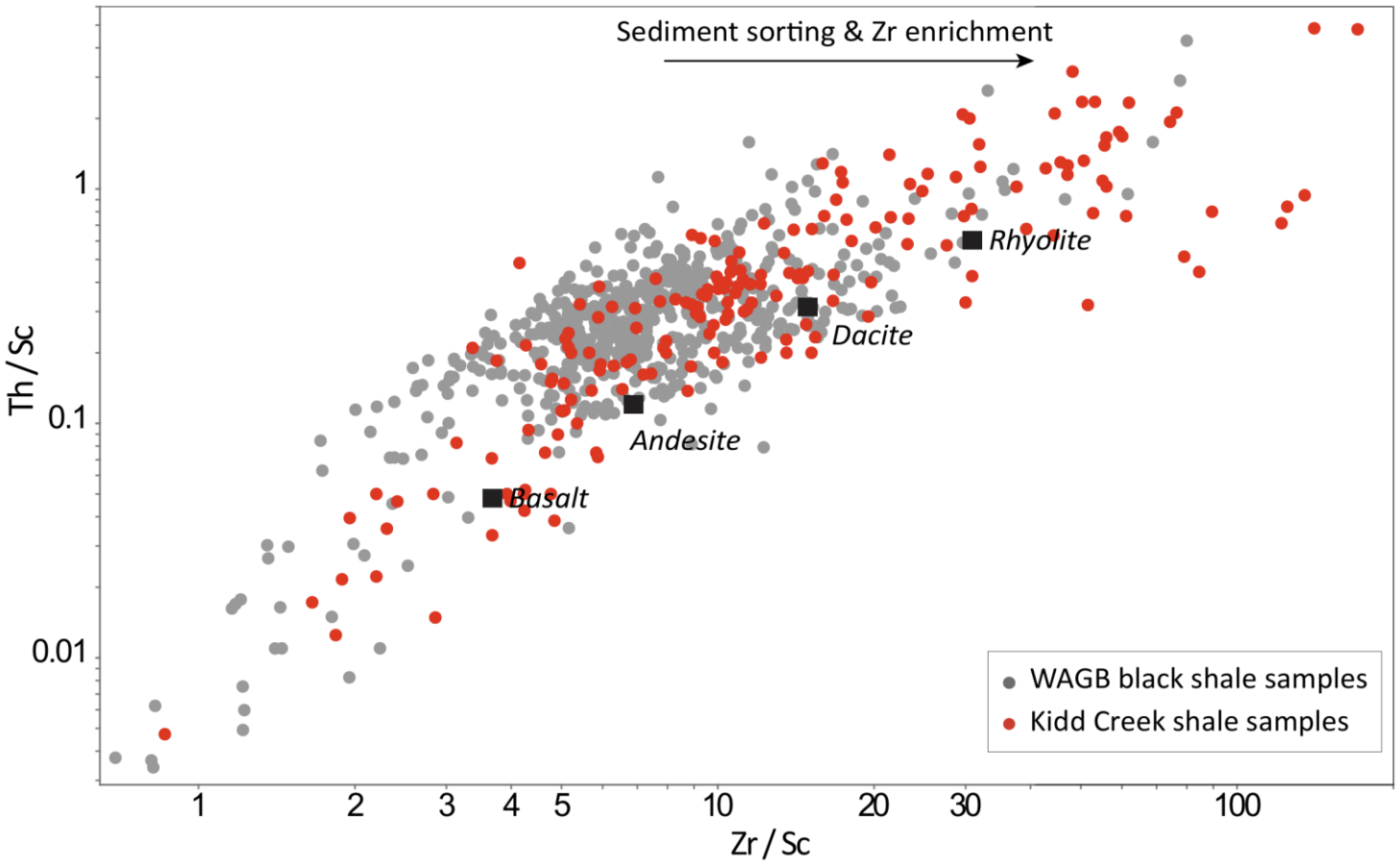


Figure 7.5. Plot of Th/Sc versus Zr/Sc modified from McLennan et al., 1993, showing western Abitibi shale samples near the Kidd Creek VMS deposit (N = 185) from Chapman et al. (2010). Both trace element ratios increase with igneous differentiation, however, in the upper right corner of the diagram shows strong effects of sediment sorting and concentration of zircon. The Kidd Creek shale samples show distinct Zr enrichment compared to the WAGB black shale samples.

Table 7.1. Summary table for the first principal components of the PCA for 564 WAGB black shale samples + 184 Kidd Creek shale samples, representing ~33% of the total variance.

Element loading	PC1 - WAGB	PC1(A) – WAGB + Kidd Creek
Positive	Sm, Hf, Al, Nd, Zr, Nb, Pr, Gd, Ga, Ta, Ce	Sm, Hf, Nd, Zr, Pr, Nb, Gd, Al, Ta, Ce
Negative	S, Hg, LOI, Cd, non-carb. C, Zn, Pb, Cu, Mo, Au, Co	C, Hg, LOI, Cd, S, Cu, Zn, Pb, Co, Mo

Given the similarity between the element loadings in each PC we can deduce that both PC1 and PC1(A) represent the REE-bearing heavy mineral component.

References:

Aitchison, J. (1982). The statistical analysis of compositional data. Journal of the Royal Statistical Society: Series B (Methodological), v. 44, issue 2, p. 139 - 160.

Anderson, T. W. (2003). An Introduction to Multivariate Statistical Analysis (3rd ed.). Wiley-Interscience, p. 459 – 486.

Armstrong, J. G. T., Parnell, J., Bullock, L. A., Perez, M., Boyce, A. J., & Feldmann, J. (2018). Tellurium, selenium and cobalt enrichment in Neoproterozoic black shales, Gwna Group, UK: Deep marine trace element enrichment during the Second Great Oxygenation Event. Terra Nova, v. 30, issue 3, p. 244 – 253.

Armstrong, J. G., Parnell, J., Bullock, L. A., Boyce, A. J., Perez, M., & Feldmann, J. (2019). Mobilisation of arsenic, selenium and uranium from Carboniferous black shales in west Ireland. Applied geochemistry, v. 109, p. 1 - 13.

Ayer, J., Amelin, Y., Corfu, F., Kamo, S., Ketchum, J., Kwok, K., & Trowell, N. (2002). Evolution of the southern Abitibi greenstone belt based on U–Pb geochronology: autochthonous volcanic construction followed by plutonism, regional deformation and sedimentation. Precambrian Research, v. 115, issue 1, p. 63 – 95.

Ayer, J.A., Berger, B.R., Hall, L.A.F., Houlé, M.G., Johns, G.W., Josey, S., Madon, Z., Rainsford, D., Trowell, N.F. & Vaillancourt, C. (2005a). Geological compilation of the central Abitibi greenstone belt: Kapuskasing Structural Zone to the Québec border; Ontario Geological Survey, Preliminary Map P.3565, scale 1:250 000.

Ayer, J.A., Thurston, P.C., Bateman, R.J., Dubé, B., Gibson, H.L., Hamilton, M.A., Hathway, B., Hocker, S., Houlé, M.G., Hudak, G., Ispolatov, V., Lafrance, B., Lesher, C.M., MacDonald, P.J., Péloquin, A.S., Piercey, S.J., Reed, L.E. & Thompson, P.H. (2005b). Overview of results from the greenstone architecture project: Discover Abitibi Initiative; Ontario Geological Survey, Open File Report 6154, p. 146.

Barrett, T. J., Cattalani, S., & MacLean, W. H. (1993). Volcanic lithogeochemistry and alteration at the Delbridge massive sulphide deposit, Noranda, Quebec. Journal of Geochemical Exploration, v. 48, issue 2, p. 135 – 173.

MacLean, W. H., & Barrett, T. J. (1993). Lithogeochemical techniques using immobile elements. Journal of Geochemical Exploration, v. 48, issue 2, p. 109 – 133.

Behnamian, A., Millard, K., Banks, S. N., White, L., Richardson, M., & Pasher, J. (2017). A systematic approach for variable selection with random forests: achieving stable variable importance values. IEEE Geoscience and Remote Sensing Letters, v. 14, issue 11, p. 1988 – 1992.

Bhatia, M. R., & Crook, K. A. W. (1986). Trace element characteristics of graywackes and tectonic setting discrimination of sedimentary basins. Contributions to Mineralogy and Petrology, v. 92, issue 2, p. 181 – 193.

Bisht, R.K., & Bisht, I.P. (2023). Investigation of the Role of Test Size, Random State, and Dataset in the Accuracy of Classification Algorithms. In Sharma, H., Shrivastava, V., Bharti, K.K., Wang, L. (Eds.), Communication and Intelligent Systems. ICCIS 2022. (Lecture Notes in Networks and Systems). Springer, v. 686, p. 715 – 726.

Bivand, R. S., Pebesma, E. J., & Gómez-Rubio, V. (2008). Chapter 7 – Spatial Point Pattern Analysis. In Applied spatial data analysis with *R*. Springer, p. 173 – 212.

Breiman, L., Friedman, J. H., Olshen, R. A., & Stone, C. J. (1984). Splitting Rules. In Classification and Regression Trees (1st ed). CRC Press, p. 93 – 129.

Breiman, L. (2001). Random Forests. Machine Learning, v. 45, issue 1, 5–32.

Breiman, L. (2002). Manual on setting up, using, and understanding random forests (Technical Report No. 1). Statistics Department University of California, Berkeley, USA, v. 1, issue 58, p. 3 - 42.

Busby, C., & Pérez, A, A. (Eds.). (2012). Tectonics of sedimentary basins: Recent advances in the tectonics of sedimentary basins. Wiley-Blackwell. p. 1 - 631.

Cao, C., Liu, X. M., & Chen, J. (2022). Cerium anomaly as a tracer for paleo-oceanic redox conditions: A thermodynamics-based Ce oxidation modeling approach. Frontiers in Earth Science, v. 10, p. 1 – 11.

Chapman, J.B., J.M. Peter, J.M. and Layton-Matthews, D. (2008). Volcanogenic massive sulphide vectors? Decoding geochemical variability in metalliferous black shales of the Kidd–Munro assemblage; in Summary of Field Work and Other Activities 2008, Ontario Geological Survey, Open File Report 6226, p.7-1 to 7-7.

Chapman, J.B., Peter, J.M., and Layton-Matthews, D. (2010). Geochemistry database for carbonaceous and sulphidic metasediment horizons of the western Neoarchean Kidd Munro assemblage, Abitibi Subprovince, Ontario; Geological Survey of Canada, Open File 6550.

Chawla, N. V., Bowyer, K. W., Hall, L. O., & Kegelmeyer, W. P. (2002). SMOTE: synthetic minority over-sampling technique. Journal of artificial intelligence research, v. 16, p. 321 - 357.

Chown, E. H., Daigneault, R., Mueller, W., & Mortensen, J. K. (1992). Tectonic evolution of the Northern Volcanic Zone, Abitibi belt, Quebec. Canadian Journal of Earth Sciences, v. 29, issue 10, p. 2211 – 2225.

Condie, K. (2001). Precambrian superplumes and supercontinents: A record in black shales, carbon isotopes, and paleoclimates? Precambrian Research, v. 106, issue 3–4, p. 239 – 260.

Cotton, S. A. (2011). Scandium, Yttrium & the Lanthanides: Inorganic & Coordination Chemistry. In Encyclopedia of Inorganic and Bioinorganic Chemistry. John Wiley & Sons, Ltd. p. 1 – 40.

Cutler, D. R., Edwards Jr, T. C., Beard, K. H., Cutler, A., Hess, K. T., Gibson, J., & Lawler, J. J. (2007). Random forests for classification in ecology. Ecology, v. 88, issue 11, p. 2783 - 2792.

Davies, J. F., & Whitehead, R. E. (1994). Molar ratios in the study of unaltered and hydrothermally altered greywackes and shales. Chemical Geology, v. 111, issue 1 - 4, p. 85 - 100.

Disha, R. A., & Waheed, S. (2022). Performance analysis of machine learning models for intrusion detection system using Gini Impurity-based Weighted Random Forest (GIWRF) feature selection technique. Cybersecurity, v. 5, issue 1, p. 1 – 22.

Babechuk, M. G., and Fedo, C. M. (2023) Analysis of chemical weathering trends across three compositional dimensions: applications to modern and ancient mafic-rock weathering profiles. Canadian Journal of Earth Sciences v. 60, issue 7, p. 839 - 864.

Dubé, B., & Mercier-Langevin, P. (2020). Chapter 32: Gold deposits of the Archean Abitibi Greenstone Belt, Canada. In R. H. Sillitoe, R. J. Goldfarb, F. Robert, & S. F. Simmons (Eds.), Geology of the World's Major Gold Deposits and Provinces. Society of Economic Geologists, v. 23, p. 553 – 602.

Dubé, B., Mercier-Langevin, P., Ayer, J., Pilote, J. L., & Monecke, T. (2020). Chapter 3: Gold Deposits of the World-Class Timmins-Porcupine Camp, Abitibi Greenstone Belt, Canada. In Richard H. Sillitoe, Richard J. Goldfarb, François Robert, Stuart F. Simmons (Eds.), *Geology of the World's Major Gold Deposits and Provinces*. Society of Economic Geologists, v. 2, p. 27 - 56.

Dumont, R., Kiss, F., Coyle, M., Potvin, J., Oneschuk, D., & Dostaler, F. (2003) Aeromagnetic survey program of the Geological Survey of Canada, 2002-2003. Geological Survey of Canada, Current Research, 2003-H1, p. 1 - 4.

Fassbender, M. L., Hannington, M., Stewart, M., Brandl, P. A., Baxter, A. T., & Diekrup, D. (2023). Geochemical signatures of felsic volcanic rocks in modern oceanic settings and implications for Archean Greenstone Belts. Economic Geology, v. 118, issue 2, p. 319 – 345.

Fassbender, M. L. (2023) Volcanism in modern back-arc regimes and their implications for ancient greenstone belts [PhD, University of Ottawa]. uOttawa Omni Library, p. 217 – 234.

Fassbender, M. L., Hannington, M., Thomas Baxter, A., Diekrup, D., Stewart, M., & A. Brandl, P. (2024). Geochemical signatures of mafic volcanic rocks in modern oceanic settings and implications for Archean mafic magmatism. Economic Geology, v. 119, issue 2, p. 445 – 470.

Fedo, C. M., Wayne Nesbitt, H., & Young, G. M. (1995). Unraveling the effects of potassium metasomatism in sedimentary rocks and paleosols, with implications for paleoweathering conditions and provenance. Geology, v. 23, issue 10, p. 921 - 924.

Feng, R. & Kerrich, R. (1990) Geochemistry of fine-grained clastic sediments in the Archaean Abitibi Greenstone Belt, Canada: Implications for provenance and tectonic setting. Geochimica et Cosmochimica Acta, v. 54, p. 1061 - 1081.

Franceschi, S., Fattorini, L., & Gregoire, T. G. (2024). Exploiting nearest-neighbour maps for estimating the variance of sample mean in equal-probability systematic sampling of spatial populations. Spatial Statistics, v. 64, Article 100865. p. 2 - 9.

Franklin, J. M., Gibson, H. L., Jonasson, I. R., Galley, A.G. (2005) Volcanogenic massive sulphide deposits. Economic Geology, p. 523 – 560.

Frieman, B. M., Kuiper, Y. D., Kelly, N. M., Monecke, T., & Kylander-Clark, A. (2017). Constraints on the geodynamic evolution of the southern Superior Province: U-Pb LA-ICP-MS analysis of detrital zircon in successor basins of the Archean Abitibi and Pontiac subprovinces of Ontario and Quebec, Canada. Precambrian Research, v. 292, p. 398 – 416.

Frontier, S. (1976). Etude de la décroissance des valeurs propres dans une analyse en composantes principales: Comparaison avec le modelé du bâton brisé. Journal of Experimental Marine Biology and Ecology, v. 25, p. 67 - 75.

Fulignati, P., Gioncada, A., & Sbrana, A. (1999). Rare-earth element (REE) behaviour in the alteration facies of the active magmatic–hydrothermal system of Vulcano (Aeolian Islands, Italy). Journal of Volcanology and geothermal research, v. 88, issue 4, p. 325 - 342.

Gaboury, D., & Pearson, V. (2008). Rhyolite Geochemical Signatures and Association with Volcanogenic Massive Sulphide Deposits: Examples from the Abitibi Belt, Canada. Economic Geology, v. 103, issue 7, p. 1531 – 1562.

Galley, A.G., Hannington, M.D., & Jonasson, I.R. (2007). Volcanogenic massive sulphide deposits. In W.D. Goodfellow, (Ed.), Mineral deposits of Canada: A Synthesis of major deposit-types, district metallogeny, the evolution of geological provinces, and exploration methods. Geological Association of Canada, Mineral Deposits Division, Special Publication No. 5, p. 141 - 161.

Gelman, A. (2004). Bayesian data analysis (2nd ed.). Chapman & Hall/CRC. P. 351 – 569.

Gholamy, A., Kreinovich, V., & Kosheleva, O. (2018). Why 70/30 or 80/20 relation between training and testing sets: A pedagogical explanation. International Journal of Intelligent Technologies and Applied Statistics, v. 11, issue 2, p. 105 – 111.

Gibson, H. L., Morton, R. L., & Hudak, G. J. (1997). Submarine volcanic processes, deposits, and environments favorable for the location of volcanic-associated massive sulfide deposits. In Barrie, C. T., Hannington, M. D. (Eds.), Volcanic-associated massive sulfide deposits: processes and examples in modern and ancient settings. Society of Economic Geologists, & Geological Association of Canada. Mineral Deposits Division. (1999). p. 13 – 48.

Giorgi, G. M., & Gigliarano, C. (2017). The gini concentration index: A review of the inference literature. Journal of Economic Surveys, v. 31, issue 4, p. 1130 – 1148.

Goldfarb, R. J., & Pitcairn, I. (2023). Orogenic gold: Is a genetic association with magmatism realistic? Mineralium Deposita, v. 58, issue 1, p. 5 – 35.

Goldhaber, M. B. (2003). Sulfur-rich Sediments. In Treatise on Geochemistry, Elsevier, p. 257 – 288.

Granitto, M, Giles, S.A., & Kelley, K.D., (2017) Global Geochemical Database for Critical Metals in Black Shales: U.S. Geological Survey data release.

Greber, N. D., & Dauphas, N. (2019). The chemistry of fine-grained terrigenous sediments reveals a chemically evolved Paleoarchean emerged crust. Geochimica et Cosmochimica Acta, v. 255, p. 247 – 264.

Gregory, D. D., Large, R. R., Halpin, J. A., Baturina, E. L., Lyons, T. W., Wu, S., Danyushevsky, L., Sack, P. J., Chappaz, A., Maslennikov, V. V., & Bull, S. W. (2015). Trace element content of sedimentary pyrite in black shales. Economic Geology and the Bulletin of the Society of Economic Geologists, v.110, issue 6, p. 1389–1410.

Gregory, D., Mukherjee, I., Olson, S. L., Large, R. R., Danyushevsky, L. V., Stepanov, A. S., Avila, J. N., Cliff, J., Ireland, T. R., Raiswell, R., Olin, P. H., Maslennikov, V. V., & Lyons, T. W. (2019). The formation mechanisms of sedimentary pyrite nodules determined by trace element and sulfur isotope microanalysis. Geochimica et Cosmochimica Acta, v. 259, p. 53 - 68.

Gribov, A., & Krivoruchko, K. (2020). Empirical Bayesian kriging implementation and usage. The Science of the Total Environment, v. 722, Article 137290. p. 2 - 20.

Hallberg, J. A. (1984). A geochemical aid to igneous rock type identification in deeply weathered terrain. Journal of Geochemical Exploration, v. 20, issue 1, p. 1 – 8.

Hannington, M. D., & Barrie, C. T. (1999). The Giant Kidd Creek Volcanogenic Massive Sulphide Deposit: Western Abitibi Subprovince, Canada. Economic Geology, v. 10, p. 1 – 661.

Hannington, M. D., Jonasson, I. R., Herzig, P. M., & Petersen, S. (1995). Physical and chemical processes of seafloor mineralization at mid-ocean ridges. In S. E. Humphris, R. A. Zierenberg, L. S. Mullineaux, & R. E. Thomson (Eds.), Seafloor Hydrothermal Systems: Physical, Chemical, Biological, and Geological Interactions. American Geophysical Union, p. 115 – 157.

Hannington, M.D., Coombs, A., van Hees, G., Duff, S. & Campos-Alvarez, N. (2012) Regional lithogeochemical study of the Kidd–Munro MEGATEM® survey areas, Timmins–Kirkland Lake, northern Ontario: Discover Abitibi Initiative; Ontario Geological Survey, Miscellaneous Release—Data 291, [PDF document], p. 1 – 209.

Harkins, W. D. (1917). The Evolution of the Elements and the Stability of Complex Atoms. I. A New Periodic System which Shows a Relation Between the Abundance of the Elements and the Structure of the Nuclei of Atoms. Journal of the American Chemical Society, v. 39, issue 5, p. 856 - 879.

Haugaard, R., White, S., Jørgensen, T. R. C., Frieman, B., Meek, D., Zhou, X., Mathieu, L., & Ayer, J. (2023). Sedimentary processes, provenance, and tectonic control on fluvial sandstone geochemistry during Superior craton stabilization. In S. J. Whitmeyer, M. L.

Williams, D. A. Kellett, & B. Tikoff, Laurentia: Turning Points in the Evolution of a Continent. Geological Society of America, p. 25 – 42.

Haus, M. & Pauk, T. (2010). Data from the PETROCH lithogeochemical database; Ontario Geological Survey, Miscellaneous Release—Data 250.

Herzig, P. M., & Hannington, M. D. (1995). Polymetallic massive sulphides at the modern seafloor a review. Ore Geology Reviews, v. 10, issue 2, p. 95 - 115.

Hesselbo, S. P. (1996). Spectral gamma-ray logs in relation to clay mineralogy and sequence stratigraphy, Cenozoic of the Atlantic margin, offshore New Jersey. In Proceedings of the Ocean Drilling Program: Scientific Results, v. 150, p. 411.

Hiebert, R. S., Bekker, A., Houlé, M. G., & Rouxel, O. J. (2018). Depositional setting of the Late Archean Fe oxide- and sulphide-bearing chert and graphitic argillite in the Shaw Dome, Abitibi greenstone belt, Canada. Precambrian Research, v. 311, p. 98 – 116.

Idrisova, E.; Gabitov, R.; Karamov, T.; Voropaev, A.; Liu, M.-C.; Bogdanovich, N.; Spasennykh, M. (2021). Pyrite Morphology and δ 34S as Indicators of Deposition Environment in Organic-Rich Shales. Geosciences, v. 11, p. 355.

Ingersoll, R. V. (1988). Tectonics of sedimentary basins. Geological Society of America Bulletin, v. 100, issue 11, p. 1704 – 1719.

Ishikawa, Y., Sawaguchi, T., Iwaya, S., & Horiuchi, M., (1976). Delineation of prospecting targets for Kuroko deposits based on modes of volcanism of underlying dacite and alteration halos: Mining Geology, v. 26, p. 105 – 117 (in Japanese with English abs.).

Jackson, D. A. (1993). Stopping rules in principal components analysis: a comparison of heuristical and statistical approaches. Ecology, v. 74, issue 8, p. 2204 - 2214.

Jackson, J. E. (1991). A User's Guide to Principal Components. Wiley. p. 1 – 592.

Jiang, S. Y., Wang, R. C., Xu, X. S., & Zhao, K. D. (2005). Mobility of high field strength elements (HFSE) in magmatic-, metamorphic-, and submarine-hydrothermal systems. Physics and Chemistry of the Earth, Parts A/B/C, v. 30, issue 17-18, p. 1020 - 1029.

Jonasson, I. R. (1999). Role of Pyrite in the Formation and Localization of Gold Mineralization at the Owl Creek Mine, Timmins, ON. In Hannington, M. D., Barrie, T. (Eds.), The Giant Kidd Creek Volcanogenic Massive Sulphide Deposit, Western Abitibi Subprovence, Canada. Economic Geology, p. 627 – 659.

Jones, J.V., III, Piatak, N.M., & Bedinger, G.M., (2017). Zirconium and hafnium, chap. V *of* Schulz, K.J., DeYoung, J.H., Jr., Seal, R.R., II, & Bradley, D.C., (Eds.), Critical mineral resources of the United States—Economic and environmental geology and prospects for future supply: U.S. Geological Survey Professional Paper, v. 1802, p. 1 – 26.

Jørgensen, T.R.C. and Gibson, H. L., (2024). Lithological compilation of the Abitibi subprovince, Superior Province, Canada. Metal Earth Project, Mineral Exploration Research Centre.

Katz, L. R., Kontak, D. J., Dubé, B., McNicoll, V., Creaser, R., & Petrus, J. A. (2021). An Archean porphyry-type gold deposit; the Côté Gold Au(-Cu) deposit, Swayze greenstone belt, Superior Province, Ontario, Canada. Economic Geology and the Bulletin of the Society of Economic Geologists, v. 116, issue 1, p. 47 – 89.

Kehew, J. (2023) Intrabasinal sediments and tectonostratigraphy of the N.E. Lau Basin: contributions to extensional models of back-arc basins. [MSc thesis, University of Ottawa. Department of Earth and Environmental Sciences].

Kelley, K.D., Scott, C.T., Polyak, D.E., & Kimball, B.E., (2017). Vanadium. In K.J. Schulz, J.H. DeYoung, Jr., R.R. Seal II, & D.C. Bradley (Eds.), Critical mineral resources of the United States—Economic and environmental geology and prospects for future supply. U.S. Geological Survey, v. 1802, p. U1 – U36.

Kerrich, R., & Wyman, D. A. (1997). Review of developments in trace-element fingerprinting of geodynamic settings and their implications for mineral exploration. Australian Journal of Earth Sciences, v. 44, issue 4, p. 465 – 487.

Kim, J., Lim, D., Jeong, D., Xu, Z., Kim, H., Kim, J., & Kim, D. (2022). Mercury (Hg) geochemistry of mid-ocean ridge sediments on the Central Indian Ridge: Chemical forms and isotopic composition. Chemical Geology, v. 604, p. 1 - 9.

Kirch, W. (Ed.). (2008). Encyclopedia of public health (1st ed. 2008.). Springer, p. 1090 – 1091.

Koopman, E. R., Hannington, M. D., Santaguida, F., Cameron, B. I., (1999). Petrology and Geochemistry of Proximal Hydrothermal Alteration in the Mine Rhyolite at Kidd Creek, In Hannington, M. D., Barrie, T. (Eds.), The Giant Kidd Creek Volcanogenic Massive Sulphide Deposit, Western Abitibi Subprovence, Canada. Economic Geology, p. 627 – 659.

Glass, J. B., & Dupont, C. L. (2017). Oceanic Nickel Biogeochemistry and the Evolution of Nickel Use. In Zamble, D., Rowińska-Żyrek, M., Kozlowski, H. (Eds.), Biological Chemistry of Nickel. Royal Society of Chemistry, v. 10, p. 12 - 26.

Large, R. R., Gemmell, J. B., & Paulick, H. (2001). The Alteration Box Plot: A simple approach to understanding the relationship between alteration mineralogy and lithogeochemistry associated with volcanic-hosted massive sulphide deposits. Economic Geology, v. 96, issue 5, p. 957 - 971.

Large, R. R., Bull, S. W., & Maslennikov, V. V. (2011). A carbonaceous sedimentary source-rock model for Carlin-type and orogenic gold deposits. Economic Geology, v. 106, issue 3, p. 331 – 358.

Le, N. D., & Zidek, J. V. (2006). Chapter 5 Modeling. In Statistical analysis of environmental space-time processes. Springer Science + Business Media, p. 53 - 79.

Lesher, C. M., Goodwin, A. M., Campbell, I. H., & Gorton, M. P. (1986). Trace-element geochemistry of ore-associated and barren, felsic metavolcanic rocks in the Superior Province, Canada. Canadian Journal of Earth Sciences, v. 23, issue 2, p. 222 – 237.

Lesher, C. M., Keays, R. R., & Cabri, L. J. (2002). Komatiite-associated Ni-Cu-PGE deposits: Geology, mineralogy, geochemistry and genesis. Canadian Institute of Mining, Metallurgy and Petroleum, v. 54, p. 579 - 618.

Liu, Q., Li, P., Jin, Z., Liang, X., Zhu, D., Wu, X., Meng, Q., Liu, J., Fu, Q., & Zhao, J. (2021). Preservation of organic matter in shale linked to bacterial sulfate reduction (BSR) and volcanic activity under marine and lacustrine depositional environments. Marine and Petroleum Geology, v. 127, Article 104950, p. 1 - 19.

Liu, W., Etschmann, B., Migdisov, A., Boukhalfa, H., Testemale, D., Müller, H., Hazemann, J.L., & Brugger, J. (2017). Revisiting the hydrothermal geochemistry of europium (II/III) in light of new in-situ XAS spectroscopy results. Chemical Geology, v. 459, p. 61 - 74.

Maynard, B.J. (2013). Manganiferous Sediments, Rocks, and Ores. In In Holland. H.D., Turekian, K.K. (Eds.), Treatise on Geochemistry: Second Edition, v. 9, p. 327 – 349.

McClarren, R. G. (2021). Decision Trees and Random Forests for Regression and Classification. Machine Learning for Engineers. Springer International Publishing, p. 55 – 82.

McDunough, W. F., & Sun, S. S. (1995). The composition of the Earth. Chemical Geology, v. 120, issue 3 - 4, p. 223 – 253.

McLennan, S. M. (1993). Weathering and Global Denudation. The Journal of Geology, v. 101, issue 2, p. 295 – 303.

McLennan, S. M., Hemming, S., McDaniel, D. K., Hanson, G. N. (1993). Geochemical approaches to sedimentation, provenance, and tectonics. In Johnsson, M. J., & Basu, A. (Eds.), Processes Controlling the Composition of Clastic Sediments. Geological Society of America. p. 21 – 40.

McLennan, S. M. (2018). Rare earth elements in sedimentary rocks: Influence of Provenance and sedimentary processes. In B. R. Lipin & G. A. McKay (Eds.), Geochemistry and Mineralogy of Rare Earth Elements. Walter de Gruyter GmbH. Originally published 1989, v. 21, p. 169 – 200.

McLennan, S.M., Brock B., Hemming, S.R., Hurowitz, J.A., Lev S.M., & McDaniel, D.K, (2003). The roles of provenance and sedimentary processes in the geochemistry of sedimentary rocks: Evolutionary considerations to mineral deposit-forming environments: Geological Association of Canada, GeoText 4, p. 7 - 38.

Mercier-Langevin, P., Hannington, M. D., Dubé, B., & Bécu, V. (2011). The gold content of volcanogenic massive sulphide deposits. Mineralium Deposita, v. 46, issue 5, p. 509–539.

Mercier-Langevin, P., Dubé, B., Houlé, M. G., Bécu, V., Sappin, A., Pilote, J., Castonguay, S., & Decrée, S. (2023). Metallogeny of the Abitibi Greenstone Belt, Canada. In Metallic Resources 2. John Wiley and Sons, Inc, p. 63 – 141.

Monecke, T., Mercier-Langevin, P., Dubé, B., & Frieman, B. M. (2017). Geology of the Abitibi Greenstone Belt. In T. Monecke, P. Mercier-Langevin, & B. Dubé (Eds.), Archean base and precious metal deposits, Southern Abitibi Greenstone Belt, Canada Society of Economic Geologists, Reviews in Economic Geology, v. 19, p. 1 - 40.

Mole, D.R., Thurston, P.C., Marsh, J.H., Stern, R.A., Ayer, J.A., Martin, L.A.J., and Lu, Y.J., (2021). The formation of Neoarchean continental crust in the south-east Superior Craton by two distinct geodynamic processes: Precambrian Research, v. 356, article 106104.

Morton, A. C. (1985). Heavy minerals in provenance studies. In G. G. Zuffa (Ed.), Provenance of Arenites. Springer Netherlands, p. 249 – 277.

Morton, A.C., & Hallsworth, C.R. (1994). Identifying provenance-specific features of detrital heavy mineral assemblages in sandstones. Sedimentary Geology, v. 90, p. 241 - 256.

Morton, A. C., & Hallsworth, C. R. (1999). Processes controlling the composition of heavy mineral assemblages in sandstones. Sedimentary Geology, v. 124, issue 1–4, p. 3 – 29.

Mueller, W. U., Daigneault, R., Mortensen, J. K., & Chown, E. H. (1996). Archean terrane docking: Upper crust collision tectonics, Abitibi greenstone belt, Quebec, Canada. Tectonophysics, v. 265, issue 1–2, p. 127 – 150.

Mueller, W., & Donaldson, J. A. (1992). Development of sedimentary basins in the Archean Abitibi belt, Canada: An overview. Canadian Journal of Earth Sciences, v. 29, issue 10, p. 2249 – 2265.

Mueller, W., Donaldson, J. A., & Doucet, P. (1994). Volcanic and tectono-plutonic influences on sedimentation in the Archaean Kirkland Basin, Abitibi greenstone belt, Canada. Precambrian Research, v. 68, issue 3–4, p. 201 – 230.

Mueller, W. U., Stix, J., Corcoran, P. L., & Daigneault, R. (2009). Subaqueous calderas in the Archean Abitibi greenstone belt: An overview and new ideas. Ore Geology Reviews, v. 35, issue 1, p. 4 - 46.

Nesbitt, H. W., & Young, G. M. (1982). Early Proterozoic climates and plate motions inferred from major element chemistry of lutites. Nature, v. 299, issue 5885, p. 715 - 717.

Nesbitt, H. W., & Young, G. M. (1984). Prediction of some weathering trends of plutonic and volcanic rocks based on thermodynamic and kinetic considerations. Geochimica et Cosmochimica Acta, v. 48, issue 7, p. 1523 - 1534.

Nesbitt, H. W., Young, G. M., McLennan, S. M., & Keays, R. R. (1996). Effects of chemical weathering and sorting on the petrogenesis of siliciclastic sediments, with implications for provenance studies. The Journal of Geology, v. 104, issue 5, p. 525 – 542.

Niels H. Schovsbo (2002) Uranium enrichment shorewards in black shales: A case study from the Scandinavian Alum Shale, Geological Society of Sweden (GFF), v. 124, issue 2, p. 107 - 115.

Ohkouchi N, Kuroda J, & Taira A. (2015) The origin of Cretaceous black shales: a change in the surface ocean ecosystem and its triggers. Proceedings of the Japan Academy, Series B Physical and Biological Sciences v. 91, issue 7, p. 273 - 91.

Oliver, M.A., & R. Webster. (1990) Kriging: a method of interpolation for geographical information systems. International Journal of Geographic Information Systems, v. 4, issue 3, p. 313 - 332.

Oosterman, D., (n.d.) Provenance Study of the Kidd-Munro Argillites Near Timmins, Ontario [Unpublished Masters thesis]. University of Ottawa. p. 1 - 58.

Oshiro, T.M., Perez, P.S., & Baranauskas, J.A. (2012). How many trees in a random forest? In: Perner, P. (Ed.) Machine learning and data mining in pattern recognition. MLDM 2012. Lecture Notes in Computer Science, Springer, Berlin, Heidelberg, v. 7376.

Pašava, J., Ackerman, L., Žák, J., Svojtka, M., Magna, T., Pour, O., Trubač, J., & Veselovský, F. (2023). Multi-stage metal enrichment and formation of gold mineralization in black shales: The role of high heat flow in a rift setting. Mineralium Deposita, v. 58, issue 6, p. 1051 – 1073.

Pawlowsky-Glahn, V., Egozcue, J. J., & Tolosana-Delgado, R. (2007). Lecture notes on compositional data analysis. Universitat de Girona, Girona.

Penner, R., Hannington, M. D., & University of Ottawa. Department of Earth and Environmental Sciences. (2023). Trace element geochemistry of volcanogenic massive sulphide deposits in Archean Greenstone Belts: implications for metal endowment and geodynamic settings [MSc thesis, Université d'Ottawa / University of Ottawa].

Percival, J. (2007). Geology and Metallogeny of the Superior Province, Canada. In Geological Association of Canada, Mineral Deposits Division, Special Publication, v. 5, p. 903 – 928.

Piercey, S.J., 2009, Lithogeochemistry of volcanic rocks associated with volcanogenic massive sulphide deposits and applications to exploration, in Submarine Volcanism and Mineralization: Modern through Ancient, (Eds.), B. Cousens and S.J. Piercey; Geological Association of Canada, Short Course 29-30 May 2008, Quebec City, Canada, p. 15 - 40.

Piercey, S. J. (2010). An overview of petrochemistry in the regional exploration for volcanogenic massive sulphide (VMS) deposits. Geochemistry: Exploration, Environment, Analysis, v. 10, issue 2, p. 119 – 136.

Piercey, S. J. (2011). The setting, style, and role of magmatism in the formation of volcanogenic massive sulphide deposits. Mineralium Deposita, v. 46, issue 5–6, p. 449 – 471.

Pilote, J.-L., Jackson, S.E., Mercier-Langevin, P., Dubé, B., & Rhys, D., (2019). Characteristics of diagenetic and epigenetic sulphides in deformed and metamorphosed Archean carbonaceous metasedimentary rocks of the Timmins-Matheson corridor: establishing a framework for fingerprinting ore-forming processes in shear zone-hosted orogenic gold systems; in Targeted Geoscience Initiative: 2018 report of activities, (ed.) N. Rogers; Geological Survey of Canada, Open File 8549, p. 33–41.

Potter, P. E., Maynard, J. B., & Pryor, W. A. (1980). Sedimentology of Shale: Study Guide and Reference Source. Springer-Verlag, p. 3 – 276.

Pyrcz, M. J., & Deutsch, C. V. (2006). Semivariogram Models Based on Geometric Offsets. Mathematical Geology, v. 38, issue 4, p. 475 – 488.

Rasool, A., Pertile, E., Brožová, K. Halfar, J., Čabanová, K., Malíková, P., Chromíková, J., Motyka, O., Drabinová, S., Heviánková, S. (2025) Mechanistic insights and environmental ramifications of Cr(III) oxidation to Cr(VI) in soil and groundwater systems: bridging geochemical mechanisms and emerging remediation strategies. Environ Geochem Health 48, p. 1 - 22.

Rickard, D., Mussmann, M., & Steadman, J. A. (2017). Sedimentary Sulphides. Elements, v. 13, issue 2, p. 117 – 122.

Rottier, B., Scheffer, C., Beaudoin, G.. Casanova, V., Quesnel, B., Chelle-Michou, C., Laflamme, C., Herzog, M. (2025). Quartz and gold remobilization in orogenic Au deposits of the Val-d'Or vein field (Abitibi, Canada) from quartz in situ SIMS oxygen isotope and LA-ICP-MS trace element composition. Miner Deposita. p. 1 - 20.

Rudnick, R.L. and Gao, S. (2003). The Composition of the Continental Crust. In: Holland, H.D. and Turekian, K.K., (Eds.), Treatise on Geochemistry, The Crust, Elsevier-Pergamon, Oxford, v. 3, p. 1 - 64.

Scott, C., Kelley, K. D., & Slack, J. F. (2014). The geobiology of sediment-hosted mineral deposits. In K. D. Kelley & H. C. Golden (Eds.), Building Exploration Capability for the 21st Century. Society of Economic Geologists. p. 17 - 31.

Shanks III, & W.C. Pat (2012). Hydrothermal alteration in volcanogenic massive sulphide occurrence model: U.S. Geological Survey Scientific Investigations Report 2010–5070 –C, chap. 11, p. 12.

Shlens, J. (2014). A tutorial on principal component analysis. Internation Journal of Remote Sensing. p. 1 - 13.

Singh, P., Singh, N., Singh, K. K., & Singh, A. (2021). Chapter 5 - Diagnosing of disease using machine learning. In Machine Learning and the Internet of Medical Things in Healthcare. Elsevier Inc, p. 89 – 111.

Sokal, R.R. and Rohlf, F.J. (1995). Biometry: The Principles and Practice of Statistics in Biological Research. 3rd Edition, W.H. Freeman and Co., New York. p. 826 - 837.

Spirakis, C. S. (1996). The roles of organic matter in the formation of uranium deposits in sedimentary rocks. Ore Geology Reviews, v. 11, issue 1-3, p. 53 - 69.

Sprague, D. D., & Vermaire, J. C. (2018). The landscape-scale relationship between lake sediment geochemistry and catchment bedrock composition from the Temagami and Gowganda areas of Northeastern Ontario, Canada. Environmental Earth Sciences, v. 77, p. 1 - 19.

Stewart, C., Camsell, C., & Collins, W.H. (1925). Summary Report, 1925, Part C. Canada Department of Mines, Geological Survey.

Tanaka, E., Yasukawa, K., Dunlea, A. G., Hendy, I., Miyazaki, T., & Vaglarov, B. S. (2025). Intermediate water sources and sediment provenance in the high-latitude South Pacific Ocean (Campbell Plateau) during the Paleogene. Geochemistry, Geophysics, Geosystems: G3, v. 26, issue 9, Article e2025GC012314, p. 10 – 24.

Taylor, S. R. & McLennan, S. M. (1985) The continental crust: Its composition and evolution. Blackwell Scientific Publications (Oxford), p. 312.

Thurston, P. C. (2015). Igneous Rock Associations 19. Greenstone Belts and Granite−Greenstone Terranes: Constraints on the Nature of the Archean World. Geoscience Canada, v. 42, issue 4, p. 437 – 484.

Thurston, P. C., Ayer, J. A., Goutier, J., & Hamilton, M. A. (2008). Depositional gaps in Abitibi Greenstone Belt stratigraphy: A key to exploration for syngenetic mineralization. Economic Geology, v. 103, issue 6, p. 1097 – 1134.

Tissot, B. P., & Welte, D. H. (1984). Petroleum Formation and Occurrence (2nd, rev. ed.). Springer-Verlag.

Todorov, V., & Filzmoser, P. (2013). Comparing classical and robust sparse PCA. In synergies of soft computing and statistics for intelligent data analysis. Springer Berlin Heidelberg, p. 283 – 291.

Totten, M. W., & Hanan, M. A. (2007). Chapter 12 Heavy minerals in shales. In Mange, M. A., Wright, D.T. (Eds.), Developments in Sedimentology, v. 58, p. 323 – 341.

Tourtelot, E. (1970). Selected annotated bibliography of minor-element content of marine black shales and related sedimentary rocks, 1930-65 (Report No. 1293; Bulletin). USGS Publications Warehouse.

Tourtelot, H. A. (1979). Black Shale—Its deposition and diagenesis. Clays and Clay Minerals, v. 27, issue 5, p. 313 – 321.

Valiev, N. G., Bagazeev, V. K., Davydov, S. Y., Apakashev, R. A., & Boikov, I. S. (2022). Fine-grained ore minerals – Raw materials for the production of refractories. Refractories and Industrial Ceramics, v. 62, issue 5, p. 487 – 491.

Veizer, J., & Mackenzie, F.T. (2005). Chapter 7.15 Evolution of sedimentary rocks. In Mackenzie, F. T., Holland, H. D., & Turekian, K. K. (Eds.), Sediments, diagenesis, and sedimentary rocks. Elsevier, v. 7, 1st ed. p. 369 – 408.

Verdhan, V., (2020). Supervised learning with Python: concepts and practical implementation using Python. 1st ed. 2020., Springer Link, Apress (Springer Science + Business Media). p. 47 – 113.

Vine, J. D., & Tourtelot, E. B. (1969). Geochemical investigations of some black shales and associated rocks. (U.S. Geological Survey Bulletin No. 1314). Government Printing Office, p. 1 – 43.

Wang, Y. (2024). Refining vanadium hyper-enrichment in black shales of the Late Devonian–Early Mississippian Bakken Formation (USA). Terra Nova, v. 36, issue 4, p. 239 - 249.

Waxman, M.H., & Smits, L.J.M. (1968). Electrical conductivities in oil-bearing shaly sands. Society of Petroleum Engineers Journal, v. 8, issue 2, p. 107 – 122.

Weaver, C. E. (1980). Fine-Grained Rocks: Shales or Physilites. Sedimentary Geology., v. 27, no. 4, p. 301 – 313.

Weaver, C. E. (1989). Marine Transport and Deposition. Clays, Muds, and Shales. Elsevier Science & Technology, v. 44, p. 314 – 320.

Winchester, J. A., & Floyd, P. A. (1977). Geochemical discrimination of different magma series and their differentiation products using immobile elements. Chemical geology, v. 20, p. 325 - 343.

Zanin, Y. N., Zamirailova, A. G., & Eder, V. G. (2016). Uranium, thorium, and potassium in black shales of the Bazhenov Formation of the West Siberian marine basin. Lithology and Mineral Resources, v. 51, issue 1, p. 74 - 85.

Zhu, G., Wang, P., Li, T., Zhao, K., Yan, H., Li, J., & Zhou, L. (2021). Nitrogen geochemistry and abnormal mercury enrichment of shales from the lowermost Cambrian Niutitang Formation in South China: Implications for the marine redox conditions and hydrothermal activity. Global and Planetary Change, v. 199, article 103449, p. 1 - 12.

Appendix:

Appendix A1. Sample analysis techniques on 564 whole-rock samples of carbonaceous argillite reproduced from the MDR Report 291

Appendix A2. Matrix of Pearson's coefficient of correlation (r) for N=564 samples of carbonaceous argillite from the Timmins–Kirkland Lake region

Appendix A3. Sample and field data description / core log entry for N=564 samples of carbonaceous argillite from the Timmins-Kirkland Lake region.

Appendix A4. Centered log ratio transformed data used for PCA and Random Forest

Appendix A5. Statistical summary of major element and trace element concentrations grouped by shale lithotype, associated mineralization, and lithostratigraphic assemblage

Appendix A6. Principal component scores for PC1 - 4 for every black shale sample

Appendix A7. PCA loadings for PC1 – 4 for individual elements

Appendix A8. Eigenvalues and Variance for each Principal Component adding up to 100% cumulative variance

Appendix A9. Complementary figures for Empirical Bayesian Kriging in Chapter 5

Appendix A10. Python Code for shale lithotype, associated mineralization style, and lithostratigraphic assemblage Random Forest classifiers, adapted from Fassbender et al. (2023)

Appendix A11. Example decision tree for shale lithotypes Random Forest classifier

Appendix A12. Example decision tree for associated mineralization style Random Forest classifier

Appendix A1. Sample analysis techniques on 564 whole-rock samples of carbonaceous argillite reproduced from the MDR Report 291.

Sample Preparation

Drill-core samples selected for analysis were washed on-site and dried before shipping to the University of Ottawa. The core was then split for crushing to less than 0.5 mm in a mechanical jaw crusher. The crushed material was mechanically split into 0.5 to 1 kg subsamples that were shipped for additional processing at Activation Laboratories in Ancaster, Ontario. Blind duplicates of crushed samples (every 100 samples) were included among the samples shipped for processing and analysis.

At Activation Laboratories, the entire sample (minimum 500 g of crushed material) was further reduced to a nominal –10 mesh (1.7 mm), mechanically split to obtain a representative subsample and then pulverized in mild steel mill to at least 95% –150 mesh (106 μm), with maximum contamination less than 0.2% Fe. As a routine practice, Activation Laboratories uses cleaner sand between each sample, and the quality of crushing and pulverization was routinely checked as part of their quality assurance program.

Sample Analysis

A total of 564 whole-rock samples were analyzed using research-grade inductively coupled plasma optical emission spectrometry (ICP–OES), inductively coupled plasma mass spectrometry (ICP–MS), instrumental neutron activation analysis (INAA) and single-element techniques to achieve a complete geochemical characterization of the argillites. The analyses were carried out by Activation Laboratories using their Code 4E-Research ICPMS+INAA+TD-ICP+Fusion ICPMS package plus Code 4F-B, 4F-C,S, 4F-CO2 Coulometry, 4F-F Specific Ion Electrode, and 4F-Hg Cold Vapour methods. Ten different analytical methods were used to achieve a total analysis. The methods used for each element or groups of elements are described below and listed in the Table 1.1.

SiO_2, Al_2O_3, Fe_2O_3(T), MnO, MgO, CaO, Na_2O, K_2O, TiO_2, P_2O_5, Ba, Be, Sr, V, Y − These elements were determined by ICP–OES following a lithium metaborate–lithium tetraborate fusion. In this technique, a 0.2 to 0.25 g sample is mixed with a mixture of lithium metaborate–lithium tetraborate and fused, then the fused sample is dissolved in 5% nitric acid. All elements

are solubilized. The solutions are analyzed by ICP–OES using the method of internal standardization (Code 4E Fusion ICP).

Bi, Cs, Ga, Ge, Hf, In, Mo, Nb, Rb, Sn, Tl, Ta, Th, U, Zr, La, Ce, Pr, Nd, Sm, Eu, Gd, Tb, Dy, Ho, Er, Tm, Yb, Lu − These elements were determined by ICP–MS following the lithium metaborate lithium tetraborate fusion noted above. All elements are solubilized. The fused samples are diluted and analyzed by ICP–MS (Code 4E ICPMS).

Au, As, Br, Co, Cr, Hg, Ir, Sb, Sc, Se, W − These elements were determined by INAA, which measures gamma radiation induced in a solid sample by irradiation with neutrons in a nuclear reactor. A 1 g aliquot is encapsulated in a polyethylene vial and irradiated with flux wires (to monitor neutron flux) and an internal standard. Once activated, each element emits a specific gamma radiation that can be measured and quantified. After a 7-day delay to allow 24Na to decay, the samples are counted on a high-purity germanium detector (Code 4F-INAA). The detection limits reported here are a function of the counting times for each element.

Cd, Cu, Ni, Pb, Ag, Zn, S − These elements were determined by ICP–OES following a four-acid dissolution. A 0.25 g sample is digested with 4 acids, beginning with hydrofluoric and followed by a mixture of nitric and perchloric acids, and then heated in several ramping and holding cycles which take the samples to dryness. The samples are then brought back into solution using hydrochloric acid and analyzed using ICP–OES and the method of internal standardization (Code 4E TD-ICP). Only sulphide sulphur is determined by this method.

C-total and S-total − These elements were determined by combusting a 0.2 g sample in pure oxygen in an induction furnace coupled to infrared (IR) detectors. During combustion, carbon-bearing compounds release all carbon in the sample, which binds with the oxygen to form CO2. Sulphur-bearing compounds release sulphur, which binds with oxygen to form SO2. Carbon dioxide and SO2 gases flow through the IR cells where the concentrations are determined by absorption of IR energy at different wavelengths (Code 4F-C,S IR).

CO_2 − Carbon present mainly in carbonate was determined by combusting a 0.2 g sample in pure nitrogen in an resistance furnace, in which temperatures can be precisely controlled. CO_2 from the furnace is determined on a CO_2/H_2O analyzer as well as by coulometry (Code 4F-CO_2

Coulometry). Non-carbonate carbon in the sample can then be calculated from this analysis by the difference between C-total and CO_2.

Hg − Mercury was determined using a flow-injection cold-vapour absorption spectrometer (Code 4F-Hg FIMS). In this analysis, a 0.5 g sample is digested with aqua regia to leach out soluble mercury. The mercury in the resulting solution is oxidized to the stable divalent form and mixed with a potassium permanganate. The Hg(II) in solution is reduced using stannous chloride and the resulting mercury atoms are carried as vapour by argon bubbled through the mixture into an absorption cell.

F − Fluorine was determined using a combination of lithium metaborate–lithium tetraborate fusion and an ion specific electrode (Code 4F-F ISE). A 0.2 g sample is first fused and then dissolved in dilute nitric acid, prior to direct analysis with a fluoride ion electrode immersed in the solution.

B − Boron was determined by prompt gamma neutron activation analysis (Code 4F-B PGNAA). A 1 g sample is encapsulated in a polyethylene vial and placed in a beam of neutrons produced from a nuclear reactor. Samples are measured for the doppler broadened prompt gamma ray at 478 KeV using a high purity germanium detector.

LOI (loss on ignition) − The LOI, which includes H_2O+, CO_2, S and other volatiles, is determined from the weight loss after roasting the sample at 1050°C for 2 hours.

Table 1.1. The analysis method, detection limit, and unit symbol for each of the elements analyzed in MRD report 291.

Analyte Symbol	Unit Symbol	Detection Limit	Analysis Method
SiO_2	%	0.01	FUS-ICP
Al_2O_3	%	0.01	FUS-ICP
Fe_2O_3	%	0.01	FUS-ICP
MnO	%	0.001	FUS-ICP
MgO	%	0.01	FUS-ICP
CaO	%	0.01	FUS-ICP
Na_2O	%	0.01	FUS-ICP
K_2O	%	0.01	FUS-ICP
TiO_2	%	0.001	FUS-ICP
P_2O_5	%	0.01	FUS-ICP
LOI	%	0.01	FUS-ICP
Au	ppb	1	INAA
Ag	ppm	0.5	TD-ICP
As	ppm	1	INAA
Ba	ppm	1	FUS-ICP
Be	ppm	1	FUS-ICP
Bi	ppm	0.1	FUS-ICP
Br	ppm	0.5	INAA
Cd	ppm	0.5	TD-ICP
Co	ppm	0.1	INAA
Cr	ppm	0.5	INAA
Cs	ppm	0.1	FUS-ICP
Cu	ppm	1	TD-ICP
Ga	ppm	1	FUS-MS
Ge	ppm	0.5	FUS-MS
Hf	ppm	0.1	FUS-MS
Hg	ppm	1	INAA

In	ppm	0.1	FUS-MS
Ir	ppb	1	INAA
Mo	ppm	2	FUS-MS
Nb	ppm	0.2	FUS-MS
Ni	ppm	1	TD-ICP
Pb	ppm	5	TD-ICP
Rb	ppm	1	FUS-MS
S	%	0.001	TD-ICP
Sb	ppm	0.1	INAA
Sc	ppm	0.01	INAA
Se	ppm	0.5	INAA
Sn	ppm	1	FUS-MS
Sr	ppm	2	FUS-MS
Ta	ppm	0.01	FUS-MS
Th	ppm	0.05	FUS-MS
Tl	ppm	0.05	FUS-MS
U	ppm	0.01	FUS-MS
V	ppm	5	FUS-ICP
W	ppm	1	INAA
Y	ppm	1	FUS-ICP
Zn	ppm	1	TD-ICP
Zr	ppm	1	FUS-MS
La	ppm	0.05	FUS-MS
Ce	ppm	0.05	FUS-MS
Pr	ppm	0.01	FUS-MS
Nd	ppm	0.05	FUS-MS
Sm	ppm	0.01	FUS-MS
Eu	ppm	0.005	FUS-MS
Gd	ppm	0.01	FUS-MS
Tb	ppm	0.01	FUS-MS
Dy	ppm	0.01	FUS-MS

Ho	ppm	0.01	FUS-MS
Er	ppm	0.01	FUS-MS
Tm	ppm	0.005	FUS-MS
Yb	ppm	0.01	FUS-MS
Lu	ppm	0.002	FUS-MS
C-Total	%	0.01	IR
Total S	%	0.01	IR
CO_2	%	0.01	COUL
F	%	0.01	FUS-ISE
B	ppm	2	PGNAA
Hg	ppb	5	FIMS

Appendix A2. Matrix of Pearson's coefficient of correlation (r) for N=564 samples of carbonaceous argillite from the Timmins–Kirkland Lake region.

Correlation - 564 rows	SiO2_pct	Al2O3_pc	Fe2O3_pc	FeO_pct	MnO_pct	MgO_pct	CaO_pct	Na2O_pct	K2O_pct	TiO2_pct	P2O5_pct	LOI_pct	Au_ppb	Ag_ppm	As_ppm	Ba_ppm	Be_ppm	Bi_ppm	Br_ppm	Cd_ppm	Co_ppm	Cr_ppm	Cs_ppm	Cu_ppm	Ga_ppm	Ge_ppm	Hf_ppm	In_ppm	Mo_ppm	Nb_ppm	Ni_ppm	Pb_ppm	Rb_ppm	Sb_ppm	Sc_ppm
SiO2_pct	1.00000																																	
Al2O3_pct	0.20299	1.00000																																
Fe2O3_pct	-0.62223	-0.44803	1.00000	1.00000																														
FeO_pct	-0.62223	-0.44803	1.00000	1.00000																														
MnO_pct	-0.35771	-0.30439	0.51984	0.51984	1.00000																													
MgO_pct	-0.43021	-0.04066	0.27010	0.27010	0.26957	1.00000																												
CaO_pct	-0.56254	-0.39952	0.24814	0.24814	0.43167	0.28335	1.00000																											
Na2O_pct	0.05306	0.33340	-0.21135	-0.21135	-0.19507	-0.12869	-0.17051	1.00000																										
K2O_pct	0.28442	0.65220	-0.40540	-0.40540	-0.31878	-0.29523	-0.39741	-0.19660	1.00000																									
TiO2_pct	-0.00140	0.76730	-0.15952	-0.15952	-0.04119	0.11606	-0.14771	0.21241	0.41189	1.00000																								
P2O5_pct	0.12109	0.65858	-0.27355	-0.27355	-0.20546	-0.04859	-0.23527	0.27245	0.46506	0.62397	1.00000																							
LOI_pct	-0.70221	-0.50954	0.30893	0.30893	0.04290	0.03896	0.33071	-0.15798	-0.32292	-0.41833	-0.35706	1.00000																						
Au_ppb	-0.03701	-0.06879	0.00511	0.00511	0.06828	0.03957	0.09246	-0.06792	-0.00064	-0.02244	-0.07813	0.04700	1.00000																					
Ag_ppm	-0.18479	-0.09422	0.09446	0.09446	-0.04859	-0.06899	-0.01492	0.05398	-0.03518	-0.09857	-0.12209	0.23602	0.20616	1.00000																				
As_ppm	-0.33197	-0.25046	0.11535	0.11535	0.11642	-0.00983	0.19678	-0.09574	-0.07980	-0.20418	-0.21655	0.46135	0.50766	0.24407	1.00000																			
Ba_ppm	0.22030	0.55967	-0.33111	-0.33111	-0.26830	-0.21520	-0.32632	-0.10060	0.77711	0.37187	0.41908	-0.27620	-0.01928	-0.06160	-0.10967	1.00000																		
Be_ppm	0.14733	0.54642	-0.24350	-0.24350	-0.18612	-0.06333	-0.22153	-0.02557	0.52698	0.34707	0.33429	-0.29991	-0.02992	-0.06983	-0.12368	0.47182	1.00000																	
Bi_ppm	-0.06170	-0.00502	0.00529	0.00529	-0.04272	-0.03193	-0.02930	0.15017	-0.06478	-0.04997	-0.01548	0.07674	-0.00734	0.38333	-0.00887	-0.05371	-0.02704	1.00000																
Br_ppm	-0.14344	-0.23875	0.06865	0.06865	-0.07554	-0.12007	-0.05185	-0.11105	-0.05682	-0.19882	-0.15132	0.40825	-0.01485	0.06068	0.19777	-0.05793	-0.17097	0.01349	1.00000															
Cd_ppm	-0.09325	-0.10601	0.05162	0.05162	0.01671	0.01301	0.05243	0.07106	-0.11996	0.06431	-0.01213	0.09747	-0.00642	0.12612	0.05963	-0.09897	-0.09435	-0.00584	0.05534	1.00000														
Co_ppm	-0.48782	-0.34838	0.43655	0.43655	0.08054	0.25729	0.20851	-0.12256	-0.26960	-0.19025	-0.23519	0.46453	-0.01899	0.28732	0.35421	-0.22852	-0.22324	0.01613	0.17594	0.13899	1.00000													
Cr_ppm	-0.19913	0.02778	0.10374	0.10374	0.09301	0.59475	0.06474	-0.07528	-0.13210	0.10546	-0.04356	0.00290	-0.01130	-0.05268	0.05725	-0.09132	-0.04472	-0.02323	-0.00861	0.00261	0.27738	1.00000												
Cs_ppm	0.15554	0.49229	-0.24725	-0.24725	-0.15900	-0.14044	-0.22821	-0.08424	0.48083	0.35999	0.25241	-0.22642	-0.01641	-0.07881	0.01203	0.40942	0.42384	-0.06912	-0.09032	-0.09377	-0.18444	-0.01683	1.00000											
Cu_ppm	-0.10688	-0.09175	0.06842	0.06842	-0.02773	0.02538	-0.01500	0.09893	-0.11974	-0.09944	-0.12107	0.11450	0.00043	0.75353	0.04054	-0.11603	-0.07385	0.41427	-0.00284	0.03767	0.21609	-0.01407	-0.09791	1.00000										
Ga_ppm	0.12168	0.88647	-0.34952	-0.34952	-0.28707	-0.04653	-0.38913	0.15086	0.67942	0.69090	0.55997	-0.37271	-0.05148	-0.01075	-0.16964	0.54997	0.55336	-0.01492	-0.17086	-0.08473	-0.18680	0.01581	0.49220	-0.06283	1.00000									
Ge_ppm	-0.12688	0.04614	0.01205	0.01205	-0.04557	0.00766	0.03921	-0.09109	0.04179	0.08437	0.02168	0.13680	0.00064	0.18108	0.18747	0.05236	0.09194	-0.00692	-0.06945	0.15934	0.33787	0.05280	0.04762	0.06187	0.20659	1.00000								
Hf_ppm	0.21028	0.53686	-0.31873	-0.31873	-0.27458	-0.18905	-0.30016	0.14333	0.48934	0.27917	0.30530	-0.27648	-0.06020	-0.01483	-0.15974	0.38457	0.42008	-0.00146	-0.09046	-0.02004	-0.25641	-0.18582	0.20673	-0.07075	0.57569	0.00944	1.00000							
In_ppm	-0.12453	-0.08156	0.03058	0.03058	-0.06383	-0.09295	0.06967	-0.06333	0.01104	-0.02867	0.05079	0.20527	-0.01075	0.20295	0.12455	-0.01309	-0.01411	0.01217	-0.01035	0.25250	0.27157	-0.04479	-0.07072	0.09571	0.09079	0.51882	-0.02351	1.00000						
Mo_ppm	-0.39419	-0.25284	0.19437	0.19437	-0.12833	-0.01013	0.08610	0.12745	-0.23328	-0.27304	-0.19384	0.55137	0.02360	0.38861	0.22780	-0.20132	-0.15297	0.31782	0.19421	0.08604	0.41683	-0.05362	-0.21660	0.29018	-0.20146	0.10184	-0.09229	0.14710	1.00000					
Nb_ppm	0.10773	0.35480	-0.18304	-0.18304	-0.18086	-0.11668	-0.17215	0.09387	0.33452	0.17328	0.22154	-0.17626	-0.04297	0.00387	-0.12212	0.25185	0.33128	-0.00436	-0.05317	-0.00900	-0.17470	-0.12821	0.09953	-0.04681	0.39613	-0.03321	0.79022	0.02321	-0.05420	1.00000				
Ni_ppm	-0.38061	-0.18916	0.21396	0.21396	0.01482	0.36174	0.11014	-0.07933	-0.20778	-0.13701	-0.16292	0.38788	-0.02041	0.05103	0.31468	-0.14777	-0.15201	0.00582	0.15878	0.05994	0.67058	0.67707	-0.11035	0.03120	-0.14223	0.08533	-0.22650	0.14306	0.27123	-0.16212	1.00000			
Pb_ppm	-0.04033	-0.02592	0.00802	0.00802	0.01393	0.03766	0.00671	0.11911	-0.09651	0.09623	0.00009	0.02193	-0.00548	0.11502	0.01139	-0.09789	-0.05576	-0.00142	0.06522	0.66469	0.01727	-0.01111	-0.05732	0.17954	-0.05765	0.00985	-0.01007	0.01481	0.04121	-0.02469	-0.00586	1.00000		
Rb_ppm	0.27915	0.65987	-0.40186	-0.40186	-0.30932	-0.27991	-0.39338	-0.17655	0.94305	0.40958	0.44096	-0.32802	-0.01261	0.00549	-0.07771	0.72101	0.58305	-0.05910	-0.07943	-0.10768	-0.26895	-0.11418	0.54451	-0.07148	0.69289	0.10569	0.48073	0.03978	-0.22282	0.34262	-0.20160	-0.08867	1.00000	
Sb_ppm	-0.18779	-0.16657	0.11901	0.11901	-0.05283	-0.08095	0.02158	-0.07282	-0.04152	-0.13497	-0.09308	0.33479	0.03813	0.11891	0.34761	-0.04932	-0.05392	-0.00155	0.25264	0.03577	0.15924	0.02303	0.06829	-0.02829	-0.12019	0.06183	-0.08465	0.04509	0.14660	-0.04721	0.16755	0.02123	-0.04546	1.00000
Sc_ppm	-0.34104	0.40466	0.05134	0.05134	0.07652	0.38629	0.11309	0.08781	0.06789	0.67814	0.23026	-0.00817	-0.02074	-0.00936	-0.00237	0.10506	0.11738	0.01652	-0.06707	0.07675	0.16549	0.37993	0.15163	-0.00155	0.37082	0.16318	-0.04855	-0.00097	-0.00012	-0.05413	0.24108	0.09364	0.09327	-0.04595	1.00000
Se_ppm	-0.40652	-0.33911	0.28603	0.28603	-0.06261	-0.03838	0.15624	-0.06720	-0.19935	-0.24125	-0.21266	0.55627	-0.01982	0.21638	0.30886	-0.15599	-0.17423	0.03191	0.20247	0.18666	0.55418	-0.03956	-0.17218	0.18900	-0.18043	0.26315	-0.14736	0.27500	0.43483	-0.09107	0.33215	0.08667	-0.20108	0.17556	0.00707
Sn_ppm	-0.18913	-0.12606	0.08788	0.08788	-0.12295	-0.15369	0.00109	-0.10169	0.07609	-0.09740	-0.02979	0.33551	0.02213	0.33389	0.21388	0.05073	-0.03475	0.01773	0.07916	0.24124	0.40210	-0.08285	-0.10036	0.14761	0.11982	0.61538	0.09926	0.75280	0.27700	0.08619	0.14869	0.03675	0.09955	0.18010	-0.04887
Sr_ppm	0.08023	0.42743	-0.26992	-0.26992	-0.02966	-0.02439	0.05532	0.32797	0.09468	0.32714	0.32429	-0.27335	-0.04116	-0.15198	-0.10705	0.21613	0.23507	-0.03081	-0.17037	-0.10193	-0.27516	-0.04879	0.33312	-0.11494	0.30651	-0.09429	0.11630	-0.17736	-0.22488	0.01648	-0.17038	-0.02742	0.11075	-0.10907	0.12443
Ta_ppm	0.14681	0.35703	-0.21681	-0.21681	-0.22041	-0.13457	-0.23028	0.05486	0.36419	0.12409	0.13521	-0.16711	-0.04886	-0.00485	-0.11705	0.27563	0.35174	-0.00226	-0.03624	-0.04285	-0.17845	-0.14915	0.10356	-0.05796	0.41932	-0.02786	0.89703	-0.03670	-0.03078	0.86077	-0.16214	-0.03025	0.36524	-0.05065	-0.08638
Th_ppm	0.08747	0.49409	-0.32386	-0.32386	-0.33632	-0.11450	-0.28407	0.19783	0.41304	0.13291	0.25173	-0.09831	-0.05990	0.06820	-0.03949	0.41621	0.52912	0.06985	-0.04694	-0.08579	-0.16615	-0.11271	0.26921	0.01871	0.46328	-0.00220	0.59591	-0.08029	0.09050	0.49843	-0.08043	-0.01766	0.47613	-0.00804	0.03008
Tl_ppm	0.16772	0.13281	-0.20820	-0.20820	-0.27591	-0.29069	-0.32171	-0.19071	0.38679	-0.02253	0.06068	0.07175	-0.04031	0.13186	0.07775	0.26359	0.14798	0.01392	0.12351	-0.02279	-0.04678	-0.14770	0.15786	0.04998	0.21532	0.21603	0.19801	0.07224	0.01696	0.13110	-0.04668	-0.02815	0.45014	0.07930	-0.05152
V_ppm	-0.20929	0.54861	0.02532	0.02532	0.12186	0.35034	0.03275	0.10205	0.17771	0.85433	0.36447	-0.23432	0.08671	-0.05715	-0.07023	0.20531	0.21877	-0.02715	-0.15849	0.04097	0.00110	0.32545	0.27502	-0.05381	0.48747	0.10839	-0.03904	-0.04413	-0.16369	-0.05406	0.07897	0.08434	0.19225	-0.09686	0.87791
W_ppm	0.13228	-0.00309	-0.08207	-0.08207	-0.02832	-0.04353	-0.07835	-0.06665	0.10083	-0.01573	-0.07596	-0.07308	0.29685	-0.04048	0.15183	0.12775	0.04022	-0.03307	0.03626	-0.04235	-0.09980	-0.03061	0.07628	-0.06642	-0.00546	-0.05654	-0.03977	-0.04489	-0.08089	-0.00341	-0.07681	-0.05020	0.05975	0.06417	-0.05516
Y_ppm	-0.02597	0.05503	-0.01836	-0.01836	-0.05197	-0.00841	-0.01192	-0.04794	0.08448	0.04061	-0.01454	0.02067	-0.00880	-0.01276	-0.01258	0.05800	0.11317	-0.00583	-0.01996	0.02198	-0.00171	-0.04744	-0.01633	-0.03435	0.14132	0.00692	0.47390	0.03057	0.05553	0.51097	-0.00990	0.01334	0.08158	-0.00479	0.02768
Zn_ppm	-0.16370	-0.18741	0.06497	0.06497	-0.05121	-0.07865	0.05787	0.02974	-0.11745	-0.07240	-0.05254	0.27336	-0.00376	0.21427	0.17012	-0.07947	-0.12533	0.00080	0.08898	0.86869	0.29699	-0.03169	-0.13626	0.07722	-0.09282	0.33928	-0.04347	0.50683	0.21808	-0.01699	0.15173	0.44417	-0.09865	0.10750	0.01097
Zr_ppm	0.22810	0.55605	-0.34516	-0.34516	-0.30411	-0.21219	-0.32244	0.16313	0.50630	0.30159	0.35554	-0.28015	-0.06962	-0.01213	-0.17046	0.39940	0.40508	0.00798	-0.08313	-0.01737	-0.26759	-0.20403	0.20822	-0.06831	0.58325	0.01782	0.97821	-0.00901	-0.09525	0.73350	-0.24181	-0.00699	0.48916	-0.08536	-0.06099
La_ppm	0.14021	0.49929	-0.31154	-0.31154	-0.28243	-0.12607	-0.26806	0.13985	0.43954	0.23031	0.37142	-0.18347	-0.05593	-0.03432	-0.09933	0.43913	0.49113	0.00879	-0.05336	-0.11935	-0.20191	-0.12632	0.26393	-0.06018	0.48903	-0.02799	0.61945	-0.06941	-0.06248	0.50358	-0.13890	0.00655	0.44462	-0.06586	0.00689
Ce_ppm	0.13286	0.50669	-0.31165	-0.31165	-0.29349	-0.12562	-0.27099	0.14852	0.44376	0.23999	0.38271	-0.17923	-0.05754	-0.02491	-0.10159	0.43415	0.48847	0.02342	-0.06465	-0.11345	-0.19815	-0.13336	0.25227	-0.05362	0.50188	-0.02157	0.66760	-0.05470	-0.04381	0.55318	-0.13913	0.00387	0.44964	-0.06611	0.01371
Pr_ppm	0.11665	0.50157	-0.29194	-0.29194	-0.28396	-0.11227	-0.25670	0.14241	0.43390	0.25722	0.38392	-0.17602	-0.05427	-0.02771	-0.10486	0.42261	0.48495	0.02151	-0.07541	-0.10745	-0.18452	-0.12641	0.25340	-0.05845	0.50957	-0.01462	0.67991	-0.04410	-0.03984	0.56717	-0.13246	-0.00536	0.43972	-0.06556	0.03332
Nd_ppm	0.10568	0.50114	-0.27648	-0.27648	-0.27094	-0.10181	-0.24531	0.13481	0.43228	0.28076	0.39690	-0.17896	-0.05166	-0.03803	-0.11154	0.41326	0.47679	0.01434	-0.07813	-0.09837	-0.17835	-0.12153	0.24526	-0.07299	0.51496	-0.00146	0.69155	-0.03068	-0.04182	0.58755	-0.13097	-0.01422	0.43822	-0.06386	0.05570
Sm_ppm	0.02044	0.41089	-0.19329	-0.19329	-0.22418	-0.05499	-0.17282	0.09741	0.35415	0.25815	0.31255	-0.09799	-0.04416	-0.02536	-0.08306	0.33422	0.40770	0.02434	-0.06321	-0.05979	-0.09981	-0.10441	0.17873	-0.06216	0.46192	0.02464	0.71366	0.01170	0.02562	0.64707	-0.08116	-0.01567	0.36169	-0.03837	0.10191
Eu_ppm	-0.32024	0.14176	-0.03602	-0.03602	-0.20042	-0.10284	0.04118	0.09946	0.13155	0.10124	0.17189	0.38341	-0.04276	0.05927	0.18865	0.20054	0.19329	-0.03225	0.04985	0.03896	0.23162	-0.11220	0.05394	-0.07572	0.22751	0.26842	0.30464	0.21034	0.32454	0.24996	0.16010	0.00237	0.12919	0.10892	0.20080
Gd_ppm	-0.03537	0.24836	-0.08547	-0.08547	-0.13063	-0.01128	-0.07555	0.02421	0.22577	0.18750	0.16635	-0.03179	-0.02754	-0.02800	-0.05206	0.20398	0.27067	0.00441	-0.04427	-0.01423	-0.02923	-0.07290	0.08348	-0.05889	0.33214	0.03076	0.65657	0.03480	0.05477	0.64131	-0.03715	-0.00295	0.22938	-0.01714	0.10480
Tb_ppm	-0.05292	0.13768	-0.03076	-0.03076	-0.08835	-0.00029	-0.03271	-0.02254	0.14474	0.10805	0.05343	0.01459	-0.02107	-0.02309	-0.02781	0.11793	0.18013	0.00012	-0.02386	0.01445	0.00949	-0.05624	0.01247	-0.04911	0.23548	0.02430	0.61727	0.03613	0.07753	0.63613	-0.00957	0.00869	0.14448	-0.00249	0.08110
Dy_ppm	-0.06438	0.10009	-0.01159	-0.01159	-0.06881	0.01169	-0.01591	-0.03735	0.11186	0.08216	0.01142	0.03442	-0.01644	-0.01381	-0.01251	0.08140	0.14473	-0.00250	-0.02088	0.02421	0.02224	-0.04262	-0.00133	-0.04061	0.20175	0.02400	0.58308	0.04029	0.08208	0.61029	0.00592	0.01520	0.11205	0.00069	0.07675
Ho_ppm	-0.06531	0.06903	0.00225	0.00225	-0.05105	0.01460	-0.00540	-0.04662	0.08531	0.06164	-0.01359	0.04270	-0.01406	-0.00912	-0.00505	0.05468	0.11614	-0.00471	-0.01326	0.03379	0.02601	-0.03730	-0.01627	-0.03625	0.16852	0.02081	0.54124	0.03913	0.08350	0.57585	0.01033	0.02238	0.08535	0.00275	0.06668
Er_ppm	-0.06943	0.05368	0.00483	0.00483	-0.04822	0.01223	-0.00261	-0.04913	0.07317	0.04555	-0.02640	0.05698	-0.01441	0.00068	0.00321	0.04275	0.10619	-0.00049	-0.00083	0.04056	0.03096	-0.03854	-0.02418	-0.02823	0.15361	0.02172	0.52344	0.04133	0.09335	0.55829	0.01559	0.02767	0.07339	0.00754	0.05924
Tm_ppm	-0.07526	0.03401	0.00872	0.00872	-0.04306	0.01495	0.00413	-0.05078	0.05481	0.02636	-0.04804	0.07333	-0.01513	0.00948	0.01255	0.02986	0.09243	0.00382	0.00542	0.04521	0.03810	-0.03688	-0.03317	-0.01969	0.13653	0.02498	0.51010	0.04341	0.10305	0.54730	0.02340	0.03044	0.05414	0.01112	0.05557
Yb_ppm	-0.09379	0.03095	0.00784	0.00784	-0.04554	0.01118	0.01091	-0.04448	0.05162	0.02261	-0.04863	0.09847	-0.01648	0.02680	0.02518	0.02511	0.09532	0.01067	0.01520	0.05843	0.04957	-0.04339	-0.03972	-0.00838	0.13602	0.03526	0.51725	0.05534	0.12876	0.55008	0.03049	0.03850	0.05135	0.01797	0.06469
Lu_ppm	-0.12473	0.00981	0.01429	0.01429	-0.04780	0.01261	0.02628	-0.04030	0.03180	0.00343	-0.06042	0.14427	-0.02223	0.05142	0.04677	0.00917	0.08133	0.02601	0.03515	0.07134	0.07622	-0.04842	-0.05176	0.01373	0.11865	0.05053	0.49603	0.07273	0.16577	0.52888	0.05089	0.04637	0.03342	0.03264	0.07306
F_pct	0.03070	0.05681	-0.03746	-0.03746	0.00103	-0.01015	0.00197	-0.02306	0.07193	0.08362	0.18742	-0.05613	-0.00699	-0.02848	-0.04803	0.07862	0.04623	-0.01789	-0.04097	-0.02477	-0.05884	-0.01243	0.01565	-0.02483	0.02382	-0.05528	0.01376	-0.02932	-0.04579	0.04989	-0.04339	-0.01415	0.06212	-0.03845	0.00371
B_ppm	-0.05065	0.03257	0.01231	0.01231	-0.01866	-0.05378	0.03231	-0.09389	0.06333	0.00947	0.00983	0.06018	0.08541	-0.00714	0.03307	0.05437	0.04519	-0.01334	0.10840	0.00020	-0.01628	-0.05799	0.10201	-0.04868	0.03936	-0.02580	0.00381	0.02733	0.01204	0.00468	-0.02152	-0.03054	0.06210	0.17544	-0.01585
Hg_ppb	-0.27827	-0.25772	0.10989	0.10989	-0.09970	-0.09358	0.09222	-0.02757	-0.15573	-0.21349	-0.15160	0.49336	0.01466	0.18755	0.38327	-0.12193	-0.16256	0.01301	0.16400	0.20827	0.35243	0.00072	-0.10764	0.06473	-0.14875	0.28626	-0.11602	0.34662	0.26415	-0.05077	0.31724	0.04962	-0.14582	0.42357	-0.02047
U	-0.00084	0.31243	-0.15554	-0.15554	-0.18502	-0.03808	-0.15152	0.14790	0.21773	0.13225	0.20029	-0.05054	-0.03368	0.03455	-0.02544	0.26218	0.34672	0.05809	-0.05210	-0.04731	-0.08294	-0.03489	0.21848	0.02109	0.31587	-0.00090	0.31413	-0.04489	0.05317	0.29314	-0.03298	-0.02250	0.27030	-0.00224	0.07106
Total S_%	-0.48476	-0.55362	0.72618	0.72618	0.17464	-0.13055	0.13442	-0.16655	-0.26048	-0.42461	-0.34392	0.54647	-0.00905	0.19177	0.28122	-0.24267	-0.29648	0.03081	0.24745	0.08875	0.35380	-0.08181	-0.24663	0.08196	-0.43287	-0.02005	-0.24515	0.11122	0.30899	-0.13642	0.18287	0.02102	-0.26710	0.30581	-0.23224
C_in_CO2_ppm	-0.49819	-0.33903	0.23743	0.23743	0.57595	0.15256	0.77986	-0.18930	-0.25903	-0.16285	-0.22441	0.32655	0.18631	-0.04091	0.28433	-0.22756	-0.18491	-0.04925	-0.01386	-0.00633	0.00705	-0.01504	-0.06954	-0.06631	-0.33200	-0.07362	-0.28902	0.01569	-0.02216	-0.16356	-0.00666	-0.03443	-0.25682	0.12067	-0.03326
Non_carb._C_ppm	-0.51509	-0.39917	0.09802	0.09802	-0.15667	-0.01906	0.16301	-0.02448	-0.26836	-0.37996	-0.28281	0.89254	-0.02923	0.24321	0.35188	-0.21229	-0.23987	0.10329	0.39309	0.10850	0.44180	-0.03525	-0.22859	0.15099	-0.28642	0.15142	-0.19839	0.19961	0.58299	-0.13776	0.36029	0.03960	-0.27496	0.22257	0.00067

Appendix A2. Matrix of Pearson's coefficient of correlation (r) for N=564 samples of carbonaceous argillite from the Timmins–Kirkland Lake region.

Correlation - 564 rows	Se_ppm	Sn_ppm	Sr_ppm	Ta_ppm	Th_ppm	Tl_ppm	V_ppm	W_ppm	Y_ppm	Zn_ppm	Zr_ppm	La_ppm	Ce_ppm	Pr_ppm	Nd_ppm	Sm_ppm	Eu_ppm	Gd_ppm	Tb_ppm	Dy_ppm	Ho_ppm	Er_ppm	Tm_ppm	Yb_ppm	Lu_ppm	F_pct	B_ppm	Hg_ppb	U	Total S_%	C_in_CO2	Non_carb._C_ppm
SiO2_pct																															
Al2O3_pct																															
Fe2O3_pct																															
FeO_pct																															
MnO_pct																															
MgO_pct																															
CaO_pct																															
Na2O_pct																															
K2O_pct																															
TiO2_pct																															
P2O5_pct																															
LOI_pct																															
Au_ppb																															
Ag_ppm																															
As_ppm																															
Ba_ppm																															
Be_ppm																															
Bi_ppm																															
Br_ppm																															
Cd_ppm																															
Co_ppm																															
Cr_ppm																															
Cs_ppm																															
Cu_ppm																															
Ga_ppm																															
Ge_ppm																															
Hf_ppm																															
In_ppm																															
Mo_ppm																															
Nb_ppm																															
Ni_ppm																															
Pb_ppm																															
Rb_ppm																															
Sb_ppm																															
Sc_ppm																															
Se_ppm	1.00000																														
Sn_ppm	0.46864	1.00000																													
Sr_ppm	-0.21127	-0.27938	1.00000																												
Ta_ppm	-0.08090	0.08898	0.01117	1.00000																											
Th_ppm	-0.06946	0.01498	0.14576	0.59154	1.00000																										
Tl_ppm	0.04545	0.23921	-0.13902	0.16860	0.25776	1.00000																									
V_ppm	-0.14998	-0.13506	0.23771	-0.10664	-0.00543	-0.13376	1.00000																								
W_ppm	-0.10755	-0.05637	-0.01474	-0.04279	-0.00230	-0.02478	-0.00070	1.00000																							
Y_ppm	0.04272	0.10839	-0.08720	0.52602	0.21510	0.02906	-0.02133	0.00273	1.00000																						
Zn_ppm	0.33126	0.51103	-0.19064	-0.05505	-0.07691	0.06221	-0.08357	-0.04056	0.02799	1.00000																					
Zr_ppm	-0.14363	0.10219	0.14439	0.82338	0.56273	0.20747	-0.04663	-0.03514	0.41823	-0.03950	1.00000																				
La_ppm	-0.12944	-0.03780	0.22565	0.55561	0.68770	0.15793	0.03333	0.01980	0.37625	-0.12829	0.60765	1.00000																			
Ce_ppm	-0.11759	-0.01566	0.22251	0.60634	0.68982	0.16135	0.03055	0.00751	0.43052	-0.11829	0.65345	0.99169	1.00000																		
Pr_ppm	-0.10643	-0.00346	0.21859	0.61996	0.66090	0.14241	0.04842	0.00156	0.47017	-0.11409	0.66293	0.97833	0.99321	1.00000																	
Nd_ppm	-0.10375	0.01100	0.20389	0.63310	0.63247	0.13466	0.07029	0.00234	0.51095	-0.10504	0.67155	0.95986	0.98147	0.99398	1.00000																
Sm_ppm	-0.03321	0.07731	0.11739	0.69416	0.56248	0.10299	0.07927	-0.01826	0.67384	-0.05652	0.67796	0.86489	0.90536	0.93492	0.95966	1.00000															
Eu_ppm	0.36707	0.31341	0.04728	0.28666	0.37614	0.09635	0.05440	-0.09509	0.41457	0.18431	0.30328	0.54143	0.55731	0.57880	0.59337	0.64546	1.00000														
Gd_ppm	0.01849	0.11325	0.00731	0.68254	0.40290	0.05310	0.06172	-0.03104	0.86954	-0.00888	0.60356	0.68080	0.73125	0.77477	0.81474	0.93408	0.61056	1.00000													
Tb_ppm	0.05267	0.12801	-0.05961	0.67740	0.31599	0.03915	0.01633	-0.02780	0.94797	0.01943	0.55452	0.52194	0.58116	0.62513	0.66832	0.82731	0.52843	0.96645	1.00000												
Dy_ppm	0.06280	0.13186	-0.08290	0.65125	0.27999	0.03194	0.00818	-0.02596	0.97003	0.02967	0.51694	0.45332	0.51365	0.55762	0.60054	0.76891	0.48415	0.93548	0.99262	1.00000											
Ho_ppm	0.06408	0.12722	-0.09795	0.60871	0.24587	0.02635	-0.00016	-0.02247	0.98475	0.03744	0.47616	0.39962	0.45913	0.50197	0.54459	0.71636	0.44383	0.90323	0.97750	0.99478	1.00000										
Er_ppm	0.07122	0.13103	-0.10689	0.58734	0.23845	0.03168	-0.01202	-0.02246	0.98785	0.04618	0.46168	0.37855	0.43817	0.47992	0.52149	0.69373	0.43031	0.88564	0.96663	0.98821	0.99782	1.00000									
Tm_ppm	0.08067	0.13560	-0.11406	0.57628	0.22926	0.03204	-0.02405	-0.02386	0.98355	0.05274	0.44966	0.35535	0.41617	0.45794	0.49872	0.67453	0.41757	0.87031	0.95664	0.98099	0.99279	0.99752	1.00000								
Yb_ppm	0.10046	0.15211	-0.12299	0.57946	0.24563	0.04087	-0.02715	-0.03086	0.97336	0.07129	0.45862	0.35978	0.42186	0.46408	0.50449	0.68098	0.43755	0.86984	0.95214	0.97489	0.98554	0.99197	0.99645	1.00000							
Lu_ppm	0.13297	0.17194	-0.13457	0.55455	0.24687	0.04947	-0.03756	-0.03820	0.96168	0.09467	0.44164	0.34843	0.41045	0.45208	0.49179	0.66932	0.45968	0.85643	0.93821	0.96156	0.97341	0.98211	0.98889	0.99632	1.00000						
F_pct	-0.04270	-0.05115	0.05670	0.01733	0.07597	0.01754	0.00540	-0.03930	0.02219	-0.04176	0.01172	0.07093	0.07752	0.06391	0.06829	0.05179	0.01558	0.02621	0.02019	0.01356	0.01313	0.00926	0.00429	0.00070	-0.00433	1.00000					
B_ppm	-0.08703	0.03461	0.04934	0.00889	0.07297	-0.02038	0.01332	0.08625	0.02313	0.04143	0.00104	0.06936	0.06644	0.05659	0.05012	0.04087	0.06478	0.03093	0.02515	0.02173	0.01981	0.02087	0.01813	0.01744	0.01611	-0.00916	1.00000				
Hg_ppb	0.44056	0.43438	-0.18190	-0.07338	-0.02208	0.19765	-0.15741	-0.05447	0.03436	0.41692	-0.11404	-0.07640	-0.07333	-0.07274	-0.07053	-0.02399	0.33847	0.01191	0.03503	0.04038	0.04112	0.04727	0.05388	0.06880	0.09667	-0.03625	-0.05396	1.00000			
U	-0.03225	-0.00333	0.12982	0.32791	0.59010	0.09837	0.07405	-0.01117	0.11380	-0.04546	0.29330	0.54699	0.52036	0.50943	0.46862	0.39378	0.27914	0.27819	0.20824	0.18114	0.15557	0.15008	0.14043	0.15116	0.15069	0.01793	0.06147	-0.01836	1.00000		
Total S_%	0.38557	0.24967	-0.31953	-0.14948	-0.20303	0.09273	-0.33367	-0.04045	0.00104	0.18751	-0.25637	-0.24141	-0.24101	-0.23866	-0.23740	-0.17508	0.06156	-0.08783	-0.02692	-0.00839	0.00595	0.01506	0.02367	0.03105	0.04723	-0.05777	0.04348	0.35076	-0.12710	1.00000	
C_in_CO2_ppm	0.02631	-0.04850	0.08357	-0.22948	-0.25028	-0.27669	-0.02072	0.05857	-0.05828	0.00173	-0.31320	-0.21097	-0.22598	-0.22156	-0.21589	-0.17866	-0.06180	-0.11383	-0.09000	-0.07586	-0.06392	-0.06130	-0.05869	-0.05658	-0.05205	-0.01017	0.11198	0.05400	-0.11026	0.18159	1.00000
Non_carb._C_ppm	0.55426	0.32265	-0.22760	-0.10345	0.00146	0.08903	-0.24131	-0.09289	0.02976	0.28365	-0.19324	-0.10042	-0.09030	-0.09044	-0.09774	-0.03131	0.44461	0.00329	0.03524	0.04832	0.05073	0.06380	0.08001	0.10622	0.15317	-0.05469	0.01982	0.43597	0.00088	0.36041	0.07139	1.00000

Appendix A3. Sample and field data description / core log entry for N=564 samples of carbonaceous argillite from the Timmins-Kirkland Lake region.

Sample #	Township	Company	Hole #	MNDM #	Sub_Assemb	Assemblage	Contact	Commodity	Ti/Zr_Source_Rock	Host	Analyzed Sample	From_	To	ft_m
4001	Duff	MNDM-T	255-B-82-4	TI0064	-	Deloro	-	Base Metal	felsic	Volcanic	Graphitic Argillite	201.00	201.50	ft
4002	Duff	MNDM-T	255-B-82-5	TI0065	-	Deloro	-	Base Metal	felsic	Volcanic	Graphitic Argillite	236.00	236.50	ft
4003	Duff	MNDM-T	255-B-81-3	TI0059	-	Deloro	-	Base Metal	felsic	Volcanic	Argillite/Siltstone	205.00	205.50	ft
4004	Aubin	MNDM-T	K-81-9	TI1089	Upper	Blake River	-	Base Metal	felsic	Volcanic	Graphitic Argillite	153.60	153.80	m
4005	Aubin	MNDM-T	K-81-8	TI1088	Upper	Blake River	-	Base Metal	felsic	Volcanic	Argillite/Siltstone	181.60	181.70	m
4006	Aubin	MNDM-T	K-81-6B	TI1085	Upper	Blake River	-	Base Metal	intermediate	Volcanic	Argillite/Siltstone	142.00	142.60	m
4007	Aubin	MNDM-T	K-81-7	TI1086	Upper	Blake River	-	Base Metal	mafic	Volcanic	Argillite/Siltstone	207.00	207.35	m
4008	Dargavel	MNDM-T	K-83-2	TI1674	Upper	Blake River	-	Base Metal	felsic	Volcanic	Graphitic Argillite	293.00	293.50	ft
4010	Aubin	MNDM-T	K-83-4	TI1673	Upper	Blake River	-	Base Metal	felsic	Volcanic	Argillite/Siltstone	131.40	132.00	ft
4011	Lennox	MNDM-T	K-85-7	TI1041	-	Deloro	-	Base Metal	mafic	Volcanic	Siltstone	86.60	86.80	m
4012	Hanna	MNDM-T	7602-78-23	TI0214	-	Stoughton-Roquemare	-	Base Metal	felsic	Volcanic	Graphitic Argillite	69.80	69.90	m
4013	Hanna	MNDM-T	7602-78-26	TI0217	-	Stoughton-Roquemare	-	Base Metal	mafic	Volcanic	Argillite/Siltstone	71.40	71.90	m
4014	Hanna	MNDM-T	7602-78-31	TI0222	-	Stoughton-Roquemare	-	Base Metal	felsic	Volcanic	Graphitic Argillite	313.70	314.00	ft
4015	Dargavel	MNDM-T	K-81-4	TI1083	Upper	Blake River	-	Base Metal	felsic	Volcanic	Graphitic Argillite	106.80	107.10	m
4016	Evelyn	MNDM-T	ED-05	TI2383	Lower	Tisdale	Tisdale/Porcupine	Orogenic Au	intermediate	Volcanic/Sediment	Graphitic Argillite	796.40	797.40	ft
4017	Kingsmill	MNDM-T	K-84-5	TI1680	Upper	Blake River	-	Base Metal	intermediate	Volcanic	Graphitic Argillite	198.30	198.60	m
4018	Little	MNDM-T	AF-5	TI3425	Upper	Tisdale	-	Base Metal	felsic	Volcanic	Graphitic Argillite	53.10	53.40	m
4019	Little	MNDM-T	TP-198	TI0039	-	Tisdale	Tisdale/Porcupine	Orogenic Au	intermediate	Volcanic/Sediment	Argillite/Siltstone	419.00	420.00	ft
4020	Little	MNDM-T	P-1980-9	TI0042	Upper	Tisdale	-	Base Metal	felsic	Volcanic	Argillite/Siltstone	130.30	130.80	ft
4021	Ottaway	MNDM-T	OT-81-1	TI0349	Upper	Kidd-Munro	Kidd-Munro/Porcupine	Base Metal	felsic	Volcanic	Graphitic Argillite	467.10	468.10	ft
4022	Hanna	MNDM-T	7602-78-33	TI0224	-	Stoughton-Roquemare	-	Base Metal	felsic	Volcanic	Argillite/Siltstone	119.20	119.50	m
4023	Hanna	MNDM-T	7602-78-36	TI0226	Upper	Tisdale	Tisdale/Stoughton-Roquemare	Base Metal	mafic	Volcanic	Graphitic Argillite	106.20	106.80	m
4024	Little	MNDM-T	T80-7	TI1532	Upper	Kidd-Munro	-	Base Metal	felsic	Volcanic	Graphitic Argillite	457.00	457.40	ft
4025	Ottaway	MNDM-T	OT-81-3	TI0351	-	Stoughton-Roquemare	-	Base Metal	felsic	Volcanic	Graphitic Argillite	368.30	368.60	ft
4026	Ottaway	MNDM-T	OT-81-4	TI0352	-	Stoughton-Roquemare	-	Base Metal	intermediate	Volcanic	Graphitic Argillite	313.80	314.80	ft
4027	Ottaway	MNDM-T	OT-81-5	TI0353	-	Stoughton-Roquemare	Stoughton-Roquemare/Porcupine	Base Metal	felsic	Volcanic	Graphitic Argillite	253.50	254.30	ft
4028	Ottaway	MNDM-T	OT-81-6	TI0354	-	Stoughton-Roquemare	-	Base Metal	felsic	Volcanic	Graphitic Argillite	351.40	352.00	ft
4029	Ottaway	MNDM-T	OT-81-7	TI0355	-	Stoughton-Roquemare	-	Base Metal	intermediate	Volcanic	Graphitic Argillite	390.40	391.00	ft
4030	Wilhelmina	MNDM-T	I	TI3510	Upper	Blake River	Blake River/Kidd-Munro	Base Metal	mafic	Volcanic	Graphitic Argillite	136.50	136.90	m
4031	Wilhelmina	MNDM-T	1566-1	TI3513	Upper	Blake River	Blake River/Kidd-Munro	Base Metal	mafic	Volcanic	Argillite/Siltstone	76.30	76.60	m
4032	Aubin	MNDM-T	K-81-10	TI1087	Upper	Blake River	-	Base Metal	mafic	Volcanic	Argillite/Siltstone	111.30	111.60	m
4033	Aubin	MNDM-T	K85-1	TI0380	Upper	Blake River	-	Base Metal	felsic	Volcanic	Graphitic Argillite w abundant sulfide	167.40	167.90	m
4034	Little	MNDM-T	AF-7	TI3426	-	Stoughton-Roquemare	-	Base Metal	felsic	Volcanic	Graphitic Argillite	380.00	381.00	ft
4035	Little	MNDM-T	TP-82-7	TI0422	Upper	Tisdale	-	Base Metal	intermediate	Volcanic	Graphitic Argillite	223.50	224.50	ft
4036	Little	MNDM-T	AF-1	TI3423	-	Stoughton-Roquemare	-	Base Metal	intermediate	Volcanic	Graphitic Argillite	84.50	84.90	m
4037	McCart	MNDM-T	AF-3	TI3424	Upper	Tisdale	-	Base Metal	intermediate	Volcanic	Graphitic Argillite	78.50	78.80	m
4038	Reaume	MNDM-T	R-82-2	TI0188	-	Stoughton-Roquemare	Stoughton-Roquemare/Tisdale	Base Metal	felsic	Volcanic	Graphitic Argillite	418.30	419.00	ft
4039	Mann	MNDM-T	7602-78-11A	TI0203	Upper	Tisdale	-	Base Metal	felsic	Volcanic	Graphitic Argillite	202.00	203.00	ft
4040	Clergue	MNDM-T	CS-81-1	TI0174	Lower	Kidd-Munro	Kidd-Munro/Porcupine	Base Metal	felsic	Volcanic	Graphitic Argillite	479.00	479.50	ft
4041	Reaume	MNDM-T	7602-78-8	TI0200	Upper	Tisdale	Tisdale/Stoughton-Roquemare	Base Metal	felsic	Volcanic	Graphitic Argillite	131.00	131.40	m
4042	Reaume	MNDM-T	7602-78-10	TI0202	-	Stoughton-Roquemare	-	Base Metal	felsic	Volcanic	Graphitic Argillite	72.40	72.70	m
4043	Reaume	MNDM-T	7602-78-13	TI0205	-	Stoughton-Roquemare	-	Base Metal	felsic	Volcanic	Argillite/Siltstone	71.30	71.60	m
4044	Reaume	MNDM-T	7602-78-2	TI0194	-	Stoughton-Roquemare	-	Base Metal	felsic	Volcanic	Graphitic Argillite	62.60	62.90	m
4045	Mahaffy	MNDM-T	R-90-2	TI3547	Upper	Blake River	-	Base Metal	intermediate	Volcanic	Graphitic Argillite	91.40	91.70	m
4046	Clergue	MNDM-T	034-06-1	TI1033	-	Blake River	Blake River/Porcupine	Base Metal	felsic	Volcanic	Graphitic Argillite	108.50	108.80	m
4047	Clergue	MNDM-T	034-07-1	TI1034	-	Blake River	Blake River/Porcupine	Base Metal	felsic	Volcanic	Graphitic Argillite	60.70	61.10	m
4048	Lennox	MNDM-T	LX-55-4	TI2269	-	Deloro	-	Base Metal	felsic	Volcanic	Graphitic Argillite	173.00	173.40	m
4049	Mahaffy	MNDM-T	RM-79-2	TI0159	Upper	Blake River	-	Base Metal	felsic	Volcanic	Graphitic Argillite	128.00	128.50	ft
4050	Mahaffy	MNDM-T	R-90-1	TI3546	Upper	Blake River	-	Base Metal	felsic	Volcanic	Graphitic Argillite	315.50	316.00	ft
4051	Lucas	MNDM-T	Lu-54-01	TI1850	-	Deloro	-	Base Metal	felsic	Volcanic	Graphitic Argillite	148.10	148.70	m
4052	Lucas	MNDM-T	C-83-4	TI1667	-	Deloro	-	Base Metal	felsic	Volcanic	Graphitic Argillite	264.50	265.50	ft
4053	Lucas	MNDM-T	C-83-1	TI1664	-	Deloro	-	Base Metal	felsic	Volcanic	Graphitic Argillite	264.30	265.20	ft
4054	Lucas	MNDM-T	C-83-3	TI1666	-	Deloro	-	Base Metal	felsic	Volcanic	Graphitic Argillite	244.80	245.50	ft
4055	Lucas	MNDM-T	LU-44-01	TI1513	-	Deloro	-	Base Metal	felsic	Volcanic	Graphitic Argillite	98.30	98.70	m
4056	Lucas	MNDM-T	7602-78-21	TI0212	-	Deloro	-	Base Metal	felsic	Volcanic	Graphitic Argillite	110.90	111.30	m
4057	Lucas	MNDM-T	7602-78-24	TI0215	-	Deloro	-	Base Metal	felsic	Volcanic	Argillite	66.30	66.60	m
4058	Reaume	MNDM-T	7602-78-19	TI0210	Upper	Tisdale	-	Base Metal	felsic	Volcanic	Argillite	252.50	254.00	ft
4059	Reaume	MNDM-T	7602-78-20	TI0211	-	Stoughton-Roquemare	Stoughton-Roquemare/Tisdale	Base Metal	felsic	Volcanic	Graphitic Argillite	96.30	96.70	m
4060	Reaume	MNDM-T	7602-78-37	TI0227	Upper	Tisdale	-	Base Metal	felsic	Volcanic	Graphitic Argillite	234.50	235.50	ft
4061	Reaume	MNDM-T	7602-78-38	TI0228	-	Stoughton-Roquemare	-	Base Metal	intermediate	Volcanic	Argillite/Siltstone	146.00	147.00	ft

Appendix A3. Sample and field data description / core log entry for N=564 samples of carbonaceous argillite from the Timmins-Kirkland Lake region.

Sample #	Easting_83	Northing_83	Sample Type	Field Description/Core Log Entry	Interval Available	Hanging wall	Footwall
4001	485174.00	5405674.00	Graphitic Argillite	Massive to nodular py with graphite	201-207 ft	Chert	Tuff Breccia
4002	485395.00	5405449.00	Graphitic Argillite	Graphite w/ nodular pyrite	228-259 ft	Black Chert	Sericite Schist
4003	485565.00	5405329.00	Argillite/Siltstone	Bedded argillite, greywacke, conglomerate	190-205.9ft	Intermediate breccia	Rhyolite Tuff
4004	461781.00	5415349.00	Graphitic Argillite	Carbonatized Graphitic Metasediment - 10-40% po, trace cpy	153-155.1m	Andesite	Andesite
4005	460371.00	5416899.00	Argillite/Siltstone	Lithic wacke -dark grey to black, aphanitic, 10-15% carbonate	174.7-192.6m	Rhyolitic tuff	EOH
4006	463721.00	5416309.00	Argillite/Siltstone	Graphite - dark grey/black, pyritic	141-146.1m	Rhyolitic tuff	Rhyolitic tuff
4007	461176.00	5415434.00	Argillite/Siltstone	Graphitic Metasediment - 5-10% po, py nodules	207-215.20m	Andesite	Wacke
4008	456094.00	5426062.00	Graphitic Argillite	Black, Cherty Graphitic, Silty Argillite, very conductive, pyrite	289-309ft	Mafic/UM? Volcanic	Gabbro Intrusion/Felsic Tuff
4010	458421.00	5417379.00	Argillite/Siltstone	Silty Argillite, not conductive	124-232 ft	Overburden	Argillaceous siltstone
4011	466161.00	5425129.00	Siltstone	Black, fine-grained	88.9-89.1	Siltstone/Chl Schist	Siltstone/Chl Schist
4012	498146.00	5414772.00	Graphitic Argillite	Black to dark grey, fine-grained, graphitic laminae	66.93-69.95m	Intermediate volcanic and chert	Intermediate volcanics
4013	497400.00	5414729.00	Argillite/Siltstone	Graphitic Argillite - chert and py (5 to 40%)	68.57-71.2m	Intermediate volcanic tuff	Peridoite
4014	494615.00	5420684.00	Graphitic Argillite	Graphite - carbonaceous, 5 to 100% po, trace py, cpy	95-96.2 m	Intermediate volcanic	Intermediate volcanic
4015	458216.00	5432139.00	Graphitic Argillite	Black, fine-grained, siliceous, pyrr nodules	105.9-111.7	Ultramafic flow	Ultramafic flow
4016	495495.00	5389194.00	Graphitic Argillite	Mudstone - thinly bedded locally pyritic, with greywacke,	697-801ft	Greywacke	Argillite
4017	455831.00	5420919.00	Graphitic Argillite	Black to dk grey, fine-grained, locally siliceous and silty laminae	198.3-206.2 m	Diabase	Felsic Tuffite
4018	503550.00	5402964.00	Graphitic Argillite	Graphitic Sediments, py nodules	47.2-49.5 m	Polymictic Agglomerate	Ash Tuff
4019	495590.00	5399159.00	Argillite/Siltstone	Black, fine-grained	112.47-112.5m	Dacitic tuff	Cherty graphitic tuff
4020	501025.00	5403939.00	Argillite/Siltstone	Metasediments - banded greywacke and some argillite	39.3-47.9m	Intermediate volcanic	Cherty tuff
4021	476076.00	5427089.00	Graphitic Argillite	Graphitic Argillite; black, some carb with minor po	466-486.9 ft	Greywacke	UM and Mafic flows
4022	498060.00	5420269.00	Argillite/Siltstone	Cherty calcareous argillite -laminations of chert and pyrite	103.4-120.89 m	Diorite	Intermediate feldspar porphyry
4023	496325.00	5418139.00	Graphitic Argillite	Graphitic argillite - carbonaceous and calcareous, 15-25% py	104-108.6 m	Argillite	Argillite
4024	495070.00	5396799.00	Graphitic Argillite	Graphitic pyritic sediment -up to 30% collorform and nodular pyrite	456.9-476 ft	Basalt	Basalt
4025	477541.00	5426789.00	Graphitic Argillite	Argillaceous graphite with po	367.1-368.6 ft	Intermediate tuff	UM flows
4026	477441.00	5426589.00	Graphitic Argillite	Interbedded graphite and greywacke, local pyrite nodules	144-320.5 ft	Casing	UM and Mafic flows
4027	475841.00	5426199.00	Graphitic Argillite	Graphitic Argillite, minor py	216-270.4ft	Casing	Interbedded greywacke and graphite
4028	478101.00	5424739.00	Graphitic Argillite	Argillte/graphitic argillite with interbedded greywacke and dike	190-383.4 ft	Basalt and UM	Mafic and UM tuffs/flows
4029	476541.00	5426719.00	Graphitic Argillite	Graphitic Argillite, black, fine-grained	337.1-409.6 ft	Greywacke	Mafic and UM tuffs/flows
4030	444962.00	5408959.00	Graphitic Argillite	Graphitic Argillite, black, fine-grained	137.8-138.3 m	Mafic Volcanic Schist	Mafic Volcanic Schist
4031	437917.00	5407579.00	Argillite/Siltstone	Sediments and graphitic sediments-pyritic	77.3-86.9	Sediments	Felsic to intermediate tuff
4032	462511.00	5415679.00	Argillite/Siltstone	Graphitic metasediment, 10% CO3, pyritic	103.9-113 m	Andesite, fault	Dacitic tuff
4033	460691.00	5417999.00	Graphitic Argillite w/ abundant sulfide	Graphite/pyrite horizon with 40% graphite, 50% pyrite, 10% carbonate	167.4-167.9m	Intermediate volcanic and tuff	Intermediate tuff
4034	503855.00	5404514.00	Graphitic Argillite	Altered Sediments with graphitic zones and py nodules at 110-118	107.0-135.5	Mafic-Intermediate Volcanics	Mafic-Intermediate Volcanics
4035	502730.00	5402849.00	Graphitic Argillite	Graphite - black, pyrite nodules	67.67-69.31m	Andesite and small sulfide zone at 50m	Basalt
4036	502160.00	5403984.00	Graphitic Argillite	Graphitic Sediments, py nodules, poss fault at 85.8	84.5-85.8 m	Intermediate Ash Tuff	Ash Tuff/Graphitic Sediments
4037	504600.00	5401649.00	Graphitic Argillite	Argillaceous Greywacke; black, graphitic, conductive layers with py nodules	63.4-112.8m	Overburden	Mafic Volcanics
4038	487218.00	5419573.00	Graphitic Argillite	Graphitic Sediments; interbedded with chert, py and po nodules	418.2-430.3	Basalt flows	Basalt Flows
4039	498220.00	5406449.00	Graphitic Argillite	Graphitic Argillite - black, strongly carbonaceous, disseminated and nodular pyrite	57.3-66m	Rhyolite	Rhyolite tuff
4040	521764.00	5385819.00	Graphitic Argillite	Graphite; black, py nodules, minor carb	467.5-473.9 ft	UM Volcanics	Chert/UM Volcanics
4041	493097.00	5417633.00	Graphitic Argillite	Graphitic Argillite, moderately conductive, py, qtz-veins	131.7-132.4 m	Intermediate Volcanic Flow	Intermediate Volcanic Flow and Breccia
4042	486720.00	5420549.00	Graphitic Argillite	Graphitic Argillite, massive from 59.44-61.26 and 63.09-64.31 with py nodules, chert and minor	59.12-74.80 m	Overburden	Intermediate Volcanic Tuff
4043	485125.00	5420974.00	Argillite/Siltstone	Graphitic Argillite; moderately conductive b/w 79.92-80.85 and 82.20-84.54, very conductive between 87.83-88.20, qtz-carb veins	61.95-116.0 m	Intermediate Volcanic Flow	Intermediate Volcanics? With Argillite interbeds
4044	489040.00	5420909.00	Graphitic Argillite	Graphitic Argillite; chert laminae, py nodules; qtz-carb veinlets	62.48-78.64 m	Arkose	Intermediate Volcanics
4045	465526.00	5406559.00	Graphitic Argillite	Graphitic Argillite - laminated, black, fine-grained, local nodular and semi-massive pyrite	89.83-95.31 m	Intermediate tuff	Brecciated mudstone
4046	521789.00	5394359.00	Graphitic Argillite	Graphitic Argillite - Conductive minor py	102-126.7m	Greywacke	Greywacke
4047	523079.00	5394129.00	Graphitic Argillite	Graphitic Argillite - conductive	60.2-63.1m	Greywacke	Greywacke
4048	473341.00	5432299.00	Graphitic Argillite	Graphitic Argillite with py nodules; graphitic content becoming lesser towards bottom	167-179.5m	Magnetite IF and Mafic Volcanic	Mafic Volcanic
4049	459051.00	5406159.00	Graphitic Argillite	Graphite, py	130-133 ft	Overburden	Massive Pyrite
4050	464681.00	5406614.00	Graphitic Argillite	Intercalated graphitic tuff and graphitic feldspathic tuff - black, fine-grained, nodular pyrite	90.85-96.56 m	Andesite	Carbonated, brecciated siliceous mudstone
4051	481086.00	5411979.00	Graphitic Argillite	Graphitic argillite - black graphitic, conductive	149.1-150.3 m	Mafic volcanic	Mafic volcanic
4052	480721.00	5410599.00	Graphitic Argillite	Graphitic Argillite - conductor -interbedded with greywacke -trace py	208-300 ft	Overburden	EOH
4053	478331.00	5411729.00	Graphitic Argillite	Graphitic Argillite	206.5-353 ft	Semi-Massive to Massive Pyrite	EOH
4054	480741.00	5411339.00	Graphitic Argillite	Graphitic Argillite with greywacke -lamined black to grey, conductor; 10% py	167-251ft	Felsic lapilli tuff	EOH
4055	481731.00	5411269.00	Graphitic Argillite	Graphitic Argillite	97.7-99.8 m	Mafic-Intermediate Volcanics	Mafic Volcanics (Brecciated)
4056	478641.00	5414329.00	Graphitic Argillite	Graphitic Argillite, strongly carbonaceous, interbedded massive py, qtz str and pods	110.9-114.8 m	Felsic Carbonaceous Tuff	Mineralization (10-100% py)
4057	481625.00	5407181.00	Argillite	Interbedded Argillite and Intermediate Schistose Tuff	57.9-82.8 m	Overburden	Intermediate Lapilli Tuff/Agglomerate (pyroclastics?)
4058	485770.00	5414824.00	Argillite	Argillaceous cherty sediment - carbonaceous and siliceous, slightly conductive	69.5-97.8m	Felsic tuff and cherty sediments	Felsic tuff
4059	488280.00	5417679.00	Graphitic Argillite	Graphitic Argillite - pyritic, very conductive	92.96-96.74m	Chert	Graphitic tuff
4060	485229.00	5419086.00	Graphitic Argillite	Argillite - graphite content increases downhole, slightly conductive	54.86-81.69m	Overburden	Intermediate volcanic
4061	489080.00	5421434.00	Argillite/Siltstone	Intermedded argillite and intermediate volcanics	20.12-46.1m	Intermediate volcanic	Graphitic argillaceous tuff

Appendix A3. Sample and field data description / core log entry for N=564 samples of carbonaceous argillite from the Timmins-Kirkland Lake region.

Sample #	Township	Company	Hole #	MNDM #	Sub_Assemb	Assemblage	Contact	Commodity	Ti/Zr_Source_Rock	Host	Analyzed Sample	From_	To	ft_m
4062	Lucas	MNDM-T	L-81-21A	TI0411	-	Deloro	-	Base Metal	intermediate	Volcanic	Argillite/Siltstone	771.50	772.00	ft
4063	Reaume	MNDM-T	7602-78-7	TI0199	-	Stoughton-Roquemare	-	Base Metal	mafic	Volcanic	Graphitic Argillite	267.50	268.50	ft
4064	Reaume	MNDM-T	7602-78-25	TI0216	-	Stoughton-Roquemare	Stoughton-Roquemare/Tisdale	Base Metal	felsic	Volcanic	Graphitic Argillite	248.00	248.50	ft
4065	Reaume	MNDM-T	7602-78-22	TI0213	-	Stoughton-Roquemare	Stoughton-Roquemare/Tisdale	Base Metal	felsic	Volcanic	Graphitic Argillite	349.50	350.50	ft
4066	Lucas	MNDM-T	LU-45-01	TI1628	-	Deloro	-	Base Metal	felsic	Volcanic	Argillite/Siltstone	456.00	457.00	ft
4067	Evelyn	MNDM-T	EVE-6	TI3057	-	Porcupine	-	Orogenic Au	intermediate	Sediment	Tuff	41.60	42.00	m
4068	Evelyn	MNDM-T	EVE-7	TI3058	-	Porcupine	-	Orogenic Au	intermediate	Sediment	Argillite/Siltstone	131.70	132.00	m
4069	Nesbitt	MNDM-T	NE-92-32	TI4208	-	Deloro	-	Base Metal	mafic	Volcanic	Argillite/Siltstone green	67.70	68.20	m
4070	Kingsmill	MNDM-T	KL-92-31	TI4209	Upper	Blake River	-	Base Metal	felsic	Volcanic	Argillite	107.40	107.70	m
4071	Lennox	MNDM-T	K-85-5	TI4243	-	Deloro	-	Base Metal	mafic	Volcanic	Greywacke/Siltstone	57.70	58.00	m
4072	Dargavel	MNDM-T	K-85-9	TI4245	-	Deloro	-	Base Metal	mafic	Volcanic	Shale/Siltstone	70.10	70.40	m
4073	Kingsmill	MNDM-T	KI-92-29	TI4211	Upper	Blake River	-	Base Metal	felsic	Volcanic	Argillite/Siltstone	29.70	29.90	m
4074	Nesbitt	MNDM-T	NE-91-18	TI4236	-	Deloro	-	Base Metal	felsic	Volcanic	Graphitic Argillite	106.50	106.80	m
4075	Taylor	St Andrew Goldfields Ltd.	TA-11-001	-	Lower	Tisdale	Tisdale/Porcupine	Orogenic Au	intermediate	Volcanic/Sediment	Argillite w qtz vein	182.60	182.90	m
4076	Taylor	St Andrew Goldfields Ltd.	TA-11-008	-	Lower	Tisdale	Tisdale/Porcupine	Orogenic Au	intermediate	Volcanic/Sediment	Argillite/Siltstone cherty	667.60	667.90	m
4077	Taylor	St Andrew Goldfields Ltd.	TA-11-003	-	Lower	Tisdale	Tisdale/Porcupine	Orogenic Au	intermediate	Volcanic/Sediment	Argillite	488.50	488.70	m
4078	Taylor	St Andrew Goldfields Ltd.	TA-11-006	-	Lower	Tisdale	Tisdale/Porcupine	Orogenic Au	intermediate	Volcanic/Sediment	Argillite/Siltstone	458.50	458.70	m
4079	Edwards	MNDM-KL	057-02-2	KL0480	-	Stoughton-Roquemare	-	Base Metal	felsic	Volcanic	Graphitic Siltstone/Mudstone	156.00	156.50	m
4080	Teefy	MNDM-KL	034-15-1	KL0435	-	Stoughton-Roquemare	Stoughton-Roquemare/Tisdale	Base Metal	felsic	Volcanic	Graphitic Argillite	163.60	164.10	m
4081	Edwards	MNDM-KL	057-02-4	KL0482	-	Stoughton-Roquemare	-	Base Metal	felsic	Volcanic	Graphitic Argillite fault gouge	105.60	106.50	m
4082	Edwards	MNDM-KL	057-02-1	KL0479	-	Stoughton-Roquemare	-	Base Metal	felsic	Volcanic	Graphitic Argillite fault gouge	0.00	0.00	-
4083	Michaud	MNDM-KL	M-82-2	KL0295	Lower	Blake River	-	Orogenic Au	mafic	Volcanic/Sediment	Argillite/Siltstone	341.90	342.10	m
4084	Munro	MNDM-KL	839-13-1	KL0031	Lower	Kidd-Munro	-	Base Metal	felsic	Volcanic	Graphitic Argillite	40.10	40.45	m
4085	Kerrs	MNDM-KL	JL-85-K	KL1830	-	Stoughton-Roquemare	-	Base Metal	intermediate	Volcanic	Graphitic Argillite	297.50	299.00	ft
4086	Munro	MNDM-KL	839-15-1	KL1003	Lower	Kidd-Munro	-	Base Metal	felsic	Volcanic	Graphitic Argillite w sulfide	67.50	67.95	m
4087	Garrison	MNDM-KL	AG883	KL1991	Lower	Kidd-Munro	-	Base Metal	felsic	Volcanic	Interflow Sediment/Siltstone	383.50	383.80	ft
4090	Harker	MNDM-KL	839-39-7	KL0470	-	Kidd-Munro	Kidd-Munro/Timiskaming	Orogenic Au	intermediate	Volcanic/Sediment	Mudstone/Siltstone	41.00	41.40	m
4091	Edwards	MNDM-KL	057-02-3	KL0481	-	Stoughton-Roquemare	-	Base Metal	felsic	Volcanic	Graphitic Shale/Siltstone	108.30	108.60	m
4092	Teefy	MNDM-KL	034-15-3	KL0436	-	Stoughton-Roquemare	-	Base Metal	felsic	Volcanic	Graphitic Argillite	127.30	127.60	m
4093	Teefy	MNDM-KL	034-15-2	KL0434	-	Stoughton-Roquemare	-	Base Metal	felsic	Volcanic	Graphitic Argillite	105.10	105.30	m
4094	Stoughton	MNDM-KL	ST-88-1	KL2178	-	Kidd-Munro	Kidd-Munro/Stoughton-Roquemare	Base Metal	felsic	Volcanic	Graphitic Argillite/Siltstone brecciated	111.00	112.00	ft
4095	Munro	MNDM-KL	839-10-9	KL0637	-	Kidd-Munro	-	Base Metal	felsic	Volcanic	Argillite/Siltstone	205.80	206.00	m
4096	Munro	MNDM-KL	839-10-8	KL0636	-	Kidd-Munro	-	Base Metal	felsic	Volcanic	Argillite/Siltstone	78.80	80.20	m
4097	Stoughton	MNDM-KL	ST-88-1	KL2178	-	Kidd-Munro	Kidd-Munro/Stoughton-Roquemare	Base Metal	felsic	Volcanic	Graphitic Argillite/Siltstone	300.10	300.30	ft
4098	Ossian	MNDM-KL	KL-3	KL0661	Lower	-	-	Orogenic Au	felsic	Volcanic/Sediment	Graphitic Argillite	115.40	115.70	m
4099	Rickard	MNDM-KL	1035-03-1	KL0036	Upper	Tisdale	Tisdale/Stoughton-Roquemare	Base Metal	felsic	Volcanic	Graphitic Argillite interflow sediment	72.90	73.20	m
4100	Stoughton	MNDM-KL	ST-88-5	KL2180	-	Kidd-Munro	-	Base Metal	felsic	Volcanic	Graphitic Argillite/Siltstone	514.00	515.00	ft
4101	Rickard	MNDM-KL	1035-04-1	KL0038	-	Stoughton-Roquemare	-	Base Metal	felsic	Volcanic	Graphitic Argillite	122.50	122.80	m
4102	Kerrs	MNDM-KL	JL-84-GSE	KL1837	-	Stoughton-Roquemare	-	Base Metal	felsic	Volcanic	Graphitic Argillite	131.50	12.00	ft
4103	McCool	MNDM-KL	839-29-1	KL0658	Lower	Kidd-Munro	-	Base Metal	mafic	Volcanic	Graphitic Argillite	64.50	64.70	m
4104	Wilkie	MNDM-KL	WI-81-1	KL0224	Lower	Kidd-Munro	Kidd-Munro/Porcupine	Base Metal	intermediate	Volcanic	Graphitic Argillite/Siltstone	1074.00	1075.00	ft
4105	Wilkie	MNDM-KL	WI-81-2	KL0225	Lower	Kidd-Munro	Kidd-Munro/Porcupine	Base Metal	felsic	Volcanic	Graphitic Argillite	198.50	199.50	ft
4106	Michaud	MNDM-KL	M-82-1	KL0294	Lower	Blake River	-	Orogenic Au	intermediate	Volcanic/Sediment	Graphitic Argillite	438.50	439.20	ft
4107	Munro	MNDM-KL	839-10-3	KL0718	Lower	Kidd-Munro	-	Base Metal	felsic	Volcanic	Graphitic Argillite	65.80	66.00	m
4108	Michaud	MNDM-KL	M-86-12	KL1820	Lower	Blake River	-	Orogenic Au	mafic	Volcanic/Sediment	Graphitic Argillite	446.50	447.00	ft
4109	Warden	MNDM-KL	839-27-1	KL0039	-	Kidd-Munro	Kidd-Munro/Porcupine	Orogenic Au	felsic	Volcanic/Sediment	Graphitic Argillite	114.00	114.30	m
4110	Marathon	MNDM-KL	MA-84-2	KL1771	-	Porcupine	-	Orogenic Au	felsic	Sediment	Graphitic Argillite	532.30	533.30	ft
4111	Wesley	MNDM-KL	MO-84-1	KL1770	-	Stoughton-Roquemare	Stoughton-Roquemare/Porcupine	Orogenic Au	felsic	Volcanic/Sediment	Graphitic Argillite	1009.00	1009.50	ft
04111B	Wesley	MNDM-KL	MO-84-1	KL1770	-	Stoughton-Roquemare	Stoughton-Roquemare/Porcupine	Orogenic Au	felsic	Volcanic/Sediment	Graphitic Argillite (not a duplicate)	0.00	0.00	-
4112	Michaud	MNDM-KL	M-86-10	KL1818	Lower	Blake River	-	Orogenic Au	intermediate	Volcanic/Sediment	Graphitic Argillite	322.60	323.20	ft
04112B	Michaud	MNDM-KL	M-86-10	KL1818	Lower	Blake River	-	Orogenic Au	intermediate	Volcanic/Sediment	Graphitic Argillite (not a duplicate)	0.00	0.00	-
4113	Coulson	MNDM-KL	056-01-4	KL1044	Lower	Kidd-Munro	-	Base Metal	felsic	Volcanic	Graphitic Argillite	51.80	52.10	m
4114	Marathon	MNDM-KL	MA-84-1	KL1772	-	Porcupine	-	Orogenic Au	felsic	Sediment	Graphitic Argillite	172.20	172.50	m
4115	Galna	MNDM-KL	JL-85-D2	KL1331	-	Stoughton-Roquemare	-	Base Metal	felsic	Volcanic	Argillite	439.00	439.50	ft
4116	Marriot	MNDM-KL	049-04-9	KL1016	Lower	Blake River	-	Orogenic Au	felsic	Volcanic	Interbedded chert and cherty graphitic argillite	142.00	142.20	m
4117	Rickard	MNDM-KL	R 92-1	KL2354	-	Stoughton-Roquemare	-	Base Metal	felsic	Volcanic	Graphitic Shale	486.50	487.20	ft
04117B	Rickard	MNDM-KL	R 92-1	KL2354	-	Stoughton-Roquemare	-	Base Metal	intermediate	Volcanic	Graphitic Shale (not a duplicate)	0.00	0.00	-
4118	Holloway	MNDM-KL	010-45-31	KL1148	-	Kidd-Munro	Kidd-Munro/Timiskaming	Orogenic Au	intermediate	Volcanic/Sediment	Graphitic Argillite/Siltstone	40.70	41.00	m
4119	Harker	MNDM-KL	86-8	KL1470	Lower	Blake River	-	Orogenic Au	felsic	Sediment	Graphitic Argillite	104.80	105.20	m
4120	McCool	MNDM-KL	183-82-6	KL1341	Lower	Kidd-Munro	-	Base Metal	felsic	Volcanic	Argillite/Siltstone/Tuff	71.20	71.50	m
4121	Kerrs	MNDM-KL	JL-85-ASE	KL1335	-	Stoughton-Roquemare	-	Base Metal	intermediate	Volcanic	Silicified Argillite, hematitic stain	41.10	41.60	ft
4122	Holloway	MNDM-KL	I-84-4	KL1142	Lower	Blake River	-	Orogenic Au	felsic	Sediment	Graphitic Argillite	62.00	62.60	ft
4123	Moody	MNDM-KL	JL-84-A	KL1841	-	Stoughton-Roquemare	Stoughton-Roquemare/Porcupine	Orogenic Au	felsic	Volcanic/Sediment	Graphitic Argillite	442.20	443.20	ft
4124	Holloway	MNDM-KL	AS-85-2	KL1677	Lower	Blake River	-	Orogenic Au	felsic	Sediment	Graphitic Argillite w vein	2618.50	2619.20	ft
4125	Holloway	MNDM-KL	839-42-6	KL0605	-	Kidd-Munro	Kidd-Munro/Timiskaming	Orogenic Au	felsic	Volcanic/Sediment	Graphitic Argillite	49.20	49.40	m
4126	Harker	MNDM-KL	M-85-4	KL1655	Lower	Blake River	-	Orogenic Au	felsic	Sediment	Shale/Siltstone	376.20	376.70	ft
4127	Marriot	MNDM-KL	049-03-2	KL0822	Lower	Blake River	Blake River/Kidd-Munro	Orogenic Au	felsic	Volcanic	Graphitic Argillite	129.50	129.70	m

Appendix A3. Sample and field data description / core log entry for N=564 samples of carbonaceous argillite from the Timmins-Kirkland Lake region.

Sample #	Easting_83	Northing_83	Sample Type	Field Description/Core Log Entry	Interval Available	Hanging wall	Footwall
4062	484019.00	5406997.00	Argillite/Siltstone	Graphitic, black to dk grey, fine-grained	795-802 ft	Mineralized Zone/Graphitic-Crystal Poor Tuff	Felsic Tuff
4063	486745.00	5421074.00	Graphitic Argillite	Graphitic Argillite, py nodules, minor cpy	78.49-79.86 m	Graphitic Tuff/Intermediate Volcanic Breccia	Graphitic Tuff/Intermediate Volcanic Flow
4064	487280.00	5418499.00	Graphitic Argillite	Graphitic, black to dk grey, fine-grained	74.83-76.5m	Intermediate volcanic	cherty argillaceous sedimentary breccia
4065	487880.00	5417899.00	Graphitic Argillite	Graphitic, black to dk grey, fine-grained	107.68-113.2m	Intermediate volcanic	Intermediate porphyry
4066	482421.00	5410779.00	Argillite/Siltstone	Massive pyrite, pyritic carbonaceous sediment - mostly colloform and nodular pyrite	143.1-147.5 m	Iron formation	Intermediate lapilli tuff
4067	496000.00	5388099.00	Tuff	Argillite, graphitic?, diss py	38.9-42.9 m	Greywacke	Greywacke
4068	496260.00	5387839.00	Argillite/Siltstone	Argillite, dark grey, fine-grained	91.1-143.8 m	Greywacke	Greywacke
4069	465661.00	5418959.00	Argillite/Siltstone green	Graphitic, black to dk grey, fine-grained	67.65-68.2 m	Mafic Volcanic	Mafic/UM Volcanic/Intrusive
4070	452791.00	5422729.00	Argillite	Argillite; minor graphite, minor sulfide	98.8-109.5 m	Basalt	Dacite tuff
4071	465921.00	5424579.00	Greywacke/Siltstone	Graphitic Schist-Black Shale; core loss b/w 60-62; fault?	60.6-61.7 m	Mafic	Mafic/UM
4072	465511.00	5425439.00	Shale/Siltstone	Black, fine-grained, shaley cleavage	69-70 m	Calcareous siltstone	Mix of siltstone, felsic volcanic, and mafic flows
4073	450231.00	5424389.00	Argillite/Siltstone	Graphitic argillite, mod. Conductive, minor py	28-32.5m	Overburden	Basalt/dacite
4074	469220.00	5417499.00	Graphitic Argillite	Graphitic argillite - 3-5% py stringers	38.7-41.4m	Lapilli tuff	Chert
4075	526501.07	5378862.50	Argillite w/ qtz vein	Argillite interbedded with greywacke; pervasive chloritization and sericitation; Shoot zone	-		
4076	527806.64	5378991.86	Argillite/Siltstone cherty	Footwall to the Main West Porphyry deposit	-		
4077	527753.82	5378830.71	Argillite	West Porphyry area, not footwall, possibly interflow seds	-		
4078	528011.38	5378999.31	Argillite/Siltstone	West Porphyry area, possibly interflow seds	-		
4079	527924.00	5414199.00	Graphitic Siltstone/Mudstone	Siliceous, black, graphitic, py and po, conductive	155.5-201.6	Siltstone	Siltstone
4080	527219.00	5398879.00	Graphitic Argillite	fg, well-bedded, py diss, lam, and nod, conductive	98.8-100.7 m	Greywacke	Greywacke
4081	528699.00	5411769.00	Graphite Argillite fault gouge	Hard, black, graphitic, py nod, qtz veins, conductive	7.30-109.7	Greywacke	Diabase
4082	528124.00	5414569.00	Graphite Argillite fault gouge	Silicified, dark grey-black interbeds, qtz veins, py diss, lam, and nod	138.6-152.0	Silicified Zone Graphite/Mafic	Silicified Zone
4083	571678.00	5368699.00	Argillite/Siltstone	vfg, well-bedded, py	343.5-352.8	Volcanics	EOH
4084	558250.00	5379300.00	Graphitic Argillite	Black, laminated, graphitic, py nodules, calcite, highly conductive	40.4-41.44	Graphite Breccia	Andeiste
4085	553673.00	5405644.00	Graphitic Argillite	10% py	272-303ft	Overburden	Graphitic Argillite
4086	554498.00	5385499.00	Graphitic Argillite w/ sulfide	Black, massive, graphitic, conductor, up to 30% nodular pyrite	66.8-75.25m	Mafic and ultramafic volcanics	Graphitic breccia and siliceous sediments
4087	575508.00	5376679.00	Interflow Sediment/Siltstone	Black turbidite, weakly graphitic	383-392.5ft	Basalt	Basalt
4090	584297.00	5375309.00	Mudstone/Siltstone	GW interbeds, dark green, vfg, massive (some laminae), qtz-carb veinlets, ser alt, minor sulphides	8.45-80.85	Green Carb Rock	Iron Formation
4091	529424.00	5414049.00	Graphitic Shale/Siltstone	Grey/black, well-bedded, fg, graphitic, py and po	103.05-147.51	MetaBasalt	MetaBasalt
4092	526739.00	5401059.00	Graphitic Argillite	Tuff interbeds, py, conductive	125.5-135.7	Mafic Flow	Polymictic Breccia
4093	526779.00	5401269.00	Graphitic Argillite	fg, bedded, py, trace sph	106.3-106.9	Mafic Flow	Mafic Flow
4094	605577.00	5378079.00	Graphitic Argillite/Siltstone brecciated	Black, well-lam, gw interbeds, py and po	89.46-92.05	Arenaceous Sediments	Arenaceous Sediments
4095	558123.00	5385649.00	Argillite/Siltstone	Interbedded with blk chert and felsic sediments, graphitic, slightly conductive, py and po,	195.2-218.24	Mafic Rock	Mafic Rock
4096	558648.00	5385319.00	Argillite/Siltstone	Chert interbeds, dark grey/black, finely lam, graphitic, qtz-carb veins	71.37-82.95	Variolitic Fragments	Variolitic UM Flow
4097	605577.00	5378079.00	Graphitic Argillite/Siltstone	Black, well-lam, gw interbeds, py and po	89.46-92.05	Arenaceous Sediments	Arenaceous Sediments
4098	606247.00	5319799.00	Graphitic Argillite	Black, fine-grained, massive, carb stringers, weakly bedded. 2-3$ pyrite blebs	113.1-124.97	Intermediate volcanic breccia	EOH
4099	535819.00	5397609.00	Graphitic Argillite interflow sediment	Mafics with interflow sediments	72.6-73.4	Mafics	Mafics
4100	602967.00	5378189.00	Graphitic Argillite/Siltstone	fg, black, poorly bedded, gw interbeds	152.43-164.9	Arenaceous Sediments Volcanic Agglomerate	Altered Volcanics
4101	541439.00	5398659.00	Graphitic Argillite	Black, graphitic, py nodules, lam, diss	124-129	w/ interbedded graphite	Greywacke
4102	559263.00	5404114.00	Graphitic Argillite	Thinly bedded, jet black, pyritic	429-432ft	Dacite	Dacite
4103	568348.00	5383949.00	Graphitic Argillite	Black, fg, qtz-carb, py diss, lam, nod, conductive, locally graphitic	54.0-81.2	Overburden	Rhyolite
4104	534979.00	5387009.00	Graphitic Argillite/Siltstone	vfg, thinly laminated, black, py lam and diss	1073.8-1075.2	Argillite	EOH
4105	535849.00	5386919.00	Graphitic Argillite	fg, black, py	198.1-204.3	UM volcanics	Greywacke
4106	572038.00	5368719.00	Graphitic Argillite	vfg, black, py, qtz-carb veins	425.7-447.6	Mafic Fragmental	Chert
4107	558023.00	5385799.00	Graphitic Argillite	Black graphitic argillite, py nodules, finely lam, mod to highly conductive	64.2-66.5	Mafic Flow	Chert Breccia
4108	571908.00	5368879.00	Graphitic Argillite	pyritic	439-449ft	Mafic volcanic	Mafic volcanic
4109	562568.00	5388659.00	Graphitic Argillite	Black, fg, graphitic, highly conductive, py nodules, calcite	95-138	Boulders	Graphitic Lapilli Tuff
4110	544879.00	5416889.00	Graphitic Argillite	Conductive, black, fg, py	527.4-536.5	Greywacke	Carbonaceous Sediment
4111	542429.00	5411744.00	Graphitic Argillite	Highly conductive, py nod, chert clasts	1003.4-1012.7	Intermediate Breccia	Intermediate Tuff Breccia
04111B	542429.00	5411744.00	Graphitic Argillite (not a duplicate)				
4112	572318.00	5368429.00	Graphitic Argillite	Grey to black, bedded	258-338ft	Altered basalt	Mafic volcanic
04112B	572318.00	5368429.00	Graphitic Argillite (not a duplicate)				
4113	553248.00	5387819.00	Graphitic Argillite	Conductor, up to 25% pyrite, quartz-carbonated veined	37.1-54.1m	Felsic lapilli tuff	Felsic agglomerate
4114	545999.00	5417919.00	Graphitic Argillite	Very conductive - black with cherty clasts, 30-35% po	559.6-567.5ft	Diabase	Rhyodacite tuff
4115	556598.00	5410969.00	Argillite	Black, fine-grained, hard, graphitic, thinly bedded, up to 7% py and 3% po, trace cpy, interbedded with chert	433.5-444ft	Ultramafic volcanic	Sheared, altered rock (altered mafic volcanic?)
4116	608872.00	5376149.00	Interbedded chert and cherty graphitic argillite	Dark grey - black, laminated, chlorite	144.76-147.85m	Graphitic tuff	Felsic pyroclastic (V9 and
4117	538129.00	5398989.00	Graphitic Shale	Black, lam, py, gn and sph	120.52-167.64	Basalt	EOH
04117B	538129.00	5398989.00	Graphitic Shale (not a duplicate)				
4118	597547.00	5375869.00	Graphitic Argillite/Siltstone	Black and grey, laminated, chlorite, carbonate, 2-3% py	32.8-41.5m	Intermediate tuff	Cherty-carbonate
4119	589347.00	5372969.00	Graphitic Argillite	Greywacke with interbedded argillites	66.14-152.4m	Basalt	EOH
4120	569218.00	5378019.00	Argillite/Siltstone/Tuff	Dark grey, fg, banding, disseminated py	70.73-73.78m	Basalt	Basalt
4121	557198.00	5402869.00	Silicified Argillite, hematitic stain	Thinly bedded, nodular pyrite, very fg	340-344.5 ft	Basalt	Metasediment
4122	593172.00	5370194.00	Graphitic Argillite	Highly graphitic, 8% py bands and nodules	56-67.3ft	Mafic metavolcanic	Mafic intrusive
4123	550773.00	5412314.00	Graphitic Argillite	Thinly bedded, locally mineralized	entire hole	Greywacke	Greywacke
4124	594197.00	5373769.00	Graphitic Argillite w/ vein	Black, shale, minor silicification, py	2616.8-2622.0	Tuff	Tuff
4125	595172.00	5375949.00	Graphitic Argillite	py, slightly conductive	45.0-45.63	Acid Tuff	Acid Fragmental Tuff
4126	591447.00	5371469.00	Shale/Siltstone	Locally silicified and graphitic, black/grey, py, minor cpy	375.2-379.6	Mafic Volcanics	Mafic Volcanics
4127	601347.00	5376469.00	Graphitic Argillite	Black, highly conductive, laminated, py nodules, carb-chl-rich sections	126.5-130.0	Carb-Chl Schist	Basalt

Appendix A3. Sample and field data description / core log entry for N=564 samples of carbonaceous argillite from the Timmins-Kirkland Lake region.

Sample #	Township	Company	Hole #	MNDM #	Sub_Assemb	Assemblage	Contact	Commodity	Ti/Zr_Source_Rock	Host	Analyzed Sample	From_	To	ft_m
4128	Teck	MNDM-KL	LS-58	KL0785	-	Timiskaming	-	Orogenic Au	intermediate	Sediment	Graphitic Argillite	135.90	136.35	m
4129	Garrison	MNDM-KL	897-12-3	KL0019	Lower	Kidd-Munro	-	Orogenic Au	felsic	Volcanic	Graphitic Argillite	68.40	68.60	m
4130	Garrison	MNDM-KL	839-04-01	KL0686	Lower	Blake River	-	Orogenic Au	felsic	Volcanic/Sediment	Graphitic Argillite	122.00	122.40	m
4131	Garrison	MNDM-KL	897-12-2	KL0018	Lower	Kidd-Munro	-	Base Metal	felsic	Volcanic	Graphitic Argillite	175.50	179.50	m
4132	Moody	MNDM-KL	JL-85-NWA	KL1834	-	Porcupine	-	Orogenic Au	felsic	Sediment	Graphitic Argillite thinly bedded	358.90	359.20	m
4133	Harker	MNDM-KL	839-24-1	KL0023	Lower	Blake River	-	Orogenic Au	felsic	Volcanic/Sediment	Graphitic Argillite	97.30	97.60	m
4134	Moody	MNDM-KL	JL-85-F7	KL1832	-	Stoughton-Roquemare	Stoughton-Roquemare/Porcupine	Orogenic Au	mafic	Volcanic/Sediment	Graphitic Argillite	483.00	484.00	ft
4135	Moody	MNDM-KL	JL-85-NWB1	KL1854	-	Stoughton-Roquemare	Stoughton-Roquemare/Porcupine	Orogenic Au	felsic	Volcanic/Sediment	Graphitic Argillite	393.40	394.10	ft
4136	Moody	MNDM-KL	JL-85-NWC	KL1855	-	Porcupine	-	Orogenic Au	felsic	Sediment	Graphitic Argillite	431.10	432.10	ft
4137	Harker	MNDM-KL	839-39-2	KL0464	Lower	Kidd-Munro	-	Base Metal	intermediate	Volcanic	Graphitic Argillite/Greywacke/Mudstone	66.70	67.00	m
4138	Holloway	MNDM-KL	HW-90-91	KL2410	Lower	Kidd-Munro	Kidd-Munro/Timiskaming	Orogenic Au	intermediate	Volcanic/Sediment	Argillite/Siltstone	225.70	225.95	m
04138D	Holloway	MNDM-KL	HW-90-91	KL2410	Lower	Kidd-Munro	Kidd-Munro/Timiskaming	Orogenic Au	intermediate	Volcanic/Sediment	Argillite/Siltstone	225.70	225.95	m
4139	Mann	Xstrata	MAN24-14	-	Upper	Tisdale	-	Base Metal	felsic	Volcanic	Graphitic Argillite	110.50	110.70	m
4140	MacDiarmid	Xstrata	MCD32-01	-	Upper	Kidd-Munro	-	Base Metal	felsic	Volcanic	Argillite/Siltstone	169.15	169.35	m
4141	MacDiarmid	Xstrata	MCD41-02	-	Upper	Kidd-Munro	-	Base Metal	felsic	Volcanic	Graphitic Argillite	152.60	152.80	m
4142	MacDiarmid	Xstrata	MCD25-01	-	Upper	Blake River	-	Base Metal	intermediate	Volcanic	Graphitic Argillite	123.25	123.50	m
4143	MacDiarmid	Xstrata	MCD41-03	-	Upper	Kidd-Munro	-	Base Metal	intermediate	Volcanic	Graphitic Argillite/Siltstone	125.70	125.85	m
4144	MacDiarmid	Xstrata	MCD52-01	-	Upper	Kidd-Munro	-	Base Metal	intermediate	Volcanic	Graphitic Argillite	163.00	163.22	m
4145	Mahaffy	Xstrata	MF13-06	-	Upper	Blake River	-	Base Metal	felsic	Volcanic	Graphitic Argillite	211.00	211.30	m
4146	Mahaffy	Xstrata	MF12-22	-	Upper	Blake River	-	Base Metal	felsic	Volcanic	Graphitic Argillite/Siltstone	475.70	476.00	m
4147	Loveland	Xstrata	L66-01	-	Upper	Kidd-Munro	-	Base Metal	felsic	Volcanic	Graphitic Argillite/Siltstone	101.50	101.65	m
4148	MacDiarmid	Xstrata	MCD61-01	-	Upper	Blake River	-	Base Metal	intermediate	Volcanic	Graphitic Argillite	116.70	116.95	m
4149	MacDiarmid	Xstrata	MCD61-02	-	Upper	Blake River	-	Base Metal	intermediate	Volcanic	Graphitic Argillite cherty	248.50	248.70	m
4150	Mahaffy	Xstrata	MF14-01	-	Upper	Kidd-Munro	-	Base Metal	felsic	Volcanic	Graphitic Argillite	0.00	0.00	-
4151	Mahaffy	Xstrata	MF12-24	-	Upper	Blake River	-	Base Metal	intermediate	Volcanic	Graphitic Argillite	86.40	86.70	m
4152	Mann	Xstrata	MAN24-08	-	-	Tisdale	-	Base Metal	intermediate	Volcanic	Argillite	152.00	152.20	m
4153	Gowan	Xstrata	GO15-01	-	Lower	Tisdale	-	Base Metal	felsic	Volcanic	Graphitic Argillite	95.20	95.40	m
4154	Gowan	Xstrata	GO15-02	-	Lower	Tisdale	-	Base Metal	felsic	Volcanic	Mudstone/Graphitic Argillite	104.55	104.80	m
4155	Gowan	Xstrata	GO15-03	-	Lower	Tisdale	-	Base Metal	felsic	Volcanic	Graphitic Argillite	124.30	124.45	m
4156	Gowan	Xstrata	GO26-02	-	Lower	Tisdale	-	Base Metal	mafic	Volcanic	Graphitic Argillite/Tuff green	134.45	134.60	m
4157	Gowan	Xstrata	GO22-01	-	Lower	Tisdale	-	Base Metal	felsic	Volcanic	Graphitic Argillite	142.10	142.30	m
4158	Gowan	Xstrata	GO42-01	-	Lower	Tisdale	-	Base Metal	felsic	Volcanic	Graphitic Argillite	84.15	84.40	m
4159	Gowan	Xstrata	GO52-01	-	Lower	Tisdale	Tisdale/Porcupine	Orogenic Au	felsic	Volcanic	Graphitic Argillite	135.50	135.67	m
4160	Gowan	Xstrata	GO52-03	-	-	Tisdale	Tisdale/Porcupine	Orogenic Au	felsic	Volcanic	Mudstone/Graphitic Argillite	115.70	115.90	m
4161	MacDiarmid	Xstrata	MCD35-03	-	Upper	Blake River	-	Base Metal	intermediate	Volcanic	Siliceous Argillite	63.20	63.50	m
4162	Gowan	Xstrata	GO52-02	-	-	Tisdale	Tisdale/Porcupine	Orogenic Au	felsic	Volcanic	Graphitic Argillite	75.70	75.90	m
4163	Mahaffy	Xstrata	MF16-03	-	Upper	Blake River	-	Base Metal	intermediate	Volcanic	Silicified Graphitic Argillite	158.50	158.70	m
4164	Little	Xstrata	LIT66-01	-	-	Stoughton-Roquemare	-	Base Metal	intermediate	Volcanic	Graphitic Argillite	62.40	62.60	m
04164B	Little	Xstrata	LIT66-01	-	-	Stoughton-Roquemare	-	Base Metal	felsic	Volcanic	Graphitic Argillite (not a duplicate)	0.00	0.00	-
4165	Duff	Xstrata	DUF46-01	-	Upper	Tisdale	-	Base Metal	felsic	Volcanic	Graphitic Argillite	97.80	98.00	m
4166	Mann	Xstrata	MAN52-02	-	Upper	Tisdale	-	Base Metal	felsic	Volcanic	Graphitic Argillite/Siltstone	97.40	97.60	m
4167	Mann	Xstrata	MAN54-02	-	-	Stoughton-Roquemare	Stoughton-Roquemare/Tisdale	Base Metal	felsic	Volcanic	Argillite	84.10	84.35	m
4168	Hanna	Xstrata	HAN11-01	-	Upper	Tisdale	Tisdale/Stoughton-Roquemare	Base Metal	felsic	Volcanic	Argillite/Siltstone	88.80	89.10	m
4169	Aurora	Xstrata	AUR22-01	-	-	Stoughton-Roquemare	-	Base Metal	mafic	Volcanic	Argillite/Siltstone	124.50	124.70	m
4170	Aurora	Xstrata	AUR22-02	-	-	Stoughton-Roquemare	-	Base Metal	mafic	Volcanic	Argillite/Siltstone (A), w cpy-sp vein (B)	115.00	115.30	m
4171	Beck	Xstrata	BEC11-02	-	Upper	Blake River	-	Base Metal	felsic	Volcanic	Argillite	150.30	150.50	m
04171B	Beck	Xstrata	BEC11-02	-	Upper	Blake River	-	Base Metal	felsic	Volcanic	Argillite (not a duplicate)	0.00	0.00	-
4172	Nesbitt	Xstrata	NES46-02	-	-	Deloro	-	Base Metal	felsic	Volcanic	Graphitic Argillite	136.30	136.50	m
4173	Nesbitt	Xstrata	NES46-01	-	-	Deloro	-	Base Metal	felsic	Volcanic	Graphitic Argillite	80.50	80.80	m
4174	Beck	Xstrata	BEC12-01	-	-	Deloro	-	Base Metal	intermediate	Volcanic	Sulfidic Graphitic Argillite/Siltstone	99.80	100.05	m
4175	Beck	Xstrata	BEC12-02	-	-	Deloro	-	Base Metal	felsic	Volcanic	Graphitic Argillite	69.20	69.50	m
4176	Beck	Xstrata	BEC42-02	-	Upper	Kidd-Munro	-	Base Metal	felsic	Volcanic	Graphitic Argillite cherty	172.30	172.50	m
4177	Beck	Xstrata	BEC52-02	-	Upper	Kidd-Munro	-	Base Metal	felsic	Volcanic	Graphitic Argillite cherty	152.70	153.00	m
04177B	Beck	Xstrata	BEC52-02	-	Upper	Kidd-Munro	-	Base Metal	felsic	Volcanic	Graphitic Argillite cherty (not a duplicate)	0.00	0.00	-
4178	Beck	Xstrata	BEC43-02	-	Upper	Kidd-Munro	-	Base Metal	felsic	Volcanic	Graphitic Argillite cherty	172.30	172.50	m
4179	Lennox	Xstrata	LEN26-01	-	Upper	Kidd-Munro	-	Base Metal	felsic	Volcanic	Graphitic Argillite	70.25	70.50	m
4180	Lennox	Xstrata	LEN26-02	-	Upper	Kidd-Munro	-	Base Metal	felsic	Volcanic	Argillite	172.00	172.30	m
04180B	Lennox	Xstrata	LEN26-02	-	Upper	Kidd-Munro	-	Base Metal	felsic	Volcanic	Argillite (not a duplicate)	0.00	0.00	-
4181	Lennox	Xstrata	LEN25-03	-	Upper	Kidd-Munro	-	Base Metal	felsic	Volcanic	Graphitic Argillite w greywacke	122.10	122.20	m
4182	Lennox	Xstrata	LEN24-01	-	Upper	Kidd-Munro	-	Base Metal	felsic	Volcanic	Graphitic Argillite/Siltstone	147.60	147.90	m
4183	Lennox	Xstrata	LEN16-02	-	Upper	Kidd-Munro	-	Base Metal	intermediate	Volcanic	Graphitic Argillite	91.10	91.40	m

Appendix A3. Sample and field data description / core log entry for N=564 samples of carbonaceous argillite from the Timmins-Kirkland Lake region.

Sample #	Easting_83	Northing_83	Sample Type	Field Description/Core Log Entry	Interval Available	Hanging wall	Footwall
4128	570653.00	5333159.00	Graphitic Argillite	Intervals don't match			
4129	583147.00	5376319.00	Graphitic Argillite	Black, fg, poorly bedded, py diss/seams/nodules, calcite veinlets, graphitic, conductive	61.54-72.5	Lamprophyre Dyke	Sediment
4130	575548.00	5367619.00	Graphitic Argillite	Grey/black, quartite interbeds, py, good conductor	67.25-126.25	Overburden	Dacite
4131	576888.00	5375619.00	Graphitic Argillite	Black, carbonaceous, graphitic, thin beds, py nodules, highly conductive	176.7-177.4	Fsp Porphyry	Andesite Tuff
4132	546888.00	5413999.00	Graphitic Argillite thinly bedded	Pyritic, nodular pyrite	347-375ft	Intermediate tuff	Intermediate lapilli tuff
4133	587827.00	5372299.00	Graphitic Argillite	Black, fg, very conductive, py nodules/stringers, magnetic po, qtz-carb veins	96.94-104.70	Andesite	Andesite
4134	552023.00	5409944.00	Graphitic Argillite	Black, fine-grained, graphitic	473-504ft	Andesite	Andesite
4135	546099.00	5412129.00	Graphitic Argillite	Jet black, thinly bedded, 10% nodular pyrite, bands	390.5-395ft	Metasediments	Metasediment
4136	546479.00	5412639.00	Graphitic Argillite	Pyritic (5%) as nodules, thinly bedded, jet black,	407-451.5ft	Greywacke	Ultramafic volcanic
4137	585487.00	5375709.00	Graphitic Argillite/ Greywacke/Mudstone	Thin, black, argillaceous sections up to 20cm wide, py, conductive, ankerite	55.19-71.50	Andesite	Tuffaceous Sediment
4138	592427.00	5375319.00	Argillite/Siltstone	Black, finely lam, minor gw beds, py	225-252.2	Argillite/Greywacke	Mafic Flow
04138D	592427.00	5375319.00	Argillite/Siltstone	Black, finely lam, minor gw beds, py	225-252.2	Argillite/Greywacke	Mafic Flow
4139	499755.26	5406800.66	Graphitic Argillite	Pyritic, nodular pyrite	109-126.5m	Intermediate volcanic	Felsic Intrusive
4140	458932.58	5389708.49	Argillite/Siltstone	black,fine-grained, nodular po, strongly conductive	162.4-169.6m	Mafic volcanic	Variolitic mafic volcanic
4141	457296.54	5391633.80	Graphitic Argillite	8% po	152.7-155.58m	Mafic volcanic	Mafic volcanic
4142	462592.69	5389356.15	Graphitic Argillite	Black, fine-grained, silicified, pyritic, weak calcite	120.6-134.75m	Mafic volcanic	Ultramafic volcanic
4143	457590.55	5390746.83	Graphitic Argillite/Siltstone	black, fg, weakly bedded, pyritic and po	124.01-132.58m	Mafic Intrusive	Intermediate tuff
4144	457727.54	5392366.80	Graphitic Argillite	Black to medium grey-green in colour, chaotic mixture of strongly magnetic and conductive argillite intermixed on the centimetre scale with breccia and amygduloidal mafic volcanic flow material, volcanic-sedimentary contact varies about 10 TCA, amygdules are fill by quartz-ankerite which has been partially replaced by pyrite, the argillite intervals contain 3-4% blebby Po replacing Py and 1-2% pyrite, 1-2% magnetite is present within the conductive argillite sections, minor fault surfaces are at 50 TCA	158.65-163.69m	Ultramafic volcanic	Mafic volcanic
4145	459886.74	5406792.82	Graphitic Argillite	Locally massive pyrite	210.8-211.71m	Sericitized quartz-phyric rhyolite	Sericitized quartz-phyric rhyolite
4146	458777.48	5406004.49	Graphitic Argillite/Siltstone	Locally massive pyrite, black and brass coloured	471.6-478m	Mafic volcanic	Mafic or felsic tuff
4147	455882.52	5395013.29	Graphitic Argillite/Siltstone	Black and fine-grained, very conductive	101.5-103.3m	Intermediate tuff	Mafic volcanic -pillow basalt
4148	465162.84	5394154.11	Graphitic Argillite	Interflow seds?	116.7-117m	Mafic volcanic	Mafic volcanic
4149	464799.82	5393934.24	Graphitic Argillite cherty	Black, fine-grained, 3-5% py nodules and less po layers	247.55-251.7m	Mafic volcanic	Mafic volcanic
4150	461567.79	5405513.65	Graphitic Argillite				
4151	458698.41	5405568.75	Graphitic Argillite	Black, graphitic, up to 20% pyrite nodules and disseminations	85.75-87.9m	Mafic volcanic + massive sulfide	Mafic volcanic
4152	499529.26	5407484.66	Argillite	Locally graphitic and interbedded with chert	151.7-157.1m	Felsic volcanic + Sedimentary Fine Grained Graphitic/Argillaceous	Felsic volcanic
4153	492713.12	5386421.76	Graphitic Argillite	Sedimentary fine grained graphitic/argillaceous	75.9-107.98m	above a fault zone	Greywacke
4154	492743.11	5385851.76	Mudstone/Graphitic Argillite	Part of greywacke turbidite sequence, gradational	87.36-115.74m	Interbedded greywacke and argillite	Greywacke and argillite, locally graphitic
4155	492413.12	5387121.76	Graphitic Argillite	Sedimentary Fine Grained Graphitic/Argillaceous	102.81-135.52m	Sediments, brecciated?	Mafic volcanic
4156	494363.15	5388549.72	Graphitic Argillite/Tuff green	Black/dark black, fine-grained, blebs of reddish sphalerite	129.98-135.13m	Mafic volcanic	Greywacke
4157	487938.12	5388964.82	Graphitic Argillite	Dark black/grey, up to 25% po, nodular pyrite, trace cpy	138.42-148.39m	Mafic volcanic	Greywacke
4158	487103.13	5391491.81	Graphitic Argillite	Graphitic/argillaceous	80.67-87.55m	Graphitic argillite above fault	Heterolithic volcanic tuff above thick mafic volcanics
4159	486978.14	5392876.80	Graphitic Argillite	Black, fine-grained, po-py	116.81-149.07m	Greywacke	Greywacke
4160	487139.15	5393291.80	Mudstone/Graphitic Argillite	Black fine-grained, apart of greywacke sequence	113.63-118.52m	Greywacke	Greywacke
4161	464307.76	5389829.98	Siliceous Argillite	Dark grey, fine-grained, 3-4% pyrite	63.24-63.98m	Mafic volcanic	Ultramafic volcanic
4162	487278.15	5393276.80	Graphitic Argillite	Black, fine-grained, weak silicification, 3-5% sulfides	72.22-89.58m	Felsic dyke	Felsic volcanic
4163	464206.90	5405733.19	Silicified Graphitic Argillite	Chert-graphite, up to 30% po lamine, conductive	158.4-159m	Diorite	Mafic volcanic -pillow basalt
4164	503909.88	5404447.81	Graphitic Argillite	Black to dark grey, fine-grained, 3% py nodules	49.9-69.5m	Mafic tuff	Mafic mediate volcanic
04164B	503909.88	5404447.81	Graphitic Argillite (not a duplicate)				
4165	493180.91	5411143.52	Graphitic Argillite	Medium to dark grey, 1% py nodules	88.65-117.45m	Intermediate porphyry intrusive	Greywacke
4166	496439.27	5412477.67	Graphitic Argillite/Siltstone	Very conductive, apart of greywacke sequence	96.11-96.6m	Mafic volcanic - pillow basalt	Ultramafic volcanic
4167	500925.57	5412286.48	Argillite	Black, fine-grained	85-85.6m	Mafic volcanic	Mafic volcanic
4168	495546.82	5415697.77	Argillite/Siltstone	Black, fine-grained, 0.5% pyrite	85.8-103.29m	Intermediate porphyry intrusive	Mafic volcanic -pillow basalt
4169	516377.87	5406578.82	Argillite/Siltstone	Interflow sediment?	not logged as arg	Mafic volcanic	Mafic volcanic
4170	516796.88	5408229.47	Argillite/Siltstone (A), w/ cpy-sp vein (B)	Siliceous sediments, medium grey, fine-grained	116.05-120.25m	Mafic volcanic	Mafic volcanic -pillow basalt
4171	475498.31	5415470.31	Argillite	Black, fine-grained, 3-4% pyrite	148.13-153.85m	Mafic volcanic	Ultramafic volcanic
04171B	475498.31	5415470.31	Argillite (not a duplicate)				
4172	473569.17	5419794.91	Graphitic Argillite	Black, fine-grained	135.33-139.5m	Volcanics/Ash/Lapilli Tuff	Mafic/UM volcanic
4173	473759.34	5420023.54	Graphitic Argillite	Black, fine-grained; foliated/layered; graphitic unit containing pyrite and minor carbonate	80.58-81.51m	Felsic/Mafic Volcanic	Diorite/UM volcanic
4174	477438.89	5414830.16	Sulfidic Graphitic Argillite/Siltstone	Black, fine-grained, up to 25% nodular pyrite	98.65-106.52m	Mafic volcanic	Mafic volcanic
4175	477478.10	5416128.84	Graphitic Argillite	Black, fine-grained, conductor 1 of 2	65.68-80m	Felsic tuff	Felsic ash
4176	477097.96	5421298.21	Graphitic Argillite cherty	Black, fine-grained, laminated	172.13-172.8m	Felsic Fragmental/Mafic	Mafic volcanic
4177	477534.63	5422296.99	Graphitic Argillite cherty	Black, fine-grained, 10-15% py + po, local nodules	152.23-153.88m	Mafic volcanic	Mafic volcanic
04177B	477534.63	5422296.99	Graphitic Argillite cherty (not a duplicate)				
4178	478572.98	5421073.51	Graphitic Argillite cherty	Dark grey to black, fine-grained, 2-3% laminar and fracture pyrite	171.11-182.05m	Sediments	Sediments
4179	474234.63	5426241.30	Graphitic Argillite	Black, fine-grained, good bedding, locally semi-massive po (magnetic) with lesser py	70.76-73.80m	Mafic volcanic	Ultramafic volcanic
4180	475027.33	5426939.14	Argillite	Dark grey to black, fine-grained, thinly bedded, locally graphitic	73-177.47m	Overburden	Mafic volcanic
04180B	475027.33	5426939.14	Argillite (not a duplicate)				
4181	473345.70	5427052.26	Graphitic Argillite w/ greywacke	Black, fine-grained	121.97-122.2m	Mafic volcanic	Mafic volcanic
4182	471320.00	5427111.50	Graphitic Argillite/Siltstone	Black, fine-grained, 5% po, apart of chert and BIF sequence	133.99-161.22m	Mafic volcanic	Mafic intrusive
4183	474017.59	5425045.55	Graphitic Argillite	Black, fine-grained	90.97-93.65m	Mafic volcanic	Mafic volcanic

Appendix A3. Sample and field data description / core log entry for N=564 samples of carbonaceous argillite from the Timmins-Kirkland Lake region.

Sample #	Township	Company	Hole #	MNDM #	Sub_Assemb	Assemblage	Contact	Commodity	Ti/Zr_Source_Rock	Host	Analyzed Sample	From_	To	ft_m
4184	Lennox	Xstrata	LEN36-02	-	-	Deloro	-	Base Metal	felsic	Volcanic	Graphitic Argillite/Siltstone	169.80	170.00	m
4185	Lennox	Xstrata	LEN55-02	-	-	Deloro	-	Base Metal	felsic	Volcanic	Graphitic Argillite	133.90	134.10	m
4186	Ottaway	Xstrata	OTT21-01	-	Upper	Kidd-Munro	Kidd-Munro/Porcupine	Base Metal	felsic	Volcanic	Graphitic Argillite	112.50	112.70	m
4187	Nesbitt	Xstrata	NES35-10A	-	-	Deloro	-	Base Metal	intermediate	Volcanic	Graphitic Argillite	102.00	102.20	m
4188	Aurora	Xstrata	AUR11-02	-	-	Stoughton-Roquemare	-	Base Metal	felsic	Volcanic	Siltstone	117.80	117.95	m
4189	Lennox	Xstrata	LEN56-02	-	-	Deloro	-	Base Metal	felsic	Volcanic	Black Mudstone w po streaks	180.80	181.04	ft
4190	Mann	Xstrata	MAN24-01	-	Upper	Tisdale	-	Base Metal	felsic	Volcanic	Graphitic Argillite w irregular py laminae	68.00	68.20	m
4191	Mahaffy	Xstrata	MF13-04	-	Upper	Blake River	-	Base Metal	felsic	Volcanic	Graphitic Argillite w minor euhedral py and qtz vein	202.70	202.90	m
4192	Currie	Metals Creek	TX08-002	-	Lower	Tisdale	-	Base Metal	felsic	Volcanic	Black Graphitic Argillite w cpy replacing py nodules	61.00	0.00	m
04192B	Currie	Metals Creek	TX08-002	-	Lower	Tisdale	-	Base Metal	felsic	Volcanic	Black Graphitic Argillite w cpy replacing py nodules (not a duplicate)	0.00	0.00	-
4193	Currie	Metals Creek	TX08-003	-	Lower	Tisdale	-	Base Metal	felsic	Volcanic	Black Graphitic Argillite w cpy and sp replacing py	59.00	0.00	m
04193B	Currie	Metals Creek	TX08-003	-	Lower	Tisdale	-	Base Metal	felsic	Volcanic	Black Graphitic Argillite w cpy and sp replacing py (not a duplicate)	0.00	0.00	-
4194	Currie	Metals Creek	TX08-004	-	Lower	Tisdale	-	Base Metal	intermediate	Volcanic	Black Graphitic Argillite w trace py	110.80	0.00	m
4195	Currie	Metals Creek	TX08-005	-	Lower	Tisdale	-	Base Metal	felsic	Volcanic	Black Graphitic Argillite w large 3 cm cpy-replaced nodule and cpy in hairline fractures; section with cpy nodule not sampled	99.20	0.00	m
4196	Currie	Metals Creek	TX08-007	-	Lower	Tisdale	-	Base Metal	felsic	Volcanic	Black Graphitic Argillite w cy-sp-carb lining microfractures	114.00	0.00	m
4197	Currie	Metals Creek	TX08-010	-	Lower	Tisdale	-	Base Metal	felsic	Volcanic	Black Graphitic Argillite w abundant white fractures	54.50	0.00	m
04198A	Ogden	Metals Creek	TOG-10-04	-	Lower	Tisdale	Tisdale/Timiskaming	Base Metal	intermediate	Volcanic/Sediment	Grey Argillite/Siltstone w py streaks	150.50	0.00	m
04198B	Ogden	Metals Creek	TOG-10-04	-	Lower	Tisdale	Tisdale/Timiskaming	Base Metal	intermediate	Volcanic/Sediment	Grey Argillite/Siltstone w py streaks and sp on fracture surface	0.00	0.00	-
4199	Ogden	Metals Creek	TOG-11-01	-	Lower	Tisdale	Tisdale/Timiskaming	Base Metal	intermediate	Volcanic/Sediment	Grey Argillite/Siltstone w white carb and minor controted py laminae	353.00	0.00	m
4200	Tully	MNDM-T	T0-77-5A-2	TI1216	Upper	Kidd-Munro	-	Base Metal	felsic	Volcanic	Black Graphitic Argillite w minor recrystallized py streaks	207.00	0.00	ft
4301	Tully	Gowest Gold	GW-10-126	-	Upper	Kidd-Munro	-	Base Metal	intermediate	Volcanic	Graphitic Argillite w carb vein and nodule	146.10	146.25	m
4303	Tully	Gowest Gold	GW-10-141	-	Upper	Kidd-Munro	-	Base Metal	felsic	Volcanic	Graphitic Argillite w py nodules	106.00	106.30	m
04307A	Tully	Gowest Gold	GW-10-107	-	Upper	Kidd-Munro	-	Base Metal	felsic	Volcanic	Black Graphitic Siltstone w po bodules (A) and py vein/deformed laminae (B)	153.60	153.80	m
4308	Tully	Gowest Gold	GW-10-54	-	Upper	Kidd-Munro	-	Base Metal	felsic	Volcanic	Graphitic Argillite w py nodules	897.60	898.00	m
4309	Tully	Gowest Gold	GW-10-60WA	-	Upper	Kidd-Munro	-	Base Metal	felsic	Volcanic	Graphitic Argillite w py nodules	638.20	638.60	m
04309B	Tully	Gowest Gold	GW-10-60WA	-	Upper	Kidd-Munro	-	Base Metal	felsic	Volcanic	Graphitic Argillite w py nodules (not a duplicate)	0.00	0.00	-
4311	Tully	Gowest Gold	GW-10-91	-	Upper	Kidd-Munro	-	Base Metal	felsic	Volcanic	Graphitic Argillite w py nodules	65.40	65.65	m
4312	Tully	Gowest Gold	GW-11-157	-	Upper	Kidd-Munro	-	Base Metal	felsic	Volcanic	Graphitic Argillite w py nodules and pink carb veinlet	222.65	222.80	m
4314	Tully	Gowest Gold	GW-10-53	-	Upper	Kidd-Munro	-	Base Metal	felsic	Volcanic	Black Graphitic Siltstone w large isolated py nodule	98.10	98.35	m
4315	Tully	Gowest Gold	GW-10-121	-	Upper	Kidd-Munro	-	Base Metal	felsic	Volcanic	Graphitic Argillite w large isolated py nodule	567.00	567.20	m
4316	Tully	Gowest Gold	GW-10-96	-	Upper	Kidd-Munro	-	Base Metal	intermediate	Volcanic	Black Graphitic Siltstone w po streaks	629.00	629.30	m
04316B	Tully	Gowest Gold	GW-10-96	-	Upper	Kidd-Munro	-	Base Metal	intermediate	Volcanic	Black Graphitic Siltstone w po streaks (not a duplicate)	0.00	0.00	-
4319	Hoyle	Lake Shore Gold	V-10-52	-	Lower	Tisdale	Tisdale/Porcupine	Orogenic Au	felsic	Volcanic/Sediment	Graphitic Argillite w py streaks	348.25	348.47	m
04319B	Hoyle	Lake Shore Gold	V-10-52	-	Lower	Tisdale	Tisdale/Porcupine	Orogenic Au	felsic	Volcanic/Sediment	Graphitic Argillite w py streaks (not a duplicate)	0.00	0.00	-
4320	Hoyle	Lake Shore Gold	S-09-07D	-	Lower	Tisdale	Tisdale/Porcupine	Orogenic Au	felsic	Volcanic/Sediment	Graphitic Argillite w py streaks and qtz-carb	771.50	771.70	m
04320B	Hoyle	Lake Shore Gold	S-09-07D	-	Lower	Tisdale	Tisdale/Porcupine	Orogenic Au	intermediate	Volcanic/Sediment	Graphitic Argillite w py streaks and qtz-carb (not a duplicate)	0.00	0.00	-
4323	Thorburn	MNDM-T	LT#13	TI1131	Upper	Kidd-Munro	-	Base Metal	felsic	Volcanic	Black Graphitic Argillite w 1 cm thick py nodule and carb bands	329.00	0.00	ft
4324	Tully	SGX	SGX-11-27	-	Upper	Kidd-Munro	-	Base Metal	felsic	Volcanic	Graphitic Argillite w py laminae	92.60	92.75	m
4325	Tully	SGX	SGX-11-30	-	Upper	Kidd-Munro	-	Base Metal	intermediate	Volcanic	Graphitic Argillite w dissem. py euhedra	52.90	53.00	m
4326	Tully	SGX	SGX-11-84	-	Upper	Kidd-Munro	Kidd-Munro/Porcupine	Base Metal	intermediate	Volcanic	Graphitic Argillite w qtz-carb, large py euhedra, and minor pink carb	194.80	195.00	m
4327	Tully	SGX	SGX-11-101	-	Upper	Kidd-Munro	-	Base Metal	felsic	Volcanic	Graphitic Argillite w fine carb-py laminae	104.50	104.65	m
04329A	Ogden	San Gold	SG-09-13	-	-	Porcupine	-	Orogenic Au	intermediate	Sediment	Argillite/Mudstone cherty w tr sp on fracture (A) and graphitic (B)	52.60	52.90	m
4330	Ogden	San Gold	SG-09-14	-	-	Porcupine	-	Orogenic Au	intermediate	Sediment	Graphitic Argillite	56.00	56.30	m
4331	Ogden	San Gold	SG-09-11	-	-	Tisdale	Tisdale/Porcupine	Orogenic Au	intermediate	Volcanic/Sediment	Argillite/Mudstone	106.90	107.10	m
4332	Ogden	San Gold	SG-09-07	-	Lower	Tisdale	Tisdale/Porcupine	Orogenic Au	mafic	Volcanic/Sediment	Graphitic Argillite w heterolith frag. and dissem. py euhedra	91.85	92.00	m
4333	Ogden	San Gold	SG-09-12	-	-	Tisdale	Tisdale/Porcupine	Orogenic Au	intermediate	Volcanic/Sediment	Argillite/Mudstone	66.15	66.40	m
4334	Tully	SGX	SGX-11-43	-	Upper	Kidd-Munro	-	Base Metal	intermediate	Volcanic	Graphitic Argillite w pinstripe carb	121.10	121.25	m
4335	Munro	Constantine	MC-11-C6	-	Lower	Kidd-Munro	Kidd-Munro/Porcupine	Base Metal	mafic	Volcanic	Interflow Sediment w volcanic clasts	18.70	18.95	m
4336	Munro	Constantine	MC-11-C7	-	Lower	Kidd-Munro	Kidd-Munro/Porcupine	Base Metal	mafic	Volcanic	Interflow Sediment w broken carb vein and dissem. py	10.25	10.48	m
4337	Munro	Constantine	MC-11-C8	-	Lower	Kidd-Munro	Kidd-Munro/Porcupine	Base Metal	intermediate	Volcanic	Interflow Sediment w broken carb vein and dissem. py	9.70	9.86	m
4338	Munro	Constantine	MC-11-26A	-	Lower	Kidd-Munro	Kidd-Munro/Porcupine	Base Metal	mafic	Volcanic	Interflow Sediment w volcanic clasts	214.17	214.42	m
4339	Tully	SGX	SGX-11-77	-	Upper	Kidd-Munro	-	Base Metal	intermediate	Volcanic	Graphitic Argillite w pinstripe carb	206.30	206.41	m
4340	Garrison	St Andrew Goldfields Ltd.	GC-10-001	-	Lower	Tisdale	-	Orogenic Au	intermediate	Volcanic/Sediment	Green Siltstone	302.20	302.50	m
4341	Garrison	St Andrew Goldfields Ltd.	GC-10-002B	-	Lower	Blake River	-	Orogenic Au	intermediate	Volcanic/Sediment	Greywacke/Argillite	500.15	500.30	m
4342	Garrison	St Andrew Goldfields Ltd.	GC-10-003	-	Lower	Tisdale	-	Orogenic Au	intermediate	Volcanic/Sediment	Greywacke/Argillite w minor carb veins	432.80	433.13	m

Appendix A3. Sample and field data description / core log entry for N=564 samples of carbonaceous argillite from the Timmins-Kirkland Lake region.

Sample #	Easting_83	Northing_83	Sample Type	Field Description/Core Log Entry	Interval Available	Hanging wall	Footwall
4184	474047.08	5429145.29	Graphitic Argillite/Siltstone	Black, fine-grained, thinly laminated, some chlorite, up to 3% po and minor py	160.94-173.85m	Mafic Intrusive	Mafic intrusive
4185	473014.27	5431681.37	Graphitic Argillite	Sedimentary Fine Grained Graphitic/Argillaceous	131.8-134.79m	Mafic volcanic	Felsic Intrusive
4186	475861.29	5426991.71	Graphitic Argillite	5g	109.5-117.28m	Mafic volcanic	Mafic volcanic
4187	472114.50	5418891.19	Graphitic Argillite	Black to dark grey, fine-grained, Siliceous and Carbonaceous Interflow Sediments, 1-3% pyrite laminae,	103.2-105.2m	Mafic volcanic	Mafic volcanic
4188	513851.67	5405822.19	Siltstone	dark brown with oxide staining, 3% disseminated pyrite	117-118.53m	Overburden	Interbedded greywacke and mudstone below fault
4189	474243.08	5431110.69	Black Mudstone w/ po streaks	Part of greywacke turbidite sequence, gradational	39-149.6m	Interbedded greywacke and argillite	Mafic tuff
4190	500019.87	5407885.16	Graphitic Argillite w/ irregular py laminae	Part ofintercalated tuffaceous sediment horizon	40-70.15m	Felsic volcanic	Ultramafic intrusive
4191	459359.70	5405854.99	Graphitic Argillite w/ minor euhedral py and qtz vein	3-5% euhedral pyrite, moderately strong conductor	201.25-204.35m	3f intermediate vol?	Mafic volcanic below a fault and 2m of sediments
4192	532981.20	5371429.40	Black Graphitic Argillite w/ cpy replacing py nodules	blk, vfg, finely lam, cpy str, diss & blebs (4-5%)	30.95-68.0m	Overburden	Fsp-Porphyry
04192B	532981.20	5371429.40	Black Graphitic Argillite w/ cpy replacing py nodules (not a duplicate)				
4193	532976.40	5371473.50	Black Graphitic Argillite w/ cpy and sp replacing py	Interbedded GW & ARG; green-grey, fg, tr cpy as diss & sm blebs, minor folds	50.63-61.50m	Fsp-Porphyry	Andesite
04193B	532976.40	5371473.50	Black Graphitic Argillite w/ cpy and sp replacing py (not a				
4194	532981.10	5371479.90	Black Graphitic Argillite w/ trace py	blk, vfg, finely lam, moderate cpy	105.55-122.13m	Dacite	Andesite
4195	532965.40	5371447.10	Black Graphitic Argillite w/ large 3cm cpy-replaced nodule and cpy in hairline fractures; section with cpy nodule not sampled	blk-dk grey, vfg, finely lam, minor graph, siliceous str, cpy str & blebs (~4%)	74.80-107.95m	Qtz-Fsp Porphyry	Greywacke
4196	533003.20	5371457.40	Black Graphitic Argillite w/ cy-sp-carb lining microfractures	blk-dk-grey, strongly fractured, felsic wisps, forest green alt min on fracture faces (epidote?), tr py and cpy as cubes & blebs	110.43-115.18m	Dacite	Andesite
4197	533022.40	5371471.30	Black Graphitic Argillite w/ abundant white fractures	Interbedded GW & ARG; black-dk grey, vfg, lam, minor graph, qtz-fsp str, tr cpy as elongate blebs & str	50.26-68.30m	Basalt	Basalt
04198A	471785.80	5362813.60	Grey Argillite/Siltstone w/ py streaks	blk-dk grey, vfg, lam, qtz veinlets, tr py	147.73-153.56m	Greywacke	Greywacke
04198B	471785.80	5362813.60	Grey Argillite/Siltstone w/ py streaks and sp on fracture surface				
4199	471521.80	5362663.40	Grey Argillite/Siltstone w/ white carb and minor contorted py	blk-dk grey, vfg, lam, qtz str, very fine cleavage, lrg py cubes & blebs	318.10-361.52m	Greywacke	Altered Ultramafics
4200	492980.00	5396759.00	Black Graphitic Argillite w/ minor recystallized py streaks	blk-dk grey, vfg, lam, qcv & str along lam	280-306 or 395-441ft	Overburden OR Intermediate/mafic volcanic	Intermediate/mafic volcanic or mafic volcanic
4301	486797.00	5398806.00	Graphitic Argillite w/ carn vein and nodule		144.9-149.8m	Mafic volcanic	Mafic volcanic
4303	486600.00	5398735.00	Graphitic Argillite w/ py nodules		105.7-107.4m	Mafic/ultramafic volcanic	Mafic volcanic
04307A	487049.80	5398893.00	Black Graphitic Siltstone w/ po nodules (A) and py vein/deformed laminae (B)		153-154.5m	Ultramafic volcanic	Mafic volcanic
4308	486296.90	5399159.70	Graphitic Argillite w/ py nodules		888.2-900.2m	Mafic volcanic	Mafic volcanic
4309	486786.00	5399222.20	Graphitic Argillite w/ py nodules		638.1-639.4m	Ultramafic volcanic	Mafic volcanic
04309B	486786.00	5399222.20	Graphitic Argillite w/ py nodules (not a duplicate)				
4311	486352.70	5398629.50	Graphitic Argillite w/ py nodules		59.93-66.05m	Mafic volcanic	Mafic volcanic
4312	486450.00	5398800.00	Graphitic Argillite w/ py nodules and pink carb veinlet		222.65-222.8m	Mafic volcanic	Mafic volcanic
4314	487099.70	5399048.20	Black Graphitic Siltstone w/ large isolated py nodule		93-100m	Mafic volcanic	Mafic volcanic
4315	486598.40	5399354.70	Graphitic Argillite w/ large isolated py nodule		567-567.2m	Mafic volcanic	Mafic volcanic
4316	486998.00	5399374.00	Black Graphitic Siltstone w/ po streaks		607-613.7m	Mafic volcanic	Mafic volcanic
04316B	486998.00	5399374.00	Black Graphitic Siltstone w/ po streaks (not a duplicate)				
4319	488432.33	5376965.42	Graphitic Argillite w/ py streaks	Black, fine-grained, pyritic, minor qtz-carb-pyrite veins, possibly trace of cpy	341-360m	Interbedded greywacke and argillite	Altered Mafic volcanic
04319B	488432.33	5376965.42	Graphitic Argillite w/ py streaks (not a duplicate)	Black, fine-grained, pyritic, minor qtz-carb-pyrite veins, possibly trace of cpy	341-360m	Interbedded greywacke and argillite	Altered Mafic volcanic
4320	487315.06	5376959.78	Graphitic Argillite w/ py streaks and qtz-carb	dk grey-black, fine-grained, strong banded graphite, up to 7% pyrite locally, <5% qcv	700-798m	Mafic volcanic	Mafic volcanic breccia
04320B	487315.06	5376959.78	Graphitic Argillite w/ py streaks and qtz-carb (not a duplicate)	dk grey-black, fine-grained, strong banded graphite, up to 7% pyrite locally, <5% qcv	700-798m	Mafic volcanic	Mafic volcanic breccia
4323	453450.00	5401420.00	Black Graphitic Argillite w/ 1cm thick py nodule and carb bands	blk-grey, well-bedded with alternating mud & silt beds, coarse py nod/blebs mostly along beds (>15%), qc (10-15%)	220-250 or 380-387 ft	Casing or Argillite	Sericite tuff (250ft) or argillite
4324	486250.00	5396722.00	Graphitic Argillite w/ py laminae		88-94.8m	Altered intermediate-mafic tuff with VG	Altered intermediate-mafic tuff
4325	486275.00	5396719.00	Graphitic Argillite w/ dissem py euhedra		48.5-54.6m	Overburden	Argillite with interbedded greywacke/fault zone
4326	486650.00	5395865.00	Graphitic Argillite w/ qtz-carb, large py euhedra, and minor pink carb		174-198m	Greywacke and argillite	Fault and greywacke with interbedded argillite
4327	486525.00	5396750.00	Graphitic Argillite w/ fine carb-py laminae		54-107.14m	Overburden	Mafic tuff
04329A	469481.00	5364965.00	Argillite/Mudstone cherty w/ trace sp on fracture (A) and graphitic (B)	Dark grey to black, fine-grained ,sharp contact with greywacke	0-161m	Overburden	Greywacke
4330	469485.00	5364487.00	Graphitic Argillite	dk grey to black, fg, rare qcv, <1% py	44.01-60.8m	Overburden	Greywacke
4331	469084.00	5366018.00	Argillite/Mudstone	Dark grey to black, fine-grained ,banded, sharp contact with greywacke	0-125m	Overburden	Greywacke
4332	474735.00	5365711.00	Graphitic Argillite w/ heterolith frag and dissem py euhedra	Mafic tuff and interbedded graphitic argillite, py is bands, qcv parallel to foliation	39.95-128.25m	Graphitic mafic flow and lapilli tuff -pyrite disseminated, barren	Massive mafic flow and interlayered mafic tuff
4333	468894.00	5364950.00	Argillite/Mudstone	Dark grey, fine-grained, white carbonate veins, <1% disseminated py	0-176m	Overburden	Greywacke
4334	486275.00	5396755.00	Graphitic Argillite w/ pinstripe carb		104.8-170.4m	Argillite with interbeded greywacke	Argillite with interbeded greywacke
4335	555620.00	5377737.50	Interflow Sediment w volcanic clasts	Black, fine-grained matrix of hyaloclastite	18.7-18.95m	Mafic volcanic	Mafic volcanic
4336	555620.00	5377737.50	Interflow Sediment w broken carb vein and dissem. py	Black, fine-grained, pyritic (<1%), qcv, thin massive po vein	10.25-10.48m	Mafic volcanic	Mafic volcanic
4337	555620.00	5377737.50	Interflow Sediment w broken carb vein and dissem. py	Black, fine-grained, minor cubic py, pervasive carb alt/veinlets	9.7-9.86m	Mafic volcanic	Mafic volcanic
4338	555710.00	5377722.20	Interflow Sediment w volcanic clasts	Black, fine-grained, 5-7% pyrite	214.17-214.42m	Mafic volcanic	Mafic volcanic
4339	486600.00	5396875.00	Graphitic Argillite w pinstripe carb				
4340	575000.90	5372397.68	Green Siltstone		219.82-375.00m	Hematized Fsp	EOH
4341	574767.89	5371256.69	Greywacke/Argillite		462.46-506.48m	Greywacke/Mafic Intrusive	EOH
4342	575048.90	5372307.68	Greywacke/Argillite w minor carb veins		425.5-435.0m	Mafic Volcanic	EOH

Appendix A3. Sample and field data description / core log entry for N=564 samples of carbonaceous argillite from the Timmins-Kirkland Lake region.

Sample #	Township	Company	Hole #	MNDM #	Sub_Assemb	Assemblage	Contact	Commodity	Ti/Zr_Source_Rock	Host	Analyzed Sample	From_	To	ft_m
4343	Garrison	St Andrew Goldfields Ltd.	GC-10-004	-	Lower	Blake River	-	Orogenic Au	intermediate	Volcanic/Sediment	Greywacke/Argillite	505.80	506.10	m
4344	Garrison	St Andrew Goldfields Ltd.	GC-10-006	-	-	Blake River	-	Orogenic Au	mafic	Volcanic/Sediment	Dark Grey Siltsone/Mudstone	602.25	602.50	m
4345	Garrison	St Andrew Goldfields Ltd.	GC-10-12	-	Lower	Tisdale	-	Orogenic Au	intermediate	Volcanic/Sediment	Greywacke/Argillite w very fine py	80.24	80.46	m
4346	Garrison	St Andrew Goldfields Ltd.	GC-10-14	-	Lower	Tisdale	-	Orogenic Au	intermediate	Volcanic/Sediment	Greywacke/Argillite w very fine py	76.55	76.80	m
4347	Garrison	St Andrew Goldfields Ltd.	GC-10-017	-	Lower	Tisdale	-	Orogenic Au	intermediate	Volcanic/Sediment	Greywacke/Argillite green w very fine py	453.00	453.17	m
4348	Taylor	St Andrew Goldfields Ltd.	TA-10-010	-	Lower	Tisdale	Tisdale/Porcupine	Orogenic Au	intermediate	Volcanic/Sediment	Greywacke/Argillite green, weakly sericitic	494.40	494.63	m
4350	Holloway	St Andrew Goldfields Ltd.	GH-10-003	-	-	Blake River	Blake River/Timiskaming	Orogenic Au	intermediate	Sediment	Fine-grained sediment w siderite veins and laminae	1005.00	1005.18	m
4353	Holloway	St Andrew Goldfields Ltd.	GH-10-10	-	Lower	Blake River	Blake River/Timiskaming	Orogenic Au	intermediate	Volcanic/Sediment	Grey Green Mudstone with possible sid/ank bands or laminae	645.33	645.56	m
4355	Holloway	St Andrew Goldfields Ltd.	GH-10-014	-	Lower	Blake River	Blake River/Timiskaming	Orogenic Au	intermediate	Volcanic/Sediment	Dark Grey Black Mudstone	1298.42	1298.60	m
4356	Holloway	St Andrew Goldfields Ltd.	GH-10-76W2	-	Lower	Blake River	Blake River/Timiskaming	Orogenic Au	intermediate	Volcanic/Sediment	Grey Mudstone w tr py and ptygmatic qtz veinlet	1320.40	1320.58	m
4357	Holloway	St Andrew Goldfields Ltd.	GH-11-002	-	Lower	Blake River	Blake River/Timiskaming	Orogenic Au	intermediate	Volcanic/Sediment	Dark Green Mudstone finely laminated w minor hematitic bands	296.55	296.80	m
4358	Holloway	St Andrew Goldfields Ltd.	GH-11-007	-	Lower	Blake River	Blake River/Timiskaming	Orogenic Au	intermediate	Volcanic/Sediment	Mudstone/Graphitic Argillite w minor py laminae	458.32	458.57	m
4359	Hoyle	Lake Shore Gold	S-10-12	-	-	Tisdale	Tisdale/Porcupine	Orogenic Au	felsic	Volcanic/Sediment	Graphitic/Argillite w py nodules	1559.64	1559.78	m
4360	Hoyle	Lake Shore Gold	S-10-11A	-	Lower	Tisdale	Tisdale/Porcupine	Orogenic Au	felsic	Volcanic/Sediment	Graphitic/Argillite w py nodules and carb	1116.00	1116.20	m
04360B	Hoyle	Lake Shore Gold	S-10-11A	-	Lower	Tisdale	Tisdale/Porcupine	Orogenic Au	felsic	Volcanic/Sediment	Graphitic/Argillite w py nodules and carb (not a duplicate)	0.00	0.00	-
4361	Hoyle	Lake Shore Gold	BC-10-91	-	Lower	Tisdale	Tisdale/Porcupine	Orogenic Au	intermediate	Volcanic/Sediment	Graphitic/Argillite w py nodules, carb, and po streaks	931.11	931.32	m
4362	Hoyle	Lake Shore Gold	WM-10-01	-	Lower	Tisdale	Tisdale/Porcupine	Orogenic Au	intermediate	Volcanic/Sediment	Graphitic/Argillite w py nodules, carb, and qtz-sid vein	185.11	185.32	m
4363	Hoyle	Lake Shore Gold	S-09-07E	-	Lower	Tisdale	Tisdale/Porcupine	Orogenic Au	felsic	Volcanic/Sediment	Graphitic/Argillite w py nodules, carb, and qtz-sid vein	1380.13	1380.38	m
4364	Hoyle	Lake Shore Gold	WM-10-04	-	-	Tisdale	Tisdale/Porcupine	Orogenic Au	felsic	Volcanic/Sediment	Graphitic/Argillite w py nodules	86.85	87.00	m
4365	Hoyle	Lake Shore Gold	BC-09-63	-	Lower	Tisdale	Tisdale/Porcupine	Orogenic Au	felsic	Volcanic/Sediment	Graphitic/Argillite w py nodules and carb nodules	861.26	861.50	m
4366	Hoyle	Lake Shore Gold	V-10-45	-	Lower	Tisdale	Tisdale/Porcupine	Orogenic Au	mafic	Volcanic/Sediment	Argillite/Siltstone w tr py	169.60	169.75	m
4367	Hoyle	Lake Shore Gold	V-10-51	-	Lower	Tisdale	Tisdale/Porcupine	Orogenic Au	mafic	Volcanic/Sediment	Argillite/Siltstone w tr py	165.60	165.80	m
4368	Hoyle	Lake Shore Gold	MH-10-04	-	-	Tisdale	Tisdale/Porcupine	Orogenic Au	felsic	Volcanic/Sediment	Graphitic/Argillite w minor py nodules	540.53	540.67	m
4369	Hoyle	Lake Shore Gold	BC-09-69	-	Lower	Tisdale	Tisdale/Porcupine	Orogenic Au	felsic	Volcanic/Sediment	Graphitic/Argillite w streaky py nodules and carb	1215.70	1215.90	m
4370	Hoyle	Lake Shore Gold	BC-09-69	-	Lower	Tisdale	Tisdale/Porcupine	Orogenic Au	felsic	Volcanic/Sediment	Graphitic/Argillite w abundant contorted carb laminae and py-po-cpy?	1003.64	1003.85	m
4371	Hoyle	Lake Shore Gold	BC-09-04	-	Lower	Tisdale	Tisdale/Porcupine	Orogenic Au	felsic	Volcanic/Sediment	Black Graphitic Argillite w minor py-carb nodules	289.20	289.32	m
4372	Coulson	Rogue Resources	GCAE6-24	-	-	Stoughton-Roquemare	Stoughton-Roquemare/Porcupine	Orogenic Au	felsic	Volcanic/Sediment	Black Argillite/Siltstone (hematitic fractures not sampled)	113.95	114.12	m
4373	Warden	Rogue Resources	GCAE6-25	-	-	Stoughton-Roquemare	Stoughton-Roquemare/Porcupine	Orogenic Au	felsic	Volcanic/Sediment	Black Graphitic Argillite w 1 cm py nodules	263.78	264.01	m
04373B	Warden	Rogue Resources	GCAE6-25	-	-	Stoughton-Roquemare	Stoughton-Roquemare/Porcupine	Orogenic Au	felsic	Volcanic/Sediment	Black Graphitic Argillite w 1 cm py nodules (not a duplicate)	0.00	0.00	-
4374	Warden	Rogue Resources	GCAE7-02	-	-	Stoughton-Roquemare	Stoughton-Roquemare/Porcupine	Orogenic Au	felsic	Volcanic/Sediment	Grey Argillite	442.50	442.60	m
4375	Warden	Rogue Resources	GCAE7-03	-	-	Stoughton-Roquemare	Stoughton-Roquemare/Porcupine	Orogenic Au	felsic	Volcanic/Sediment	Black Graphitic Argillite w flattened py nodules	213.55	213.70	m
4376	Warden	Rogue Resources	GCAE7-04	-	-	Stoughton-Roquemare	Stoughton-Roquemare/Porcupine	Orogenic Au	felsic	Volcanic/Sediment	Black Graphitic Argillite w rare 1 cm py nodules	54.30	54.50	m
04376B	Warden	Rogue Resources	GCAE7-04	-	-	Stoughton-Roquemare	Stoughton-Roquemare/Porcupine	Orogenic Au	felsic	Volcanic/Sediment	Black Graphitic Argillite w rare 1 cm py nodules (not a duplicate)	0.00	0.00	-
4377	Warden	Rogue Resources	GCAE7-05	-	-	Stoughton-Roquemare	Stoughton-Roquemare/Porcupine	Orogenic Au	felsic	Volcanic/Sediment	Argillite/Cherty laminated	88.66	88.80	m
4378	Warden	Rogue Resources	GCAE7-06	-	-	Stoughton-Roquemare	Stoughton-Roquemare/Porcupine	Orogenic Au	intermediate	Volcanic/Sediment	Black Argillite/ Brecciated	75.83	76.00	m
4379	Warden	Rogue Resources	GCAE7-07	-	-	Stoughton-Roquemare	Stoughton-Roquemare/Porcupine	Orogenic Au	felsic	Volcanic/Sediment	Black Graphitic Argillite w streaky py nodules	74.83	75.03	m
4380	Warden	Rogue Resources	GCAE7-08	-	-	Stoughton-Roquemare	Stoughton-Roquemare/Porcupine	Orogenic Au	felsic	Volcanic/Sediment	Black Argillite siliceous w tr py	162.00	162.20	m
4381	Warden	Rogue Resources	GCAE7-09	-	-	Stoughton-Roquemare	Stoughton-Roquemare/Porcupine	Orogenic Au	felsic	Volcanic/Sediment	Black Argillite siliceous w tr py	188.80	188.96	m
4382	Warden	Rogue Resources	GCAE7-10	-	-	Stoughton-Roquemare	Stoughton-Roquemare/Porcupine	Orogenic Au	intermediate	Volcanic/Sediment	Black Argillite siliceous	135.04	135.19	m
4383	Warden	Rogue Resources	GCAE7-13	-	-	Stoughton-Roquemare	Stoughton-Roquemare/Porcupine	Orogenic Au	felsic	Volcanic/Sediment	Black Argillite w fractures and tr py	330.23	330.40	m
4384	Coulson	Rogue Resources	GCAE7-14	-	-	Stoughton-Roquemare	Stoughton-Roquemare/Porcupine	Orogenic Au	felsic	Volcanic/Sediment	Black Argillite w fractures and tr py	212.15	212.38	m
4385	Warden	Rogue Resources	GCAE7-16	-	-	Stoughton-Roquemare	Stoughton-Roquemare/Porcupine	Orogenic Au	felsic	Volcanic/Sediment	Black Graphitic Argillite	643.20	643.45	m
4386	Warden	Rogue Resources	GCAE7-16B	-	-	Stoughton-Roquemare	Stoughton-Roquemare/Porcupine	Orogenic Au	felsic	Volcanic/Sediment	Black Graphitic Argillite w sp vein	638.40	638.46	m
4387	Coulson	Rogue Resources	GCAE8-01	-	-	Stoughton-Roquemare	Stoughton-Roquemare/Porcupine	Orogenic Au	felsic	Volcanic/Sediment	Black Graphitic Argillite w minor py laminae	367.70	367.90	m
4388	Warden	Rogue Resources	GCAE7-17	-	-	Stoughton-Roquemare	Stoughton-Roquemare/Porcupine	Orogenic Au	felsic	Volcanic/Sediment	Black Grey Graphitic Argillite w py laminae	253.50	253.67	m
04389A	McCart	Bridgeport Ventures	MC-08-1	-	-	Stoughton-Roquemare	-	Base Metal	felsic	Volcanic	Black Argillite w carb and py nodules	66.45	66.70	m
04389B	McCart	Bridgeport Ventures	MC-08-1	-	-	Stoughton-Roquemare	-	Base Metal	felsic	Volcanic	Black Argillite w carb and py nodules, black matrix	0.00	0.00	-
4390	McCart	Bridgeport Ventures	MC-08-2	-	-	Stoughton-Roquemare	-	Base Metal	felsic	Volcanic	Black Graphitic Argillite w py-carb nodules	73.00	73.30	m
4391	McCart	Bridgeport Ventures	MC-08-3	-	-	Stoughton-Roquemare	-	Base Metal	felsic	Volcanic	Black Graphitic Argillite w po and py-carb nodules	117.42	117.79	m
4392	Hoyle	Lake Shore Gold	BC-08-23A	-	Lower	Tisdale	Tisdale/Porcupine	Orogenic Au	felsic	Volcanic/Sediment	Black Argillite w small py-carb nodules	675.60	675.85	m
4393	Hoyle	Lake Shore Gold	BC-08-08	-	Lower	Tisdale	Tisdale/Porcupine	Orogenic Au	intermediate	Volcanic/Sediment	Black Graphitic Argillite phyllitic w carb-py vein	129.10	129.28	m
4394	Hoyle	Lake Shore Gold	BC-08-16	-	Lower	Tisdale	Tisdale/Porcupine	Orogenic Au	intermediate	Volcanic/Sediment	Black Argillite w contorted po-py-carb laminae (carb vein not sampled)	1022.90	1023.08	m
4395	Hoyle	Lake Shore Gold	BC-11-104A	-	Lower	Tisdale	Tisdale/Porcupine	Orogenic Au	felsic	Volcanic/Sediment	Black Graphitic Argillite w py nodules and laminae	292.57	292.72	m
4396	Marriot	Plato Gold	MP-09	-	Lower	Blake River	-	Orogenic Au	mafic	Volcanic/Sediment	Black Graphitic Argillite w abundant py nodules and laminae	128.05	128.20	m
4397	Holloway	na	GH-08-27	-	-	-	-	-	intermediate	-	Black Graphitic Argillite w minor py nodules	na	na	na
4398	Marriot	Plato Gold	MP-03	-	Lower	Blake River	-	Orogenic Au	mafic	Volcanic	Black Argillite w minor streaky py	108.70	108.92	m
4399	Marriot	Plato Gold	MP-07	-	Lower	Blake River	-	Orogenic Au	felsic	Volcanic	Black Graphitic Argillite	88.55	88.70	m
4400	Guibord	Plato Gold	G-09-06	-	Lower	Tisdale	Tisdale/Porcupine	Orogenic Au	intermediate	Volcanic/Sediment	Argillite	403.93	404.10	m
4401	Guibord	Plato Gold	G-09-06	-	Lower	Tisdale	Tisdale/Porcupine	Orogenic Au	felsic	Volcanic/Sediment	Black Graphitic Argillite w abundant py nodules and laminae	0.00	0.00	-

Appendix A3. Sample and field data description / core log entry for N=564 samples of carbonaceous argillite from the Timmins-Kirkland Lake region.

Sample #	Easting_83	Northing_83	Sample Type	Field Description/Core Log Entry	Interval Available	Hanging wall	Footwall
4343	575442.62	5371799.39	Greywacke/Argillite		341.46-511.50m	Syenite Intrusion	EOH
4344	575346.37	5371661.14	Dark Grey Siltsone/Mudstone		549.80-613.00m	Syenite Intrusion	EOH
4345	574392.88	5372845.69	Greywacke/Argillite w very fine py		64.0-219.3m	OVB	Felsic Intrusion
4346	574350.88	5373077.69	Greywacke/Argillite w very fine py		54.0-241.55m	OVB	Fault Zone
4347	575348.91	5372447.68	Greywacke/Argillite green w very fine py		408.07-494.9m	Intermediate Dyke	Intermediate Dyke
4348	527319.44	5378874.43	Greywacke/Argillite green, weakly sericitic				
4350	595705.29	5374846.47	Fine-grained sediment w siderite veins and laminae	Within conglomerates		Ultramafic volcanic	EOH
4353	596061.29	5374849.47	Grey Green Mudstone with possible sid/ank bands or laminae	Interbedded ARG/GW/Congl sequence; tr py	626.95-659.33m	Syenitic Intrusion	Mafic Volcanics
4355	595981.29	5374687.46	Dark Grey Black Mudstone	Interbedded GW & ARG sequence; ARG is blk, vfg, patchy sil & alb alt, locally fol	1294.20-1311.55m	Ultramafic Volcanics	Argillite/Conglomerate
4356	596007.99	5374789.64	Grey Mudstone w tr py and ptygmatic qtz veinlet	Dk to lt grey, bedded, tr py along bedding	1316.11-1322.25m	Mafic Volcanics	Fault Zone
4357	596101.29	5374807.46	Dark Green Mudstone finely laminated w minor hematitic bands	Interbedded Arg/GW/IF sequence	292.54-299.35m	Greywacke	Greywacke
4358	596030.29	5374722.46	Mudstone/Graphitic Argillite w minor py laminae	Part of greywacke turbidite sequence, gradational		Mafic volcanic	Quartz breccia
4359	487351.95	5376170.56	Graphitic/Argillite w py nodules	Black, fine-grained, up to 5-7% nodular pyrite, minor qtz-carb	1540-1574.8m	Interbedded greywacke and argillite	Interbedded greywacke and argillite
4360	487315.62	5376960.15	Graphitic/Argillite w py nodules and carb	Black, fine-grained, coarse pyrite. minor Carb-qtz veins	1103-1121m	Massive mafic volcanic	Pillowed mafic volcanic
04360B	487315.62	5376960.15	Graphitic/Argillite w py nodules and carb (not a duplicate)	Black, fine-grained, coarse pyrite. minor Carb-qtz veins	1103-1121m	Massive mafic volcanic	Pillowed mafic volcanic
4361	486774.69	5377412.13	Graphitic/Argillite w py nodules, carb, and po streaks	Black, fine-grained, graphitic, laminated, foliated, abundant po, disseminated py	927-932.6m	Altered mafic volcanic	Massive mafic volcanic
4362	487878.00	5376600.00	Graphitic/Argillite w py nodules, carb, and qtz-sid vein	Graphitic alteration zone' in mafic volcanics with abundant po and py locally	184-185.45	Mafic volcanic	Mafic volcanic
4363	487315.06	5376959.78	Graphitic/Argillite w py nodules, carb, and qtz-sid vein	Dark grey to black, fg, coarse and disseminated py (2%), qcv	1319.6-1396m	Altered mafic volcanic	EOH
4364	487827.00	5378899.00	Graphitic/Argillite w py nodules	Black, fine-grained, nodular pyrite, weak carb	78.8-94.3m	Interbedded greywacke and argillite	Massive mafic volcanic
4365	487213.57	5377376.52	Graphitic/Argillite w py nodules and carb nodules	Black, fine-grained, pyritic, minor qtz-carb veins	856.6-863.1m	Altered mafic volcanic	Massive mafic volcanic
4366	488492.76	5377160.36	Argillite/Siltstone w tr py	blk to dk grey, fine-grained, Trace py and po 'chlorite fracture fill zone'	168.5-171.1m	Pillowed Mafic volcanic	Pillowed Mafic volcanic
4367	488412.52	5377060.41	Argillite/Siltstone w tr py	Part of greywacke turbidite sequence, gradational; dark grey to black, fine-grained	39-171m	Overburden	Argillite
4368	487827.00	5378899.00	Graphitic/Argillite w minor py nodules	Part of greywacke turbidite sequence, gradational; dark grey to black, fine-grained	521.5-547.2m	Interbedded greywacke-argillite	Pillowed mafic volcanic
4369	486973.94	5377345.45	Graphitic/Argillite w streaky py nodules and carb	Black, variably silicified, laminated, significant blebby and disseminated concordant py	1214.2-1218.85m	Dark grey alteration zone	Massive mafic volcanic
4370	486973.94	5377345.45	Graphitic/Argillite w abundant contorted carb laminae and py-po-cpy?	Black to dark grey, fine-grained, silicified, veined, nodular to disseminated pyrite	999.95-1003.8m	Mafic metavolcanic	Dark grey alteration zone' silicified, local graphite
4371	487264.65	5377666.03	Black Graphitic Argillite w minor py-carb nodules	Black, laminated, nodular pyrite, minor qcv	261.3-300m	Light grey alteration zone	EOH
4372	552032.00	5394305.00	Black Argillite/Siltstone (hematitic fractures not sampled)	blk, vfg, sericitic bands (~5%), coarse py (~1%), slightly graphitic fractures	113.5-115.2m	Rhyolite Tuff	Altered Porphyritic Dyke/Gabbro
4373	553826.00	5394030.00	Black Graphitic Argillite w 1 cm py nodules	blk, fg, very coarse nod py (2-3%), carb str (~2%), sil alt, local weak foliation, patchy grey alt	246.7-272.2m	Argillite	Greywacke
04373B	553826.00	5394030.00	Black Graphitic Argillite w 1 cm py nodules (not a duplicate)				
4374	553400.68	5394199.64	Grey Argillite	blk-grey, fg, hard, py str (1-2%), qtz-carb str (1-2%), mod sil alt, rare carb-filled fractures, weak fol	428.9-459.2m	Sediments	Sediments
4375	553999.71	5393953.23	Black Graphitic Argillite w flattened py nodules	blk, fg, carb str, coarse py with local py diss & lam (1%), chl- and graph-filled fractures, qcv with tr cpy, variable fol	202.3-225.2m	Fault Zone below argillaceous sediments	Sediments/tuff
4376	554167.15	5394100.32	Black Graphitic Argillite w rare 1 cm py nodules	blk, fg, tr coarse py, local sil alt & graph fractures, carb str	53.6-92.7m	Rhyolite Tuff	Sediment/Gabbro
04376B	554167.15	5394100.32	Black Graphitic Argillite w rare 1 cm py nodules (not a duplicate)				
4377	554367.41	5394091.21	Argillite/Cherty laminated	blk, fg, massive, coarse & fine py (1%), carb str, weak sil alt, patchy grey alt, weak fol	87.2-99m	Gabbro	Basalt
4378	554479.33	5394091.94	Black Argillite/ Brecciated	blk, fg, tr coarse py, carb str, local intense sil alt, patchy mod sericite alt, local graph fractures	73.2-79.1m	Rhyolite Tuff	Graphitic sediments
4379	554653.87	5394055.39	Black Graphitic Argillite w streaky py nodules	blk, fg, massive, py blebs, str & diss (1%), carb str (~2%), local qcv, rare graph fractures, weak sil	65.7-109.3m	Rhyolite Tuff	Porphyritic sediment
4380	554756.49	5394059.84	Black Argillite siliceous w tr py	blk-dk grey, coarse, fine & diss py (~1%), carb- and graph-filled fractures, local weak sil alt, weak	157.5-168.8m	Debris flow	Fault Zone above greywacke
4381	555149.58	5393997.90	Black Argillite siliceous w tr py	blk, fg, massive, mod sil alt, tr coarse & diss py, rare carb str, weak fol	176.5-200m	Fault Zone	EOH
4382	555555.21	5393852.83	Black Argillite siliceous	blk-dk grey, fg, hard, tr coarse py in fractures, carb- and graph-filled fractures, carb str, weak sil alt, patchy ser alt, weak fol	123.1-138.1m	Lapilli tuff	Polymictic breccia
4383	554514.00	5394310.00	Black Argillite w fractures and tr py	blk-grey, fg, bedded, very hard, locally massive, coarse & diss py (<3%), carb str (2%), int sil alt, patchy ser alt, fol	308.6-369.9m	Gabbro	Polymictic breccia
4384	551400.00	5394575.00	Black Argillite w fractures and tr py	blk-dk grey, fg, hard, chl- & carb-filled fractures, qtz-carb str (~2%), local weak fol	204.9-215.3	Lapilli tuff	Lapilli tuff
4385	553400.03	5394304.68	Black Graphitic Argillite	Interbedded GW & ARG sequence; blk-grey, bedded, fol, tr py veins/str/diss, qcv, sil alt	607.7-658.4m	Sediment (altered GW & ARG)	Debris Flow with cherty horizons
4386	553400.03	5394304.68	Black Graphitic Argillite w sp vein	Interbed GW & ARG sequence; blk-grey, fg, bedded, hard, tr py & cpy, rare chl- & carb-filled fractures, local weak sil & ser alt, fol	617.3-657.1m	Gabbro	Argillite in Fault Zone above greywacke
4387	553310.00	5394300.00	Black Graphitic Argillite w minor py laminae	Interbed siltstone, mdst, chert, wacke & arg sequence; blk, fg, bedded, tr coarse py, graph fractures, carb str	363.3-369.8m	Pillow Basalt	Gabbro
4388	553470.00	5394069.00	Black Grey Graphitic Argillite w py laminae	Interbed arg & wackes (felsic tuff); blk, bedded (with some chert beds), hard, sil alt, local ser alt, tr py, slightly graph with local graph fractures, minor carb- & chl-filled fractures,	242-251.5m	Gabbro	Greywacke
04389A	508799.00	5402424.00	Black Argillite w carb and py nodules	Interbedded GW & ARG; blk-light grey, vfg, lam, hard, tight folds, qtz-carb veintlets to fractures (2-3%), py diss & lam (~5%)	57.35-77.6m	Peridotite	Komatiitic Basalt
04389B	508799.00	5402424.00	Black Argillite w carb and py nodules, black matrix				
4390	508880.00	5402485.00	Black Graphitic Argillite w py-carb nodules	Mixed unit of ARG & Kom.Basalt; ARG is black, vfg, mod hard, non-bedded, py diss & ovoids (7-	67.45-80.8m	Komatiitic Basalt	Argillite/Greywacke
4391	508953.00	5402544.00	Black Graphitic Argillite w po and py-carb nodules	Mixed unit of ARG & Kom.Basalt; ARG is black, vfg, soft, qcv (~3%), py diss & lam (2%), po diss & stretched ovoids (2%)	106.7-139.0m	Komatiitic Basalt	Greywacke
4392	487218.88	5377516.27	Black Argillite w small py-carb nodules	Dark black, fg, weak pervasive calcite	621.1-684.25m	Light grey alteration zone with vg	EOH
4393	486266.64	5377240.53	Black Graphitic Argillite phyllitic w carb-py vein	Black, fine-grained, <5% qtz-carb veins	105.5-148.5m	Ultramafic volcanic	Mafic volcanic breccia
4394	486890.69	5377385.68	Black Argillite w contorted po-py-carb laminae (carb vein not sampled)	Dark grey graphite alteration zone' , dark grey to black, fg, 2-3% po, tr cp and minor py	1019.95-1026.5	Massive mafic volcanic	Pillowed mafic volcanic
4395	486389.00	5377728.00	Black Graphitic Argillite w py nodules and laminae	dk grey to black, fine-grained, nodular pyrite, minor qcv	276-312m	Overburden	EOH
4396	606091.00	5374454.00	Black Graphitic Argillite w abundant py nodules and laminae		125.6-130.4m	Greywacke/Mg tholeiite basalt	Fe-tholeiite basalt
4397	na	na	Black Graphitic Argillite w minor py nodules				
4398	608949.00	5374757.00	Black Argillite w minor streaky py		108.4-115.1m	Greywacke	Greywacke
4399	606886.00	5374541.00	Black Graphitic Argillite		85.8-92.8m	Fe-tholeiite basalt	Fe-tholeiite basalt
4400	554193.59	5372622.24	Argillite		373.25-420m	Greywacke	Greywacke
4401	554193.59	5372622.24	Black Graphitic Argillite w abundant py nodules and laminae	Black, fine-grained, pyrite nodules	354.9-362.25m	Mafic volcanic	Pillow basalt

Appendix A3. Sample and field data description / core log entry for N=564 samples of carbonaceous argillite from the Timmins-Kirkland Lake region.

Sample #	Township	Company	Hole #	MNDM #	Sub_Assemb	Assemblage	Contact	Commodity	Ti/Zr_Source_Rock	Host	Analyzed Sample	From_	To	ft_m
4402	Lamplugh	Solid Gold	SG-10-14	-	-	Stoughton-Roquemare	Stoughton-Roquemare/Kidd-Munro	Base Metal	intermediate	Volcanic	Graphitic Argillite sheared	175.75	175.95	m
4403	Lamplugh	Solid Gold	SG-10-15	-	Lower	Kidd-Munro	-	Base Metal	intermediate	Volcanic	Argillite	284.00	284.15	m
4404	Lamplugh	Solid Gold	SG-10-07	-	Lower	Kidd-Munro	-	Base Metal	intermediate	Volcanic	Cherty Argillite	135.57	135.77	m
4405	Lamplugh	Solid Gold	SG-10-06	-	Lower	Kidd-Munro	-	Base Metal	intermediate	Volcanic	Green Argillite w recrystallized py nodule	208.03	208.23	m
04405D	Lamplugh	Solid Gold	SG-10-06	-	Lower	Kidd-Munro	-	Base Metal	mafic	Volcanic	Green Argillite w recrystallized py nodule	208.03	208.23	m
4406	Hoyle	Goldcorp	OC10936AW2	-	Lower	Tisdale	Tisdale/Porcupine	Orogenic Au	felsic	Volcanic/Sediment	Graphitic Argillite w siderite vein and pyrite, minor white laminae	584.60	584.85	m
4408	Hoyle	Goldcorp	OC10936AW	-	Lower	Tisdale	Tisdale/Porcupine	Orogenic Au	felsic	Volcanic/Sediment	Black Carbonaceous Argillite w minor qtz-py laminae, silicified	715.50	715.75	m
4409	Hoyle	Goldcorp	OC10934	-	Lower	Tisdale	Tisdale/Porcupine	Orogenic Au	felsic	Volcanic/Sediment	Black Carbonaceous Argillite w minor qtz-py laminae, silicified	477.25	477.45	m
4410	Hoyle	Goldcorp	OC10928	-	Lower	Tisdale	Tisdale/Porcupine	Orogenic Au	mafic	Volcanic/Sediment	Gritty Black Carbonaceous Argillite w minor qtz-py laminae, 1-2 cm carbonaceous band silicified	474.10	474.27	m
4411	Hoyle	Goldcorp	OC10930	-	Lower	Tisdale	Tisdale/Porcupine	Orogenic Au	felsic	Volcanic/Sediment	Black Carbonaceous Argillite w 1 cm py nodule, silicified	636.08	636.30	m
4412	Hoyle	Goldcorp	OC10931	-	Lower	Tisdale	Tisdale/Porcupine	Orogenic Au	mafic	Volcanic/Sediment	Black Carbonaceous Argillite	560.28	560.45	m
4413	Hoyle	Goldcorp	OC10932	-	Lower	Tisdale	Tisdale/Porcupine	Orogenic Au	felsic	Volcanic/Sediment	Black Carbonaceous Argillite w 1 cm py nodule, silicified	447.35	447.56	m
4414	Hoyle	Goldcorp	OC10927	-	Lower	Tisdale	Tisdale/Porcupine	Orogenic Au	felsic	Volcanic/Sediment	Black Carbonaceous Argillite w 1 cm py-carb nodule	859.26	859.45	m
4416	Hoyle	Goldcorp	OC10929A	-	Lower	Tisdale	Tisdale/Porcupine	Orogenic Au	felsic	Volcanic/Sediment	Black Carbonaceous Argillite w 1 cm py-carb nodule	548.00	548.22	m
4417	Hoyle	Goldcorp	OC10933	-	Lower	Tisdale	Tisdale/Porcupine	Orogenic Au	intermediate	Volcanic/Sediment	Black Carbonaceous Argillite w minor carb vein	371.61	371.79	m
4418	Hoyle	Goldcorp	OC10926	-	Lower	Tisdale	Tisdale/Porcupine	Orogenic Au	felsic	Volcanic/Sediment	Highly Graphitic Argillite w few 1 cm py nodule	924.84	925.00	m
4421	Tisdale/Dome	Goldcorp	32998	-	-	Tisdale	Tisdale/Timiskaming/Porcupine	Orogenic Au	intermediate	Volcanic/Sediment	Black Carbonaceous Argillite w few 1 cm py nodule and carb laminae	3873.00	3873.80	ft
4426	Tisdale/Dome	Goldcorp	19000	-	-	Tisdale	Tisdale/Porcupine	Orogenic Au	intermediate	Volcanic/Sediment	Graphitic Argillite	211.60	211.80	m
4434	Whitney/Pamour	Goldcorp	19152	-	-	Tisdale	Tisdale/Porcupine	Orogenic Au	intermediate	Volcanic/Sediment	Black Graphitic Argillite w rare <1 cm py nodules	89.00	89.20	m
4435	Whitney/Pamour	Goldcorp	19144	-	-	Tisdale	Tisdale/Porcupine	Orogenic Au	felsic	Volcanic/Sediment	Black Graphitic Argillite w rare <1 cm py nodules	126.70	126.90	m
4437	Whitney/Pamour	Goldcorp	19130	-	-	Tisdale	Tisdale/Porcupine	Orogenic Au	intermediate	Volcanic/Sediment	Mudstone	38.15	38.35	m
4438	Whitney/Pamour	Goldcorp	19133	-	-	Tisdale	Tisdale/Porcupine	Orogenic Au	intermediate	Volcanic/Sediment	Mudstone	89.17	89.33	m
4441	Whitney/Pamour	Goldcorp	19153	-	-	Tisdale	Tisdale/Porcupine	Orogenic Au	felsic	Volcanic/Sediment	Black Graphitic Argillite w 1 cm py nodules	167.28	167.43	m
4445	Hoyle	Goldcorp	TV-11-02	-	-	Porcupine	Tisdale/Porcupine	Orogenic Au	felsic	Sediment	Black Graphitic Argillite w rare 1 cm py nodules	94.83	95.00	m
4446	Hoyle	Goldcorp	TV-11-02	-	-	Porcupine	Tisdale/Porcupine	Orogenic Au	felsic	Sediment	Black Graphitic Argillite w <1 cm white carb nodules or spots	116.70	116.90	m
4447	Hoyle	Goldcorp	TV-11-02	-	-	Porcupine	Tisdale/Porcupine	Orogenic Au	intermediate	Sediment	Black Argillite w 1 cm py-carb-qtz vein (not included)	152.40	152.59	m
4448	Hoyle Trend	Goldcorp	MT-04-01	-	-	Timiskaming	-	Orogenic Au	intermediate	Sediment	Grey Argillite	44.65	44.85	m
4449	Hoyle Trend	Goldcorp	18945	-	-	Tisdale	Tisdale/Porcupine	Orogenic Au	felsic	Volcanic/Sediment	Mixed sample, mafic volcanic with black argillite	166.93	167.10	m
4450	Hoyle/Bell Creek	Goldcorp	TW-04-01	-	Lower	Tisdale	Tisdale/Timiskaming	Orogenic Au	felsic	Volcanic/Sediment	Graphitic Argillite w tr euhedral dissem py	152.76	152.98	m
4451	Hoyle/Bell Creek	Goldcorp	TW-04-02A	-	Lower	Tisdale	Tisdale/Timiskaming	Orogenic Au	felsic	Volcanic/Sediment	Graphitic Argillite	118.45	118.60	m
4452	Hoyle/Bell Creek	Goldcorp	TW-04-02A	-	Lower	Tisdale	Tisdale/Timiskaming	Orogenic Au	intermediate	Volcanic/Sediment	Argillite	295.25	295.45	m
4453	Hoyle/Bell Creek	Goldcorp	TW-04-07	-	-	Tisdale	Tisdale/Timiskaming	Orogenic Au	felsic	Volcanic/Sediment	Graphitic Argillite w qtz-carb-py deformed white laminae and band	248.00	248.13	m
4454	Hoyle/Bell Creek	Goldcorp	TW-04-03	-	Lower	Tisdale	Tisdale/Timiskaming	Orogenic Au	intermediate	Volcanic/Sediment	Graphitic Argillite w qtz-carb-py deformed white laminae and band	93.10	93.26	m
4456	Hoyle/Bell Creek	Goldcorp	TW-05-15	-	Lower	Tisdale	Tisdale/Timiskaming	Orogenic Au	intermediate	Volcanic/Sediment	Graphitic Argillite/Siltstone	150.27	150.47	m
4457	Hoyle	Goldcorp	OC10919	-	Lower	Tisdale	Tisdale/Porcupine	Orogenic Au	felsic	Volcanic/Sediment	Black Graphitic Argillite	189.95	190.08	m
4458	Hoyle	Goldcorp	OC10922	-	-	Porcupine	Tisdale/Porcupine	Orogenic Au	intermediate	Sediment	Black Graphitic Argillite w isolated 1 cm py nodule	108.16	108.36	m
4459	Hoyle	Goldcorp	OC10895	-	Lower	Tisdale	Tisdale/Porcupine	Orogenic Au	felsic	Volcanic/Sediment	Black Graphitic Argillite w isolated 1 cm py nodule	145.60	145.76	m
4460	Hoyle	Goldcorp	OC10909	-	-	Porcupine	Tisdale/Porcupine	Orogenic Au	intermediate	Sediment	Black Graphitic Argillite w isolated 1 cm py nodule, highly deformed	170.64	170.78	m
4461	Whitney/Pamour	Goldcorp	19007	-	-	Tisdale	Tisdale/Porcupine	Orogenic Au	felsic	Volcanic/Sediment	Black Graphitic Argillite w minor <1 cm py nodule	216.10	216.30	m
4462	Whitney/Pamour	Goldcorp	19005A	-	-	Tisdale	Tisdale/Porcupine	Orogenic Au	intermediate	Volcanic/Sediment	Black Graphitic Argillite w minor <1 cm py nodule, possible volcaniclastci component	165.35	165.60	m
4463	Whitney/Pamour	Goldcorp	18973	-	-	Tisdale	Tisdale/Porcupine	Orogenic Au	felsic	Volcanic/Sediment	Black Graphitic Argillite w minor <1 cm py nodule, possible volcaniclastci component	170.00	170.20	m
4464	Munro	Golden Valley	GM-07-06	-	Lower	Kidd-Munro	-	Base Metal	felsic	Volcanic	Black Graphitic Argillite w tr dissem py	186.00	186.30	m
4465	Munro	Golden Valley	GM-07-06	-	Lower	Kidd-Munro	-	Base Metal	felsic	Volcanic	Black Graphitic Argillite w tr dissem py	204.00	204.30	m
4466	Munro	Golden Valley	GM-07-10	-	Lower	Kidd-Munro	-	Base Metal	felsic	Volcanic	Black Graphitic Argillite w tr dissem py	208.79	209.00	m
4469	Kirkland Lake/Bernhardt	Golden Valley	GA-03-01	-	Lower	Blake River	-	Orogenic Au	felsic	Volcanic/Sediment	Black Graphitic Argillite w rare <1 cm py nodules	316.30	317.30	ft
4470	Kirkland Lake/Bernhardt	Golden Valley	GA-03-02	-	Lower	Blake River	-	Orogenic Au	felsic	Volcanic/Sediment	Black Graphitic Argillite w rare <1 cm py nodules	73.77	73.87	m
4471	German	Sage Gold Inc.	CL-11-20	-	-	Kidd-Munro	Porcupine/Kidd-Munro	Orogenic Au	intermediate	Volcanic/Sediment	Argillite w strong cleavage	157.30	157.46	m
4473	Stock	Sage Gold Inc.	CL-11-19	-	-	Kidd-Munro	Kidd-Munro/Porcupine	Orogenic Au	intermediate	Volcanic/Sediment	Black Graphitic Argillite w <1 cm py nodules, strong cleavage	512.60	512.85	m
4474	Stock	Sage Gold Inc.	CL-11-17	-	-	Kidd-Munro	Kidd-Munro/Porcupine	Orogenic Au	intermediate	Volcanic/Sediment	Black Graphitic Argillite w strong cleavage	463.18	463.42	m

Appendix A3. Sample and field data description / core log entry for N=564 samples of carbonaceous argillite from the Timmins-Kirkland Lake region.

Sample #	Easting_83	Northing_83	Sample Type	Field Description/Core Log Entry	Interval Available	Hanging wall	Footwall
4402	588460.00	5381726.00	Graphitic Argillite sheared	Dark grey-black, lam, not graph, soft-sed def, py lam, qtz-carb str		Mafic Metavolcanics	Intercalated Arg-Rhyolite
4403	587243.00	5381603.00	Argillite	lam, mod hard	275.4-284.1m	Intercalated Mafic Flows & Tuffs	Int. Volcanics
4404	584490.00	5382380.00	Cherty Argillite	med-grey to grey-green, laminated	133.15-149.5m	Mafic Xstl Tuff/Fragmental	Mafic to UM Volcanics
4405	583980.00	5382610.00	Green Argillite w recrystallized py nodule	3-5% py rounded nod	202.2-217.05m	Brecciated IF & Clastic Metaseds	Iron Formation
04405D	583980.00	5382610.00	Green Argillite w recrystallized py nodule	3-5% py rounded nod	202.2-217.05m	Brecciated IF & Clastic Metaseds	Iron Formation
4406	489969.82	5378068.68	Graphitic Argillite w siderite vein and pyrite, minor white laminae	blk-dk grey, vfg, lam, qcv (1-2%) with tr py, Fe-carb alt	5.0m	Volc	Gwk
4408	489969.82	5378068.68	Black Carbonaceous Argillite w minor qtz-py laminae, silicified	blk, vfg, finely lam, py vein & str along lam + blebs, tr qcv; Sample @ EOH	>35.5m	Volc	Unk
4409	489774.13	5377917.85	Black Carbonaceous Argillite w minor qtz-py laminae, silicified	blk, vfg, lam, py vein, str, nod along lam, qcv assoc with py	25.0m	Volc	Gwk
4410	489908.90	5377927.00	Gritty Black Carbonaceous Argillite w minor qtz-py laminae, 1-2 cm carbonaceous band silicified	blk, vfg, lam, pervasive diss py thro-out (some alt to Fe-carb) + along lam (~5%), tr coarse py, qc assoc with py, graph fractures; Sample @ EOH	>23.8m	Volc	Unk
4411	489919.43	5378019.95	Black Carbonaceous Argillite w 1 cm py nodule, silicified	blk, vfg, finely lam, coarse py nod + veinlets/str along lam (2-3%), tr qc assoc with py, tr silt along	63.6m	Volc	Gwk
4412	489709.16	5377899.75	Black Carbonaceous Argillite	blk-dk grey, vfg, lam, tr py srt along lam & tr py blebs, tr qcv cutting across lam + some along lam; Sample @ EOH	>40.7m	Volc	Unk
4413	489744.27	5377867.95	Black Carbonaceous Argillite w 1 cm py nodule, silicified	blk, vfg, f.lam, coarse py nod/blebs + str & diss along lam, qc mostly assoc with py, graph on	16.0m	Volc	Gwk
4414	489934.46	5378067.19	Black Carbonaceous Argillite w 1 cm py-carb nodule	blk-dk grey, vfg-fg, lam, folding is evident, coarse py nod, some with concentric zoning with arg, and py diss & blebs mostly along lam (~5%), qc along lam and assoc with py (~5%), graph?	10.5m	Volc	Gwk
4416	489909.15	5377944.55	Black Carbonaceous Argillite w 1 cm py-carb nodule	blk, vfg. Lam, coarse py nod/stretched nod/blebs + veinlets/str/diss mostly following lam (~3%), tr qc along lam and assoc with py; Sample @ EOH	>57.0m	Volc	Unk
4417	489775.94	5377826.88	Black Carbonaceous Argillite w minor carb vein	blk, vfg, f.lam, py nod/stretched nod/veinlets/str/diss mostly along lam (~5%), tr qc veins/veinlets curring lam, with some assoc with py; Sample @ EOH	>27.5m	Volc	Unk
4418	489983.60	5378144.76	Highly Graphitic Argillite w few 1 cm py nodule	blk, vfg, lam?, coarse py nod/stretched nod/blebs (2-3%), qc blebs/wisps, some assoc with py, some following lam? (2-3%)	7.4m	Volc	Gwk
4421	481559.32	5368953.62	Black Carbonaceous Argillite w few 1 cm py nodule and carb	blk, vfg, lam, coarse py nod/lam (~2%), qc str & assoc with py (1%)	15.80	Krist	Volc
4426	492049.07	5375466.58	Graphitic Argillite	blk, vfg, lam, py nod/veinlets/blebs/diss (3-5%); qcv and blebs, & assoc with py	2.0m	Gwk	Volc
4434	492194.42	5375383.48	Black Graphitic Argillite w rare <1 cm py nodules	Black, fine-grained, laminated, <1% nodular pyrite, <1% carb-quartz veins/pressure shadows around nodules	12.2m	Gwk	Volc
4435	492124.14	5375419.85	Black Graphitic Argillite w rare <1 cm py nodules	Black, fine-grained, laminated, <1% nodular pyrite, <1% carb-quartz veins/pressure shadows around nodules	6.8m	Gwk	Volc
4437	491136.81	5375283.85	Mudstone	Arg band in Gwk; dk grey, fine-grained, laminated, <1% qtz-carb vein	Unk	Gwk	Gwk
4438	492036.99	5375360.87	Mudstone	Arg band in Gwk; dk grey, fine-grained, laminated, 3% qtz-carb vein	Unk	Gwk	Gwk
4441	492167.28	5375473.10	Black Graphitic Argillite w 1 cm py nodules	Black, fine-grained, laminated, 5-7% pyrite nodules with carb +/- qtz pressure shadows, <1% carb-qtz veins	7.5m	Gwk	Volc
4445	490792.40	5377537.19	Black Graphitic Argillite w rare 1 cm py nodules	Black, fine-grained, laminated, very strongly graphitic, 2-3% nodular pyrite, 3-4% qtz-carb pressure shadows/veins	6.0m	Volc	Volc
4446	490792.40	5377537.19	Black Graphitic Argillite w <1 cm white carb nodules or spots	Black, fine-grained, laminated, 1% py nodules, 1 % qtz-carb veins/ pressure shadows around	19.6m	Volc	Gwk
4447	490792.40	5377537.19	Black Argillite w 1 cm py-carb-qtz vein (not included)	Arg band in Gwk; Black to dk grey, fine-grained, weakly graphitic, 3% qtz-carb veins, 3% pyrite as a single disseminated vein, crenulation cleavage throughout	Unk	Gwk	Gwk
4448	498937.52	5376298.51	Grey Argillite	Arg band in Gwk; Black, fine-grained, trace of qtz-carb	Unk	Gwk	Gwk
4449	492050.27	5375412.40	Mixed sample, mafic volcanic with black argillite	Black, fine-grained, massive looking and feeling, 2% disseminated cubic pyrite, 3% carb-qtz +/- py veins; few pieces look more like argillite but most look a bit off	0.3m	Gwk	Volc
4450	472547.84	5363004.81	Graphitic Argillite w tr euhedral dissem py	Black, fine-grained, very graphitic, laminated, avg 2% py, veins + disseminated, <1% qtz-carb	1.7m	Gwk	Gwk
4451	472550.29	5363165.01	Graphitic Argillite	Arg band in Gwk; Black, fine-grained, laminated (10% brownish laminae), 1% disseminated cubic pyrite following broadly lamination, 1% qtz-carb veins	Unk	Gwk	Gwk
4452	472550.29	5363165.01	Argillite	Arg band in Gwk; Black, fine-grained, laminated, 1% qtz-carb (with some iron staining) +/- py	Unk	Gwk	Gwk
4453	472544.93	5362905.24	Graphitic Argillite w qtz-carb-py deformed white laminae and band	Black, fine-grained, laminated (20% light grey silty mud? Laminae), 4% py as veins, 2% carb-qtz veins +/- py	14.0m	Gwk	Volc
4454	472248.55	5362970.19	Graphitic Argillite w qtz-carb-py deformed white laminae and band	Black, fine-grained, laminated, 1% nodular pyrite, 20% carb-py-qtz veins running parallel to core axis; Collared in Arg	>47.0m	OVB	Dacite
4456	487777.48	5373274.21	Graphitic Argillite/Siltstone	Arg band in Gwk; Black, fine-grained, laminated, 1% qtz-carb-py veins	Unk	Gwk	Gwk
4457	489857.26	5377690.16	Black Graphitic Argillite	Black, fine-grained, laminated, trace pyrite and qtz-carb veins	44.1m	Gwk	Gwk
4458	489434.18	5377418.01	Black Graphitic Argillite w isolated 1 cm py nodule	Black, fine-grained, laminated, <1% nodular pyrite, <1% carb-quartz veins/pressure shadows around nodules	32.6m	Gwk	Gwk
4459	490308.92	5377730.73	Black Graphitic Argillite w isolated 1 cm py nodule	Black, fine-grained, laminated, 1-2% nodular pyrite, <1% carb-quartz veins/pressure shadows around nodules	>9.8m	Volc	Unk
4460	490708.06	5377592.95	Black Graphitic Argillite w isolated 1 cm py nodule, highly	blk-dk grey, vfg, lam, tr py blebs/nod/str, tr qc	35.4m	Volc	Gwk
4461	492281.68	5375538.45	Black Graphitic Argillite w minor <1 cm py nodule	blk, vfg, lam, py nod/blebs/str/diss (~2%), tr qc	2.8m	Gwk	Volc
4462	492297.63	5375489.17	Black Graphitic Argillite w minor <1 cm py nodule, possible volcaniclastci component	blk-dk grey, vfg, lam, py blebs/diss (1-2%), qc str and assoc with py (~2%)	6.0m	Gwk	Volc
4463	492159.67	5375470.24	Black Graphitic Argillite w minor <1 cm py nodule, possible volcaniclastci component	blk, vfg, py blebs/str/diss (1-2%), tr qc veinlets/str	11.7m	Gwk	Volc
4464	560188.00	5381528.00	Black Graphitic Argillite w tr dissem py	Black, fine-grained, laminated, 1% pyrite, graphitic			
4465	560188.00	5381528.00	Black Graphitic Argillite w tr dissem py	Dark grey to black, fine-grained, minor graphite, disseminated euhedral pyrite (1%)			
4466	560172.00	5381495.00	Black Graphitic Argillite w tr dissem py	Black, fine-grained, graphitic, trace pyrite (disseminated + nodular), very minor carb-qtz veinlets			
4469	567270.00	5338977.00	Black Graphitic Argillite w rare <1 cm py nodules	Black, fine-grained, graphitic, trace pyrite and minor qtz-carb veinlets			
4470	566994.00	5338658.00	Black Graphitic Argillite w rare <1 cm py nodules	Black, fine-grained, graphitic, trace disseminated pyrite, very minor qtz-carb veinlets			
4471	513263.17	5384436.30	Argillite w strong cleavage	Dark grey, fine-grained, laminated, <3% silicified silt/fine sand layers	150.35-160.6m	Intercalated argillite and greywacke	Intercalated argillite and greywacke
4473	514312.16	5384343.27	Black Graphitic Argillite w <1 cm py nodules, strong cleavage	Black, fine-grained, 1-2% pyrite, locally nodular, <1% minor qtz veinlets	503.7-519.6m	Sericite altered fragmental ultramafic volcanic	Sericite altered fragmental ultramafic volcanic
4474	514252.16	5384349.27	Black Graphitic Argillite w strong cleavage	Black/dark grey, brecciated, fine-grained, graphitic, 4% carb-qtz veinlets	459.1-465.1m	Sericite altered fragmental ultramafic volcanic	Sericite altered fragmental ultramafic volcanic

Appendix A3. Sample and field data description / core log entry for N=564 samples of carbonaceous argillite from the Timmins-Kirkland Lake region.

Sample #	Township	Company	Hole #	MNDM #	Sub_Assemb	Assemblage	Contact	Commodity	Ti/Zr_Source_Rock	Host	Analyzed Sample	From_	To	ft_m
4475	German	Sage Gold Inc.	CL-11-20	-	-	Kidd-Munro	Porcupine/Kidd-Munro	Orogenic Au	intermediate	Volcanic/Sediment	Green Slate w pink carb vein and fine dissem py euhedra	72.50	72.65	m
4476	German	St Andrew Goldfields Ltd.	CL-04-01	-	-	Kidd-Munro	Porcupine/Kidd-Munro	Orogenic Au	intermediate	Volcanic/Sediment	Green Slate w pink carb vein	304.50	304.63	m
4477	German	St Andrew Goldfields Ltd.	CL-04-01	-	-	Kidd-Munro	Porcupine/Kidd-Munro	Orogenic Au	felsic	Volcanic/Sediment	Black Graphitic Argillite	427.70	427.81	m
4478	Stock	St Andrew Goldfields Ltd.	CL-04-02	-	-	Kidd-Munro	Kidd-Munro/Porcupine	Orogenic Au	intermediate	Volcanic/Sediment	Black Slate w white laminae, strong cleavage	283.47	283.60	m
4479	Stock	St Andrew Goldfields Ltd.	CL-04-03	-	-	Kidd-Munro	Kidd-Munro/Porcupine	Orogenic Au	intermediate	Volcanic/Sediment	Black Slate w fine white laminae, tr py, strong cleavage	50.60	50.76	m
4480	Stock	St Andrew Goldfields Ltd.	CL-04-03	-	-	Kidd-Munro	Kidd-Munro/Porcupine	Orogenic Au	intermediate	Volcanic/Sediment	Black Slate w tr py, strong cleavage	273.77	273.97	m
4481	Stock	St Andrew Goldfields Ltd.	CL-04-04	-	-	Kidd-Munro	Kidd-Munro/Porcupine	Orogenic Au	intermediate	Volcanic/Sediment	Graphitic Argillite/Slate w Fe-carb vein and laminae	226.25	226.40	m
4482	Stock	St Andrew Goldfields Ltd.	CL-04-06	-	-	Kidd-Munro	Kidd-Munro/Porcupine	Orogenic Au	intermediate	Volcanic/Sediment	Slate	197.80	198.02	m
4483	German	St Andrew Goldfields Ltd.	CL-04-09	-	-	Kidd-Munro	Porcupine/Kidd-Munro	Orogenic Au	intermediate	Volcanic/Sediment	Slate w minor siderite-carb vein	42.65	42.75	m
4487	German	Sage Gold Inc.	CL-11-02	-	-	Kidd-Munro	Porcupine/Kidd-Munro	Orogenic Au	intermediate	Volcanic/Sediment	Black Argillite w white laminae, strong cleavage	125.50	125.68	m
4488	German	Sage Gold Inc.	CL-11-04	-	-	Kidd-Munro	Porcupine/Kidd-Munro	Orogenic Au	intermediate	Volcanic/Sediment	Black Slate	147.90	148.15	m
4489	Stock	Sage Gold Inc.	CL-11-12	-	-	Kidd-Munro	Kidd-Munro/Porcupine	Orogenic Au	intermediate	Volcanic/Sediment	Black Slate	70.67	70.77	m
4490	Tisdale	Moneta	MM-11-2	-	Lower	Tisdale	Tisdale/Timiskaming/Porcupine	Orogenic Au	intermediate	Volcanic/Sediment	Graphitic Argillite w 1 cm recrystallized py laminae/bands, strong cleavage	17.40	17.58	m
4491	Michaud/55 Zone	Moneta	M55-10-11	-	Lower	Tisdale	Tisdale/Timiskaming	Orogenic Au	intermediate	Volcanic/Sediment	Green Mudstone w pink carb vein	171.51	171.69	m
4492	Michaud/55 Zone	Moneta	M55-10-17	-	Lower	Tisdale	Tisdale/Timiskaming	Orogenic Au	intermediate	Volcanic/Sediment	Green Mudstone	147.60	147.87	m
4493	Michaud	Moneta	M-87-26	-	Lower	Blake River	-	Orogenic Au	intermediate	Volcanic/Sediment	Black Argillite/Siltstone	0.00	0.00	ft
4495	Michaud	Moneta	M-87-91	-	Lower	Blake River	-	Orogenic Au	intermediate	Volcanic/Sediment	Green Mudstone (small sample)	380.15	381.50	ft
4496	Michaud	Moneta	M-87-91	-	Lower	Blake River	-	Orogenic Au	intermediate	Volcanic/Sediment	Green Mudstone (small sample)	0.00	402.50	ft
4498	Michaud/55 Zone	Moneta	MA-02-H6-H232	-	-	Blake River	Blake River/Timiskaming	Orogenic Au	intermediate	Volcanic/Sediment	Green Mudstone/Siltstone	197.55	197.75	m
4499	Michaud/Southwest Zone	Moneta	MSW-10-162D1	-	-	Tisdale	Tisdale/Timiskaming	Orogenic Au	intermediate	Volcanic/Sediment	Silty Mudstone w tr py, silicified	894.00	894.42	m
4500	Michaud/Southwest Zone	Moneta	MSW-10-162G	-	-	Tisdale	Tisdale/Timiskaming	Orogenic Au	intermediate	Volcanic/Sediment	Dark Green Mudstone	463.66	463.89	m
7401	Michaud/Southwest Zone	Moneta	MSW-10-162G	-	-	Tisdale	Tisdale/Timiskaming	Orogenic Au	intermediate	Volcanic/Sediment	Light Grey Mudstone, cherty w py on fractures	897.55	897.62	m
7402	Michaud/Southwest Zone	Moneta	MSW-10-267	-	Lower	Blake River	Blake River/Timiskaming	Orogenic Au	intermediate	Volcanic/Sediment	Green Grey Silty Mudstone w pink carb vein	450.85	451.11	m
7403	Michaud/Southwest Zone	Moneta	MSW-10-267	-	Lower	Blake River	Blake River/Timiskaming	Orogenic Au	intermediate	Volcanic/Sediment	Dark Grey Silty Mudstone	809.18	809.43	m
7404	Michaud/Southwest Zone	Moneta	MSW-10-267	-	Lower	Blake River	Blake River/Timiskaming	Orogenic Au	intermediate	Volcanic/Sediment	Light Grey Silty Mudstone w tr py and carb on fractures	1206.19	1206.42	m
7405	Michaud/55 Zone	Moneta	M55-01	-	Lower	Tisdale	Tisdale/Timiskaming	Orogenic Au	intermediate	Volcanic/Sediment	Graphitic Argillite breccia w white carb and tr py	68.14	68.35	m
7406	Michaud/55 Zone	Moneta	M55-01	-	Lower	Tisdale	Tisdale/Timiskaming	Orogenic Au	intermediate	Volcanic/Sediment	Black Graphitic Argillite w isolated py nodules	140.50	140.95	m
7407	Michaud/Last Chance/Landing/Twin Creeks	Moneta	MU-89-100	-	Lower	Tisdale	-	Orogenic Au	intermediate	Volcanic/Sediment	Dark Grey Silty Mudstone	224.66	224.81	m
7408	Michaud/Windjammer	Moneta	MWJ-09-24	-	-	Tisdale	Tisdale/Timiskaming	Orogenic Au	intermediate	Volcanic/Sediment	Very Light Grey Silty Mudstone w minor quartz veins	247.85	248.00	m
7409	Michaud/Windjammer	Moneta	MWJ-09-25	-	-	Tisdale	Tisdale/Timiskaming	Orogenic Au	intermediate	Volcanic/Sediment	Grey Green Silty Mudstone	355.83	355.93	m
7410	Michaud/Windjammer	Moneta	WJ-87-3	-	-	Tisdale	Tisdale/Timiskaming	Orogenic Au	intermediate	Volcanic/Sediment	Grey Green Silty Mudstone	632.50	0.00	ft
7411	Michaud/55 Zone	Moneta	MA-08-47	-	-	Tisdale	Tisdale/Timiskaming	Orogenic Au	intermediate	Volcanic/Sediment	Grey Green Silty Mudstone w tr py	59.25	59.37	m
7412	Michaud/55 Zone	Moneta	MA-08-46	-	-	Tisdale	Tisdale/Timiskaming	Orogenic Au	intermediate	Volcanic/Sediment	Green Silty Mudstone/Volcaniclastic w wispy py-carb	176.17	176.39	m
7413	Michaud/55 Zone	Moneta	M55-08	-	Lower	Tisdale	Tisdale/Timiskaming	Orogenic Au	intermediate	Volcanic/Sediment	Black Graphitic Argillite w minor py nodules	85.05	85.21	m
07413D	Michaud/55 Zone	Moneta	M55-08	-	Lower	Tisdale	Tisdale/Timiskaming	Orogenic Au	intermediate	Volcanic/Sediment	Black Graphitic Argillite w minor py nodules	85.05	85.21	m
7414	Michaud/55 Zone	Moneta	M55-08	-	Lower	Tisdale	Tisdale/Timiskaming	Orogenic Au	felsic	Volcanic/Sediment	Black Graphitic Argillite, strong cleavage	105.57	105.76	m
7416	Hoyle Trend	Goldcorp	18662	-	-	Tisdale	Tisdale/Timiskaming	Orogenic Au	intermediate	Volcanic/Sediment	Black Graphitic Argillite	118.23	118.35	m
7417	Hoyle Trend	Goldcorp	18654	-	-	Tisdale	Tisdale/Timiskaming	Orogenic Au	intermediate	Volcanic/Sediment	Black Graphitic Argillite	50.81	50.89	m
7418	Hoyle Trend	Goldcorp	18654	-	-	Tisdale	Tisdale/Timiskaming	Orogenic Au	intermediate	Volcanic/Sediment	Black Graphitic Argillite w tr py	86.09	86.19	m
7420	Hoyle Trend	Goldcorp	18666	-	-	Tisdale	Tisdale/Timiskaming	Orogenic Au	intermediate	Volcanic/Sediment	Grey Argillite	213.00	214.00	ft
7421	Hoyle Trend	Goldcorp	18695	-	Lower	Tisdale	Tisdale/Timiskaming	Orogenic Au	intermediate	Volcanic/Sediment	Dark Grey Argillite w 1/2 cm sericite vein	320.00	321.00	ft
7422	Hoyle Trend	Goldcorp	16442	-	-	Tisdale	Tisdale/Porcupine	Orogenic Au	felsic	Volcanic/Sediment	Black Graphitic Argillite w deformed py nodules	475.61	475.86	m
7423	Hoyle Trend	Goldcorp	16400	-	-	Tisdale	Tisdale/Porcupine	Orogenic Au	felsic	Volcanic/Sediment	Black Carbonaceous Argillite w deformed py nodules and py-carb laminae	459.90	460.02	m
7424	Hoyle Trend	Goldcorp	16442	-	-	Tisdale	Tisdale/Porcupine	Orogenic Au	intermediate	Volcanic/Sediment	Black Carbonaceous Argillite w deformed py nodules and py-carb laminae	706.36	706.53	m
7425	Hoyle Trend	Goldcorp	17147	-	-	Tisdale	Tisdale/Porcupine	Orogenic Au	felsic	Volcanic/Sediment	Black Carbonaceous Argillite w deformed py nodules and py-po-carb laminae	235.70	236.00	m
7427	Hoyle Trend	Goldcorp	17147	-	-	Tisdale	Tisdale/Porcupine	Orogenic Au	felsic	Volcanic/Sediment	Black Carbonaceous Argillite w deformed py nodules	288.40	288.62	m
7428	Hoyle Trend	Goldcorp	15614	-	-	Tisdale	Tisdale/Porcupine	Orogenic Au	felsic	Volcanic/Sediment	Black Carbonaceous Argillite w deformed py nodules	177.50	177.75	m
7429	Hislop	Brigus Gold	10-BF-504	-	-	Tisdale	Tisdale/Porcupine	Orogenic Au	intermediate	Volcanic/Sediment	Argillite w pink calcite vein	67.25	67.55	m
7430	Hislop	Brigus Gold	10-BF-504	-	-	Tisdale	Tisdale/Porcupine	Orogenic Au	intermediate	Volcanic/Sediment	Black Argillite w white carb nodules/veins	172.21	172.40	m
7431	Hislop	Brigus Gold	10-BF-517	-	Lower	Tisdale	Tisdale/Porcupine	Orogenic Au	felsic	Volcanic/Sediment	Argillite, cherty	811.87	812.18	m
7432	Hislop	Brigus Gold	05-BF-411	-	-	Tisdale	Tisdale/Porcupine	Orogenic Au	intermediate	Volcanic/Sediment	Black Argillite w white carb laminae/vein	366.32	366.65	m

Appendix A3. Sample and field data description / core log entry for N=564 samples of carbonaceous argillite from the Timmins-Kirkland Lake region.

Sample #	Easting_83	Northing_83	Sample Type	Field Description/Core Log Entry	Interval Available	Hanging wall	Footwall
4475	513263.17	5384436.30	Green Slate w pink carb vein and fine dissem py euhedra	Dark grey-green, 10-15% silt? Laminae, minor Mn-carbonate veins, make sure to clean off edge of sample	70.1-78.15m	Greywacke	Greywacke
4476	513804.74	5384402.47	Green Slate w pink carb vein	dk grey-black, fine-grained, laminated, <1% qtz-carb veins with trace pyrite; 1 large carbonate vein (w minor Fe) please remove!	304.5-307.5m	Greywacke	Argillite
4477	513804.74	5384402.47	Black Graphitic Argillite	Black, fine-grained, laminated, graphitic, 2% pyrite along discontinuous qtz veins	424.5-428.3m	Argillite	Sericite altered fragmental ultramafic volcanic
4478	513895.12	5384327.92	Black Slate w white laminae, strong cleavage	dk grey, fine-grained, laminated, 2% qtz carb-pyrite veins as tension gashes and bedding parallel, trace sphalerite?	267.5-291.3m	Greywacke	Intercalated greywacke and argillite
4479	514034.51	5384448.61	Black Slate w fine white laminae, tr py, strong cleavage	dk grey-black, fine-grained, laminated, trace qtz-carb veins	21-59m	Intercalated argillite and greywacke	Greywacke
4480	514034.51	5384448.61	Black Slate w tr py, strong cleavage	dk grey-black, fine-grained, laminated, <2% thin qtz-carb veins	258-293.95m	Intercalated argillite and greywacke	Greywacke
4481	514097.46	5384458.93	Graphitic Argillite/Slate w Fe-carb vein and laminae	dk grey-black, fine-grained bedded to laminated, <5% qtz-py-carb veins; pyrite is abundantly disseminated in veins	215-231.2m	Greywacke	Greywacke
4482	514104.74	5384403.96	Slate	dk grey - black, fine-grained, laminated, < 2% qtz-carb veins (commonly oxidized; py? Or fe-carb (but certainly not typical ankerite))	197-217.5m	Intercalated greywacke and argillite	Greywacke
4483	512770.47	5384656.31	Slate w minor siderite-carb vein	dk grey - black, fine-grained, laminated, < 2% qtz-carb veins (commonly oxidized; py? Or fe-carb (but certainly not typical ankerite))	28-80.5m	Argillite	Sericite altered fragmental ultramafic volcanic
4487	512543.88	5384620.77	Black Argillite w white laminae, strong cleavage	Black to dk brown, 50/50 black and brown mudstone laminae, <2% qtz-carb veins, minor yellow qtz-sericite? Veins (look at ends for grain size, drill imparts notches in brown mudstone; silty	116.9-142.3m	Greywacke	Sericite altered fragmental ultramafic volcanic
4488	512513.42	5384607.68	Black Slate	dk grey - black, fine-grained, laminated with paler brown-grey muddy laminae, < 2% qtz-carb veins (minor oxidation; likely a bit of Fe in the calcite)	143-193.4m	Argillite	Sericite altered fragmental ultramafic volcanic
4489	514787.16	5384498.26	Black Slate	dak grey, fine-grained, laminated, <2% qtz-carb veins	66.4-88.45m	Intercalated argillite and greywacke	Carbonate altered fragmental ultramafic volcanic
4490	475885.27	5368674.52	Graphitic Argillite w 1 cm recrystallized py laminae/bands, strong cleavage	Black/dark grey, fine-grained, laminated, graphitic, <5% pyrite, oxidized pyritic veinlets and minor white carbonate	-		
4491	569712.76	5369099.74	Green Mudstone w pink carb vein	Dark green, fine-grained, laminated, <5% carbonate veins + minor mn-carbonate	-		
4492	568780.74	5368730.96	Green Mudstone	Green/grey, fine-grained, laminated, some silt content likely, but still very fine-grained	-		
4493	571405.32	5369293.18	Black Argillite/Siltstone	Black, fine-grained, laminated, pyritic (1%), trace qtz-carb veinlets	-		
4495	571405.32	5369293.18	Green Mudstone (small sample)	Green-grey, fine-grained, <5% minor fine sand	-		
4496	571405.32	5369293.18	Green Mudstone (small sample)	Green-grey, fine-grained, qtz-silt laminae (10%)	-		
4498	569266.75	5368592.74	Green Mudstone/Siltstone	Green, fine-grained, laminated, slight cleavage, 10% qtz veinlets	-		
4499	570980.79	5369582.72	Silty Mudstone w tr py, silicified	Green, fine-grained, laminated, <1% qtz-carb +/- py veins; py makes up 0.5-1%	-		
4500	570980.79	5369582.72	Dark Green Mudstone	Green, fine-grained (contains silt?) , laminated, trace pyrite, minor qtz +/-graphite? Veinlets	-		
7401	570980.79	5369582.72	Light Grey Mudstone, cherty w py on fractures	Creamy olive green, fine-grained, laminated, minor qtz-carb-py veinlets with 3mm sericite halo around few	-		
7402	570980.79	5368867.71	Green Grey Silty Mudstone w pink carb vein	Green, laminated, fine-grained, 3% carb-qtz-py veins, 2% quartzite? Lenses	-		
7403	570980.79	5368867.71	Dark Grey Silty Mudstone	Green, bedded to laminated, fine-grained, <1% carb-qtz-py veins; some copper staining from drill	-		
7404	570980.79	5368867.71	Light Grey Silty Mudstone w tr py and carb on fractures	Olive green-grey, fine-grained, weakly laminated, 1cm sandstone bed in middle, trace qtz-carb-py	-		
7405	569230.75	5368907.75	Graphitic Argillite breccia w white carb and tr py	Black, fine-grained, graphitic, minor carbonate veins, trace pyrite: **Half sample has 15% carbonate veins, make sure to use other half and save veined sample for reference	-		
7406	569200.00	5369000.00	Black Graphitic Argillite w isolated py nodules	Black, fine-grained, laminated, 0.5-1% boudinaged pyrite nodules, 1% carb-qtz veins	-		
7407	569980.77	5370207.74	Dark Grey Silty Mudstone	Green, fine-grained, thin qtz-carb-py veinlets throughout with chorite? Altered margins; 1-2% py	-		
7408	572180.83	5370407.72	Very Light Grey Silty Mudstone w minor quartz veins	Beige, fine-grained, bedded, 3% disseminated pyrite throughout, trace qtz-carb-py veins	-		
7409	572180.83	5370407.72	Grey Green Silty Mudstone	Green, bedded to laminated, fine-grained, <1% carb-qtz-py veins	box 67		
7410	572496.37	5370942.17	Grey Green Silty Mudstone	Green, fine-grained, laminated, 1% oxidized pyrite stringers, half sample has large sandstone lens; send other half to lab	-		
7411	569436.75	5368730.74	Grey Green Silty Mudstone w tr py	Med. Grey-beige-brown, 15% discontinuous tqz lens/veins with pyrite, py ~1%, weak streaky hematite alteration	-		
7412	569442.75	5368784.74	Green Silty Mudstone/Volcaniclastic w wispy py-carb	Olive green-grey, fine-grained, weakly laminated to bedded, weak to moderately silicified, rare brown silty? Beds, 5-7% massive pyrite veins/veinlets, 2% carb-qtz	-		
7413	569230.75	5368907.75	Black Graphitic Argillite w minor py nodules	Black ,fine-grained, graphitic, laminated, 1% nodular pyrite, 1-2% qtz-carb	-		
07413D	569230.75	5368907.75	Black Graphitic Argillite w minor py nodules	Black ,fine-grained, graphitic, laminated, 1% nodular pyrite, 1-2% qtz-carb	-		
7414	569230.75	5368907.75	Black Graphitic Argillite, strong cleavage	Black ,fine-grained, graphitic, laminated, 1% nodular pyrite, 1-2% qtz-carb	-		
7416	488059.82	5373082.19	Black Graphitic Argillite	Arg band in Gwk; dk grey, vfg, lam, tr py, tr qc str	8.5m	Gwk	Volc
7417	487649.62	5372868.28	Black Graphitic Argillite	Arg band in Gwk; blk-dk grey, vfg, tr py, tr qc str	Unk	Gwk	Gwk
7418	487649.62	5372868.28	Black Graphitic Argillite w tr py	Arg band in Gwk; blk-dk grey, vfg, lam, tr py blebs & str, tr qc	Unk	Gwk	Gwk
7420	488475.59	5373293.65	Grey Argillite	Arg band in Gwk; dk grey, vfg, lam, tr qc	Unk	Gwk	Gwk
7421	487039.66	5372789.51	Dark Grey Argillite w 1/2 cm sericite vein	Arg band in Gwk; dk grey, vfg-fg, lam, tr qc veins/veinlets/str	Unk	Volc	Gwk
7422	492969.07	5378170.00	Black Graphitic Argillite w deformed py nodules	Arg bed in Volc; blk, vfg, lam, py blebs/str/diss mostly along lam, some Fe-carb alt, qc mostly assoc with py	14.9m	Volc	Volc
7423	492969.07	5378170.00	Black Carbonaceous Argillite w deformed py nodules and py-carb laminae	Arg bed in Volc; blk, vfg, f.lam, py str/diss mostly along lam (~1%), qc veinlets/str (~1%)	2.8m	Volc	Volc
7424	492969.07	5378170.00	Black Carbonaceous Argillite w deformed py nodules and py-carb laminae	Arg bed in Volc; blk-dk grey, vfg-fg, lam, py blebs/str/diss (2-3%), qc veinlets/str & assoc with py (~2%)	Unk	Volc	Volc
7425	493062.22	5377591.63	Black Carbonaceous Argillite w deformed py nodules and py-po-carb laminae	blk-dk grey, vfg-fg, lam, py nod/blebs/str/diss (~2%), qc str & assoc with py	15.6m	Volc	Gwk
7427	493062.22	5377591.63	Black Carbonaceous Argillite w deformed py nodules	blk, vfg, lam, py nod/blebs/str/diss (2-3%), tr qc	16.5m	Gwk	Gwk
7428	492984.34	5377725.75	Black Carbonaceous Argillite w deformed py nodules	blk, vfg, lam, py nod/blebs/str (1-2%), qc (~1%)	Unk	Volc	Unk
7429	549855.76	5375594.47	Argillite w pink calcite vein	Interbedded gw & arg; black, fg, lam, qcv	Interbedded, large horizons with variable	Interbedded greywacke and argillite	Interbedded greywacke and argillite
7430	549855.76	5375594.47	Black Argillite w white carb nodules/veins	blk, fg, sil alt, minor qcv	Interbedded, large horizons with variable	Interbedded greywacke and argillite	Interbedded greywacke and argillite
7431	549060.90	5375396.70	Argillite, cherty	vfg, very alt, sil alt, pervasive str	Interbedded, large horizons with variable	Mafic volcanic	Interbedded greywacke and argillite
7432	549512.10	5375921.00	Black Argillite w white carb laminae/vein	blk, vfg, lam, ~5% qcv, sil alt?	Interbedded, large horizons with variable	Mafic volcanic	Interbedded greywacke and argillite

Appendix A3. Sample and field data description / core log entry for N=564 samples of carbonaceous argillite from the Timmins-Kirkland Lake region.

Sample #	Township	Company	Hole #	MNDM #	Sub_Assemb	Assemblage	Contact	Commodity	Ti/Zr_Source_Rock	Host	Analyzed Sample	From_	To	ft_m
7433	Hislop	Brigus Gold	05-BF-409	-	-	Tisdale	Tisdale/Porcupine	Orogenic Au	intermediate	Volcanic/Sediment	Grey Argillite/Siltstone	298.80	299.00	m
7434	Hislop	Brigus Gold	05-BF-400	-	-	Tisdale	Tisdale/Porcupine	Orogenic Au	intermediate	Volcanic/Sediment	Black Graphitic Argillite w white carb-py veins/laminae	185.42	185.69	m
7435	Hoyle	Goldcorp	TV-11-10	-	-	Porcupine	Tisdale/Porcupine	Orogenic Au	mafic	Sediment	Black Argillite w <1 cm py euhedra	86.85	87.13	m
7436	Hoyle	Goldcorp	TV-11-10	-	-	Porcupine	Tisdale/Porcupine	Orogenic Au	intermediate	Sediment	Black Argillite w white carb-py laminae and fractures	167.00	167.20	m
7437	Hoyle	Goldcorp	TV-11-10	-	-	Porcupine	Tisdale/Porcupine	Orogenic Au	intermediate	Sediment	Black Argillite w white carb-py laminae, nodules, fractures	292.29	292.49	m
7438	Hoyle	Goldcorp	TV-11-17	-	-	Tisdale	Tisdale/Porcupine	Orogenic Au	felsic	Volcanic/Sediment	Black Graphitic Argillite w deformed py nodules	134.76	134.93	m
7439	Hoyle	Goldcorp	TV-11-17	-	-	Tisdale	Tisdale/Porcupine	Orogenic Au	felsic	Volcanic/Sediment	Black Graphitic Argillite w isolated py nodules	91.80	92.00	m
7440	Hoyle	Goldcorp	TV-11-17	-	-	Tisdale	Tisdale/Porcupine	Orogenic Au	intermediate	Volcanic/Sediment	Black Graphitic Argillite w 1 cm py nodules, py-carb bands, tr dissem py	41.55	41.78	m
7441	Hoyle	MNDM-T	3	TI1040	-	Porcupine	Tisdale/Porcupine	Orogenic Au	mafic	Sediment	Black Argillite	417.00	418.00	ft
7442	Hoyle	MNDM-T	1	TI1038	-	Porcupine	Tisdale/Porcupine	Orogenic Au	mafic	Sediment	Grey Argillite w siderite vein	337.20	338.00	ft
7443	Carscallen	MNDM-T	BM-3	TI1574	-	Deloro	Deloro/Kidd-Munro	Base Metal	intermediate	Volcanic	Grey Argillite w siderite band	0.00	0.00	ft
7444	Carscallen	MNDM-T	BM-9	TI1580	-	Deloro	Deloro/Kidd-Munro	Base Metal	felsic	Volcanic	Black Argillite w recrystallized py band	96.50	97.00	ft
7445	Carscallen	MNDM-T	BM-1	TI1572	-	Deloro	Deloro/Kidd-Munro	Base Metal	mafic	Volcanic	Black Argillite w grey carb ban, >1 cm py euhedra in band	0.00	0.00	ft
7446	Thornloe	MNDM-T	T-18	TI4125	-	Porcupine	Porcupine/Tisdale	Orogenic Au	intermediate	Sediment	Black Argillite w contorted white lam inae and rare < 1 cm py nodules	0.00	0.00	ft
7447	Thornloe	MNDM-T	T-15	TI4122	-	Porcupine	Porcupine/Tisdale	Orogenic Au	intermediate	Sediment	Dark Grey Argillite w brown siderite veinlets	0.00	0.00	ft
7448	Thornloe	MNDM-T	T-13	TI4120	-	Porcupine	Porcupine/Tisdale	Orogenic Au	intermediate	Sediment	Black Argillite w brown siderite veinlets and tr euhedral py	0.00	0.00	ft
7449	Thornloe	MNDM-T	T-10	TI4119	-	Porcupine	Porcupine/Tisdale	Orogenic Au	intermediate	Sediment	Graphitic Argillite w contorted white bands and dissem py euhedra	297.48	297.70	m
7450	Thornloe	MNDM-T	T-21	TI4127	-	Porcupine	Porcupine/Tisdale	Orogenic Au	intermediate	Sediment	Black Argillite w contorted siderite bands and deformed py nodules/bands	255.14	255.32	m
7451	Thornloe	MNDM-T	T-22	TI4128	-	Porcupine	Porcupine/Tisdale	Orogenic Au	intermediate	Sediment	Dark Grey Argillite w thin controted white laminae	0.00	0.00	ft
7452	Deloro	MNDM-T	DEL82005	TI1050	Lower	Tisdale	Tisdale/Porcupine	Orogenic Au	intermediate	Volcanic/Sediment	Dark Grey Argillite w contorted white and pale brown laminae	0.00	0.00	ft
7453	Deloro	MNDM-T	DEL82003	TI1048	Lower	Tisdale	Tisdale/Porcupine	Orogenic Au	intermediate	Volcanic/Sediment	Argillite w minor white to pale brown carb laminae/bands, strong cleavage	222.05	222.15	m
7454	Deloro	MNDM-T	DEL83005	TI1052	Lower	Tisdale	Tisdale/Porcupine	Orogenic Au	intermediate	Volcanic/Sediment	Black Graphitic Argillite w minor carb-py bands/laminae	793.70	793.94	m
7455	Ogden	MNDM-T	OG-1-1	TI2334	-	Deloro	-	Orogenic Au	felsic	Volcanic/Sediment	Black Argillite w py band (small sample)	0.00	0.00	ft
7456	German	MNDM-T	GE6-3-75	TI2309	-	Porcupine	Porcupine/Kidd-Munro	Orogenic Au	intermediate	Sediment	Black Argillite (small sample)	0.00	0.00	ft
7458	Stock	MNDM-T	ST-81-3	TI0181	-	Kidd-Munro	Kidd-Munro/Porcupine	Orogenic Au	intermediate	Volcanic/Sediment	Black Argillite w minor white laminae	0.00	0.00	ft
7459	Stock	MNDM-T	ST-81-1	TI0179	-	Kidd-Munro	Kidd-Munro/Porcupine	Orogenic Au	intermediate	Volcanic/Sediment	Black Argillite w white and brown carb laminae, minor py	0.00	0.00	ft
7460	Murphy	MNDM-T	045-07-153	TI0173	-	Tisdale	Tisdale/Porcupine	Orogenic Au	felsic	Volcanic/Sediment	Black Argillite w minor white laminae, tr euhedral py	147.51	147.86	m
7461	Shaw	MNDM-T	WS-81-5	TI0327	-	Deloro	Deloro/Tisdale	Base Metal	intermediate	Volcanic	Black Graphitic Argillite w white carb-py laminae	0.00	0.00	ft
7462	Hoyle	MNDM-T	045-04-205	TI0308	-	Porcupine	Tisdale/Porcupine	Orogenic Au	intermediate	Sediment	Black Argillite w minor white carb laminae and spots	200.45	200.60	m
7463	Hoyle	MNDM-T	045-01-213	TI0388	Lower	Tisdale	Tisdale/Porcupine	Orogenic Au	intermediate	Volcanic/Sediment	Grey Mudstone w tr py	46.10	46.25	m
7464	Langmuir	MNDM-T	FR-81-2	TI0382	Lower	Tisdale	-	Base Metal	mafic	Volcanic	Graphitic Argillite	0.00	0.00	ft
7465	Langmuir	MNDM-T	FR-81-3	TI0383	Lower	Tisdale	-	Base Metal	mafic	Volcanic	Graphitic Argillite	0.00	0.00	ft
7466	Langmuir	MNDM-T	FR-81-4	TI0384	Lower	Tisdale	-	Base Metal	intermediate	Volcanic	Graphitic Argillite	0.00	0.00	ft
7467	Ogden	MNDM-T	1043-03-1	TI1976	Lower	Deloro	-	Orogenic Au	intermediate	Volcanic/Sediment	Black Shale, cherty?, strong cleavage	85.43	85.57	m
7468	Cody	MNDM-T	NH-84-1	TI0360	-	Porcupine	Tisdale/Porcupine	Orogenic Au	intermediate	Sediment	Black Mudstone	0.00	0.00	ft
7469	Cody	MNDM-T	NH-84-2	TI0361	Lower	Tisdale	Tisdale/Porcupine	Orogenic Au	felsic	Volcanic/Sediment	Argillite/Shale, strong cleavage	0.00	0.00	ft
7470	Carman	MNDM-T	NH-84-3	TI0362	Lower	Tisdale	Tisdale/Porcupine	Orogenic Au	felsic	Volcanic/Sediment	Black Argillite	37.83	38.00	m
7471	Carman	MNDM-T	NH-84-3	TI0362	Lower	Tisdale	Tisdale/Porcupine	Orogenic Au	felsic	Volcanic/Sediment	Black Graphitic Argillite w pinstripe py and brown carb, strong cleavage	70.54	70.67	m
7472	Cody	MNDM-T	NH-84-4	TI0363	-	Porcupine	Tisdale/Porcupine	Orogenic Au	felsic	Sediment	Black Argillite	53.40	53.55	m
7474	Murphy	MNDM-T	95-1	TI4286	-	Porcupine	-	Orogenic Au	felsic	Sediment	Massive Black Mudstone w tr euhedral py and minor py-carb on fractures	175.20	175.47	m
7475	Murphy	MNDM-T	95-1	TI4286	-	Porcupine	-	Orogenic Au	felsic	Sediment	Massive Black Mudstone w tr py	52.00	52.19	m
7476	Murphy	MNDM-T	95-2	TI4287	-	Porcupine	-	Orogenic Au	intermediate	Sediment	Massive Black Argillite	59.72	59.92	m
7477	Murphy	MNDM-T	95-3	TI4288	-	Porcupine	-	Orogenic Au	intermediate	Sediment	Massive Black Graphitic Argillite w minor py nodules and py-carb laminae	101.51	101.70	m
7478	Murphy	MNDM-T	95-3	TI4288	-	Porcupine	-	Orogenic Au	felsic	Sediment	Massive Black Graphitic Argillite w minor deformed py	78.52	78.70	m
7479	Murphy	MNDM-T	95-4	TI4289	-	Porcupine	-	Orogenic Au	felsic	Sediment	Massive Black Graphitic Argillite w minor deformed py	74.67	74.88	m
7480	Matheson	MNDM-T	79-1	TI3562	-	Porcupine	-	Orogenic Au	felsic	Sediment	Black Argillite w minor thin carb laminae	0.00	0.00	ft
7481	Hoyle	MNDM-T	H12-81	TI3574	Lower	Tisdale	Tisdale/Porcupine	Orogenic Au	felsic	Volcanic/Sediment	Black Graphitic Argillite w isolated 1 cm py nodules	0.00	0.00	ft
7482	Jessop	MNDM-T	TP-83-2	TI0420	Upper	Blake River	Blake River/Porcupine	Orogenic Au	felsic	Volcanic/Sediment	Black Graphitic Argillite w isolated 1 cm py nodules, minor white carb	0.00	0.00	ft
7483	Thornloe	MNDM-T	T-19	TI3581	-	Porcupine	Porcupine/Tisdale	Orogenic Au	intermediate	Sediment	Black Graphitic Argillite w contorted white and brown siderite bands	0.00	0.00	ft
7485	Matheson	MNDM-T	76-1	TI3561	-	Porcupine	-	Orogenic Au	mafic	Sediment	Dark Grey Argillite	0.00	0.00	ft
7486	Whitney	MNDM-T	TN-1-90	TI3489	Lower	Tisdale	Tisdale/Porcupine	Orogenic Au	intermediate	Volcanic/Sediment	Black Argillite w tr dissem py and white spots	33.72	33.80	m
7487	Whitney	MNDM-T	S-2-90	TI3488	-	Deloro	Deloro/Porcupine	Orogenic Au	felsic	Volcanic/Sediment	Black Argillite w tr dissem py	0.00	0.00	ft
7488	Whitney	MNDM-T	M-88-1	TI3587	-	Timiskaming	Timiskaming/Porcupine	Orogenic Au	intermediate	Sediment	Black Argillite	56.55	56.70	m
7489	Whitney	MNDM-T	298-84-5	TI1377	Lower	Tisdale	-	Orogenic Au	intermediate	Volcanic/Sediment	Black Graphitic Argillite w po-py streaks and py-carb clots	0.00	0.00	ft
7490	Tisdale	MNDM-T	297-84-1	TI1371	Lower	Tisdale	Tisdale/Timiskaming/Porcupine	Orogenic Au	felsic	Volcanic/Sediment	Black Graphitic Argillite w deformed py-carb nodules and laminae	0.00	0.00	ft
7491	Whitney	MNDM-T	NM-83-3	TI1364	Lower	Tisdale	Tisdale/Timiskaming	Orogenic Au	intermediate	Volcanic/Sediment	Graphitic Argillite w white carb bands and one py-carb band	0.00	0.00	ft
7492	Mountjoy	MNDM-T	GS-84-1	TI0389	-	Porcupine	-	Orogenic Au	intermediate	Sediment	Argillite	0.00	0.00	ft
7495	Whitney	MNDM-T	OW-17-82	TI1398	Lower	Tisdale	Tisdale/Timiskaming/Porcupine	Orogenic Au	intermediate	Volcanic/Sediment	Argillite w minor white laminae, strong cleavage	0.00	0.00	ft
7496	German	MNDM-T	K-87-9	TI2739	-	Porcupine	Porcupine/Kidd-Munro	Orogenic Au	felsic	Sediment	Black Argillite w minor deformed py-carb nodules	195.15	195.38	m
7498	German	MNDM-T	K-87-6	TI2740	-	Porcupine	Porcupine/Kidd-Munro	Orogenic Au	intermediate	Sediment	Argillite w minor white carb and tr euhedral py on fractures	96.45	96.65	m
7500	German	MNDM-T	K-87-7	TI2741	-	Porcupine	Porcupine/Kidd-Munro	Orogenic Au	intermediate	Sediment	Black Graphitic Argillite	178.50	178.80	m
8501	Jessop	MNDM-T	K2-87-01	TI1332	Upper	Blake River	Blake River/Porcupine	Orogenic Au	felsic	Volcanic/Sediment	Graphitic Argillite w minor white carb laminae and tr py	0.00	0.00	ft
8502	Jessop	MNDM-T	JESS-20-1	TI1543	-	Porcupine	-	Orogenic Au	intermediate	Sediment	Black Graphitic Argillite w py nodules	0.00	0.00	ft
8503	Deloro	MNDM-T	DEL82004	TI1049	Lower	Tisdale	Tisdale/Porcupine	Orogenic Au	intermediate	Volcanic/Sediment	Black Graphitic Argillite w deformed py-carb nodules	109.34	109.48	m

Appendix A3. Sample and field data description / core log entry for N=564 samples of carbonaceous argillite from the Timmins-Kirkland Lake region.

Sample #	Easting_83	Northing_83	Sample Type	Field Description/Core Log Entry	Interval Available	Hanging wall	Footwall
7433	549512.10	5375921.00	Grey Argillite/Siltstone	blk, vfg to fg	Interbedded, large horizons with variable	Mafic volcanic	Interbedded greywacke and argillite
7434	549513.50	5375870.80	Black Graphitic Argillite w white carb-py veins/laminae	blk, vfg, lam, qcv, tr. py, tr. Fe-carb alt	Interbedded, large horizons with variable	Mafic volcanic	Interbedded greywacke and argillite
7435	491087.45	5377382.21	Black Argillite w <1 cm py euhedra	sm (~10cm) to lrg (~1m) fault zones thro-out horizon	10.5m	Gwk	Gwk
7436	491087.45	5377382.21	Black Argillite w white carb-py laminae and fractures	Arg bed in Gwk; blk, vfg, minor qtz veins, minor py lam, int gw & arg?	Unk	Gwk	Gwk
7437	491087.45	5377382.21	Black Argillite w white carb-py laminae, nodules, fractures	blk, vfg, lam, minor qtz veins, tr to minor py lam	7.6m	Gwk	Gwk
7438	490348.28	5377629.71	Black Graphitic Argillite w deformed py nodules	blk, vfg, minor qtz and py; Collared in Arg	>116.8m	OVB	Gwk
7439	490348.28	5377629.71	Black Graphitic Argillite w isolated py nodules	black, vfg, minor qtz and py lam; Collared in Arg	>116.8m	OVB	Gwk
7440	490348.28	5377629.71	Black Graphitic Argillite w 1 cm py nodules, py-carb bands, tr dissem py	blk, vfg, lam, minor py lam & nod, minor qcv; Collared in Arg	>116.8m	OVB	Gwk
7441	489550.00	5377530.00	Black Argillite	Dark grey to black, fg, thinly bedded, pyritic	374-701ft	Argillite	Altered tuff with interflow argillite
7442	489630.00	5377490.00	Grey Argillite w siderite vein	dk grey, slatey, minor qcv & Fe-carb veins; depth is rough estimation (bx8, tag1255)	213-526ft	Tuffaceous fragmental, bedded	Greywacke and argillite
7443	454105.00	5360460.00	Grey Argillite w siderite band	blk, vfg, lam, cubic py, Fe-carb alt (tag1318)	134-213ft	Metasediment	Silicified metasediments
7444	454150.00	5360280.00	Black Argillite w recrystallized py band	blk, vfg, lam, minor silt lam, py lam, minor qcv	95-106ft	Metasediment	Metasediment
7445	454135.00	5360490.00	Black Argillite w grey carb ban, >1 cm py euhedra in band	blk-dk grey, vfg, lam, coarse cubic py, Fe-carb lam	97-191ft	Pyritic gneiss	EOH
7446	460980.00	5355280.00	Black Argillite w contorted white lam inae and rare < 1 cm py nodules	blk, vfg, lam, qcv, minor py lam	236.5-246.2m	Ser-Schist	EOH
7447	460610.00	5355220.00	Dark Grey Argillite w brown siderite veinlets	blk, vfg, minor silt lam, qcv, minor py & Fe-carb	152.6-156.7m	Lithic Arenite	EOH
7448	460610.00	5355220.00	Black Argillite w brown siderite veinlets and tr euhedral py	blk, vfg, lam, py, Fe-carb lam, graph.phyllite?	138.7-154.23m	Conglomerate	EOH
7449	460470.00	5355040.00	Graphitic Argillite w contorted white bands and dissem py euhedra	blk, vfg, lam, py, qcv, Fe-carb	256.3-298.9m	Lithic Arenite	Ser-Schist
7450	461080.00	5355200.00	Black Argillite w contorted siderite bands and deformed py nodules/bands	blk, vfg, lam, py, Fe-carb	229.7-258.2m	Lithic Arenite	Qtz Porphyry
7451	461230.00	5355140.00	Dark Grey Argillite w thin controted white laminae	blk, vfg, lam, minor silt lam, minor qcv, py	191.8-208.9m	Lithic Arenite	Lithic Arenite
7452	476344.00	5364355.00	Dark Grey Argillite w contorted white and pale brown laminae	blk, fg, ~5% qcv, tr py	120-130.1m	Mg Tholeiite	Mg Tholeiite
7453	475973.00	5364510.00	Argillite w minor white to pale brown carb laminae/bands, strong cleavage	blk, fg, lam, ~10% sand lam, Fe-staining	221.9-266.5m	Mg Tholeiite	Mg Tholeiite
7454	476905.00	5364720.00	Black Graphitic Argillite w minor carb-py bands/laminae	blk, vfg, lam, qcv, minor py lam	790.7-793.2m	Iron tholeiite	Basaltic komatite
7455	468665.00	5361250.00	Black Argillite w py band (small sample)	blk, vfg, lam, py (telescoped core)	246.5-257ft	Dacite	Dacite Fragmental
7456	508880.00	5378210.00	Black Argillite (small sample)	blk, vfg, lam (telescoped core)	758.5-790ft	Greywacke & Arg interbeds	Greywacke & Arg interbeds
7458	517075.00	5384250.00	Black Argillite w minor white laminae	blk, fg, py, carb	260.2-289.6ft	Overburden	Siliceous argillite
7459	517190.00	5384130.00	Black Argillite w white and brown carb laminae, minor py		164-729ft	Overburden	Ultramafic breccia/tuff
7460	480430.00	5378720.00	Black Argillite w minor white laminae, tr euhedral py	blk, vfg, lam, minor qcv, py lam & cubes	136.78-168.19m	Felsic volcanic breccia	Carbonatized greywacke
7461	490600.00	5365270.00	Black Graphitic Argillite w white carb-py laminae		16-63ft	Overburden	Ultramafic volcanic?
7462	485915.00	5380440.00	Black Argillite w minor white carb laminae and spots	blk-dk grey, fg, qcv, py lam& cubes	92-204m	Greywacke	EOH
7463	486935.00	5376085.00	Grey Mudstone w tr py	dk grey, Fe-staining, tr py	43.2-117m	Overburden	Greywacke
7464	497530.00	5349220.00	Graphitic Argillite	blk, vfg, Fe-staining, tr py, sharp planar UC	258-259ft	Andesite	Peridotite
7465	499850.00	5349160.00	Graphitic Argillite	blk-dk grey, vfg	246-269ft	Ultramafic volcanic	Basalt
7466	498730.00	5349175.00	Graphitic Argillite	blk, fg	245-246ft	Ultramafic volcanic	Ultramafic volcanic
7467	473650.00	5359990.00	Black Shale, cherty?, strong cleavage	dk grey, shaley (HW-IF; FW-rhy or chem seds?)	85.3-98.3m	Iron formation	Interbedded chert and graphite
7468	497420.00	5369060.00	Black Mudstone	blk, fg, Fe-staining	69.2-72.4m	Interbedded argillite and greywacke	Interbedded argillite and greywacke
7469	496980.00	5366710.00	Argillite/Shale, strong cleavage	blk-grey, py lam, qcv, minor silt lam	64.5-71.7m	Greywacke	Greywacke
7470	496851.00	5366734.00	Black Argillite	blk, vfg, minor carb veinlets	35.1-40m	Argillite breccia	Greywacke/argillite
7471	496851.00	5366734.00	Black Graphitic Argillite w pinstripe py and brown carb, strong cleavage	blk, vfg, lam, minor qcv with Fe-carb, tr to minor py lam	68.1-89m	Argillite breccia	Greywacke/argillite
7472	497810.00	5370430.00	Black Argillite	blk, vfg, finely lam, tr qcv	50.4-63.6m	Green	Tuff argillite
7474	476390.00	5379696.00	Massive Black Mudstone w tr euhedral py and minor py-carb on fractures	dk grey, vfg, minor py lam & nod, qcv	49-200m	OVB	EOH
7475	476390.00	5379696.00	Massive Black Mudstone w tr py	dk grey, vfg, no lam evident, prob bedded mdst, tr py, tr qcv, graph?	49-200m	OVB	EOH
7476	476600.00	5379500.00	Massive Black Argillite	dk grey, fg, tr py, weathered yellow & orange	37.0-88.75m	OVB	Greywacke
7477	476275.00	5379500.00	Massive Black Graphitic Argillite w minor py nodules and py-carb laminae	blk, vfg, lam, qcv, +/-py; bottom of horizon	59.0-104.0m	OVB	Greywacke
7478	476275.00	5379500.00	Massive Black Graphitic Argillite w minor deformed py	blk, vfg, tr py & qcv; middle of horizon; top is a fault	59.0-104.0m	OVB	Greywacke
7479	476275.00	5379250.00	Massive Black Graphitic Argillite w minor deformed py	blk, vfg, lam, minor py, tr qcv; mid-horizon	68.0-92.5m	Mafic Volcanic	Carbonatized Sediment
7480	497175.00	5380940.00	Black Argillite w minor thin carb laminae	blk, vfg, finely lam, minor py lam, minor qcv, discy	1851.5-1955.0ft	Intermediate Volcanics	EOH
7481	487988.00	5376752.00	Black Graphitic Argillite w isolated 1 cm py nodules	blk, vfg, lam, py nod, qcv; mid-horizon	266.35-295.5m	Sediments	Pillowed Mafics
7482	469832.00	5384640.00	Black Graphitic Argillite w isolated 1 cm py nodules, minor white carb	blk, vfg, finely lam, py nod & lam, qcv, minor silt lam	84.43-86.53m	Chert	Chert
7483	460870.00	5355300.00	Black Graphitic Argillite w contorted white and brown siderite	blk, fg, lam, 5-10% ank-qtz-carb, some silt lam, minor py	179.9-193.5m	Ser-Schist	Conglomerate
7485	494645.00	5380960.00	Dark Grey Argillite	blk, vfg to fg, tr fine sand lam, tr qcv & py; interbedded sandst & arg sequence	263-271ft	Greywacke	Intermediate Volcanics
7486	493544.00	5373000.00	Black Argillite w tr dissem py and white spots	blk, fg, minor py nod mostly alt to Fe-carb, minor qcv	19.66-40.5m	Greywacke	Greywacke
7487	493137.00	5369254.00	Black Argillite w tr dissem py	blk, fg, lam, qcv, minor silt lam	60.4-61.6m	Dacite	Andesite
7488	503625.00	5376410.00	Black Argillite	blk, vfg, finely lam, tr py & qcv	52-67m	Greywacke	Conglomerate
7489	486670.00	5373695.00	Black Graphitic Argillite w po-py streaks and py-carb clots	blk, vfg, lam, po diss & lam (3-5%), minor qcv	655.7-674.2ft	Basalt	Basalt
7490	481820.00	5373370.00	Black Graphitic Argillite w deformed py-carb nodules and laminae	blk, vfg, py lam & nod (~3-5%), minor qcv	311-396.5ft	Pillow basalt	Lithic wacke
7491	488360.00	5373755.00	Graphitic Argillite w white carb bands and one py-carb band	blk, vfg, lam, minor qcv, minor po nod, py lam	687-691.8ft	Basaltic andesite	Andesite to dacite
7492	471960.00	5373305.00	Argillite	interbedded GW & ARG sequence; black-dk grey, massive	50-306ft	Overburden	EOH
7495	491835.00	5373400.00	Argillite w minor white laminae, strong cleavage	interbedded GW & ARG sequence; dk grey, vfg, lam, minor recessive Fe-carb str, tr qtz str, tr py	800-831ft	Sediments	EOH
7496	505800.00	5385330.00	Black Argillite w minor deformed py-carb nodules	blk, vfg, lam, minor py nod & lam, minor qcv	192.1-232.5ft	UM	EOH
7498	506010.00	5385130.00	Argillite w minor white carb and tr euhedral py on fractures	Interbedded GW & ARG sequence; blk, vfg, lam, tr py along fractures	68.8-233.4ft	OVB	EOH
7500	505990.00	5385250.00	Black Graphitic Argillite	blk, vfg, lam, qcv (~2%), tr py	156.6-215.2ft	Altered UM	EOH
8501	466810.00	5376410.00	Graphitic Argillite w minor white carb laminae and tr py	Interbedded GW & ARG sequence; blk, vfg, lam, minor silt lam	394.5-438ft	Felsic crystal tuff	EOH
8502	474520.00	5384050.00	Black Graphitic Argillite w py nodules	blk, vfg, minor py nod mostly weathered/altered, qcv	117.1-118.6m	Andesite tuff	Andesite tuff
8503	476090.00	5364870.00	Black Graphitic Argillite w deformed py-carb nodules	blk, vfg, lam, some silt lam, ~10% py, qcv, minor fault below & larger one above	108-111.9m	Iron tholeiite	Iron tholeiite

Appendix A3. Sample and field data description / core log entry for N=564 samples of carbonaceous argillite from the Timmins-Kirkland Lake region.

Sample #	Township	Company	Hole #	MNDM #	Sub_Assemb	Assemblage	Contact	Commodity	Ti/Zr_Source_Rock	Host	Analyzed Sample	From_	To	ft_m
8504	Ogden	MNDM-T	026-29-2	TI0034	Lower	Tisdale	Tisdale/Porcupine	Orogenic Au	intermediate	Volcanic/Sediment	Black Graphitic Argillite w deformed py-carb nodules	0.00	0.00	ft
8505	Carscallen	MNDM-T	BM-2	TI1573	-	Deloro	Deloro/Kidd-Munro	Base Metal	intermediate	Volcanic	Black Graphitic Argillite w carb vein and single large py euhedra, strong cleavage	0.00	0.00	ft
8506	Thomas	MNDM-T	TH-83-1	TI1585	Lower	Tisdale	-	Base Metal	intermediate	Volcanic	Black Graphitic Argillite w isolated row of coalesced 1 cm py nodules	0.00	0.00	ft
8507	Hoyle	MNDM-T	H12-49	TI3572	Lower	Porcupine	Tisdale/Porcupine	Orogenic Au	intermediate	Sediment	Black Graphitic Argillite	104.65	104.80	m
8508	Whitney	MNDM-T	297-84-3	TI1481	Lower	Tisdale	-	Orogenic Au	intermediate	Volcanic/Sediment	Black Argillite w white fractures and tr po-py clots	784.60	784.71	m
8509	Dundonald	Xstrata	DUN25-20	-	Lower	Kidd-Munro	-	Base Metal	felsic	Volcanic	Black Graphitic Argillite w < 1 cm po nodules and bands	193.08	193.28	m
8510	Dundonald	Xstrata	DUN25-22	-	Lower	Kidd-Munro	-	Base Metal	felsic	Volcanic	Black Graphitic Argillite	149.26	149.34	m
8511	Dundonald	Xstrata	DUN25-22	-	Lower	Kidd-Munro	-	Base Metal	intermediate	Volcanic	Black Graphitic Argillite w <1 cm py nodules and bands (green oxide)	88.66	88.82	m
8512	Dundonald	Xstrata	DUN25-18	-	Lower	Kidd-Munro	-	Base Metal	intermediate	Volcanic	Black Graphitic Argillite w isolated py nodules	0.00	0.00	ft
8513	Dundonald	Xstrata	DUN25-18	-	Lower	Kidd-Munro	-	Base Metal	felsic	Volcanic	Black Graphitic Argillite w 1 cm py bands and nodules (green oxide)	304.94	305.09	m
8514	Dundonald	Xstrata	DUN25-08	-	Lower	Kidd-Munro	-	Base Metal	felsic	Volcanic	Black Graphitic Argillite w py-po-carb-biotite on fractures (green oxide)	98.55	98.70	m
8515	Dundonald	Xstrata	DUN25-15	-	Lower	Kidd-Munro	-	Base Metal	felsic	Volcanic	Black Graphitic Argillite (green oxide on fracture)	0.00	0.00	ft
8516	Dundonald	Xstrata	DUN25-15	-	Lower	Kidd-Munro	-	Base Metal	felsic	Volcanic	Black Graphitic Argillite w isolated 0.5-1 cm py-po nodules	228.50	228.70	m
8517	Dundonald	Xstrata	DUN25-24	-	Lower	Kidd-Munro	-	Base Metal	felsic	Volcanic	Black Graphitic Argillite w isolated py-po nodule, white carb on fractures (green oxide)	43.70	43.90	m
8518	Dundonald	Xstrata	DUN89-06	-	-	Kidd-Munro	-	Base Metal	felsic	Volcanic	Black Graphitic Argillite w <1 cm py nodules	604.18	604.41	m
8519	Thornloe	Lake Shore Gold	TH-11-81	-	-	Porcupine	Porcupine/Tisdale	Orogenic Au	intermediate	Sediment	Black Argillite w minor white laminae and tr py	272.24	272.38	m
8520	Thornloe	Lake Shore Gold	TH-11-74	-	-	Porcupine	Porcupine/Tisdale	Orogenic Au	intermediate	Sediment	Grey Black Silty Mudstone w white laminae	423.00	423.06	m
8521	Thornloe	Lake Shore Gold	TH-10-60	-	-	Porcupine	Porcupine/Tisdale	Orogenic Au	intermediate	Sediment	Black Argillite w minor white laminae	219.34	219.46	m
8522	Thornloe	Lake Shore Gold	TH-10-58	-	-	Porcupine	Porcupine/Tisdale	Orogenic Au	intermediate	Sediment	Graphitic Argillite w minor white laminae	185.10	185.26	m
8523	Thornloe	Lake Shore Gold	TH-10-53	-	-	Porcupine	Porcupine/Tisdale	Orogenic Au	intermediate	Sediment	Graphitic Argillite w minor white lamniae and tr euhedral py	597.88	598.12	m
8524	Thornloe	Lake Shore Gold	TH-10-29	-	-	Porcupine	Porcupine/Tisdale	Orogenic Au	intermediate	Sediment	Graphitic Argillite w minor white lamniae and tr euhedral py	44.10	44.30	m
8525	Thornloe	Lake Shore Gold	TH-10-24	-	-	Porcupine	Porcupine/Tisdale	Orogenic Au	intermediate	Sediment	Graphitic Argillite w brown carb laminae and minor py	129.34	129.49	m
8526	Thornloe	Lake Shore Gold	TH-10-55	-	-	Porcupine	Porcupine/Tisdale	Orogenic Au	intermediate	Sediment	Black Graphitic Argillite w minor grey laminae and minor py	333.12	333.80	m
8527	Thornloe	Lake Shore Gold	TH-10-52	-	-	Porcupine	Porcupine/Tisdale	Orogenic Au	intermediate	Sediment	Graphitic Argillite w tr py	153.01	153.09	m
8528	Thornloe	Lake Shore Gold	TH-10-50	-	-	Porcupine	Porcupine/Tisdale	Orogenic Au	intermediate	Sediment	Black Graphitic Argillite	211.80	211.88	m
8529	Thornloe	Lake Shore Gold	TH-10-69	-	-	Porcupine	Porcupine/Tisdale	Orogenic Au	intermediate	Sediment	Black Mudston/Argillite	221.27	221.39	m
8530	Thornloe	Lake Shore Gold	TH-10-65A	-	-	Porcupine	Porcupine/Tisdale	Orogenic Au	intermediate	Sediment	Black Argillite w minor white carb vein and tr euhedral py	542.58	542.74	m
8531	Thornloe	Lake Shore Gold	TH-10-26C	-	-	Porcupine	Porcupine/Tisdale	Orogenic Au	felsic	Sediment	Black Graphitic Argillite w contorted white carb laminae, minor euhedral py	652.00	652.20	m
8532	Thornloe	Lake Shore Gold	TH-10-70	-	-	Porcupine	Porcupine/Tisdale	Orogenic Au	intermediate	Sediment	Dark Grey Argillite	86.18	86.33	m
8533	Thornloe	Lake Shore Gold	TH-11-75	-	-	Porcupine	Porcupine/Tisdale	Orogenic Au	intermediate	Sediment	Dark Grey Argillite w dissem euhedral py and white carb bands	624.10	624.30	m
8534	Hoyle	Lake Shore Gold	BC-10-92	-	Lower	Tisdale	Tisdale/Porcupine	Orogenic Au	felsic	Volcanic/Sediment	Graphitic Argillite w minor <1 cm py nodules and white carb clots	1855.97	1856.10	m
8535	Hoyle	Lake Shore Gold	BC-11-97	-	Lower	Tisdale	Tisdale/Porcupine	Orogenic Au	intermediate	Volcanic/Sediment	Graphitic Argillite w streaky to diffuse py bands, strong cleavage	769.86	770.00	m
8536	Thornloe	Lake Shore Gold	TH-10-18	-	-	Porcupine	Porcupine/Tisdale	Orogenic Au	intermediate	Sediment	Dark Grey Argillite	195.07	195.15	m
8537	Thornloe	Lake Shore Gold	TH-10-12	-	-	Porcupine	Porcupine/Tisdale	Orogenic Au	intermediate	Sediment	Graphitic Argillite w contorted Fe-carb vein	153.70	153.93	m
8538	Bristol	Lake Shore Gold	TG-06-96	-	Lower	Tisdale	Tisdale/Porcupine	Orogenic Au	intermediate	Volcanic/Sediment	Graphitic Argillite w contorted white bands up to 1 cm, minor py	944.54	944.70	m
8539	Bristol	Lake Shore Gold	TG-05-69	-	-	Porcupine	Tisdale/Porcupine	Orogenic Au	intermediate	Volcanic/Sediment	Graphitic Argillite w thin white carb laminae	128.88	128.98	m
8540	Dundonald	First Nickel	AV-07-04	-	-	Kidd-Munro	-	Base Metal	intermediate	Volcanic	Black Graphitic Argillite w isolated 1 cm py nodules	329.28	329.82	m
8541	Dundonald	First Nickel	FNS-04-18	-	-	Kidd-Munro	-	Base Metal	felsic	Volcanic	Black Graphitic Argillite w isolated 1 cm py nodules	173.64	174.09	m
8542	Dundonald	First Nickel	FNS-04-16	-	Lower	Kidd-Munro	-	Base Metal	intermediate	Volcanic	Black Graphitic Argillite w semimassive py-po nodules	39.15	39.27	m
8543	Dundonald	First Nickel	FNS-04-12	-	Lower	Kidd-Munro	-	Base Metal	intermediate	Volcanic	Black Graphitic Argillite w coalesced po? nodules w altered rims	172.08	172.45	m
8544	Dundonald	First Nickel	FNS-04-11	-	Lower	Kidd-Munro	-	Base Metal	felsic	Volcanic	Black Graphitic Argillite w minor po? nodules w altered rims	134.10	134.30	m
8545	Dundonald	First Nickel	FND-05-50	-	-	Kidd-Munro	-	Base Metal	felsic	Volcanic	Black Graphitic Argillite w coalesced py nodules	125.11	125.36	m
8546	Dundonald	First Nickel	FND-05-46	-	-	Kidd-Munro	-	Base Metal	felsic	Volcanic	Black Graphitic Argillite w contorted white carb vein, tr py	58.00	58.20	m
8547	Dundonald	First Nickel	FND-04-31	-	-	Kidd-Munro	-	Base Metal	felsic	Volcanic	Black Graphitic Argillite w coalesced py nodules (hard)	261.92	262.17	m
8548	Dundonald	First Nickel	FND-04-31	-	-	Kidd-Munro	-	Base Metal	felsic	Volcanic	Black Graphitic Argillite w coalesced py nodules (hard)	286.76	287.00	m
8549	Dundonald	First Nickel	FND-04-26	-	-	Kidd-Munro	-	Base Metal	felsic	Volcanic	Black Graphitic Argillite w coalesced py nodules (hard)	42.44	42.64	m
8550	Dundonald	First Nickel	FND-04-11	-	-	Kidd-Munro	-	Base Metal	felsic	Volcanic	Black Graphitic Argillite w minor py nodules, weakly sheared	129.00	129.20	m
8551	Dundonald	First Nickel	FND-04-08	-	-	Kidd-Munro	-	Base Metal	felsic	Volcanic	Black Graphitic Argillite w py nodules and stringer py (hard)	88.34	88.56	m
8552	Dundonald	First Nickel	FND-04-09	-	-	Kidd-Munro	-	Base Metal	felsic	Volcanic	Black Graphitic Argillite w py nodules	113.93	114.15	m
8553	Dundonald	First Nickel	FNT-04-01	-	-	Kidd-Munro	-	Base Metal	intermediate	Volcanic	Black Graphitic Argillite w small dissem py nodules	180.39	180.70	m
8554	Dundonald	First Nickel	FNS-05-98	-	-	Kidd-Munro	-	Base Metal	felsic	Volcanic	Black Graphitic Argillite w small dissem py nodules (one 1 cm nodule included)	180.80	181.02	m
8555	Nesbitt	Xstrata	NES44-01	-	-	Deloro	-	Base Metal	felsic	Volcanic	Dark Grey Argillite w diffuse grey white laminae	186.96	187.07	m
8556	Nesbitt	Xstrata	NES16-03	-	-	Deloro	-	Base Metal	intermediate	Volcanic	Dark Grey Argillite w diffuse grey white laminae	142.30	142.42	m
8557	Nesbitt	Xstrata	NES16-04	-	Upper	Blake River	-	Base Metal	intermediate	Volcanic	Dark Grey Argillite w diffuse grey white laminae, tr py in laminae	144.50	144.56	m
8558	Nesbitt	Xstrata	NES35-04	-	-	Deloro	-	Base Metal	felsic	Volcanic	Black Argillite w regularly spaced py-po bands (2-3 mm), minor white laminae	139.37	139.57	m

Appendix A3. Sample and field data description / core log entry for N=564 samples of carbonaceous argillite from the Timmins-Kirkland Lake region.

Sample #	Easting_83	Northing_83	Sample Type	Field Description/Core Log Entry	Interval Available	Hanging wall	Footwall
8504	474290.00	5364410.00	Black Graphitic Argillite w deformed py-carb nodules	blk, vfg, lam, py nod & lam (2-3%), qcv (5%)	ministry erroro	Greywacke	Greywacke
8505	454135.00	5360490.00	Black Graphitic Argillite w carb vein and single large py euhedra, strong cleavage	blk-dk grey, lam, minor qcv & py	154-188ft	Pyritic shale	Greywacke
8506	513230.00	5365375.00	Black Graphitic Argillite w isolated row of coalesced 1 cm py	blk, vfg, no lam evident, py nod from mm's to few cm's, tr qcv	1119.1-1146.1ft	Felsic tuff	Felsic tuff
8507	487534.00	5376876.00	Black Graphitic Argillite	blk, vfg, very weathered/altered, py nod remnants, tr Fe-card & py	82.75-109.20m	Sediments	Altered Mafic
8508	485260.00	5374025.00	Black Argillite w white fractures and tr po-py clots	blk, vfg, lam, po lam & nod (~2%), qcv (~2%), tr py	783.6-788.5ft	Exhalite? and pillow lava	Mafic volcanic?
8509	512144.29	5388060.72	Black Graphitic Argillite w < 1 cm po nodules and bands	blk, vfg, py nod (1-2%), po vein, carb wisps? (~1m horizon with fault (gr core) above (30cm) & below (1m))	192.59-196.62	Ultramafic volcanic	Ultramafic volcanic
8510	512224.09	5388052.32	Black Graphitic Argillite	blk, vfg, tr diss & nod py, oxidized on surface, sm faults (gr core) above & below	not logged as arg	Ultramafic	Ultramafic volcanic
8511	512224.09	5388052.32	Black Graphitic Argillite w <1 cm py nodules and bands (green oxide)	blk, vfg, lam, py nod (1-2%), tr po, fairly lrg fault (gr core) above	not logged as arg	Ultramafic	Ultramafic volcanic
8512	511316.09	5387724.15	Black Graphitic Argillite w isolated py nodules	blk, vfg, nod py, qcv (approx middle of 1m horizon)	403.38-404.45m	Ultramafic	Ultramafic volcanic
8513	511316.09	5387724.15	Black Graphitic Argillite w 1 cm py bands and nodules (green	blk, vfg, py nod (~2%), qcv	303.41-306.12m	Ultramafic	Ultramafic volcanic
8514	511965.19	5387966.73	Black Graphitic Argillite w py-po-carb-biotite on fractures (green oxide)	blk, vfg, py nod (mostly oxidized), qcv	96.18-99.25m	Ultramafic	Ultramafic volcanic
8515	512134.29	5388061.23	Black Graphitic Argillite (green oxide on fracture)	blk, vfg, qcv, py (interflow seds?)	not logged as arg	Ultramafic	Ultramafic volcanic
8516	512134.29	5388061.23	Black Graphitic Argillite w isolated 0.5-1 cm py-po nodules	blk, vfg, no lam evident, po nod (~2-3%), qcv (~3-5%), very competent	226.47-229.47m	Ultramafic	Ultramafic volcanic
8517	512200.19	5387911.32	Black Graphitic Argillite w isolated py-po nodule, white carb on fractures (green oxide)	blk, vfg, no lam evident, alt py nod, ~15% veins (weathered/altered/oxidized) w/ chrysotile along edges of veins	42.95-52.44m	Ultramafic	Ultramafic volcanic
8518	511649.18	5386251.32	Black Graphitic Argillite w <1 cm py nodules	blk, vfg, no lam evident, py nod (2-3%), qcv (~1%)		Ultramafic	Ultramafic volcanic
8519	462080.00	5355150.00	Black Argillite w minor white laminae and tr py	blk, fg-vfg, laminated, quartz-carb vein (qcv), trace pyrite, some silty laminae	271.6-273.6m	Greywacke	Greywacke
8520	462040.00	5355205.00	Grey Black Silty Mudstone w white laminae	blk-dk-grey, fg-vfg, foliated, minor qcv, trace pyrite	415.3-428.0m	Wacke	EOH
8521	460700.00	5355600.00	Black Argillite w minor white laminae	blk, vfg, qcv (~1%), graphitic foliation throughout	218.85-225.0m	Qtz-Sericite Schist	EOH
8522	460680.00	5355600.00	Graphitic Argillite w minor white laminae	blk, vfg, laminated, py (<1%), qcv (~3%)	182.9-200.2m	Wacke	Siltstone
8523	461700.00	5355605.00	Graphitic Argillite w minor white lamniae and tr euhedral py	blk, vfg, laminatede, py (<1%), qcv (1-2%)	594.9-604.0m	Siltstone	Siltstone
8524	460920.00	5355400.00	Graphitic Argillite w minor white lamniae and tr euhedral py	blk-dk grey, fg-vfg, qcv (3-5%), py (1%)	38.0-67.95m	Overburden	Pelite/Mudstone
8525	460950.00	5355475.00	Graphitic Argillite w brown carb laminae and minor py	blk, vfg-fg, laminated, qcv (3%), py (<1%)	126.5-149.5m	Pelite/Mudstone	Pelite/Mudstone
8526	460980.00	5355600.00	Black Graphitic Argillite w minor grey laminae and minor py	blk, vfg, laminated, trace py - disseminated +vein/lam, qcv (1-2%)	332.0-342.0m	Siltstone	Siltstone
8527	461720.00	5355250.00	Graphitic Argillite w tr py	blk-dk grey, laminated, fg-vfg, some silt laminae, trace qcv + py	141.8-158.7m	Siltstone	Altered Siltstone
8528	460880.00	5355550.00	Black Graphitic Argillite	blk, vfg, laminated, qcv (1%), trace pyrite	192.0-243.0m	Wacke	Greywacke/Argillite
8529	459100.00	5355800.00	Black Mudston/Argillite	blk, vfg, trace py +qcv, 40cm above large brittle fault, undistrubed	189.0-226.0m	Wacke	Altered Sediments
8530	461517.00	5355605.00	Black Argillite w minor white carb vein and tr euhedral py	blk, vfg, laminated, py (<1%), qcv (~1-2%), minor graphite	535.4-546.0m	Wacke	Wacke
8531	461467.00	5355605.00	Black Graphitic Argillite w contorted white carb laminae, minor euhedral py	blk, vfg, laminated + foliated, qcv (3-5%), py (1%)	645.1-660.2m	Wacke	Wacke
8532	458880.00	5355436.00	Dark Grey Argillite	blk, vfg-fg, laminated, trace qcv + py, minor graphite and silt laminae	75.2-89.8m	Qtz-Sericite Schist	Altered Sediments
8533	461600.00	5355600.00	Dark Grey Argillite w dissem euhedral py and white carb bands	vfg-fg, py (3-5%), trace qcv, graphitic foliation	581.0-634.2m	Altered Sediments	Altered Sediments
8534	487523.48	5376527.09	Graphitic Argillite w minor <1 cm py nodules and white carb clots	blk, vfg, laminated, sm. Nodular pyrite, trace qcv	1839.8-1880.1m	Interbedded greywacke and argillite + altered mafic volcanics	Pillowed mafic volcanic
8535	486389.00	5377728.00	Graphitic Argillite w streaky to diffuse py bands, strong cleavage	blk, vfg, laminated, nodular pyrite + py laminae/veins, 1% qcv	753-793m	Interbedded greywacke and argillite + altered mafic volcanics	Mafic volcanic breccia
8536	459340.00	5355658.00	Dark Grey Argillite	blk-dk grey, fg, gradation from silty mud to mud grain size	180.0-216.9m	Pelite/Mudstone	Lithic Greywacke
8537	459541.00	5355622.00	Graphitic Argillite w contorted Fe-carb vein	blk-dk grey, fg,mud + silt laminae, py, qcv	139.10-159.45m	Int. GW & ARG w/ veining	Altered Sediments
8538	458719.00	5360030.59	Graphitic Argillite w contorted white bands up to 1 cm, minor py	blk-dk grey, mostly mud + moderate silt, lam/bedded, py blebs along silt (1%) tr qcv	942.9-947.4m	Silificified Debris Flow	Silicified Debris Flow
8539	460270.76	5360542.18	Graphitic Argillite w thin white carb laminae	dk grey, laminated, vfg-fg, 1% qcv	122.4-132.6m	Felsic Quartz Feldspar Porphyry Dyke	Greywacke
8540	511700.00	5386304.00	Black Graphitic Argillite w isolated 1 cm py nodules	blk, vfg, coarse po nod (1%), qcv, weathered, grey alt; sm horizon in UMs - interflow seds?		Komatiite Mesocumulate Peridotite Flow	EOH
8541	511772.00	5386376.00	Black Graphitic Argillite w isolated 1 cm py nodules	blk, vfg, coarse py nod (~3%), minor 'wispy' qcv			
8542	512023.00	5386364.00	Black Graphitic Argillite w semimassive py-po nodules	blk, vfg, weathered, ~25% py +/- po (~2%) coarse to fine nod, etc.; mostly massive py in argillite	38.4-42.3m		
8543	512072.00	5386354.00	Black Graphitic Argillite w coalesced po? nodules w altered rims	blk, vfg, coarse po nod & po str, nod rimmed with something?, graph fractures; sm horizon - interflow seds?	-		
8544	512072.00	5386355.00	Black Graphitic Argillite w minor po? nodules w altered rims	blk, vfg, po nod (>1%), tr qcv, serp veins, graph, massive fault above 134m	-		
8545	511600.00	5386546.00	Black Graphitic Argillite w coalesced py nodules	blk, vfg, py nod & veins (~3%), chyrsotile wisps/veinlets/along py edges, tr qc str, graph?	-		
8546	511652.00	5386592.00	Black Graphitic Argillite w contorted white carb vein, tr py	blk, vfg, tr diss po in qcv & discont po str	-		
8547	511516.00	5386481.00	Black Graphitic Argillite w coalesced py nodules (hard)	blk, vfg, coarse py nod (1-2%), qcv	-		
8548	511516.00	5386481.00	Black Graphitic Argillite w coalesced py nodules (hard)	blk, vfg, po nod (~1%), tr qcv	-		
8549	511371.00	5386618.00	Black Graphitic Argillite w coalesced py nodules (hard)	blk, vfg, coarse po nod (1%) +/- py veins cross-cutting po nod	-		
8550	511462.00	5386540.00	Black Graphitic Argillite w minor py nodules, weakly sheared	blk, vfg, py nod (~1%), chyrsotile, qcv	-		
8551	511486.00	5386537.00	Black Graphitic Argillite w py nodules and stringer py (hard)	blk, vfg, massive, coarse po nod + veins (2%), qcv, chyrsotile	-		
8552	511486.00	5386536.00	Black Graphitic Argillite w py nodules	blk, vfg, coarse po nod, some with py rims, finely lam, graph?	-		
8553	511524.00	5386578.00	Black Graphitic Argillite w small dissem py nodules	blk, vfg, coarse py nod (2%)	-		
8554	511782.00	5386323.00	Black Graphitic Argillite w small dissem py nodules (one 1 cm nodule included)	blk, vfg, coarse po nod w/ py rims, po str, tr qcv	-		
8555	471609.09	5419527.89	Dark Grey Argillite w diffuse grey white laminae	blk, fg, lam, po str/lam/blebs (2-3%), qc str cutting lam, qc along lam	185.11-187.12m	1m Felsic tuff below large heterolithic lapilli tuff	Heterolithic lapilli tuff
8556	474506.06	5416326.93	Dark Grey Argillite w diffuse grey white laminae	dk grey, fg, 3 cm mud? bed In lrg sandstone sequence	142.3-142.42m	Mixed (Mafic, Intermediate, felsic) fragmental	Mixed (Mafic, Intermediate, felsic) fragmental
8557	474964.04	5415745.77	Dark Grey Argillite w diffuse grey white laminae, tr py in laminae	blk, fg, lam, qtz str/veinlets (>10%), py blebs & str (1-2%); dirty mud? Bed in fg sandstone	144.5-149.5m	Pillowed Mafic volcanic	Mafic volcanic
8558	472220.79	5418860.33	Black Argillite w regularly spaced py-po bands (2-3 mm), minor white laminae	blk, vfg, lam/bed, po blebs/veinlets along lam + diss (3-4%), qc veinlets assoc with po	138.7-140.63m	Carbonaceous felsic to intermediate tuff	Carbonaceous felsic to intermediate tuff

Appendix A3. Sample and field data description / core log entry for N=564 samples of carbonaceous argillite from the Timmins-Kirkland Lake region.

Sample #	Township	Company	Hole #	MNDM #	Sub_Assemb	Assemblage	Contact	Commodity	Ti/Zr_Source_Rock	Host	Analyzed Sample	From_	To	ft_m
8559	Lucas	Xstrata	LUC61-01	-	-	Deloro	-	Base Metal	felsic	Volcanic	Black Graphitic Argillite w minor discontinuous py-carb bands	225.15	225.47	m
8560	Ottaway	Xstrata	OTT31-03	-	Upper	Kidd-Munro	Kidd-Munro/Porcupine	Base Metal	felsic	Volcanic	Black Argillite	165.05	165.35	m
8561	Ottaway	Xstrata	OTT31-01	-	-	Deloro	-	Base Metal	intermediate	Volcanic	Black Argillite w tr py on fractures and minor py streaks, strong cleavage	118.52	118.74	m
8562	Lennox	Xstrata	LEN64-02	-	-	Deloro	-	Base Metal	intermediate	Volcanic	Black Graphitic Argillite w dissem py and deformed carb? clots	176.00	176.15	m
8563	Reaume	Xstrata	REA24-01	-	Upper	Stoughton-Roquemare	-	Orogenic Au	intermediate	Volcanic/Sediment	Black Graphitic Argillite w py nodules and laminae	61.31	61.58	m
8564	Tisdale/Dome	Goldcorp	Dome1	-	Lower	Tisdale	Tisdale/Porcupine	Orogenic Au	mafic	Volcanic/Sediment	Black Graphitic Argillite w minor qtz and dissem py euhedra, strongly deformed	491.05	0.00	m
8565	Tisdale/Dome	Goldcorp	Dome2	-	Lower	Tisdale	Tisdale/Porcupine	Orogenic Au	intermediate	Volcanic/Sediment	Argillite	491.96	0.00	m
8566	Tisdale/Dome	Goldcorp	Dome3	-	-	Tisdale	Tisdale/Porcupine	Orogenic Au	mafic	Volcanic/Sediment	Argillite	471.54	0.00	m
8567	Mann	Xstrata	MAN43-03	-	-	Tisdale	-	Base Metal	felsic	Volcanic	Black Argillite w grey silty bands and fine dissem py	50.80	50.97	m
8568	Geary	Xstrata	GY31-04	-	Upper	Blake River	-	Base Metal	felsic	Volcanic	Shale/Argillite	147.60	147.85	m
8569	Godfrey	Xstrata	G33-15	-	Upper	Blake River	-	Base Metal	felsic	Volcanic	Argillite w minor white laminae, isolated carb spots, and coalesced py	75.30	75.60	m
8570	Calvert	Xstrata	CAL63-01	-	-	Stoughton-Roquemare	-	Base Metal	mafic	Volcanic	Argillite w minor white laminae	41.37	41.57	m
8571	Jessop	Xstrata	JS51-01	-	Upper	Blake River	-	Base Metal	intermediate	Volcanic	Black Argillite w isolated py euhedra (3 mm)	151.68	152.00	m
8572	Jessop	Xstrata	JS44-01	-	Upper	Blake River	Blake River/Porcupine	Base Metal	felsic	Volcanic/Sediment	Black Argillite w thin white carb laminae , minor py nodules	151.00	151.35	m
8573	Lucas	Xstrata	LU41-05	-	-	Deloro	-	Base Metal	felsic	Volcanic	Black Argillite w minor white laminae and minor py nod	257.77	258.03	m
8574	Munro	Xstrata	MUN62-01	-	Lower	Kidd-Munro	-	Base Metal	intermediate	Volcanic	Black Argillite w 0.5-1 cm py nodules and minor white carb	103.20	103.48	m
08574D	Munro	Xstrata	MUN62-01	-	Lower	Kidd-Munro	-	Base Metal	intermediate	Volcanic	Black Argillite w 0.5-1 cm py nodules and minor white carb	103.20	103.48	m
8575	Walker	Xstrata	WA55-01	-	Lower	Kidd-Munro	Kidd-Munro/Porcupine	Base Metal	felsic	Volcanic	Black Argillite w volcaniclastic component, dissem py and py nodules	92.85	92.97	m
8576	Wilkie	Xstrata	WI21-14	-	Lower	Kidd-Munro	-	Base Metal	felsic	Volcanic	Black Argillite w abundant white carb bands and py nodules	179.58	179.70	m
8577	Wilkie	Xstrata	WI23-02	-	Lower	Kidd-Munro	-	Base Metal	felsic	Volcanic	Black Argillite w recrystallized py bands	263.85	264.00	m
8578	Whitney	Xstrata	WH66-37	-	-	Tisdale	Tisdale/Timiskaming	Orogenic Au	intermediate	Volcanic/Sediment	Black Argillite/Mudstone w few round py nodules	121.15	121.30	m
8579	Whitney	Xstrata	WH66-15	-	Lower	Tisdale	Tisdale/Porcupine	Orogenic Au	intermediate	Volcanic/Sediment	Black Argillite w strong cleav, tr py	776.19	776.42	m
8580	Whitney	Xstrata	WH66-20	-	-	Tisdale	Tisdale/Timiskaming	Orogenic Au	intermediate	Volcanic/Sediment	Argillite	30.68	30.80	m
8581	Jessop	Xstrata	JS12-06	-	Upper	Blake River	-	Base Metal	intermediate	Volcanic	Black Argillite w recrystallized py laminae	256.58	256.74	m
8582	Jessop	Xstrata	JS12-04	-	Upper	Blake River	-	Base Metal	felsic	Volcanic	Black Argillite	168.10	168.30	m
8583	Jessop	Xstrata	JS23-01	-	Upper	Blake River	-	Base Metal	felsic	Volcanic	Black Argillite w white carb-qtz laminae, t py nodules	106.20	106.41	m
8584	Jessop	Xstrata	JS12-05	-	-	Blake River	Blake River/Porcupine	Base Metal	intermediate	Volcanic/Sediment	Dark Grey Argillite/Mudstone, tr py laminae	96.07	96.31	m
8585	Rickard	MNDM-KL	-	KL2357	-	Stoughton-Roquemare	-	Base Metal	intermediate	Volcanic	Black Graphitic Argillite w minor py nodules	129.80	130.05	m
8586	Beatty	MNDM-KL	-	KL1943	Lower	Kidd-Munro	-	Orogenic Au	intermediate	Volcanic/Sediment	Grey Black Argillite w two 1 cm quartz-siderite veins	0.00	0.00	ft
8587	Moody	MNDM-KL	-	KL1851	-	Stoughton-Roquemare	Stoughton-Roquemare/Porcupine	Orogenic Au	intermediate	Volcanic/Sediment	Black Argillite w minor qtz veining, strong cleavage	0.00	0.00	ft
8588	Michaud	MNDM-KL	-	KL1821	Lower	Blake River	-	Orogenic Au	felsic	Volcanic/Sediment	Black Graphitic Argillite w coalesced py nodules	0.00	0.00	ft
8589	Michaud	MNDM-KL	-	KL1821	Lower	Blake River	-	Orogenic Au	intermediate	Volcanic/Sediment	Black Argillite w minor fine py on fractures and single band of py	0.00	0.00	ft
8590	Beatty	MNDM-KL	-	KL1931	-	Porcupine	-	Orogenic Au	intermediate	Sediment	Greywacke w 3 cm argillite interbed	0.00	0.00	ft
8591	Beatty	MNDM-KL	-	KL1934	Lower	Kidd-Munro	-	Orogenic Au	intermediate	Volcanic/Sediment	Siltstone	0.00	0.00	ft
8592	Munro	Millstream	S97-09	-	Lower	Kidd-Munro	-	Base Metal	felsic	Volcanic	Black Graphitic Argillite w py nodules	324.20	324.50	m
8595	Munro	Millstream	S97-09	-	Lower	Kidd-Munro	-	Base Metal	intermediate	Volcanic	Black Graphitic Argillite w py nodules	515.15	515.45	m
8599	Munro	Millstream	S97-09	-	Lower	Kidd-Munro	-	Base Metal	felsic	Volcanic	Black Graphitic Argillite w py nodules	602.60	602.95	m
8600	Munro	Millstream	S98-01	-	Lower	Kidd-Munro	-	Base Metal	felsic	Volcanic	Black Graphitic Argillite w py nodules	542.00	542.20	m
8601	Munro	Millstream	S98-02	-	Lower	Kidd-Munro	-	Base Metal	felsic	Volcanic	Black Graphitic Argillite w py nodules	633.05	633.25	m
8602	Munro	Millstream	S00-01	-	Lower	Kidd-Munro	-	Base Metal	intermediate	Volcanic	Black Graphitic Argillite w py nodules	373.55	373.75	m
8604	Munro	Millstream	S07-07	-	Lower	Kidd-Munro	-	Base Metal	felsic	Volcanic	Black Graphitic Argillite w py nodules	588.00	588.40	m
8605	Munro	Millstream	S07-22	-	Lower	Kidd-Munro	-	Base Metal	mafic	Volcanic	Black Graphitic Argillite w py nodules	609.30	609.45	m
8606	Munro	Millstream	S07-24	-	Lower	Kidd-Munro	-	Base Metal	intermediate	Volcanic	Black Graphitic Argillite w py nodules	396.70	396.95	m

Appendix A3. Sample and field data description / core log entry for N=564 samples of carbonaceous argillite from the Timmins-Kirkland Lake region.

Sample #	Easting_83	Northing_83	Sample Type	Field Description/Core Log Entry	Interval Available	Hanging wall	Footwall
8559	477034.42	5414489.17	Black Graphitic Argillite w minor discontinuous py-carb bands	blk, vfg, py nod with qc	185.56-230.67m	Mafic breccia - carbonaceous, sulfide-rich insitu breccia	Carbonaceous sediments and tuff
8560	475498.22	5427691.69	Black Argillite	blk-dk grey, vfg, lam, tr py in tr qc	154.35-168.84m	Mafic Volcanic	Graphitic Argillite below a fault zone
8561	475737.57	5427955.40	Black Argillite w tr py on fractures and minor py streaks, strong cleavage	blk, vfg, lam, tr qcv +/- py	111.28-128m	Mafic Intrusive	Mafic volcanic
8562	471429.62	5432594.95	Black Graphitic Argillite w dissem py and defomred carb? clots	blk, fg, lam, py nod (1%), some altered, qcv (10-15%)	176-176.15m	Mafic volcanic	Mafic volcanic
8563	489954.33	5417309.18	Black Graphitic Argillite w py nodules and laminae	blk, vfg, lam, tr py nod with tr qc, tr py str/lam	59.97-62.71m	Mafic volcanic	Felsic tuff
8564	482733.89	5368348.01	Black Graphitic Argillite w minor qtz and dissem py euhedra, strongly deformed		-	Tisdale Mafic Volcanics	Tisdale Mafic Volcanics
8565	482993.13	5368307.19	Argillite	Interbedded ARG & GW sequence; more arg than gw; folded (some tight folds), should be very little fluid flow through this horizon "control sample", sample taken in middle of horizon	-	OVB	Tisdale Mafic Volcanics
8566	482866.12	5368687.10	Argillite	Interbedded ARG & GW sequence, not graph, sm amt of carb veins	-	OVB	Tisdale Mafic Volcanics
8567	498593.85	5410667.73	Black Argillite w grey silty bands and fine dissem py	blk, vfg-fg, lam, brownish-silt lam?, tr py diss along lam, tr qc str, minor oxidation on surface, minor rubbly faults above and below	41.67-53.57m	Mafic Volcanic	Mafic Volcanic
8568	447172.05	5408845.22	Shale/Argillite	blk-green, vfg-fg, lam, chl-alt?, shaley, in fold hinge?, rubbly faults above and below	144.2-152.9m	Mafic Tuff	Mafic Tuff
8569	459495.44	5369934.28	Argillite w minor white laminae, isolated carb spots, and coalesced py	blk, vfg, lam, tr py nod/blebs, tr qc assoc with py & in veinlets/str + recessive Fe-carb veinlets/str; 5cm rubbly section below	72.4-78.7m	Felsic volcanic	Felsic volcanic
8570	516748.30	5404331.53	Argillite w minor white laminae	dk grey-green, fg, bedded, qc veinlets/str along bedding, chl-alt? around qcv	37-43.65m	Mafic volcanic	Mafic volcanic
8571	466402.79	5383184.35	Black Argillite w isolated py euhedra (3 mm)	blk, vfg, lam/bed, tr py blebs/cubes/str, tr po blebs, tr qc str	137.2-158.9m	Argillite	Argillite
8572	466662.80	5382184.11	Black Argillite w thin white carb laminae , minor py nodules	blk-dk grey, vfg, lam, tr py nod/blebs/cubes, some alt to Fe-carb, qc veinlets/str, graph	144.5-155.28m	Greywacke	Greywacke
8573	475519.13	5410842.36	Black Argillite w minor white laminae and minor py nod	blk, vfg, lam, graph, py nod (~2%), qc str (1%)	225.95-379m	Mafic Volcanic	EOH
8574	556428.89	5384916.08	Black Argillite w 0.5-1 cm py nodules and minor white carb	blk, vfg, py nod/blebs (3-5%), qc str & assoc with py (~1-2%)	93.9-104.2m	Ultramafic volcanic	Mafic volcanic
08574D	556428.89	5384916.08	Black Argillite w 0.5-1 cm py nodules and minor white carb	blk, vfg, py nod/blebs (3-5%), qc str & assoc with py (~1-2%)	93.9-104.2m	Ultramafic volcanic	Mafic volcanic
8575	531352.35	5392374.92	Black Argillite w volcaniclastic component, dissem py and py nodules	blk, vfg, contains plag glomerocrysts (~5%), felsic lithic frags, py nod/blebs (~2%), qc veinlets/str; "dirty argillite"	92.85-92.97m	Tholeiitic Mafic volcanic	Tholeiitic Mafic volcanic
8576	534406.42	5388388.04	Black Argillite w abundant white carb bands and py nodules	Small horizon in mafic volcanic sequence; blk, vfg, py (~10%), tr qc, rusty oxidation, ser alt?; "dirty arg"	174.84-184.6m	Pillowed Mafic volcanic	Pillowed Mafic volcanic
8577	537026.21	5388155.35	Black Argillite w recrystallized py bands	Small horizon; blk, vfg, lam, py blebs/str (~5%), qc str (<1%), graph on fractures	263.65-264.25m	Felsic volcanic (coherent and tuff)	Pillowed Mafic volcanic
8578	494432.10	5375066.68	Black Argillite/Mudstone w few round py nodules		37-156.9m	Greywacke	Greywacke
8579	493939.10	5375520.69	Black Argillite w strong cleav, tr py		676.28-786.38m	Porcupine Reworked Fragmental (5F)	EOH
8580	494007.10	5374988.69	Argillite		16-108.3	Overburden	EOH
8581	467581.82	5377078.20	Black Argillite w recrystallized py laminae	blk, fg, lam, diss py (2-3%), tr qcv	78.22-78.28m	Overburden	Greywacke
8582	468813.89	5377777.00	Black Argillite	blk-dk grey, vfg, lam, graph, tr py (mostly alt to Fe-carb), tr qc str	167-172.1m	Mafic volcanic	Mafic volcanic
8583	470328.97	5378212.67	Black Argillite w white carb-qtz laminae, t py nodules	blk, vfg, lam, qc str (~5%), tr py	104.5-111.5m	Fault zone below graphitic argillite	Interbedded greywacke and argillite
8584	468315.86	5377893.12	Dark Grey Argillite/Mudstone, tr py laminae	blk-dk grey, vfg, lam, tr qcv, tr py	48-136.8m	Overburden	Fault zone above mafic
8585	538089.00	5398989.00	Black Graphitic Argillite w minor py nodules	blk, py nod (~1%), oxidation on surface	117.7-158.4	Graphitic Shale and Massive Pyrite	Felsic Volcanics
8586	543524.00	5383769.00	Grey Black Argillite w two 1 cm quartz-siderite veins	dk grey, vfg, lam, qtz veins with Fe-carb staining	426-436ft	Porphyry dike	Sericite alteration
8587	550918.00	5410309.00	Black Argillite w minor qtz veining, strong cleavage	blk, lam, qc (2-3%), graph fractures, tr py	595.5-626.7ft	Carbonate tuff	Caronatized dacite tuff
8588	571993.00	5368884.00	Black Graphitic Argillite w coalesced py nodules	blk, lam, py nod (~3%), qc, graph	418-470ft	Mafic volcanic	Argillite
8589	571993.00	5368884.00	Black Argillite w minor fine py on fractures and single band of py	dk grey-grey, lam/bedded, qc along lam, tr py	470-557ft	Graphitic argillite	Greywacke
8590	543299.00	5383769.00	Greywacke w 3 cm argillite interbed	Small 5 cm horizon of dk grey sediments within a larger sandstone sequence	291-328ft	Wacke - (turbidites?)	Wacke - (turbidites?)
8591	543199.00	5383944.00	Siltstone	Small 5" horizon in large sandstone sequence; horizon is grey-blk, fg, lam, Fe-carb alt	267-390ft	Granule conglomerate	Wacke - (turbidites?)
8592	557900.00	5383300.00	Black Graphitic Argillite w py nodules	blk, vfg, coarse po nod (~2%), qcv (~3%)	-		
8595	557900.00	5383300.00	Black Graphitic Argillite w py nodules	blk, vfg, graph, po blebs/str (~5%) +/-py, qcv/str	-		
8599	557900.00	5383300.00	Black Graphitic Argillite w py nodules	blk, vfg, po blebs/str/diss (5-8%), minor oxid on surface	-		
8600	557850.00	5383350.00	Black Graphitic Argillite w py nodules	blk, vfg, lrg po vein + blebs/diss +/- py (~25%), qcv/str, contact w/ breccia	-	BSDK	HC
8601	558100.00	5383400.00	Black Graphitic Argillite w py nodules	blk, vfg, po nod/blebs/str/diss (5-8%), qcv	-	A_HC	HC
8602	559000.00	5383000.00	Black Graphitic Argillite w py nodules	blk, vfg, coarse po nod + str/diss (3-5%), qc veinlets/str (2-3%)	-		
8604	557923.00	5382942.00	Black Graphitic Argillite w py nodules	blk, vfg, po blebs/str (10-20%), minor qcv, some oxid on surface	-	BSDK	HC
8605	557845.00	5382948.00	Black Graphitic Argillite w py nodules	blk, vfg, po blebs/str/diss (3-5%)	-	BSDK	BSDK/KUFS
8606	557845.00	5382948.00	Black Graphitic Argillite w py nodules	blk, vfg, po blebs/str (5-8%), minor qcv	-		

Appendix A4. Centered log ratio transformed data used for PCA and Random Forest.

Sample	Si	Al	Fe	Mn	Mg	Ca	Na	K	Ti	P	LOI	C-Total	C_in_CO2	Non_carb._C	Total S	Cu	Zn	Pb	Cd	Hg	Sn	Tl	In	As	Co	Ni	Se	Mo	Ge	Sb	Ag	Au	W	Bi	B	Rb	Sr	Cs	Ba	Be	Zr
4001	8.88	6.43	10.41	6.72	6.93	5.35	4.63	4.81	3.12	0.01	10.16	8.20	9.44	5.39	10.03	1.12	2.14	-0.44	-2.38	-3.81	-3.07	-4.68	-5.38	3.50	1.54	3.05	-3.77	-1.69	-3.77	0.47	-3.07	-6.99	-3.07	-3.99	-1.28	-0.77	0.88	-3.30	1.12	-3.07	0.26
4002	10.35	7.49	7.15	2.10	3.47	3.07	5.41	5.95	4.09	-0.19	7.99	7.10	2.72	7.10	6.94	2.97	3.72	0.36	-2.58	-4.88	-1.19	-3.18	-5.58	1.72	0.62	1.29	-3.97	-1.19	-1.79	-0.19	-3.97	-7.19	-0.79	-2.58	0.71	0.36	1.70	-2.40	2.54	-3.27	1.20
4003	9.30	7.74	8.89	5.46	6.74	7.45	4.25	4.51	4.68	2.27	8.72	7.15	8.24	5.51	7.11	-0.11	2.58	-1.21	-3.01	-6.51	-3.70	-5.13	-6.00	0.73	0.54	2.00	-4.39	-2.31	-2.67	-2.74	-4.39	-10.83	-3.70	-4.21	2.50	-0.93	2.11	-3.70	0.71	-3.70	1.64
4004	8.79	7.48	7.94	2.88	5.80	6.44	5.84	6.62	4.62	2.09	7.42	5.95	5.61	5.74	7.35	2.05	4.24	-0.27	-2.01	-5.84	-0.93	-3.49	-5.24	-0.93	0.28	0.57	-1.51	-2.03	-3.16	-4.15	-3.23	-6.45	-4.33	-2.89	0.24	0.91	-0.27	-2.94	3.37	-4.33	1.47
4005	9.85	8.50	7.34	2.52	5.85	6.56	7.03	7.03	5.05	2.90	7.39	4.82	3.17	4.77	6.22	0.51	1.36	-0.88	-4.21	-10.65	-3.52	-3.52	-5.82	0.27	-0.08	0.51	-4.21	-2.83	-2.56	-2.73	-4.21	-6.74	-3.52	-3.05	0.35	1.11	3.13	-2.04	3.30	-2.83	1.95
4006	9.95	8.61	7.75	3.98	6.56	7.94	7.48	6.03	5.42	2.90	7.73	5.57	6.77	3.22	3.73	0.73	1.58	-1.75	-4.06	-10.50	-3.36	-5.33	-5.67	0.33	0.12	0.33	-4.06	-2.67	-2.49	-3.18	-4.06	-7.27	-1.06	-4.28	-2.67	0.27	2.93	-3.36	2.60	-3.36	2.16
4007	9.82	8.76	9.02	5.01	7.96	8.86	6.15	4.12	6.17	2.53	7.84	4.94	5.28	4.45	4.30	2.23	1.99	-1.59	-3.89	-10.33	-3.20	-5.03	-5.50	0.76	1.58	2.14	-3.89	-2.50	-1.67	-2.73	-3.89	-10.33	-3.20	-5.50	0.06	-1.81	2.37	-4.80	-0.10	-3.20	1.41
4008	9.52	8.35	7.44	2.81	5.93	6.90	7.09	7.00	5.06	2.60	7.67	5.32	2.66	5.30	7.08	2.04	0.32	-1.10	-4.43	-7.65	-2.35	-3.60	-6.04	-0.05	0.10	0.18	-4.43	-2.35	-2.64	-3.40	-4.43	-10.87	-3.74	-3.55	-0.27	1.51	1.85	-1.94	3.26	-3.04	2.13
4010	10.05	8.69	7.37	3.12	6.40	7.16	7.44	7.06	4.99	2.93	7.29	4.61	5.40	3.68	4.96	0.45	1.87	-1.72	-4.02	-10.47	-3.33	-3.75	-5.63	0.13	-0.27	0.31	-4.02	-1.25	-2.54	-5.63	-4.02	-6.14	-1.25	-3.15	-0.15	1.17	3.55	-1.76	3.75	-3.33	2.06
4011	9.76	8.69	8.53	4.56	7.72	7.56	5.64	7.47	5.93	2.37	8.51	6.27	7.63	-10.48	5.13	1.22	2.41	-1.74	-3.35	-10.48	-3.35	-4.08	-5.65	-0.02	0.98	2.18	-4.04	-2.65	-1.82	-3.17	-4.04	-10.48	-0.57	-4.96	2.06	1.50	1.44	-1.15	5.16	-3.35	1.41
4012	8.65	7.47	7.06	2.51	5.82	6.08	3.29	6.83	4.14	1.83	8.77	8.48	6.84	8.43	6.61	1.42	1.08	-2.74	-4.16	-8.26	-2.27	-3.89	-6.65	1.73	0.96	0.96	-5.04	-1.45	-2.78	-3.76	-5.04	-6.65	-1.86	-2.70	0.01	0.88	-0.28	-3.39	3.25	-3.65	1.29
4013	10.04	8.52	8.85	4.64	8.88	6.88	3.00	4.96	5.43	2.47	8.83	6.05	6.67	5.33	4.97	2.53	3.21	-1.49	-3.79	-10.24	-2.41	-4.30	-5.40	1.56	1.29	3.69	-3.79	-2.41	-2.00	-5.40	-3.79	-5.91	-3.10	-4.02	-1.31	-0.62	0.16	-2.51	1.81	-3.10	1.35
4014	8.93	7.56	7.82	2.72	5.89	6.62	7.04	5.24	4.35	1.34	8.94	8.68	7.31	8.61	7.07	2.11	3.66	-1.74	-2.32	-7.96	-2.66	-5.76	-6.35	-1.05	0.18	1.81	-1.15	-0.95	-3.46	-3.46	-4.74	-7.26	-4.04	-1.51	-3.35	-0.58	0.78	-4.27	1.93	-4.04	1.32
4015	9.66	7.75	7.56	2.10	4.87	6.68	6.85	5.07	4.59	1.48	8.83	8.72	4.10	8.72	6.81	1.49	4.49	-1.38	-1.55	-10.82	-2.99	-4.95	-5.98	-0.59	0.73	1.94	-4.37	-0.04	-2.99	-5.98	-3.68	-7.59	-3.68	-2.30	-1.20	-0.59	1.20	-4.19	2.79	-3.68	1.67
4016	9.14	7.96	7.38	1.90	5.61	5.44	5.82	7.17	4.85	2.08	7.69	6.55	5.98	6.38	6.89	1.67	3.74	0.77	-2.41	-11.23	-1.79	-3.52	-6.40	-1.10	0.42	1.80	-4.79	-1.79	-3.40	-3.91	-3.00	-8.01	-1.79	-2.04	1.97	1.27	0.80	-2.45	2.71	-3.40	1.35
4017	9.76	7.81	7.64	3.68	5.86	4.74	5.58	6.78	4.64	2.16	7.70	6.37	4.65	6.32	6.80	1.97	4.04	1.35	-2.26	-10.83	-1.90	-3.51	-5.99	-0.43	0.58	1.19	-4.39	-1.90	-2.17	-3.51	-3.36	-6.22	-0.80	-2.17	0.18	0.83	1.13	-3.10	2.38	-3.69	1.35
4018	9.15	7.73	7.25	2.41	5.56	6.05	5.95	6.11	4.54	2.35	8.94	8.60	6.73	8.56	6.21	1.33	0.17	-2.38	-4.68	-6.11	-3.99	-4.16	-6.29	0.32	0.47	1.53	-4.68	-1.22	-2.89	-3.30	-4.68	-7.90	-3.99	-3.40	0.49	0.04	1.52	-3.40	2.30	-3.99	1.64
4019	9.47	8.42	7.76	2.26	6.88	4.69	6.88	6.86	5.31	2.78	7.47	4.24	0.83	4.23	4.17	1.05	1.44	-1.00	-4.46	-6.30	-3.77	-3.64	-6.07	0.36	0.20	1.70	-4.46	-2.38	-2.55	-2.05	-4.46	-10.91	-3.77	-3.30	1.86	1.21	2.04	-2.12	3.13	-2.38	1.67
4020	10.01	8.29	8.06	3.56	6.49	8.02	5.87	6.73	4.65	2.87	8.70	6.88	8.20	-10.44	7.00	1.59	1.68	-1.70	-4.00	-10.44	-3.31	-4.58	-5.61	0.72	0.28	0.97	-4.00	-1.92	-2.61	-2.84	-4.00	-7.22	-3.31	-3.12	0.82	0.72	3.59	-2.97	3.03	-3.31	1.88
4021	9.44	7.64	8.02	3.54	5.75	5.54	6.99	6.05	4.27	1.74	8.46	8.14	5.11	8.13	7.07	1.68	4.26	-2.22	-1.68	-6.64	-2.04	-4.24	-6.13	-0.49	0.52	0.93	-4.52	-1.34	-2.66	-3.49	-4.52	-6.64	-1.75	-3.36	-0.74	-0.24	1.20	-3.49	2.04	-3.83	1.44
4022	9.63	8.08	7.39	2.92	5.74	6.47	6.95	6.60	5.10	2.71	7.04	5.11	3.32	5.07	6.00	1.10	2.79	-2.16	-3.43	-10.90	-1.98	-3.59	-6.07	-0.08	-0.24	0.29	-4.46	-2.38	-1.98	-3.77	-4.46	-7.68	-3.77	-3.59	-0.19	0.71	2.60	-3.77	3.03	-3.08	2.45
4023	9.75	8.64	8.74	5.14	7.65	8.74	7.53	4.41	6.10	2.38	9.20	7.61	8.85	4.76	1.42	0.73	1.97	-1.58	-3.88	-10.32	-3.19	-6.00	-5.49	0.84	1.25	1.81	-3.88	-2.49	-1.90	-5.49	-3.88	-6.40	-3.19	-3.70	-0.30	-1.11	2.98	-4.80	-0.41	-3.19	1.36
4024	8.34	6.87	8.65	2.15	4.34	5.28	5.21	5.32	3.55	1.24	8.83	7.60	5.66	7.56	8.80	1.88	4.21	0.90	-1.84	-2.73	-2.24	-2.73	-6.63	2.18	0.35	1.12	-1.55	-2.02	-3.37	-0.46	-3.04	-7.54	-4.32	-2.94	0.48	0.01	0.26	-2.00	1.31	-4.32	0.90
4025	9.41	7.84	7.24	2.70	5.48	6.52	4.37	7.16	4.69	2.41	7.92	7.12	6.49	6.97	6.65	1.55	4.67	-2.32	-1.30	-6.23	-2.14	-3.50	-6.23	-0.19	0.05	0.53	-3.46	-1.85	-2.40	-3.34	-4.62	-6.74	-2.54	-3.14	2.48	0.98	0.02	-3.75	4.00	-3.93	1.75
4026	9.35	7.23	7.79	3.01	7.05	6.17	5.30	4.62	4.45	1.45	8.51	8.09	6.01	8.06	6.69	2.36	4.38	0.02	-1.76	-5.90	-2.14	-4.35	-5.54	0.26	0.94	2.64	-1.53	-1.63	-3.24	-2.60	-3.75	-6.74	-3.93	-2.07	1.11	-1.16	-0.35	-4.15	1.33	-3.93	1.01
4027	9.48	8.07	6.95	1.66	5.76	5.75	6.41	6.97	4.85	2.75	8.01	6.75	2.83	6.74	6.29	1.34	2.60	-0.97	-2.83	-6.67	-2.47	-3.25	-6.16	0.60	0.12	2.02	-1.73	-2.06	-2.90	-3.52	-4.55	-7.77	-3.86	-3.39	0.86	1.06	2.15	-2.63	3.09	-3.86	1.77
4028	9.35	8.10	6.92	1.82	5.44	5.93	7.35	6.58	4.87	2.81	7.55	6.56	5.02	6.50	6.54	1.41	2.24	-0.01	-3.78	-5.48	-2.58	-3.72	-6.27	-0.32	0.02	1.61	-4.66	-1.88	-2.86	-3.37	-4.66	-11.10	-3.96	-2.68	0.06	0.56	2.81	-3.49	3.05	-3.27	1.92
4029	9.70	6.97	7.80	2.70	5.04	6.09	5.73	5.95	4.05	1.66	8.62	8.11	5.84	8.08	7.83	1.16	4.22	0.75	-2.16	-4.03	-1.65	-3.27	-6.03	1.97	0.37	1.61	-1.81	-1.93	-3.14	-2.04	-4.42	-10.86	-1.09	-2.50	-0.47	0.23	1.24	-3.03	2.02	-3.72	0.80
4030	9.75	8.66	9.04	5.26	7.89	8.43	7.05	5.50	6.42	3.01	8.02	5.94	7.26	-10.39	6.20	2.59	2.07	-1.64	-3.95	-10.39	-3.25	-4.97	-5.56	-1.46	1.48	1.41	-3.95	-2.56	-1.82	-3.48	-3.95	-10.39	-3.25	-4.17	-2.56	-0.61	2.53	-5.56	2.04	-3.25	1.97
4031	9.30	8.28	7.66	3.69	6.11	7.27	6.78	7.12	5.35	2.83	7.87	6.14	6.90	5.27	6.87	1.39	1.87	-1.20	-4.53	-10.97	-2.45	-4.61	-6.14	-1.76	0.45	0.92	-4.53	-1.76	-2.50	-4.35	-4.53	-10.97	-0.84	-3.25	-1.20	0.97	2.98	-3.05	3.98	-3.14	1.52
4032	9.01	8.00	8.76	4.91	6.90	8.10	4.85	5.77	5.32	2.32	8.80	7.36	8.49	5.51	6.44	1.72	2.19	-0.98	-3.29	-6.98	-1.97	-5.72	-6.06	1.39	0.96	1.56	-4.45	-3.06	-1.42	-2.73	-4.45	-10.89	-3.76	-4.27	-0.42	0.46	2.00	-3.06	2.46	-3.06	0.83
4033	8.57	6.86	10.47	3.93	6.89	6.92	2.54	2.65	3.66	1.72	9.78	5.61	6.89	1.64	10.15	5.14	1.98	-1.55	-2.20	-6.38	-3.16	-5.97	-5.46	0.79	2.12	3.33	-0.88	-1.37	-3.16	-3.67	-1.21	-3.03	-3.16	0.02	-2.46	-2.46	-0.07	-5.46	-0.86	-3.16	0.53
4034	9.07	7.47	7.33	0.59	4.39	4.42	4.13	6.50	4.34	2.25	8.27	7.56	2.45	7.56	7.36	1.01	3.29	-0.01	-3.36	-7.05	-1.93	-3.48	-6.54	1.80	-0.13	0.57	-3.44	-1.75	-2.71	-1.12	-3.20	-7.05	-2.44	-3.20	0.12	0.31	0.12	-3.54	2.05	-4.23	1.98
4035	9.07	7.24	7.59	0.63	4.26	3.74	4.97	5.93	4.01	1.66	9.16	8.94	3.81	8.94	7.35	1.17	2.05	0.25	-3.87	-5.08	-1.98	-3.71	-6.36	2.11	0.27	1.62	-1.93	-1.06	-3.18	-1.21	-3.47	-7.28	-2.67	-2.49	1.34	0.16	0.46	-2.96	2.40	-4.06	0.75
4036	9.41	6.88	7.41	1.93	4.19	5.03	5.18	4.97	3.74	1.26	9.07	8.83	5.57	8.82	7.46	1.68	1.93	0.80	-3.31	-5.62	-2.51	-3.59	-6.20	2.12	0.67	1.70	-2.33	-1.01	-3.21	-0.50	-3.31	-6.43	-2.51	-2.38	0.09	-0.50	0.90	-3.03	1.42	-3.90	0.48
4037	9.64	7.51	8.06	3.27	7.34	6.42	5.58	4.87	4.69	1.67	8.33	7.27	7.87	6.58	7.32	1.15	1.41	-0.25	-4.41	-6.02	-1.41	-4.13	-5.32	1.91	0.22	1.35	-4.41	-1.41	-2.93	-2.03	-3.53	-10.85	-2.33	-1.80	0.76	-0.94	-0.13	-3.94	1.59	-3.71	1.28
4038	9.33	7.40	8.65	2.44	6.01	4.67	5.85	6.28	4.38	1.81	7.71	5.42	3.59	5.37	8.19	3.34	4.15	-0.65	-1.85	-6.43	-0.91	-4.01	-4.82	-0.27	1.82	2.07	-0.99	-1.60	-2.52	-3.57	-3.32	-7.82	-2.11	-2.68	-1.02	0.68	-0.73	-3.57	2.70	-3.91	1.24
4039	9.33	7.90	6.37	4.22	6.10	6.64	5.64	6.85	4.34	2.36	8.10	6.84	7.28	6.29	6.31	0.24	2.67	-0.89	-4.68	-5.95	-3.29	-2.61	-6.29	1.87	-0.90	0.37	-4.68	-2.19	-2.26	-2.55	-4.68	-7.90	-2.60	-3.65	0.42	1.13	2.01	-2.46	2.96	-3.29	1.81
4040	9.09	7.96	7.66	1.56	4.72	5.42	7.68	4.05	4.47	2.33	8.58	8.07	5.92	8.03	7.16	1.43	4.02	1.29	-1.52	-4.98	-1.71	-6.82	-5.62	-4.01	0.70	2.10	-1.86	-0.68	-4.01	-2.91	-3.83	-7.92	-4.01	-1.59	-0.92	-2.22	1.50	-5.62	0.42	-4.01	1.49
4041	9.18	7.15	8.73	5.09	7.20	8.08	2.67	2.09	3.91	1.85	9.04	8.11	8.57	7.54	8.09	2.54	3.23	-1.08	-1.59	-5.43	-3.72	-6.02	-6.02	0.41	0.73	1.24	-1.27	-1.64	-2.69	-2.69	-4.41	-7.63	-2.33	-3.38	-0.03	-3.03	2.03	-5.33	-0.19	-3.72	0.82
4042	11.08	7.56	6.65	1.98	4.64	5.35	6.76	6.06	3.99	1.91	8.79	8.61	3.44	8.61	5.52	1.23	4.38	-0.94	-1.86	-5.77	-2.55	-3.17	-4.86	1.14	0.26	1.57	-3.25	-1.17	-3.25	-2.55	-3.25	-9.69	0.09	-3.47	-0.25	0.44	2.05	-3.06	2.28	-2.55	0.91
4043	9.99	8.51	7.22	3.31	6.21	7.37	6.96	7.25	4.91	2.68	7.32	5.54	4.39	5.45	3.00	0.47	1.91	-1.79	-4.09	-10.53	-2.70	-3.67	-5.70	0.66	-0.85	0.24	-4.09	-2.01	-2.37	-3.62	-4.09	-10.53	-1.09	-3.40	0.19	1.32	3.61	-2.37	3.90	-3.40	2.37
4044	10.18	6.95	7.03	2.26	5.23	5.51	3.71	6.18	3.88	1.51	8.95	8.77	3.32	8.77	6.77	1.09	3.72	0.16	-2.20	-4.39	-1.98	-3.14	-5.67	1.89	0.47	1.55	-4.06	-1.29	-3.19	-1.72	-4.06	-7.28	-0.88	-2.90	-0.37	0.69	0.22	-3.37	2.85	-3.37	1.09
4045	8.92	7.52	7.01	0.21	3.88	4.16	6.59	5.87	4.22	1.59	9.13	8.96	3.80	8.95	6.88	0.98	2.46	-0.15	-4.83	-5.56	-2.06	-3.41	-5.05	2.13	0.57	1.73	-2.49	-0.80	-3.55	-1.63	-3.66	-6.66	-4.13	-2.28	-0.67	0.53	0.90	-2.38	1.78	-4.13	0.88
4046	8.78	7.53	6.67	0.80	5.12	4.70	6.45	6.36	4.20	1.23	8.57	8.13	3.16	8.13	6.67	0.58	2.31	0.81	-5.03	-4.40	-2.03	-2.54	-6.64	2.07	-0.15	1.24	-2.85	-1.70	-2.54	-0.36	-3.46	-6.30	-2.26	-2.73	0.05	1.02	0.43	-2.39	2.26	-3.64	1.17
4047	9.53	8.03	7.27	2.83	5.82	5.90	5.77	7.10	5.07	2.33	7.51	5.70	6.31	5.00	4.23	-0.32	1.30	-2.23	-4.54	-6.66	-2.46	-2.81	-6.15	-0.38	-0.94	-0.59	-4.54	-3.15	-2.62	-2.97	-4.54	-7.76	-1.36	-3.84	0.63	1.27	1.23	-2.09	3.22	-3.15	2.38
4048	8.99	7.61	7.68	2.83	5.57	6.28	6.67	5.52	4.21	1.38	8.04	7.23	2.49	7.23	7.72	1.64	3.76	0.11	-2.47	-7.00	-2.80	-4.21	-6.49	1.84	0.56	0.99	-4.88	-1.89	-2.50	-2.43	-4.01	-8.10	-1.10	-2.54	0.44	-0.06	1.96	-2.43	1.47	-3.50	1.57
4049	9.27	7.40	7.39	0.68	4.83	2.43	4.44	6.38	3.95	1.24	7.53	5.77	3.35	5.75	7.20	-1.15	1.40	-1.66	-4.84	-5.22	-2.06	-3.31	-6.44	0.74	-1.04	0.08	-4.84	-2.06	-3.27	-3.35	-4.84	-11.28	-1.50	-3.04	2.17	0.78	0.46	-2.57	2.50	-3.45	1.69
4050	8.59	7.18	7.55	1.71	4.27	5.48	5.59	6.04	3.55	1.29	8.56	8.07	5.48	8.04	7.64	1.41	3.97	-0.44	-2.52	-5.57	-2.35	-3.01	-6.74	1.76	-0.26	1.35	-2.64	-1.54	-3.48	-1.60	-3.85	-6.74	-2.35	-2.55	1.71	0.67	1.11	-2.58	2.03	-3.74	0.79
4051	9.10	7.52	8.54	4.64	6.63	6.88	1.71	1.82	4.18	1.73	8.33	7.24	6.97	7.01	7.28	3.17	4.50	-0.04	-1.59	-4.29	-1.91	-5.26	-6.29	-0.81	1.38	2.16	-1.98	-1.68	-2.19	-3.11	-3.80	-7.21	-1.50	-2.60	-2.60	-3.29	-0.07	-6.29	-3.99	-3.99	1.49
4052	9.57	8.26	6.74	0.34	4.80	4.96	7.20	6.93	4.90	2.99	7.81	6.90	3.13	6.90	6.73	1.09	2.35	-1.48	-4.47	-5.50	-2.40	-3.00	-6.08	0.80	-0.11	1.12	-4.47	-2.40	-2.62	-2.83	-4.47	-10.92	-1.30	-3.60	-0.26	1.12	2.58	-1.84	3.05	-3.09	1.78
4053	9.63	7.75	6.83	3.07	6.04	6.54	6.74	6.14	4.38	1.91	7.61	6.63	6.48	6.36	5.83	0.90	3.12	-1.33	-3.48	-5.78	-3.81	-3.65	-6.12	0.14	0.23	1.81	-3.48	-2.02	-2.78	-3.48	-4.51	-7.73	-0.82	-3.12	0.38	0.52	1.49	-2.20	2.30	-3.81	1.21
4054	9.55	8.09	6.84	1.62	5.19	6.25	6.31	6.87	4.70	2.95	7.70	6.01	6.84	5.01	6.30	1.19	2.28	-2.22	-3.82	-10.96	-3.82	-3.75	-6.13	-0.09	-0.24	0.33	-4.52	-2.03	-3.04	-3.49	-3.82	-7.74	-1.75	-2.66	1.19	0.98	2.79	-2.03	3.34	-3.13	2.07
4055	9.20	7.27	7.76	2.98	5.07	3.54	4.51	5.48	4.20	1.44	8.22	7.73	2.78	7.73	6.97	1.22	5.25	-0.87	-0.94	-3.90	-0.87	-3.33	-4.64	1.15	0.95	1.74	-3.66	-1.49	-2.65	-2.56	-3.66	-7.35	-1.64	-2.34	0.09	-0.30	0.94	-3.34	2.04	-4.13	1.02
4056	9.73	6.90	8.37	3.41	5.58	5.72	4.46	4.33	3.75	1.49	8.62	7.81	6.41	7.74	8.08	2.26	3.05	-0.27	-2.72	-6.49	-2.29	-0.67	-5.97	1.27	0.79	1.89	-1.27	-1.37	-2.51	-1.78	-4.36	-6.89	-0.90	-2.80	-1.03	-1.19	1.06	-4.18	0.73	-3.67	0.76
4057	9.33	7.96	6.91	2.91	5.90	6.40	6.67	6.44	4.64	2.36	7.94	6.96	7.02	6.62	5.54	0.21	2.05	-2.37	-4.67	-5.49	-3.28	-3.48	-6.28	0.48	-0.46	0.88	-4.67	-2.19	-2.95	-2.81	-4.67	-7.89	-2.19	-3.28	0.83	0.65	1.97	-2.12	2.60	-3.28	1.61
4058	10.55	8.02	6.99	3.80	5.52	7.23	7.05	6.55	4.79	2.55	8.16	7.31	7.29	7.00	4.68	0.51	0.57	-1.41	-3.71	-10.15	-3.02	-3.98	-5.32	-0.94	-0.35	0.57	-2.83	-1.63	-2.83	-3.93	-3.71	-10.15	0.08	-3.53	-0.53	0.86	2.76	-2.23	3.00	-3.02	1.85
4059	9.10	7.74	7.05	2.76	5.72	6.42	6.10	6.47	4.61	2.26	7.93	6.90	6.95	6.56	6.36	1.27	2.38	-1.38	-3.82	-5.67	-2.77	-4.12	-6.46	0.77	0.09	1.72	-4.85	-2.36	-3.37	-2.88	-4.85	-8.07	-2.08	-3.20	1.49	0.70	2.39	-2.43	3.24	-3.46	1.45
4060	9.66	8.14	7.01	2.36	6.01	5.28	6.61	7.13	4.73	2.37	8.01	7.14	0.89	7.14	6.25	1.08	2.19	-1.23	-4.40	-7.62	-2.32	-2.82	-6.01	1.08	0.69	2.48	-4.40	-1.92	-2.92	-3.71	-4.40	-10.85	-1.92	-2.68	-0.53	1.34	1.56	-2.10	3.30	-3.71	1.61
4061	9.43	8.42	8.11	3.69	7.46	6.05	6.75	6.96	5.24	2.53	7.66	4.66	2.26	4.64	4.71	1.16	1.49	-2.12	-4.42	-10.86	-3.03	-3.54	-6.03	-0.33	0.75	2.52	-4.42	-2.34	-2.29	-3.95	-4.42	-7.64	-3.73	-3.14	0.14	1.16	2.50	-2.20	3.28	-3.03	1.54
4062	9.54	8.39	7.83	3.85	6.20	7.19	7.42	6.50	5.58	3.40	8.34	6.89	8.04	4.96	4.44	-0.30	1.23	-2.03	-4.33	-10.77	-2.94	-4.60	-5.94	0.32	-0.46	1.01	-4.33	-2.25	-3.05	-3.45	-4.33	-7.55	-3.63	-5.24	0.87	0.52	2.88	-2.54	2.77	-2.94	2.06
4063	8.85	7.63	7.56	3.94	6.38	7.81	5.36	6.50	4.67	1.07	8.61	7.41	7.81	6.89	7.56	1.89	3.34	-0.14	-2.34	-6.62	-1.61	-5.70	-6.40	2.79	1.46	3.95	-4.79	-2.71	-1.59	-1.85	-4.09	-7.31	-4.09	-3.22	-0.36	0.86	0.79	-2.61	2.79	-4.09	0.31
4064	9.60	8.38	8.04

Appendix A4. Centered log ratio transformed data used for PCA and Random Forest.

Sample	Hf	Nb	Ta	Ga	Sc	V	Cr	Th	U	Y	La	Ce	Pr	Nd	Sm	Eu	Gd	Tb	Dy	Ho	Er	Tm	Yb	Lu	Br	F
4001	-3.07	-2.60	-5.04	-1.28	-1.73	0.39	-3.77	-3.35	-3.73	-0.99	-1.34	-0.75	-2.84	-1.46	-3.00	-3.59	-2.93	-4.59	-2.75	-4.15	-3.02	-4.79	-2.77	-4.50	-3.77	1.53
4002	-2.58	-2.40	-4.70	-0.50	-0.40	1.31	0.89	-2.98	-3.93	-1.19	-1.03	-0.31	-2.43	-1.01	-2.49	-3.82	-2.77	-4.55	-2.84	-4.55	-3.47	-5.39	-3.52	-5.39	-1.55	1.33
4003	-2.13	-1.46	-4.06	-0.37	-0.60	1.12	0.95	-2.40	-3.70	-0.37	-0.76	0.03	-2.05	-0.56	-2.00	-3.31	-2.07	-3.87	-2.11	-3.72	-2.61	-4.47	-2.52	-4.24	-2.31	0.91
4004	-2.27	-1.57	-4.10	-0.30	-0.92	0.95	-0.01	-2.48	-3.61	-0.74	-0.73	0.08	-2.03	-0.63	-2.17	-3.27	-2.25	-4.08	-2.35	-3.98	-2.91	-4.77	-2.91	-4.66	-5.02	0.28
4005	-1.80	-1.54	-3.93	0.17	-0.56	1.39	0.87	-1.82	-3.11	-1.03	0.31	1.07	-1.06	0.27	-1.55	-2.85	-1.96	-4.00	-2.39	-4.10	-3.09	-5.03	-3.14	-4.95	-1.54	1.09
4006	-1.60	-1.17	-3.54	0.22	-0.07	1.91	0.76	-2.02	-3.47	-0.03	0.02	0.67	-1.51	-0.14	-1.73	-2.94	-1.75	-3.56	-1.86	-3.47	-2.40	-4.28	-2.44	-4.23	-1.57	1.24
4007	-2.17	-1.47	-4.27	0.39	1.21	3.19	2.70	-3.67	-5.03	0.54	-1.23	-0.32	-2.24	-0.58	-1.70	-2.68	-1.46	-3.10	-1.28	-2.80	-1.71	-3.55	-1.70	-3.47	-3.89	1.41
4008	-1.61	-0.86	-3.17	-0.15	-0.75	1.08	0.40	-1.66	-2.98	-0.15	0.05	0.76	-1.41	-0.06	-1.69	-2.83	-1.80	-3.68	-1.96	-3.60	-2.55	-4.39	-2.52	-4.32	-4.43	0.87
4010	-1.64	-1.51	-3.88	0.45	-0.76	1.25	0.78	-1.69	-2.93	-0.85	0.33	1.05	-1.08	0.24	-1.61	-2.98	-2.03	-3.99	-2.47	-4.20	-3.17	-5.05	-3.25	-5.05	-4.02	1.27
4011	-2.18	-1.87	-4.62	0.29	1.04	3.07	2.83	-3.48	-4.69	0.18	-1.34	-0.46	-2.40	-0.82	-2.00	-3.18	-1.77	-3.39	-1.55	-3.10	-2.02	-3.86	-2.01	-3.83	-4.04	1.26
4012	-2.40	-1.84	-4.29	-0.47	-0.63	0.85	0.46	-2.02	-3.29	-0.56	0.33	0.81	-1.45	-0.16	-1.77	-2.93	-1.95	-3.87	-2.20	-3.87	-2.77	-4.67	-2.74	-4.52	-0.87	0.26
4013	-2.31	-1.77	-4.61	0.59	0.43	2.29	4.41	-3.28	-4.37	-0.46	-1.55	-0.73	-2.72	-1.14	-2.42	-3.46	-2.34	-3.92	-2.16	-3.88	-2.75	-4.61	-2.78	-4.61	-3.79	1.50
4014	-2.44	-1.78	-4.32	-0.95	-0.66	0.69	0.74	-2.20	-3.32	-0.41	-0.70	0.12	-1.98	-0.56	-2.02	-3.19	-2.09	-3.86	-2.10	-3.68	-2.62	-4.52	-2.64	-4.37	-1.45	0.56
4015	-2.11	-1.96	-4.04	-0.42	-0.32	0.70	1.07	-1.72	-2.87	-0.50	-0.54	0.41	-1.66	-0.29	-1.72	-2.61	-1.91	-3.64	-1.94	-3.72	-2.74	-4.70	-2.77	-4.46	-2.30	0.92
4016	-2.30	-1.66	-4.08	-0.27	-0.33	1.43	1.23	-1.72	-2.90	-1.00	-0.26	0.49	-1.64	-0.27	-1.96	-3.33	-2.25	-4.22	-2.63	-4.32	-3.26	-5.17	-3.17	-4.92	-4.79	0.51
4017	-2.41	-1.87	-4.24	-0.36	-1.06	0.95	0.19	-2.47	-3.69	-0.92	-0.66	0.11	-2.01	-0.61	-2.22	-3.40	-2.36	-4.24	-2.62	-4.27	-3.22	-5.12	-3.29	-4.96	-2.31	0.91
4018	-2.13	-1.54	-3.99	-0.66	-0.76	0.76	0.23	-2.13	-3.48	-0.25	-0.34	0.44	-1.69	-0.31	-1.85	-2.75	-1.92	-3.77	-2.02	-3.64	-2.55	-4.50	-2.57	-4.26	-0.13	0.62
4019	-1.98	-1.39	-3.88	0.10	-0.01	2.00	2.30	-1.19	-2.56	-0.44	0.34	1.11	-1.02	0.37	-1.36	-2.81	-1.74	-3.69	-2.04	-3.71	-2.63	-4.59	-2.71	-4.46	-2.29	0.83
4020	-1.82	-1.74	-4.17	0.03	0.22	1.87	0.57	-1.53	-2.91	-0.53	0.51	1.23	-0.95	0.35	-1.57	-2.94	-1.98	-4.04	-2.42	-4.08	-2.98	-4.82	-2.91	-4.73	-2.28	1.30
4021	-2.30	-2.00	-3.98	-0.74	-1.04	0.56	0.22	-2.32	-3.43	-0.57	-1.10	-0.28	-2.36	-0.92	-2.31	-3.33	-2.33	-4.00	-2.24	-3.87	-2.78	-4.60	-2.77	-4.52	-2.55	0.78
4022	-1.32	-0.82	-3.26	-0.13	-0.56	0.84	0.07	-1.76	-3.11	0.29	-0.50	0.54	-1.43	0.02	-1.42	-2.88	-1.49	-3.17	-1.43	-3.02	-1.97	-3.77	-1.91	-3.71	-4.46	0.84
4023	-2.23	-1.70	-4.61	0.22	1.16	3.11	2.77	-4.15	-4.70	0.40	-1.61	-0.66	-2.51	-0.87	-1.94	-3.05	-1.57	-3.17	-1.32	-2.88	-1.77	-3.70	-1.79	-3.51	-3.88	1.42
4024	-2.84	-2.04	-4.62	-1.14	-1.45	0.06	-0.41	-2.48	-3.77	-1.06	-1.00	-0.23	-2.33	-0.91	-2.58	-4.12	-2.82	-4.57	-2.80	-4.36	-3.31	-5.19	-3.32	-5.06	-1.79	0.28
4025	-1.98	-1.48	-4.08	-0.29	-1.19	0.75	-0.14	-2.43	-3.65	-0.84	-0.60	0.15	-2.01	-0.66	-2.31	-3.42	-2.48	-4.26	-2.52	-4.13	-3.05	-4.95	-3.13	-4.90	-4.62	0.68
4026	-2.77	-2.21	-4.62	-0.93	-0.56	1.19	3.05	-2.60	-3.73	-0.67	-1.58	-0.70	-2.79	-1.40	-2.64	-3.62	-2.54	-4.18	-2.46	-4.08	-2.98	-4.85	-3.01	-4.80	-4.62	0.68
4027	-1.94	-1.68	-4.13	-0.17	-0.77	1.33	1.43	-1.93	-3.41	-0.86	-0.52	0.35	-1.71	-0.31	-1.97	-3.39	-2.29	-4.16	-2.47	-4.16	-3.06	-5.00	-3.06	-4.93	-4.55	0.75
4028	-1.79	-1.56	-4.00	-0.38	-0.83	1.18	0.91	-1.66	-3.23	-0.63	0.23	1.05	-1.04	0.31	-1.50	-3.07	-1.95	-3.92	-2.30	-3.98	-2.93	-4.83	-2.94	-4.70	-4.66	0.64
4029	-2.94	-2.39	-4.69	-0.95	-1.06	0.66	1.51	-2.78	-3.95	-0.95	-1.49	-0.66	-2.70	-1.29	-2.78	-3.31	-2.78	-4.46	-2.74	-4.34	-3.27	-5.15	-3.21	-5.00	-4.42	0.88
4030	-1.64	-1.10	-3.83	0.44	1.38	3.30	1.05	-2.82	-4.17	0.74	-0.57	0.31	-1.63	-0.09	-1.30	-2.39	-1.09	-2.75	-0.95	-2.49	-1.42	-3.27	-1.37	-3.18	-3.95	1.35
4031	-2.19	-1.64	-4.28	-0.05	-0.32	1.83	-0.40	-2.52	-3.76	-0.25	-0.20	0.53	-1.55	-0.16	-1.78	-2.81	-1.88	-3.69	-2.01	-3.65	-2.59	-4.49	-2.60	-4.42	-2.40	0.77
4032	-2.88	-2.07	-4.78	-0.29	0.47	2.38	1.92	-3.64	-4.72	-0.23	-1.42	-0.64	-2.66	-1.10	-2.35	-3.18	-2.18	-3.84	-2.02	-3.54	-2.47	-4.37	-2.50	-4.27	-4.45	0.85
4033	-3.16	-2.82	-5.46	-0.86	-0.58	1.30	0.55	-3.60	-3.54	-0.67	-0.49	0.10	-2.10	-0.74	-2.47	-4.03	-2.55	-4.24	-2.42	-3.85	-2.77	-4.58	-2.75	-4.43	-1.55	1.45
4034	-1.75	-1.23	-3.68	-0.65	-0.44	1.03	-0.36	-2.38	-3.69	-0.01	-0.75	0.03	-2.11	-0.74	-2.30	-3.56	-2.17	-3.73	-1.81	-3.29	-2.18	-3.97	-2.05	-3.80	-1.97	0.37
4035	-2.96	-2.30	-4.57	-0.88	-0.75	0.66	0.27	-2.17	-3.65	-0.97	-0.84	-0.05	-2.19	-0.82	-2.37	-3.35	-2.47	-4.16	-2.45	-4.06	-2.99	-4.83	-2.93	-4.67	-0.99	0.55
4036	-3.11	-2.47	-4.72	-0.91	-0.82	0.51	0.20	-2.64	-3.77	-1.26	-0.81	0.04	-2.01	-0.57	-2.11	-3.35	-2.43	-4.29	-2.70	-4.38	-3.37	-5.25	-3.38	-5.17	-0.66	0.70
4037	-2.49	-1.92	-4.45	-0.82	-0.36	1.40	1.03	-2.33	-3.48	-0.62	-1.37	-0.45	-2.57	-1.22	-2.44	-3.41	-2.37	-4.04	-2.23	-3.84	-2.79	-4.68	-2.77	-4.58	-1.92	0.89
4038	-2.52	-1.93	-4.35	-0.51	-0.90	0.68	0.24	-2.71	-3.74	-0.65	-1.70	-0.75	-2.66	-1.08	-2.26	-3.07	-2.25	-3.95	-2.24	-3.89	-2.87	-4.77	-2.92	-4.60	-3.03	0.70
4039	-2.01	-1.57	-4.05	-0.46	-1.61	0.27	-0.52	-1.65	-3.08	-0.99	0.08	0.84	-1.34	-0.03	-1.95	-3.26	-2.37	-4.34	-2.74	-4.43	-3.32	-5.26	-3.33	-5.12	-2.07	0.62
4040	-2.18	-1.54	-3.93	-1.01	-0.91	0.81	0.51	-1.31	-2.86	-0.54	-0.94	-0.03	-2.05	-0.61	-2.00	-2.81	-2.11	-3.83	-2.11	-3.75	-2.66	-4.52	-2.61	-4.36	-1.88	0.60
4041	-2.93	-2.33	-4.86	-0.95	-0.79	0.69	0.91	-2.98	-4.23	-0.39	-1.04	-0.29	-2.41	-0.98	-2.40	-3.31	-2.26	-3.94	-2.11	-3.64	-2.49	-4.30	-2.41	-4.11	-1.52	0.89
4042	-2.78	-2.37	-4.67	-1.17	-1.37	0.22	0.65	-2.53	-3.69	-1.17	-1.04	-0.28	-2.40	-1.05	-2.57	-3.83	-2.59	-4.16	-2.53	-4.16	-3.21	-5.08	-3.25	-5.08	-1.27	2.05
4043	-1.37	-1.06	-3.46	0.19	-1.20	0.66	-0.21	-1.21	-2.55	-0.62	0.74	1.50	-0.69	0.60	-1.37	-2.83	-1.78	-3.88	-2.30	-4.01	-3.01	-4.91	-3.06	-4.74	-2.12	1.21
4044	-2.78	-2.27	-4.71	-0.88	-1.41	0.22	0.13	-2.64	-3.75	-0.88	-1.06	-0.31	-2.44	-1.08	-2.61	-3.07	-2.64	-4.39	-2.63	-4.28	-3.17	-5.08	-3.22	-4.88	-1.11	1.24
4045	-2.80	-2.16	-4.46	-0.67	-0.77	0.78	0.71	-2.14	-3.50	-0.61	-0.99	-0.12	-2.19	-0.80	-2.32	-3.28	-2.38	-4.08	-2.20	-3.77	-2.66	-4.52	-2.64	-4.31	-1.68	0.47
4046	-2.51	-1.98	-4.53	-0.81	-0.51	0.76	0.79	-1.81	-3.26	-0.93	-1.09	-0.23	-2.33	-0.88	-2.42	-3.42	-2.61	-4.46	-2.71	-4.24	-3.10	-4.99	-2.99	-4.61	-1.51	0.27
4047	-1.36	-0.92	-3.47	-0.16	-0.71	0.18	-4.54	-1.88	-3.31	0.38	0.50	1.31	-0.78	0.61	-1.08	-2.59	-1.29	-3.14	-1.41	-2.99	-1.89	-3.77	-1.86	-3.63	-2.68	0.76
4048	-2.06	-1.52	-3.87	-0.61	-1.11	0.58	-0.18	-2.11	-3.27	-0.72	-0.44	0.31	-1.82	-0.46	-2.07	-3.37	-2.23	-4.08	-2.38	-3.99	-2.94	-4.77	-2.85	-4.67	-4.88	0.42
4049	-1.80	-0.62	-3.47	-0.56	-1.88	-0.15	-4.84	-1.81	-3.00	2.30	0.54	1.35	-0.71	0.72	-0.64	-2.31	-0.23	-1.77	0.17	-1.27	-0.15	-2.05	-0.23	-2.05	-4.84	0.46
4050	-2.75	-2.11	-4.38	-0.97	-1.12	0.28	-0.14	-2.18	-3.53	-0.65	-1.19	-0.38	-2.48	-1.10	-2.57	-3.45	-2.64	-4.32	-2.54	-4.07	-2.95	-4.82	-2.84	-4.58	-2.28	0.17
4051	-2.23	-1.61	-4.11	-0.46	-0.37	1.28	0.43	-2.01	-3.14	-0.12	-0.54	0.26	-1.81	-0.36	-1.82	-3.01	-1.84	-3.58	-1.81	-3.40	-2.30	-4.18	-2.24	-4.01	-2.71	0.62
4052	-1.99	-1.65	-4.03	-0.04	-0.77	1.24	0.68	-1.93	-3.27	-0.38	0.08	0.89	-1.21	0.15	-1.64	-2.99	-1.94	-3.93	-2.33	-3.96	-2.93	-4.80	-2.91	-4.70	-4.47	0.82
4053	-2.48	-1.73	-4.14	-0.72	-0.88	0.77	1.81	-2.07	-3.37	-1.17	0.67	1.30	-0.99	0.22	-1.87	-3.19	-2.45	-4.51	-2.91	-4.63	-3.55	-5.42	-3.48	-5.24	-2.48	0.79
4054	-1.67	-1.48	-3.98	-0.24	-1.27	0.84	-0.16	-1.51	-2.64	-0.65	0.59	1.40	-0.75	0.56	-1.36	-2.85	-1.89	-3.98	-2.39	-4.13	-3.03	-4.96	-3.16	-4.90	-2.66	0.78
4055	-2.74	-2.13	-4.57	-0.60	-0.54	0.91	0.48	-2.81	-3.83	-0.87	-1.12	-0.30	-2.39	-0.97	-2.47	-3.63	-2.55	-4.35	-2.59	-4.19	-3.10	-4.99	-3.03	-4.78	-2.02	0.48
4056	-2.98	-2.39	-4.75	-1.19	-0.90	0.49	0.49	-3.00	-4.18	-0.90	-1.34	-0.51	-2.59	-1.16	-2.57	-3.76	-2.61	-4.36	-2.60	-4.22	-3.14	-5.02	-3.06	-4.81	-1.82	0.93
4057	-2.06	-1.60	-4.00	-0.34	-0.58	1.17	0.62	-1.80	-3.20	-0.58	0.00	0.75	-1.40	-0.06	-1.81	-3.25	-2.18	-4.10	-2.44	-4.08	-2.96	-4.84	-2.93	-4.67	-2.64	0.63
4058	-1.92	-1.41	-3.71	-0.53	-0.85	0.62	0.36	-2.12	-3.26	-0.53	-0.38	0.41	-1.76	-0.41	-2.13	-3.53	-2.34	-4.16	-2.46	-4.04	-2.92	-4.73	-2.88	-4.63	-1.45	1.59
4059	-2.27	-1.78	-4.28	-0.52	-0.76	1.09	1.49	-2.27	-3.58	-0.82	-0.38	0.39	-1.74	-0.37	-2.10	-3.57	-2.37	-4.28	-2.62	-4.26	-3.11	-5.02	-3.10	-4.85	-2.43	0.45
4060	-2.06	-1.74	-4.16	-0.13	-0.19	1.53	2.65	-1.85	-3.22	-0.82	-0.29	0.47	-1.68	-0.34	-2.04	-3.40	-2.30	-4.16	-2.46	-4.04	-2.96	-4.85	-2.84	-4.58	-2.18	0.89
4061	-2.29	-1.65	-4.08	0.06	0.33	2.19	3.12	-1.66	-2.89	-0.26	-0.15	0.63	-1.51	-0.12	-1.78	-2.98	-1.90	-3.79	-2.03	-3.67	-2.57	-4.46	-2.58	-4.38	-2.85	0.88
4062	-1.72	-1.02	-3.72	0.10	-0.38	1.72	-0.44	-2.07	-3.31	-0.30	0.11	0.90	-1.22	0.17	-1.54	-2.83	-1.73	-3.65	-1.99	-3.63	-2.61	-4.50	-2.63	-4.41	-4.33	0.97
4063	-3.40	-2.87	-5.70	-0.51	0.15	1.94	4.64	-3.93	-4.96	-0.76	-2.51	-1.77	-3.73	-2.13	-3.27	-4.14	-2.91	-4.48	-2.64	-4.16	-3.08	-4.96	-3.05	-4.87	-1.68	0.51
4064	-1.83	-1.46	-3.91	-0.19	-0.62	1.23	0.43	-1.96	-2.99	-0.33	-1.56	-0.58	-2.58	-1.10	-2.32	-3.25	-2.16	-3.83	-2.06	-3.63	-2.49	-4.36	-2.40	-4.20	-2.15	1.02
4065	-2.37	-1.37	-4.13	-1.13	-1.26	0.34	0.62	-1.95	-3.01	-0.54	-0.39	0.38	-1.74	-0.37	-1.99	-3.09	-2.11	-3.92	-2.22	-3.87	-2.84	-4.74	-2.86	-4.64	-2.79	0.38
4066	-4.48	-2.69	-4.99	-0.79	-1.42	0.30	1.05	-3.53	-3.53	-0.79	-1.16	-0.58	-2.76	-1.32	-2.91	-3.61	-3.00	-4.71	-3.05	-4.48	-3.38	-4.99	-3.32	-5.40	-0.79	2.42
4067	-2.09	-1.24	-3.80	0.03	0.00	1.79	2.33	-1.19	-2.19	-0.30	0.15	0.94	-1.20	0.17	-1.52	-3.02	-1.75	-3.66	-1.98	-3.65	-2.60	-4.53	-2.69	-4.50	-2.85	0.73
4068	-2.00	-1.13	-3.64	0.16	0.14	1.96	2.47	-1.11	-2.38	-0.53	0.25	1.05	-1.07	0.30	-1.39	-2.84	-1.70	-3.71	-2.12	-3.87	-2.86	-4.76	-2.77	-4.56	-4.48	0.82
4069	-2.89	-2.60	-5.59	-0.07	1.17	2.78	5.53	-4.42	-5.19	0.02	-2.06	-1.24	-3.15	-1.53	-2.55	-3.34	-2.09	-3.58	-1.74	-3.24	-2.15	-3.99	-2.06	-3.85	-1.85	1.54
4070	-1.50	-1.41	-3.56	0.28	-1.11	0.43	0.18	-1.83	-3.13	-0.72	0.15	0.83	-1.40	-0.11	-1.82	-3.24	-2.12	-3.97	-2.47	-4.09	-3.09	-4.97	-3.11	-4.87	-2.48	1.25
4071	-2.47	-2.10	-4.98	-0.17	1.34	2.84	4.37	-3.74	-4.87	0.20	-1.43	-0.59	-2.58	-1.00	-2.14	-3.24	-1.85	-3.44	-1.64	-3.17	-2.13	-4.08	-2.16	-3.92	-1.93	1.34
4072	-2.18	-1.80	-4.58	0.13	1.08	2.96	0.09	-3.43	-4.64	0.53	-1.05	-0.17	-2.13	-0.53	-1.71	-2.86	-1.42	-3.06	-1.25	-2.80	-1.72	-3.58	-1.72	-3.52	-1.88	1.04
4073	-1.25	-0.86	-3.28	0.58	-0.40	1.34	0.43	-1.58	-2.87	-0.42	0.13	0.83	-1.33	-0.01	-1.70	-2.96	-1.89	-3.76	-2.08	-3.79	-2.74	-4.59	-2.71	-4.43	-4.21	1.09
4074	-2.48	-1.74	-4.27	-0.46	-0.61	0.78	0.63	-2.42	-3.41	-0.87	-0.65	0.14	-1.99	-0.64	-2.18	-3.93	-2.29	-4.04	-2.42	-4.01	-2.91	-4.62	-2.61	-4.22	-4.04	1.25
4075	-2.32	-1.51	-4.14	0.04	-0.23	1.87	2.01	-1.53	-2.79	-0.41	0.11	0.86	-1.26	0.11	-1.63	-3.31	-2.03	-3.91	-2.21	-3.84	-2.80	-4.76	-2.85	-4.66	-2.76	0.46
4076	-1.89	-1.29	-3.92	-0.01	-0.16	1.78	2.21	-1.30	-2.62	-0.31	0.47	1.22	-0.91	0.45	-1.30	-2.76	-1.66	-3.71	-2.06	-3.76	-2.71	-4.66	-2.78	-4.53	-4.53	0.77
4077	-1.98	-1.13	-3.67	0.11	0.06	1.99	2.41	-1.06	-2.28	-0.06	0.31	1.09	-1.06	0.31	-1.33	-2.96	-1.61	-3.55	-1.88	-3.52	-2.50	-4.42	-2.54	-4.35	-2.77	0.80
4078	-1.80	-0.97	-3.57	0.20	0.18	1.95	2.53	-1.06	-2.27	-0.29	0.46	1.19	-0.97	0.40	-1.32	-2.84	-1.66	-3.65	-1.96	-3.63	-2.56	-4.45	-2.58	-4.32	-4.32	0.98
4079	-2.53	-1.90	-4.37	-0.82	-0.65	0.94	0.76	-2.10	-3.26	-0.69	-1.04	-0.20	-2.29	-0.88	-2.37	-3.27	-2.42	-4.14	-2.37	-3.96	-2.84	-4.70	-2.74	-4.49	-2.88	0.39
4080	-2.93	-2.39	-4.74	-1.08	-1.00	0.53	0.55	-2.52	-3.68	-0.95	-1.70	-0.84	-2.93	-1.51	-2.94	-3.80	-2.94	-4.54	-2.82	-4.46	-3.38	-5.24	-3.44	-5.15	-1.69	0.88
4081	-2.29	-1.64	-4.17	-0.33	-0.36	1.07	1.29	-1.59	-2.82	-0.93	-0.15	0.59	-1.57	-0.23	-1.93	-3.22	-2.25	-4.20	-2.49	-4.13	-3.04	-4.89	-2.92	-4.62	-2.83	0.49
4082	-2.49	-1.82	-4.39	-0.68	-0.70	1.00	1.61	-2.19	-3.36	-0.68	-1.02	-0.21	-2.33	-0.96	-2.46	-3.44	-2.50	-4.29	-2.48	-4.08	-2.98	-4.84	-2.94	-4.76	-2.98	0.46
4083	-2.15	-1.60	-4.26	0.10	0.66	2.58	2.46	-2.43	-3.46	0.10	-0.61	0.21	-1.86	-0.41	-1.81	-2.89	-1.80	-3.51	-1.75	-3.32	-2.26	-4.16	-2.28	-4.10	-2.40	0.93
4084	-2.87	-2.02	-4.58	-1.05	-0.93	0.30	1.47	-2.60	-3.56	-0.84	-1.21	-0.36	-2.44	-1.02	-2.47	-3.48	-2.44	-4.18	-2.43	-4.06	-3.05	-4.89	-3.00	-4.82	-2.48	0.30

Appendix A4. Centered log ratio transformed data used for PCA and Random Forest.

Sample	Si	Al	Fe	Mn	Mg	Ca	Na	K	Ti	P	LOI	C-Total	C_in_CO2	Non_carb._C	Total S	Cu	Zn	Pb	Cd	Hg	Sn	Tl	In	As	Co	Ni	Se	Mo	Ge	Sb	Ag	Au	W	Bi	B	Rb	Sr	Cs	Ba	Be	Zr
4085	9.57	8.22	7.09	2.03	5.83	5.77	6.89	7.14	5.11	2.32	7.95	6.26	0.85	6.26	6.43	1.23	2.06	-0.58	-4.45	-6.57	-3.06	-2.15	-6.06	1.24	0.64	1.48	-4.45	-1.96	-2.97	-2.42	-4.45	-7.67	-3.76	-2.88	0.30	1.13	1.67	-2.03	2.99	-3.06	1.77
4086	10.22	6.25	9.10	2.49	4.79	7.23	5.16	5.02	3.08	-0.06	9.28	8.01	7.27	7.87	9.20	1.83	3.95	0.39	-2.45	-2.03	-1.75	-4.34	-5.44	2.54	0.81	1.70	-0.56	-1.06	-2.80	-1.53	-3.83	-7.05	-0.37	-2.55	-0.65	-0.65	-0.05	-3.65	0.81	-3.14	0.04
4087	9.39	7.73	7.08	2.87	6.32	5.55	4.61	6.57	3.85	0.44	7.22	4.89	5.46	4.22	4.80	0.28	2.66	-2.41	-3.55	-6.84	-1.72	-3.62	-6.33	-4.02	-1.78	-0.85	-1.11	-2.23	-2.80	-4.54	-4.02	-7.94	-4.02	-4.25	0.73	0.97	-0.77	-3.24	2.62	-2.64	2.54
4090	9.30	8.26	7.67	2.76	6.80	5.46	6.83	6.91	5.22	2.66	7.43	4.67	5.88	2.22	4.12	0.76	1.47	-1.40	-4.58	-11.02	-3.19	-3.58	-6.19	0.80	0.31	1.70	-4.58	-2.10	-2.66	-2.13	-4.58	-7.80	-1.58	-3.70	1.11	1.16	1.84	-2.66	3.30	-2.50	1.59
4091	9.58	8.06	7.42	3.07	5.98	6.42	7.20	6.29	5.08	2.06	6.84	5.97	3.29	5.95	5.58	1.41	3.17	-1.31	-2.92	-10.93	-1.72	-4.05	-6.10	-0.33	0.31	1.02	-4.49	-2.01	-2.04	-6.10	-3.62	-10.93	-3.80	-3.10	0.26	0.79	2.10	-2.41	3.24	-3.10	2.29
4092	10.46	6.92	7.89	2.53	5.16	6.49	5.48	5.62	3.65	-0.02	8.74	8.29	6.50	8.25	7.63	2.50	3.60	-0.01	-2.92	-7.01	-2.41	-4.24	-5.40	0.59	0.78	2.05	-1.31	-1.02	-3.79	-2.76	-3.79	-7.01	-0.61	-2.92	0.16	-0.21	0.16	-3.61	2.01	-3.10	0.73
4093	9.98	6.77	8.52	4.00	6.30	5.09	2.70	4.55	3.44	1.07	9.16	8.63	6.32	8.61	8.17	3.46	4.90	1.92	-1.27	-5.12	-1.61	-4.75	-5.70	-1.61	0.95	2.41	-4.09	-1.10	-2.71	-2.45	-3.40	-6.21	-2.02	-1.68	-1.10	-0.92	-0.92	-4.32	1.12	-3.40	0.47
4094	9.67	7.53	8.55	4.13	6.60	8.29	3.11	3.56	4.36	1.66	8.76	7.69	8.52	6.70	5.63	0.88	1.59	-1.02	-4.19	-3.50	-3.50	-6.32	-5.80	1.30	0.45	0.63	-1.20	-1.71	-2.55	0.26	-4.19	-7.41	-3.50	-3.03	-2.81	-1.71	1.02	-4.01	-0.61	-3.50	1.60
4095	9.33	8.31	7.04	2.98	5.53	5.26	4.58	7.46	4.56	1.91	7.34	4.06	0.66	4.05	5.34	-0.37	1.96	-2.34	-4.64	-6.07	-1.18	-2.56	-6.25	-1.06	-1.18	-1.06	-4.64	-3.26	-3.36	-4.17	-3.48	-11.08	-3.95	-3.61	1.05	1.71	-0.12	-2.30	3.27	-3.26	2.95
4096	8.96	7.54	6.98	1.71	5.15	5.69	5.86	6.35	3.94	1.02	7.39	6.20	4.30	6.16	6.73	0.82	2.56	-1.10	-3.57	-5.97	-1.72	-3.41	-6.66	0.67	-0.71	0.14	-5.06	-2.06	-3.49	-3.20	-5.06	-11.50	-2.98	-3.26	-0.67	0.65	1.19	-3.20	2.37	-2.98	1.96
4097	9.54	7.86	7.53	1.51	4.88	5.35	5.20	6.68	4.68	1.86	7.93	6.58	5.48	6.49	7.22	1.06	0.01	0.05	-4.56	-3.21	-2.07	-3.45	-6.17	1.87	1.02	1.00	-4.56	-2.07	-2.91	0.61	-3.68	-7.78	-3.86	-2.48	1.45	0.70	0.49	-2.99	2.30	-2.48	1.59
4098	9.01	7.41	6.79	1.49	4.84	6.36	6.02	6.31	4.12	1.73	8.32	7.88	6.11	7.84	6.85	2.77	3.94	0.12	-2.30	-5.67	-1.94	-3.42	-6.54	2.21	0.42	1.88	-4.93	-1.25	-3.29	-2.07	-3.65	-7.46	-4.24	-2.27	-0.33	0.76	0.34	-2.59	2.80	-4.24	0.95
4099	9.46	7.25	7.91	1.92	5.08	4.86	6.18	6.08	4.24	2.07	8.46	7.87	3.00	7.87	7.37	1.53	2.98	-2.30	-2.81	-6.72	-2.52	-3.30	-6.21	-0.38	0.90	2.56	-1.39	-1.42	-3.32	-4.82	-4.60	-7.82	-1.83	-2.26	-1.60	0.40	-0.44	-2.88	2.47	-3.91	1.17
4100	9.50	8.33	7.34	2.48	5.39	5.87	4.51	7.44	5.06	2.29	7.84	5.65	5.88	5.24	6.77	0.34	0.31	-2.18	-4.48	-4.20	-2.40	-3.96	-6.09	0.27	-0.26	0.00	-4.48	-3.09	-2.76	-0.70	-3.79	-10.92	-3.79	-3.79	2.00	1.30	0.59	-2.51	3.26	-2.40	1.98
4101	8.79	7.35	7.55	2.09	5.21	5.58	5.51	6.44	4.32	2.15	8.30	7.56	5.31	7.53	7.56	1.24	3.49	2.87	-1.83	-5.68	-2.54	-3.06	-6.64	1.72	0.33	1.35	-5.03	-1.70	-3.17	-1.73	-3.31	-7.15	-4.34	-2.81	0.25	0.80	-0.24	-3.24	2.55	-3.64	1.16
4102	8.45	6.94	7.70	1.40	4.97	5.51	4.99	5.64	3.85	1.66	8.60	8.09	6.15	8.05	7.76	2.03	1.65	0.09	-4.04	-4.74	-3.13	-3.39	-6.82	2.50	0.55	1.69	-0.88	-1.52	-3.72	-1.49	-3.64	-6.48	-1.87	-1.39	2.00	-0.08	1.38	-3.29	2.25	-3.82	0.90
4103	9.52	8.00	8.49	4.01	8.39	6.71	2.54	2.94	5.21	2.17	8.76	7.58	6.65	7.46	6.24	1.88	2.43	-1.25	-2.77	-4.63	-2.86	-4.58	-5.86	1.74	1.82	3.89	-4.25	-1.76	-2.22	-0.87	-4.25	-7.47	-3.55	-3.37	-2.86	-1.48	0.23	-3.37	-1.48	-3.55	0.83
4104	9.37	8.18	6.50	3.08	5.69	6.90	6.44	7.15	4.84	2.64	7.88	6.34	7.35	4.94	4.33	0.99	-0.65	-2.30	-4.60	-11.05	-3.22	-4.04	-6.21	1.75	0.12	1.28	-4.60	-2.12	-2.69	-0.33	-3.91	-6.72	-3.91	-3.12	1.71	1.50	2.32	-1.51	3.33	-2.53	1.60
4105	9.13	7.89	7.62	2.38	6.19	5.03	7.33	4.65	4.56	2.53	7.98	6.88	2.83	6.88	7.29	1.64	2.94	0.94	-3.89	-5.59	-2.28	-4.30	-6.38	1.02	0.68	2.41	-4.77	-2.00	-2.91	-1.50	-4.77	-7.29	-4.08	-2.13	0.31	-1.18	1.08	-3.61	1.75	-3.38	1.49
4106	9.25	8.04	7.56	2.14	6.05	5.04	3.77	7.31	4.90	2.61	7.79	5.90	4.59	5.83	7.20	0.93	0.30	-0.67	-4.69	-7.22	-2.61	-3.12	-6.30	2.28	0.68	1.51	-4.69	-2.21	-2.84	-3.21	-3.66	-3.27	-1.52	-2.39	0.66	1.57	-0.74	-3.21	2.95	-3.31	1.44
4107	9.92	6.80	8.20	2.47	4.83	7.34	6.05	5.23	3.70	1.67	8.95	8.16	7.45	8.02	8.28	1.61	4.16	-0.23	-2.06	-3.31	-1.70	-3.85	-5.79	2.03	0.52	1.49	-4.19	-1.41	-2.80	-2.21	-4.19	-10.63	-3.49	-2.54	-0.85	-0.23	1.03	-3.49	0.84	-3.49	0.73
4108	8.82	7.15	8.47	3.87	6.12	8.36	4.88	5.19	4.94	1.79	8.64	7.35	8.55	4.99	8.17	3.01	2.63	2.96	-3.24	-7.15	-3.93	-6.74	-6.23	0.13	1.12	1.59	-4.62	-2.14	-3.34	-2.98	-3.59	-11.07	-3.93	-3.34	-0.94	-0.40	0.77	-3.24	2.13	-3.93	0.63
4109	8.33	6.90	7.50	2.22	5.18	5.97	4.46	5.53	3.83	1.50	8.63	8.02	6.39	7.97	7.69	1.52	3.17	0.00	-2.89	-2.94	-2.79	-3.33	-6.88	2.12	0.42	1.80	-1.67	-1.58	-3.30	-1.39	-4.11	-6.70	-4.58	-2.34	-0.30	-0.22	1.02	-3.05	1.86	-3.89	0.85
4110	9.48	8.03	7.10	2.05	5.87	5.82	6.89	6.74	4.68	2.47	7.78	6.78	5.46	6.71	6.88	0.97	3.73	-0.69	-2.91	-7.09	-2.08	-3.17	-6.17	1.53	0.57	1.66	-4.56	-1.57	-3.08	-2.91	-4.56	-11.00	-3.87	-2.30	-1.38	1.09	2.21	-2.11	3.32	-3.18	1.54
4111	9.12	7.33	7.34	1.63	5.07	4.66	5.70	6.25	4.11	1.86	8.74	8.45	4.83	8.44	7.35	1.98	4.34	-0.05	-2.06	-4.50	-1.22	-2.89	-5.72	1.89	0.81	1.44	-4.80	-1.34	-2.25	-2.35	-3.77	-8.02	-2.03	-2.35	-0.20	0.68	0.11	-2.72	2.69	-4.11	1.15
4112	9.16	7.94	7.03	1.97	5.88	5.97	5.66	7.09	4.70	2.38	7.77	6.38	5.85	6.20	6.60	0.06	0.12	-0.07	-4.79	-5.93	-2.31	-2.92	-6.40	1.61	0.34	1.04	-4.79	-2.02	-2.94	-2.71	-3.63	-5.81	-2.31	-2.34	0.58	1.46	0.06	-3.14	3.07	-3.41	1.48
4113	8.36	6.66	6.77	1.70	4.23	4.90	3.82	5.73	3.39	1.40	8.64	8.41	5.47	8.40	6.85	2.17	4.41	0.22	-1.90	-3.23	-1.68	-3.23	-6.28	2.33	0.69	2.05	-1.59	-1.15	-3.34	0.22	-2.99	-5.95	-2.37	-2.14	0.06	0.11	0.14	-3.15	1.58	-3.29	0.28
4114	8.74	7.27	8.51	2.47	5.39	4.74	6.40	5.92	4.00	1.78	9.04	8.82	3.52	8.82	8.05	2.71	4.59	-0.61	-1.90	-6.20	-1.59	-3.64	-6.38	-1.30	1.02	1.92	-1.13	-1.08	-3.49	-6.38	-4.77	-11.21	-1.59	-1.37	-1.44	0.14	1.04	-2.91	2.77	-4.08	1.00
4115	9.08	7.84	7.40	1.81	5.08	5.63	7.47	5.88	4.54	2.24	8.77	8.57	5.61	8.55	7.05	2.17	-0.28	-2.41	-4.71	-7.93	-4.02	-6.83	-6.32	1.97	0.86	1.71	-4.71	-0.69	-3.06	-2.58	-4.71	-7.24	-4.02	-2.74	-1.38	-0.19	1.14	-2.79	2.36	-4.02	1.54
4116	9.33	7.49	7.41	3.50	5.87	7.01	4.04	6.48	4.38	2.33	8.05	6.65	7.68	5.21	5.71	0.18	1.12	-2.40	-3.82	-3.84	-2.62	-4.83	-6.31	0.58	0.05	0.47	-4.70	-2.21	-2.78	-0.92	-3.82	-6.13	-1.52	-3.82	0.40	0.49	0.35	-2.78	2.25	-4.01	1.85
4117	8.74	7.29	6.55	1.72	5.25	5.32	6.36	5.95	3.79	1.42	7.59	6.93	4.98	6.89	6.61	1.68	3.86	2.51	-1.61	-6.16	-2.76	-3.62	-6.85	1.76	-0.28	0.98	-1.75	-2.25	-3.07	-2.63	-3.96	-11.69	-2.07	-2.86	-0.56	0.49	1.30	-3.12	2.21	-3.16	1.67
4118	9.66	8.11	6.64	1.80	5.36	5.53	5.03	7.11	5.00	2.40	7.47	5.70	6.06	5.20	4.89	0.96	0.39	-1.47	-4.47	-5.74	-3.08	-3.47	-6.08	1.37	-0.31	0.70	-4.47	-2.39	-2.55	-1.98	-4.47	-7.69	-1.29	-2.67	3.23	1.39	0.79	-2.29	3.18	-3.08	1.59
4119	9.05	7.79	7.40	1.84	5.81	5.91	7.11	6.02	4.46	2.18	7.77	6.59	5.79	6.46	7.23	1.49	2.31	-1.27	-3.82	-6.28	-2.08	-4.89	-6.46	0.17	0.13	1.24	-4.85	-1.39	-2.82	-3.98	-4.85	-4.33	-1.86	-2.51	-0.57	0.41	1.40	-3.82	2.73	-2.77	1.48
4120	9.06	7.97	7.66	3.10	5.98	3.90	4.61	7.15	4.32	1.42	7.43	4.48	1.15	4.47	6.63	0.96	2.65	-1.15	-3.19	-6.96	-1.38	-3.43	-6.45	-0.24	-0.52	-0.09	-4.84	-2.36	-2.93	-2.62	-3.56	-8.06	-4.15	-3.46	0.76	1.76	-1.06	-2.62	2.65	-2.76	2.70
4121	9.71	7.31	9.19	4.68	6.79	7.58	3.81	3.52	4.05	1.08	9.18	7.69	8.45	6.82	8.71	2.56	1.87	0.44	-3.39	-4.41	-2.69	-4.66	-5.69	1.92	1.93	2.06	-1.78	-1.59	-2.29	-0.54	-1.95	-5.69	-3.39	-2.22	-0.90	-1.59	0.35	-3.61	-0.61	-3.39	0.83
4122	8.73	7.46	7.09	1.26	5.19	4.26	3.34	6.82	4.25	1.80	8.49	7.98	4.39	7.97	7.08	2.61	2.08	-0.15	-2.51	-5.72	-1.88	-2.80	-5.98	2.25	0.50	1.59	-5.06	-1.60	-2.98	-2.01	-4.37	-8.28	-4.37	-1.97	0.35	1.22	-1.11	-2.40	2.80	-2.98	1.06
4123	9.26	7.20	7.32	2.00	5.32	4.68	5.08	5.95	4.00	1.73	9.01	8.77	2.69	8.77	7.38	1.95	3.88	-0.90	-2.51	-4.77	-1.91	-2.62	-6.30	1.40	0.82	1.76	-1.29	-1.10	-2.83	-3.12	-4.69	-7.91	-1.91	-2.38	-0.21	0.51	0.36	-2.56	2.47	-3.99	1.14
4124	9.16	8.07	7.25	2.36	5.95	6.18	3.83	7.34	4.65	2.48	7.75	5.82	6.12	5.36	6.86	1.83	0.46	-0.81	-4.76	-5.34	-2.27	-3.09	-6.37	1.46	0.27	1.12	-4.76	-1.58	-2.78	-1.70	-3.88	-5.67	-4.06	-2.46	1.02	1.44	0.18	-1.32	3.05	-2.27	1.61
4125	9.19	7.73	7.70	1.19	4.63	4.54	5.47	6.36	4.31	2.23	7.86	5.61	4.58	5.51	7.58	1.45	1.68	-0.20	-3.93	-4.02	-1.34	-3.61	-6.42	2.17	-0.19	0.81	-4.81	-2.32	-2.51	-0.11	-3.78	-4.50	-1.48	-2.95	2.15	0.64	1.00	-2.68	2.59	-3.42	1.41
4126	9.34	7.98	7.62	2.20	6.04	5.31	6.03	7.03	4.66	2.54	7.59	4.72	4.35	4.51	7.28	3.54	2.45	-0.77	-2.99	-6.76	-0.95	-3.89	-4.45	0.66	0.15	1.12	-4.64	-2.15	-2.42	-3.94	-3.76	-6.47	-3.94	-2.26	0.51	1.33	-0.31	-3.94	2.49	-3.94	1.82
4127	8.67	7.42	7.64	2.14	5.80	4.85	7.01	3.72	4.45	2.10	8.23	7.50	4.35	7.49	7.46	2.10	0.72	1.05	-3.91	-2.75	-1.39	-3.89	-6.69	2.38	1.21	3.06	-1.51	-1.39	-3.05	0.97	-2.95	-6.35	-4.38	-2.10	-1.49	-1.90	0.20	-4.90	0.12	-4.38	1.26
4129	9.62	8.05	6.73	2.87	6.54	6.02	7.46	6.04	4.37	1.81	7.68	6.84	5.58	6.76	5.70	1.46	3.04	-0.87	-3.07	-5.37	-2.37	-4.20	-6.06	0.89	0.04	1.67	-4.45	-1.97	-2.48	-3.76	-4.45	-10.89	-3.76	-2.80	1.01	0.07	2.13	-3.98	2.92	-3.07	1.83
4130	9.20	8.00	6.79	2.16	5.75	5.58	6.29	6.74	4.64	2.07	7.49	5.92	5.44	5.73	6.32	0.86	2.36	-0.12	-3.64	-7.32	-2.72	-2.85	-6.41	0.86	-0.24	1.02	-4.80	-2.03	-2.88	-3.01	-4.80	-7.32	-4.11	-2.72	1.48	1.32	1.49	-2.13	3.07	-2.72	1.62
4131	9.09	7.00	8.34	1.76	4.55	5.91	5.75	6.37	3.78	1.31	8.36	7.31	5.81	7.25	8.31	2.01	3.93	0.59	-1.73	-4.30	-2.28	-3.51	-6.38	1.69	1.05	1.89	-1.28	-1.18	-3.74	-0.12	-3.20	-6.60	-4.08	-2.55	-0.20	0.64	-0.34	-3.74	2.68	-4.08	0.97
4132	9.42	8.02	7.20	0.61	4.84	4.22	5.79	7.04	4.62	2.34	7.94	6.61	3.68	6.60	7.14	0.71	2.93	-0.92	-4.61	-4.89	-2.53	-2.32	-6.22	1.90	0.36	1.19	-4.61	-1.84	-2.64	-2.64	-4.61	-7.83	-3.92	-2.76	0.38	1.31	1.60	-2.10	3.31	-3.23	1.55
4133	9.25	8.01	7.93	2.61	5.95	6.14	7.64	3.84	4.70	1.66	8.13	7.06	5.94	6.97	7.75	1.54	2.52	-1.14	-3.32	-6.21	-2.12	-6.72	-6.21	1.38	0.62	1.63	-4.60	0.94	-3.44	-3.44	-3.58	-6.03	-3.91	-0.57	-0.82	-1.83	-0.13	-4.42	-0.92	-3.22	1.72
4134	8.56	7.48	6.94	2.61	6.09	6.09	5.69	6.13	4.75	1.75	8.52	8.09	3.52	8.08	6.93	1.42	2.92	-0.06	-2.53	-3.86	-1.65	-2.75	-6.03	1.54	0.56	1.30	-5.11	-1.65	-1.61	-2.44	-4.42	-7.64	-4.42	-3.03	0.06	0.64	0.82	-2.50	2.36	-4.42	0.68
4135	8.94	7.33	7.77	1.91	4.76	5.38	5.33	5.88	4.06	1.66	8.66	8.11	5.88	8.08	7.87	1.44	3.57	0.26	-2.54	-5.80	-1.89	-3.21	-6.50	0.92	0.88	1.26	-1.30	-1.55	-2.62	-2.00	-3.72	-7.01	-4.19	-2.44	-0.36	0.47	0.98	-2.44	2.53	-4.19	1.34
4136	9.43	8.12	7.23	0.97	5.57	4.64	6.74	6.22	4.64	1.54	8.29	7.56	3.75	7.55	7.06	1.08	4.41	-0.11	-4.54	-6.15	-2.06	-2.61	-6.15	0.80	0.33	1.72	-4.54	-2.06	-3.26	-2.51	-4.54	-10.98	-3.85	-2.28	1.45	0.53	2.45	-2.32	2.81	-3.15	1.53
4137	8.78	7.29	7.94	3.97	7.67	8.03	2.13	1.15	3.90	1.60	9.05	8.42	8.15	8.19	6.48	1.84	2.75	-0.02	-1.91	-2.02	-2.58	-6.78	-6.27	0.62	0.58	2.48	-2.21	-1.33	-3.18	-0.62	-3.63	-6.09	-3.97	-2.53	-1.48	-2.18	1.80	-4.88	-0.38	-3.97	0.62
4138	9.40	8.11	7.21	3.01	6.43	6.82	5.68	6.96	4.88	2.63	8.04	6.42	7.54	4.59	4.44	0.75	1.09	-1.22	-4.55	-6.67	-3.16	-3.72	-6.16	1.28	0.02	1.23	-4.55	-2.06	-2.83	-1.61	-4.55	-10.99	-3.85	-3.38	1.53	1.36	2.23	-1.88	3.24	-2.47	1.56
4139	9.81	6.96	7.69	1.33	3.58	4.65	5.03	5.33	3.83	2.57	9.03	8.73	3.99	8.73	7.64	3.62	2.15	0.52	-4.30	-4.81	-2.91	-2.89	-5.91	1.50	0.26	1.78	-4.30	-0.84	-2.27	-1.31	-3.27	-7.52	-1.53	-2.73	1.73	-0.21	1.79	-2.73	1.88	-3.61	0.80
4140	9.20	8.00	7.34	3.03	6.52	5.65	3.43	7.42	5.15	2.43	7.49	5.87	2.35	5.86	6.76	1.14	1.11	-2.44	-4.74	-11.19	-2.26	-2.80	-6.35	1.82	0.63	-0.72	-1.00	-2.26	-2.89	-2.66	-4.05	-7.96	-1.57	-4.56	-0.41	1.85	0.25	-2.00	3.18	-3.36	2.18
4141	8.90	6.75	8.42	3.30	7.68	8.69	4.35	3.66	4.02	2.13	7.63	7.16	3.84	7.15	7.58	2.79	0.74	-1.30	-3.76	-7.86	-3.25	-6.76	-6.25	2.66	1.79	3.14	-0.68	-0.25	-3.15	-4.17	-4.64	-11.08	-3.94	-1.49	-1.86	-1.46	3.06	-4.45	1.20	-2.56	1.11
4142	8.69	7.02	7.35	2.95	5.87	7.42	4.04	5.86	3.81	1.24	8.47	7.61	7.84	7.19	7.18	3.73	4.77	-0.75	-1.30	-4.91	-1.00	-4.84	-5.25	2.02	1.51	2.94	-1.43	-1.69	-3.74	-1.10	-3.86	-6.86	-4.33	-3.86	1.51	0.54	0.28	-1.78	2.42	-4.33	0.33
4143	9.59	8.04	7.58	2.04	5.00	6.03	7.02	6.80	5.30	2.80	8.01	7.59	1.55	7.59	7.01	0.84	0.21	-2.14	-4.44	-10.88	-3.05	-3.65	-6.05	0.41	0.79	1.54	-4.44	-1.67	-3.56	-4.26	-3.16	-10.88	-3.75	-2.14	0.21	1.25	1.33	-2.47	3.22	-3.05	1.84
4144	8.89	7.07	8.35	2.78	6.09	7.50	2.95	3.38	4.30	1.72	8.41	7.99	5.88	7.96	7.79	3.10	1.41	0.84	-3.26	-4.43	-1.24	-5.96	-6.43	-2.05	1.44	2.34	-0.93	-1.24	-2.34	-2.00	-3.03	-5.85	-4.13	-1.63	-1.36	-1.49	0.77	-4.13	-1.36	-4.13	0.82
4145	9.22	7.38	9.26	2.53	5.05	5.07	3.72	6.75	4.30	2.18	9.09	6.83	5.67	6.74	9.36	0.51	1.18	0.38	-3.34	-3.35	-2.98	-3.37	-5.98	2.73	0.58	0.91	-4.37	-1.88	-3.68	-1.01	-4.37	-10.81	-3.68	-3.68	0.06	0.73	-0.21	-2.29	2.01	-3.68	1.49
4146	9.17	7.51	7.07	2.50	3.95	6.34	5.22	6.25	3.14	-1.13	7.60	6.20	6.58	5.69	6.88	-1.03	2.36	-2.60	-3.51	-7.43	-1.90	-4.27	-6.51	0.73	-1.01	0.40	-4.90	-1.90	-3.04	-2.68	-4.90	-8.12	-4.21	-3.62	0.82	0.53	0.91	-2.26	2.31	-2.82	1.84
4147	9.03	7.45	6.70	2.46	6.14	5.28	6.29	6.00	3.78	0.57	7.64	7.20	4.82	7.17	5.51	0.32	0.43	-2.70	-5.00	-4.85	-2.52	-4.14	-6.61	-0.52	-0.39	0.70	-5.00	-1.82	-3.61	-3.84	-4.13	-8.22	-4.31	-3.97	-0.18	0.32	0.86	-3.35	3.62	-2.01	2.41
4148	8.54	6.95	7.10	2.09	4.74	6.18	5.66	5.79	3.87	1.74	8.07	7.43	5.92	7.37	7.27	3.35	5.02	0.19	-1.22	-2.80	-1.51	-3.14	-4.82	2.28	0.94	1.76	-1.15	-1.71	-2.30	-1.15	-3.26	-7.41	-4.60	-1.95	-0.65	0.27	-0.24	-3.26	2.02	-3.21	0.37
4149	8.63	7.32	7.64	2.00	5.75	5.55	4.05	6.51	4.14	1.62	8.62	8.33	-11.49	8.33	7.21	3.40	4.74	-0.66	-1.33	-3.01	-1.36	-3.32	-4.57	3.34	2.60	4.38	-0.76	-1.17	-3.25	-2.38	-3.40	-8.26	-4.35	-2.74	0.13	0.79	-0.95	-2.43	2.78	-4.35	0.59
4150	9.66	7.63	6.81

Appendix A4. Centered log ratio transformed data used for PCA and Random Forest.

Sample	Hf	Nb	Ta	Ga	Sc	V	Cr	Th	U	Y	La	Ce	Pr	Nd	Sm	Eu	Gd	Tb	Dy	Ho	Er	Tm	Yb	Lu	Br	F
4085	-1.96	-1.43	-3.86	-0.07	-0.31	1.45	1.28	-1.81	-3.05	-0.67	-0.57	0.26	-1.88	-0.54	-2.15	-3.27	-2.41	-4.14	-2.37	-3.98	-2.91	-4.78	-2.86	-4.62	-4.45	0.85
4086	-3.65	-2.96	-5.44	-1.35	-1.18	0.04	0.24	-2.92	-3.62	-1.75	-1.62	-0.84	-3.02	-1.64	-3.12	-4.01	-3.29	-4.97	-3.34	-4.97	-3.96	-5.66	-3.83	-5.44	-1.45	1.47
4087	-1.09	-0.03	-2.62	-0.20	-1.70	-1.54	-0.72	-1.24	-2.50	1.09	0.71	1.57	-0.50	0.91	-0.62	-2.81	-0.66	-2.41	-0.61	-2.18	-1.08	-2.92	-0.99	-2.75	-2.74	0.58
4090	-2.10	-1.40	-3.95	0.03	0.07	1.88	2.32	-1.53	-2.76	-0.36	0.08	0.85	-1.27	0.11	-1.56	-2.94	-1.78	-3.70	-2.01	-3.70	-2.64	-4.50	-2.64	-4.47	-2.79	0.72
4091	-1.40	-1.05	-3.50	-0.16	-0.47	1.02	0.62	-1.88	-3.15	0.19	-0.08	0.73	-1.37	0.05	-1.45	-3.04	-1.47	-3.24	-1.52	-3.13	-2.07	-3.93	-2.06	-3.88	-4.49	0.81
4092	-3.10	-2.51	-4.81	-1.02	-1.25	0.37	0.33	-2.72	-3.64	-1.02	-1.15	-0.39	-2.52	-1.16	-2.67	-3.58	-2.72	-4.53	-2.84	-4.45	-3.37	-5.22	-3.35	-5.22	-0.67	1.51
4093	-3.22	-2.71	-5.01	-0.76	-1.13	0.51	0.93	-2.44	-3.79	-0.92	-1.70	-0.79	-2.87	-1.49	-2.91	-3.48	-2.93	-4.54	-2.80	-4.37	-3.27	-5.01	-3.09	-4.83	-1.00	1.20
4094	-1.98	-1.03	-3.86	-0.51	-0.98	0.59	0.07	-2.31	-3.63	-0.24	-1.19	-0.27	-2.24	-0.68	-1.92	-3.15	-1.98	-3.78	-2.01	-3.52	-2.33	-4.12	-2.10	-3.80	-1.68	1.10
4095	-0.39	0.59	-1.71	0.30	-0.66	-0.55	-4.64	-0.46	-1.87	1.29	0.80	1.67	-0.45	0.92	-0.57	-2.96	-0.52	-2.12	-0.24	-1.82	-0.80	-2.72	-0.91	-2.82	-4.64	0.66
4096	-1.47	-0.24	-2.80	-0.58	-1.09	-0.11	-1.14	-1.52	-2.83	0.96	0.36	1.23	-0.85	0.55	-0.90	-3.10	-0.91	-2.64	-0.87	-2.47	-1.41	-3.27	-1.38	-3.21	-5.06	0.24
4097	-2.14	-1.62	-3.97	-0.28	-0.92	0.92	0.24	-2.48	-3.70	-0.53	-0.31	0.35	-1.80	-0.46	-2.31	-3.97	-2.44	-4.14	-2.40	-3.99	-2.95	-5.00	-3.15	-5.00	-4.56	0.74
4098	-2.76	-2.09	-4.49	-0.78	-0.90	0.71	0.29	-2.22	-3.44	-0.78	-1.07	-0.26	-2.38	-1.01	-2.53	-3.39	-2.66	-4.35	-2.62	-4.20	-3.06	-4.93	-3.01	-4.69	-1.74	0.36
4099	-2.62	-1.93	-4.49	-1.13	-0.50	0.72	2.30	-2.89	-3.95	-0.22	-0.59	0.26	-1.82	-0.40	-1.97	-3.31	-2.06	-3.81	-2.04	-3.63	-2.53	-4.45	-2.52	-4.29	-1.39	0.70
4100	-1.71	-1.01	-3.48	0.08	-0.79	1.13	0.45	-2.09	-3.45	-0.32	0.01	0.74	-1.42	-0.07	-1.74	-3.29	-2.00	-3.79	-2.04	-3.69	-2.63	-4.56	-2.59	-4.40	-2.83	0.82
4101	-2.45	-1.79	-4.34	-0.75	-0.94	0.67	0.67	-2.19	-3.63	-0.81	-1.51	-0.64	-2.63	-1.14	-2.55	-4.01	-2.59	-4.42	-2.66	-4.17	-3.01	-4.88	-2.99	-4.69	-1.32	0.27
4102	-2.79	-2.10	-4.57	-1.18	-1.59	0.24	0.01	-2.52	-3.79	-1.18	-0.70	-0.03	-2.21	-0.91	-2.71	-3.89	-2.96	-4.71	-2.94	-4.51	-3.35	-5.25	-3.29	-5.06	-0.41	0.09
4103	-2.77	-2.22	-4.90	-0.38	0.68	2.40	4.95	-3.44	-4.63	-0.22	-1.98	-1.06	-2.98	-1.36	-2.44	-3.91	-2.13	-3.64	-1.80	-3.41	-2.34	-4.21	-2.35	-4.13	-4.25	1.05
4104	-2.06	-1.46	-4.02	-0.13	-0.46	1.39	1.88	-1.50	-2.67	-0.92	0.23	0.94	-1.22	0.13	-1.67	-3.00	-2.04	-4.06	-2.43	-4.13	-3.07	-4.99	-3.07	-4.88	-4.60	0.69
4105	-2.16	-1.59	-4.10	-0.61	-0.51	1.01	1.00	-1.60	-3.07	-0.55	-0.23	0.50	-1.64	-0.28	-1.94	-3.25	-2.15	-3.96	-2.28	-3.89	-2.82	-4.81	-2.86	-4.62	-4.77	0.53
4106	-2.24	-1.72	-4.22	-0.22	-0.37	1.41	1.79	-1.62	-2.94	-0.67	-1.23	-0.33	-2.38	-0.91	-2.25	-3.48	-2.28	-4.04	-2.33	-3.98	-2.87	-4.82	-2.92	-4.78	-3.12	0.60
4107	-2.90	-2.27	-4.70	-1.19	-1.26	0.25	0.20	-2.62	-3.55	-1.01	-1.09	-0.37	-2.50	-1.07	-2.61	-3.49	-2.69	-4.36	-2.71	-4.36	-3.29	-5.21	-3.23	-5.01	-1.39	1.11
4108	-2.98	-2.32	-4.90	-0.84	-0.38	1.71	-0.77	-2.62	-4.06	-0.15	-0.41	0.28	-1.80	-0.26	-1.75	-3.18	-1.68	-3.58	-1.85	-3.40	-2.34	-4.26	-2.37	-4.15	-2.21	0.67
4109	-2.86	-2.06	-4.66	-1.11	-1.11	0.42	0.74	-2.76	-3.97	-0.80	-1.02	-0.23	-2.33	-0.93	-2.40	-3.25	-2.47	-4.17	-2.44	-4.03	-2.92	-4.80	-2.88	-4.60	-2.05	0.02
4110	-2.15	-1.67	-4.23	-0.54	-0.63	1.04	1.04	-1.85	-3.00	-1.23	-0.37	0.35	-1.78	-0.41	-2.12	-3.49	-2.38	-4.31	-2.71	-4.45	-3.31	-5.22	-3.36	-5.22	-2.34	0.74
4111	-2.54	-2.03	-4.59	-0.71	-0.74	0.64	0.58	-2.77	-3.91	-1.11	-1.17	-0.36	-2.47	-1.05	-2.57	-3.58	-2.67	-4.41	-2.70	-4.31	-3.20	-5.03	-3.14	-4.84	-4.80	0.50
4112	-2.18	-1.61	-4.08	-0.27	-0.41	1.29	1.31	-1.49	-2.82	-0.63	-1.40	-0.44	-2.44	-1.01	-2.35	-3.34	-2.37	-4.06	-2.24	-3.88	-2.85	-4.79	-2.95	-4.79	-2.21	0.51
4113	-3.39	-2.65	-5.03	-1.09	-1.22	0.35	0.39	-2.46	-3.84	-1.09	-1.10	-0.38	-2.51	-1.15	-2.73	-3.60	-2.74	-4.48	-2.73	-4.32	-3.29	-5.15	-3.28	-4.98	-1.07	-0.07
4114	-2.64	-2.10	-4.46	-0.82	-0.76	1.06	0.65	-2.07	-3.27	-0.82	-0.99	-0.18	-2.29	-0.87	-2.34	-3.11	-2.42	-4.16	-2.41	-4.06	-2.94	-4.81	-2.93	-4.69	-2.43	0.53
4115	-2.13	-1.47	-4.02	-0.38	-0.03	0.98	0.70	-1.83	-2.99	-0.55	-0.27	0.49	-1.64	-0.24	-1.78	-3.10	-2.02	-3.87	-2.16	-3.77	-2.63	-4.46	-2.52	-4.24	-0.36	0.59
4116	-1.93	-0.95	-3.49	-0.67	-1.26	0.02	-1.32	-2.42	-3.66	0.02	-0.20	0.60	-1.51	-0.07	-1.59	-3.00	-1.60	-3.41	-1.68	-3.31	-2.23	-4.16	-2.20	-4.03	-4.70	0.60
4117	-2.03	-1.44	-4.11	-0.86	-1.28	0.17	0.36	-1.40	-2.79	-0.64	0.08	0.81	-1.40	-0.11	-1.96	-3.76	-2.31	-4.13	-2.32	-3.89	-2.75	-4.57	-2.62	-4.37	-2.86	0.05
4118	-2.12	-1.51	-4.10	-0.14	-0.35	1.54	1.76	-1.57	-2.62	-0.44	0.03	0.70	-1.46	-0.13	-1.90	-3.23	-2.18	-4.05	-2.37	-3.95	-2.87	-4.79	-2.87	-4.64	-4.47	0.83
4119	-2.18	-1.58	-4.10	-0.42	-0.60	1.06	0.95	-1.47	-2.81	-0.83	-0.14	0.57	-1.57	-0.23	-1.95	-3.37	-2.23	-4.08	-2.41	-4.06	-3.01	-4.93	-2.94	-4.70	-4.85	0.45
4120	-0.89	0.09	-2.53	-0.06	-1.14	-0.57	-1.53	-1.25	-2.89	0.73	-0.17	0.76	-1.32	0.12	-1.28	-3.08	-1.20	-2.79	-0.98	-2.56	-1.55	-3.63	-1.87	-3.74	-2.67	0.46
4121	-2.92	-2.43	-5.00	-0.50	-1.46	0.53	0.59	-3.29	-4.59	-1.31	-1.20	-0.57	-2.75	-1.34	-2.89	-4.08	-2.88	-4.59	-2.99	-4.59	-3.51	-5.51	-3.56	-5.22	-4.08	1.22
4122	-2.61	-1.94	-4.41	-0.63	-0.39	0.81	0.74	-1.71	-2.99	-0.90	-0.80	0.14	-1.95	-0.58	-2.16	-2.87	-2.39	-4.15	-2.37	-4.01	-2.87	-4.70	-2.65	-4.35	-1.97	0.24
4123	-2.61	-2.17	-4.61	-0.82	-0.65	0.57	0.15	-2.48	-3.75	-0.66	-1.24	-0.44	-2.51	-1.07	-2.41	-3.47	-2.44	-4.08	-2.29	-3.90	-2.84	-4.73	-2.79	-4.57	-4.69	0.61
4124	-2.06	-1.55	-4.06	-0.15	-0.55	1.22	0.93	-1.42	-2.67	-0.73	-1.41	-0.52	-2.57	-1.10	-2.53	-3.79	-2.51	-4.26	-2.50	-4.03	-2.86	-4.68	-2.79	-4.58	-4.76	0.54
4125	-2.26	-1.87	-4.36	-0.38	-0.94	0.87	0.25	-2.20	-3.48	-0.71	-0.86	-0.06	-2.18	-0.75	-2.25	-3.88	-2.33	-4.16	-2.44	-4.04	-2.96	-4.85	-2.91	-4.69	-4.81	0.49
4126	-1.92	-1.58	-4.07	-0.16	-0.75	0.83	0.11	-2.16	-3.43	-0.31	-1.02	-0.16	-2.21	-0.73	-2.16	-3.39	-2.14	-3.85	-2.11	-3.68	-2.57	-4.45	-2.44	-4.30	-3.07	0.66
4127	-2.41	-1.65	-4.19	-0.86	-0.53	0.99	2.49	-2.04	-3.13	-0.56	-2.33	-1.07	-2.83	-1.19	-2.27	-3.25	-2.23	-3.98	-2.22	-3.85	-2.76	-4.61	-2.65	-4.36	-5.08	0.22
4129	-1.97	-1.87	-3.93	-0.23	-0.72	0.40	1.21	-1.72	-2.99	-0.58	-0.06	0.69	-1.48	-0.15	-1.91	-3.29	-2.15	-3.96	-2.28	-3.91	-2.84	-4.73	-2.80	-4.53	-4.45	0.85
4130	-2.05	-1.47	-3.94	-0.19	-0.67	1.07	1.11	-1.27	-2.41	-0.93	-0.09	0.62	-1.56	-0.21	-1.93	-3.13	-2.17	-4.09	-2.51	-4.15	-3.17	-5.07	-3.17	-4.97	-2.88	0.50
4131	-2.74	-2.07	-4.62	-0.98	-1.36	-0.01	0.35	-2.91	-3.94	-0.82	-1.45	-0.58	-2.62	-1.20	-2.58	-3.83	-2.54	-4.32	-2.57	-4.12	-3.04	-4.94	-3.14	-4.85	-4.77	0.53
4132	-2.13	-1.54	-4.00	-0.18	-0.50	1.05	0.99	-1.58	-2.91	-0.92	0.01	0.71	-1.45	-0.11	-1.84	-3.26	-2.20	-4.17	-2.48	-4.17	-3.11	-5.00	-3.16	-4.89	-4.61	0.69
4133	-1.97	-1.33	-3.82	-0.45	-0.65	1.56	0.45	-1.24	-2.60	-0.65	-0.60	0.21	-1.88	-0.47	-1.99	-3.21	-2.21	-3.99	-2.27	-3.83	-2.72	-4.57	-2.59	-4.33	-4.60	0.69
4134	-2.94	-2.29	-5.03	-0.55	-0.23	1.74	1.24	-2.88	-3.89	-0.55	-1.47	-0.62	-2.67	-1.21	-2.55	-3.14	-2.38	-4.04	-2.25	-3.84	-2.77	-4.62	-2.76	-4.55	-2.31	0.19
4135	-2.37	-1.91	-4.44	-0.67	-1.16	0.56	-0.31	-2.57	-3.81	-0.93	-0.85	-0.08	-2.19	-0.80	-2.32	-3.49	-2.50	-4.30	-2.58	-4.21	-3.09	-5.01	-3.09	-4.81	-4.89	0.41
4136	-2.12	-1.87	-4.26	-0.32	-0.47	1.29	1.05	-1.95	-3.46	-0.85	-0.39	0.32	-1.85	-0.47	-2.12	-2.82	-2.29	-4.15	-2.38	-4.02	-2.99	-4.87	-2.95	-4.67	-4.54	0.76
4137	-3.09	-2.53	-5.05	-1.20	-0.68	0.84	2.56	-1.92	-3.51	-0.79	-0.50	0.12	-1.94	-0.59	-2.05	-3.06	-2.14	-4.07	-2.47	-4.12	-3.05	-4.99	-3.06	-4.79	-2.36	0.64
4138	-2.13	-1.55	-4.08	-0.12	-0.32	1.43	1.67	-1.68	-2.78	-0.68	-0.07	0.67	-1.46	-0.09	-1.78	-3.12	-2.03	-3.92	-2.27	-3.94	-2.91	-4.82	-2.96	-4.72	-4.55	0.75
4139	-2.91	-2.44	-4.75	-0.97	-0.07	0.13	1.90	-2.71	-3.83	-1.53	-0.91	-0.17	-2.30	-0.85	-2.42	-3.46	-2.62	-4.43	-2.81	-4.43	-3.41	-5.22	-3.22	-4.88	-4.30	1.00
4140	-1.57	-1.03	-3.42	-0.18	-1.94	0.92	0.05	-1.99	-3.33	0.04	0.00	0.69	-1.47	-0.08	-1.65	-2.73	-1.66	-3.45	-1.71	-3.32	-2.26	-4.18	-2.24	-4.03	-1.83	0.55
4141	-2.61	-1.84	-4.56	-1.64	0.34	1.22	1.00	-2.04	-3.20	0.05	-0.53	0.41	-1.68	-0.27	-1.62	-2.59	-1.65	-3.38	-1.61	-3.21	-2.11	-3.94	-1.98	-3.62	-4.64	0.66
4142	-3.30	-2.76	-5.35	-1.15	-1.01	0.52	1.47	-3.09	-4.23	-1.15	-1.78	-1.00	-3.13	-1.73	-3.16	-4.08	-2.99	-4.66	-2.86	-4.39	-3.34	-5.30	-3.34	-5.06	-2.09	0.28
4143	-1.74	-0.87	-3.37	-0.22	-0.29	1.73	0.81	-1.15	-2.68	-0.11	0.07	0.88	-1.27	0.11	-1.45	-2.89	-1.58	-3.44	-1.80	-3.48	-2.54	-4.52	-2.67	-4.52	-4.44	0.86
4144	-2.75	-1.91	-4.52	-0.95	-0.62	1.09	2.30	-2.45	-3.65	-0.55	-0.95	-0.06	-2.16	-0.72	-2.18	-2.74	-2.20	-3.97	-2.27	-3.87	-2.80	-4.75	-2.81	-4.58	-2.16	0.47
4145	-2.15	-1.55	-4.19	-0.79	-1.13	0.01	-0.33	-2.51	-3.76	-0.50	-0.50	0.31	-1.82	-0.43	-2.00	-3.30	-2.12	-3.87	-2.12	-3.76	-2.70	-4.59	-2.66	-4.45	-4.37	0.93
4146	-1.47	-0.26	-2.89	-0.29	-2.51	-1.72	-1.41	-1.44	-2.93	1.37	0.55	1.39	-0.68	0.72	-0.75	-2.87	-0.70	-2.37	-0.55	-2.09	-1.00	-2.88	-1.00	-2.82	-4.90	0.40
4147	-1.16	-0.37	-2.74	-0.72	-1.98	0.19	-0.71	-0.52	-1.78	0.66	0.92	1.63	-0.58	0.72	-0.91	-2.31	-1.08	-2.89	-1.16	-2.77	-1.71	-3.60	-1.72	-3.54	-5.00	0.30
4148	-3.32	-2.74	-5.47	-0.96	-1.09	0.66	0.67	-3.32	-4.45	-0.77	-1.10	-0.36	-2.48	-1.08	-2.62	-3.32	-2.65	-4.49	-2.74	-4.34	-3.24	-5.14	-3.23	-4.96	-5.29	0.01
4149	-3.02	-2.49	-5.08	-0.71	-0.49	1.23	3.44	-2.88	-3.86	-0.77	-1.25	-0.45	-2.59	-1.20	-2.64	-3.39	-2.61	-4.27	-2.45	-4.01	-2.86	-4.74	-2.84	-4.57	-1.64	0.25
4150	-2.02	-1.33	-3.54	-0.64	-1.29	0.01	-0.25	-1.32	-2.74	0.06	0.00	0.77	-1.38	-0.05	-1.66	-3.37	-1.81	-3.52	-1.78	-3.40	-2.32	-4.17	-2.30	-4.12	-4.51	0.79
4151	-2.23	-1.76	-4.38	-0.11	-0.26	1.78	2.03	-2.31	-3.54	-0.88	-0.60	0.17	-1.95	-0.57	-2.18	-3.42	-2.22	-3.99	-2.29	-3.87	-2.78	-4.72	-2.76	-4.59	-4.21	1.09
4152	-2.42	-1.94	-4.30	-0.52	-0.81	1.00	0.61	-2.27	-3.40	-0.68	-0.85	-0.04	-2.21	-0.84	-2.35	-3.08	-2.43	-4.18	-2.45	-4.08	-3.01	-4.88	-2.96	-4.68	-4.55	0.75
4153	-2.43	-1.83	-4.43	-0.47	-0.82	0.84	0.33	-1.89	-3.39	-0.57	-1.32	-0.26	-2.32	-0.95	-2.31	-3.33	-2.37	-4.08	-2.32	-3.94	-2.85	-4.77	-2.88	-4.74	-4.85	0.45
4154	-2.35	-1.65	-4.17	-0.48	-0.76	0.70	0.87	-1.32	-2.73	-0.77	-0.26	0.47	-1.72	-0.41	-2.12	-3.28	-2.36	-4.28	-2.55	-4.19	-3.16	-5.04	-3.14	-4.86	-4.86	0.43
4155	-2.52	-1.95	-4.42	-0.65	-0.74	0.60	0.92	-1.85	-3.06	-0.99	-0.53	0.20	-1.99	-0.68	-2.35	-3.58	-2.65	-4.47	-2.74	-4.39	-3.35	-5.19	-3.35	-5.09	-3.07	0.43
4156	-2.30	-1.56	-3.97	-0.04	0.51	2.35	2.21	-1.63	-2.68	-0.08	-0.55	0.21	-1.88	-0.45	-1.90	-3.17	-1.93	-3.67	-1.88	-3.47	-2.42	-4.31	-2.46	-4.22	-4.56	0.74
4157	-2.02	-1.39	-4.01	-0.38	-0.51	1.00	1.00	-1.30	-2.52	-0.33	0.06	0.79	-1.37	-0.07	-1.82	-3.22	-2.07	-3.91	-2.18	-3.80	-2.69	-4.62	-2.74	-4.51	-4.66	0.64
4158	-1.75	-1.20	-3.87	0.17	-0.27	1.28	1.35	-1.15	-2.30	-0.44	0.30	1.01	-1.17	0.16	-1.57	-2.91	-1.85	-3.78	-2.20	-3.90	-2.89	-4.78	-2.88	-4.62	-2.91	0.91
4159	-1.90	-1.34	-3.93	-0.12	-0.58	1.01	0.92	-1.15	-2.38	-0.55	0.18	0.86	-1.33	-0.03	-1.79	-3.18	-2.15	-4.01	-2.34	-4.01	-2.88	-4.82	-2.91	-4.60	-3.48	0.66
4160	-2.10	-1.68	-4.06	-0.36	-0.55	0.92	0.87	-1.24	-2.47	-0.70	-0.21	0.55	-1.59	-0.26	-1.99	-3.25	-2.28	-4.12	-2.49	-4.08	-3.01	-4.92	-3.01	-4.72	-4.79	0.51
4161	-1.93	-2.06	-4.82	-0.21	-0.82	0.89	1.27	-3.36	-4.32	-0.65	-0.94	-0.05	-2.07	-0.63	-2.19	-3.34	-2.32	-4.28	-2.57	-4.20	-3.14	-5.06	-3.16	-4.97	-2.59	1.06
4162	-1.99	-1.45	-3.94	-0.38	-0.71	0.99	0.29	-1.24	-2.55	-0.22	0.04	0.77	-1.39	-0.06	-1.69	-3.21	-1.92	-3.76	-2.08	-3.66	-2.58	-4.44	-2.52	-4.32	-4.86	0.44
4163	-2.41	-1.82	-4.28	-0.59	-0.78	0.97	0.68	-2.82	-4.04	-0.80	-1.04	-0.26	-2.34	-0.91	-2.39	-3.68	-2.41	-4.14	-2.35	-3.96	-2.90	-4.75	-2.85	-4.64	-3.27	0.55
4164	-2.03	-1.86	-4.37	0.07	-0.39	1.48	1.18	-2.39	-3.80	-1.08	-0.28	0.37	-1.84	-0.55	-2.15	-3.19	-2.34	-4.23	-2.57	-4.23	-3.20	-5.15	-3.22	-4.99	-4.41	0.89
4165	-2.02	-1.54	-4.04	-0.32	-1.02	0.78	0.33	-2.18	-3.52	-0.85	-0.13	0.60	-1.50	-0.17	-1.92	-3.18	-2.22	-4.09	-2.48	-4.09	-3.04	-4.93	-3.04	-4.81	-2.09	0.76
4166	-1.10	-0.61	-3.13	0.56	-0.38	1.35	0.89	-1.24	-2.69	-0.14	-0.49	0.27	-1.84	-0.38	-1.78	-2.70	-1.79	-3.58	-1.84	-3.38	-2.29	-4.10	-2.15	-3.87	-3.82	1.47
4167	-2.41	-2.03	-4.58	-0.43	-1.07	0.61	0.22	-2.79	-3.97	-0.71	-0.56	0.13	-2.02	-0.62	-2.23	-3.55	-2.31	-4.17	-2.44	-4.09	-2.98	-4.86	-2.92	-4.67	-4.58	0.71
4168	-1.87	-1.40	-3.84	0.03	-0.61	1.44	0.86	-2.06	-3.51	-0.48	-0.31	0.48	-1.66	-0.32	-1.95	-3.28	-2.11	-3.94	-2.20	-3.77	-2.65	-4.58	-2.60	-4.36	-4.36	0.94
4169	-2.32	-2.01	-5.07	0.36	1.48	3.26	3.43	-4.13	-4.94	0.58	-1.52	-0.60	-2.45	-0.75	-1.85	-2.71	-1.48	-3.13	-1.29	-2.81	-1.73	-3.58	-1.74	-3.49	-3.80	1.50
4170	-2.08	-1.52	-4.31	-0.23	0.91	2.90	2.10	-3.89	-5.21	0.18	-1.25	-0.33	-2.25	-0.70	-1.86	-3.26	-1.64	-3.27	-1.45	-2.99	-1.93	-3.82	-1.90	-3.67	-2.08	0.91
4171	-1.86	-1.42	-3.76	-0.03	-0.92	0.50	0.17	-1.71	-3.18	-0.46	-0.60	0.18	-2.00	-0.70	-2.29	-3.19	-2.41	-4.02	-2.28	-3.85	-2.76	-4.59	-2.70	-4.45	-4.41	0.89

Appendix A4. Centered log ratio transformed data used for PCA and Random Forest.

Sample	Si	Al	Fe	Mn	Mg	Ca	Na	K	Ti	P	LOI	C-Total	C_in_CO2	Non_carb._C	Total S	Cu	Zn	Pb	Cd	Hg	Sn	Tl	In	As	Co	Ni	Se	Mo	Ge	Sb	Ag	Au	W	Bi	B	Rb	Sr	Cs	Ba	Be	Zr
4172	10.05	8.05	8.04	3.15	7.08	6.12	6.98	5.13	4.80	2.62	8.45	8.06	3.74	8.06	5.97	1.56	0.78	-0.87	-4.04	-7.26	-3.35	-4.56	-5.65	-0.26	1.14	1.97	-4.04	-1.27	-4.04	-4.96	-4.04	-7.26	-0.46	-4.27	-0.58	-0.71	1.10	-3.35	1.48	-3.35	1.62
4173	9.09	7.63	7.79	2.03	6.78	6.90	6.98	5.00	4.42	2.38	8.77	8.45	3.28	8.45	7.44	2.97	-0.23	-1.32	-4.66	-7.88	-3.96	-5.68	-6.27	-1.88	1.28	2.67	-0.19	-0.38	-3.78	-3.96	-4.66	-7.88	-3.96	-1.99	-0.09	-0.97	1.12	-4.19	0.95	-3.96	1.23
4174	8.85	7.74	7.96	3.40	5.53	7.70	6.84	5.94	5.19	2.85	8.84	7.89	7.94	7.55	8.10	0.05	1.89	-2.40	-4.01	-7.93	-2.63	-6.83	-6.32	1.61	0.10	0.81	-4.71	-3.32	-3.32	-2.04	-4.71	-6.13	-4.01	-4.93	0.11	0.59	1.85	-2.58	2.54	-3.32	1.61
4175	9.47	8.08	7.22	1.91	6.17	4.55	6.00	6.71	4.77	2.54	7.97	7.25	0.73	7.25	6.03	1.76	2.99	-1.24	-4.57	-7.79	-2.49	-3.68	-6.18	0.58	0.16	1.65	-4.57	-2.08	-3.00	-4.10	-3.41	-7.79	-3.88	-2.59	1.60	0.91	2.86	-2.65	3.46	-2.49	1.66
4176	10.65	7.18	7.73	3.58	4.62	6.35	6.45	5.75	3.72	1.53	8.88	8.74	6.42	8.71	6.88	0.97	4.34	-1.33	-1.99	-10.08	-2.94	-5.76	-5.24	-1.15	0.64	2.21	-3.63	-0.86	-2.61	-3.16	-3.63	-6.85	-0.17	-3.16	0.52	0.15	0.84	-3.16	2.15	-2.94	0.80
4177	9.98	6.87	9.22	4.96	6.18	6.54	5.89	4.24	3.82	1.11	8.48	7.29	6.62	7.14	8.76	2.41	4.75	-0.10	-1.33	-4.43	-1.56	-6.17	-5.66	-0.02	0.72	1.68	-4.05	-1.97	-2.77	-2.89	-4.05	-7.27	-0.87	-3.36	2.97	-1.05	0.05	-3.87	0.95	-3.36	0.70
4178	9.55	8.22	6.95	2.19	5.95	6.33	6.83	7.21	4.90	2.90	7.73	6.60	6.07	6.43	6.06	1.28	2.77	-1.00	-4.46	-10.90	-3.08	-3.48	-6.07	-1.98	-0.04	1.13	-4.46	-2.38	-2.98	-3.99	-3.77	-10.90	-1.47	-3.08	-0.08	1.34	2.63	-2.29	3.33	-3.08	1.92
4179	9.18	7.64	7.86	1.76	4.93	5.57	6.32	6.56	4.35	1.83	8.35	8.01	4.49	8.00	7.42	1.31	4.65	-0.29	-1.68	-7.24	-1.72	-3.75	-5.63	-0.93	0.87	1.99	-4.72	-1.38	-3.69	-2.05	-4.02	-6.33	-4.02	-3.15	0.00	0.31	0.87	-4.25	3.58	-3.33	1.38
4180	9.51	8.01	7.01	3.62	6.82	7.46	7.02	6.70	3.97	2.44	8.43	7.88	7.18	7.73	6.07	1.14	3.04	0.30	-3.04	-6.95	-1.65	-4.65	-6.03	-3.73	-0.28	0.85	-4.42	-2.34	-2.77	-3.95	-4.42	-10.87	-3.73	-3.39	0.18	0.91	2.18	-3.14	2.63	-2.34	1.58
4181	8.64	6.89	8.39	3.28	5.90	8.24	5.34	4.99	3.97	1.69	8.78	8.44	8.29	8.17	7.81	2.43	3.63	-0.39	-1.95	-7.94	-3.34	-6.85	-6.33	-2.65	1.32	2.10	-4.73	-0.63	-3.85	-2.81	-3.85	-6.33	-4.03	-2.06	-1.26	-0.77	1.00	-4.03	1.83	-4.03	0.99
4182	9.74	7.67	8.84	5.55	6.78	6.99	5.59	6.77	4.52	1.87	8.07	6.84	7.20	6.35	7.32	1.51	3.22	-0.18	-3.05	-10.65	-2.13	-4.10	-5.82	-3.52	0.35	0.43	-4.21	-2.82	-2.42	-3.74	-3.05	-6.74	-3.52	-3.52	-2.82	1.15	0.01	-1.16	2.10	-3.52	1.69
4183	9.70	7.84	8.86	5.28	6.38	6.76	6.54	6.76	4.79	2.03	8.35	6.90	7.49	6.21	8.28	0.52	1.90	-0.76	-3.20	-10.67	-3.54	-4.36	-5.84	-0.90	-0.39	1.77	-1.54	-2.15	-3.20	-2.26	-3.35	-10.67	-3.54	-3.35	1.81	1.25	2.05	-1.46	2.62	-3.54	1.33
4184	10.20	8.65	8.67	4.63	8.65	5.21	5.88	4.95	4.29	1.42	8.78	7.49	3.86	7.48	3.64	-2.36	3.63	-1.44	-3.74	-10.18	-3.05	-3.87	-5.35	0.35	1.27	2.59	-1.10	0.04	-2.02	-5.35	-3.74	-10.18	-3.05	-5.35	-2.36	-0.97	0.48	-3.27	0.42	-3.05	1.80
4185	9.67	8.30	7.59	3.09	6.36	7.31	6.88	6.67	4.54	2.35	8.01	7.29	6.36	7.17	6.81	0.94	2.53	-1.14	-4.31	-10.76	-2.93	-4.44	-5.92	-3.62	-0.09	1.00	-4.31	-1.54	-2.59	-5.92	-4.31	-7.53	-3.62	-3.44	-0.44	1.08	3.03	-2.40	3.39	-2.93	2.01
4186	8.47	7.06	7.77	2.33	5.15	5.87	4.17	6.27	3.70	1.42	8.67	8.19	5.55	8.17	7.85	2.59	4.56	0.02	-1.70	-4.06	-1.44	-3.02	-5.35	1.83	0.78	1.63	-1.04	-1.35	-2.44	-2.65	-3.56	-8.35	-4.44	-2.18	-1.10	0.65	0.21	-3.10	2.61	-4.44	0.71
4187	8.60	7.15	8.05	3.34	6.52	7.07	4.85	5.57	4.48	1.37	8.05	7.14	7.03	6.86	7.45	3.27	4.36	-0.05	-1.82	-6.18	-2.05	-5.62	-5.96	-4.35	0.76	2.40	-1.35	-1.87	-3.48	-2.70	-3.25	-6.65	-4.35	-2.05	2.08	-0.05	0.15	-3.88	3.20	-4.35	0.89
4188	10.19	7.63	7.69	2.86	5.79	4.71	6.66	6.34	4.24	1.81	8.36	7.83	3.05	7.83	7.14	2.86	3.75	-0.35	-2.07	-10.48	-2.65	-3.12	-5.65	-0.57	0.86	2.30	-1.06	-1.04	-1.96	-5.65	-4.04	-7.26	-0.71	-3.57	-1.56	0.60	1.26	-3.16	2.68	-3.35	1.32
4189	10.44	7.36	8.82	5.60	6.32	7.22	5.64	5.92	4.20	1.42	8.45	7.13	7.56	6.58	8.33	1.36	2.11	-1.44	-3.74	-10.18	-3.05	-5.01	-5.35	-0.74	2.08	3.35	-3.74	-2.35	-2.35	-3.05	-3.74	-6.96	-3.05	-2.17	-0.41	0.42	1.92	-2.86	1.91	-3.05	1.14
4190	8.66	7.68	7.12	1.63	5.62	4.64	4.07	7.06	4.50	2.09	8.58	8.27	4.86	8.26	6.85	2.99	3.80	-2.72	-2.57	-6.85	-2.54	-3.81	-5.94	2.84	0.83	1.32	-1.22	-1.07	-2.85	-3.63	-3.63	-7.14	-4.33	-2.01	-1.15	0.89	-0.34	-3.54	2.70	-4.33	1.47
4191	9.56	8.06	7.54	4.06	5.59	6.57	5.71	6.68	4.17	1.79	7.95	6.39	7.23	5.39	6.33	-0.26	1.44	-2.17	-4.47	-7.69	-2.40	-4.40	-6.08	-1.01	-1.01	-0.45	-4.47	-2.40	-2.75	-3.78	-3.44	-10.92	-3.78	-4.00	2.81	0.92	1.32	-2.13	2.62	-3.09	2.39
4192	9.24	7.96	6.66	0.91	5.33	3.65	5.74	7.04	4.66	0.85	8.20	7.76	0.58	7.76	6.60	5.88	0.20	-0.39	-4.72	-7.94	-2.64	-2.36	-6.33	1.82	0.08	0.99	-4.72	-1.54	-2.93	-2.64	-1.25	-7.24	-4.02	-2.05	0.96	1.69	1.01	-2.05	3.16	-3.33	1.47
4193	8.92	8.05	6.99	1.64	5.60	4.16	7.29	6.12	4.67	1.98	8.48	8.22	2.30	8.22	6.63	5.81	0.38	-0.14	-4.79	-8.01	-2.30	-3.19	-6.40	-0.18	-0.46	0.88	-4.79	0.68	-2.57	-6.40	-0.43	-7.31	-4.09	1.39	-0.84	0.64	1.27	-3.14	2.36	-3.40	1.58
4194	9.00	7.96	6.70	2.36	6.24	4.47	7.02	6.54	4.88	2.29	8.87	8.74	1.95	8.74	5.62	5.64	0.52	-0.17	-4.74	-11.18	-1.74	-2.66	-6.35	1.14	0.55	0.76	-2.25	-0.71	-3.17	-6.35	-1.67	-7.96	-1.56	-0.05	-1.27	1.11	1.09	-2.77	3.10	-2.66	1.46
4195	9.73	8.04	6.95	1.99	5.76	5.28	7.54	5.80	4.42	2.44	8.43	8.23	0.97	8.23	6.26	6.26	0.46	-2.03	-4.33	-10.77	-2.25	-3.22	-5.94	0.05	-0.77	0.84	-4.33	-0.38	-2.54	-3.64	-1.46	-7.55	-3.64	-0.03	-2.25	0.35	2.21	-3.45	1.67	-2.94	1.78
4196	9.29	8.09	7.45	2.89	6.08	5.46	7.52	5.89	4.77	2.51	8.07	7.72	0.70	7.72	5.24	5.46	1.24	0.52	-4.60	-11.04	-3.91	-4.18	-6.21	-3.91	-0.26	0.68	-4.60	-0.04	-3.21	-6.21	-1.69	-6.72	-3.91	2.30	-0.51	0.08	1.86	-4.13	2.31	-3.21	1.67
4197	9.37	7.99	7.45	3.41	6.85	4.70	7.36	4.95	4.49	2.27	7.82	7.19	3.00	7.18	5.27	5.83	2.83	5.25	-2.80	-7.82	-3.90	-4.35	-6.21	-0.07	0.11	1.24	-4.60	-0.91	-3.21	-6.21	-2.08	-11.04	-3.90	-2.57	-1.42	-0.64	1.09	-3.90	0.50	-3.21	1.45
4199	9.52	8.41	7.71	3.26	6.54	6.56	6.58	6.86	5.33	2.46	7.69	5.59	6.58	4.26	4.76	0.95	1.61	-1.41	-4.41	-6.53	-3.71	-3.91	-6.02	0.31	0.13	1.80	-4.41	-3.02	-2.49	-3.38	-4.41	-10.85	-3.71	-3.53	1.55	1.07	2.40	-2.93	3.14	-3.02	1.77
4200	9.43	7.97	7.30	3.28	6.19	4.78	6.24	6.78	4.53	2.05	7.75	6.00	4.47	5.94	6.53	1.64	2.88	-1.28	-3.45	-5.89	-2.53	-2.91	-6.22	0.49	0.22	2.16	-1.64	-2.53	-2.44	-2.89	-4.61	-11.06	-3.92	-3.05	1.26	1.08	0.53	-3.92	3.16	-3.23	1.41
4301	8.84	6.52	8.38	3.46	6.85	7.74	5.45	6.08	3.60	1.17	9.08	7.98	8.55	7.31	8.25	1.53	2.94	-0.25	-3.04	-3.81	-3.30	-6.81	-6.29	2.76	0.27	1.57	-4.69	-1.91	-3.12	1.35	-2.77	-3.13	-1.51	-2.71	-1.10	0.03	1.28	-3.99	2.14	-3.99	0.03
4303	9.03	7.01	7.81	2.20	5.20	5.88	3.32	6.37	3.91	1.61	8.13	7.39	5.88	7.32	7.57	1.33	3.88	0.63	-2.30	-4.47	-1.61	-4.03	-6.55	-0.99	0.19	1.26	-1.95	-1.76	-3.46	-1.03	-3.78	-7.06	-2.86	-2.49	2.41	0.45	-1.07	-4.47	3.08	-4.25	0.92
4308	8.32	7.20	8.45	3.69	6.63	7.01	6.44	5.15	3.68	-1.13	8.85	7.71	7.78	7.36	8.36	2.82	3.12	-0.63	-2.69	-5.83	-3.52	-7.03	-6.52	2.27	0.49	1.21	-4.91	-1.91	-3.26	-0.81	-3.88	-5.24	-1.04	-2.73	3.85	-0.96	1.28	-4.73	0.74	-4.22	0.94
4309	8.19	6.77	7.77	2.30	5.32	6.88	5.87	4.42	3.54	1.20	8.73	8.38	7.02	8.30	7.41	1.15	4.41	0.11	-1.94	-5.25	-2.03	-5.60	-6.13	1.61	1.03	2.21	-3.13	-0.83	-4.05	-0.04	-3.73	-6.82	-3.13	-2.14	3.89	-1.43	0.89	-4.33	0.61	-4.52	0.38
4311	8.93	7.11	7.62	2.28	4.61	6.08	5.88	6.22	3.88	1.46	8.42	7.87	6.28	7.81	7.57	0.83	4.00	-0.31	-2.16	-5.00	-1.96	-4.39	-6.56	1.38	0.35	1.46	-3.10	-1.78	-3.57	-0.54	-3.93	-7.07	-4.26	-2.58	0.30	0.53	-0.48	-4.26	2.33	-4.26	1.14
4312	8.56	6.90	7.89	1.60	4.74	4.41	5.64	6.40	4.01	1.79	8.35	7.69	4.68	7.68	7.91	1.19	3.51	0.68	-2.41	-6.77	-2.39	-4.02	-6.77	2.32	0.43	1.35	-5.16	-1.70	-3.78	0.33	-3.51	-5.16	-4.47	-2.61	1.13	0.25	-1.14	-4.00	2.76	-4.47	0.94
4314	8.71	6.99	7.65	1.53	4.60	6.51	6.27	6.22	3.77	1.47	8.98	8.68	6.53	8.65	7.74	2.48	3.93	0.08	-2.36	-3.48	-1.95	-4.53	-6.55	2.24	0.70	2.11	-1.67	-1.07	-4.07	-0.64	-4.07	-7.47	-4.25	-2.17	-3.56	-0.30	1.03	-5.17	2.88	-4.25	0.69
4315	8.47	7.04	7.09	1.79	4.93	3.73	6.50	5.54	3.80	1.41	8.93	8.81	4.15	8.81	6.88	1.47	4.75	-0.11	-1.33	-3.95	-2.65	-3.68	-5.36	1.97	0.83	2.13	-2.62	-1.11	-3.98	-0.47	-4.11	-6.75	-4.45	-1.85	-0.39	-0.81	-0.32	-4.67	1.92	-4.45	1.19
4316	8.28	6.94	7.90	1.97	6.36	6.23	5.99	6.33	4.22	1.55	8.23	7.78	4.06	7.77	7.67	2.18	3.96	0.34	-2.27	-3.64	-1.89	-4.92	-6.14	1.64	0.75	1.85	-2.15	-1.54	-3.66	-2.19	-3.84	-8.44	-4.53	-2.21	-0.37	-0.10	0.54	-5.04	2.99	-4.53	0.82
4319	8.89	7.30	7.20	0.34	4.06	4.23	3.88	6.46	3.99	1.63	8.34	7.94	4.00	7.93	7.31	1.61	4.25	0.43	-2.31	-3.79	-1.86	-2.83	-6.65	2.37	0.67	1.86	-1.76	-1.25	-2.77	-0.82	-3.39	-6.06	-2.96	-1.89	0.85	0.92	0.09	-2.46	2.49	-4.34	0.83
4320	8.40	7.43	7.03	1.17	4.59	5.17	4.58	6.43	4.43	2.40	7.52	6.35	5.24	6.25	6.95	2.71	3.84	-0.21	-2.53	-4.58	-1.31	-3.23	-5.22	-1.45	0.03	0.43	-3.83	-2.92	-3.18	-3.10	-3.68	-7.52	-2.40	-2.38	0.78	0.84	0.33	-2.71	2.56	-4.01	1.68
4323	8.86	7.41	8.09	3.24	6.19	7.12	5.54	5.76	4.24	2.41	8.57	7.00	7.81	6.05	8.07	0.60	1.29	-0.05	-4.83	-5.86	-3.45	-5.57	-6.44	1.87	-0.36	0.22	-4.83	-2.35	-3.45	-0.33	-3.27	-4.62	-2.75	-3.80	0.38	0.08	1.58	-2.81	1.88	-4.14	1.36
4324	8.93	7.73	7.77	2.50	5.60	6.34	7.00	6.01	4.52	2.14	7.98	6.58	6.77	6.17	7.54	1.47	1.53	-0.24	-4.89	-6.72	-2.81	-7.01	-6.50	1.34	0.08	1.09	-4.89	-2.40	-3.41	-1.26	-3.41	-5.80	-1.56	-2.86	0.16	0.28	1.01	-3.32	2.62	-3.50	1.45
4325	9.14	8.10	7.27	1.61	5.91	4.34	6.56	6.56	4.85	2.49	7.31	5.53	2.97	5.51	6.10	0.83	2.17	-1.13	-4.12	-7.34	-2.74	-3.56	-6.42	1.18	0.00	1.38	-4.81	-2.33	-2.96	-3.09	-3.94	-7.34	-4.12	-2.20	2.13	1.04	1.45	-2.51	2.92	-3.43	1.62
4326	9.28	7.89	7.22	3.23	6.31	6.36	5.91	6.63	4.80	2.06	7.70	6.11	7.05	4.91	6.00	1.28	2.13	-0.44	-4.71	-7.93	-2.63	-3.58	-6.32	0.41	-0.05	1.35	-4.71	-2.63	-3.07	-2.69	-4.02	-7.93	-4.02	-2.41	1.47	1.03	1.29	-2.80	2.70	-3.33	1.43
4327	9.02	7.68	6.83	0.69	4.70	4.42	6.73	6.37	4.34	2.01	8.00	7.53	4.48	7.51	6.69	1.97	2.32	0.00	-4.94	-5.45	-2.46	-3.65	-6.55	1.84	-0.03	1.10	-2.92	-1.77	-3.30	-0.87	-3.38	-6.78	-4.25	-3.15	0.18	0.86	0.35	-3.09	2.83	-3.56	1.42
4330	9.59	8.49	7.56	2.92	6.58	4.40	7.07	6.98	5.33	2.16	7.61	5.85	3.91	5.82	3.40	0.61	1.60	-0.17	-4.39	-7.60	-2.31	-3.38	-5.99	-0.51	-0.80	1.21	-4.39	-3.00	-2.66	-3.51	-3.51	-10.83	-3.69	-2.66	1.98	1.44	2.64	-1.52	3.26	-2.31	1.96
4331	9.84	8.72	7.87	3.53	6.98	7.43	7.63	6.64	5.72	3.13	7.33	1.19	3.83	-10.55	4.65	0.74	1.79	-1.81	-4.11	-10.55	-2.73	-4.20	-5.72	0.16	0.56	1.83	-4.11	-1.12	-2.03	-4.34	-3.24	-10.55	-3.42	-3.64	0.89	1.06	3.82	-1.89	3.34	-2.73	2.19
4332	9.11	7.61	8.92	5.70	7.87	8.92	2.69	2.39	5.08	1.75	9.27	8.37	9.47	6.69	7.56	2.71	3.67	-1.80	-1.98	-4.03	-2.72	-6.23	-5.71	0.37	0.80	1.52	-4.11	-2.72	-2.38	-3.23	-4.11	-10.55	-3.41	-2.82	-0.52	-2.72	1.75	-5.71	-1.11	-3.41	0.99
4333	9.66	8.52	7.83	3.41	6.78	6.26	7.34	6.35	5.49	2.94	7.33	3.77	4.73	2.51	4.09	1.18	1.67	-0.72	-4.30	-7.52	-3.61	-3.97	-5.91	-0.84	0.33	1.76	-4.30	-2.92	-2.74	-4.12	-4.30	-10.75	-3.61	-3.27	0.69	0.89	2.68	-2.13	2.71	-3.61	1.89
4334	9.35	8.17	7.13	2.72	6.06	6.18	7.08	6.52	4.92	2.33	7.67	6.36	6.74	5.85	5.91	1.10	2.40	-0.94	-3.75	-7.15	-2.55	-3.93	-6.24	0.67	-0.13	1.21	-4.63	-2.55	-3.06	-2.90	-4.63	-7.85	-3.93	-2.90	1.02	0.98	1.54	-2.60	2.88	-3.24	1.66
4335	9.52	7.40	8.56	5.73	6.81	9.26	3.06	2.48	4.97	1.83	9.01	8.29	9.40	6.55	7.27	2.44	3.45	-0.69	-1.85	-6.55	-3.33	-6.14	-5.63	-1.54	0.64	1.21	-2.11	-2.64	-2.86	-2.05	-2.74	-4.94	-3.33	-4.25	-0.56	-2.64	2.06	-5.63	-1.25	-3.33	0.73
4336	9.40	6.61	8.49	5.55	6.76	8.82	4.87	5.29	4.14	1.63	9.16	8.25	9.27	6.81	7.65	2.22	3.96	-0.35	-1.65	-6.06	-3.53	-6.35	-5.83	-0.07	0.55	0.87	-4.23	-2.84	-3.35	-1.33	-4.23	-6.75	-3.53	-4.45	0.56	-0.35	2.19	-3.53	2.21	-3.53	-0.01
4337	10.05	5.98	9.07	5.55	6.69	8.79	3.51	4.72	2.97	1.37	9.50	8.47	9.26	7.55	8.70	2.69	3.94	0.43	-1.57	-5.91	-3.10	-5.91	-5.40	1.91	0.88	1.15	-1.38	-2.41	-3.10	-0.58	-3.79	-5.40	-3.10	-3.32	-2.41	-0.80	2.18	-4.02	1.62	-3.10	-0.46
4338	8.74	6.38	9.46	6.28	7.21	9.00	5.62	4.25	3.96	1.53	9.48	8.76	9.83	7.16	8.49	2.44	2.55	-1.74	-1.40	-7.26	-3.35	-6.16	-5.65	4.48	0.18	0.64	-1.27	-2.66	-4.04	-1.15	-4.04	-3.86	-3.35	-3.35	-1.27	-1.56	2.17	-4.26	0.12	-3.35	-0.09
4339	9.05	8.75	7.44	2.60	6.46	5.45	6.38	7.44	5.79	2.27	7.71	5.16	5.18	4.83	2.78	0.38	1.63	-2.29	-4.59	-11.04	-2.51	-3.32	-6.20	0.85	0.60	1.32	-4.59	-2.51	-2.51	-3.21	-4.59	-11.04	-1.42	-5.51	2.04	1.78	2.55	-1.60	3.72	-2.51	2.28
4340	9.49	8.38	7.80	3.13	7.00	6.35	6.62	7.48	5.31	3.16	7.63	5.00	6.33	-10.84	4.89	0.92	1.47	-2.09	-4.39	-10.84	-3.01	-3.45	-6.00	-0.93	0.35	1.71	-4.39	-1.40	-2.54	-2.67	-3.52	-4.67	-0.93	-3.92	-1.06	1.91	2.25	-1.57	4.02	-2.32	1.77
4341	9.79	8.68	8.24	3.51	7.20	5.78	8.27	7.06	5.66	3.25	6.33	3.26	3.26	2.95	4.71	1.01	1.91	-1.81	-4.11	-10.56	-3.42	-6.23	-5.72	-2.73	0.39	2.21	-4.11	-0.94	-2.46	-5.72	-4.11	-7.33	-3.42	-4.34	-0.24	1.59	2.34	-1.98	2.63	-2.03	1.94
4342	9.41	8.22	7.57	3.23	6.78	6.66	6.63	7.27	5.13	2.86	7.61	5.45	6.71	2.21	4.49	0.70	1.38	-2.19	-4.49	-10.94	-3.80	-4.05	-6.10	-0.02	0.10	1.45	-4.49	-3.11	-2.58	-2.52	-4.49	-7.71	-1.32	-4.02	0.74	1.55	2.33	-1.98	3.69	-2.42	1.55
4343	9.50	8.49	7.90	3.65	7.07	6.16	7.88	7.15	5.35	2.80	6.20	3.23	4.25	1.78	3.70	1.14	1.83	0.72	-4.38	-10.82	-2.99	-6.50	-5.99	-2.30	0.55	1.89	-4.38	-0.10	-2.35	-4.19	-4.38	-7.59	-3.68	-1.96	-0.69	2.03	2.81	-0.97	2.99	-2.30	1.70
4344	9.83	8.73	8.04	3.88	7.10	6.97	8.25	6.85	5.87	2.60	7.25	5.14	6.49	-10.51	5.10	2.02	2.01	-0.04	-4.07	-10.51	-2.68	-6.19	-5.68	-2.68	0.87	1.96	-4.07	-1.29	-2.34	-5.68	-4.07	-10.51	-3.37	-3.37	-0.73	1.33	2.99	-1.52	3.19	-1.99	1.90
4345	9.26	8.23	7.67	3.26	6.88	6.10	6.23	7.08	5.16	2.75	7.42	4.47	5.49	3.06	4.21	0.85	1.73	-0.59	-3.23	-7.83	-3.23	-4.00	-6.22	0.44	0.20	1.59	-4.61	-3.23	-2.70	-2.96	-4.61	-7.83	-1.62	-4.14	0.46	1.33	2.02	-2.13	3.66	-2.53	1.44
4346	9.10	8.15	7.41	2.92	6.51	5.67	6.26	7.10	4.89	2.33	7.08	7.38	4.05	7.37	6.48	0.60	1.19	-0.75	-4.77	-7.99	-3.39	-3.70	-6.38	0.56	-0.05	1.26	-4.77	-2.69	-2.92	-2.80	-4.77	-7.99	-4.08	-3.90	0.53	1.58	2.13	-2.08	3.27	-2.69	1.41
4347	9.41	8.46	7.97	3.61	7.16	6.00	7.88	5.02	5.39	2.98	7.22	7.40	3.51	7.39	7.26	0.91	1.75	-2.13	-4.43	-10.87	-3.04	-5.08	-6.04	-0.96	0.28	1.79	-4.43	-3.04	-2.64	-2.95	-4.43	-10.87	-3.73	-4.65	0.25	-0.84	2.82	-3.96	1.84	-2.35	1.74
4348	9.39	8.33	7.61

Appendix A4. Centered log ratio transformed data used for PCA and Random Forest.

Sample	Hf	Nb	Ta	Ga	Sc	V	Cr	Th	U	Y	La	Ce	Pr	Nd	Sm	Eu	Gd	Tb	Dy	Ho	Er	Tm	Yb	Lu	Br	F
4172	-2.13	-1.70	-4.13	-0.46	-0.37	1.48	0.83	-2.00	-3.12	-0.58	-0.47	0.37	-1.76	-0.43	-1.98	-2.93	-2.15	-3.90	-2.19	-3.83	-2.79	-4.70	-2.72	-4.43	-2.76	1.25
4173	-2.48	-1.81	-4.35	-0.63	0.12	1.51	2.20	-1.89	-3.05	-0.18	-0.45	0.36	-1.75	-0.38	-1.83	-2.90	-1.90	-3.61	-1.86	-3.44	-2.35	-4.21	-2.28	-4.05	-4.66	0.64
4174	-2.10	-1.23	-3.99	-0.61	-0.57	1.27	1.26	-3.08	-4.14	-0.38	-0.71	0.13	-1.95	-0.54	-2.04	-3.23	-2.09	-3.87	-2.16	-3.77	-2.67	-4.63	-2.68	-4.49	-4.71	0.59
4175	-1.99	-1.50	-4.03	-0.24	-0.49	1.26	1.06	-1.46	-3.02	-0.62	0.22	0.96	-1.21	0.11	-1.65	-3.05	-2.04	-4.03	-2.40	-4.10	-3.05	-4.95	-2.97	-4.74	-4.57	0.73
4176	-2.94	-2.76	-4.77	-1.15	-0.83	0.32	0.83	-2.15	-3.36	-0.64	-0.89	-0.09	-2.21	-0.89	-2.50	-3.45	-2.63	-4.29	-2.59	-4.21	-3.14	-5.06	-3.12	-4.91	-1.91	1.66
4177	-3.02	-2.57	-5.48	-0.87	-0.80	0.56	0.68	-3.17	-4.05	-1.28	-1.22	-0.42	-2.56	-1.12	-2.64	-3.44	-2.75	-4.50	-2.74	-4.32	-3.16	-5.07	-3.12	-4.78	-4.05	1.25
4178	-1.77	-1.39	-3.92	-0.08	-0.50	1.23	1.16	-1.57	-2.94	-0.51	0.21	0.99	-1.16	0.17	-1.60	-2.83	-1.91	-3.85	-2.22	-3.85	-2.82	-4.74	-2.82	-4.59	-4.46	0.84
4179	-2.30	-1.78	-4.17	-0.56	-0.84	0.84	0.40	-1.94	-3.17	-0.69	-0.67	0.12	-2.06	-0.71	-2.34	-3.22	-2.42	-4.17	-2.48	-4.11	-3.04	-4.94	-3.08	-4.85	-4.72	0.58
4180	-1.97	-1.49	-4.00	-0.26	-1.38	0.10	-0.43	-1.97	-2.72	-0.26	0.05	0.71	-1.56	-0.31	-2.10	-3.37	-2.34	-4.15	-2.30	-3.86	-2.67	-4.46	-2.49	-4.21	-4.42	0.88
4181	-2.75	-2.18	-4.65	-1.26	-0.50	0.79	2.10	-2.11	-3.02	-0.51	-0.62	0.16	-1.96	-0.59	-2.06	-2.54	-2.11	-3.80	-2.07	-3.68	-2.62	-4.54	-2.60	-4.28	-4.73	0.57
4182	-2.04	-1.49	-4.17	-0.43	-1.09	0.54	0.19	-2.30	-3.62	-0.43	-0.44	0.37	-1.73	-0.35	-1.94	-2.91	-2.01	-3.82	-2.05	-3.67	-2.59	-4.48	-2.58	-4.34	-4.21	1.09
4183	-2.37	-2.06	-4.81	-0.45	-0.68	1.39	1.67	-2.45	-3.66	-1.23	-0.73	0.01	-2.09	-0.74	-2.39	-3.58	-2.62	-4.45	-2.77	-4.36	-3.31	-5.15	-3.29	-5.05	-4.23	1.07
4184	-1.44	-0.42	-2.41	0.21	-0.18	1.08	0.71	-0.57	-1.42	0.04	-0.78	0.18	-1.89	-0.54	-1.95	-3.59	-1.96	-3.59	-1.76	-3.27	-2.07	-3.83	-1.88	-3.59	-3.74	1.56
4185	-1.70	-1.30	-3.47	0.02	-0.84	0.88	0.49	-1.60	-2.87	-0.44	-0.30	0.51	-1.64	-0.33	-1.89	-2.93	-1.98	-3.80	-2.09	-3.73	-2.70	-4.59	-2.64	-4.40	-4.31	0.98
4186	-3.00	-2.29	-4.74	-0.80	-1.02	0.43	0.00	-2.75	-3.60	-0.97	-1.21	-0.43	-2.57	-1.23	-2.72	-3.41	-2.72	-4.44	-2.69	-4.31	-3.27	-5.13	-3.19	-4.98	-3.05	0.17
4187	-2.78	-1.85	-4.48	-1.02	-0.57	1.19	2.76	-2.65	-3.76	-0.71	-1.44	-0.52	-2.65	-1.35	-2.70	-3.65	-2.63	-4.24	-2.42	-4.00	-2.94	-4.83	-2.92	-4.77	-2.87	0.25
4188	-2.56	-2.12	-4.55	-0.57	-0.68	0.71	2.37	-1.87	-3.31	-1.04	-1.01	-0.14	-2.30	-1.03	-2.69	-3.79	-2.93	-4.62	-2.83	-4.49	-3.31	-5.06	-3.04	-4.77	-2.32	1.26
4189	-2.71	-2.26	-4.47	-0.74	-0.95	0.78	0.94	-2.78	-3.46	-0.74	-0.97	-0.25	-2.42	-1.16	-2.67	-3.56	-2.65	-4.47	-2.72	-4.32	-3.22	-5.01	-3.20	-4.88	-3.74	1.56
4190	-2.30	-1.65	-4.21	-0.54	-0.67	0.98	0.43	-2.20	-3.36	-0.74	-0.30	0.47	-1.70	-0.41	-2.01	-3.33	-2.18	-3.98	-2.28	-3.94	-2.89	-4.84	-2.89	-4.66	-5.02	0.28
4191	-1.30	-0.98	-3.47	-0.09	-1.00	-0.45	-4.47	-1.52	-3.08	0.58	0.53	1.32	-0.82	0.48	-1.19	-2.77	-1.24	-2.97	-1.19	-2.74	-1.65	-3.50	-1.58	-3.39	-4.47	0.82
4192	-2.20	-1.72	-4.32	-0.33	-0.12	1.33	1.23	-1.60	-2.95	-0.77	-0.19	0.62	-1.52	-0.20	-1.85	-3.86	-2.23	-4.20	-2.52	-4.15	-3.00	-4.76	-2.81	-4.47	-4.72	0.58
4193	-2.09	-1.44	-3.93	-0.22	-0.42	1.35	0.92	-1.04	-2.24	-0.92	-0.84	0.06	-2.10	-0.81	-2.34	-3.95	-2.60	-4.34	-2.52	-4.11	-2.95	-4.71	-2.68	-4.29	-4.79	0.51
4194	-2.29	-1.32	-4.11	-0.31	-0.36	1.42	0.93	-1.84	-2.57	-0.95	-1.40	-0.46	-2.58	-1.29	-2.71	-4.27	-2.77	-4.46	-2.72	-4.24	-3.09	-4.87	-2.84	-4.43	-2.16	0.56
4195	-1.91	-1.44	-3.96	-0.64	-0.87	0.72	0.46	-1.07	-2.26	-0.46	-0.36	0.46	-1.67	-0.38	-1.97	-3.60	-2.18	-3.91	-2.12	-3.76	-2.66	-4.60	-2.62	-4.29	-4.33	0.97
4196	-2.02	-1.55	-4.04	-0.27	-0.13	1.52	1.08	-1.40	-2.32	-0.32	0.32	1.16	-0.98	0.34	-1.31	-3.65	-1.66	-3.66	-2.00	-3.68	-2.60	-4.52	-2.58	-4.26	-4.60	0.70
4197	-2.22	-1.75	-4.32	-0.64	-0.65	1.09	0.83	-1.44	-2.95	-0.44	0.59	1.29	-0.98	0.20	-1.74	-3.35	-2.08	-4.01	-2.24	-3.81	-2.68	-4.56	-2.63	-4.35	-1.99	0.70
4199	-1.96	-1.54	-4.10	0.16	-0.18	1.87	2.10	-1.74	-2.83	-0.54	0.12	0.88	-1.27	0.02	-1.65	-2.98	-1.96	-3.89	-2.18	-3.84	-2.79	-4.68	-2.81	-4.58	-4.41	0.89
4200	-2.31	-1.84	-4.34	-0.28	-0.49	1.25	1.98	-2.11	-3.43	-0.66	0.20	0.83	-1.38	-0.11	-1.85	-3.06	-2.10	-4.03	-2.36	-3.96	-2.91	-4.74	-2.84	-4.61	-4.61	0.68
4301	-3.52	-2.89	-5.42	-1.91	-1.36	0.65	1.45	-3.19	-4.38	-1.35	-1.44	-0.63	-2.73	-1.34	-2.87	-3.95	-2.90	-4.61	-2.89	-4.50	-3.49	-5.34	-3.52	-5.27	-2.20	0.61
4303	-2.81	-2.01	-4.63	-0.99	-1.26	0.41	0.23	-2.74	-3.84	-0.30	-1.01	-0.09	-2.19	-0.83	-2.21	-3.48	-2.18	-3.91	-2.14	-3.68	-2.61	-4.50	-2.66	-4.47	-2.56	0.36
4308	-2.73	-2.27	-4.46	-1.33	-1.48	0.71	-0.46	-2.26	-3.53	-1.04	-0.82	-0.05	-2.23	-0.92	-2.50	-3.82	-2.63	-4.44	-2.72	-4.32	-3.21	-5.08	-3.17	-4.95	-1.31	0.39
4309	-3.35	-2.52	-5.06	-1.52	-1.10	0.37	0.30	-2.32	-3.31	-0.93	-0.88	-0.11	-2.26	-0.96	-2.48	-3.10	-2.61	-4.35	-2.61	-4.22	-3.13	-5.00	-3.07	-4.79	-1.76	0.09
4311	-2.58	-1.86	-4.46	-1.08	-1.11	0.38	0.64	-2.58	-3.75	-0.24	-1.31	-0.37	-2.43	-1.07	-2.39	-3.65	-2.18	-3.86	-2.04	-3.60	-2.53	-4.41	-2.55	-4.34	-2.74	0.34
4312	-2.78	-1.72	-4.51	-1.38	-1.49	0.25	0.53	-2.74	-3.81	-0.22	-0.71	0.15	-1.94	-0.56	-1.99	-3.57	-2.00	-3.77	-1.98	-3.55	-2.46	-4.39	-2.51	-4.30	-1.44	0.14
4314	-3.03	-2.36	-4.91	-1.26	-1.02	0.41	0.35	-2.55	-3.56	-0.99	-0.99	-0.15	-2.27	-0.93	-2.47	-3.62	-2.56	-4.33	-2.59	-4.23	-3.15	-5.03	-3.11	-4.87	-1.84	0.35
4315	-2.47	-1.78	-4.31	-1.19	-1.13	0.24	0.11	-2.29	-3.34	-0.76	-0.54	0.27	-1.91	-0.63	-2.40	-3.84	-2.73	-4.53	-2.71	-4.14	-2.91	-4.69	-2.68	-4.35	-1.52	0.16
4316	-2.81	-2.00	-4.55	-1.27	-0.83	1.01	1.94	-2.50	-3.65	-0.79	-1.09	-0.25	-2.34	-0.99	-2.44	-3.27	-2.46	-4.18	-2.43	-4.05	-2.99	-4.86	-2.93	-4.73	-1.89	0.07
4319	-2.82	-2.15	-4.70	-0.82	-0.98	0.49	0.45	-1.94	-3.19	-1.16	-0.75	-0.01	-2.20	-0.93	-2.62	-3.55	-2.83	-4.67	-2.95	-4.54	-3.44	-5.31	-3.36	-5.08	-3.18	0.26
4320	-2.04	-1.47	-4.12	-0.61	-0.96	0.60	-0.50	-2.34	-3.58	-0.19	-0.25	0.58	-1.51	-0.17	-1.73	-3.23	-1.90	-3.68	-1.94	-3.54	-2.46	-4.32	-2.39	-4.15	-3.83	-0.10
4323	-2.38	-1.82	-4.36	-0.96	-1.32	0.34	-0.13	-2.41	-3.67	-0.36	-0.56	0.18	-1.96	-0.64	-2.16	-3.42	-2.11	-3.88	-2.13	-3.76	-2.68	-4.56	-2.62	-4.42	-3.45	0.46
4324	-2.19	-1.65	-4.30	-0.56	-1.10	0.89	0.10	-1.67	-3.09	-0.73	-0.12	0.64	-1.52	-0.24	-1.89	-3.26	-2.13	-4.05	-2.44	-4.08	-3.01	-4.89	-3.01	-4.81	-2.86	0.41
4325	-2.07	-1.56	-4.12	-0.17	-0.61	1.40	1.21	-1.45	-2.80	-0.38	0.41	1.18	-0.99	0.27	-1.50	-3.04	-1.84	-3.76	-2.04	-3.70	-2.65	-4.63	-2.76	-4.57	-3.33	0.48
4326	-2.26	-1.62	-4.22	-0.33	-0.57	1.35	1.07	-1.84	-3.12	-0.56	-0.04	0.73	-1.43	-0.15	-1.80	-3.17	-2.04	-3.89	-2.23	-3.89	-2.85	-4.76	-2.87	-4.68	-2.69	0.58
4327	-2.28	-1.58	-4.10	-0.61	-0.93	0.75	0.52	-1.39	-2.82	-0.72	-0.08	0.68	-1.51	-0.24	-1.96	-3.35	-2.29	-4.17	-2.47	-4.09	-2.97	-4.87	-2.96	-4.73	-2.64	0.35
4330	-1.72	-1.08	-3.63	0.26	0.06	2.01	1.98	-0.89	-2.44	-0.43	-0.43	0.44	-1.70	-0.44	-2.03	-3.38	-2.29	-3.92	-2.12	-3.67	-2.57	-4.43	-2.48	-4.27	-4.39	0.91
4331	-1.50	-0.93	-3.55	0.49	0.41	2.43	2.25	-0.97	-2.33	0.16	0.69	1.52	-0.59	0.74	-0.95	-2.33	-1.20	-3.14	-1.47	-3.13	-2.12	-4.04	-2.18	-3.96	-4.11	1.19
4332	-2.82	-2.38	-5.24	-0.52	0.69	2.44	0.97	-2.94	-3.92	-0.08	-1.54	-0.61	-2.60	-1.11	-2.17	-3.01	-1.97	-3.66	-1.86	-3.41	-2.29	-4.19	-2.31	-4.03	-4.11	1.19
4333	-1.79	-1.23	-3.89	0.13	0.12	2.15	2.16	-1.46	-2.80	-0.21	0.39	1.16	-0.97	0.32	-1.37	-2.85	-1.65	-3.57	-1.88	-3.53	-2.47	-4.39	-2.47	-4.30	-2.66	0.99
4334	-1.99	-1.47	-4.04	-0.10	-0.55	1.38	0.91	-1.55	-2.76	-0.68	-0.17	0.62	-1.53	-0.22	-1.91	-3.36	-2.18	-4.08	-2.37	-4.04	-2.94	-4.85	-2.90	-4.67	-4.63	0.67
4335	-2.86	-2.23	-5.16	-0.69	0.00	1.86	0.50	-3.60	-4.53	-0.07	-1.54	-0.63	-2.63	-1.07	-2.26	-3.46	-2.05	-3.78	-2.00	-3.53	-2.40	-4.25	-2.26	-3.95	-2.30	1.28
4336	-3.53	-2.94	-6.06	-1.23	-0.19	1.41	-0.18	-4.23	-5.14	-0.13	-2.02	-1.14	-3.07	-1.40	-2.38	-3.11	-2.13	-3.86	-2.09	-3.57	-2.43	-4.19	-2.17	-3.83	-2.10	1.07
4337	-4.02	-3.61	-6.32	-1.71	-0.86	0.64	-0.40	-4.37	-5.62	-0.80	-2.03	-1.38	-3.35	-1.68	-2.53	-3.35	-2.38	-4.24	-2.52	-4.12	-2.92	-4.81	-2.79	-4.37	-1.66	1.51
4338	-3.86	-3.01	-5.87	-1.56	-0.78	0.78	-0.11	-4.26	-4.96	-0.71	-2.34	-1.47	-3.45	-1.80	-2.78	-3.60	-2.53	-4.32	-2.40	-3.89	-2.71	-4.49	-2.43	-4.17	-1.82	1.26
4339	-1.38	-0.76	-3.31	0.40	0.22	2.29	1.75	-1.30	-2.60	-0.37	0.39	1.16	-0.99	0.35	-1.38	-2.74	-1.74	-3.75	-2.07	-3.72	-2.62	-4.45	-2.54	-4.29	-4.59	0.70
4340	-1.88	-1.22	-3.83	0.13	-0.05	1.97	2.24	-1.26	-2.51	-0.18	0.32	1.10	-1.05	0.31	-1.39	-2.86	-1.69	-3.64	-1.94	-3.61	-2.58	-4.52	-2.57	-4.39	-3.23	0.90
4341	-1.73	-1.22	-3.87	0.36	0.31	2.41	2.40	-1.49	-2.83	-0.09	0.32	1.11	-1.04	0.32	-1.36	-2.75	-1.55	-3.48	-1.78	-3.42	-2.36	-4.29	-2.37	-4.15	-4.11	1.19
4342	-2.11	-1.27	-4.13	-0.06	-0.25	1.67	2.12	-1.52	-2.70	-0.54	0.20	0.97	-1.20	0.15	-1.57	-3.03	-1.89	-3.88	-2.20	-3.86	-2.83	-4.77	-2.85	-4.72	-2.58	0.80
4343	-2.00	-1.18	-3.91	0.19	0.13	2.13	2.48	-1.33	-2.29	-0.35	-0.04	0.82	-1.28	0.15	-1.45	-2.93	-1.68	-3.62	-1.91	-3.57	-2.55	-4.50	-2.58	-4.38	-4.38	0.92
4344	-1.76	-1.15	-3.88	0.50	0.79	2.75	2.74	-1.51	-2.52	0.09	0.18	0.98	-1.17	0.21	-1.37	-2.71	-1.48	-3.31	-1.55	-3.16	-2.08	-4.03	-2.10	-3.92	-4.07	1.23
4345	-2.23	-1.45	-4.02	-0.09	-0.08	1.86	2.19	-1.45	-2.74	-0.39	0.00	0.83	-1.31	0.04	-1.59	-3.10	-1.86	-3.81	-2.11	-3.81	-2.75	-4.74	-2.77	-4.65	-4.61	0.69
4346	-2.22	-1.27	-3.85	-0.17	-0.31	1.58	1.91	-1.06	-2.14	-0.61	0.06	0.82	-1.38	-0.04	-1.74	-3.09	-2.08	-3.98	-2.35	-4.02	-2.96	-4.90	-2.94	-4.77	-2.69	0.53
4347	-1.91	-1.15	-3.82	0.22	0.09	2.10	2.45	-1.15	-2.45	-0.15	0.47	1.27	-0.89	0.48	-1.25	-2.77	-1.52	-3.50	-1.85	-3.55	-2.51	-4.43	-2.50	-4.39	-4.43	0.87
4348	-2.05	-1.32	-3.94	-0.05	-0.17	1.82	2.15	-1.17	-2.39	-0.44	0.39	1.13	-1.05	0.30	-1.42	-2.83	-1.74	-3.74	-2.07	-3.74	-2.69	-4.61	-2.71	-4.53	-4.53	0.77
4350	-2.67	-1.75	-4.41	-0.50	-0.66	1.33	1.67	-1.63	-2.76	-0.81	-0.15	0.59	-1.57	-0.22	-1.93	-3.36	-2.21	-4.18	-2.48	-4.17	-3.14	-5.06	-3.16	-5.01	-4.97	0.32
4353	-2.35	-1.69	-4.37	-0.36	-0.45	1.48	1.87	-1.79	-3.06	-0.81	-0.13	0.64	-1.53	-0.17	-1.86	-3.34	-2.18	-4.16	-2.49	-4.14	-3.09	-5.01	-3.09	-4.92	-2.92	0.46
4355	-2.79	-1.89	-4.60	-0.69	-0.61	1.23	1.77	-1.69	-2.82	-0.69	-0.22	0.49	-1.69	-0.34	-1.84	-3.00	-2.06	-4.06	-2.43	-4.19	-3.16	-5.19	-3.23	-5.09	-2.62	1.03
4356	-2.15	-1.41	-4.04	-0.03	0.00	1.99	2.82	-1.41	-2.67	-0.31	0.12	0.87	-1.28	0.09	-1.58	-2.94	-1.78	-3.72	-2.04	-3.70	-2.61	-4.54	-2.61	-4.41	-2.23	0.89
4357	-2.01	-1.32	-3.84	0.03	-0.24	1.78	2.04	-1.60	-2.84	-0.33	0.05	0.83	-1.32	0.03	-1.66	-3.20	-1.90	-3.86	-2.13	-3.72	-2.64	-4.53	-2.67	-4.44	-4.35	0.94
4358	-2.42	-1.34	-3.82	-0.36	-0.89	1.04	1.52	-0.77	-1.87	-0.88	0.17	0.80	-1.47	-0.22	-2.04	-3.48	-2.36	-4.29	-2.62	-4.29	-3.22	-5.11	-3.20	-5.11	-4.83	0.47
4359	-2.72	-2.17	-4.73	-1.02	-0.89	0.57	0.52	-1.99	-3.24	-1.20	-0.60	0.12	-2.08	-0.77	-2.42	-3.36	-2.66	-4.53	-2.83	-4.51	-3.36	-5.22	-3.22	-4.88	-1.67	0.00
4360	-1.82	-1.37	-3.58	-0.41	-1.01	0.70	-0.40	-0.67	-2.00	-0.41	-0.17	0.54	-1.67	-0.37	-2.01	-3.03	-2.16	-3.97	-2.21	-3.77	-2.59	-4.46	-2.43	-4.19	-2.53	0.50
4361	-2.20	-1.48	-4.21	-0.64	-0.72	1.00	0.62	-2.47	-3.78	-0.64	-0.34	0.52	-1.57	-0.18	-1.79	-3.40	-2.00	-3.98	-2.33	-3.99	-2.92	-4.81	-2.88	-4.70	-4.92	0.38
4362	-2.44	-2.39	-5.08	-0.41	-0.47	1.31	2.64	-3.80	-4.42	-0.41	-1.36	-0.45	-2.52	-1.06	-2.46	-3.69	-2.45	-4.18	-2.35	-3.88	-2.80	-4.61	-2.80	-4.57	-4.57	0.73
4363	-2.38	-1.61	-4.14	-0.74	-0.89	0.50	0.56	-1.06	-2.34	-0.80	0.01	0.68	-1.56	-0.29	-2.05	-3.41	-2.34	-4.23	-2.56	-4.16	-3.07	-4.94	-3.02	-4.71	-2.15	0.28
4364	-2.20	-1.57	-4.06	-0.70	-0.88	0.46	0.08	-1.22	-2.77	-0.59	-0.55	0.26	-1.90	-0.54	-2.10	-3.01	-2.26	-4.07	-2.32	-3.91	-2.77	-4.62	-2.61	-4.33	-3.29	0.03
4365	-2.46	-1.77	-4.37	-0.73	-1.19	0.52	0.20	-1.88	-3.12	-1.19	-0.62	0.12	-2.06	-0.73	-2.40	-3.92	-2.76	-4.69	-2.91	-4.52	-3.34	-5.13	-3.14	-4.90	-2.73	0.09
4366	-2.70	-2.29	-5.22	0.07	1.09	2.92	1.09	-4.60	-5.36	0.01	-2.13	-1.08	-2.92	-1.29	-2.35	-3.52	-1.99	-3.61	-1.78	-3.30	-2.16	-4.05	-2.14	-3.90	-4.08	1.21
4367	-2.08	-1.30	-3.73	0.06	0.42	2.43	2.28	-1.45	-2.47	-0.08	-0.29	0.47	-1.67	-0.28	-1.79	-3.16	-1.80	-3.59	-1.79	-3.35	-2.22	-4.19	-2.25	-4.05	-4.46	0.83
4368	-1.73	-1.45	-4.20	-1.00	-1.01	-0.24	-1.23	-2.19	-3.52	-0.05	-0.44	0.39	-1.70	-0.29	-1.81	-3.40	-1.90	-3.67	-1.86	-3.43	-2.33	-4.18	-2.23	-4.02	-2.72	0.28
4369	-2.33	-1.74	-4.43	-0.75	-0.60	0.81	0.97	-1.79	-3.02	-0.98	-0.14	0.61	-1.57	-0.25	-2.01	-3.39	-2.44	-4.40	-2.70	-4.35	-3.23	-5.12	-3.21	-4.85	-1.89	0.45
4370	-2.39	0.56	-3.95	-0.75	-1.39	0.17	-0.17	-2.23	-3.62	-0.99	-0.92	-0.10	-2.21	-0.77	-2.35	-3.78	-2.53	-4.35	-2.64	-4.23	-3.14	-4.94	-3.00	-4.73	-4.77	0.53
4371	-2.15	-1.57	-4.14	-0.42	-0.53	1.05	0.71	-1.70	-2.89	-0.92	-0.20	0.56	-1.61	-0.29	-2.02	-3.62	-2.38	-4.29	-2.55	-4.17	-3.02	-4.83	-2.88	-4.64	-2.68	0.35
4372	-1.99	-1.21	-3.81	-0.32	-0.56	1.10	0.42	-1.90	-2.98	-0.32	-0.60	0.20	-1.94	-0.53	-1.96	-3.18	-2.03	-3.78	-2.04	-3.63	-2.52	-4.35	-2.46	-4.18	-2.30	0.70
4373	-3.05	-2.09	-4.55	-1.00	-1.00	0.70	0.59	-1.91	-3.36	-1.24	-0.59	0.21	-1.96	-0.64	-2.36	-3.66	-2.78	-4.71	-3.01	-4.58	-3.36	-5.15	-3.09	-4.77	-1.19	0.28

Appendix A4. Centered log ratio transformed data used for PCA and Random Forest.

Sample	Si	Al	Fe	Mn	Mg	Ca	Na	K	Ti	P	LOI	C-Total	C_in_CO2	Non_carb._C	Total S	Cu	Zn	Pb	Cd	Hg	Sn	Tl	In	As	Co	Ni	Se	Mo	Ge	Sb	Ag	Au	W	Bi	B	Rb	Sr	Cs	Ba	Be	Zr
4374	9.55	8.29	7.73	3.14	6.94	4.84	6.20	7.27	5.25	2.88	7.65	5.20	2.26	5.19	6.35	-0.74	0.89	-0.47	-4.42	-7.64	-2.34	-3.17	-6.03	0.93	0.52	0.97	-4.42	-2.34	-2.94	-2.94	-3.26	-7.64	-3.73	-3.73	0.77	1.22	1.12	-2.40	3.60	-3.04	2.23
4375	9.18	7.63	6.79	1.82	5.22	5.89	7.06	5.83	4.40	2.16	8.40	8.00	6.14	7.95	6.67	1.60	-0.07	0.62	-4.79	-6.40	-2.31	-4.27	-6.40	1.78	0.47	0.89	-4.79	-1.10	-3.31	-2.49	-3.07	-6.91	-4.10	-2.37	-0.51	-0.11	1.35	-3.91	1.28	-4.10	1.60
4376	9.20	7.71	7.16	1.30	5.76	4.02	5.96	6.60	4.42	2.00	8.28	7.55	2.83	7.55	7.10	2.11	1.38	1.58	-4.77	-5.15	-2.28	-2.65	-6.38	2.47	0.35	1.66	-4.77	-2.28	-3.12	-1.51	-2.55	-7.29	-4.07	-2.98	0.33	0.81	0.64	-3.04	2.86	-3.38	1.45
4377	10.27	8.51	7.39	3.30	6.17	6.04	8.02	5.78	5.13	3.21	6.73	4.40	4.40	4.08	3.20	0.71	1.30	-0.56	-3.89	-10.33	-3.20	-3.93	-5.50	-0.43	-0.62	-0.31	-3.89	-2.51	-2.10	-4.12	-3.89	-10.33	-3.20	-4.12	0.38	-0.20	2.87	-4.12	2.12	-2.51	2.69
4378	9.28	7.89	8.15	4.21	7.82	6.95	5.65	4.41	4.89	2.64	8.14	5.79	6.79	4.43	5.96	1.06	2.96	-2.23	-3.05	-7.06	-2.45	-5.67	-6.14	0.49	0.68	2.45	-4.53	-3.15	-2.81	-3.66	-4.53	-10.97	-3.84	-3.37	-0.66	-1.54	1.24	-4.06	0.41	-3.84	1.61
4379	9.59	8.02	6.95	2.39	5.96	5.83	6.25	6.99	4.30	2.19	7.98	6.99	5.41	6.93	6.80	1.43	2.05	-0.26	-4.48	-6.31	-2.40	-3.16	-6.09	1.32	-0.13	0.82	-4.48	-1.99	-2.91	-2.91	-3.78	-7.70	-2.40	-3.45	0.49	1.23	1.36	-2.56	3.10	-3.09	1.65
4380	9.74	8.24	7.31	2.43	6.25	5.43	7.15	6.51	4.79	2.53	7.56	6.32	5.21	6.22	5.71	1.06	0.96	-0.24	-4.34	-6.46	-2.95	-3.68	-5.95	0.55	-0.31	0.66	-4.34	-2.95	-2.69	-3.06	-3.31	-10.78	-3.64	-2.95	0.14	0.86	2.03	-3.06	2.75	-3.64	2.03
4381	10.38	8.80	7.23	3.14	5.97	6.58	8.02	7.20	4.96	2.91	7.48	5.70	6.21	5.10	4.80	0.46	2.20	-1.45	-3.76	-10.20	-3.06	-3.24	-5.36	-0.07	-0.63	-0.07	-3.76	-2.37	-2.37	-5.36	-3.76	-10.20	-3.06	-3.57	0.12	1.29	2.95	-2.88	3.55	-3.06	2.13
4382	9.63	8.41	7.70	2.90	6.72	7.08	7.13	6.75	5.15	2.71	8.07	6.55	7.10	5.91	5.83	1.38	1.29	-1.14	-4.32	-7.54	-2.24	-3.88	-5.93	0.56	0.06	1.05	-4.32	-2.24	-2.84	-3.85	-4.32	-10.76	-3.63	-4.14	0.24	0.75	2.01	-3.16	2.96	-3.63	1.69
4383	9.92	8.28	7.10	3.42	5.68	7.54	7.46	6.78	5.11	2.87	7.93	6.42	7.49	4.82	5.01	0.75	1.75	-0.98	-4.16	-10.60	-2.08	-3.88	-5.77	0.06	-0.43	-0.21	-4.16	-2.77	-3.13	-3.69	-4.16	-10.60	-3.47	-5.77	-0.29	0.66	2.54	-3.13	2.82	-3.47	2.24
4384	9.66	8.20	7.06	2.72	5.72	6.40	7.12	6.96	4.73	2.55	7.47	5.44	6.15	4.62	6.36	1.20	1.92	-0.08	-3.53	-7.62	-2.33	-3.77	-6.02	0.16	-0.42	0.07	-4.41	-1.92	-3.24	-3.53	-4.41	-10.85	-1.92	-4.22	-0.62	1.02	2.03	-2.19	3.12	-3.02	1.98
4385	8.61	7.50	5.66	0.23	5.21	3.84	6.20	6.37	4.41	1.80	8.54	8.44	3.48	8.43	5.35	3.83	4.46	1.51	-1.70	-5.97	-1.46	-3.46	-6.76	1.25	0.44	1.31	-1.74	-1.13	-3.36	-2.54	-2.89	-6.98	-4.46	-2.74	-0.36	0.63	0.48	-3.29	2.10	-4.46	1.26
4386	9.67	8.10	6.86	2.39	6.22	4.80	7.73	3.73	5.13	2.86	6.99	4.95	0.92	4.94	6.84	2.53	7.30	4.60	1.87	-3.11	-2.30	-6.50	-5.99	-1.60	-0.65	0.31	-2.00	-1.60	-3.50	-2.99	-2.52	-10.82	-3.68	-4.60	-0.51	-3.68	1.55	-5.99	-0.43	-3.68	2.30
4387	8.32	7.96	7.60	3.10	6.05	6.12	5.31	7.01	4.79	2.14	7.78	6.33	6.16	6.07	6.61	1.92	0.59	0.55	-5.16	-6.43	-1.83	-4.09	-6.77	1.13	0.83	0.90	-1.67	-1.69	-4.46	-2.61	-2.94	-7.68	-4.46	-6.77	1.17	1.00	-0.13	-3.37	2.42	-3.08	1.98
4388	9.17	7.80	7.31	2.26	5.22	5.13	7.24	5.49	4.46	2.20	8.30	8.04	3.43	8.04	6.65	2.15	2.47	-0.04	-3.37	-7.97	-1.58	-4.00	-6.37	1.14	0.40	1.39	-1.42	-1.42	-3.19	-2.54	-2.73	-7.28	-4.06	-2.73	0.03	-0.37	0.92	-4.57	1.41	-4.06	1.61
4390	8.87	7.26	7.51	1.70	5.01	5.81	6.39	5.92	3.94	1.59	8.58	8.18	6.47	8.13	7.50	2.02	4.51	0.12	-1.88	-6.23	-1.49	-3.65	-5.87	1.41	1.14	1.47	-0.97	-1.00	-3.39	-3.16	-4.08	-11.40	-4.26	-3.23	-1.49	0.24	0.76	-2.61	2.23	-4.26	0.99
4391	8.77	7.33	7.98	2.56	6.13	5.79	5.85	5.34	4.04	1.86	8.67	8.42	5.62	8.41	7.00	2.44	5.04	0.03	-1.14	-5.42	-1.74	-3.83	-5.14	-2.43	1.52	1.78	-4.91	-0.75	-2.43	-6.52	-3.53	-8.13	-4.22	-1.90	-0.96	-0.19	0.26	-3.34	1.57	-4.22	1.05
4392	9.01	7.70	6.42	1.67	4.97	5.58	6.33	6.54	4.35	2.13	7.75	7.02	5.95	6.92	6.49	2.51	4.02	-0.33	-2.40	-3.42	-2.49	-3.28	-6.59	1.74	-0.08	1.16	-4.98	-2.21	-3.12	-1.89	-3.95	-7.10	-4.29	-3.26	1.86	0.87	0.74	-3.12	2.76	-3.59	1.28
4393	8.71	7.56	7.19	2.60	5.54	6.62	3.29	6.96	4.73	2.58	7.79	6.28	6.64	5.79	7.25	2.46	3.95	0.02	-2.33	-4.26	-1.32	-2.76	-6.02	1.45	-0.25	0.51	-1.45	-2.62	-2.66	-1.95	-3.46	-6.94	-4.41	-3.83	0.98	1.39	-0.16	-3.13	2.75	-3.72	1.23
4394	8.87	7.47	8.07	3.38	6.03	6.82	4.47	6.60	4.60	2.32	7.91	6.67	6.90	6.25	7.54	3.00	4.58	-0.31	-1.60	-4.84	-1.45	-3.89	-4.73	-2.43	0.39	1.02	-1.76	-1.74	-2.70	-2.37	-3.44	-5.36	-4.22	-3.44	0.64	0.84	0.00	-4.22	2.57	-3.53	1.05
4395	8.68	7.35	6.36	1.10	4.78	5.41	4.71	6.20	4.18	1.75	7.83	7.30	5.34	7.26	6.45	1.60	3.85	-0.04	-2.51	-3.89	-1.49	-3.00	-5.50	1.47	-0.23	0.94	-1.79	-1.95	-2.67	-2.22	-3.71	-7.40	-4.59	-3.36	0.68	0.64	1.46	-2.61	2.40	-3.20	1.33
4396	8.51	7.37	8.14	2.27	5.20	5.51	3.49	6.52	4.73	1.86	8.27	6.74	6.08	6.59	8.17	1.82	1.98	0.30	-3.61	-7.62	-2.32	-3.72	-6.71	1.70	0.36	1.26	-1.84	-2.10	-3.30	-1.18	-3.18	-4.65	-1.92	-3.45	0.88	0.59	0.03	-3.45	2.88	-3.71	0.89
4397	8.41	7.54	7.18	1.04	5.04	5.69	4.22	6.86	4.45	1.79	8.59	8.07	5.92	8.04	7.28	1.63	2.12	0.38	-3.25	-7.69	-1.38	-3.28	-6.77	1.62	0.62	1.81	-2.23	-0.17	-3.59	-1.39	-3.37	-6.59	-3.08	-2.94	0.33	1.08	-1.00	-3.68	2.50	-3.08	1.03
4398	9.09	7.78	7.41	3.51	5.65	7.21	4.56	6.76	5.35	3.31	7.99	6.53	7.23	5.73	6.28	0.70	1.46	-1.62	-4.79	-5.62	-3.41	-2.88	-6.40	0.35	-0.53	-0.08	-4.79	-2.31	-3.63	-2.72	-3.92	-8.01	-4.10	-6.40	0.94	0.97	0.69	-3.31	3.08	-4.10	1.41
4399	10.25	7.62	6.99	2.40	5.41	5.72	6.02	6.53	4.40	2.23	7.90	7.46	5.95	7.39	5.46	1.69	1.99	-1.73	-4.03	-5.64	-3.34	-3.75	-5.64	1.04	0.45	1.14	-4.03	-1.26	-2.31	-2.65	-4.03	-7.25	-3.34	-4.25	0.94	0.79	0.69	-3.16	2.66	-3.34	1.40
4400	9.44	8.47	7.87	3.31	7.00	5.92	6.45	7.21	5.30	3.08	7.45	3.75	1.55	3.72	5.05	1.08	1.57	-1.44	-4.44	-10.88	-3.05	-3.50	-6.05	-0.85	0.32	1.90	-4.44	-2.36	-2.65	-3.05	-4.44	-7.66	-3.74	-4.26	0.53	1.62	2.31	-1.48	3.66	-2.36	1.68
4401	8.75	7.52	7.45	1.78	4.91	6.12	6.11	6.45	4.34	2.05	8.09	7.29	5.73	7.23	7.53	1.57	3.19	-0.24	-3.20	-6.33	-2.06	-2.57	-6.67	2.19	-0.11	1.14	-5.06	-2.06	-2.84	-1.75	-3.89	-8.27	-4.36	-3.20	0.30	0.98	1.60	-2.26	3.18	-3.67	1.23
4402	9.13	7.68	7.39	2.85	6.07	6.98	5.25	6.51	5.23	2.65	7.70	6.20	6.88	5.42	5.67	3.05	4.65	-0.29	-1.59	-4.90	-1.64	-3.51	-5.73	0.40	0.72	1.10	-2.33	-1.82	-3.65	-2.96	-3.02	-8.03	-4.12	-6.42	-0.72	0.44	0.85	-3.65	2.14	-4.12	1.46
4403	9.45	8.25	7.41	3.22	6.92	6.25	7.47	6.80	5.20	3.36	7.01	3.56	4.43	2.52	4.85	1.97	3.08	0.06	-2.25	-4.47	-1.73	-4.59	-6.12	-0.56	0.04	1.57	-3.12	-2.43	-3.48	-4.32	-3.63	-7.73	-3.81	-4.04	-0.56	0.35	2.76	-4.73	3.80	-3.81	1.88
4404	9.90	8.72	8.05	3.88	7.67	7.47	7.78	6.92	5.69	3.84	8.03	4.88	6.35	-10.44	3.60	1.56	1.94	-1.70	-4.00	-7.22	-2.61	-4.58	-5.61	-1.92	0.53	2.12	-4.00	-2.61	-2.52	-3.31	-4.00	-10.44	-3.31	-4.22	-0.53	0.60	3.08	-3.82	3.66	-2.61	2.34
4405	9.73	8.17	8.99	4.09	7.23	6.31	7.08	3.61	5.24	3.27	8.11	4.48	5.67	2.21	7.56	2.67	2.61	-1.84	-4.15	-5.98	-1.66	-3.16	-5.76	-1.15	0.59	1.41	-1.57	-2.76	-1.57	-3.45	-4.15	-10.59	-3.45	-3.96	0.01	-3.45	0.98	-3.96	0.18	-2.76	1.46
4406	9.09	7.67	6.71	1.85	5.00	6.03	5.33	6.62	4.31	2.12	7.81	6.89	6.46	6.70	6.66	1.52	-1.05	-0.27	-4.92	-4.92	-2.43	-3.55	-6.53	1.84	-0.36	1.00	-4.92	-1.92	-3.00	-0.82	-3.75	-5.25	-1.92	-3.00	0.28	0.94	0.51	-3.13	2.77	-2.84	1.54
4408	8.82	7.50	6.78	1.54	4.09	5.58	6.66	5.62	4.30	2.06	7.80	7.13	5.83	7.05	6.93	2.17	5.00	0.18	-1.27	-3.25	-0.89	-3.72	-4.08	1.28	-0.49	0.88	-3.09	-2.34	-2.70	-2.10	-3.47	-6.25	-2.12	-3.26	-0.55	-0.06	0.73	-4.08	1.71	-4.42	1.26
4409	8.93	7.60	6.88	0.78	4.40	4.83	6.13	6.32	4.25	1.90	7.75	6.92	5.17	6.87	6.99	1.92	3.69	0.04	-2.75	-4.36	-1.88	-2.67	-6.66	1.58	-0.20	1.15	-3.03	-0.72	-2.54	-1.54	-3.67	-6.08	-2.28	-3.26	0.41	0.62	0.69	-3.33	2.63	-3.67	1.21
4410	8.38	7.68	7.46	4.26	7.14	7.88	6.09	6.30	5.03	1.69	8.88	7.88	8.55	7.10	7.56	1.36	2.01	-0.38	-4.85	-4.70	-1.86	-6.97	-6.46	1.41	0.15	0.82	-3.28	-2.08	-3.06	-2.59	-4.85	-7.38	-4.16	-4.67	0.43	0.63	1.89	-2.68	2.69	-4.16	0.40
4411	8.93	7.66	6.68	1.45	4.96	5.34	6.19	6.33	4.37	2.08	7.94	7.27	5.91	7.20	6.83	0.94	2.97	-0.38	-3.37	-4.31	-2.25	-2.39	-6.63	1.47	-0.01	1.41	-2.33	-2.03	-2.38	-1.72	-3.74	-8.24	-4.33	-3.30	0.25	0.82	1.50	-2.51	2.70	-3.64	1.19
4412	9.26	8.37	8.13	3.85	7.17	6.12	6.75	6.58	5.53	2.50	7.56	4.68	5.20	4.07	4.30	1.58	1.81	-0.84	-4.53	-7.75	-3.14	-4.03	-6.14	0.08	0.71	1.90	-4.53	-2.45	-2.67	-3.14	-4.53	-10.97	-2.45	-4.75	0.59	0.95	1.47	-2.55	2.87	-3.14	1.44
4413	8.52	7.36	6.52	1.38	4.75	5.22	5.26	6.22	4.07	1.83	7.89	7.30	5.77	7.24	6.65	2.05	4.36	-0.15	-2.04	-4.11	-1.76	-2.77	-5.16	1.60	0.02	1.40	-2.55	-2.01	-2.55	-1.57	-3.87	-7.18	-2.86	-3.22	0.06	0.57	0.87	-3.17	2.38	-3.96	0.92
4414	8.83	7.52	6.90	1.82	5.49	6.07	6.15	6.06	4.14	1.91	8.21	7.65	6.77	7.53	6.75	1.87	3.91	-1.09	-2.56	-4.77	-2.05	-3.65	-5.96	1.63	-0.08	1.20	-5.05	-1.87	-2.87	-2.13	-4.17	-5.43	-2.05	-3.25	-0.08	0.33	1.24	-3.40	2.38	-3.66	1.11
4416	8.65	7.35	7.08	1.20	4.87	5.38	5.82	5.99	4.08	1.54	7.93	7.15	5.98	7.06	7.22	2.28	3.96	0.16	-2.41	-3.78	-1.77	-2.82	-5.46	1.84	0.10	1.49	-2.46	-1.77	-2.97	-2.20	-3.58	-7.07	-3.85	-3.20	-0.71	0.46	0.80	-2.82	2.30	-3.85	1.12
4417	8.62	7.42	6.82	2.67	5.01	6.20	6.14	5.99	4.47	2.17	7.69	6.47	6.60	6.10	6.99	2.72	4.52	0.01	-1.87	-3.82	-1.22	-3.20	-4.77	1.03	-0.04	0.57	-2.52	-2.25	-2.50	-1.99	-3.76	-7.77	-4.55	-3.68	-0.05	0.30	0.80	-3.68	2.11	-3.86	1.14
4418	8.86	7.61	7.02	1.25	4.77	5.27	5.15	6.49	4.15	2.09	8.26	7.74	5.75	7.70	7.11	1.56	3.25	0.06	-3.16	-4.68	-1.84	-3.28	-6.63	2.08	0.07	1.34	-5.02	-1.84	-2.64	-1.27	-3.54	-5.24	-2.53	-3.37	0.17	0.86	0.98	-2.80	2.72	-3.63	1.14
4421	9.16	7.93	6.44	2.47	5.51	6.21	6.69	6.30	4.70	2.36	7.81	6.75	6.83	6.40	6.30	1.10	2.17	-1.23	-4.12	-5.47	-2.74	-3.09	-6.43	1.52	-0.44	0.91	-4.82	-2.04	-2.74	-2.96	-4.12	-8.04	-4.12	-3.94	1.20	0.80	2.05	-2.18	2.67	-3.43	1.44
4426	8.86	7.51	7.45	2.04	5.85	5.57	6.73	5.62	4.39	1.86	7.96	7.04	6.14	6.92	7.38	1.33	4.05	0.35	-2.40	-4.64	-2.01	-4.27	-6.61	1.41	0.38	1.64	-2.74	-1.67	-3.36	-2.43	-3.84	-7.13	-4.31	-2.49	1.13	-0.12	0.51	-3.28	2.10	-4.31	1.08
4434	8.89	7.74	6.73	2.69	5.61	6.28	6.51	6.55	4.58	2.19	7.86	6.99	6.86	6.72	6.49	0.91	3.30	-0.66	-3.60	-4.95	-2.00	-3.85	-6.60	1.33	-0.38	1.00	-4.99	-0.56	-3.27	-2.15	-4.12	-7.11	-4.30	-3.83	0.54	0.87	0.59	-2.77	2.70	-3.60	1.34
4435	8.67	7.46	7.09	2.12	5.25	6.18	6.44	6.00	4.09	1.96	8.03	7.41	6.45	7.30	6.88	2.26	4.02	-0.42	-2.37	-4.43	-1.68	-4.75	-6.06	0.57	-0.06	1.43	-2.73	0.00	-3.57	-2.19	-3.76	-6.75	-2.66	-3.66	0.00	0.30	0.73	-3.06	2.42	-4.45	1.11
4437	9.73	8.69	7.58	3.18	6.55	6.44	7.50	7.37	5.26	2.74	7.62	5.15	6.33	2.99	3.98	0.94	1.71	-1.03	-4.21	-7.43	-2.82	-3.58	-5.82	-0.05	0.22	1.57	-4.21	-2.82	-2.82	-4.43	-4.21	-10.65	-3.52	-5.12	1.60	1.43	2.55	-2.23	3.29	-3.52	1.85
4438	9.45	8.43	7.59	2.91	6.53	5.76	6.77	7.11	5.41	2.75	7.34	4.33	4.27	4.04	4.07	0.66	1.59	-1.49	-4.49	-7.71	-3.10	-3.90	-6.10	0.33	0.14	1.53	-4.49	-2.01	-2.77	-4.02	-4.49	-7.71	-3.10	-4.71	2.17	1.29	1.70	-2.46	3.45	-3.10	1.75
4441	8.76	7.48	7.19	2.00	4.92	6.25	5.99	6.49	4.19	1.93	7.93	7.03	6.29	6.89	7.22	1.88	3.50	0.29	-2.80	-4.45	-1.92	-3.78	-6.71	1.91	-0.01	1.24	-5.10	-1.77	-3.45	-1.27	-3.62	-5.83	-4.41	-3.13	1.21	0.85	0.68	-2.52	2.69	-3.71	1.16
4445	8.50	7.46	6.77	-0.10	4.08	3.80	4.40	6.43	4.14	1.85	8.03	7.43	1.77	7.43	6.78	2.31	4.36	0.19	-2.46	-3.81	-1.74	-3.01	-6.24	1.92	0.27	1.67	-5.32	-1.74	-3.02	-0.79	-3.24	-5.11	-2.15	-2.94	0.34	0.82	0.62	-2.18	2.71	-3.24	1.05
4446	9.18	7.79	6.74	2.13	5.05	5.53	6.63	6.47	4.45	2.25	7.66	6.58	6.05	6.41	6.78	1.27	2.81	-0.29	-3.69	-4.64	-2.78	-3.07	-6.47	2.03	-0.29	1.15	-4.86	-2.08	-2.44	-1.30	-3.69	-6.69	-4.16	-3.47	0.42	0.85	1.45	-2.34	2.80	-3.47	1.54
4447	9.53	8.15	6.95	2.51	5.93	5.81	6.14	6.95	4.89	2.50	7.51	6.34	5.69	6.18	3.65	0.99	3.10	-0.26	-2.97	-5.68	-2.46	-3.27	-6.15	-0.67	-0.28	1.31	-3.51	-2.46	-2.75	-3.84	-4.54	-7.76	-2.46	-4.76	1.36	1.24	1.90	-2.41	3.31	-3.15	1.58
4449	9.10	7.60	7.39	3.47	6.35	7.15	7.31	4.65	4.17	2.44	8.35	7.22	7.85	6.51	7.29	1.75	3.42	-0.22	-2.76	-4.70	-2.66	-6.86	-6.35	1.51	-0.04	1.33	-4.74	-1.27	-3.57	-1.35	-4.74	-6.57	-2.25	-2.95	1.69	-1.15	1.33	-4.56	0.79	-4.04	1.15
4450	9.20	7.86	6.82	2.16	5.34	5.96	6.52	6.86	4.68	2.38	7.57	6.22	6.49	5.77	6.26	0.56	1.02	-1.21	-4.80	-6.92	-2.31	-3.86	-6.41	0.35	-0.80	0.25	-4.80	-1.33	-2.94	-1.80	-3.77	-8.01	-2.02	-4.10	0.35	1.17	1.77	-2.22	3.22	-2.72	1.78
4451	9.10	7.95	6.94	3.34	5.48	6.70	6.93	6.70	4.94	2.70	7.76	6.41	7.27	5.39	6.09	-0.72	1.18	-2.51	-4.82	-6.65	-2.04	-5.26	-6.42	0.97	-0.69	0.04	-4.82	-1.64	-3.02	-2.47	-3.94	-5.73	-1.64	-4.35	0.21	0.85	2.27	-3.02	2.88	-3.43	1.81
4452	9.77	8.66	7.65	2.86	6.80	4.88	7.10	7.21	5.40	2.46	7.59	4.88	3.17	4.83	2.88	0.84	1.70	-1.90	-4.21	-7.42	-2.82	-3.23	-5.81	0.82	0.43	2.26	-4.21	-1.72	-2.56	-2.35	-4.21	-10.65	-3.51	-4.43	1.42	1.29	2.67	-2.64	3.43	-2.82	1.91
4453	9.07	7.56	6.67	2.01	4.89	5.78	6.05	6.58	4.26	1.91	7.73	7.10	5.88	7.01	6.16	1.08	3.61	0.02	-2.73	-5.23	-1.96	-3.86	-6.56	0.12	-0.13	0.93	-4.95	-1.78	-3.10	-2.31	-3.67	-7.07	-4.26	-2.98	-0.73	0.81	1.94	-3.10	3.19	-3.57	1.56
4454	8.71	7.51	6.98	2.05	4.89	5.63	5.61	6.62	4.72	2.23	7.75	6.86	5.97	6.74	6.87	1.13	3.17	-1.50	-3.16	-5.32	-2.19	-3.92	-6.80	0.97	-0.19	0.81	-2.17	-1.72	-3.27	-1.47	-3.80	-6.46	-2.01	-4.31	-0.09	0.80	1.39	-3.16	3.10	-3.11	1.43
4456	9.60	8.51	7.71	3.15	6.58	5.83	6.97	6.73	5.41	2.60	7.46	4.47	4.20	4.23	4.12	0.90	1.57	-2.06	-4.36	-7.58	-2.97	-4.11	-5.97	-0.03	0.34	1.83	-4.36	-2.97	-2.38	-3.33	-3.48	-10.80	-3.66	-4.58	0.96	1.00	2.55	-2.79	3.06	-2.97	1.86
4457	9.14	7.69	6.20	1.87	5.22	5.63	5.92	6.51	4.00	1.65	7.97	7.35	6.27	7.25	6.21	1.33	2.61	-0.87	-4.20	-5.02	-2.12	-2.79	-6.51	1.21	-0.49	0.92	-2.26	-1.90	-2.44	-2.23	-4.90	-8.11	-4.20	-3.87	0.23	0.97	1.55	-2.38	2.88	-2.82	1.31
4458	8.32	7.15	6.79	0.98	4.42	4.73	6.02	5.74	3.89	1.46	8.26	7.90	5.20	7.88	6.94	2.35	4.33	0.59	-1.96	-4.02	-1.71	-3.12	-6.32	2.03	0.54	1.98	-1.36	-1.45	-2.73	-1.04	-3.23	-6.67	-2.22	-2.63	-0.58	0.29	0.38	-2.88	1.95	-4.02	0.61
4459	8.77	7.46	6.55	-0.63	3.99	4.19	5.55	6.35	4.20	1.10	8.12	7.63	2.22	7.63	6.70	1.51	2.82	0.12	-3.77	-3.04	-1.29	-2.58	-6.07	1.43	-0.36	0.75	-1.51	-1.57	-2.61	-0.83	-3.18	-7.28	-1.98	-2.82	0.36	0.81	0.83	-2.08	2.57	-3.08	1.16
4460	9.21	7.75	6.46

Appendix A4. Centered log ratio transformed data used for PCA and Random Forest.

Sample	Hf	Nb	Ta	Ga	Sc	V	Cr	Th	U	Y	La	Ce	Pr	Nd	Sm	Eu	Gd	Tb	Dy	Ho	Er	Tm	Yb	Lu	Br	F
4374	-1.56	-1.33	-3.73	0.10	-0.28	1.28	0.14	-1.78	-2.92	0.22	-1.00	-0.02	-2.07	-0.65	-2.23	-4.01	-2.29	-4.12	-2.15	-3.58	-2.33	-4.15	-2.20	-3.98	-2.30	0.87
4375	-2.12	-1.34	-3.98	-1.01	-0.88	0.64	0.11	-2.34	-3.43	-0.41	0.46	1.21	-0.98	0.33	-1.54	-3.29	-1.99	-3.98	-2.18	-3.72	-2.54	-4.43	-2.43	-4.30	-4.79	0.51
4376	-2.32	-1.64	-4.27	-0.55	-0.57	0.98	1.12	-1.56	-2.96	-0.90	-0.40	0.39	-1.81	-0.51	-2.18	-3.66	-2.47	-4.35	-2.57	-4.14	-3.02	-4.85	-2.93	-4.62	-4.77	0.53
4377	-1.05	-0.94	-3.26	0.13	-0.79	0.27	-0.22	-1.04	-2.39	0.63	0.82	1.64	-0.50	0.84	-0.87	-2.47	-1.06	-2.89	-1.15	-2.77	-1.62	-3.59	-1.62	-3.47	-3.89	1.41
4378	-1.98	-0.95	-3.71	-0.51	0.07	1.70	3.17	-1.81	-3.38	0.26	-0.09	0.82	-1.21	0.25	-1.26	-2.87	-1.44	-3.25	-1.51	-3.13	-2.01	-3.90	-1.96	-3.80	-4.53	0.77
4379	-1.96	-1.56	-3.93	-0.20	-1.21	0.44	0.24	-1.85	-3.17	-0.79	-0.41	0.39	-1.77	-0.48	-2.11	-3.57	-2.36	-4.23	-2.55	-4.14	-3.04	-4.99	-3.03	-4.80	-4.48	0.82
4380	-1.62	-1.52	-3.84	-0.06	-1.00	0.86	-0.28	-1.69	-2.98	-0.18	0.12	0.88	-1.28	0.05	-1.69	-3.32	-1.94	-3.77	-1.98	-3.60	-2.51	-4.42	-2.50	-4.34	-2.12	0.96
4381	-1.49	-1.27	-3.51	0.40	-0.89	0.77	0.41	-1.43	-2.60	-0.42	0.21	0.99	-1.21	0.09	-1.60	-3.06	-1.96	-3.88	-2.22	-3.88	-2.78	-4.78	-2.82	-4.67	-3.76	1.54
4382	-1.98	-1.80	-4.32	0.01	-0.40	1.62	0.73	-2.06	-3.43	-0.54	0.08	0.86	-1.28	0.09	-1.67	-3.17	-2.01	-3.93	-2.24	-3.83	-2.77	-4.71	-2.80	-4.54	-4.32	0.98
4383	-1.41	-1.03	-3.51	-0.21	-0.85	0.52	-0.81	-1.60	-3.16	0.17	0.30	1.14	-0.99	0.40	-1.30	-2.88	-1.51	-3.32	-1.61	-3.24	-2.18	-4.12	-2.16	-3.98	-4.16	2.52
4384	-1.74	-1.39	-3.80	-0.19	-1.08	0.64	0.05	-1.80	-2.98	0.02	0.31	1.03	-1.16	0.14	-1.62	-3.17	-1.83	-3.71	-1.92	-3.51	-2.47	-4.37	-2.55	-4.41	-4.41	0.89
4385	-2.35	-1.72	-4.17	-0.33	-0.43	1.12	2.24	-2.07	-3.22	-0.93	-0.85	-0.02	-2.18	-0.86	-2.60	-4.21	-2.85	-4.66	-2.86	-4.28	-3.05	-4.94	-2.89	-4.59	-0.88	0.15
4386	-1.32	-1.06	-3.53	-0.69	-0.94	0.67	2.49	-1.58	-2.78	0.10	-1.25	-0.23	-2.29	-0.76	-2.19	-4.01	-2.14	-3.72	-1.88	-3.30	-2.09	-3.93	-1.91	-3.64	-2.20	0.92
4387	-1.63	-1.22	-3.76	-0.08	-0.87	1.16	-0.24	-1.86	-3.26	-0.25	-0.17	0.56	-1.65	-0.32	-2.01	-3.36	-2.14	-3.87	-2.08	-3.63	-2.57	-4.53	-2.60	-4.39	-2.71	0.14
4388	-2.03	-1.47	-4.00	-0.37	-0.62	0.85	0.21	-2.06	-3.26	-0.60	-1.15	-0.25	-2.30	-0.84	-2.24	-3.62	-2.30	-4.04	-2.32	-3.83	-2.75	-4.68	-2.68	-4.39	-1.05	0.54
4390	-2.73	-2.00	-4.48	-0.86	-0.68	0.65	0.17	-2.53	-3.59	-0.68	-0.87	0.00	-2.09	-0.69	-2.16	-3.52	-2.27	-4.13	-2.37	-4.00	-2.94	-4.88	-2.94	-4.71	-2.34	0.34
4391	-2.61	-1.88	-4.49	-0.69	-0.57	0.76	0.39	-2.51	-3.46	-0.75	-0.59	0.21	-1.95	-0.53	-2.08	-3.26	-2.21	-3.99	-2.28	-3.91	-2.86	-4.80	-2.87	-4.58	-2.36	0.38
4392	-2.31	-1.68	-4.27	-0.65	-0.75	0.78	0.64	-1.60	-2.82	-1.03	-0.19	0.54	-1.69	-0.37	-2.14	-3.57	-2.47	-4.39	-2.72	-4.35	-3.26	-5.15	-3.21	-4.94	-4.98	0.32
4393	-2.50	-1.59	-4.37	-0.72	-0.90	1.13	0.49	-2.82	-4.11	-0.89	-0.74	0.12	-2.00	-0.56	-2.21	-3.70	-2.41	-4.25	-2.56	-4.18	-3.17	-5.15	-3.25	-4.99	-5.11	0.19
4394	-2.66	-1.96	-4.70	-0.70	-0.70	1.24	0.92	-2.90	-4.22	-1.13	-0.97	-0.12	-2.25	-0.80	-2.43	-3.80	-2.59	-4.50	-2.77	-4.37	-3.34	-5.30	-3.33	-5.04	-4.92	0.38
4395	-2.28	-1.83	-4.25	-0.80	-1.25	0.56	-0.35	-1.70	-3.12	-0.56	-0.19	0.58	-1.64	-0.29	-1.97	-3.22	-2.22	-4.04	-2.31	-3.92	-2.86	-4.81	-2.92	-4.71	-5.28	0.02
4396	-2.72	-1.93	-4.60	-0.94	-0.89	1.33	0.09	-2.10	-3.47	-0.82	-0.63	0.13	-2.06	-0.69	-2.42	-4.00	-2.66	-4.36	-2.57	-4.14	-3.03	-4.95	-3.07	-4.85	-2.37	0.20
4397	-2.61	-1.85	-4.47	-0.60	-0.73	1.43	0.20	-2.10	-3.48	-0.52	-1.69	-0.74	-2.79	-1.26	-2.57	-3.47	-2.47	-4.19	-2.40	-3.89	-2.76	-4.67	-2.66	-4.39	-2.47	0.13
4398	-2.28	-0.99	-3.92	-0.52	-0.39	1.02	-0.92	-1.99	-3.49	0.23	-0.01	0.83	-1.30	0.13	-1.52	-2.90	-1.65	-3.44	-1.68	-3.21	-2.14	-4.06	-2.23	-4.04	-3.41	2.30
4399	-2.24	-1.69	-4.25	-0.57	-1.05	1.02	0.40	-1.93	-3.21	-0.57	-0.47	0.37	-1.83	-0.45	-2.13	-3.85	-2.32	-4.07	-2.36	-3.88	-2.73	-4.61	-2.61	-4.36	-2.11	1.27
4400	-1.95	-1.09	-3.76	0.13	0.05	2.02	2.33	-1.06	-2.40	-0.28	-0.10	0.80	-1.36	0.02	-1.53	-3.01	-1.75	-3.63	-1.95	-3.60	-2.60	-4.57	-2.64	-4.44	-4.44	2.25
4401	-2.36	-1.80	-4.47	-0.72	-1.15	0.70	-0.28	-1.80	-3.12	-0.67	-0.65	0.12	-2.07	-0.67	-2.25	-3.33	-2.34	-4.18	-2.41	-4.01	-2.93	-4.87	-2.94	-4.72	-3.08	0.24
4402	-2.21	-1.37	-4.06	-0.54	-0.63	1.42	0.35	-2.63	-3.97	-0.54	-0.66	0.19	-1.95	-0.53	-2.12	-3.48	-2.21	-4.04	-2.33	-3.96	-2.90	-4.86	-2.94	-4.70	-3.33	0.48
4403	-1.84	-1.15	-3.74	-0.41	-0.77	1.54	1.29	-1.50	-2.89	-0.64	0.41	1.14	-1.09	0.25	-1.59	-2.91	-1.99	-3.96	-2.31	-4.01	-3.01	-4.95	-3.03	-4.84	-4.51	0.79
4404	-1.39	-0.67	-3.31	0.28	-0.10	2.06	2.27	-1.07	-2.53	-0.22	0.81	1.55	-0.66	0.68	-1.15	-2.38	-1.53	-3.53	-1.88	-3.53	-2.53	-4.58	-2.59	-4.13	-4.00	1.30
4405	-2.17	-1.77	-4.53	-0.05	-0.24	1.88	1.57	-2.42	-3.81	-0.19	-0.35	0.48	-1.62	-0.20	-1.72	-2.59	-1.82	-3.63	-1.94	-3.56	-2.51	-4.47	-2.50	-4.23	-2.58	1.15
4406	-2.12	-1.49	-4.18	-0.54	-0.82	0.67	0.51	-1.50	-2.80	-0.76	-0.02	0.73	-1.43	-0.10	-1.85	-3.36	-2.18	-4.17	-2.45	-4.04	-2.97	-4.92	-2.89	-4.61	-4.92	0.38
4408	-2.42	-1.87	-4.62	-0.43	-1.40	0.46	-0.26	-2.51	-3.80	-0.68	-0.77	0.01	-2.17	-0.75	-2.38	-3.75	-2.44	-4.31	-2.51	-4.07	-3.01	-4.97	-3.00	-4.72	-3.55	0.18
4409	-2.39	-1.86	-4.42	-1.27	-0.85	0.62	0.30	-1.76	-2.99	-1.27	-0.31	0.44	-1.77	-0.44	-2.20	-3.55	-2.56	-4.47	-2.76	-4.45	-3.38	-5.33	-3.38	-5.10	-3.08	0.24
4410	-3.13	-2.34	-5.43	-0.52	0.10	1.93	0.94	-3.40	-4.46	-0.58	-0.91	-0.13	-2.24	-0.83	-2.20	-3.29	-2.25	-4.10	-2.33	-3.91	-2.89	-4.81	-2.95	-4.78	-3.00	0.45
4411	-2.41	-1.78	-4.41	-0.69	-0.56	0.85	0.76	-1.72	-2.94	-1.15	-0.27	0.47	-1.74	-0.39	-2.17	-3.34	-2.66	-4.55	-2.82	-4.46	-3.35	-5.25	-3.23	-4.95	-3.17	0.27
4412	-2.11	-1.30	-3.74	-0.01	0.47	2.44	2.30	-1.47	-2.61	-0.10	-0.26	0.49	-1.67	-0.26	-1.78	-3.16	-1.83	-3.60	-1.81	-3.38	-2.31	-4.22	-2.31	-4.08	-4.53	0.77
4413	-2.68	-2.00	-4.60	-0.67	-0.97	0.59	0.26	-1.93	-3.23	-0.87	-0.50	0.25	-1.96	-0.60	-2.34	-3.49	-2.60	-4.41	-2.66	-4.22	-3.15	-5.10	-3.09	-4.76	-3.17	-0.05
4414	-2.50	-1.83	-4.35	-0.71	-1.04	0.47	0.24	-1.67	-3.01	-1.09	-0.37	0.36	-1.87	-0.53	-2.27	-3.40	-2.65	-4.58	-2.88	-4.50	-3.40	-5.32	-3.30	-5.01	-3.13	0.25
4416	-2.57	-1.93	-4.46	-0.85	-1.05	0.47	0.12	-1.90	-3.14	-0.90	-0.60	0.17	-1.99	-0.66	-2.35	-3.52	-2.55	-4.41	-2.62	-4.22	-3.12	-5.02	-3.06	-4.84	-3.44	0.07
4417	-2.50	-1.73	-4.53	-0.64	-1.01	0.84	0.33	-2.71	-3.96	-0.68	-0.85	-0.01	-2.13	-0.71	-2.31	-3.61	-2.39	-4.17	-2.43	-4.02	-2.95	-4.88	-2.97	-4.68	-3.39	0.05
4418	-2.47	-1.81	-4.29	-0.59	-0.92	0.64	0.22	-1.75	-2.95	-1.07	-0.80	-0.01	-2.20	-0.85	-2.52	-3.63	-2.73	-4.57	-2.79	-4.39	-3.32	-5.24	-3.24	-4.94	-3.16	0.28
4421	-2.15	-1.43	-4.07	-0.34	-0.70	1.14	1.13	-1.45	-2.69	-0.95	0.01	0.74	-1.48	-0.14	-1.91	-3.28	-2.34	-4.23	-2.54	-4.25	-3.16	-5.15	-3.17	-4.90	-3.25	0.48
4426	-2.52	-1.78	-4.49	-0.91	-0.95	0.72	0.79	-1.92	-3.17	-0.85	-0.55	0.22	-2.00	-0.64	-2.35	-3.87	-2.58	-4.37	-2.62	-4.20	-3.12	-5.01	-3.09	-4.82	-3.28	0.29
4434	-2.27	-1.66	-4.24	-0.56	-0.78	0.97	0.97	-1.69	-3.00	-0.90	-0.28	0.47	-1.71	-0.35	-2.08	-3.35	-2.39	-4.28	-2.56	-4.20	-3.14	-5.07	-3.10	-4.84	-3.20	0.31
4435	-2.42	-2.05	-4.53	-0.87	-1.08	0.64	-0.05	-2.00	-3.27	-0.87	-0.71	0.04	-2.10	-0.74	-2.40	-3.56	-2.53	-4.37	-2.60	-4.16	-3.05	-4.96	-2.99	-4.70	-3.29	0.16
4437	-1.72	-1.36	-3.99	0.27	-0.13	1.86	1.97	-1.67	-2.91	-0.52	-0.16	0.64	-1.47	-0.06	-1.75	-3.14	-1.99	-3.84	-2.12	-3.74	-2.67	-4.65	-2.66	-4.43	-2.64	1.09
4438	-1.82	-1.31	-3.86	0.07	0.08	2.12	2.03	-1.39	-2.77	-0.27	0.13	0.95	-1.18	0.21	-1.50	-2.89	-1.80	-3.68	-1.94	-3.57	-2.50	-4.49	-2.56	-4.31	-4.49	0.81
4441	-2.38	-1.89	-4.39	-0.67	-0.99	0.74	0.42	-1.66	-2.96	-1.15	-0.59	0.16	-2.01	-0.67	-2.42	-3.68	-2.68	-4.61	-2.87	-4.49	-3.41	-5.27	-3.29	-4.99	-3.18	0.20
4445	-2.48	-1.85	-4.32	-0.54	-0.87	0.58	0.48	-1.62	-3.14	-0.89	-0.34	0.41	-1.80	-0.44	-2.17	-3.27	-2.50	-4.34	-2.59	-4.22	-3.12	-5.05	-3.07	-4.76	-2.91	-0.03
4446	-2.06	-1.66	-4.23	-0.76	-0.88	0.82	0.75	-1.74	-3.16	-0.99	-0.22	0.54	-1.65	-0.30	-2.06	-3.42	-2.41	-4.29	-2.58	-4.20	-3.13	-5.08	-3.14	-4.86	-4.86	0.44
4447	-1.99	-1.46	-4.04	-0.21	-0.51	1.34	1.02	-1.36	-2.57	-0.67	0.06	0.77	-1.47	-0.13	-1.88	-3.25	-2.33	-4.17	-2.45	-4.09	-3.02	-4.98	-3.03	-4.87	-4.54	2.15
4449	-2.48	-1.94	-4.43	-1.05	-1.18	0.17	0.68	-1.79	-3.14	-0.71	-0.23	0.48	-1.76	-0.42	-2.17	-3.41	-2.42	-4.24	-2.47	-4.04	-2.99	-4.91	-3.00	-4.74	-4.74	0.56
4450	-1.82	-1.19	-3.71	-0.47	-1.14	0.81	-0.06	-1.89	-3.19	-0.27	-0.21	0.55	-1.57	-0.17	-1.82	-3.32	-1.95	-3.78	-2.01	-3.57	-2.50	-4.46	-2.51	-4.30	-2.77	0.50
4451	-1.82	-1.15	-3.74	-0.43	-0.90	1.04	0.20	-2.02	-3.21	-0.34	-0.21	0.56	-1.56	-0.16	-1.79	-3.21	-1.94	-3.79	-2.05	-3.64	-2.59	-4.57	-2.60	-4.40	-2.96	0.48
4452	-1.72	-1.27	-3.74	0.36	0.05	2.02	2.53	-1.55	-2.83	-0.42	0.09	0.83	-1.33	0.04	-1.68	-3.02	-1.91	-3.81	-2.10	-3.74	-2.68	-4.59	-2.69	-4.48	-4.21	1.09
4453	-2.09	-1.50	-3.95	-0.73	-1.25	0.28	0.08	-1.65	-3.06	-0.57	-0.23	0.50	-1.68	-0.33	-2.00	-3.53	-2.14	-4.00	-2.28	-3.84	-2.79	-4.71	-2.81	-4.56	-1.59	0.34
4454	-2.25	-1.15	-3.86	-0.76	-1.06	0.79	0.17	-2.33	-3.59	-0.71	-0.49	0.27	-1.86	-0.46	-2.11	-3.46	-2.26	-4.16	-2.42	-4.05	-3.03	-4.94	-3.04	-4.85	-2.70	0.11
4456	-1.75	-1.27	-3.89	0.21	0.10	2.05	2.22	-1.57	-2.86	-0.41	0.38	1.13	-1.03	0.32	-1.43	-2.96	-1.72	-3.73	-2.02	-3.66	-2.62	-4.58	-2.60	-4.40	-2.50	0.94
4457	-2.29	-1.47	-3.94	-0.57	-1.13	0.32	0.41	-0.67	-2.37	-1.02	0.20	0.81	-1.48	-0.24	-2.12	-3.14	-2.48	-4.43	-2.73	-4.31	-3.20	-5.07	-3.10	-4.86	-2.52	0.40
4458	-3.02	-2.37	-4.98	-0.84	-0.80	0.42	0.54	-2.25	-3.69	-1.18	-0.75	0.00	-2.16	-0.78	-2.45	-3.33	-2.68	-4.59	-2.85	-4.45	-3.38	-5.29	-3.27	-4.91	-2.63	-0.10
4459	-2.49	-1.93	-4.41	-0.68	-0.81	0.67	0.36	-1.75	-3.12	-0.88	-0.41	0.32	-1.83	-0.48	-2.19	-3.33	-2.48	-4.37	-2.61	-4.17	-3.04	-4.94	-2.91	-4.62	-2.94	0.14
4460	-2.41	-1.68	-4.30	-1.13	-0.89	0.62	1.07	-1.80	-3.01	-1.04	-0.33	0.41	-1.74	-0.39	-2.08	-3.24	-2.27	-4.21	-2.54	-4.19	-3.21	-5.15	-3.18	-4.91	-4.82	0.48
4461	-2.42	-1.92	-4.41	-0.75	-0.90	0.73	0.77	-1.70	-3.02	-0.81	-0.18	0.54	-1.64	-0.29	-2.00	-3.35	-2.29	-4.22	-2.53	-4.15	-3.11	-5.10	-3.15	-4.90	-2.89	0.33
4462	-2.59	-1.95	-4.59	-0.84	-0.93	0.79	0.56	-2.21	-3.49	-0.98	-0.59	0.11	-2.05	-0.66	-2.33	-3.68	-2.48	-4.39	-2.67	-4.24	-3.17	-5.10	-3.12	-4.89	-4.93	0.37
4463	-2.10	-1.59	-4.05	-1.16	-1.02	0.46	0.27	-1.33	-2.73	-0.43	-0.40	0.37	-1.77	-0.39	-2.01	-3.33	-2.08	-3.94	-2.17	-3.73	-2.65	-4.52	-2.58	-4.32	-5.03	0.26
4464	-2.27	-1.80	-4.26	-0.53	-0.84	0.50	0.95	-1.81	-3.04	-0.82	-0.36	0.40	-1.75	-0.42	-2.13	-3.21	-2.37	-4.28	-2.57	-4.18	-3.11	-5.00	-3.01	-4.76	-2.53	0.39
4465	-1.61	-1.36	-3.85	-0.24	-0.59	1.19	0.97	-1.91	-3.25	-0.14	-0.15	0.72	-1.33	0.09	-1.54	-2.87	-1.72	-3.60	-1.84	-3.44	-2.38	-4.32	-2.34	-4.12	-2.23	0.73
4466	-2.23	-1.74	-4.19	-0.59	-0.70	0.54	1.07	-1.86	-3.10	-0.49	-0.51	0.30	-1.83	-0.45	-2.03	-3.16	-2.14	-4.00	-2.26	-3.81	-2.74	-4.68	-2.69	-4.45	-4.92	0.38
4469	-2.37	-1.69	-4.22	-0.84	-1.29	0.30	0.00	-1.49	-2.85	-0.84	-1.30	-0.36	-2.38	-0.87	-2.40	-3.68	-2.54	-4.44	-2.66	-4.19	-3.12	-5.00	-3.05	-4.78	-1.90	0.18
4470	-2.59	-1.95	-4.51	-0.86	-0.71	0.76	0.53	-1.95	-3.41	-0.86	-0.75	0.10	-1.99	-0.62	-2.25	-3.10	-2.42	-4.28	-2.52	-4.13	-3.08	-4.99	-3.03	-4.72	-1.79	0.16
4471	-2.01	-1.33	-4.01	-0.11	-0.25	1.76	2.00	-1.43	-2.76	-0.60	0.18	0.94	-1.17	0.20	-1.57	-3.03	-1.94	-3.88	-2.21	-3.85	-2.77	-4.76	-2.81	-4.64	-4.76	0.54
4473	-2.61	-1.92	-4.49	-0.68	-0.36	1.40	3.40	-1.87	-3.06	-0.86	-0.64	0.10	-2.03	-0.67	-2.30	-3.72	-2.47	-4.26	-2.50	-4.06	-2.99	-4.92	-2.99	-4.74	-2.14	0.34
4474	-2.50	-1.91	-4.49	-0.33	-0.06	1.69	4.10	-1.91	-3.09	-1.03	-0.78	-0.01	-2.14	-0.75	-2.42	-3.63	-2.55	-4.44	-2.70	-4.21	-3.16	-4.94	-3.04	-4.80	-2.88	0.94
4475	-1.85	-1.14	-3.73	0.12	0.03	1.98	2.37	-1.14	-2.40	-0.71	0.35	1.11	-1.00	0.37	-1.35	-2.75	-1.73	-3.81	-2.24	-3.91	-2.82	-4.73	-2.74	-4.44	-4.40	0.90
4476	-1.86	-1.13	-3.79	0.08	0.06	1.99	2.22	-1.23	-2.53	-0.35	0.26	1.06	-1.04	0.35	-1.35	-2.61	-1.67	-3.62	-1.95	-3.62	-2.56	-4.57	-2.62	-4.40	-1.99	0.85
4477	-2.05	-1.67	-4.25	-0.39	-0.86	1.05	0.78	-1.50	-2.82	-0.85	-0.05	0.68	-1.48	-0.13	-1.91	-3.21	-2.21	-4.18	-2.48	-4.09	-3.06	-4.94	-3.03	-4.80	-2.20	0.58
4478	-1.73	-1.11	-3.74	0.21	0.01	2.00	2.26	-1.20	-2.42	-0.39	0.32	1.07	-1.03	0.33	-1.42	-2.86	-1.69	-3.69	-2.02	-3.62	-2.60	-4.51	-2.61	-4.37	-4.55	0.75
4479	-1.95	-1.15	-3.74	0.01	-0.09	1.88	2.20	-1.09	-2.42	-0.38	0.37	1.12	-1.07	0.26	-1.50	-2.94	-1.77	-3.78	-2.04	-3.70	-2.66	-4.55	-2.72	-4.47	-4.47	0.83
4480	-1.74	-0.95	-3.60	0.25	0.22	2.19	2.36	-1.01	-2.34	-0.13	0.43	1.19	-0.93	0.45	-1.25	-2.74	-1.55	-3.53	-1.82	-3.48	-2.45	-4.39	-2.46	-4.24	-4.35	0.95
4481	-1.98	-1.14	-3.82	-0.33	-0.21	1.72	1.50	-2.19	-3.48	-0.29	-0.47	0.34	-1.74	-0.32	-1.87	-3.40	-1.93	-3.74	-1.97	-3.53	-2.50	-4.40	-2.44	-4.24	-4.89	0.41
4482	-2.04	-1.15	-3.79	0.00	-0.19	1.79	2.16	-1.16	-2.40	-0.47	0.31	1.03	-1.12	0.23	-1.47	-2.92	-1.77	-3.79	-2.08	-3.70	-2.71	-4.60	-2.69	-4.52	-2.53	0.74
4483	-1.96	-1.02	-3.73	0.11	-0.08	1.95	2.23	-1.09	-2.35	-0.38	0.30	1.04	-1.11	0.26	-1.47	-2.88	-1.75	-3.73	-2.06	-3.68	-2.66	-4.62	-2.69	-4.43	-4.54	0.76
4487	-1.90	-1.22	-3.86	-0.07	-0.27	1.76	1.94	-1.23	-2.48	-0.64	0.13	0.87	-1.28	0.08	-1.65	-3.11	-1.92	-3.88	-2.23	-3.86	-2.84	-4.81	-2.85	-4.63	-4.59	0.71

Appendix A4. Centered log ratio transformed data used for PCA and Random Forest.

Sample	Si	Al	Fe	Mn	Mg	Ca	Na	K	Ti	P	LOI	C-Total	C_in_CO2	Non_carb._C	Total S	Cu	Zn	Pb	Cd	Hg	Sn	Tl	In	As	Co	Ni	Se	Mo	Ge	Sb	Ag	Au	W	Bi	B	Rb	Sr	Cs	Ba	Be	Zr
4488	9.37	8.38	7.50	2.79	6.50	5.64	6.74	6.96	5.26	2.62	7.50	5.15	6.12	3.88	3.92	0.97	1.42	-1.22	-4.56	-7.77	-3.17	-3.92	-6.16	0.49	0.21	1.44	-4.56	-1.78	-2.83	-1.24	-4.56	-11.00	-3.86	-4.09	1.32	1.33	2.43	-1.73	3.33	-2.48	1.71
4489	9.20	8.17	7.65	3.42	6.51	6.27	6.05	6.82	5.46	2.56	7.66	5.68	6.82	3.73	3.87	0.67	1.42	-2.38	-4.68	-7.90	-2.60	-4.01	-6.29	0.89	0.23	1.30	-4.68	-2.60	-2.77	-2.02	-4.68	-7.90	-3.99	-4.91	2.17	1.13	2.11	-2.27	2.88	-2.60	1.76
4490	9.35	7.48	7.74	1.25	4.27	3.95	6.53	5.16	4.68	2.36	7.68	6.61	3.04	6.60	7.06	3.94	3.89	0.30	-1.24	-3.46	-0.06	-4.14	-3.58	0.97	0.78	0.96	-1.39	-1.97	-1.46	-2.95	-2.62	-6.58	-4.05	-2.44	-0.36	-0.59	0.25	-3.02	1.32	-4.05	0.97
4491	10.05	8.91	8.45	3.75	7.18	6.95	8.36	5.17	5.82	3.32	7.78	5.18	6.48	-10.30	5.03	1.46	1.97	-1.55	-3.86	-10.30	-3.16	-3.58	-5.47	-0.17	1.14	2.72	-3.86	-1.78	-2.00	-5.47	-3.86	-10.30	-3.16	-3.16	-0.52	-0.68	1.36	-4.08	2.37	-3.16	2.22
4492	9.86	8.80	8.14	2.82	7.13	5.88	7.28	7.47	5.71	3.37	7.85	4.25	5.77	-10.49	4.25	1.31	2.06	-0.71	-4.05	-10.49	-2.66	-3.31	-5.66	-0.71	0.66	1.86	-4.05	-1.97	-2.07	-5.66	-4.05	-10.49	-3.35	-3.35	1.73	1.59	0.95	-2.77	2.94	-2.66	2.19
4493	9.82	8.60	9.16	4.56	7.55	6.24	6.95	6.95	5.54	3.58	7.89	1.31	3.11	-10.43	6.33	0.24	2.06	-0.40	-3.98	-10.43	-3.29	-3.74	-5.59	-0.99	0.72	2.03	-3.98	-2.60	-1.64	-3.11	-3.98	-10.43	-3.29	-2.95	0.90	1.35	2.53	-1.47	3.74	-2.60	1.94
4495	9.62	8.55	8.05	3.20	7.11	5.49	7.18	6.99	5.46	3.14	7.65	3.91	4.81	2.81	4.02	0.48	1.78	-1.97	-4.27	-7.49	-2.89	-3.71	-5.88	-1.28	0.36	1.54	-4.27	-2.19	-2.42	-5.88	-4.27	-10.72	-3.58	-4.09	0.37	1.30	2.24	-2.48	3.62	-2.89	2.02
4496	9.95	8.84	8.45	3.63	7.36	5.50	7.42	7.29	5.79	3.50	7.89	2.72	4.11	-10.41	4.42	1.39	2.15	-1.66	-3.96	-10.41	-2.58	-3.52	-5.57	-0.50	0.74	1.90	-3.96	-2.58	-2.05	-5.57	-3.96	-10.41	-3.27	-3.78	0.60	1.56	2.38	-2.24	3.77	-2.58	2.21
4498	9.72	8.61	8.24	3.12	7.15	5.06	7.54	6.72	5.57	3.31	7.53	3.17	3.87	2.39	4.09	1.33	2.00	-1.90	-4.20	-7.42	-2.82	-4.05	-5.81	-3.51	0.41	1.77	-4.20	-1.72	-2.23	-5.81	-4.20	-10.65	-3.51	-4.02	0.36	0.97	1.50	-2.63	2.63	-2.82	2.01
4499	9.69	8.57	7.94	3.44	6.97	6.73	7.03	7.44	5.60	3.15	7.77	4.73	6.22	-10.65	3.98	1.35	1.57	-1.91	-4.21	-10.65	-2.82	-3.60	-5.82	0.07	0.62	1.77	-4.21	-1.73	-2.49	-3.33	-4.21	-6.74	-3.52	-4.03	0.70	1.65	1.81	-2.24	3.83	-2.82	1.96
4500	9.73	8.57	8.38	3.62	7.02	7.09	6.76	7.38	5.52	3.37	8.09	5.68	7.02	-10.58	4.42	0.96	1.68	-1.84	-4.14	-10.58	-3.45	-3.53	-5.75	-0.67	0.39	1.65	-4.14	-2.06	-2.11	-3.45	-4.14	-10.58	-3.45	-3.96	0.83	1.81	2.05	-1.45	3.79	-2.75	1.87
7401	9.47	8.45	7.81	3.38	6.76	6.71	7.07	7.12	5.43	2.89	7.43	3.77	4.80	2.35	5.34	1.83	1.39	-2.11	-4.41	-10.86	-3.03	-3.80	-6.02	-0.46	0.62	1.75	-4.41	-1.64	-2.77	-3.38	-4.41	-10.86	-3.72	-3.72	0.58	1.48	2.84	-2.56	3.52	-3.03	1.78
7402	9.64	8.53	8.02	3.31	7.01	6.40	7.64	6.65	5.51	3.05	7.83	4.45	5.87	-10.69	6.04	1.46	1.72	-1.94	-4.25	-7.47	-2.86	-4.13	-5.86	-0.30	0.66	1.67	-4.25	-1.76	-2.33	-5.86	-4.25	-6.37	-3.55	-3.78	0.08	1.01	2.32	-2.52	3.11	-2.17	1.93
7403	9.70	8.63	8.12	3.45	7.06	5.78	7.27	7.17	5.57	3.16	7.61	3.73	3.73	3.42	3.58	0.18	1.77	-1.90	-4.20	-10.64	-2.82	-3.47	-5.81	-1.21	0.37	1.75	-4.20	-2.12	-2.29	-5.81	-4.20	-10.64	-3.51	-4.43	1.01	1.45	2.19	-2.29	3.55	-2.12	1.95
7404	9.63	8.56	7.81	3.21	6.86	6.32	7.29	7.44	5.47	2.81	7.40	3.77	4.33	3.12	4.64	1.04	1.35	-2.00	-4.30	-10.74	-2.91	-3.51	-5.91	-0.21	0.37	1.75	-4.30	-1.31	-2.82	-5.91	-4.30	-10.74	-3.61	-4.12	1.07	1.78	2.38	-2.58	3.65	-2.91	1.89
7405	9.87	7.83	7.34	2.84	4.97	7.56	7.41	5.39	4.56	2.03	8.32	7.34	7.62	6.89	7.19	0.20	2.94	-0.36	-2.84	-7.45	-2.84	-5.50	-5.84	2.04	0.19	1.44	-4.23	-1.74	-2.66	-2.74	-4.23	-10.67	-3.53	-3.20	0.56	-0.20	1.46	-3.53	1.03	-3.53	1.29
7406	9.09	7.91	6.71	1.75	5.70	5.47	6.47	6.74	4.65	1.91	7.91	7.21	4.66	7.19	6.58	1.60	3.36	-0.22	-3.07	-6.98	-2.09	-2.52	-6.47	1.79	-0.11	1.09	-4.86	-2.09	-2.41	-2.09	-3.70	-11.30	-2.78	-3.47	1.06	1.18	0.99	-2.17	2.67	-3.47	1.38
7407	9.69	8.64	8.02	3.35	7.23	5.55	6.79	7.53	5.60	2.66	7.70	3.39	4.08	2.60	3.86	1.18	1.88	-1.91	-4.21	-10.65	-2.82	-3.69	-5.82	1.15	0.96	2.78	-4.21	-2.82	-2.64	-5.82	-4.21	-10.65	-3.52	-4.43	1.29	1.80	1.13	-2.18	3.77	-2.82	1.93
7408	9.58	8.52	7.80	3.20	6.74	6.52	6.02	7.85	5.53	3.12	8.27	6.49	7.83	-10.73	4.65	1.01	1.33	-1.99	-4.29	-10.73	-2.90	-3.52	-5.90	-1.11	0.45	1.64	-4.29	-2.21	-2.37	-3.41	-4.29	-10.73	-0.96	-3.41	1.49	1.97	1.57	-1.68	3.96	-2.21	2.01
7409	9.66	8.66	8.13	3.27	7.31	6.13	7.05	7.46	5.60	3.05	7.95	5.27	6.71	-10.63	5.10	1.35	1.93	-1.89	-4.19	-10.63	-2.81	-3.54	-5.80	-1.20	0.73	2.48	-4.19	-1.42	-2.22	-5.80	-4.19	-7.41	-3.50	-4.01	0.56	1.66	1.00	-2.34	3.32	-2.11	1.95
7410	9.85	8.93	8.22	2.89	7.29	5.28	7.26	7.81	5.96	3.29	7.89	2.67	4.87	-10.45	4.38	-1.24	2.00	-1.71	-4.01	-10.45	-2.62	-3.36	-5.62	-3.32	0.55	2.46	-4.01	-1.93	-2.04	-3.83	-4.01	-7.23	-3.32	-4.23	0.81	2.07	1.09	-1.98	3.78	-2.62	2.17
7411	9.64	8.43	8.21	3.21	6.97	6.73	6.95	7.21	5.35	3.10	7.99	5.31	6.73	-10.70	6.79	1.76	1.67	-1.27	-4.26	-10.70	-3.57	-3.90	-5.87	0.59	0.40	1.48	-4.26	-2.18	-2.18	-3.39	-4.26	-6.10	-0.93	-3.57	0.56	1.51	1.02	-2.09	2.91	-2.88	1.82
7412	9.59	8.61	8.42	2.94	6.75	6.03	7.89	6.79	5.36	2.88	7.99	4.59	5.99	-10.67	7.57	0.74	2.19	-0.76	-4.23	-10.67	-2.84	-4.31	-5.84	0.10	0.41	1.54	-4.23	-2.15	-2.44	-3.20	-3.36	-5.66	-3.54	-3.76	0.52	1.13	1.09	-3.20	2.29	-2.84	1.92
7413	9.12	7.90	6.95	1.09	5.54	4.04	6.33	6.87	4.70	2.04	8.02	7.21	3.46	7.21	6.85	1.19	2.91	0.17	-3.35	-6.26	-2.35	-2.62	-6.44	1.87	-0.17	0.99	-4.83	-2.06	-2.53	-2.53	-3.67	-8.05	-4.14	-3.35	0.53	1.29	0.51	-2.41	2.82	-3.44	1.42
7414	9.02	7.81	6.66	2.05	5.35	6.14	6.72	6.58	4.48	2.22	8.15	7.54	5.98	7.48	6.60	1.38	2.94	-0.50	-3.40	-6.49	-2.40	-3.20	-6.49	1.49	-0.46	0.86	-4.88	-2.11	-2.54	-2.66	-3.85	-8.10	-3.50	-3.50	0.65	0.93	1.18	-2.66	2.27	-3.50	1.33
7416	9.47	8.46	7.52	3.21	6.85	5.43	6.72	7.20	5.21	2.65	7.39	4.02	2.64	3.95	3.62	0.67	1.37	0.19	-4.45	-10.90	-3.07	-3.20	-6.06	-0.18	-0.26	1.57	-4.45	-3.07	-2.81	-3.29	-3.42	-10.90	-2.37	-3.17	0.92	1.70	2.48	-1.29	3.55	-2.37	1.55
7417	9.63	8.51	7.57	3.35	6.85	5.97	6.72	7.21	5.21	2.83	7.52	4.41	3.94	4.23	4.04	0.53	1.50	-0.40	-4.35	-10.79	-2.96	-3.23	-5.96	0.37	-0.05	1.38	-4.35	-1.87	-2.87	-3.32	-4.35	-10.79	-2.27	-3.66	1.10	1.65	2.57	-1.40	3.64	-2.27	1.74
7418	9.41	8.41	7.41	3.07	6.79	5.74	6.99	7.13	5.20	2.73	7.27	3.68	2.18	3.62	4.74	0.54	1.56	-0.18	-4.51	-10.95	-3.12	-3.26	-6.12	0.77	0.03	1.59	-4.51	-2.02	-2.79	-3.63	-3.82	-7.73	-3.82	-3.48	0.85	1.60	2.83	-1.16	3.77	-2.43	1.74
7420	9.42	8.53	7.81	3.07	7.04	4.90	6.57	7.08	5.35	3.07	7.59	3.74	3.34	3.54	4.73	0.93	1.64	-2.14	-4.44	-10.89	-3.06	-3.22	-6.05	-0.29	0.07	1.62	-4.44	-1.96	-2.53	-3.28	-4.44	-10.89	-2.36	-3.97	2.03	1.42	2.45	-1.72	3.58	-2.36	1.69
7421	9.56	8.49	7.92	3.64	6.88	5.95	6.43	7.11	5.33	3.05	7.53	4.03	3.58	3.84	0.94	0.94	1.67	-0.58	-4.36	-10.80	-2.97	-3.59	-5.97	0.12	0.16	1.65	-4.36	-2.28	-2.64	-2.97	-4.36	-10.80	-3.67	-3.67	3.13	1.42	2.15	-1.69	3.07	-2.28	1.81
7422	9.06	7.77	6.93	0.33	4.67	4.71	6.96	6.38	4.25	2.28	7.97	7.68	5.03	7.67	6.42	2.09	4.03	-0.07	-2.44	-7.42	-1.90	-4.33	-6.50	-1.43	0.15	1.54	-4.89	-1.56	-3.33	-2.52	-3.51	-6.03	-1.43	-2.59	-0.21	0.59	0.18	-3.25	2.57	-3.51	1.57
7423	8.68	7.73	6.64	0.20	4.98	4.28	5.94	6.89	4.37	2.06	7.65	7.20	4.50	7.18	6.01	1.78	3.87	-1.40	-2.49	-7.30	-1.72	-3.95	-6.79	-0.62	-0.10	1.25	-5.18	-1.85	-3.33	-3.05	-3.80	-6.61	-1.09	-2.21	0.67	0.99	-0.33	-2.88	3.49	-2.70	1.54
7424	8.74	7.47	6.93	2.80	5.36	6.98	4.36	6.45	4.57	2.18	7.77	6.66	7.08	6.13	6.46	2.61	4.50	-0.96	-1.80	-6.73	-1.25	-3.82	-4.65	0.07	0.19	0.71	-5.12	-2.35	-2.54	-1.64	-3.84	-6.55	-2.13	-3.96	2.79	0.67	0.44	-2.78	2.58	-4.43	1.09
7425	8.80	7.52	6.65	1.81	5.45	6.09	4.43	6.49	4.09	1.84	8.06	7.51	6.48	7.41	6.11	1.68	3.80	-0.47	-2.60	-6.72	-1.94	-3.38	-6.72	0.91	0.22	1.45	-5.11	-1.78	-2.94	-2.63	-3.55	-7.23	-2.63	-3.20	3.77	0.68	0.83	-2.60	3.02	-3.73	1.03
7427	8.99	7.59	6.86	1.94	5.24	6.28	5.22	6.64	4.15	2.15	7.99	7.41	6.65	7.27	6.37	1.79	4.08	0.14	-2.27	-6.57	-1.78	-3.16	-6.57	-0.40	0.05	1.38	-4.96	-1.78	-2.88	-2.99	-3.68	-7.08	-2.88	-3.11	2.31	0.89	1.06	-2.38	2.67	-3.58	1.12
7428	9.00	7.79	6.80	1.45	5.44	5.61	6.41	6.63	4.38	2.03	7.86	7.17	6.06	7.08	6.38	1.59	2.49	-0.10	-3.76	-7.04	-1.93	-3.07	-6.53	-0.10	-0.28	1.14	-4.92	-1.75	-2.44	-2.84	-4.05	-6.53	-2.44	-2.84	2.26	0.89	1.02	-2.37	2.79	-3.54	1.36
7429	9.57	8.17	7.19	3.09	6.49	7.04	6.38	7.05	4.98	2.35	7.92	6.35	7.34	5.01	3.18	2.06	1.07	-1.43	-4.42	-10.86	-3.04	-4.00	-6.03	0.90	-0.08	1.29	-4.42	-1.94	-2.85	-3.04	-4.42	-7.64	-3.73	-3.39	0.95	1.46	2.25	-1.70	3.34	-3.04	1.73
7430	9.62	8.51	7.51	2.73	6.71	5.97	5.77	7.30	5.28	2.30	7.70	5.45	6.41	4.21	2.32	1.49	1.60	-1.19	-4.37	-10.81	-2.98	-3.41	-5.98	1.47	0.45	2.44	-4.37	-1.88	-2.80	-2.51	-4.37	-10.81	-3.67	-3.90	0.97	1.65	2.29	-1.64	3.53	-2.29	1.68
7431	9.82	8.51	7.49	2.92	6.64	6.30	5.32	7.65	4.98	2.75	7.76	4.96	6.29	-10.65	4.09	1.47	3.00	0.77	-2.48	-7.42	-2.82	-3.05	-5.81	1.28	-0.03	1.50	-4.20	-1.43	-2.64	-2.35	-3.17	-10.65	-3.51	-3.51	1.15	2.08	1.22	-1.46	3.73	-2.13	1.90
7432	9.31	8.16	7.31	3.13	6.45	6.93	5.57	7.04	5.03	2.48	7.73	5.88	6.98	4.17	2.98	1.28	1.11	-0.02	-4.62	-11.07	-3.24	-3.33	-6.23	0.77	0.00	1.25	-4.62	-1.45	-2.90	-1.55	-2.65	-7.84	-3.93	-3.24	0.89	1.50	1.92	-2.01	3.23	-2.54	1.62
7433	9.74	8.44	7.50	3.21	6.70	7.11	5.84	7.29	5.30	2.60	7.97	5.87	7.14	2.18	3.52	0.68	1.55	0.62	-4.26	-10.70	-3.57	-3.72	-5.87	1.20	0.33	2.32	-4.26	-2.88	-2.78	-1.88	-4.26	-10.70	-3.57	-4.08	0.79	1.70	2.25	-1.85	3.55	-2.88	1.67
7434	8.95	7.71	6.59	0.18	4.23	4.19	4.95	6.75	4.47	2.13	7.68	6.87	3.72	6.85	6.63	0.42	4.67	3.31	-0.94	-5.87	-2.56	-3.57	-6.65	1.79	-0.01	1.44	-5.04	-2.27	-2.25	-0.37	-2.18	-6.47	-4.35	-3.56	0.92	1.22	1.29	-2.56	2.75	-2.97	1.20
7435	9.16	8.18	7.98	3.83	6.97	6.27	6.72	6.15	5.37	2.46	7.67	5.76	6.38	5.05	5.45	1.49	1.78	-0.87	-4.65	-7.87	-3.26	-3.77	-6.26	0.26	0.64	1.69	-4.65	-3.26	-2.62	-3.77	-4.65	-11.09	-3.96	-3.62	1.60	0.56	1.49	-2.73	2.28	-3.26	1.39
7436	9.03	7.89	6.91	2.07	5.79	4.75	5.65	6.74	4.70	2.00	7.45	6.36	4.44	6.31	5.91	1.87	2.34	-0.31	-3.67	-5.53	-2.46	-3.50	-6.56	0.53	0.50	2.68	-4.95	-2.46	-2.87	-3.09	-3.47	-7.48	-2.46	-2.69	0.88	1.11	1.25	-2.25	3.11	-2.87	1.23
7437	9.46	8.15	7.06	2.57	6.04	6.04	6.37	6.96	4.91	2.46	7.43	6.13	6.00	5.85	5.00	1.00	3.04	-0.62	-3.01	-6.70	-2.09	-3.82	-6.18	0.24	-0.02	1.40	-4.58	-2.09	-2.60	-3.88	-4.58	-11.02	-3.88	-3.88	2.80	1.29	1.93	-1.94	3.14	-3.19	1.66
7438	9.13	7.86	6.62	1.90	5.06	5.61	6.55	6.53	4.48	2.09	7.81	6.97	6.08	6.85	6.67	1.64	3.13	-0.71	-3.22	-4.32	-2.38	-2.67	-6.48	1.41	-0.01	1.27	-4.87	-2.09	-2.69	-2.53	-3.84	-11.31	-4.17	-3.08	-0.01	0.94	1.50	-2.26	2.73	-3.48	1.49
7439	9.23	7.93	6.82	-0.25	4.34	3.96	6.06	6.76	4.56	2.08	8.07	7.43	2.30	7.43	6.84	1.77	3.79	-0.76	-3.62	-4.11	-2.01	-2.26	-6.39	1.41	0.33	1.87	-4.79	-1.61	-2.87	-2.57	-3.62	-11.23	-4.09	-3.50	0.24	1.19	1.52	-1.79	2.97	-2.71	1.51
7440	8.62	7.47	7.01	-0.39	4.01	3.66	5.58	6.22	4.21	1.56	8.17	7.57	2.39	7.57	7.07	2.87	4.03	0.44	-2.09	-3.32	-1.43	-2.23	-6.13	1.38	0.50	1.91	-2.39	-2.03	-2.37	-2.07	-3.42	-7.74	-2.73	-2.73	-0.42	0.69	0.74	-2.52	2.54	-3.83	0.97
7441	9.46	8.44	8.10	3.50	7.22	5.28	7.26	6.42	5.51	2.47	7.54	4.54	4.96	4.00	4.43	1.51	1.86	-0.82	-3.71	-7.62	-3.01	-3.86	-6.01	0.08	0.58	1.77	-4.40	-3.01	-2.54	-3.37	-4.40	-10.84	-3.71	-3.93	0.92	0.82	1.13	-2.68	2.58	-3.01	1.62
7442	9.09	8.17	7.98	3.90	7.02	6.65	6.62	6.47	5.35	2.29	7.93	6.05	7.22	3.95	5.62	1.38	1.32	-2.36	-4.66	-7.88	-2.58	-4.24	-6.27	0.70	0.53	1.59	-4.66	-2.58	-2.68	-3.09	-4.66	-11.10	-1.19	-3.97	0.44	0.82	1.08	-2.80	2.43	-3.27	1.29
7443	8.83	7.81	6.97	0.54	5.48	4.54	4.13	6.88	4.88	2.22	7.11	5.67	4.80	5.55	5.22	2.70	5.34	-0.48	-0.77	-6.36	-0.37	-3.42	-3.92	1.12	0.57	0.59	-3.29	-1.62	-1.62	-2.71	-3.06	-6.51	-2.60	-3.60	2.41	1.42	0.17	-2.82	2.84	-2.60	1.16
7444	8.92	7.56	7.32	0.93	5.55	3.72	5.13	6.16	4.40	1.97	7.48	6.49	2.87	6.49	6.32	2.68	4.43	0.62	-1.78	-5.98	-0.79	-2.64	-4.60	1.56	1.15	1.19	-1.68	-1.89	-1.71	-2.25	-2.13	-6.34	-4.37	-2.09	2.01	0.79	0.01	-3.09	1.77	-2.99	1.25
7445	8.87	7.65	6.75	1.61	5.44	5.95	4.01	6.83	4.77	2.22	7.32	5.97	6.61	5.24	5.44	2.43	5.33	-0.14	-0.81	-6.36	-0.75	-3.65	-4.06	1.03	0.50	0.36	-5.08	-1.62	-1.89	-2.74	-3.23	-6.92	-4.39	-3.60	1.70	1.39	0.55	-2.87	2.68	-2.60	0.93
7446	9.06	7.96	7.25	2.72	5.86	6.52	5.50	6.83	4.92	2.19	7.84	6.17	7.24	4.58	6.51	0.90	0.54	-1.51	-4.84	-8.06	-2.76	-4.07	-6.45	1.91	-0.11	1.11	-4.84	-2.35	-2.71	-1.31	-3.68	-7.36	-2.07	-4.15	1.95	1.08	2.10	-0.87	2.86	-2.76	1.38
7447	9.30	8.15	7.35	3.22	6.17	6.91	6.53	6.88	5.16	2.41	7.92	6.44	7.49	4.92	5.34	1.03	0.59	-1.62	-3.59	-11.06	-3.23	-4.18	-6.23	1.93	0.11	1.33	-4.62	-3.23	-2.70	-1.39	-4.62	-7.84	-3.93	-3.93	1.04	1.15	1.66	-0.87	2.82	-3.23	1.52
7448	9.14	8.10	7.29	2.65	6.12	5.83	6.29	6.91	5.06	2.27	7.73	6.25	7.22	4.98	5.32	1.10	1.58	-1.18	-4.77	-7.99	-3.38	-3.80	-6.38	1.58	0.00	1.32	-4.77	-3.38	-2.98	-1.04	-4.07	-7.99	-2.69	-4.59	1.57	1.14	1.78	-0.79	2.80	-3.38	1.44
7449	9.37	8.23	7.45	2.89	6.45	6.34	6.82	6.78	5.17	2.39	7.77	6.21	6.96	5.36	5.06	1.39	1.03	-2.26	-4.57	-11.01	-3.18	-3.78	-6.17	2.41	0.26	1.56	-4.57	-3.18	-2.59	-1.57	-4.57	-7.78	-3.87	-3.69	1.25	1.04	1.78	-0.95	2.73	-3.18	1.63
7450	9.30	7.97	7.17	2.57	5.49	5.81	4.87	7.01	4.78	2.15	7.58	5.62	6.79	3.51	6.38	1.03	1.93	-1.25	-3.84	-7.93	-3.33	-3.76	-6.32	1.53	-0.20	1.25	-4.71	-3.33	-2.54	-0.37	-3.84	-5.45	-1.02	-5.63	2.19	1.36	1.81	-0.47	3.12	-2.63	1.32
7451	9.32	8.10	6.99	2.54	5.92	6.55	5.98	7.02	4.98	2.45	7.76	6.15	7.24	4.50	5.10	0.86	1.09	-0.87	-4.66	-11.10	-3.27	-3.69	-6.27	2.90	0.19	1.48	-4.66	-2.17	-2.53	-0.78	-4.66	-11.10	-1.32	-3.78	2.15	1.44	2.50	-0.51	3.28	-2.58	1.53
7452	9.16	8.36	7.50	2.78	6.37	6.78	6.26	6.92	5.19	2.72	7.77	5.77	6.97	3.42	2.96	0.70	1.26	-1.46	-4.64	-11.08	-2.56	-3.87	-6.25	0.24	0.19	1.56	-4.64	-2.16	-2.56	-3.36	-4.64	-11.08	-1.18	-4.17	2.59	1.40	1.49	-1.69	3.38	-2.56	1.61
7453	9.17	8.33	7.62	3.24	6.34	6.96	6.60	6.69	5.14	2.75	8.08	6.36	7.59	3.67	2.99	0.67	1.38	-2.31	-4.61	-7.13	-3.22	-4.16	-6.22	0.69	-0.02	1.53	-4.61	-2.53	-2.31	-2.39	-4.61	-11.05	-3.92	-4.43	2.20	1.16	2.21	-1.72	3.02	-2.53	1.63
7454	9.25	7.74	7.30	2.39	5.65	5.18	4.62	6.83	4.68	2.17	7.83	6.92	5.04	6.88	6.74	2.07	4.26	0.10	-1.77	-5.60	-2.30	-4.60	-5.70	-2.01	0.28	1.58	-4.78	-1.79	-2.75	-2.26	-4.09	-7.31	-4.09	-3.06	2.60	0.59	-0.91	-3.50	2.55	-3.40	1.37
7455	8.76	7.10	8.27

Appendix A4. Centered log ratio transformed data used for PCA and Random Forest.

Sample	Hf	Nb	Ta	Ga	Sc	V	Cr	Th	U	Y	La	Ce	Pr	Nd	Sm	Eu	Gd	Tb	Dy	Ho	Er	Tm	Yb	Lu	Br	F
4488	-1.89	-1.24	-3.60	0.01	-0.10	1.90	1.87	-1.36	-2.59	-0.46	0.12	0.88	-1.25	0.14	-1.57	-2.85	-1.85	-3.79	-2.13	-3.77	-2.71	-4.64	-2.73	-4.52	-4.56	0.74
4489	-1.84	-1.00	-3.67	-0.21	-0.01	1.93	1.43	-2.14	-3.37	0.00	-0.25	0.55	-1.53	-0.10	-1.64	-3.07	-1.66	-3.50	-1.72	-3.31	-2.25	-4.19	-2.25	-4.05	-4.68	0.61
4490	-2.67	-1.86	-4.53	-0.47	-0.74	1.19	0.81	-2.88	-4.03	-0.87	-1.22	-0.39	-2.43	-0.96	-2.43	-3.63	-2.51	-4.35	-2.57	-4.09	-3.04	-4.87	-2.93	-4.60	-4.75	0.55
4491	-1.37	-0.97	-3.61	0.57	0.59	2.54	3.20	-1.25	-2.50	0.10	0.20	1.01	-1.09	0.38	-1.25	-2.55	-1.41	-3.29	-1.57	-3.22	-2.16	-4.08	-2.17	-4.03	-3.86	1.44
4492	-1.41	-0.84	-3.33	0.43	0.28	2.28	2.36	-0.83	-1.98	0.05	0.63	1.39	-0.76	0.63	-1.10	-2.54	-1.34	-3.28	-1.60	-3.26	-2.20	-4.13	-2.19	-3.97	-4.05	1.25
4493	-1.68	-1.16	-3.80	0.29	0.30	2.26	2.40	-1.42	-2.70	0.04	0.18	0.96	-1.13	0.29	-1.33	-2.71	-1.49	-3.44	-1.70	-3.31	-2.21	-4.16	-2.25	-3.98	-3.98	1.31
4495	-1.61	-0.99	-3.62	0.29	0.05	2.06	2.05	-1.32	-2.54	-0.12	0.38	1.13	-0.99	0.42	-1.33	-2.67	-1.56	-3.50	-1.78	-3.38	-2.35	-4.32	-2.38	-4.16	-4.27	1.02
4496	-1.42	-0.77	-3.35	0.51	0.39	2.38	2.44	-0.98	-2.31	0.06	0.62	1.39	-0.74	0.65	-1.05	-2.40	-1.33	-3.27	-1.58	-3.21	-2.17	-4.09	-2.22	-3.96	-3.96	1.33
4498	-1.59	-0.96	-3.57	0.32	0.16	2.19	2.20	-1.29	-2.57	-0.11	0.46	1.22	-0.90	0.49	-1.19	-2.59	-1.44	-3.38	-1.72	-3.34	-2.31	-4.29	-2.33	-4.13	-2.12	1.10
4499	-1.60	-0.98	-3.58	0.27	0.21	2.20	2.26	-1.38	-2.68	0.01	0.37	1.15	-0.97	0.45	-1.19	-2.55	-1.44	-3.39	-1.70	-3.32	-2.28	-4.21	-2.29	-4.10	-4.21	1.09
4500	-1.76	-1.16	-3.67	0.24	0.09	2.13	2.21	-1.35	-2.65	0.14	0.36	1.13	-0.97	0.44	-1.19	-2.38	-1.34	-3.23	-1.56	-3.22	-2.23	-4.22	-2.29	-4.10	-4.14	1.16
7401	-1.83	-1.11	-3.72	0.19	0.07	2.09	2.15	-1.62	-2.90	-0.14	0.04	0.84	-1.27	0.15	-1.46	-2.83	-1.68	-3.56	-1.84	-3.46	-2.43	-4.34	-2.41	-4.20	-4.41	0.88
7402	-1.70	-1.04	-3.68	0.23	0.15	2.18	2.18	-1.41	-2.69	-0.09	0.33	1.10	-1.01	0.40	-1.28	-2.58	-1.52	-3.46	-1.77	-3.41	-2.40	-4.37	-2.38	-4.21	-4.25	1.05
7403	-1.69	-1.01	-3.62	0.32	0.23	2.18	2.21	-1.31	-2.61	-0.04	0.36	1.15	-0.96	0.43	-1.24	-2.66	-1.45	-3.40	-1.70	-3.34	-2.31	-4.24	-2.32	-4.13	-4.20	1.10
7404	-1.75	-1.09	-3.67	0.26	0.23	2.19	2.21	-1.44	-2.78	-0.02	0.16	0.95	-1.15	0.28	-1.35	-2.78	-1.61	-3.49	-1.77	-3.38	-2.34	-4.30	-2.36	-4.15	-4.30	1.00
7405	-2.37	-1.51	-3.92	-1.05	-0.86	0.59	0.52	-1.87	-3.27	-0.28	-0.46	0.32	-1.85	-0.47	-2.05	-3.60	-2.14	-3.89	-2.05	-3.57	-2.53	-4.40	-2.46	-4.23	-4.23	1.07
7406	-2.22	-1.46	-3.90	-0.38	-0.70	1.11	0.56	-1.82	-3.12	-0.58	-0.45	0.31	-1.85	-0.47	-2.07	-3.24	-2.23	-4.04	-2.27	-3.87	-2.82	-4.75	-2.74	-4.52	-4.86	0.44
7407	-1.76	-1.28	-3.90	0.31	0.37	2.32	3.06	-1.65	-2.98	-0.12	0.32	1.10	-1.04	0.28	-1.39	-2.76	-1.65	-3.56	-1.81	-3.44	-2.42	-4.34	-2.47	-4.25	-4.21	1.09
7408	-1.62	-1.02	-3.70	0.32	0.11	2.13	2.13	-1.36	-2.64	-0.07	0.34	1.12	-1.00	0.41	-1.25	-2.72	-1.51	-3.50	-1.77	-3.43	-2.40	-4.37	-2.37	-4.18	-4.29	1.01
7409	-1.67	-1.00	-3.65	0.45	0.32	2.27	2.68	-1.24	-2.59	-0.10	0.39	1.16	-0.96	0.45	-1.22	-2.64	-1.50	-3.46	-1.74	-3.37	-2.35	-4.27	-2.30	-4.15	-4.19	1.11
7410	-1.43	-0.99	-3.52	0.71	0.66	2.68	2.86	-1.20	-2.56	0.27	0.56	1.34	-0.78	0.63	-1.05	-2.42	-1.29	-3.24	-1.50	-3.10	-2.05	-4.01	-2.06	-3.86	-4.01	1.29
7411	-1.85	-1.23	-3.87	0.17	-0.10	1.88	1.98	-1.53	-2.92	-0.39	0.12	0.89	-1.26	0.15	-1.55	-2.90	-1.82	-3.74	-2.00	-3.65	-2.61	-4.54	-2.65	-4.44	-4.26	1.04
7412	-1.68	-1.20	-3.84	0.33	0.03	2.08	2.13	-1.44	-2.69	-0.07	0.18	0.95	-1.16	0.26	-1.41	-2.76	-1.64	-3.60	-1.81	-3.44	-2.36	-4.31	-2.37	-4.19	-4.23	1.07
7413	-2.19	-1.35	-3.82	-0.35	-0.79	1.04	0.32	-1.62	-2.94	-0.61	-0.16	0.59	-1.59	-0.23	-1.93	-3.21	-2.21	-4.08	-2.37	-4.01	-2.93	-4.87	-2.91	-4.65	-3.26	0.47
7414	-2.27	-1.64	-4.11	-0.50	-0.89	0.87	0.18	-1.94	-3.29	-0.66	-0.37	0.41	-1.75	-0.36	-2.06	-3.20	-2.25	-4.13	-2.37	-3.99	-2.89	-4.81	-2.81	-4.57	-3.23	0.42
7416	-1.97	-1.17	-3.65	0.23	-0.21	1.90	2.27	-0.79	-2.25	-0.36	0.45	1.17	-1.01	0.33	-1.41	-2.87	-1.76	-3.70	-2.01	-3.67	-2.64	-4.58	-2.66	-4.41	-2.97	0.84
7417	-1.83	-1.00	-3.68	0.21	-0.26	1.82	2.02	-0.69	-2.00	-0.57	0.05	0.75	-1.44	-0.06	-1.74	-3.11	-2.02	-3.88	-2.15	-3.81	-2.76	-4.68	-2.75	-4.52	-4.35	0.95
7418	-1.93	-1.03	-3.78	0.14	-0.19	1.93	2.15	-0.65	-1.88	-0.48	0.08	0.85	-1.30	0.06	-1.65	-3.33	-2.00	-3.88	-2.13	-3.74	-2.66	-4.64	-2.67	-4.47	-4.51	0.79
7420	-1.96	-1.13	-3.77	0.20	0.05	2.12	2.29	-1.11	-2.43	-0.42	0.43	1.15	-1.01	0.40	-1.34	-2.77	-1.68	-3.71	-2.00	-3.64	-2.56	-4.53	-2.56	-4.33	-4.44	0.85
7421	-1.84	-1.10	-3.80	0.20	-0.02	2.09	2.22	-1.12	-2.40	-0.20	0.82	1.54	-0.64	0.70	-1.08	-2.61	-1.52	-3.50	-1.84	-3.52	-2.50	-4.44	-2.58	-4.32	-4.36	0.94
7422	-2.07	-1.51	-3.97	-0.56	-1.13	0.59	-0.27	-1.05	-2.35	-0.56	-0.21	0.53	-1.63	-0.27	-1.98	-3.47	-2.22	-4.16	-2.39	-3.99	-2.87	-4.75	-2.78	-4.48	-3.10	0.40
7423	-2.07	-1.35	-3.88	-0.62	-1.10	0.66	-0.32	-1.08	-2.43	-0.30	0.16	0.86	-1.34	0.02	-1.69	-3.19	-1.93	-3.87	-2.08	-3.69	-2.60	-4.51	-2.58	-4.32	-3.33	0.12
7424	-2.60	-1.82	-4.53	-0.60	-0.72	1.20	0.70	-2.93	-4.20	-0.69	-0.99	-0.14	-2.23	-0.74	-2.25	-3.82	-2.29	-4.18	-2.39	-4.00	-2.94	-4.84	-2.87	-4.60	-3.26	0.18
7425	-2.56	-1.86	-4.22	-0.68	-0.99	0.59	0.21	-1.61	-2.95	-0.89	-0.20	0.51	-1.74	-0.41	-2.13	-3.28	-2.43	-4.33	-2.65	-4.27	-3.18	-5.08	-3.12	-4.87	-2.99	0.18
7427	-2.51	-1.87	-4.37	-0.63	-0.87	0.69	0.33	-1.69	-2.97	-1.09	-0.37	0.36	-1.84	-0.48	-2.23	-3.42	-2.54	-4.44	-2.71	-4.35	-3.30	-5.19	-3.21	-4.96	-3.24	0.34
7428	-2.26	-1.62	-4.12	-0.40	-0.78	0.94	0.57	-1.38	-2.67	-1.14	-0.13	0.57	-1.64	-0.31	-2.08	-3.34	-2.49	-4.53	-2.81	-4.45	-3.28	-5.20	-3.16	-4.85	-3.36	0.37
7429	-1.97	-1.24	-3.86	-0.09	-0.49	1.46	1.66	-1.24	-2.47	-0.84	0.19	0.88	-1.33	0.00	-1.76	-2.92	-2.13	-4.09	-2.44	-4.11	-3.07	-5.00	-2.99	-4.81	-2.57	0.88
7430	-1.91	-1.41	-3.97	0.24	-0.05	1.98	2.32	-1.69	-3.02	-0.49	0.06	0.81	-1.35	0.05	-1.65	-3.00	-1.90	-3.85	-2.11	-3.69	-2.66	-4.59	-2.71	-4.49	-2.72	0.93
7431	-1.72	-1.15	-3.69	0.23	-0.51	1.46	1.53	-0.85	-2.16	-0.52	0.27	0.96	-1.26	0.07	-1.65	-3.09	-1.98	-3.90	-2.19	-3.84	-2.82	-4.78	-2.88	-4.65	-2.35	1.09
7432	-2.07	-1.40	-4.04	-0.15	-0.42	1.55	1.62	-1.32	-2.53	-0.60	0.06	0.78	-1.41	-0.02	-1.75	-2.94	-2.00	-3.95	-2.25	-3.89	-2.87	-4.85	-2.94	-4.71	-3.05	0.67
7433	-2.00	-1.47	-4.05	0.17	-0.09	1.93	2.33	-1.82	-3.15	-0.68	-0.06	0.69	-1.48	-0.06	-1.73	-3.19	-2.07	-3.99	-2.20	-3.87	-2.80	-4.77	-2.80	-4.54	-2.88	1.04
7434	-2.50	-1.94	-4.48	-0.52	-0.76	1.01	1.34	-1.74	-3.13	-1.26	-0.19	0.51	-1.70	-0.33	-2.17	-3.23	-2.60	-4.71	-3.04	-4.65	-3.50	-5.37	-3.34	-5.01	-2.97	0.25
7435	-2.23	-1.41	-3.92	-0.17	0.27	2.25	2.08	-1.57	-2.85	-0.17	-0.40	0.34	-1.78	-0.35	-1.89	-3.23	-1.90	-3.71	-1.90	-3.47	-2.38	-4.34	-2.41	-4.18	-3.08	0.65
7436	-2.40	-1.79	-4.36	-0.47	-0.36	1.40	2.55	-1.77	-3.12	-0.79	-0.34	0.41	-1.79	-0.43	-2.12	-3.45	-2.34	-4.26	-2.48	-4.11	-3.04	-4.99	-3.07	-4.84	-3.23	0.35
7437	-2.00	-1.43	-3.94	-0.19	-0.45	1.33	1.35	-1.36	-2.57	-0.79	-0.16	0.59	-1.59	-0.22	-1.97	-3.26	-2.24	-4.16	-2.49	-4.13	-3.06	-4.96	-3.04	-4.80	-3.01	0.72
7438	-2.17	-1.59	-4.12	-1.00	-0.73	0.89	0.69	-1.40	-2.75	-0.77	-0.04	0.68	-1.53	-0.18	-1.93	-3.17	-2.25	-4.17	-2.46	-4.12	-3.05	-4.99	-3.05	-4.79	-3.39	0.43
7439	-2.18	-1.59	-4.07	-0.83	-0.51	1.03	0.82	-1.43	-2.82	-0.63	-0.14	0.62	-1.56	-0.28	-1.95	-3.18	-2.21	-4.13	-2.40	-4.02	-2.95	-4.83	-2.88	-4.60	-2.99	0.51
7440	-2.69	-1.95	-4.50	-0.69	-0.74	0.74	0.46	-1.95	-3.40	-0.83	-0.49	0.25	-1.92	-0.53	-2.24	-3.19	-2.46	-4.39	-2.60	-4.23	-3.15	-5.06	-3.06	-4.77	-3.24	0.09
7441	-1.98	-1.16	-3.69	0.12	0.38	2.35	2.15	-1.41	-2.54	-0.07	-0.25	0.49	-1.67	-0.25	-1.77	-3.15	-1.77	-3.61	-1.83	-3.40	-2.33	-4.29	-2.30	-4.12	-4.40	0.90
7442	-2.28	-1.46	-3.87	-0.18	0.30	2.24	2.15	-1.63	-2.60	-0.18	-0.52	0.22	-1.89	-0.44	-1.90	-3.20	-1.93	-3.69	-1.90	-3.44	-2.41	-4.32	-2.39	-4.19	-4.66	0.64
7443	-2.51	-1.86	-4.54	-0.37	-0.56	1.51	0.61	-2.54	-3.86	-1.21	-0.83	0.03	-2.06	-0.63	-2.23	-3.55	-2.50	-4.50	-2.79	-4.43	-3.34	-5.26	-3.29	-5.05	-2.91	0.21
7444	-2.43	-1.86	-4.39	-0.42	-1.21	0.71	-0.31	-2.44	-3.93	-1.20	-0.67	0.16	-1.98	-0.58	-2.18	-3.48	-2.42	-4.39	-2.74	-4.41	-3.40	-5.40	-3.48	-5.34	-3.28	0.23
7445	-2.74	-2.01	-4.78	-0.56	-0.66	1.39	0.57	-2.81	-3.92	-0.70	-0.76	0.06	-2.06	-0.60	-2.16	-3.43	-2.25	-4.13	-2.40	-4.03	-2.97	-4.94	-3.04	-4.84	-2.87	0.21
7446	-2.26	-1.61	-4.32	-0.36	-0.45	1.55	1.58	-1.62	-2.91	-0.74	-0.33	0.41	-1.76	-0.37	-2.08	-3.39	-2.30	-4.23	-2.45	-4.03	-3.04	-4.97	-2.99	-4.69	-4.84	0.46
7447	-2.10	-1.53	-4.20	-0.14	-0.14	1.85	1.91	-1.77	-3.08	-0.59	-0.27	0.49	-1.66	-0.27	-1.92	-3.21	-2.09	-4.01	-2.30	-3.91	-2.85	-4.79	-2.86	-4.66	-2.97	0.68
7448	-2.19	-1.59	-4.20	-0.20	-0.25	1.75	1.73	-1.69	-2.93	-0.61	-0.25	0.48	-1.68	-0.28	-1.96	-3.24	-2.17	-4.07	-2.32	-3.94	-2.89	-4.77	-2.91	-4.65	-3.38	0.53
7449	-1.99	-1.44	-4.07	-0.09	-0.11	1.80	1.98	-1.59	-2.90	-0.61	-0.14	0.61	-1.55	-0.13	-1.83	-3.18	-2.11	-4.02	-2.30	-3.89	-2.88	-4.84	-2.85	-4.65	-4.57	0.73
7450	-2.30	-1.80	-4.44	-0.33	-0.57	1.37	1.61	-1.87	-3.17	-0.93	-0.41	0.34	-1.82	-0.44	-2.14	-3.55	-2.41	-4.32	-2.60	-4.27	-3.22	-5.16	-3.21	-5.04	-2.41	0.58
7451	-2.11	-1.55	-4.19	-0.18	-0.33	1.63	1.85	-1.63	-2.87	-0.79	-0.15	0.57	-1.59	-0.22	-1.92	-3.28	-2.19	-4.16	-2.41	-4.09	-3.01	-4.93	-3.06	-4.83	-4.66	0.64
7452	-1.97	-1.14	-3.77	0.08	-0.07	1.92	2.26	-1.11	-2.35	-0.36	0.27	0.99	-1.17	0.21	-1.54	-2.98	-1.84	-3.77	-2.03	-3.67	-2.65	-4.64	-2.71	-4.46	-2.85	0.66
7453	-2.00	-1.16	-3.75	0.04	-0.14	1.85	2.27	-1.11	-2.40	-0.45	0.25	0.98	-1.20	0.18	-1.56	-2.88	-1.88	-3.84	-2.15	-3.80	-2.76	-4.74	-2.81	-4.57	-4.61	0.69
7454	-2.23	-1.91	-4.42	-0.40	-0.46	1.33	0.70	-1.91	-3.11	-0.56	-0.53	0.26	-1.84	-0.48	-2.07	-3.11	-2.17	-3.96	-2.21	-3.80	-2.74	-4.60	-2.68	-4.50	-4.78	0.52
7455	-3.01	-2.61	-5.04	-1.00	-1.25	0.37	0.20	-2.86	-4.01	-1.08	-1.07	-0.28	-2.36	-1.01	-2.56	-3.52	-2.74	-4.65	-2.88	-4.40	-3.30	-5.20	-3.22	-4.91	-1.58	0.43
7456	-2.17	-1.53	-4.11	-0.09	-0.41	1.36	1.49	-1.49	-2.65	-1.07	-0.38	0.34	-1.78	-0.47	-2.15	-3.53	-2.45	-4.44	-2.72	-4.35	-3.22	-5.10	-3.16	-4.98	-3.09	0.64
7458	-1.91	-1.27	-3.81	-0.12	-0.21	1.65	1.53	-1.43	-2.74	-0.32	0.00	0.76	-1.33	0.00	-1.61	-2.98	-1.82	-3.76	-1.97	-3.56	-2.48	-4.39	-2.57	-4.39	-4.60	0.70
7459	-1.74	-1.15	-3.75	0.08	0.00	1.98	1.93	-1.67	-2.94	-0.21	0.02	0.82	-1.28	0.10	-1.53	-2.96	-1.77	-3.68	-1.90	-3.49	-2.44	-4.30	-2.46	-4.27	-4.49	0.81
7460	-1.28	-1.08	-3.62	-0.18	-0.53	0.31	-0.52	-1.69	-2.88	0.25	-0.03	0.80	-1.23	0.15	-1.36	-3.25	-1.45	-3.30	-1.47	-3.05	-1.98	-3.76	-1.80	-3.62	-4.51	0.79
7461	-2.26	-1.82	-4.36	-0.30	-0.40	1.77	1.01	-2.52	-3.76	-0.50	-0.48	0.32	-1.72	-0.32	-1.90	-3.11	-2.04	-3.97	-2.24	-3.79	-2.77	-4.66	-2.81	-4.66	-4.78	0.52
7462	-1.80	-1.26	-3.82	0.20	-0.05	1.90	2.37	-1.22	-2.57	-0.45	0.40	1.18	-0.93	0.40	-1.36	-2.83	-1.74	-3.75	-2.11	-3.71	-2.72	-4.68	-2.86	-4.58	-4.41	0.89
7463	-1.66	-1.20	-3.71	0.32	0.18	2.15	2.22	-1.24	-2.74	-0.26	0.53	1.27	-0.81	0.54	-1.23	-2.65	-1.56	-3.57	-1.83	-3.48	-2.39	-4.36	-2.52	-4.36	-4.36	0.94
7464	-2.56	-1.95	-4.38	0.35	0.52	2.42	4.87	-2.25	-3.87	-0.12	-0.53	0.28	-1.77	-0.42	-1.85	-3.46	-1.83	-3.58	-1.69	-3.29	-2.19	-4.03	-2.14	-3.93	-4.21	1.09
7465	-2.61	-2.38	-4.49	-0.53	0.12	2.04	4.14	-2.52	-4.33	-0.31	-1.95	-1.15	-3.12	-1.50	-2.46	-3.91	-2.18	-3.91	-2.03	-3.54	-2.45	-4.25	-2.44	-4.19	-2.68	0.89
7466	-2.05	-2.12	-4.17	-0.51	0.04	1.78	3.72	-1.76	-3.53	0.41	0.27	1.08	-0.98	0.43	-1.06	-3.28	-1.19	-3.12	-1.29	-2.84	-1.78	-3.66	-1.78	-3.51	-2.15	0.63
7467	-0.82	-0.27	-2.74	0.67	0.58	2.65	2.10	-1.58	-2.94	-0.35	0.51	1.25	-0.84	0.51	-1.12	-2.64	-1.42	-3.34	-1.68	-3.32	-2.27	-4.20	-2.42	-4.32	-2.33	1.49
7468	-1.72	-1.21	-3.82	0.21	0.00	2.03	2.04	-1.89	-3.26	-0.20	-0.49	0.40	-1.61	-0.20	-1.69	-2.93	-1.82	-3.69	-1.88	-3.48	-2.39	-4.25	-2.36	-4.25	-4.36	0.94
7469	-1.37	-0.93	-3.29	0.04	-0.75	0.90	0.28	-1.61	-2.95	-0.26	-0.68	0.24	-1.80	-0.46	-2.00	-3.54	-2.19	-3.91	-1.99	-3.56	-2.39	-4.17	-2.27	-4.03	-4.48	0.82
7470	-1.79	-1.34	-3.73	0.00	-0.55	1.38	1.19	-1.74	-3.07	-0.84	-0.78	0.04	-2.03	-0.66	-2.27	-3.49	-2.49	-4.31	-2.47	-4.06	-2.93	-4.70	-2.76	-4.51	-4.43	0.87
7471	-2.13	-1.79	-4.21	-0.39	-0.85	1.03	0.81	-2.01	-3.33	0.05	1.20	1.86	-0.25	1.13	-0.59	-2.02	-0.79	-3.00	-1.47	-3.33	-2.52	-4.72	-2.96	-4.78	-2.87	0.30
7472	-1.93	-1.49	-4.06	-0.45	-0.87	1.25	1.05	-2.04	-3.45	-0.35	-0.47	0.34	-1.72	-0.32	-1.96	-3.27	-2.08	-3.93	-2.23	-3.82	-2.74	-4.70	-2.75	-4.59	-4.78	0.52
7474	-1.94	-1.63	-4.14	-0.02	-0.59	1.09	0.78	-1.63	-2.87	-0.71	-0.20	0.58	-1.54	-0.23	-1.94	-3.13	-2.13	-4.04	-2.40	-4.06	-2.96	-4.86	-2.97	-4.67	-4.58	0.72
7475	-1.80	-1.41	-3.69	0.20	-0.19	1.40	1.08	-1.10	-2.53	-0.66	-1.27	-0.32	-2.35	-0.95	-2.31	-3.49	-2.36	-4.05	-2.25	-3.92	-2.78	-4.67	-2.73	-4.44	-4.44	0.86
7476	-1.56	-1.03	-3.40	0.32	-0.15	1.84	1.26	-1.47	-3.03	-0.31	-0.08	0.75	-1.36	-0.02	-1.68	-3.11	-1.93	-3.73	-1.96	-3.61	-2.51	-4.35	-2.44	-4.20	-4.53	0.76
7477	-1.73	-1.42	-3.79	0.19	-0.14	1.43	1.25	-1.19	-2.60	-0.50	0.04	0.80	-1.31	0.00	-1.71	-2.91	-1.93	-3.88	-2.18	-3.76	-2.71	-4.60	-2.72	-4.41	-4.37	0.93
7478	-1.89	-1.37	-3.81	-0.02	-0.42	1.23	1.07	-1.24	-2.73	-0.71	0.02	0.79	-1.34	-0.05	-1.82	-3.06	-2.07	-3.95	-2.26	-3.89	-2.84	-4.71	-2.74	-4.62	-4.58	0.72

Appendix A4. Centered log ratio transformed data used for PCA and Random Forest.

Sample	Si	Al	Fe	Mn	Mg	Ca	Na	K	Ti	P	LOI	C-Total	C_in_CO2	Non_carb._C	Total S	Cu	Zn	Pb	Cd	Hg	Sn	Tl	In	As	Co	Ni	Se	Mo	Ge	Sb	Ag	Au	W	Bi	B	Rb	Sr	Cs	Ba	Be	Zr
7479	9.21	8.04	7.02	2.89	5.42	4.74	6.69	6.76	4.70	2.29	8.05	7.33	3.95	7.32	6.40	1.52	3.13	-0.79	-3.18	-11.19	-2.26	-2.87	-6.35	-1.57	0.19	1.27	-4.74	-1.97	-2.89	-4.05	-3.46	-11.19	-4.05	-2.05	2.02	1.20	2.14	-1.53	3.43	-2.67	1.76
7480	9.15	7.98	7.15	2.25	5.78	5.65	6.47	6.73	4.66	2.16	7.78	6.83	5.17	6.78	6.74	1.40	2.40	-0.84	-3.77	-6.40	-2.02	-2.99	-6.40	1.35	-0.02	1.50	-4.80	-2.02	-2.77	-2.22	-3.92	-11.24	-4.10	-3.31	1.24	1.08	1.87	-2.77	3.31	-2.72	1.48
7481	8.74	7.25	6.82	0.21	4.38	4.15	3.89	6.38	4.04	1.38	8.29	7.95	3.91	7.95	6.90	3.00	4.41	0.07	-1.91	-3.64	-1.59	-2.53	-6.09	2.09	0.36	1.87	-1.33	-1.59	-2.59	-1.42	-3.45	-7.70	-4.48	-2.91	0.13	0.87	0.46	-2.33	2.53	-3.78	0.87
7482	9.17	7.84	7.11	1.56	5.12	6.05	7.58	3.19	4.50	2.05	7.40	6.05	6.43	5.54	6.84	1.70	3.79	0.00	-2.56	-6.65	-2.74	-6.24	-6.43	2.69	0.17	1.41	-4.82	-1.64	-3.25	-3.79	-3.25	-5.73	-0.60	-3.03	0.00	-2.33	2.09	-5.73	-0.87	-4.12	1.78
7483	9.32	8.28	7.41	2.75	6.24	6.31	6.45	6.85	5.22	2.43	7.82	5.96	6.97	4.56	4.86	1.22	0.99	-2.30	-4.60	-11.04	-2.52	-3.83	-6.21	1.50	0.20	1.51	-4.60	-3.21	-2.30	-1.58	-4.60	-11.04	-3.91	-3.91	1.22	1.19	2.09	-0.76	2.93	-2.52	1.78
7485	9.28	8.37	8.07	3.19	7.20	5.39	6.39	6.93	5.54	2.43	7.80	5.16	5.97	4.20	3.95	1.51	1.85	-2.22	-4.52	-7.74	-2.44	-3.45	-6.13	0.83	0.75	1.76	-4.52	-3.14	-2.44	-3.49	-4.52	-10.97	-3.83	-4.34	0.77	1.17	0.58	-2.44	2.89	-3.14	1.48
7486	9.46	8.53	7.57	3.14	6.53	6.43	7.07	6.82	5.32	2.23	7.74	5.56	6.56	4.22	3.86	0.86	1.71	-1.10	-4.44	-10.88	-3.05	-3.87	-6.05	0.45	0.33	1.90	-2.36	-2.36	-2.36	-6.05	-3.56	-10.88	-3.74	-4.25	1.16	1.09	3.05	-2.31	3.08	-2.36	1.80
7487	9.52	8.31	6.80	3.19	5.92	7.04	7.22	7.06	4.87	2.50	7.85	6.40	7.08	5.63	5.47	2.26	3.92	-0.36	-2.33	-6.98	-1.46	-3.92	-6.07	-3.76	-0.55	1.51	-4.46	-1.28	-2.28	-6.07	-3.29	-10.90	-3.76	-3.76	2.08	1.82	1.29	-2.54	2.97	-2.38	2.00
7489	9.17	7.74	8.19	2.89	5.40	7.23	7.32	4.49	4.50	2.01	8.10	7.04	7.25	6.63	7.67	3.13	4.10	1.30	-1.72	-4.88	-2.57	-5.47	-6.26	-3.96	0.87	1.67	-0.72	-1.88	-3.27	-3.49	-3.62	-6.08	-3.96	-1.48	0.66	-1.07	1.08	-4.18	0.98	-3.96	1.10
7490	9.02	7.60	7.53	3.29	6.26	6.27	5.55	6.29	4.44	2.13	7.90	6.76	6.22	6.58	6.86	2.58	4.57	-0.42	-1.74	-4.82	-0.68	-3.38	-4.43	0.65	-0.15	1.04	-4.90	-2.13	-2.41	-2.56	-3.62	-11.34	-4.21	-3.25	0.15	0.65	0.78	-2.41	2.23	-3.51	1.40
7491	8.93	7.26	7.38	3.60	5.38	7.28	6.14	5.35	4.41	1.97	7.90	6.58	7.35	5.69	6.73	3.35	4.40	-0.55	-1.92	-4.56	-1.51	-5.49	-4.80	0.07	0.81	0.73	-4.98	-2.21	-2.95	-2.23	-3.41	-6.00	-4.29	-3.33	1.85	-0.26	0.36	-4.10	1.84	-4.29	0.90
7492	9.47	8.48	7.68	3.26	6.83	6.48	7.02	7.15	5.51	2.88	7.39	4.21	0.87	4.20	5.18	1.63	1.56	-2.12	-4.42	-10.87	-3.04	-3.75	-6.03	-0.47	0.50	1.82	-4.42	-3.04	-2.51	-3.73	-4.42	-10.87	-3.73	-3.73	0.99	1.55	2.66	-1.65	3.79	-2.34	2.06
7495	9.50	8.33	7.45	3.24	6.39	6.77	6.60	7.04	5.29	2.30	7.63	5.76	6.77	4.35	5.02	1.01	1.80	-1.14	-4.47	-10.91	-3.08	-4.10	-6.08	-0.31	0.21	1.39	-4.47	-3.08	-2.39	-3.59	-4.47	-6.99	-3.78	-3.59	2.12	1.11	2.51	-2.29	3.04	-3.08	1.75
7496	9.44	8.00	7.42	2.87	6.86	6.06	7.43	2.88	4.69	2.42	8.06	7.41	6.04	7.33	6.32	2.15	3.91	0.51	-2.51	-4.92	-2.46	-5.96	-6.14	-0.95	0.67	2.52	-4.54	-1.54	-2.74	-2.68	-3.66	-7.06	-3.84	-2.97	-0.32	-2.05	-0.20	-4.07	-1.20	-3.84	1.63
7498	9.39	8.40	7.66	3.11	6.81	5.90	6.47	7.07	5.20	2.73	7.57	4.88	5.85	3.62	3.56	1.20	1.43	-0.48	-4.51	-10.95	-3.12	-3.55	-6.12	-0.48	0.20	1.64	-4.51	-2.43	-2.59	-2.72	-4.51	-10.95	-3.81	-3.81	1.07	1.59	2.18	-1.44	3.62	-2.43	1.66
7500	9.42	7.88	8.00	3.93	8.45	7.45	3.47	3.45	4.71	1.78	8.89	7.57	8.21	6.84	3.30	0.45	3.40	-1.12	-3.14	-6.13	-2.91	-6.42	-5.91	3.48	1.24	3.55	-4.30	-1.82	-2.00	-1.30	-4.30	-10.74	-3.61	-4.52	-2.91	-1.82	2.36	-4.12	-0.97	-2.22	1.38
8501	9.54	8.35	7.01	2.88	6.11	5.64	6.28	7.33	5.10	2.47	7.40	5.68	2.20	5.67	5.35	0.56	2.05	-1.49	-4.49	-7.71	-2.00	-3.21	-6.10	-0.39	-0.48	0.61	-4.49	-3.10	-2.77	-3.79	-3.46	-10.93	-3.79	-3.61	1.13	1.54	1.31	-2.11	3.36	-2.41	1.97
8502	9.59	8.16	7.40	2.12	5.69	4.64	7.38	6.45	4.88	2.32	7.88	7.12	5.51	7.07	6.68	1.90	3.47	-0.98	-2.73	-10.89	-2.37	-3.10	-6.06	-3.76	0.60	1.49	-4.45	-1.96	-2.88	-4.27	-3.57	-10.89	-3.76	-3.17	0.34	1.17	1.65	-2.37	3.06	-3.06	1.63
8503	8.53	7.74	7.96	2.55	5.80	5.14	4.27	6.78	4.92	2.47	7.90	6.26	4.97	6.18	7.49	1.63	1.98	1.95	-5.09	-6.23	-0.09	-2.88	-6.00	-1.30	1.08	1.26	-0.66	-2.09	-2.24	-1.21	-3.17	-11.53	-4.39	-2.82	0.71	1.18	-0.81	-2.51	2.56	-3.01	1.57
8504	8.89	7.71	6.74	2.45	5.38	6.29	5.75	6.12	4.55	2.13	7.89	6.81	6.97	6.42	6.27	1.09	3.36	-0.52	-2.83	-5.13	-2.27	-3.76	-6.65	1.40	-0.29	0.93	-5.05	-2.27	-2.67	-1.23	-4.02	-8.26	-4.35	-3.56	1.80	0.52	1.43	-2.67	2.47	-3.66	1.24
8505	9.17	7.73	6.89	2.24	5.75	6.49	4.12	6.89	4.38	2.20	7.79	6.51	7.14	5.80	5.38	2.95	5.12	-0.36	-0.93	-6.44	-0.74	-3.02	-4.36	1.40	0.87	0.91	-4.83	-1.37	-1.52	-2.38	-2.86	-6.26	-4.14	-3.45	0.52	1.44	0.80	-2.71	2.89	-2.35	1.05
8506	8.55	7.44	6.98	0.45	4.57	4.28	5.68	6.24	4.47	1.81	8.98	8.80	3.24	8.80	7.12	1.69	3.74	0.32	-2.61	-4.27	-2.06	-2.74	-6.67	1.70	0.61	1.82	-5.06	-1.59	-3.27	-2.15	-3.78	-11.50	-4.37	-2.98	1.07	0.72	1.51	-1.74	2.39	-2.98	1.24
8507	9.39	7.92	6.55	1.67	5.42	3.94	5.58	6.59	5.03	1.71	7.68	6.48	0.59	6.48	6.12	2.61	4.70	-0.49	-1.58	-2.86	-1.12	-2.54	-4.52	0.44	-0.17	1.01	-4.71	-2.63	-1.65	-2.40	-3.54	-7.23	-4.01	-4.52	1.27	1.10	1.07	-2.01	2.77	-3.32	1.48
8508	8.58	7.16	7.24	2.38	4.72	6.56	4.85	6.47	4.18	2.02	7.44	6.03	6.55	5.42	6.86	3.76	5.31	1.14	-0.71	-4.63	-0.29	-4.32	-3.80	0.13	0.61	0.90	-1.32	-2.11	-2.54	-2.35	-2.09	-6.43	-4.59	-2.44	0.26	0.87	-0.81	-2.31	2.84	-3.90	0.84
8509	7.97	7.05	7.25	0.81	3.82	6.04	6.47	4.69	3.52	1.21	8.79	8.67	5.80	8.65	7.10	2.84	5.14	1.50	-1.02	-4.03	-0.55	-7.45	-5.15	2.41	0.80	2.12	-0.56	-0.77	-1.78	-0.89	-2.40	-6.61	-4.64	-2.38	-2.56	-1.46	1.31	-5.15	3.33	-4.64	0.68
8510	8.14	6.93	7.42	1.39	6.43	5.81	6.51	2.57	3.69	1.23	8.98	8.86	5.71	8.85	6.92	2.75	4.77	1.02	-1.39	-3.60	-1.49	-6.45	-5.40	2.70	1.07	2.71	-0.84	-0.85	-2.51	-1.77	-3.21	-6.61	-4.49	-2.69	-1.85	-3.10	0.86	-5.00	-0.01	-4.49	0.59
8511	7.87	6.85	7.24	0.99	4.68	4.24	6.44	3.83	3.66	1.26	9.40	9.26	3.40	9.26	7.36	3.07	4.69	0.86	-1.63	-3.51	-0.82	-5.12	-4.46	2.01	1.33	2.59	-0.77	-0.47	-2.24	-1.27	-3.03	-7.68	-4.46	-2.74	-3.77	-1.98	0.96	-4.97	1.24	-4.46	0.33
8512	8.60	6.85	7.14	3.41	7.88	9.15	5.71	3.17	3.87	1.43	9.49	8.95	9.04	8.60	6.56	2.47	3.36	0.05	-1.94	-4.39	-2.35	-6.55	-6.04	2.43	0.86	1.72	-4.43	-0.74	-2.05	-1.91	-4.43	-10.87	-3.73	-3.26	-0.56	-2.35	1.86	-5.34	-0.96	-3.73	0.51
8513	8.09	7.24	7.28	3.04	5.84	8.26	3.17	0.10	3.90	1.54	9.02	8.87	7.05	8.82	7.02	3.13	2.22	-0.49	-2.98	-5.46	-2.02	-7.13	-4.54	2.75	1.21	2.13	-1.45	-0.58	-2.34	-1.94	-3.36	-8.23	-4.32	-1.85	-2.02	-4.32	-0.10	-5.93	-1.43	-2.93	1.70
8514	8.42	7.33	7.67	1.56	4.70	6.94	7.02	2.96	3.66	0.52	8.76	8.42	7.06	8.34	7.50	2.63	5.29	2.09	-0.69	-3.11	-0.33	-7.17	-4.35	2.54	0.49	1.93	-1.80	-1.10	-1.65	-1.33	-2.97	-7.17	-4.35	-2.41	-1.36	-2.97	1.19	-6.66	1.11	-4.35	1.04
8515	8.86	7.81	8.21	3.59	8.73	6.68	2.86	2.06	4.20	1.82	9.21	8.63	5.01	8.62	4.03	3.44	3.68	-2.14	-1.47	-5.87	-2.36	-6.56	-6.05	1.47	1.29	2.81	-4.44	-0.98	-2.41	-6.05	-4.44	-6.97	-3.75	-2.65	-3.06	-3.75	-0.35	-4.26	-1.26	-3.75	2.03
8516	7.42	6.85	7.99	2.90	7.37	7.90	1.85	0.18	3.75	1.48	9.23	8.99	8.04	8.88	7.16	2.92	5.15	0.99	-1.37	-3.69	-2.17	-7.06	-5.16	2.60	1.38	2.05	-0.82	-0.42	-2.49	-5.85	-3.29	-6.08	-4.24	-2.03	-2.45	-4.24	0.87	-6.55	-1.35	-4.24	0.65
8517	7.76	6.90	8.15	3.30	7.32	7.86	2.45	0.96	3.76	1.41	9.30	8.92	7.97	8.81	7.76	2.96	4.81	1.37	-1.10	-5.07	-1.67	-6.97	-5.07	2.12	1.12	2.09	-0.90	-0.69	-2.05	-1.35	-3.37	-6.97	-4.16	-1.87	-1.38	-4.16	0.12	-6.46	-2.08	-4.16	0.67
8518	8.27	6.68	6.93	0.88	4.28	5.77	6.06	5.64	3.47	1.34	8.75	8.61	5.79	8.59	7.05	2.86	4.95	1.35	-1.23	-2.89	-0.80	-4.63	-4.85	2.44	0.78	2.26	-1.33	-0.84	-2.35	-1.45	-2.87	-7.15	-4.63	-2.19	-2.33	-0.60	0.40	-4.85	1.77	-4.63	0.27
8519	9.31	8.23	7.29	2.42	6.34	6.04	6.62	6.56	5.10	2.24	7.63	5.69	6.71	4.27	4.46	0.29	1.76	-2.32	-4.62	-7.84	-3.24	-4.34	-6.23	0.95	0.05	1.49	-4.62	-2.54	-2.97	-1.39	-3.93	-7.15	-2.54	-4.15	1.51	0.83	2.23	-1.14	2.76	-2.54	1.66
8520	9.67	8.66	6.98	1.99	5.64	5.54	6.74	6.94	5.60	2.53	7.61	5.02	6.01	3.70	3.04	0.72	1.23	-0.65	-4.33	-10.78	-2.95	-3.89	-5.94	0.74	0.07	1.30	-4.33	-2.95	-2.54	-2.07	-4.33	-10.78	-1.16	-5.25	2.10	1.16	3.08	-0.92	3.19	-2.95	2.10
8521	9.34	8.28	7.06	2.29	5.94	6.27	6.10	7.18	5.26	2.43	7.68	5.72	6.90	3.47	4.38	0.92	0.15	-2.30	-4.61	-11.05	-3.22	-3.56	-6.21	2.36	0.21	1.46	-4.61	-3.22	-2.43	-0.76	-4.61	-7.82	-1.43	-4.42	1.69	1.43	1.88	-0.51	3.14	-2.53	1.63
8522	9.33	8.24	7.28	2.58	5.96	6.34	6.39	6.98	5.14	2.34	7.76	6.14	7.00	5.11	4.96	1.15	0.17	-2.31	-4.61	-11.06	-3.92	-3.60	-6.22	2.79	0.10	1.46	-4.61	-3.23	-2.49	-0.96	-4.61	-11.06	-1.44	-4.43	3.04	1.35	1.83	-0.65	2.83	-2.54	1.64
8523	9.25	8.18	7.19	2.17	6.08	5.95	6.57	6.79	4.94	2.26	7.54	5.58	6.57	4.23	4.91	1.04	1.40	-0.47	-4.69	-11.13	-3.31	-4.13	-6.30	1.55	-0.15	1.23	-4.69	-3.31	-2.77	-1.26	-3.82	-6.81	-1.51	-3.04	0.90	1.25	2.04	-0.89	3.09	-3.31	1.65
8524	9.42	8.36	7.14	3.10	5.93	6.81	6.31	7.11	5.25	2.36	8.05	6.43	7.48	4.90	4.75	0.78	1.03	-2.20	-4.50	-10.95	-3.12	-4.50	-6.11	2.00	0.15	1.63	-4.50	-3.12	-2.71	-1.06	-4.50	-10.95	-3.81	-5.42	1.54	1.44	2.32	-0.54	3.10	-3.12	1.74
8525	9.21	8.12	7.26	3.12	5.72	5.68	5.92	6.78	5.15	2.22	7.83	6.28	7.27	4.96	5.51	1.09	1.63	-2.43	-4.73	-7.95	-3.34	-4.23	-6.34	3.39	-0.06	1.23	-4.73	-3.34	-2.70	-0.54	-4.73	-11.17	-1.14	-4.55	2.46	1.14	2.11	-0.82	2.80	-2.65	1.49
8526	9.24	8.14	7.40	3.42	6.05	6.57	6.27	6.76	5.24	2.46	8.13	6.68	7.80	4.85	4.44	0.82	1.21	-1.31	-4.64	-11.09	-3.26	-4.40	-6.25	1.61	0.18	1.44	-4.64	-3.26	-2.79	-0.42	-4.64	-7.86	-3.95	-4.17	1.19	1.14	2.49	-0.81	2.82	-3.26	1.56
8527	9.56	8.44	7.72	2.65	6.65	5.85	6.55	6.76	5.44	2.79	7.73	5.13	6.40	1.57	4.00	1.04	1.87	-1.06	-4.39	-10.83	-3.70	-4.28	-6.00	1.14	0.31	1.87	-4.39	-3.00	-2.53	-1.28	-4.39	-10.83	-3.70	-5.31	1.45	1.17	2.49	-0.65	2.96	-3.00	1.88
8528	9.42	8.31	7.61	2.93	6.36	6.37	6.03	6.97	5.29	2.43	7.88	6.20	7.04	5.21	3.26	1.02	1.67	-0.94	-4.53	-10.97	-3.14	-3.40	-6.14	1.60	0.27	1.62	-4.53	-3.14	-2.35	-1.21	-4.53	-10.97	-2.04	-4.06	1.52	1.34	2.15	-0.71	2.96	-3.14	1.66
8529	9.46	8.57	7.10	2.70	5.66	4.74	6.93	6.85	5.44	2.30	7.88	6.06	7.24	3.87	2.91	0.90	1.49	-1.14	-4.47	-10.91	-3.08	-4.13	-6.08	1.89	0.12	1.36	-4.47	-3.08	-2.44	-1.14	-4.47	-10.91	-1.47	-5.39	1.80	1.19	3.00	-0.60	3.26	-2.39	2.06
8530	9.45	8.23	7.13	2.35	5.98	6.25	6.70	6.96	4.94	2.63	7.69	6.04	6.93	4.96	5.62	1.09	1.50	-1.37	-4.55	-10.99	-3.16	-4.00	-6.16	1.09	-0.13	1.22	-4.55	-3.16	-2.47	-0.54	-4.55	-10.99	-1.77	-3.06	0.90	1.38	2.30	-0.83	3.09	-2.47	1.69
8531	9.30	8.08	7.17	2.29	6.09	6.05	5.70	6.94	4.86	2.34	7.61	5.68	6.54	4.64	6.07	0.95	0.48	-1.01	-4.69	-11.14	-3.31	-4.06	-6.30	1.36	-0.01	0.85	-4.69	-3.31	-2.43	-2.06	-4.69	-6.12	-1.01	-2.35	1.59	1.41	2.04	-0.62	3.03	-2.62	1.71
8532	9.47	8.44	7.32	2.67	5.75	4.68	6.92	7.03	5.34	2.19	7.87	6.26	7.42	4.25	2.90	1.17	1.81	-1.30	-4.48	-7.00	-3.09	-4.11	-6.08	1.02	0.08	1.42	-4.48	-3.09	-2.62	-1.75	-3.45	-10.92	-3.78	-4.01	1.85	1.35	2.71	-0.53	3.64	-3.09	1.88
8533	9.34	8.09	7.18	2.73	6.07	6.48	6.40	6.89	4.91	2.40	7.98	6.38	7.59	3.89	5.86	1.18	1.54	0.31	-4.63	-11.07	-3.94	-4.24	-6.24	1.84	0.01	1.28	-4.63	-3.24	-2.71	-0.66	-4.63	-7.85	-2.14	-3.06	1.51	1.29	2.05	-0.68	2.95	-3.24	1.56
8534	9.17	7.83	6.48	1.75	4.95	5.38	6.49	6.63	4.30	1.91	7.76	6.99	5.89	6.90	6.55	0.74	3.15	-0.18	-3.48	-4.09	-2.78	-3.29	-6.47	1.63	-0.26	1.32	-3.58	-2.09	-3.07	-2.56	-3.99	-8.08	-4.17	-3.22	0.28	1.02	1.57	-3.01	2.97	-3.48	1.53
8535	9.04	7.88	6.70	1.30	5.56	5.38	6.10	6.72	4.68	1.96	7.80	6.82	5.46	6.75	6.77	1.17	3.20	-0.02	-3.18	-4.25	-1.91	-2.14	-6.51	1.70	-0.05	1.45	-4.90	-2.42	-2.06	-2.49	-3.87	-11.34	-4.21	-3.11	0.78	1.22	1.59	-1.72	2.93	-3.52	1.31
8536	9.46	8.47	7.39	2.90	6.14	5.60	6.84	7.07	5.39	2.33	8.08	6.42	7.67	3.42	3.16	0.93	0.44	-2.14	-4.45	-6.97	-3.06	-3.81	-6.05	0.97	0.20	1.54	-4.45	-3.06	-2.59	-1.11	-4.45	-10.89	-3.75	-4.67	1.53	1.42	2.71	-0.61	3.25	-3.06	1.90
8537	9.40	8.47	6.81	2.64	5.47	5.32	6.66	7.02	5.39	2.22	7.75	5.91	7.05	3.94	3.05	1.11	1.20	-1.09	-4.55	-7.77	-3.16	-4.08	-6.16	1.01	0.04	1.36	-4.55	-3.16	-2.58	-1.86	-3.86	-10.99	-2.07	-4.77	2.01	1.37	2.77	-0.47	3.38	-3.16	1.99
8538	9.51	8.48	7.62	3.11	6.50	6.36	7.29	6.71	5.36	2.62	7.75	6.09	6.18	5.73	5.78	0.78	0.96	-2.11	-4.42	-10.86	-3.72	-4.23	-6.02	1.43	0.43	1.83	-4.42	-3.03	-2.77	-6.02	-4.42	-10.86	-3.72	-3.54	1.84	1.16	2.83	-2.11	3.07	-3.03	1.88
8539	9.48	8.42	7.59	2.78	6.60	6.12	6.62	7.38	5.35	2.86	7.60	5.24	6.04	4.30	4.32	0.88	1.42	-2.14	-4.44	-10.88	-3.75	-3.44	-6.05	0.24	0.18	1.54	-4.44	-3.05	-2.65	-3.75	-3.75	-10.88	-3.75	-3.57	1.36	1.68	1.77	-1.72	3.57	-2.36	1.85
8540	7.75	6.79	7.47	0.55	4.34	6.20	5.99	5.34	3.61	1.05	8.93	8.87	5.98	8.86	7.05	2.77	4.83	1.11	-1.48	-3.06	-1.68	-6.79	-6.28	2.80	1.05	2.43	-0.96	-0.68	-2.75	-2.17	-2.88	-5.59	-4.67	-3.72	-3.98	-0.65	0.24	-3.45	1.89	-4.67	0.30
8541	8.14	6.78	7.48	1.60	5.92	7.81	6.40	3.48	3.56	1.30	9.31	9.09	7.80	9.01	7.55	2.92	4.88	1.56	-1.44	-3.79	-1.63	-7.08	-5.19	2.15	1.18	2.12	-0.88	-0.58	-3.32	-1.27	-3.05	-6.80	-4.27	-3.32	-3.58	-2.48	0.93	-5.19	-0.94	-4.27	0.53
8542	8.64	7.41	8.71	3.42	6.32	5.40	6.60	5.30	4.66	1.80	8.31	7.05	3.07	7.04	8.43	2.25	3.72	-0.34	-2.25	-4.59	-1.28	-4.90	-5.09	-0.48	0.62	1.03	-4.86	-1.69	-3.70	-2.84	-3.38	-11.31	-4.17	-3.30	1.96	-0.43	0.58	-4.68	1.58	-3.48	1.38
8543	8.52	7.56	8.33	2.91	7.56	7.34	6.21	3.69	4.40	2.07	9.53	9.36	6.38	9.34	7.54	3.24	0.22	-0.44	-4.60	-5.87	-3.91	-6.72	-6.21	0.40	1.51	2.74	-4.60	0.01	-3.44	-4.42	-4.60	-11.04	-3.91	-1.93	-2.52	-2.52	0.81	-4.82	0.22	-3.91	1.11
8544	8.43	7.63	8.10	3.97	8.31	8.64	2.75	1.48	4.34	2.22	9.82	9.53	8.58	9.42	5.94	2.03	0.88	-1.00	-4.33	-5.35	-3.64	-6.45	-5.94	2.03	1.29	3.26	-4.33	0.00	-3.17	-5.94	-4.33	-7.55	-3.64	-0.84	-0.86	-3.64	1.49	-5.94	-1.85	-3.64	1.13
8545	8.28	7.06	7.85	0.88	4.44	6.61	6.67	4.83	3.69	0.82	9.10	8.84	6.59	8.81	7.95	2.65	-1.45	0.85	-5.04	-3.36	-1.86	-5.77	-5.95	3.03	1.02	2.15	-0.30	-0.82	-3.18	-1.12	-2.42	-6.64	-4.34	-2.21	-2.96	-1.45	1.10	-5.26	1.02	-4.34	0.96
8546	9.08	7.48	6.88	1.58	5.23	6.71	7.11	3.76	4.17	1.58	9.21	9.12	6.52	9.09	6.15	1.45	3.14	0.07	-3.40	-4.07	-3.99	-4.77	-6.29	1.08	0.49	1.90	-4.68	-0.30	-2.71	-4.50	-4.68	-11.13	-3.99	-3.30	-1.22	-2.20	0.53	-5.60	-0.59	-3.99	1.69
8547	8.35	6.82	7.12

Appendix A4. Centered log ratio transformed data used for PCA and Random Forest.

Sample	Hf	Nb	Ta	Ga	Sc	V	Cr	Th	U	Y	La	Ce	Pr	Nd	Sm	Eu	Gd	Tb	Dy	Ho	Er	Tm	Yb	Lu	Br	F
7479	-1.85	-1.52	-3.99	-0.03	-0.50	1.20	0.90	-1.32	-2.67	-0.53	-0.13	0.61	-1.50	-0.15	-1.81	-3.08	-2.08	-3.97	-2.22	-3.80	-2.76	-4.63	-2.65	-4.41	-4.74	0.55
7480	-2.10	-1.69	-4.14	-0.19	-0.46	1.17	1.05	-1.48	-2.70	-0.84	-0.18	0.54	-1.56	-0.21	-1.96	-3.28	-2.28	-4.25	-2.51	-4.16	-3.04	-4.97	-3.08	-4.80	-4.80	0.50
7481	-2.79	-2.01	-4.48	-0.79	-1.04	0.48	0.37	-2.24	-3.26	-0.74	-0.61	0.12	-1.99	-0.67	-2.30	-3.30	-2.34	-4.14	-2.34	-3.97	-2.91	-4.86	-2.98	-4.73	-5.17	0.13
7482	-1.82	-1.21	-3.55	-0.39	-0.85	0.18	0.28	-1.00	-1.89	-0.17	0.29	0.99	-1.14	0.16	-1.54	-3.01	-1.76	-3.65	-1.88	-3.55	-2.44	-4.32	-2.44	-4.21	-4.82	0.48
7483	-1.85	-1.27	-3.77	0.12	-0.20	1.80	1.83	-1.25	-2.40	-0.32	0.00	0.70	-1.41	-0.07	-1.75	-3.02	-1.88	-3.83	-2.02	-3.58	-2.54	-4.42	-2.62	-4.42	-4.60	0.70
7485	-2.07	-1.40	-3.72	0.20	0.51	2.41	2.35	-1.47	-2.65	0.04	-0.22	0.53	-1.53	-0.12	-1.59	-3.00	-1.67	-3.49	-1.68	-3.28	-2.23	-4.08	-2.19	-4.03	-4.52	0.77
7486	-1.83	-1.40	-3.89	0.35	-0.01	1.97	2.12	-1.58	-2.96	-0.41	0.28	1.02	-1.09	0.27	-1.47	-2.77	-1.75	-3.76	-2.03	-3.70	-2.68	-4.61	-2.78	-4.56	-4.44	0.86
7487	-1.59	-1.35	-3.87	0.15	-0.73	0.88	1.45	-2.07	-3.26	-0.67	-0.90	-0.08	-2.13	-0.76	-2.30	-3.43	-2.42	-4.24	-2.39	-3.99	-2.86	-4.68	-2.77	-4.50	-4.46	0.84
7489	-2.57	-1.96	-4.54	-0.78	-0.54	0.88	1.12	-1.91	-3.21	-0.56	-1.56	-0.72	-2.75	-1.33	-2.71	-3.53	-2.53	-4.29	-2.39	-3.98	-2.92	-4.83	-2.89	-4.65	-4.65	0.64
7490	-2.26	-1.74	-4.33	-0.29	-1.07	0.75	0.37	-2.20	-3.61	-0.80	-0.78	-0.01	-2.08	-0.73	-2.27	-3.56	-2.49	-4.27	-2.47	-4.09	-2.95	-4.82	-2.89	-4.65	-4.90	0.40
7491	-2.72	-2.28	-4.87	-0.82	-1.00	0.83	0.75	-3.09	-4.35	-0.46	-0.81	0.01	-2.06	-0.62	-2.15	-3.37	-2.16	-4.04	-2.25	-3.83	-2.69	-4.56	-2.61	-4.37	-2.90	0.32
7492	-1.58	-1.01	-3.62	0.29	0.14	2.10	2.25	-1.26	-2.61	-0.33	0.31	1.10	-1.01	0.28	-1.45	-2.91	-1.68	-3.62	-1.84	-3.53	-2.49	-4.35	-2.49	-4.24	-4.42	0.87
7495	-1.92	-1.45	-3.88	0.18	-0.14	1.84	1.85	-1.72	-3.00	-0.60	-0.09	0.66	-1.42	-0.08	-1.71	-3.10	-1.93	-3.86	-2.15	-3.84	-2.80	-4.64	-2.70	-4.39	-4.47	0.83
7496	-1.99	-1.46	-3.82	-0.20	-0.53	1.10	2.47	-1.33	-2.82	-0.75	-0.16	0.58	-1.57	-0.23	-1.96	-3.35	-2.21	-4.17	-2.46	-3.97	-2.89	-4.71	-2.70	-4.50	-4.54	0.76
7498	-1.99	-1.15	-3.70	0.28	-0.05	1.93	2.35	-1.07	-2.30	-0.35	0.44	1.16	-0.96	0.38	-1.37	-2.78	-1.67	-3.68	-1.97	-3.67	-2.61	-4.51	-2.63	-4.36	-4.51	0.79
7500	-2.27	-0.95	-3.69	-0.21	-0.05	1.73	4.02	-1.56	-2.94	-0.52	-0.49	0.26	-1.85	-0.55	-2.15	-3.71	-2.27	-3.94	-2.11	-3.63	-2.52	-4.43	-2.56	-4.38	-2.65	1.00
8501	-1.58	-0.71	-2.94	0.30	-0.56	1.33	0.85	-1.27	-2.60	0.03	-0.07	0.77	-1.31	0.00	-1.57	-3.20	-1.72	-3.56	-1.67	-3.29	-2.17	-3.99	-2.06	-3.97	-4.49	0.81
8502	-1.96	-1.36	-3.66	0.03	-0.49	1.10	1.14	-1.42	-2.69	-0.66	0.19	0.95	-1.18	0.13	-1.58	-3.19	-1.88	-3.86	-2.22	-3.91	-2.77	-4.67	-2.75	-4.41	-4.45	0.85
8503	-2.11	-1.57	-4.28	-0.04	-0.86	1.21	1.10	-2.43	-3.72	-0.66	-0.70	0.12	-1.89	-0.46	-2.04	-3.41	-2.24	-4.13	-2.36	-4.00	-2.86	-4.72	-2.84	-4.62	-5.09	0.21
8504	-2.35	-1.83	-4.35	-0.44	-0.69	1.04	1.19	-1.80	-3.16	-0.89	-0.33	0.42	-1.68	-0.34	-2.08	-3.27	-2.22	-4.28	-2.54	-4.20	-3.09	-4.97	-3.05	-4.80	-2.27	0.25
8505	-2.53	-2.32	-4.62	-0.27	-0.94	0.90	0.60	-2.43	-3.70	-1.37	-0.94	-0.11	-2.18	-0.79	-2.50	-3.68	-2.77	-4.79	-3.06	-4.65	-3.60	-5.41	-3.41	-5.16	-4.83	0.46
8506	-2.39	-1.88	-4.25	-0.38	-1.12	0.82	0.58	-1.92	-3.14	-0.90	-0.49	0.25	-1.88	-0.53	-2.26	-3.48	-2.46	-4.41	-2.61	-4.23	-3.05	-4.91	-2.96	-4.72	-1.61	0.24
8507	-2.22	-1.53	-4.24	-0.14	-0.57	1.48	1.15	-2.54	-3.83	-0.61	-1.13	-0.12	-2.07	-0.62	-2.22	-3.44	-2.23	-4.03	-2.35	-3.96	-2.90	-4.79	-2.88	-4.63	-4.71	0.59
8508	-2.91	-2.14	-4.77	-0.60	-1.35	0.66	0.49	-2.96	-4.17	-0.86	-1.13	-0.28	-2.30	-0.87	-2.42	-3.75	-2.52	-4.43	-2.64	-4.26	-3.19	-5.14	-3.27	-5.04	-5.29	0.01
8509	-2.99	-2.54	-4.86	-1.24	-0.94	0.30	0.36	-2.32	-3.39	-0.86	-1.01	-0.19	-2.29	-0.94	-2.45	-2.75	-2.53	-4.33	-2.59	-4.20	-3.11	-4.97	-3.03	-4.72	-5.33	-0.04
8510	-3.10	-2.46	-4.90	-1.15	-0.82	0.66	2.19	-2.15	-3.28	-0.66	-0.75	0.00	-2.11	-0.76	-2.24	-3.00	-2.33	-4.15	-2.35	-3.92	-2.85	-4.73	-2.75	-4.47	-5.18	0.12
8511	-3.36	-2.70	-5.12	-1.06	-0.62	0.72	0.49	-2.38	-3.43	-0.59	-1.04	-0.16	-2.22	-0.85	-2.27	-2.50	-2.36	-4.10	-2.28	-3.85	-2.75	-4.61	-2.62	-4.28	-3.03	0.14
8512	-3.15	-2.71	-5.08	-1.43	-0.80	0.67	0.57	-2.24	-3.36	-0.48	-0.76	0.06	-1.99	-0.61	-2.04	-3.10	-2.15	-3.96	-2.15	-3.73	-2.66	-4.51	-2.55	-4.21	-2.51	0.87
8513	-2.00	-1.34	-3.81	-0.92	-0.85	0.22	0.32	-1.47	-2.56	-0.04	-0.22	0.58	-1.53	-0.19	-1.75	-2.80	-1.87	-3.62	-1.77	-3.32	-2.21	-4.09	-2.15	-3.91	-5.01	0.29
8514	-2.71	-2.25	-4.48	-0.83	-1.29	0.10	-0.23	-1.88	-2.89	-1.10	-0.80	-0.05	-2.20	-0.91	-2.50	-2.92	-2.68	-4.55	-2.77	-4.40	-3.35	-5.18	-3.24	-4.97	-5.05	0.25
8515	-1.67	-1.12	-3.71	-0.01	-0.48	1.00	2.24	-1.25	-2.52	0.12	-0.17	0.76	-1.35	-0.03	-1.60	-3.46	-1.68	-3.40	-1.53	-3.09	-1.97	-3.81	-1.87	-3.60	-2.87	0.86
8516	-3.02	-2.60	-5.07	-1.35	-0.04	0.91	0.74	-2.21	-3.34	-0.22	-0.62	0.19	-1.88	-0.50	-1.92	-2.44	-1.92	-3.70	-1.92	-3.52	-2.43	-4.33	-2.36	-4.05	-2.91	0.36
8517	-3.13	-2.51	-5.02	-1.06	-0.42	0.87	0.99	-2.36	-3.40	-0.52	-0.84	-0.06	-2.14	-0.75	-2.18	-2.74	-2.22	-4.02	-2.22	-3.79	-2.70	-4.60	-2.66	-4.35	-4.85	0.45
8518	-3.40	-2.98	-5.32	-1.04	-1.01	0.38	0.16	-2.54	-3.69	-0.84	-1.02	-0.25	-2.35	-1.00	-2.45	-2.84	-2.56	-4.38	-2.59	-4.18	-3.10	-4.98	-3.03	-4.71	-3.06	-0.02
8519	-2.01	-1.65	-4.18	-0.02	-0.25	1.68	1.76	-1.71	-2.97	-0.60	-0.06	0.69	-1.44	-0.10	-1.78	-3.12	-2.01	-3.97	-2.23	-3.87	-2.86	-4.80	-2.88	-4.62	-2.97	0.68
8520	-1.56	-1.24	-3.75	0.35	0.06	2.07	1.83	-1.69	-2.88	-0.24	0.05	0.81	-1.31	0.04	-1.60	-2.93	-1.81	-3.68	-1.90	-3.51	-2.42	-4.33	-2.42	-4.19	-2.77	0.96
8521	-2.09	-1.69	-4.21	0.00	-0.11	1.93	1.93	-1.69	-2.86	-0.33	-0.10	0.63	-1.48	-0.14	-1.81	-3.21	-2.01	-3.97	-2.18	-3.84	-2.76	-4.65	-2.73	-4.57	-3.12	0.69
8522	-2.03	-1.64	-4.14	-0.01	-0.21	1.78	1.88	-1.56	-2.78	-0.66	-0.16	0.60	-1.51	-0.18	-1.86	-3.24	-2.09	-4.03	-2.29	-3.92	-2.83	-4.70	-2.77	-4.61	-2.89	0.68
8523	-2.00	-1.66	-4.06	-0.05	-0.44	1.58	1.51	-1.14	-2.43	-0.67	-0.05	0.67	-1.49	-0.19	-1.87	-3.25	-2.10	-4.08	-2.30	-3.96	-2.87	-4.73	-2.84	-4.65	-3.12	0.61
8524	-1.92	-1.59	-4.11	0.10	-0.13	1.88	1.93	-1.66	-2.99	-0.48	0.03	0.78	-1.34	0.00	-1.69	-3.03	-1.93	-3.89	-2.18	-3.83	-2.77	-4.68	-2.77	-4.54	-2.78	0.80
8525	-2.18	-1.82	-4.34	-0.16	-0.21	1.84	1.73	-1.76	-2.95	-0.51	-0.25	0.51	-1.60	-0.27	-1.91	-3.25	-2.10	-3.98	-2.24	-3.85	-2.81	-4.73	-2.84	-4.58	-4.73	0.57
8526	-2.13	-1.80	-4.40	-0.12	-0.07	1.93	1.91	-1.98	-3.20	-0.48	-0.32	0.44	-1.65	-0.28	-1.87	-3.25	-2.07	-3.93	-2.18	-3.78	-2.71	-4.60	-2.69	-4.46	-2.73	0.66
8527	-1.81	-1.50	-4.08	0.22	0.12	2.15	2.32	-1.60	-2.93	-0.29	0.23	1.01	-1.08	0.27	-1.41	-2.84	-1.68	-3.66	-1.93	-3.56	-2.51	-4.47	-2.56	-4.39	-3.11	0.91
8528	-1.98	-1.64	-4.19	0.04	-0.03	2.01	2.09	-1.69	-2.93	-0.43	-0.11	0.65	-1.46	-0.10	-1.75	-3.05	-1.93	-3.85	-2.11	-3.79	-2.70	-4.61	-2.70	-4.45	-4.53	0.77
8529	-1.63	-1.24	-3.72	0.32	-0.07	1.99	1.57	-1.53	-2.70	-0.38	0.19	0.96	-1.17	0.15	-1.57	-2.98	-1.84	-3.78	-2.03	-3.65	-2.58	-4.51	-2.58	-4.36	-4.47	0.83
8530	-2.00	-1.85	-4.27	0.02	-0.52	1.54	1.44	-1.57	-2.75	-0.68	-0.07	0.67	-1.43	-0.13	-1.80	-3.21	-2.08	-4.05	-2.34	-4.00	-2.93	-4.88	-2.98	-4.72	-3.16	0.75
8531	-1.95	-1.78	-4.25	-0.13	-0.54	1.51	1.31	-1.37	-2.63	-0.74	-0.08	0.63	-1.54	-0.22	-1.90	-3.35	-2.17	-4.13	-2.40	-4.04	-3.02	-4.92	-2.98	-4.78	-3.53	0.60
8532	-1.81	-1.48	-3.93	0.17	-0.07	1.95	1.49	-1.91	-3.17	-0.38	-0.06	0.68	-1.43	-0.08	-1.73	-3.15	-1.90	-3.76	-2.02	-3.67	-2.62	-4.52	-2.66	-4.40	-4.48	0.82
8533	-2.11	-1.91	-4.35	-0.15	-0.46	1.56	1.54	-1.74	-2.89	-0.76	-0.20	0.52	-1.60	-0.28	-1.94	-3.37	-2.18	-4.14	-2.41	-4.06	-2.99	-4.90	-2.98	-4.80	-4.63	0.67
8534	-2.14	-1.85	-4.13	-0.53	-0.93	0.70	0.48	-1.18	-2.20	-0.99	-0.17	0.53	-1.62	-0.33	-2.06	-3.47	-2.40	-4.39	-2.64	-4.28	-3.20	-5.09	-3.18	-4.90	-2.45	0.43
8535	-2.38	-1.91	-4.31	-0.30	-0.58	1.18	1.19	-1.71	-2.84	-1.03	-0.25	0.45	-1.70	-0.40	-2.11	-3.43	-2.40	-4.38	-2.66	-4.34	-3.24	-5.18	-3.25	-4.99	-3.25	0.40
8536	-1.75	-1.49	-3.86	0.24	-0.03	1.99	1.72	-1.79	-3.03	-0.42	-0.05	0.71	-1.40	-0.06	-1.69	-3.08	-1.88	-3.81	-2.02	-3.64	-2.63	-4.53	-2.61	-4.45	-4.45	0.85
8537	-1.68	-1.37	-3.82	0.20	-0.05	1.98	1.56	-1.83	-3.12	-0.39	-0.09	0.69	-1.42	-0.07	-1.72	-3.09	-1.90	-3.82	-2.06	-3.66	-2.63	-4.51	-2.60	-4.37	-2.90	0.75
8538	-1.84	-1.46	-4.00	0.27	-0.06	1.92	2.09	-1.31	-2.53	-0.46	0.14	0.94	-1.18	0.13	-1.61	-3.13	-1.93	-3.85	-2.13	-3.78	-2.71	-4.64	-2.65	-4.46	-4.42	0.88
8539	-1.86	-1.53	-3.95	0.16	-0.08	1.98	1.94	-1.35	-2.69	-0.42	0.32	1.09	-1.02	0.31	-1.41	-2.95	-1.72	-3.71	-1.99	-3.69	-2.62	-4.57	-2.66	-4.44	-3.05	0.86
8540	-3.39	-2.85	-5.18	-1.09	-0.72	0.60	0.32	-2.40	-3.50	-0.61	-0.94	-0.09	-2.17	-0.80	-2.25	-2.56	-2.34	-4.13	-2.33	-3.93	-2.85	-4.71	-2.74	-4.41	-2.57	-0.07
8541	-3.11	-2.59	-5.05	-1.18	-0.60	0.64	0.29	-2.29	-3.41	-0.69	-1.04	-0.19	-2.26	-0.90	-2.35	-2.88	-2.44	-4.19	-2.38	-3.98	-2.91	-4.78	-2.79	-4.47	-4.96	0.33
8542	-2.25	-1.67	-4.15	-0.48	-0.57	1.25	0.77	-2.05	-3.19	-0.30	-0.71	0.12	-1.95	-0.57	-2.01	-3.50	-1.98	-3.79	-2.00	-3.56	-2.53	-4.39	-2.51	-4.30	-4.86	0.43
8543	-2.62	-2.11	-4.45	-0.91	-0.05	1.41	2.34	-1.79	-2.90	0.01	-0.45	0.51	-1.52	-0.13	-1.61	-2.52	-1.71	-3.51	-1.71	-3.30	-2.20	-4.08	-2.13	-3.83	-4.60	0.70
8544	-2.54	-2.11	-4.50	-1.33	0.00	1.20	1.31	-1.67	-3.14	0.05	-0.26	0.54	-1.55	-0.17	-1.67	-2.83	-1.77	-3.54	-1.74	-3.32	-2.20	-4.08	-2.10	-3.81	-4.33	0.97
8545	-2.73	-2.29	-4.54	-1.08	-0.71	0.59	0.62	-2.09	-3.10	-0.51	-0.58	0.21	-1.93	-0.62	-2.20	-2.57	-2.30	-4.08	-2.24	-3.80	-2.68	-4.54	-2.58	-4.28	-5.04	0.26
8546	-1.99	-1.31	-3.73	-1.22	-0.62	0.78	1.21	-1.24	-2.39	0.07	-0.12	0.75	-1.33	0.01	-1.54	-2.67	-1.64	-3.45	-1.63	-3.20	-2.11	-3.91	-1.98	-3.68	-2.46	0.61
8547	-2.86	-2.38	-4.66	-0.98	-0.67	0.51	0.65	-2.10	-2.95	-0.65	-0.81	-0.04	-2.14	-0.81	-2.25	-2.82	-2.34	-4.09	-2.27	-3.85	-2.77	-4.66	-2.69	-4.40	-5.08	0.22
8548	-2.70	-2.13	-4.58	-0.95	-0.54	0.80	1.29	-1.90	-2.90	-0.11	0.02	0.76	-1.38	-0.05	-1.59	-3.11	-1.70	-3.50	-1.72	-3.34	-2.32	-4.24	-2.35	-4.11	-4.82	0.47
8549	-3.09	-2.53	-4.91	-0.87	-0.64	0.66	1.07	-2.24	-3.30	-0.55	-0.95	-0.12	-2.18	-0.79	-2.22	-2.82	-2.28	-4.07	-2.24	-3.84	-2.76	-4.57	-2.63	-4.30	-2.18	-0.01
8550	-3.15	-2.64	-5.02	-1.15	-0.66	0.80	0.73	-2.29	-3.37	-0.42	-0.96	-0.11	-2.16	-0.79	-2.21	-2.82	-2.26	-4.01	-2.20	-3.79	-2.70	-4.57	-2.62	-4.29	-4.94	0.36
8551	-2.83	-2.83	-4.90	-1.08	-0.01	0.95	0.99	-2.10	-3.45	-0.34	-1.10	-0.19	-2.18	-0.76	-2.13	-2.76	-2.14	-3.90	-2.11	-3.68	-2.57	-4.39	-2.41	-4.04	-4.86	0.44
8552	-3.29	-2.78	-5.12	-1.05	-0.77	0.64	0.72	-2.39	-3.43	-0.58	-1.04	-0.17	-2.23	-0.85	-2.28	-2.52	-2.40	-4.17	-2.35	-3.93	-2.83	-4.70	-2.72	-4.42	-5.26	0.03
8553	-2.93	-2.56	-4.93	-0.83	0.24	1.87	4.28	-2.24	-3.34	-0.63	-1.09	-0.33	-2.44	-1.08	-2.53	-3.49	-2.50	-4.23	-2.39	-3.94	-2.83	-4.74	-2.78	-4.59	-4.41	0.88
8554	-2.51	-2.00	-4.36	-1.17	-1.05	0.15	0.41	-1.91	-2.91	-0.54	-1.09	-0.12	-2.17	-0.83	-2.28	-3.20	-2.36	-4.10	-2.27	-3.83	-2.73	-4.60	-2.66	-4.39	-4.64	0.66
8555	-2.45	-2.26	-4.80	-0.60	0.24	0.97	0.53	-2.37	-3.65	-0.79	-0.78	-0.07	-2.13	-0.80	-2.42	-3.51	-2.55	-4.29	-2.44	-3.96	-2.80	-4.65	-2.56	-4.33	-4.48	0.82
8556	-1.41	-0.78	-3.33	0.26	0.25	2.17	1.53	-2.02	-3.45	-0.15	-0.13	0.61	-1.46	-0.12	-1.76	-2.89	-1.86	-3.63	-1.88	-3.48	-2.39	-4.29	-2.33	-4.10	-1.99	1.28
8557	-2.20	-1.76	-4.10	-0.26	-0.48	1.50	0.77	-2.53	-3.86	-0.50	-0.86	-0.19	-2.26	-0.97	-2.50	-3.42	-2.50	-4.21	-2.40	-3.95	-2.82	-4.67	-2.69	-4.46	-4.28	1.02
8558	-2.21	-1.71	-4.20	-0.36	-0.74	1.12	0.70	-2.35	-3.47	-0.60	-0.31	0.38	-1.71	-0.41	-2.12	-3.05	-2.27	-4.17	-2.40	-3.99	-2.95	-4.89	-2.96	-4.66	-4.38	0.92
8559	-2.24	-1.88	-4.18	-0.57	-1.14	0.27	0.64	-2.18	-3.55	-0.85	-0.52	0.19	-1.95	-0.66	-2.32	-3.05	-2.45	-4.33	-2.64	-4.31	-3.23	-5.11	-3.19	-4.95	-4.72	0.57
8560	-1.80	-1.06	-3.46	-0.22	-0.63	1.36	0.73	-1.63	-3.01	-0.12	0.01	0.75	-1.33	-0.04	-1.74	-3.16	-1.83	-3.70	-1.96	-3.58	-2.52	-4.40	-2.48	-4.27	-4.55	0.75
8561	-2.44	-1.86	-4.38	-0.50	-0.84	1.35	1.04	-2.61	-4.05	-0.97	-0.93	-0.13	-2.15	-0.84	-2.43	-3.53	-2.63	-4.51	-2.77	-4.38	-3.28	-5.17	-3.23	-4.93	-3.27	0.64
8562	-2.72	-2.09	-4.56	-0.95	-0.86	0.88	2.09	-2.43	-3.55	-0.76	-0.99	-0.21	-2.23	-0.89	-2.43	-2.93	-2.50	-4.33	-2.55	-4.12	-3.04	-4.90	-2.92	-4.64	-4.98	0.32
8563	-2.10	-1.60	-4.04	-0.32	-0.44	1.60	1.40	-2.29	-3.72	-0.63	-0.43	0.33	-1.66	-0.36	-2.04	-3.37	-2.23	-4.14	-2.40	-4.02	-2.94	-4.83	-2.91	-4.72	-2.21	0.50
8564	-3.15	-2.74	-5.30	-1.13	-0.84	2.03	0.41	-4.06	-5.05	-0.69	-2.08	-1.19	-3.05	-1.54	-2.78	-3.81	-2.55	-4.33	-2.51	-4.09	-3.02	-4.94	-3.01	-4.89	-4.72	0.58
8565	-1.96	-1.50	-4.00	-0.14	0.08	1.62	2.09	-1.34	-2.56	-0.20	0.08	0.79	-1.26	0.06	-1.62	-3.00	-1.85	-3.68	-1.95	-3.63	-2.58	-4.54	-2.64	-4.46	-4.42	0.88
8566	-2.55	-1.99	-4.78	-0.03	0.82	2.92	2.94	-4.30	-5.26	-0.03	-1.89	-0.95	-2.69	-1.09	-2.24	-3.35	-2.02	-3.68	-1.86	-3.33	-2.29	-4.21	-2.22	-3.94	-4.12	1.18
8567	-2.35	-1.85	-4.27	-0.08	-1.25	0.31	-0.03	-2.51	-3.74	-0.81	-0.55	0.13	-1.92	-0.61	-2.21	-2.95	-2.38	-4.19	-2.49	-4.11	-3.09	-5.03	-3.05	-4.79	-4.90	0.40
8568	-1.47	-0.93	-3.44	0.01	-0.47	1.45	-0.09	-1.82	-3.24	0.25	0.86	1.50	-0.60	0.70	-1.09	-2.34	-1.16	-3.17	-1.52	-3.18	-2.24	-4.27	-2.45	-4.23	-1.93	1.03

Appendix A4. Centered log ratio transformed data used for PCA and Random Forest.

Sample	Si	Al	Fe	Mn	Mg	Ca	Na	K	Ti	P	LOI	C-Total	C_in_CO2	Non_carb._C	Total S	Cu	Zn	Pb	Cd	Hg	Sn	Tl	In	As	Co	Ni	Se	Mo	Ge	Sb	Ag	Au	W	Bi	B	Rb	Sr	Cs	Ba	Be	Zr
8569	9.15	7.78	7.47	1.17	5.14	3.53	3.35	7.29	4.52	1.84	7.70	6.00	2.77	5.99	7.47	0.68	2.35	-0.04	-3.55	-7.35	-2.06	-3.61	-6.44	1.48	-0.48	0.56	-4.83	-2.75	-3.26	-1.72	-3.26	-5.75	-4.14	-3.35	0.58	1.43	-0.80	-3.55	2.89	-2.34	2.18
8570	9.27	8.10	8.35	5.05	6.69	7.95	7.02	5.23	6.24	2.74	6.89	5.42	6.56	3.48	4.82	1.41	2.83	-0.92	-3.47	-10.95	-2.42	-6.11	-6.11	-0.35	0.87	0.87	-1.92	-3.12	-2.53	-2.94	-3.63	-6.11	-3.81	-6.11	-0.35	-0.55	1.74	-3.63	1.55	-3.12	1.58
8571	9.30	8.18	6.87	2.40	5.89	5.69	6.72	6.57	4.96	2.26	7.41	6.03	5.08	5.91	5.80	0.64	2.11	-1.00	-4.69	-7.91	-2.61	-2.96	-6.30	0.28	-0.43	0.68	-1.58	-2.61	-3.13	-2.61	-3.82	-6.81	-4.00	-3.82	1.59	0.97	2.32	-2.39	2.71	-2.61	1.69
8572	9.47	7.85	6.35	2.16	5.19	5.39	6.00	6.97	4.23	1.90	7.51	6.53	5.86	6.38	5.72	0.88	2.96	-0.77	-3.48	-7.86	-2.16	-3.47	-6.25	0.21	-0.38	0.63	-4.64	-1.87	-2.85	-2.67	-4.64	-6.76	-3.95	-3.61	-0.04	1.30	1.06	-2.38	3.04	-3.26	1.41
8573	9.27	7.94	7.16	1.88	5.57	5.52	6.59	6.69	4.61	2.30	7.88	7.03	2.36	7.03	7.06	0.93	2.64	-0.35	-4.73	-4.69	-3.34	-2.44	-6.34	2.13	0.31	1.20	-2.43	-2.24	-3.01	-1.24	-3.70	-11.17	-4.04	-3.70	0.09	0.86	2.23	-1.68	3.07	-3.34	1.52
8574	8.70	6.97	8.06	2.48	6.17	7.57	6.44	3.85	4.23	1.01	8.87	8.04	7.61	7.85	8.14	2.49	4.22	0.32	-2.07	-3.52	-1.85	-4.08	-6.46	2.18	1.02	2.30	-4.85	-1.38	-3.28	-1.32	-3.82	-8.07	-4.15	-2.93	-3.46	-1.67	0.93	-4.38	0.00	-4.15	0.68
8575	9.10	7.36	7.97	2.39	4.39	6.14	6.03	6.03	4.15	1.30	8.55	7.62	6.36	7.54	8.03	1.46	0.76	0.39	-4.78	-5.11	-2.70	-3.19	-6.39	2.05	0.33	1.19	-4.78	-1.60	-3.21	-0.79	-3.30	-7.31	-4.09	-3.13	0.16	0.45	0.79	-3.13	2.43	-4.09	1.21
8576	9.20	7.10	7.53	2.85	4.77	4.01	2.87	6.53	4.17	1.51	7.60	6.21	5.76	6.02	7.24	2.35	4.04	1.72	-2.18	-5.42	-2.13	-3.93	-6.51	-0.52	0.65	1.34	-4.90	-1.91	-3.74	-1.57	-2.21	-7.03	-4.21	-2.73	0.12	0.70	-1.73	-2.42	2.54	-4.21	1.35
8577	9.25	7.24	7.60	1.93	4.36	6.05	5.17	5.55	3.14	0.32	7.95	6.85	6.10	6.71	7.43	3.31	1.42	0.54	-3.81	-7.36	-2.07	-4.92	-6.45	0.55	-0.27	0.85	-4.84	-2.35	-3.12	-1.48	-3.27	-8.06	-4.15	-3.19	1.32	-0.02	1.40	-2.98	1.74	-2.76	1.37
8578	9.18	8.43	7.70	2.34	6.69	4.34	6.58	6.91	5.24	2.76	7.41	4.43	3.13	4.36	3.83	1.61	1.98	-2.35	-3.62	-11.09	-3.26	-3.45	-6.26	0.96	0.20	1.53	-4.65	-2.16	-2.73	-1.56	-3.77	-7.17	-1.32	-4.47	-3.26	1.26	2.26	-1.10	3.51	-2.16	1.65
8579	9.10	8.25	7.36	2.44	6.48	5.18	5.88	7.22	5.00	2.55	7.32	4.82	5.00	4.43	4.93	0.75	1.43	-0.97	-4.75	-11.19	-2.67	-3.36	-6.36	0.35	0.06	1.50	-4.75	-2.27	-3.27	-2.53	-4.75	-6.87	-1.06	-3.72	2.02	1.63	1.40	-1.34	3.65	-2.27	1.50
8580	9.17	8.44	7.63	2.09	6.69	4.39	6.61	7.07	5.42	2.88	7.36	3.55	1.36	3.52	2.74	1.24	1.84	-0.21	-2.84	-11.08	-2.56	-3.42	-6.25	0.15	-0.72	1.54	-4.64	-3.25	-2.72	-2.91	-4.64	-11.08	-3.94	-3.76	2.26	1.53	2.21	-1.09	3.63	-2.15	1.88
8581	9.50	8.24	6.93	2.62	5.73	6.57	7.02	6.66	4.96	2.34	7.61	6.24	6.59	5.75	5.13	0.45	1.75	-1.53	-4.52	-7.74	-2.44	-3.47	-6.13	0.23	-0.35	0.47	-4.52	-2.44	-2.87	-2.95	-3.83	-7.05	-3.83	-4.34	1.10	1.04	2.14	-2.30	2.81	-3.14	1.73
8582	9.37	7.75	6.61	2.03	4.99	5.51	6.56	6.65	4.02	1.53	7.39	6.71	5.55	6.62	5.85	0.73	3.69	-0.40	-2.70	-11.17	-1.96	-3.82	-6.34	0.15	-0.79	0.68	-4.73	-2.25	-3.25	-3.57	-3.70	-7.26	-4.04	-3.70	0.02	1.05	0.34	-3.70	3.41	-2.65	2.11
8583	9.53	8.20	6.52	1.69	5.58	5.48	6.48	7.10	4.92	2.44	7.73	7.01	5.33	6.95	4.31	1.91	3.39	-1.52	-2.95	-10.96	-2.44	-2.94	-6.13	1.59	-0.32	1.16	-4.52	-2.03	-2.87	-2.54	-3.64	-6.64	-3.82	-4.33	-0.49	1.35	1.89	-1.72	3.00	-2.44	1.71
8584	9.40	8.35	7.50	3.26	6.26	6.34	6.29	6.79	5.26	2.96	7.59	5.29	6.04	4.42	3.63	0.86	1.78	-0.97	-4.55	-11.00	-3.17	-3.84	-6.16	1.68	0.12	1.29	-4.55	-3.17	-2.99	-4.37	-4.55	-7.08	-3.86	-4.37	0.93	1.07	2.40	-2.21	2.96	-3.17	1.91
8585	9.02	7.71	7.00	1.65	5.17	4.90	6.14	6.83	4.49	2.19	8.05	7.33	2.46	7.33	7.10	0.18	2.83	1.18	-2.79	-6.05	-2.14	-2.57	-6.52	2.57	0.19	1.38	-4.92	-1.74	-3.12	-1.94	-3.63	-7.44	-4.22	-3.19	0.26	1.35	1.08	-2.70	2.80	-3.53	1.22
8586	8.85	8.22	7.09	2.76	6.15	6.58	5.43	7.29	5.15	3.01	7.97	6.36	7.65	1.21	2.23	1.27	0.50	-0.53	-4.86	-8.08	-2.78	-4.05	-6.47	1.91	-0.10	1.16	-4.86	-2.78	-2.83	-0.84	-3.38	-6.29	-4.17	-4.68	1.96	1.59	2.68	-0.92	3.51	-2.38	1.57
8587	10.00	6.72	7.41	2.29	4.19	5.62	3.65	5.79	3.59	0.92	8.62	8.36	4.75	8.35	7.18	2.26	3.99	0.55	-2.45	-3.72	-1.75	-2.89	-5.85	2.74	0.88	2.20	-4.24	-0.90	-2.11	-1.42	-4.24	-6.76	-3.54	-2.67	0.84	0.28	0.09	-2.67	1.95	-3.54	0.28
8588	9.06	7.61	6.88	1.56	5.35	5.75	5.28	6.71	4.13	1.70	7.70	6.67	5.74	6.56	6.81	0.94	2.39	0.25	-3.57	-5.18	-2.48	-2.89	-6.57	1.66	-0.46	0.66	-4.96	-2.19	-3.39	-2.07	-3.17	-7.49	-4.27	-3.31	0.25	1.23	0.79	-2.83	2.88	-2.88	1.53
8589	9.28	8.24	7.54	3.04	6.45	5.62	6.05	7.01	5.25	2.31	7.39	5.04	4.44	4.87	4.87	1.07	1.85	-2.34	-4.64	-7.86	-3.26	-3.20	-6.25	0.90	0.30	1.51	-1.52	-2.56	-3.00	-3.16	-4.64	-7.86	-3.95	-3.95	0.80	1.38	1.50	-2.56	3.22	-2.56	1.56
8590	9.02	8.16	7.56	2.74	6.62	5.80	6.80	6.61	5.11	2.76	7.78	5.94	7.28	-11.20	4.60	0.88	1.58	-1.42	-4.76	-7.28	-2.68	-4.02	-6.37	-0.19	0.14	1.64	-4.76	-2.27	-2.84	-1.78	-3.88	-7.28	-4.06	-4.06	1.46	1.16	2.31	-1.42	3.31	-2.68	1.61
8591	8.98	8.23	7.62	2.47	6.75	5.81	6.07	7.14	5.22	2.70	7.56	5.13	6.35	2.64	4.06	0.64	1.32	-2.47	-4.77	-7.99	-2.69	-3.75	-6.38	0.20	0.12	1.54	-4.77	-2.28	-2.69	-2.00	-4.08	-6.89	-4.08	-4.08	0.88	1.49	2.11	-0.91	3.94	-2.28	1.57
8592	8.15	6.78	8.41	3.39	6.61	8.08	6.38	3.45	3.43	1.32	9.17	9.05	8.24	8.92	7.92	3.17	3.74	1.09	-2.45	-4.31	-1.98	-6.87	-6.36	1.45	1.20	2.38	-0.67	-0.66	-4.06	-4.06	-3.18	-6.87	-4.06	-2.73	-1.98	-1.76	1.80	-4.57	-0.28	-4.06	0.50
8595	8.68	6.99	8.11	4.03	6.66	7.13	6.71	3.58	3.78	1.33	8.22	7.99	1.75	7.99	7.46	5.67	5.21	1.32	-0.96	-3.39	-0.65	-5.51	-5.15	2.47	2.38	1.11	-4.93	-1.06	-2.18	-1.69	-0.67	-6.20	-4.24	-2.21	-2.16	-1.60	0.52	-5.15	-0.50	-4.24	0.41
8599	9.05	6.61	9.18	4.95	7.60	7.75	5.54	4.31	3.65	-0.76	7.15	6.11	2.55	6.10	7.45	3.01	4.56	-1.20	-1.33	-5.96	-0.26	-5.81	-5.45	1.72	2.95	1.52	-0.20	-0.67	-0.73	-2.09	-2.81	-6.37	-3.84	-2.74	-3.15	-0.75	0.38	-3.15	-0.95	-3.84	0.88
8600	8.66	7.31	8.62	3.74	6.43	8.43	7.03	4.82	4.20	1.45	7.75	7.72	8.44	6.89	8.15	2.67	2.61	-1.45	-2.97	-5.76	-2.54	-6.74	-6.23	-0.75	0.63	1.77	-4.62	-2.14	-3.75	-3.93	-4.62	-7.15	-3.93	-4.44	-1.04	-0.35	1.96	-4.15	0.92	-3.93	1.31
8601	8.69	7.67	8.46	2.67	6.30	5.60	7.23	2.85	4.43	2.05	7.68	6.26	4.72	6.20	7.96	2.89	3.86	-0.95	-2.24	-4.69	-4.21	-7.03	-6.52	1.36	2.02	3.35	-1.09	0.01	-3.74	-4.44	-2.69	-6.74	-4.21	-2.99	-2.42	-3.52	1.41	-5.13	0.77	-4.21	1.31
8602	8.37	7.21	7.98	3.47	7.06	8.11	3.47	1.64	4.40	1.55	9.00	8.92	2.92	8.92	6.97	2.04	4.09	-0.99	-2.02	-4.30	-1.86	-6.98	-5.08	-0.22	1.38	3.11	-1.21	-0.70	-2.48	-3.47	-4.86	-6.98	-4.17	-2.25	0.02	-2.78	0.08	-4.68	-1.28	-2.78	0.87
8604	10.23	6.76	8.78	3.20	6.48	4.39	4.90	4.03	3.48	1.59	7.90	6.54	2.71	6.53	8.05	6.62	2.96	-0.19	-2.94	-5.58	-3.28	-4.42	-5.58	-0.10	1.79	1.99	1.01	-0.64	-3.97	-3.28	-1.71	-6.09	-3.28	-2.33	-1.20	-0.64	-2.59	-3.28	0.25	-2.59	0.41
8605	8.50	7.50	8.73	3.09	8.08	6.65	4.06	2.83	5.05	1.31	8.23	6.87	1.92	6.87	7.40	5.34	4.15	-1.59	-1.92	-5.59	-0.55	-5.91	-6.38	0.95	2.21	1.73	-0.45	-0.55	-1.88	-3.38	-1.90	-6.38	-4.07	-2.16	-1.59	-2.28	-1.08	-4.07	-4.07	-4.07	1.24
8606	9.23	7.12	9.12	4.17	7.70	7.74	6.90	4.85	3.85	1.68	8.02	7.03	2.98	7.03	8.33	4.48	1.55	1.05	-3.52	-5.67	-1.91	-4.62	-6.00	2.42	1.67	2.54	-4.40	-0.71	-4.40	-3.70	-2.42	-6.23	-3.70	-1.81	-3.01	-0.24	0.21	-3.70	-0.93	-3.70	0.60
04111B	8.87	7.42	7.09	1.81	5.41	5.04	5.81	6.40	4.27	1.84	8.33	7.84	5.27	7.82	7.01	1.32	3.81	-0.31	-2.45	-4.85	-1.45	-2.91	-5.94	1.44	0.49	1.00	-3.05	-1.16	-2.33	-2.61	-3.75	-8.25	-2.26	-2.48	-0.24	0.81	0.19	-2.69	2.76	-4.34	1.39
04112B	9.28	8.01	7.24	1.97	5.85	6.05	6.42	6.98	4.92	2.49	7.73	6.04	5.84	5.78	6.90	0.10	0.23	-0.52	-4.68	-6.29	-2.60	-2.97	-6.29	1.78	0.41	1.10	-4.68	-2.20	-2.77	-2.42	-3.99	-6.11	-3.99	-2.66	0.63	1.35	0.69	-3.30	2.94	-3.30	1.50
04117B	8.81	7.52	6.93	1.49	5.12	5.07	6.71	6.03	4.36	2.10	8.01	7.46	3.96	7.45	7.02	2.14	3.84	1.31	-1.59	-5.99	-2.30	-3.38	-6.69	2.31	0.47	1.60	-5.08	-1.90	-3.05	-2.04	-4.05	-7.60	-4.38	-2.33	-0.11	0.61	1.61	-3.00	2.31	-3.00	1.06
04138D	9.43	8.12	7.24	3.01	6.47	6.83	5.69	6.98	4.93	2.33	8.06	6.44	7.53	4.75	4.59	0.77	1.06	-1.35	-4.53	-6.65	-3.15	-3.74	-6.14	1.27	0.03	1.21	-4.53	-2.05	-2.81	-1.54	-4.53	-10.97	-3.84	-3.37	1.58	1.39	2.25	-2.19	3.29	-3.15	1.59
04164B	9.67	8.18	7.36	2.85	5.49	6.36	6.43	6.05	4.85	2.04	8.30	7.23	6.88	7.02	7.23	0.82	1.98	-0.59	-4.37	-7.59	-2.29	-3.17	-5.98	1.16	0.16	0.45	-4.37	-2.29	-2.45	-1.96	-4.37	-10.81	-1.89	-4.19	1.71	0.48	2.02	-2.34	2.09	-3.68	1.69
04171B	9.39	7.76	7.15	1.45	5.73	3.43	4.98	6.66	4.07	1.64	8.56	8.21	2.47	8.21	6.52	-0.10	2.71	-0.02	-4.62	-5.76	-1.85	-2.62	-6.23	0.53	-0.28	0.97	-2.36	-1.44	-2.54	-3.14	-3.46	-7.84	-2.54	-2.54	1.11	1.10	0.77	-2.20	2.68	-3.93	1.71
04177B	10.79	6.80	9.38	4.92	5.92	6.90	6.08	4.49	3.49	0.38	8.77	7.65	6.98	7.50	8.97	2.49	5.43	-0.22	-0.73	-3.73	-2.01	-5.52	-5.01	1.29	1.16	2.08	-3.40	-2.01	-2.01	-2.93	-3.40	-9.84	0.29	-2.93	-0.22	-0.91	0.07	-3.62	1.08	-2.70	0.76
04180B	9.99	8.43	6.48	2.00	5.79	6.12	7.74	6.82	4.47	2.88	8.60	8.44	1.92	8.44	5.50	0.65	3.12	-1.07	-4.07	-7.29	-1.59	-3.08	-5.68	-1.99	-0.28	1.00	-4.07	-1.99	-2.91	-3.60	-4.07	-10.51	-3.38	-3.20	-2.68	1.05	2.53	-2.91	2.68	-2.68	1.95
04192B	8.87	7.73	7.68	0.98	5.18	3.37	5.65	6.86	4.50	0.31	8.17	7.53	1.84	7.53	7.73	5.75	0.15	-0.13	-4.85	-7.37	-2.36	-2.34	-6.46	1.88	0.18	0.99	-4.85	-1.38	-3.20	-2.47	-0.70	-6.97	-4.15	-1.22	0.92	1.49	0.86	-2.27	2.93	-3.46	1.36
04193B	9.34	8.37	6.98	2.02	5.94	4.75	7.82	5.49	4.88	2.49	8.68	8.47	0.84	8.47	6.08	6.14	0.64	-0.24	-4.46	-10.90	-1.97	-3.39	-6.07	-1.46	-1.11	1.20	-4.46	-0.13	-2.54	-6.07	-1.16	-7.68	-3.77	0.69	0.33	-0.03	2.09	-3.77	2.00	-3.77	1.90
04198A	9.17	8.04	7.22	3.33	6.07	6.84	7.57	5.66	4.97	1.85	7.83	6.39	7.52	4.50	6.13	1.71	1.53	0.85	-4.70	-6.31	-4.00	-6.82	-6.31	3.09	-0.12	1.56	-4.70	-3.31	-3.05	-1.22	-3.82	-5.61	-1.52	-3.82	1.92	-0.05	3.01	-4.00	2.07	-4.00	1.44
04198B	9.04	7.93	7.23	3.67	6.26	7.12	7.48	5.42	4.89	1.80	7.98	6.68	7.84	4.62	5.74	0.89	3.78	3.03	-2.05	-4.09	-4.05	-6.87	-6.36	1.68	-0.05	1.71	-4.75	-3.36	-3.02	-2.57	-3.58	-5.19	-4.05	-4.05	1.33	-0.53	3.16	-4.28	1.89	-4.05	1.30
04307A	8.56	6.99	8.78	3.47	5.41	5.17	6.43	3.89	3.59	1.30	8.30	7.45	5.76	7.40	8.33	2.41	3.83	0.60	-2.12	-8.18	-2.19	-4.42	-6.57	-2.19	1.20	1.81	-1.08	0.75	-3.68	-1.09	-3.31	-7.08	-2.48	-1.75	0.09	-1.63	-1.50	-5.19	-0.17	-4.27	0.98
04309B	8.45	6.72	7.70	2.59	5.46	7.11	5.52	4.00	3.52	1.44	8.79	8.44	7.24	8.35	7.34	0.53	4.10	0.02	-2.24	-5.15	-1.93	-5.49	-6.02	1.18	0.68	1.96	-2.66	-0.78	-3.94	-0.19	-4.08	-7.23	-3.03	-1.98	4.28	-1.77	1.12	-4.41	0.30	-4.41	0.48
04316B	8.42	7.05	7.95	1.91	6.38	6.30	6.31	6.24	4.33	1.53	8.24	7.69	3.49	7.68	7.80	1.96	3.56	0.36	-2.62	-3.94	-1.96	-4.95	-6.75	1.86	0.84	1.83	-2.03	-1.67	-3.49	-2.05	-3.86	-11.58	-4.44	-2.25	-0.28	-0.09	0.75	-4.67	2.85	-4.44	1.02
04319B	8.95	7.39	6.96	0.03	4.19	3.64	3.94	6.58	4.13	1.65	8.34	8.00	2.77	8.00	7.06	1.90	4.42	0.32	-2.10	-3.84	-1.83	-2.79	-6.62	1.98	0.54	1.87	-2.35	-1.55	-2.71	-1.03	-3.53	-6.44	-4.32	-2.08	1.39	1.05	0.18	-2.35	2.62	-4.32	0.97
04320B	8.87	7.85	6.30	1.32	5.10	5.26	5.60	6.74	4.94	2.50	7.65	7.03	5.21	6.99	5.52	2.13	4.96	-1.37	-1.26	-3.46	-1.04	-2.80	-4.37	-2.58	-0.94	0.50	-5.06	-2.58	-2.84	-4.03	-3.78	-7.59	-1.88	-3.27	1.65	1.14	0.72	-2.42	2.88	-3.67	1.59
04329A	9.34	8.25	7.65	3.43	6.87	4.75	6.38	6.52	5.12	2.38	7.53	5.55	3.72	5.50	3.82	1.15	4.30	2.48	-1.25	-5.15	-2.49	-3.65	-6.18	0.43	0.02	1.34	-4.57	-3.19	-3.00	-2.02	-3.88	-11.01	-3.88	-3.41	1.25	1.02	2.05	-2.02	2.79	-3.88	1.53
04360B	8.97	7.45	6.20	1.56	5.11	5.60	4.55	6.44	4.29	1.72	7.87	5.24	5.91	4.49	5.42	1.72	4.57	-0.67	-1.82	-4.23	-1.27	-2.73	-5.27	1.59	-0.11	1.05	-1.76	-2.28	-2.60	-2.25	-4.02	-7.17	-4.36	-3.57	0.54	0.91	0.55	-2.53	2.75	-3.67	1.29
04373B	8.25	7.01	7.32	0.78	5.36	3.69	4.87	6.09	3.78	1.12	9.18	9.03	3.79	9.03	7.43	2.23	2.12	1.79	-3.29	-6.06	-1.45	-2.85	-6.75	2.03	0.89	2.26	-1.03	-0.58	-3.98	-1.56	-1.98	-6.75	-4.45	-2.59	-0.54	0.25	-0.32	-3.06	1.58	-3.76	0.70
04376B	9.03	7.65	6.83	1.15	5.62	4.10	5.80	6.63	4.42	2.11	8.21	7.52	3.01	7.52	6.76	2.02	1.30	1.65	-4.93	-5.51	-2.44	-2.94	-6.54	2.17	0.28	1.55	-4.93	-2.15	-3.20	-1.49	-2.71	-7.45	-1.93	-3.01	0.43	0.83	0.50	-3.07	2.73	-3.54	1.25
04389A	9.47	8.10	6.87	2.31	5.53	5.87	4.69	7.47	4.58	2.55	8.05	7.23	5.82	7.16	6.71	0.49	-0.54	-1.23	-4.56	-6.39	-2.08	-2.67	-6.17	1.23	0.33	0.72	-1.87	-1.79	-2.77	-2.84	-3.87	-7.09	-3.87	-0.92	0.38	1.61	-0.08	-2.53	2.60	-2.48	1.62
04389B	9.53	7.76	7.99	3.33	5.22	7.33	4.50	7.19	4.22	2.25	8.61	7.47	7.40	7.17	8.05	1.54	1.57	-0.13	-4.41	-6.02	-3.03	-2.84	-6.02	1.69	0.62	1.15	-4.41	-2.33	-4.41	-1.89	-3.54	-6.02	-3.72	-6.02	-0.25	1.22	1.50	-2.93	2.44	-3.72	1.24
04405D	9.73	8.20	9.02	4.10	7.24	6.36	7.08	3.47	5.28	3.23	8.16	4.50	5.73	1.75	7.61	2.65	2.61	-1.83	-4.13	-5.97	-1.65	-3.13	-5.74	-1.14	0.63	1.40	-2.00	-2.75	-1.62	-3.26	-4.13	-10.57	-2.75	-3.66	-0.35	-3.44	0.99	-3.95	0.20	-2.75	1.46
07413D	9.17	7.95	6.93	1.04	5.57	4.08	6.37	6.92	4.72	2.08	8.02	7.26	3.28	7.26	6.78	1.26	2.94	0.18	-3.51	-6.40	-2.31	-2.49	-6.40	1.84	-0.14	1.03	-4.79	-2.02	-2.49	-2.53	-3.63	-11.23	-3.40	-3.40	1.06	1.35	0.55	-2.27	2.85	-3.40	1.48
08574D	8.74	6.98	8.15	2.51	6.11	7.61	6.45	3.84	4.19	1.06	8.89	8.08	7.74	7.86	8.24	2.51	4.17	0.28	-2.05	-3.77	-1.80	-4.01	-6.41	2.24	0.98	2.24	-4.80	-1.33	-3.23	-1.36	-3.64	-7.32	-4.11	-2.77	-1.01	-2.03	0.94	-4.62	-0.08	-4.11	0.68

Appendix A4. Centered log ratio transformed data used for PCA and Random Forest.

Sample	Hf	Nb	Ta	Ga	Sc	V	Cr	Th	U	Y	La	Ce	Pr	Nd	Sm	Eu	Gd	Tb	Dy	Ho	Er	Tm	Yb	Lu	Br	F
8569	-1.45	-1.12	-3.59	-0.35	-0.89	0.45	-0.94	-1.94	-3.25	0.34	0.16	0.97	-1.02	0.34	-1.34	-2.93	-1.45	-3.29	-1.48	-3.06	-1.95	-3.89	-1.91	-3.68	-4.83	0.47
8570	-1.95	-1.36	-4.17	-0.07	0.78	2.97	1.65	-3.73	-4.54	0.57	-1.41	-0.40	-2.14	-0.52	-1.63	-2.73	-1.36	-3.07	-1.22	-2.75	-1.70	-3.63	-1.68	-3.46	-4.50	0.79
8571	-1.95	-1.33	-3.72	-0.09	-0.59	1.31	0.75	-1.68	-3.05	-0.47	-0.19	0.57	-1.49	-0.19	-1.89	-3.27	-2.07	-3.96	-2.24	-3.87	-2.83	-4.82	-2.80	-4.58	-4.69	0.60
8572	-2.06	-1.15	-3.34	-0.55	-1.34	0.24	-0.08	-1.09	-2.53	-0.17	0.36	1.08	-1.05	0.15	-1.69	-3.36	-1.92	-3.80	-2.04	-3.63	-2.57	-4.46	-2.46	-4.23	-2.57	0.65
8573	-2.28	-1.77	-4.00	-0.40	-0.64	1.00	0.84	-1.85	-3.22	-0.78	-0.14	0.58	-1.49	-0.19	-1.98	-3.07	-2.25	-4.19	-2.50	-4.16	-3.10	-5.00	-3.04	-4.81	-4.73	0.57
8574	-2.93	-2.13	-4.63	-1.16	-0.66	1.06	2.65	-2.47	-3.47	-0.90	-1.17	-0.36	-2.40	-1.04	-2.51	-3.39	-2.54	-4.38	-2.57	-4.19	-3.14	-5.07	-3.10	-4.98	-1.89	0.45
8575	-2.40	-1.77	-4.19	-0.83	-1.22	0.52	0.25	-2.11	-3.38	-0.76	-0.44	0.21	-1.91	-0.67	-2.41	-3.83	-2.43	-4.19	-2.44	-4.05	-2.96	-4.82	-2.93	-4.67	-1.83	0.52
8576	-2.29	-1.63	-3.82	-1.12	-0.98	0.77	-0.09	-2.44	-3.78	0.14	-0.48	0.37	-1.56	-0.13	-1.59	-2.85	-1.69	-3.53	-1.70	-3.25	-2.13	-3.98	-2.03	-3.83	-4.90	0.39
8577	-1.97	-0.66	-3.07	-0.68	-1.39	-0.62	-0.87	-1.77	-3.36	0.16	-0.59	0.26	-1.68	-0.29	-1.67	-3.41	-1.68	-3.42	-1.57	-3.15	-2.07	-3.96	-2.00	-3.77	-1.82	0.46
8578	-1.93	-1.17	-3.77	0.11	-0.05	1.95	2.18	-1.06	-2.30	-0.17	0.40	1.11	-0.93	0.38	-1.35	-2.79	-1.64	-3.65	-1.95	-3.60	-2.56	-4.50	-2.57	-4.40	-4.65	0.65
8579	-2.06	-1.24	-3.79	-0.03	-0.26	1.74	2.19	-1.07	-2.32	-0.37	0.11	0.83	-1.23	0.05	-1.66	-3.09	-1.91	-3.87	-2.18	-3.81	-2.78	-4.75	-2.85	-4.60	-4.75	0.55
8580	-1.70	-0.76	-3.45	0.22	0.00	2.05	2.31	-0.84	-0.33	-0.16	1.08	1.72	-0.41	0.85	-0.98	-2.48	-1.33	-3.29	-1.60	-3.26	-2.20	-4.14	-2.24	-4.05	-4.64	0.66
8581	-1.86	-1.28	-3.54	-0.09	-0.65	1.18	0.63	-1.61	-3.01	-0.25	0.00	0.73	-1.32	-0.01	-1.73	-3.13	-1.91	-3.77	-2.05	-3.66	-2.61	-4.52	-2.61	-4.45	-4.52	0.78
8582	-1.47	-0.87	-3.19	-0.51	-1.39	-0.30	-0.76	-0.43	-1.79	0.24	0.63	1.31	-0.81	0.44	-1.32	-3.07	-1.47	-3.37	-1.60	-3.18	-2.13	-4.06	-2.08	-3.86	-4.73	0.57
8583	-1.88	-1.26	-3.61	-0.08	-0.52	1.16	0.96	-1.44	-2.85	-0.56	0.05	0.78	-1.29	-0.02	-1.82	-3.28	-2.12	-4.12	-2.38	-3.97	-2.91	-4.84	-2.92	-4.74	-4.52	0.78
8584	-1.94	-1.52	-3.88	0.01	-0.22	1.84	1.63	-1.29	-2.74	-0.17	0.37	1.12	-0.93	0.37	-1.39	-2.79	-1.67	-3.61	-1.88	-3.51	-2.48	-4.44	-2.55	-4.41	-2.43	0.74
8585	-2.40	-1.81	-4.35	-0.44	-0.49	1.12	1.13	-1.71	-3.06	-0.76	-0.24	0.55	-1.52	-0.26	-2.00	-3.20	-2.29	-4.24	-2.54	-4.14	-3.12	-5.00	-3.03	-4.77	-4.92	0.38
8586	-2.02	-1.31	-3.94	-0.01	-0.31	1.79	2.16	-1.41	-2.73	-0.48	0.11	0.83	-1.21	0.12	-1.61	-2.97	-1.90	-3.89	-2.21	-3.87	-2.82	-4.78	-2.80	-4.61	-4.86	0.44
8587	-3.36	-2.45	-4.97	-1.06	-0.99	0.52	0.90	-2.40	-3.56	-0.90	-1.71	-0.96	-2.97	-1.63	-2.96	-3.22	-2.99	-4.57	-2.69	-4.28	-3.11	-4.97	-3.05	-4.75	-0.99	1.06
8588	-2.05	-1.52	-3.96	-0.63	-1.01	0.40	0.34	-0.87	-2.28	-0.68	0.07	0.75	-1.37	-0.12	-1.95	-3.36	-2.31	-4.33	-2.59	-4.15	-3.02	-4.92	-2.89	-4.65	-2.54	0.34
8589	-2.01	-1.52	-4.15	-0.04	0.06	2.07	2.04	-1.61	-2.83	-0.42	-0.30	0.46	-1.55	-0.22	-1.81	-2.98	-1.96	-3.84	-2.07	-3.69	-2.67	-4.53	-2.62	-4.43	-3.08	0.65
8590	-1.98	-1.01	-3.66	0.06	-0.23	1.87	2.24	-1.09	-0.10	-0.37	0.96	1.58	-0.55	0.67	-1.18	-2.72	-1.45	-3.41	-1.69	-3.32	-2.28	-4.26	-2.32	-4.13	-4.76	0.54
8591	-1.97	-1.25	-3.93	0.11	-0.13	1.95	2.27	-1.33	-2.67	-0.49	0.12	0.88	-1.14	0.18	-1.52	-3.02	-1.85	-3.89	-2.20	-3.78	-2.75	-4.66	-2.71	-4.52	-4.77	0.53
8592	-3.10	-2.45	-4.84	-1.17	-1.19	0.24	0.28	-2.19	-3.34	-0.97	-1.13	-0.34	-2.36	-1.03	-2.51	-3.10	-2.60	-4.39	-2.62	-4.23	-3.15	-5.03	-3.10	-4.79	-2.49	0.54
8595	-3.14	-2.55	-5.10	-0.90	-0.88	0.76	2.00	-2.55	-3.62	-1.15	-1.01	-0.31	-2.41	-1.11	-2.72	-3.12	-2.80	-4.59	-2.83	-4.44	-3.39	-5.32	-3.35	-5.06	-4.93	0.37
8599	-2.74	-2.32	-4.76	-0.59	-1.24	0.49	1.55	-2.27	-3.40	-0.95	-0.79	0.08	-1.93	-0.58	-2.19	-3.84	-2.40	-4.14	-2.47	-4.04	-2.98	-4.86	-2.98	-4.76	-4.54	0.76
8600	-2.11	-1.12	-3.65	-1.04	-0.91	0.77	2.32	-2.14	-3.50	-0.35	-1.11	-0.13	-2.03	-0.65	-2.04	-3.75	-2.03	-3.76	-1.95	-3.57	-2.50	-4.41	-2.45	-4.26	-2.65	0.68
8601	-2.27	-1.62	-4.03	-0.88	-0.22	1.23	1.45	-1.36	-2.65	-0.38	-0.15	0.57	-1.47	-0.19	-1.74	-2.81	-1.88	-3.72	-1.99	-3.58	-2.57	-4.54	-2.60	-4.36	-4.91	0.39
8602	-2.64	-1.99	-4.55	-1.08	-0.46	1.19	2.44	-2.15	-3.33	-0.48	-0.61	0.05	-1.97	-0.60	-2.09	-2.52	-2.14	-3.94	-2.17	-3.80	-2.73	-4.61	-2.69	-4.42	-2.52	0.44
8604	-3.28	-2.33	-4.89	-0.98	-1.26	0.41	0.73	-2.24	-3.19	-0.64	-0.46	0.31	-1.66	-0.28	-1.78	-4.49	-1.93	-3.83	-2.21	-4.02	-3.02	-5.00	-3.08	-4.89	-2.12	1.32
8605	-2.28	-1.38	-4.00	0.05	-0.19	1.79	2.45	-2.15	-3.30	-0.20	-1.66	-0.64	-2.52	-1.08	-2.23	-4.00	-2.09	-3.77	-1.91	-3.47	-2.40	-4.30	-2.38	-4.14	-4.77	0.53
8606	-3.01	-2.05	-4.67	-0.93	-0.92	0.68	1.32	-2.08	-3.20	-0.81	-0.84	-0.03	-2.15	-0.80	-2.34	-3.20	-2.42	-4.28	-2.49	-4.09	-2.98	-4.91	-3.01	-4.72	-4.40	0.90
04111B	-2.28	-1.80	-4.34	-0.60	-0.97	0.55	-0.03	-2.45	-3.83	-1.08	-0.98	-0.21	-2.31	-0.88	-2.42	-3.39	-2.53	-4.38	-2.63	-4.26	-3.15	-5.03	-3.08	-4.78	-2.90	0.27
04112B	-2.13	-1.67	-4.21	-0.30	-0.51	1.32	1.37	-1.76	-3.01	-0.73	-0.38	0.53	-1.59	-0.27	-1.96	-3.15	-2.18	-3.97	-2.22	-3.89	-2.86	-4.81	-3.00	-4.86	-4.68	0.62
04117B	-2.62	-1.90	-4.36	-0.75	-0.52	0.99	1.31	-1.83	-3.07	-0.98	-0.32	0.43	-1.74	-0.41	-2.11	-3.57	-2.41	-4.25	-2.55	-4.22	-3.12	-5.04	-3.14	-4.89	-5.08	0.22
04138D	-2.08	-1.48	-4.09	-0.10	-0.30	1.49	1.70	-1.64	-2.75	-0.75	-0.03	0.71	-1.42	-0.07	-1.74	-3.09	-1.99	-3.90	-2.27	-3.94	-2.86	-4.81	-2.93	-4.76	-4.53	0.77
04164B	-2.15	-1.92	-4.37	-0.04	-0.42	1.23	0.73	-2.36	-3.78	-0.91	-0.44	0.27	-1.92	-0.54	-2.16	-3.27	-2.28	-4.16	-2.47	-4.12	-3.09	-4.95	-3.06	-4.88	-3.21	0.93
04171B	-1.93	-1.29	-3.81	-0.40	-0.97	0.29	-0.06	-1.97	-3.27	-0.34	-0.67	0.15	-2.02	-0.68	-2.22	-3.19	-2.22	-3.89	-2.08	-3.68	-2.60	-4.51	-2.60	-4.37	-3.23	0.68
04177B	-3.21	-3.21	-5.92	-0.91	-1.26	0.07	0.42	-3.12	-3.98	-1.32	-1.52	-0.73	-2.88	-1.41	-2.90	-3.57	-3.15	-4.82	-3.15	-4.82	-3.62	-5.52	-3.67	-5.23	-3.40	1.90
04180B	-1.69	-1.06	-3.55	0.02	-1.23	0.53	0.22	-1.32	-2.42	-0.12	0.03	0.73	-1.50	-0.27	-2.03	-3.12	-2.23	-3.96	-2.17	-3.65	-2.51	-4.40	-2.46	-4.15	-4.07	1.23
04192B	-2.33	-1.79	-4.40	-0.47	-0.39	1.22	1.02	-1.65	-3.00	-1.06	0.08	0.82	-1.39	-0.14	-1.96	-3.99	-2.44	-4.54	-2.82	-4.46	-3.23	-5.07	-3.00	-4.63	-4.85	0.45
04193B	-1.79	-1.23	-3.75	-0.08	-0.40	1.31	0.98	-1.05	-2.04	-0.59	-0.88	0.03	-2.13	-0.79	-2.17	-3.73	-2.30	-4.15	-2.41	-3.99	-2.81	-4.59	-2.50	-4.07	-4.46	0.84
04198A	-2.25	-1.78	-4.48	-0.27	-0.47	1.54	1.99	-2.21	-3.53	-0.83	-0.29	0.46	-1.71	-0.39	-2.08	-3.28	-2.30	-4.23	-2.50	-4.18	-3.14	-5.03	-3.16	-4.92	-4.70	0.60
04198B	-2.41	-1.95	-4.53	-0.37	-0.43	1.54	2.16	-2.33	-3.66	-0.96	-0.48	0.29	-1.86	-0.53	-2.19	-3.41	-2.42	-4.30	-2.60	-4.23	-3.18	-5.08	-3.15	-4.97	-4.75	0.55
04307A	-2.62	-1.80	-4.40	-1.27	-1.48	0.09	0.52	-2.46	-3.66	-0.14	-0.69	0.21	-1.89	-0.52	-1.93	-3.14	-1.89	-3.66	-1.89	-3.43	-2.32	-4.23	-2.31	-4.16	-2.66	0.34
04309B	-3.19	-2.50	-4.89	-1.42	-1.11	0.36	0.19	-2.11	-3.20	-0.89	-0.86	-0.06	-2.23	-0.92	-2.45	-3.12	-2.54	-4.32	-2.57	-4.20	-3.11	-4.99	-3.06	-4.71	-1.67	0.19
04316B	-2.62	-1.79	-4.33	-1.27	-0.79	1.00	1.99	-2.27	-3.44	-0.66	-0.89	-0.05	-2.16	-0.81	-2.27	-3.15	-2.31	-4.04	-2.30	-3.92	-2.86	-4.74	-2.83	-4.62	-1.89	0.16
04319B	-2.71	-1.98	-4.57	-0.68	-0.89	0.66	0.56	-1.90	-3.07	-0.99	-0.58	0.18	-2.01	-0.75	-2.44	-3.42	-2.67	-4.52	-2.76	-4.32	-3.24	-5.14	-3.17	-4.86	-3.10	0.29
04320B	-2.15	-1.52	-4.27	-0.31	-0.71	1.30	0.70	-2.56	-3.80	-0.46	-0.50	0.35	-1.73	-0.38	-1.93	-3.40	-2.09	-3.96	-2.23	-3.86	-2.79	-4.70	-2.75	-4.50	-5.06	0.24
04329A	-2.16	-1.38	-3.94	0.03	-0.17	1.80	1.97	-1.25	-2.79	-0.88	-0.51	0.32	-1.83	-0.54	-2.21	-3.71	-2.56	-4.42	-2.65	-4.29	-3.13	-4.96	-3.02	-4.70	-3.09	0.73
04360B	-2.36	-1.59	-4.16	-0.72	-1.07	0.63	0.22	-1.68	-2.95	-0.53	-0.26	0.46	-1.74	-0.43	-2.09	-3.43	-2.31	-4.16	-2.37	-3.94	-2.81	-4.66	-2.74	-4.51	-2.75	0.25
04373B	-2.92	-2.03	-4.45	-1.05	-0.95	0.64	0.64	-1.81	-3.24	-1.19	-0.49	0.30	-1.88	-0.58	-2.31	-3.62	-2.70	-4.67	-2.94	-4.53	-3.30	-5.10	-3.08	-4.67	-1.31	0.16
04376B	-2.47	-1.78	-4.34	-0.54	-0.56	1.00	1.11	-1.65	-3.04	-0.97	-0.18	0.56	-1.64	-0.35	-2.10	-3.54	-2.44	-4.38	-2.67	-4.29	-3.14	-5.01	-3.08	-4.74	-2.15	0.37
04389A	-2.01	-1.45	-4.07	-0.13	-1.00	0.90	0.52	-2.19	-3.55	-0.87	-0.53	0.26	-1.96	-0.67	-2.36	-3.65	-2.54	-4.25	-2.55	-4.20	-3.14	-5.07	-3.19	-5.01	-2.43	0.74
04389B	-2.44	-1.93	-4.49	-0.54	-1.15	0.64	1.48	-2.59	-3.92	-1.23	-0.27	0.41	-1.88	-0.59	-2.33	-3.61	-2.62	-4.41	-2.80	-4.45	-3.44	-5.43	-3.49	-5.23	-2.62	1.58
04405D	-2.16	-1.75	-4.58	-0.11	-0.24	1.91	1.59	-2.46	-3.83	-0.26	-0.37	0.49	-1.64	-0.21	-1.72	-2.62	-1.78	-3.69	-1.95	-3.57	-2.54	-4.46	-2.53	-4.31	-2.56	1.17
07413D	-2.12	-1.30	-3.79	-0.31	-0.72	1.10	0.39	-1.57	-2.92	-0.57	-0.15	0.61	-1.58	-0.21	-1.93	-3.20	-2.17	-4.10	-2.35	-3.95	-2.87	-4.79	-2.83	-4.61	-3.00	0.51
08574D	-2.94	-2.22	-4.76	-1.11	-0.66	1.04	2.65	-2.45	-3.50	-1.01	-1.21	-0.39	-2.41	-1.04	-2.54	-3.41	-2.59	-4.38	-2.58	-4.21	-3.17	-5.07	-3.12	-4.93	-4.80	0.50

Appendix A5. Statistical summary of major element and trace element concentrations grouped by shale lithotype, associated mineralization, and lithostratigraphic assemblage.

Shale Lithotype	SiO2_pct	Al2O3_pct	Fe2O3_pct	MgO_pct	CaO_pct	Na2O_pct	K2O_pct	TiO2_pct	P2O5_pct	MnO_pct	LOI_pct	Total S_pct	CO2_pct	C_in_CO2_ppm
felsic : Minimum	12.45	0.34	0.71	0.07	0.04	0.02	0.01	0.01	0.01	0.00	1.03	0.03	0.01	13.65
felsic : Maximum	94.54	23.62	59.30	21.76	37.23	8.12	5.80	0.87	0.28	1.16	41.33	30.20	22.80	62244.00
felsic : Mean	58.59	11.63	7.95	1.64	2.34	2.12	2.03	0.37	0.10	0.06	12.13	3.88	1.66	4527.92
felsic : Median	61.61	12.73	5.97	1.17	1.35	1.70	2.14	0.38	0.10	0.03	9.47	2.94	0.87	2293.20
felsic : Standard Deviation	13.37	4.08	6.67	1.95	3.68	1.75	1.35	0.15	0.04	0.10	8.55	3.87	2.63	7189.29
felsic : 25 percentile	53.11	8.79	3.98	0.79	0.56	0.73	0.83	0.26	0.06	0.02	6.28	1.36	0.09	245.70
felsic : 75 percentile	66.53	14.40	9.85	1.71	2.42	3.10	3.00	0.46	0.13	0.06	14.87	5.14	1.98	5419.05
felsic : 90 percentile	70.91	15.82	14.92	2.83	5.06	4.71	3.52	0.54	0.15	0.10	24.93	7.57	3.74	10281.18
intermediate : Minimum	21.55	0.83	2.37	0.16	0.08	0.03	0.01	0.04	0.02	0.00	0.86	0.01	0.01	0.00
intermediate : Maximum	81.28	29.62	29.96	18.07	27.65	8.08	6.42	1.35	0.30	1.09	52.59	14.80	28.40	77532.00
intermediate : Mean	56.92	15.30	7.77	2.84	2.37	2.33	2.49	0.62	0.13	0.07	8.27	2.01	2.16	5702.83
intermediate : Median	58.71	16.49	6.51	2.40	1.47	2.14	2.64	0.65	0.13	0.06	6.06	0.67	1.02	2784.60
intermediate : Standard Deviation	8.87	4.46	4.55	2.36	3.01	1.60	1.31	0.19	0.05	0.08	6.92	2.80	3.27	8316.70
intermediate : 25 percentile	54.87	13.17	5.36	1.54	0.75	1.31	1.63	0.52	0.10	0.04	4.25	0.13	0.16	436.80
intermediate : 75 percentile	61.50	18.23	8.22	3.37	3.02	3.05	3.34	0.74	0.17	0.08	9.02	2.95	2.98	8067.15
intermediate : 90 percentile	64.58	19.60	13.97	4.45	5.02	4.26	4.00	0.83	0.20	0.12	17.54	6.04	5.00	13546.26
mafic : Minimum	19.08	1.58	4.93	1.23	0.56	0.03	0.02	0.12	0.03	0.03	0.84	0.01	0.02	54.60
mafic : Maximum	61.77	18.81	26.02	21.71	20.59	7.54	4.51	1.93	0.38	0.99	22.94	14.40	26.40	72072.00
mafic : Mean	47.37	12.63	12.35	6.04	6.60	1.52	1.25	0.77	0.10	0.23	9.24	2.03	5.05	13789.83
mafic : Median	50.10	13.56	11.26	4.59	5.14	1.10	0.55	0.82	0.09	0.17	7.33	0.90	1.79	4886.70
mafic : Standard Deviation	9.41	4.50	4.87	4.89	5.28	1.57	1.24	0.35	0.06	0.18	5.61	2.93	6.68	18239.07
mafic : 25 percentile	43.84	10.09	8.98	2.97	2.01	0.22	0.12	0.51	0.06	0.11	4.69	0.18	0.49	1324.05
mafic : 75 percentile	53.45	16.49	15.00	6.63	10.39	2.58	2.18	0.94	0.12	0.28	14.03	2.57	7.92	21607.95
mafic : 90 percentile	57.28	17.74	19.23	13.58	15.77	3.36	3.11	1.06	0.17	0.54	16.73	6.06	16.76	45754.80

Appendix A5. Statistical summary of major element and trace element concentrations grouped by shale lithotype, associated mineralization, and lithostratigraphic assemblage.

Shale Lithotype	Non_carb._C_ppm	Cu_ppm	Zn_ppm	Pb_ppm	Cd_ppm	Hg_ppm	Sn_ppm	Tl_ppm	In_ppm	As_ppm	Co_ppm	Ni_ppm	Se_ppm	Mo_ppm
felsic : Minimum	57.00	1.00	9.00	2.50	0.25	0.00	0.50	0.03	0.05	0.50	4.70	6.00	0.25	1.00
felsic : Maximum	356481.30	10000.00	29400.00	4730.00	129.00	2.83	30.00	10.10	0.70	1400.00	446.00	960.00	36.50	76.00
felsic : Mean	64300.08	494.00	1293.18	62.52	2.92	0.27	4.43	1.03	0.08	140.18	48.77	144.65	3.49	7.58
felsic : Median	37499.40	152.00	533.00	19.00	1.20	0.07	3.00	0.77	0.05	83.00	35.80	114.00	0.25	5.00
felsic : Standard Deviation	73529.14	1537.20	2232.52	308.54	8.13	0.47	4.32	1.08	0.09	168.33	44.42	129.37	5.85	8.61
felsic : 25 percentile	15431.70	72.00	193.00	7.00	0.25	0.01	2.00	0.24	0.05	20.00	23.20	64.50	0.25	3.00
felsic : 75 percentile	83434.40	333.00	1725.00	41.00	3.55	0.33	5.00	1.47	0.05	201.50	62.55	178.50	4.95	8.00
felsic : 90 percentile	167113.96	664.00	3222.00	91.20	6.24	0.83	10.00	2.42	0.20	340.00	101.80	298.60	11.48	17.40
intermediate : Minimum	2.10	4.00	13.00	2.50	0.25	0.00	0.50	0.03	0.05	0.50	9.00	20.00	0.25	1.00
intermediate : Maximum	456645.10	10000.00	9970.00	1060.00	24.40	3.49	37.00	4.95	1.10	1090.00	521.00	3110.00	20.90	27.00
intermediate : Mean	30095.20	261.61	800.85	28.28	1.86	0.17	3.21	0.66	0.08	111.30	43.13	159.91	1.57	4.00
intermediate : Median	4043.50	70.00	123.00	9.00	0.25	0.01	1.00	0.52	0.05	51.00	29.20	106.00	0.25	3.00
intermediate : Standard Deviation	64875.08	877.48	1518.73	85.50	3.39	0.44	5.04	0.65	0.12	159.35	47.12	234.39	3.66	4.39
intermediate : 25 percentile	890.80	50.50	88.50	2.50	0.25	0.00	1.00	0.32	0.05	18.00	25.35	88.00	0.25	1.00
intermediate : 75 percentile	26956.68	163.50	645.50	24.50	1.85	0.09	3.00	0.77	0.05	145.00	44.00	139.00	0.25	4.50
intermediate : 90 percentile	84768.88	600.60	2604.00	54.60	6.06	0.47	8.00	1.34	0.10	267.60	78.78	287.20	5.28	8.60
mafic : Minimum	4.60	25.00	58.00	2.50	0.25	0.00	0.50	0.03	0.05	0.50	17.00	24.00	0.25	1.00
mafic : Maximum	134617.80	6110.00	18200.00	5000.00	143.00	0.87	19.00	2.66	0.70	2450.00	269.00	1660.00	18.70	17.00
mafic : Mean	11461.16	320.85	942.29	143.35	4.91	0.06	2.50	0.36	0.07	146.70	60.17	233.76	1.36	2.73
mafic : Median	2297.60	116.00	158.00	6.00	0.25	0.01	1.00	0.11	0.05	33.00	47.60	104.00	0.25	1.00
mafic : Standard Deviation	22781.98	945.34	3052.05	781.15	22.29	0.15	3.97	0.53	0.10	422.09	45.59	393.05	3.23	3.24
mafic : 25 percentile	808.15	94.00	101.00	2.50	0.25	0.00	0.50	0.04	0.05	14.00	35.95	56.00	0.25	1.00
mafic : 75 percentile	13853.00	179.00	445.00	13.50	2.15	0.04	2.00	0.52	0.05	81.00	62.85	143.00	0.48	3.50
mafic : 90 percentile	30274.26	452.60	888.20	38.20	3.46	0.25	6.00	1.04	0.05	218.60	127.40	839.60	3.86	7.60

Appendix A5. Statistical summary of major element and trace element concentrations grouped by shale lithotype, associated mineralization, and lithostratigraphic assemblage.

Shale Lithotype	Ge_ppm	Sb_ppm	Ag_ppm	Au_ppm	W_ppm	Bi_ppm	B_ppm	Rb_ppm	Sr_ppm	Cs_ppm	Ba_ppm	Be_ppm	Zr_ppm	Hf_ppm	Nb_ppm
felsic : Minimum	0.25	0.05	0.25	0.00	0.50	0.05	1.00	0.50	1.00	0.05	0.50	0.50	5.00	0.05	0.30
felsic : Maximum	11.20	106.00	19.50	0.57	19.00	249.00	2980.00	185.00	551.00	14.70	2187.00	5.00	497.00	17.50	51.50
felsic : Mean	1.78	5.52	1.06	0.03	2.28	3.62	87.65	56.10	107.47	1.79	406.86	0.98	127.79	3.31	6.22
felsic : Median	1.50	2.00	0.70	0.02	0.50	1.50	30.00	56.00	82.00	1.50	421.00	1.00	125.00	3.20	5.50
felsic : Standard Deviation	1.24	10.45	1.74	0.06	2.97	16.50	270.44	38.90	92.38	1.62	298.68	0.65	62.82	1.82	5.35
felsic : 25 percentile	1.10	0.50	0.25	0.00	0.50	0.80	12.50	20.00	45.00	0.50	166.50	0.50	91.50	2.30	4.00
felsic : 75 percentile	2.20	5.95	1.10	0.04	4.00	2.70	57.50	84.50	137.50	2.65	587.00	1.00	148.50	3.80	6.90
felsic : 90 percentile	3.00	13.44	1.94	0.07	6.00	4.98	152.60	105.40	213.00	3.60	724.40	2.00	183.80	4.94	8.78
intermediate : Minimum	0.25	0.05	0.25	0.00	0.50	0.05	1.00	0.50	8.00	0.10	3.00	0.50	7.00	0.20	0.30
intermediate : Maximum	8.00	104.00	17.70	6.66	50.00	27.10	681.00	168.00	696.00	17.40	1596.00	3.00	241.00	6.20	14.20
intermediate : Mean	1.82	4.29	0.70	0.07	2.24	1.21	96.56	71.97	164.57	3.47	495.45	1.30	115.19	3.00	5.65
intermediate : Median	1.60	2.00	0.25	0.01	0.50	0.60	63.00	77.00	145.00	2.30	502.00	1.00	120.00	3.10	5.80
intermediate : Standard Deviation	1.00	8.45	1.32	0.46	4.51	2.10	109.41	38.87	118.80	3.56	287.77	0.67	32.32	0.84	1.99
intermediate : 25 percentile	1.30	0.60	0.25	0.00	0.50	0.30	30.00	43.50	72.00	1.10	312.00	1.00	102.50	2.70	4.50
intermediate : 75 percentile	2.00	5.20	0.75	0.03	2.00	1.30	115.50	98.50	234.00	4.15	656.50	2.00	131.50	3.40	6.90
intermediate : 90 percentile	2.70	10.08	1.26	0.06	6.00	2.90	228.80	117.20	316.40	9.06	848.60	2.00	148.00	3.86	8.10
mafic : Minimum	0.25	0.05	0.25	0.00	0.50	0.05	1.00	0.50	5.00	0.05	0.50	0.50	13.00	0.30	0.70
mafic : Maximum	8.30	12.50	8.50	30.00	17.00	4.70	506.00	162.00	455.00	4.50	2470.00	3.00	124.00	3.20	11.20
mafic : Mean	2.18	1.87	0.71	0.76	1.99	0.65	47.10	34.80	102.39	1.19	296.13	0.74	67.93	1.83	3.61
mafic : Median	1.80	1.00	0.25	0.01	0.50	0.40	16.00	17.00	86.00	1.00	214.00	0.50	58.00	1.60	2.80
mafic : Standard Deviation	1.61	2.50	1.44	4.68	3.43	0.90	85.71	35.10	84.31	1.01	434.09	0.48	30.80	0.84	2.25
mafic : 25 percentile	1.45	0.45	0.25	0.00	0.50	0.15	7.00	4.00	48.50	0.30	17.50	0.50	41.00	1.10	1.85
mafic : 75 percentile	2.05	2.50	0.55	0.03	0.75	0.80	52.00	60.50	134.50	1.75	415.00	1.00	98.50	2.65	5.55
mafic : 90 percentile	5.06	4.66	1.56	0.10	7.60	1.30	109.20	74.80	201.40	2.28	644.60	1.00	104.60	2.88	6.38

Appendix A5. Statistical summary of major element and trace element concentrations grouped by shale lithotype, associated mineralization, and lithostratigraphic assemblage.

Shale Lithotype	Ta_ppm	Ga_ppm	Sc_ppm	V_ppm	Cr_ppm	Th_ppm	U_ppm	Y_ppm	La_ppm	Ce_ppm	Pr_ppm	Nd_ppm	Sm_ppm	Eu_ppm	Gd_ppm
felsic : Minimum	0.02	2.00	1.07	6.00	0.25	0.13	0.13	2.00	1.39	2.49	0.28	1.18	0.24	0.12	0.22
felsic : Maximum	4.70	40.00	36.40	138.00	483.00	22.10	6.24	313.00	123.00	237.00	29.00	115.00	20.50	4.91	25.00
felsic : Mean	0.51	16.77	13.11	62.39	60.45	4.92	1.38	19.03	21.10	45.46	5.37	20.66	4.08	1.16	3.50
felsic : Median	0.45	18.00	13.20	65.00	49.40	4.18	1.19	15.00	19.40	42.80	5.03	19.70	3.85	1.07	3.06
felsic : Standard Deviation	0.40	6.07	5.73	25.84	58.78	3.13	0.83	22.12	13.49	27.59	3.23	12.41	2.46	0.62	2.54
felsic : 25 percentile	0.35	13.00	9.03	44.00	28.95	2.96	0.82	12.00	12.80	28.90	3.46	13.35	2.79	0.76	2.38
felsic : 75 percentile	0.56	20.00	15.90	80.50	71.80	6.41	1.76	21.00	26.80	56.35	6.54	25.10	4.61	1.37	3.86
felsic : 90 percentile	0.74	24.00	20.24	92.00	98.84	8.53	2.30	28.00	35.30	75.50	8.35	30.66	5.95	1.93	5.26
intermediate : Minimum	0.02	2.00	3.44	21.00	7.40	0.14	0.04	4.00	1.45	2.79	0.39	2.07	0.82	0.25	0.83
intermediate : Maximum	0.94	39.00	30.70	244.00	1490.00	14.50	26.30	40.00	75.90	144.00	17.20	60.50	9.66	4.11	8.08
intermediate : Mean	0.43	21.14	18.52	125.61	182.63	4.73	1.50	15.01	21.86	46.95	5.61	21.87	4.15	1.13	3.33
intermediate : Median	0.44	22.00	19.20	129.00	148.00	4.53	1.29	15.00	21.60	47.00	5.64	21.90	4.20	1.10	3.37
intermediate : Standard Deviation	0.14	5.97	4.76	39.62	190.02	2.19	2.08	4.49	9.71	19.28	2.26	8.34	1.36	0.41	0.97
intermediate : 25 percentile	0.35	18.00	15.40	97.50	83.40	3.19	0.90	12.00	15.90	35.85	4.40	17.25	3.40	0.92	2.83
intermediate : 75 percentile	0.51	25.00	21.95	155.00	206.50	6.16	1.69	17.00	27.15	58.55	6.88	26.85	4.92	1.29	3.89
intermediate : 90 percentile	0.58	27.00	24.10	172.60	288.00	7.26	2.10	20.60	32.52	68.30	7.84	30.56	5.63	1.47	4.36
mafic : Minimum	0.04	3.00	6.54	31.00	11.80	0.13	0.06	7.00	1.37	3.10	0.45	2.32	0.84	0.35	1.07
mafic : Maximum	0.60	31.00	52.00	442.00	3120.00	5.45	1.96	40.00	29.80	69.40	8.24	34.40	6.59	1.80	5.83
mafic : Mean	0.26	17.56	31.70	217.68	448.81	1.86	0.58	19.05	9.09	20.33	2.58	11.22	2.80	0.85	3.05
mafic : Median	0.19	18.00	34.40	223.00	181.00	0.80	0.27	18.00	5.73	15.20	2.36	10.40	3.13	0.84	2.87
mafic : Standard Deviation	0.17	6.22	12.23	85.07	779.25	1.89	0.60	6.69	7.28	15.60	1.78	7.11	1.30	0.37	1.14
mafic : 25 percentile	0.11	13.00	20.65	159.50	43.05	0.40	0.12	15.00	2.67	6.36	0.99	4.91	1.69	0.53	2.10
mafic : 75 percentile	0.38	22.50	39.25	268.00	266.50	3.32	1.00	22.00	16.10	33.40	4.04	16.70	3.68	1.09	3.83
mafic : 90 percentile	0.55	24.00	49.62	333.20	2008.00	5.17	1.64	26.40	18.74	39.44	4.96	20.28	4.43	1.38	4.35

Appendix A5. Statistical summary of major element and trace element concentrations grouped by shale lithotype, associated mineralization, and lithostratigraphic assemblage.

Shale Lithotype	Tb_ppm	Dy_ppm	Ho_ppm	Er_ppm	Tm_ppm	Yb_ppm	Lu_ppm	Br_ppm
felsic : Minimum	0.04	0.21	0.05	0.15	0.03	0.16	0.02	0.25
felsic : Maximum	5.37	37.20	8.86	27.00	4.07	25.10	4.06	30.20
felsic : Mean	0.57	3.31	0.67	2.00	0.30	2.09	0.36	2.25
felsic : Median	0.47	2.66	0.54	1.61	0.25	1.71	0.30	1.40
felsic : Standard Deviation	0.48	3.07	0.68	2.03	0.31	1.96	0.32	3.60
felsic : 25 percentile	0.38	2.16	0.43	1.28	0.19	1.33	0.23	0.25
felsic : 75 percentile	0.63	3.63	0.73	2.22	0.33	2.32	0.40	2.50
felsic : 90 percentile	0.86	5.16	1.04	3.03	0.47	3.26	0.57	5.54
intermediate : Minimum	0.15	0.74	0.15	0.44	0.06	0.42	0.08	0.25
intermediate : Maximum	1.17	7.33	1.55	4.48	0.68	4.46	0.79	12.80
intermediate : Mean	0.50	2.79	0.55	1.58	0.23	1.59	0.27	1.15
intermediate : Median	0.50	2.82	0.54	1.56	0.23	1.55	0.26	0.25
intermediate : Standard Deviation	0.14	0.80	0.16	0.47	0.07	0.49	0.09	1.68
intermediate : 25 percentile	0.41	2.30	0.45	1.31	0.19	1.30	0.22	0.25
intermediate : 75 percentile	0.56	3.17	0.62	1.77	0.26	1.74	0.30	1.40
intermediate : 90 percentile	0.64	3.54	0.71	2.07	0.30	2.11	0.35	2.96
mafic : Minimum	0.19	1.28	0.23	0.71	0.11	0.69	0.11	0.25
mafic : Maximum	1.05	6.70	1.44	4.11	0.60	4.20	0.71	5.60
mafic : Mean	0.54	3.29	0.69	2.03	0.31	2.05	0.35	1.20
mafic : Median	0.53	3.11	0.65	1.97	0.29	1.95	0.33	0.25
mafic : Standard Deviation	0.19	1.13	0.24	0.68	0.10	0.66	0.11	1.29
mafic : 25 percentile	0.40	2.45	0.55	1.56	0.24	1.67	0.27	0.25
mafic : 75 percentile	0.66	3.93	0.83	2.39	0.35	2.37	0.40	2.00
mafic : 90 percentile	0.82	4.96	1.06	3.09	0.48	3.14	0.51	2.78

Appendix A5. Statistical summary of major element and trace element concentrations grouped by shale lithotype, associated mineralization, and lithostratigraphic assemblage. Concentrations of major oxides given in weight percent, and trace elements given in ppm

Associated Mineralization	SiO2_pct	Al2O3_pct	Fe2O3_pct	MgO_pct	CaO_pct	Na2O_pct	K2O_pct	TiO2_pct	P2O5_pct	MnO_pct	LOI_pct	Total S_pct	CO2_pct
Base Metal : Minimum	12.45	0.34	0.71	0.07	0.04	0.02	0.01	0.01	0.01	0.00	0.84	0.01	0.01
Base Metal : Maximum	94.54	29.62	59.30	21.76	37.23	8.03	5.78	1.93	0.30	1.16	52.59	30.20	26.40
Base Metal : Mean	55.20	10.72	9.90	2.63	3.52	1.96	1.59	0.40	0.09	0.09	12.64	4.01	2.35
Base Metal : Median	58.35	10.98	8.25	1.52	1.87	1.57	1.42	0.36	0.08	0.05	9.33	3.00	0.96
Base Metal : Standard Deviation	14.82	4.48	7.32	3.43	4.66	1.74	1.35	0.24	0.05	0.13	9.40	4.18	3.79
Base Metal : 25 percentile	45.51	7.63	5.04	0.88	0.88	0.40	0.33	0.25	0.06	0.02	5.87	0.99	0.09
Base Metal : 75 percentile	65.26	14.11	12.63	2.62	4.23	3.05	2.48	0.51	0.12	0.10	16.89	5.78	2.84
Base Metal : 90 percentile	70.91	15.99	18.08	5.91	9.01	4.26	3.32	0.67	0.15	0.21	27.74	8.97	7.37
Orogenic Au : Minimum	21.55	2.72	1.77	0.19	0.08	0.03	0.02	0.11	0.02	0.00	0.86	0.01	0.01
Orogenic Au : Maximum	84.88	23.62	28.05	14.27	19.54	8.12	6.42	1.14	0.38	1.09	41.33	14.40	28.40
Orogenic Au : Mean	58.84	15.54	6.63	2.31	1.88	2.36	2.69	0.60	0.13	0.06	8.10	1.99	1.90
Orogenic Au : Median	59.63	15.92	6.17	1.88	1.31	2.15	2.93	0.59	0.13	0.05	6.67	1.18	1.01
Orogenic Au : Standard Deviation	7.536	3.394	3.413	1.787	2.343	1.614	1.152	0.185	0.046	0.079	5.420	2.386	3.098
Orogenic Au : 25 percentile	56.30	13.65	4.60	1.13	0.68	1.29	2.07	0.46	0.11	0.03	4.37	0.17	0.19
Orogenic Au : 75 percentile	62.81	17.89	7.52	3.08	2.16	3.01	3.32	0.73	0.16	0.07	9.85	2.95	2.48
Orogenic Au : 90 percentile	66.34	19.26	9.88	4.02	3.54	4.42	4.00	0.83	0.19	0.10	14.59	5.45	4.41

Associated Mineralization	C_in_CO2_ppm	Non_carb._C_ppm	Cu_ppm	Zn_ppm	Pb_ppm	Cd_ppm	Hg_ppm	Sn_ppm	Tl_ppm	In_ppm	As_ppm	Co_ppm	Ni_ppm
Base Metal : Minimum	0.00	4.60	1.00	9.00	2.50	0.25	0.00	0.50	0.03	0.05	0.50	4.70	6.00
Base Metal : Maximum	72072.00	456645.10	10000.00	18200.00	5000.00	143.00	3.49	30.00	10.10	0.80	1400.00	521.00	3110.00
Base Metal : Mean	6383.63	65234.71	614.11	1267.13	73.61	3.26	0.25	3.93	0.70	0.08	139.66	59.86	189.26
Base Metal : Median	2566.20	29737.60	144.00	419.00	15.00	1.00	0.05	3.00	0.41	0.05	55.00	41.50	108.00
Base Metal : Standard Deviation	10334.90	83113.01	1778.87	2015.19	423.05	9.32	0.50	4.66	0.97	0.10	202.20	60.55	279.37
Base Metal : 25 percentile	245.70	9614.80	66.50	131.50	5.00	0.25	0.01	1.00	0.10	0.05	16.00	24.00	61.50
Base Metal : 75 percentile	7725.90	84159.75	393.00	1645.00	37.00	3.85	0.24	5.00	0.92	0.05	201.00	79.20	214.00
Base Metal : 90 percentile	20092.80	185437.90	855.00	3690.00	93.00	8.20	0.73	9.00	1.74	0.20	360.00	126.00	385.00
Orogenic Au : Minimum	13.65	2.10	4.00	12.00	2.50	0.25	0.00	0.50	0.03	0.05	0.50	5.70	9.00
Orogenic Au : Maximum	77532.00	356481.30	2130.00	29400.00	1970.00	129.00	2.58	37.00	4.95	1.10	2450.00	134.00	853.00
Orogenic Au : Mean	5060.01	28480.94	171.40	872.18	36.15	2.04	0.18	3.64	0.95	0.08	118.38	35.57	128.13
Orogenic Au : Median	2743.65	8592.85	88.50	158.50	13.00	0.25	0.02	2.00	0.66	0.05	62.00	29.95	108.00
Orogenic Au : Standard Deviation	7943.87	49079.26	243.73	2075.40	137.72	7.93	0.38	4.65	0.85	0.11	187.55	19.08	93.52
Orogenic Au : 25 percentile	518.70	1262.13	54.00	92.00	5.00	0.25	0.00	1.00	0.41	0.05	21.50	24.80	87.00
Orogenic Au : 75 percentile	6777.23	37788.45	190.50	1022.50	29.00	1.90	0.19	4.00	1.30	0.05	166.00	39.68	137.25
Orogenic Au : 90 percentile	11992.89	73283.07	405.30	2452.00	52.90	4.58	0.53	9.00	2.28	0.10	268.00	62.38	193.90

Appendix A5. Statistical summary of major element and trace element concentrations grouped by shale lithotype, associated mineralization, and lithostratigraphic assemblage. Concentrations of major oxides given in weight percent, and trace elements given in ppm

Associated Mineralization	Se_ppm	Mo_ppm	Ge_ppm	Sb_ppm	Ag_ppm	Au_ppm	W_ppm	Bi_ppm	B_ppm	Rb_ppm	Sr_ppm	Cs_ppm	Ba_ppm	Be_ppm	Zr_ppm
Base Metal : Minimum	0.25	1.00	0.25	0.05	0.25	0.00	0.50	0.05	1.00	0.50	1.00	0.05	0.50	0.50	5.00
Base Metal : Maximum	36.50	76.00	11.20	104.00	19.50	1.18	19.00	249.00	2980.00	185.00	679.00	6.90	2470.00	5.00	497.00
Base Metal : Mean	3.58	7.16	1.79	4.98	1.06	0.03	2.02	3.65	74.68	42.62	113.25	1.33	331.00	0.89	107.86
Base Metal : Median	0.25	4.00	1.30	1.50	0.60	0.01	0.50	1.30	22.00	37.00	80.00	0.90	270.00	0.50	102.00
Base Metal : Standard Deviation	6.11	8.29	1.45	10.36	2.05	0.09	2.77	17.05	254.05	37.95	109.59	1.24	314.44	0.64	64.99
Base Metal : 25 percentile	0.25	2.00	1.00	0.50	0.25	0.00	0.50	0.60	8.00	8.50	41.00	0.40	71.00	0.50	69.50
Base Metal : 75 percentile	4.25	9.00	2.10	4.95	1.05	0.03	3.00	2.85	50.00	66.50	150.50	2.00	510.00	1.00	132.50
Base Metal : 90 percentile	12.20	18.00	3.30	12.50	1.90	0.06	6.00	5.10	138.00	87.00	239.00	3.00	688.00	2.00	165.00
Orogenic Au : Minimum	0.25	1.00	0.50	0.05	0.25	0.00	0.50	0.05	1.00	0.50	12.00	0.05	5.00	0.50	23.00
Orogenic Au : Maximum	20.90	64.00	8.30	106.00	8.50	30.00	50.00	14.10	1800.00	165.00	696.00	17.40	2187.00	3.00	315.00
Orogenic Au : Mean	1.56	4.41	1.86	4.52	0.72	0.16	2.45	1.23	101.11	78.34	147.27	3.49	532.76	1.29	127.70
Orogenic Au : Median	0.25	3.00	1.70	2.40	0.50	0.01	0.50	0.75	58.00	83.00	122.00	2.55	525.50	1.00	125.00
Orogenic Au : Standard Deviation	3.32	5.43	0.87	8.23	0.87	1.81	4.41	1.41	150.36	33.71	102.83	3.28	274.49	0.64	34.61
Orogenic Au : 25 percentile	0.25	2.00	1.40	0.70	0.25	0.00	0.50	0.40	33.00	59.75	70.00	1.40	395.25	1.00	112.75
Orogenic Au : 75 percentile	0.25	5.00	2.00	5.43	0.80	0.03	3.25	1.50	109.25	100.00	210.25	3.82	659.00	2.00	142.00
Orogenic Au : 90 percentile	6.59	8.00	2.80	10.87	1.40	0.08	6.00	2.79	226.50	117.90	268.90	7.60	835.20	2.00	167.00
Associated Mineralization	**Hf_ppm**	**Nb_ppm**	**Ta_ppm**	**Ga_ppm**	**Sc_ppm**	**V_ppm**	**Cr_ppm**	**Th_ppm**	**U_ppm**	**Y_ppm**	**La_ppm**	**Ce_ppm**	**Pr_ppm**	**Nd_ppm**	**Sm_ppm**
Base Metal : Minimum	0.05	0.30	0.02	2.00	1.07	6.00	0.25	0.13	0.04	2.00	1.37	2.49	0.28	1.18	0.24
Base Metal : Maximum	17.50	46.70	4.70	37.00	52.00	442.00	3120.00	22.10	6.24	313.00	93.40	190.00	20.80	76.60	16.60
Base Metal : Mean	2.77	5.21	0.43	15.53	15.03	81.38	145.92	3.59	1.04	18.58	17.34	37.87	4.56	17.69	3.66
Base Metal : Median	2.60	4.50	0.38	16.00	13.60	69.00	57.60	3.21	0.93	15.00	15.10	32.50	3.94	15.30	3.43
Base Metal : Standard Deviation	1.86	4.84	0.42	6.17	9.17	61.86	360.68	2.67	0.74	22.76	12.38	26.25	3.08	11.71	2.38
Base Metal : 25 percentile	1.75	2.90	0.24	11.00	8.87	45.00	30.30	1.87	0.55	11.00	9.03	20.70	2.67	10.55	2.34
Base Metal : 75 percentile	3.40	6.10	0.50	20.00	18.15	97.00	98.00	4.68	1.35	20.00	22.50	48.50	5.78	22.35	4.38
Base Metal : 90 percentile	4.00	7.90	0.67	22.00	26.20	134.00	257.00	6.26	1.82	28.00	31.70	67.90	7.86	29.10	5.86
Orogenic Au : Minimum	0.60	1.40	0.08	6.00	4.41	16.00	7.10	0.15	0.07	7.00	1.77	5.04	0.80	3.39	0.90
Orogenic Au : Maximum	8.50	51.50	1.17	40.00	44.00	285.00	1180.00	17.10	26.30	46.00	123.00	237.00	29.00	115.00	20.50
Orogenic Au : Mean	3.35	6.33	0.48	21.54	18.29	117.52	134.24	5.56	1.68	16.22	23.51	50.14	5.92	23.04	4.34
Orogenic Au : Median	3.30	6.10	0.47	22.00	17.70	110.00	104.00	5.31	1.50	15.00	22.85	49.75	5.88	22.90	4.25
Orogenic Au : Standard Deviation	0.91	3.25	0.15	5.11	5.95	51.26	130.23	2.58	1.90	5.29	11.04	21.38	2.49	9.33	1.55
Orogenic Au : 25 percentile	2.90	5.10	0.40	19.00	14.48	77.00	59.40	3.80	1.07	13.00	18.50	39.35	4.74	18.50	3.57
Orogenic Au : 75 percentile	3.70	7.10	0.55	25.00	21.53	152.25	177.75	6.92	1.92	18.00	27.92	59.13	6.88	26.80	4.92
Orogenic Au : 90 percentile	4.40	8.30	0.65	27.00	24.67	174.90	239.80	8.34	2.28	22.00	33.29	69.49	8.05	30.87	5.72

Appendix A5. Statistical summary of major element and trace element concentrations grouped by shale lithotype, associated mineralization, and lithostratigraphic assemblage. Concentrations of major oxides given in weight percent, and trace elements given in ppm

Associated Mineralization	Eu_ppm	Gd_ppm	Tb_ppm	Dy_ppm	Ho_ppm	Er_ppm	Tm_ppm	Yb_ppm	Lu_ppm	Br_ppm
Base Metal : Minimum	0.12	0.22	0.04	0.21	0.05	0.15	0.03	0.16	0.02	0.25
Base Metal : Maximum	4.11	25.00	5.37	37.20	8.86	27.00	4.07	25.10	4.06	30.20
Base Metal : Mean	1.12	3.30	0.55	3.24	0.66	1.95	0.30	2.01	0.34	2.16
Base Metal : Median	1.01	2.93	0.46	2.64	0.52	1.55	0.24	1.65	0.28	1.10
Base Metal : Standard Deviation	0.65	2.50	0.48	3.16	0.71	2.10	0.32	2.02	0.33	3.53
Base Metal : 25 percentile	0.70	2.09	0.36	2.05	0.41	1.19	0.18	1.23	0.21	0.25
Base Metal : 75 percentile	1.33	3.80	0.63	3.58	0.72	2.10	0.32	2.20	0.38	2.50
Base Metal : 90 percentile	1.95	5.12	0.86	5.09	1.04	3.05	0.48	3.28	0.58	5.50
Orogenic Au : Minimum	0.30	0.87	0.18	1.16	0.22	0.66	0.09	0.64	0.10	0.25
Orogenic Au : Maximum	4.91	16.90	1.85	8.52	1.60	4.71	0.74	5.08	0.87	17.90
Orogenic Au : Mean	1.14	3.47	0.52	2.96	0.59	1.72	0.25	1.76	0.30	1.30
Orogenic Au : Median	1.11	3.40	0.51	2.87	0.56	1.60	0.23	1.60	0.27	0.25
Orogenic Au : Standard Deviation	0.39	1.21	0.16	0.90	0.18	0.52	0.08	0.56	0.09	1.96
Orogenic Au : 25 percentile	0.94	2.87	0.43	2.40	0.47	1.38	0.21	1.42	0.24	0.25
Orogenic Au : 75 percentile	1.30	3.91	0.57	3.26	0.65	1.90	0.28	1.97	0.33	1.60
Orogenic Au : 90 percentile	1.47	4.45	0.69	3.96	0.83	2.43	0.36	2.51	0.43	2.80

Appendix A5. Statistical summary of major element and trace element concentrations grouped by shale lithotype, associated mineralization, and lithostratigraphic assemblage. Concentrations of major oxides given in weight percent, and trace elements given in ppm

Lithostratigrapic Assemblage	SiO2_pct	Al2O3_pct	Fe2O3_pct	MgO_pct	CaO_pct	Na2O_pct	K2O_pct	TiO2_pct	P2O5_pct	MnO_pct	LOI_pct	Total S_pct	CO2_pct
Deloro : Minimum	16.62	0.34	2.40	0.07	0.04	0.02	0.02	0.01	0.01	0.00	2.15	0.02	0.01
Deloro : Maximum	94.54	18.93	51.13	13.69	8.88	4.26	4.73	1.14	0.26	1.16	27.93	24.60	13.60
Deloro : Mean	59.23	11.07	10.59	2.70	2.86	1.50	1.50	0.45	0.10	0.14	9.14	3.17	2.36
Deloro : Median	60.65	11.19	8.57	1.61	2.47	0.96	1.27	0.38	0.09	0.07	7.02	1.72	1.68
Deloro : Standard Deviation	13.48	4.54	8.90	2.88	2.38	1.40	1.24	0.28	0.06	0.21	5.95	4.38	2.70
Deloro : 25 percentile	50.87	8.43	4.83	1.27	0.69	0.32	0.45	0.27	0.06	0.03	5.46	0.68	0.07
Deloro : 75 percentile	66.07	14.76	12.40	3.10	4.26	2.71	2.37	0.56	0.13	0.17	11.31	4.14	3.09
Deloro : 90 percentile	73.54	16.04	20.67	5.81	6.16	3.83	3.02	0.87	0.20	0.35	18.63	7.54	5.70
Stoughton-Roquemare : Minimum	35.07	2.12	0.71	0.11	0.19	0.03	0.06	0.06	0.01	0.01	0.84	0.03	0.01
Stoughton-Roquemare : Maximum	89.57	23.62	20.68	13.16	10.41	6.57	5.80	1.93	0.20	0.46	41.33	12.80	7.41
Stoughton-Roquemare : Mean	60.80	11.29	7.43	1.96	1.85	2.03	1.87	0.45	0.10	0.06	11.25	3.31	1.02
Stoughton-Roquemare : Median	61.48	12.21	6.28	1.24	1.24	1.53	1.82	0.41	0.10	0.04	9.63	2.73	0.40
Stoughton-Roquemare : Std. Dev	10.76	4.11	4.21	2.24	2.06	1.64	1.24	0.29	0.05	0.07	7.92	2.77	1.47
Stoughton-Roquemare : 25 percentile	53.91	8.92	4.35	0.86	0.48	0.77	0.85	0.31	0.07	0.02	5.77	1.23	0.06
Stoughton-Roquemare : 75 percentile	67.28	13.91	9.91	2.04	2.39	3.17	2.63	0.53	0.14	0.06	14.88	4.62	1.50
Stoughton-Roquemare : 90 percentile	73.21	15.40	13.20	4.35	4.32	4.40	3.47	0.73	0.16	0.14	21.70	7.29	2.95
Kidd-Munro : Minimum	12.45	0.83	1.37	0.16	0.15	0.03	0.01	0.04	0.01	0.01	2.52	0.01	0.01
Kidd-Munro : Maximum	85.27	29.62	33.31	21.76	37.23	8.03	5.78	1.35	0.30	0.99	52.59	24.90	26.40
Kidd-Munro : Mean	50.41	10.76	10.87	3.15	4.43	2.08	1.52	0.40	0.09	0.09	14.71	4.46	3.07
Kidd-Munro : Median	55.08	9.26	9.12	2.27	2.07	1.74	1.20	0.34	0.08	0.06	10.48	3.59	1.27
Kidd-Munro : Standard Deviation	15.36	5.39	6.43	3.48	5.89	1.77	1.48	0.24	0.06	0.13	11.34	4.14	4.63
Kidd-Munro : 25 percentile	39.55	7.13	6.06	0.96	1.04	0.55	0.14	0.25	0.05	0.03	5.56	0.90	0.35
Kidd-Munro : 75 percentile	61.77	14.76	14.39	3.63	5.18	3.04	2.63	0.54	0.13	0.10	23.25	6.81	3.15
Kidd-Munro : 90 percentile	67.36	18.21	18.49	7.94	12.80	4.48	3.17	0.74	0.17	0.16	34.19	10.40	9.21
Blake River : Minimum	13.31	2.11	2.00	0.16	0.05	0.02	0.02	0.08	0.01	0.01	0.86	0.06	0.01
Blake River : Maximum	84.88	19.09	59.30	10.73	19.54	8.12	5.63	1.32	0.38	0.38	28.89	30.20	28.40
Blake River : Mean	58.53	13.75	8.73	2.06	2.43	2.24	2.42	0.53	0.12	0.07	8.21	3.30	1.79
Blake River : Median	59.72	14.16	6.79	1.64	1.47	1.72	2.34	0.51	0.12	0.05	6.06	1.80	0.72
Blake River : Standard Deviation	10.78	3.57	8.04	1.62	3.35	2.04	1.33	0.23	0.06	0.07	6.11	4.86	3.92
Blake River : 25 percentile	53.24	11.54	4.80	1.15	0.71	0.75	1.62	0.36	0.08	0.03	4.09	0.37	0.13
Blake River : 75 percentile	65.17	16.81	8.93	2.76	2.26	3.12	3.37	0.66	0.15	0.09	10.94	4.31	1.76
Blake River : 90 percentile	69.63	17.72	17.59	3.56	5.75	5.40	4.12	0.78	0.19	0.14	18.26	7.60	3.50
Tisdale : Minimum	27.33	3.66	1.58	0.11	0.08	0.03	0.02	0.14	0.02	0.00	1.03	0.01	0.01
Tisdale : Maximum	83.19	22.66	18.22	21.71	15.88	7.44	6.42	0.97	0.28	0.59	31.32	7.28	19.60
Tisdale : Mean	58.42	14.94	6.46	2.35	2.17	2.37	2.63	0.56	0.13	0.06	8.89	2.10	1.99
Tisdale : Median	58.94	15.18	6.11	1.61	1.42	2.08	2.97	0.54	0.12	0.05	8.42	1.82	1.14
Tisdale : Standard Deviation	7.71	3.39	2.93	2.72	2.47	1.71	1.24	0.17	0.05	0.07	5.00	1.93	2.92
Tisdale : 25 percentile	55.69	13.22	4.48	1.01	0.66	1.15	1.98	0.42	0.10	0.02	4.67	0.23	0.10
Tisdale : 75 percentile	62.63	17.54	7.57	2.96	2.61	3.05	3.40	0.70	0.16	0.07	10.75	3.08	2.70
Tisdale : 90 percentile	66.47	18.96	9.79	4.12	5.05	4.77	4.01	0.78	0.19	0.12	15.08	5.10	4.96
Porcupine : Minimum	39.52	7.97	2.72	0.50	0.20	0.08	0.05	0.27	0.05	0.01	3.36	0.03	0.01
Porcupine : Maximum	71.17	21.85	20.97	14.27	4.45	5.30	4.09	0.98	0.21	0.17	24.96	9.26	6.78
Porcupine : Mean	60.64	16.92	5.72	2.20	1.29	2.37	2.70	0.66	0.12	0.05	6.78	1.07	1.73
Porcupine : Median	60.97	17.08	5.29	1.66	1.13	2.37	2.92	0.69	0.12	0.04	5.97	0.41	0.99
Porcupine : Standard Deviation	5.50	2.49	2.73	1.93	0.92	0.98	0.83	0.16	0.03	0.03	3.70	1.56	1.74
Porcupine : 25 percentile	58.39	15.74	4.13	1.07	0.54	1.81	2.33	0.53	0.11	0.03	4.81	0.15	0.23

Appendix A5. Statistical summary of major element and trace element concentrations grouped by shale lithotype, associated mineralization, and lithostratigraphic assemblage. Concentrations of major oxides given in weight percent, and trace elements given in ppm

Lithostratigrapic Assemblage	SiO2_pct	Al2O3_pct	Fe2O3_pct	MgO_pct	CaO_pct	Na2O_pct	K2O_pct	TiO2_pct	P2O5_pct	MnO_pct	LOI_pct	Total S_pct	CO2_pct
Porcupine : 75 percentile	64.63	18.40	6.41	2.57	1.86	2.99	3.23	0.78	0.14	0.06	7.28	1.39	2.75
Porcupine : 90 percentile	66.86	19.52	7.98	3.80	2.78	3.52	3.54	0.86	0.17	0.09	8.96	2.68	4.34
	C_in_CO2_ppm	**Non_carb._C_ppm**	**Cu_ppm**	**Zn_ppm**	**Pb_ppm**	**Cd_ppm**	**Hg_ppm**	**Sn_ppm**	**Tl_ppm**	**In_ppm**	**As_ppm**	**Co_ppm**	**Ni_ppm**
Porcupine : 75 percentile	7493.85	19482.55	104.25	538.25	17.25	1.00	0.03	2.00	1.03	0.05	162.25	34.53	129.25
Porcupine : 90 percentile	11848.20	39807.75	191.10	1775.00	32.30	3.65	0.18	4.00	1.76	0.05	324.00	49.22	213.30
	Se_ppm	**Mo_ppm**	**Ge_ppm**	**Sb_ppm**	**Ag_ppm**	**Au_ppm**	**W_ppm**	**Bi_ppm**	**B_ppm**	**Rb_ppm**	**Sr_ppm**	**Cs_ppm**	**Ba_ppm**
Porcupine : 75 percentile	0.25	3.00	2.03	7.73	0.60	0.01	5.00	1.23	136.00	95.00	241.00	11.53	663.00
Porcupine : 90 percentile	0.25	5.00	2.50	13.62	0.80	0.04	6.00	2.54	262.60	108.40	319.70	13.34	793.20
	Be_ppm	**Zr_ppm**	**Hf_ppm**	**Nb_ppm**	**Ta_ppm**	**Ga_ppm**	**Sc_ppm**	**V_ppm**	**Cr_ppm**	**Th_ppm**	**U_ppm**	**Y_ppm**	**La_ppm**
Porcupine : 75 percentile	2.00	142.00	3.70	6.30	0.53	26.00	22.42	157.75	175.00	6.23	1.73	16.00	25.30
Porcupine : 90 percentile	2.00	160.90	4.30	7.10	0.56	28.70	24.91	178.70	247.60	7.58	2.18	19.70	28.30
	Ce_ppm	**Pr_ppm**	**Nd_ppm**	**Sm_ppm**	**Eu_ppm**	**Gd_ppm**	**Tb_ppm**	**Dy_ppm**	**Ho_ppm**	**Er_ppm**	**Tm_ppm**	**Yb_ppm**	**Lu_ppm**
Porcupine : 75 percentile	53.08	6.21	23.33	4.33	1.15	3.59	0.53	3.01	0.60	1.71	0.26	1.70	0.29
Porcupine : 90 percentile	62.89	7.62	28.94	5.24	1.32	3.99	0.61	3.34	0.69	1.97	0.30	2.09	0.38
	Br_ppm												
Porcupine : 75 percentile	1.20												
Porcupine : 90 percentile	1.61												

Appendix A5. Statistical summary of major element and trace element concentrations grouped by shale lithotype, associated mineralization, and lithostratigraphic assemblage. Concentrations of major oxides given in weight percent, and trace elements given in ppm

Lithostratigrapic Assemblage	C_in_CO2_ppm	Non_carb._C_ppm	Cu_ppm	Zn_ppm	Pb_ppm	Cd_ppm	Hg_ppm	Sn_ppm	Tl_ppm	In_ppm	As_ppm	Co_ppm	Ni_ppm
Deloro : Minimum	13.65	96.70	1.00	14.00	2.50	0.25	0.00	0.50	0.03	0.05	0.50	10.00	29.00
Deloro : Maximum	37128.00	185437.90	1020.00	8400.00	74.00	18.70	0.63	28.00	10.10	0.80	1400.00	202.00	1660.00
Deloro : Mean	6430.48	29492.52	209.63	1274.22	14.41	2.90	0.07	4.02	0.85	0.11	95.46	53.95	163.83
Deloro : Median	4586.40	15945.40	106.00	396.00	7.00	0.70	0.02	2.00	0.28	0.05	26.00	43.20	98.00
Deloro : Standard Deviation	7364.69	39119.99	235.86	2107.33	15.42	4.66	0.12	6.08	1.67	0.17	224.73	40.06	257.42
Deloro : 25 percentile	191.10	4200.30	44.50	105.00	2.50	0.25	0.00	0.50	0.14	0.05	7.00	22.10	63.00
Deloro : 75 percentile	8435.70	36316.95	295.50	1415.00	19.50	3.05	0.08	5.00	0.94	0.05	105.50	77.55	149.00
Deloro : 90 percentile	15571.92	81448.78	595.80	4890.00	36.80	11.32	0.22	14.60	2.29	0.38	231.80	104.60	338.60
Stoughton-Roquemare : Minimum	13.65	4.60	10.00	14.00	2.50	0.25	0.00	0.50	0.03	0.05	0.50	5.70	9.00
Stoughton-Roquemare : Maximum	20229.30	356481.30	1990.00	29400.00	5000.00	143.00	0.89	10.00	5.33	0.20	558.00	155.00	1560.00
Stoughton-Roquemare : Mean	2788.53	62093.11	198.34	1515.77	149.64	5.83	0.10	3.36	0.94	0.06	115.99	50.00	146.51
Stoughton-Roquemare : Median	1092.00	35718.10	133.00	384.00	18.00	1.10	0.04	3.00	0.74	0.05	72.00	41.70	117.00
Stoughton-Roquemare : Std. Dev	4025.00	70202.38	258.46	4046.77	627.72	22.20	0.17	2.48	0.88	0.03	126.22	33.19	191.94
Stoughton-Roquemare : 25 percentile	163.80	8401.90	74.00	122.00	7.50	0.25	0.01	2.00	0.37	0.05	19.50	26.65	58.00
Stoughton-Roquemare : 75 percentile	4081.35	84802.35	249.00	1400.00	47.00	3.00	0.11	4.00	1.31	0.05	191.00	65.45	165.00
Stoughton-Roquemare : 90 percentile	8053.50	154795.64	395.40	3006.00	189.00	7.50	0.30	7.60	2.08	0.10	291.80	101.60	253.20
Kidd-Munro : Minimum	13.65	53.40	18.00	9.00	2.50	0.25	0.00	0.50	0.03	0.05	0.50	4.70	9.00
Kidd-Munro : Maximum	72072.00	456645.10	10000.00	8860.00	455.00	19.50	3.49	30.00	3.76	0.50	1250.00	446.00	960.00
Kidd-Munro : Mean	8376.89	79895.91	467.25	1305.01	40.69	2.93	0.40	4.39	0.47	0.08	183.68	67.04	205.32
Kidd-Munro : Median	3467.10	30414.50	145.00	447.00	18.00	1.20	0.10	3.00	0.32	0.05	124.00	44.20	121.00
Kidd-Munro : Standard Deviation	12652.80	102530.89	1324.42	1830.10	62.99	3.79	0.64	5.12	0.56	0.08	214.87	64.24	186.05
Kidd-Munro : 25 percentile	941.85	7133.95	68.00	108.00	6.00	0.25	0.02	1.00	0.03	0.05	26.50	26.60	79.50
Kidd-Munro : 75 percentile	8585.85	110009.45	414.00	1745.00	49.00	4.05	0.52	5.00	0.67	0.05	266.50	94.05	295.50
Kidd-Munro : 90 percentile	25132.38	256057.94	852.60	4266.00	101.20	8.34	1.22	9.60	1.00	0.20	484.20	130.60	492.40
Blake River : Minimum	0.00	18.40	9.00	29.00	2.50	0.25	0.00	0.50	0.03	0.05	0.50	6.80	6.00
Blake River : Maximum	77532.00	309813.00	2010.00	7550.00	491.00	14.70	3.01	15.00	3.64	0.40	1090.00	521.00	3110.00
Blake River : Mean	4833.16	35334.39	199.21	593.29	23.87	1.38	0.16	3.16	0.79	0.07	99.55	43.62	149.35
Blake River : Median	1911.00	9389.00	66.00	150.00	8.00	0.25	0.02	2.00	0.53	0.05	33.00	29.20	87.00
Blake River : Standard Deviation	10638.67	61935.61	362.61	1221.40	58.50	2.66	0.50	3.36	0.74	0.07	162.29	62.79	364.55
Blake River : 25 percentile	286.65	2634.70	33.00	90.50	2.50	0.25	0.00	1.00	0.28	0.05	14.00	17.75	51.50
Blake River : 75 percentile	4722.90	30243.00	165.50	374.00	27.00	1.00	0.07	4.00	1.19	0.05	127.00	45.95	126.50
Blake River : 90 percentile	9303.84	115635.60	544.20	1862.00	60.40	3.56	0.28	9.20	1.86	0.12	289.20	81.72	195.40
Tisdale : Minimum	13.65	2.10	4.00	12.00	2.50	0.25	0.00	0.50	0.03	0.05	0.50	6.90	17.00
Tisdale : Maximum	53508.00	260727.00	10000.00	9970.00	4730.00	24.40	2.07	37.00	4.95	1.10	2450.00	142.00	1170.00
Tisdale : Mean	5422.36	32864.87	622.21	1023.05	60.02	2.09	0.22	4.31	1.07	0.10	113.60	36.00	135.93
Tisdale : Median	3112.20	19799.00	131.00	386.00	16.00	0.90	0.04	3.00	0.78	0.05	52.00	30.30	111.00
Tisdale : Standard Deviation	7974.77	41677.25	1900.83	1394.62	369.46	3.06	0.37	5.55	0.98	0.13	214.29	21.55	131.14
Tisdale : 25 percentile	273.00	1452.50	59.00	95.50	5.00	0.25	0.00	1.00	0.39	0.05	18.50	24.55	84.00
Tisdale : 75 percentile	7371.00	46133.05	264.00	1630.00	33.00	3.05	0.29	5.00	1.39	0.05	166.00	40.65	144.00
Tisdale : 90 percentile	13546.26	72971.74	712.40	2792.00	53.60	5.30	0.57	10.60	2.58	0.20	215.60	61.96	204.40
Porcupine : Minimum	13.65	96.70	29.00	29.00	2.50	0.25	0.00	0.50	0.03	0.05	0.50	9.00	64.00
Porcupine : Maximum	18509.40	199727.00	579.00	4210.00	289.00	7.80	1.59	10.00	2.53	0.30	835.00	95.10	640.00
Porcupine : Mean	4726.42	16662.80	108.10	558.98	18.35	1.02	0.09	2.10	0.83	0.06	125.31	33.09	134.40
Porcupine : Median	2702.70	4069.65	76.50	144.00	10.00	0.25	0.01	1.50	0.65	0.05	65.50	28.95	109.50
Porcupine : Standard Deviation	4746.95	33159.58	106.37	910.54	38.20	1.65	0.28	1.95	0.61	0.03	154.69	14.36	99.29
Porcupine : 25 percentile	614.25	1384.41	61.25	96.50	5.75	0.25	0.00	1.00	0.41	0.05	26.25	25.30	92.00

Appendix A5. Statistical summary of major element and trace element concentrations grouped by shale lithotype, associated mineralization, and lithostratigraphic assemblage. Concentrations of major oxides given in weight percent, and trace elements given in ppm

Lithostratigrapic Assemblage	Se_ppm	Mo_ppm	Ge_ppm	Sb_ppm	Ag_ppm	Au_ppm	W_ppm	Bi_ppm	B_ppm	Rb_ppm	Sr_ppm	Cs_ppm	Ba_ppm	Be_ppm	Zr_ppm
Deloro : Minimum	0.25	1.00	0.25	0.05	0.25	0.00	0.50	0.05	1.00	0.50	12.00	0.05	0.50	0.50	5.00
Deloro : Maximum	21.80	18.00	8.00	17.30	4.70	0.07	19.00	6.50	449.00	168.00	420.00	5.30	2470.00	4.00	195.00
Deloro : Mean	2.30	4.37	2.21	2.18	0.70	0.01	2.87	1.47	80.49	43.77	122.51	1.59	352.11	1.15	96.54
Deloro : Median	0.25	3.00	1.40	0.70	0.50	0.01	0.50	1.00	31.00	37.00	72.00	1.40	239.00	1.00	90.00
Deloro : Standard Deviation	4.82	3.44	1.83	3.30	0.79	0.02	4.07	1.62	116.83	41.97	111.38	1.25	418.39	0.92	45.67
Deloro : 25 percentile	0.25	2.00	1.15	0.40	0.25	0.00	0.50	0.20	7.50	9.50	44.00	0.50	65.50	0.50	64.50
Deloro : 75 percentile	1.15	6.00	2.65	2.80	0.80	0.02	5.50	1.90	93.50	60.50	183.50	2.20	527.00	1.50	131.50
Deloro : 90 percentile	9.56	8.00	5.60	5.32	1.58	0.05	8.80	4.62	286.80	123.80	329.00	3.44	684.80	3.00	156.20
Stoughton-Roquemare : Minimum	0.25	1.00	0.25	0.05	0.25	0.00	0.50	0.05	1.00	0.50	6.00	0.05	8.00	0.50	16.00
Stoughton-Roquemare : Maximum	19.00	24.00	8.30	15.00	5.90	0.07	7.00	11.30	419.00	131.00	551.00	3.40	1510.00	2.00	315.00
Stoughton-Roquemare : Mean	2.73	5.59	1.67	2.57	0.84	0.02	2.08	1.80	44.08	48.23	109.88	1.40	371.63	0.75	116.12
Stoughton-Roquemare : Median	0.25	4.00	1.40	1.40	0.50	0.01	0.50	1.40	23.00	46.00	86.00	1.40	354.00	0.50	116.00
Stoughton-Roquemare : Std. Dev	4.11	4.57	1.30	2.97	0.97	0.02	2.27	1.94	71.18	30.29	98.15	0.86	278.81	0.38	57.57
Stoughton-Roquemare : 25 percentile	0.25	2.00	1.00	0.50	0.25	0.00	0.50	0.50	13.00	24.00	39.00	0.60	158.00	0.50	85.50
Stoughton-Roquemare : 75 percentile	3.55	7.00	1.95	3.40	0.95	0.03	4.00	2.65	39.50	69.50	152.50	2.00	490.00	1.00	145.50
Stoughton-Roquemare : 90 percentile	8.68	11.60	2.96	7.34	2.02	0.04	6.00	3.32	99.00	85.60	211.20	2.60	646.00	1.00	188.40
Kidd-Munro : Minimum	0.25	1.00	0.25	0.05	0.25	0.00	0.50	0.10	1.00	0.50	1.00	0.05	0.50	0.50	7.00
Kidd-Munro : Maximum	36.50	76.00	11.20	104.00	17.70	1.18	18.00	8.20	2980.00	185.00	548.00	12.80	2187.00	5.00	497.00
Kidd-Munro : Mean	4.79	8.44	1.84	8.77	0.99	0.05	1.65	2.01	102.60	42.03	111.29	1.56	344.38	0.99	110.34
Kidd-Munro : Median	0.25	4.00	1.40	3.60	0.60	0.02	0.50	1.30	24.00	26.00	87.00	0.50	213.00	0.50	102.00
Kidd-Munro : Standard Deviation	7.47	9.60	1.52	14.22	1.69	0.12	2.76	1.83	350.65	43.57	94.63	2.12	375.14	0.72	74.13
Kidd-Munro : 25 percentile	0.25	3.00	1.00	1.05	0.25	0.00	0.50	0.60	6.00	5.00	44.50	0.30	29.00	0.50	67.50
Kidd-Munro : 75 percentile	7.30	12.00	2.00	11.35	1.15	0.04	0.50	3.25	71.00	74.50	149.00	2.10	577.50	1.00	132.00
Kidd-Munro : 90 percentile	15.32	20.60	3.60	22.22	2.00	0.09	6.00	4.90	156.60	99.60	246.80	5.00	750.00	2.00	156.60
Blake River : Minimum	0.25	1.00	0.50	0.05	0.25	0.00	0.50	0.05	1.00	1.00	8.00	0.05	5.00	0.50	20.00
Blake River : Maximum	18.10	64.00	5.20	106.00	3.50	1.04	17.00	14.10	610.00	151.00	584.00	7.80	1244.00	3.00	277.00
Blake River : Mean	1.95	5.23	1.58	4.05	0.63	0.05	1.99	1.57	64.79	68.95	121.61	2.04	448.53	1.12	123.12
Blake River : Median	0.25	3.00	1.50	1.10	0.25	0.01	0.50	0.70	36.00	69.00	80.00	1.90	432.00	1.00	120.00
Blake River : Standard Deviation	3.90	8.07	0.75	12.53	0.59	0.15	2.89	2.32	94.19	37.87	114.52	1.51	255.78	0.67	47.95
Blake River : 25 percentile	0.25	2.00	1.20	0.50	0.25	0.00	0.50	0.30	16.00	45.00	44.50	1.00	258.50	0.50	93.00
Blake River : 75 percentile	0.25	5.50	1.80	3.45	0.70	0.04	2.50	2.00	69.00	95.00	161.00	2.90	630.50	2.00	144.00
Blake River : 90 percentile	7.68	9.20	2.22	8.78	1.50	0.09	6.00	3.22	144.00	124.40	271.40	3.52	735.60	2.00	178.20
Tisdale : Minimum	0.25	1.00	0.50	0.05	0.25	0.00	0.50	0.05	1.00	1.00	5.00	0.05	3.00	0.50	36.00
Tisdale : Maximum	20.90	59.00	6.70	32.80	19.50	30.00	50.00	249.00	1800.00	165.00	696.00	8.70	1596.00	3.00	297.00
Tisdale : Mean	1.71	5.38	1.89	3.37	1.12	0.25	2.66	4.01	95.36	75.12	136.10	2.39	510.90	1.18	124.49
Tisdale : Median	0.25	4.00	1.70	2.00	0.60	0.01	0.50	1.00	52.00	81.00	103.00	2.00	520.00	1.00	124.00
Tisdale : Standard Deviation	3.21	6.30	0.89	4.56	2.20	2.33	5.08	21.19	164.74	36.32	112.13	1.66	267.97	0.63	37.43
Tisdale : 25 percentile	0.25	2.00	1.30	0.65	0.25	0.00	0.50	0.50	30.00	54.50	64.00	1.20	357.50	0.50	108.00
Tisdale : 75 percentile	1.10	6.00	2.30	4.45	1.00	0.04	4.00	1.80	97.50	98.00	177.50	3.30	646.00	2.00	138.00
Tisdale : 90 percentile	6.56	10.00	3.06	8.28	1.76	0.09	6.00	3.72	211.40	118.00	249.20	4.36	841.40	2.00	166.20
Porcupine : Minimum	0.25	1.00	0.90	0.05	0.25	0.00	0.50	0.10	1.00	3.00	19.00	0.30	7.00	0.50	73.00
Porcupine : Maximum	14.20	13.00	5.30	23.30	2.20	0.31	10.00	7.50	826.00	116.00	440.00	17.40	924.00	2.00	179.00
Porcupine : Mean	0.63	2.61	1.86	5.06	0.48	0.02	2.46	1.04	125.15	80.23	200.24	6.81	536.26	1.41	127.74
Porcupine : Median	0.25	1.50	1.70	2.85	0.25	0.00	0.50	0.55	85.50	85.00	198.50	5.25	526.50	1.00	124.50
Porcupine : Standard Deviation	2.11	2.46	0.63	5.64	0.37	0.04	2.81	1.23	136.58	24.05	91.35	4.80	187.34	0.53	21.36
Porcupine : 25 percentile	0.25	1.00	1.58	0.50	0.25	0.00	0.50	0.30	49.75	69.00	131.75	2.98	425.75	1.00	115.75

Appendix A5. Statistical summary of major element and trace element concentrations grouped by shale lithotype, associated mineralization, and lithostratigraphic assemblage. Concentrations of major oxides given in weight percent, and trace elements given in ppm

Lithostratigrapic Assemblage	Hf_ppm	Nb_ppm	Ta_ppm	Ga_ppm	Sc_ppm	V_ppm	Cr_ppm	Th_ppm	U_ppm	Y_ppm	La_ppm	Ce_ppm	Pr_ppm	Nd_ppm	Sm_ppm
Deloro : Minimum	0.05	0.30	0.03	2.00	1.07	6.00	0.25	0.13	0.06	2.00	1.37	2.49	0.28	1.18	0.24
Deloro : Maximum	5.00	8.60	0.95	28.00	52.00	340.00	2710.00	5.96	2.54	30.00	44.40	92.90	10.80	40.30	5.88
Deloro : Mean	2.45	4.21	0.35	15.68	16.18	95.44	166.73	2.43	0.73	12.73	14.14	30.72	3.72	14.54	2.89
Deloro : Median	2.40	4.30	0.36	16.00	12.30	77.00	50.30	2.38	0.69	12.00	12.30	28.10	3.54	13.30	2.72
Deloro : Standard Deviation	1.14	2.09	0.19	6.18	11.40	72.01	445.99	1.49	0.47	5.63	9.77	20.26	2.29	8.48	1.35
Deloro : 25 percentile	1.65	2.45	0.19	11.50	9.18	49.00	29.75	1.27	0.44	9.00	6.80	15.65	2.03	8.41	1.94
Deloro : 75 percentile	3.35	5.50	0.46	19.50	20.00	120.50	86.60	3.34	0.97	16.00	18.85	42.10	5.25	21.55	4.19
Deloro : 90 percentile	4.06	6.88	0.57	23.80	33.72	181.20	283.40	4.45	1.24	19.80	26.30	55.88	6.56	25.42	4.47
Stoughton-Roquemare : Minimum	0.40	0.60	0.06	2.00	1.64	8.00	7.10	0.18	0.08	2.00	2.27	4.87	0.58	2.24	0.49
Stoughton-Roquemare : Maximum	8.50	12.80	1.01	40.00	49.70	442.00	3120.00	11.70	2.92	40.00	53.80	106.00	11.70	42.40	6.70
Stoughton-Roquemare : Mean	2.89	4.94	0.40	16.44	15.15	84.26	142.24	3.23	0.90	15.18	16.06	34.95	4.14	16.21	3.24
Stoughton-Roquemare : Median	2.90	5.10	0.41	17.00	14.00	68.00	50.20	3.20	0.89	14.00	14.20	30.90	3.70	14.60	3.24
Stoughton-Roquemare : Std. Dev	1.46	2.45	0.19	5.95	9.99	73.38	383.29	1.97	0.51	7.58	11.18	22.38	2.49	9.12	1.52
Stoughton-Roquemare : 25 percentile	2.05	3.10	0.26	13.50	7.75	43.00	30.45	1.88	0.54	10.00	6.69	16.60	2.39	10.31	2.25
Stoughton-Roquemare : 75 percentile	3.55	6.05	0.50	20.00	18.05	92.50	105.50	4.14	1.15	19.00	21.40	46.40	5.62	22.10	4.25
Stoughton-Roquemare : 90 percentile	4.40	7.86	0.58	22.00	27.68	144.60	303.40	6.20	1.66	25.60	28.88	62.52	7.46	27.94	5.24
Kidd-Munro : Minimum	0.20	0.30	0.02	2.00	2.11	6.00	0.25	0.14	0.04	2.00	1.37	2.79	0.39	1.82	0.41
Kidd-Munro : Maximum	17.50	46.70	4.70	37.00	36.40	244.00	2480.00	22.10	6.24	102.00	93.40	190.00	20.80	76.60	16.00
Kidd-Munro : Mean	2.93	6.01	0.49	15.59	15.31	82.37	150.68	4.40	1.29	19.71	19.68	43.20	5.23	20.32	4.21
Kidd-Munro : Median	2.70	4.90	0.40	15.00	14.70	74.00	73.90	3.94	1.18	16.00	17.90	40.90	4.88	18.90	3.98
Kidd-Munro : Standard Deviation	2.23	6.11	0.54	7.17	7.17	47.88	283.32	2.81	0.76	14.68	12.44	26.77	3.13	12.05	2.46
Kidd-Munro : 25 percentile	1.75	3.05	0.26	10.50	9.88	50.00	38.45	2.75	0.83	13.00	11.10	26.30	3.30	13.20	2.79
Kidd-Munro : 75 percentile	3.55	6.95	0.53	20.50	20.10	105.50	157.50	5.59	1.67	22.50	25.65	56.45	6.59	25.40	5.05
Kidd-Munro : 90 percentile	4.26	8.58	0.71	24.00	25.44	159.00	300.60	7.49	2.10	29.00	32.12	67.66	7.83	30.26	6.02
Blake River : Minimum	0.50	0.70	0.05	5.00	2.73	6.00	0.25	0.31	0.08	6.00	3.56	8.87	1.30	5.60	0.99
Blake River : Maximum	7.70	25.80	1.86	30.00	51.50	352.00	1210.00	18.50	4.83	313.00	58.30	135.00	17.00	68.70	16.60
Blake River : Mean	3.21	6.10	0.49	19.30	16.10	99.35	103.11	4.63	1.29	22.52	20.49	44.39	5.40	21.16	4.22
Blake River : Median	3.10	5.80	0.44	20.00	14.40	89.00	58.00	4.26	1.14	16.00	19.10	41.20	5.14	20.00	3.79
Blake River : Standard Deviation	1.31	3.48	0.28	4.70	8.47	65.26	153.25	3.23	0.94	36.75	11.89	24.96	3.06	11.69	2.45
Blake River : 25 percentile	2.50	4.10	0.31	16.50	11.15	52.50	25.10	2.37	0.71	13.00	11.35	25.80	3.15	12.70	2.86
Blake River : 75 percentile	3.70	7.05	0.61	22.00	20.05	139.50	148.50	5.40	1.54	20.50	25.35	54.10	6.39	25.40	4.77
Blake River : 90 percentile	4.84	9.48	0.86	25.00	24.40	167.60	200.80	8.04	2.11	29.20	37.50	80.10	9.68	35.56	6.59
Tisdale : Minimum	0.90	1.40	0.08	6.00	4.36	19.00	11.10	0.15	0.07	4.00	1.77	5.04	0.80	4.10	1.21
Tisdale : Maximum	7.20	51.50	0.94	39.00	44.00	285.00	2190.00	17.10	18.60	46.00	123.00	237.00	29.00	115.00	20.50
Tisdale : Mean	3.24	6.26	0.47	20.58	17.74	109.85	134.23	5.57	1.64	16.32	23.93	50.89	5.94	23.03	4.34
Tisdale : Median	3.20	6.10	0.46	21.00	16.90	96.00	77.50	5.40	1.56	15.00	24.30	52.10	6.11	23.30	4.27
Tisdale : Standard Deviation	0.98	4.00	0.15	5.37	6.19	52.30	210.27	2.93	1.52	5.78	12.59	24.60	2.88	10.98	1.88
Tisdale : 25 percentile	2.85	4.90	0.38	18.00	14.05	73.00	51.20	3.59	0.96	12.00	17.85	38.20	4.48	17.75	3.41
Tisdale : 75 percentile	3.60	7.10	0.54	24.00	20.85	143.50	178.50	6.98	1.99	18.00	28.80	60.95	7.01	27.00	4.92
Tisdale : 90 percentile	4.40	8.26	0.64	27.00	24.16	174.00	241.20	9.01	2.52	22.00	33.96	71.34	8.15	31.36	5.88
Porcupine : Minimum	1.90	3.60	0.32	10.00	12.40	58.00	53.20	2.19	0.60	7.00	5.94	15.50	2.03	8.19	2.11
Porcupine : Maximum	4.90	10.60	0.78	32.00	38.50	257.00	1030.00	10.10	26.30	24.00	75.60	141.00	16.70	57.10	8.91
Porcupine : Mean	3.35	5.69	0.46	23.58	19.92	133.89	157.43	5.46	1.89	14.42	22.45	47.56	5.66	21.73	4.06
Porcupine : Median	3.30	5.65	0.45	24.00	19.90	144.00	142.50	5.26	1.48	14.00	21.80	46.75	5.44	21.15	3.99
Porcupine : Standard Deviation	0.56	1.22	0.10	4.30	5.31	45.60	133.72	1.61	3.18	3.43	8.90	16.68	1.95	6.69	1.00
Porcupine : 25 percentile	3.00	4.80	0.39	22.00	15.95	92.00	85.88	4.31	1.17	12.00	18.58	40.18	4.85	19.20	3.58

Appendix A5. Statistical summary of major element and trace element concentrations grouped by shale lithotype, associated mineralization, and lithostratigraphic assemblage. Concentrations of major oxides given in weight percent, and trace elements given in ppm

Lithostratigrapic Assemblage	Eu_ppm	Gd_ppm	Tb_ppm	Dy_ppm	Ho_ppm	Er_ppm	Tm_ppm	Yb_ppm	Lu_ppm	Br_ppm
Deloro : Minimum	0.12	0.22	0.04	0.21	0.05	0.15	0.03	0.16	0.02	0.25
Deloro : Maximum	1.95	4.28	0.83	5.05	1.07	3.17	0.49	3.17	0.52	6.70
Deloro : Mean	0.89	2.49	0.40	2.26	0.46	1.34	0.20	1.41	0.24	1.28
Deloro : Median	0.95	2.43	0.42	2.14	0.42	1.27	0.19	1.35	0.23	0.90
Deloro : Standard Deviation	0.40	1.04	0.17	0.99	0.21	0.60	0.09	0.62	0.10	1.35
Deloro : 25 percentile	0.63	1.81	0.29	1.73	0.35	1.02	0.15	1.04	0.18	0.25
Deloro : 75 percentile	1.15	3.34	0.49	2.72	0.57	1.64	0.25	1.75	0.29	1.95
Deloro : 90 percentile	1.33	3.92	0.64	3.62	0.72	2.07	0.30	2.07	0.35	2.78
Stoughton-Roquemare : Minimum	0.14	0.48	0.10	0.51	0.10	0.26	0.04	0.25	0.04	0.25
Stoughton-Roquemare : Maximum	2.06	5.82	1.05	6.70	1.44	4.11	0.65	4.44	0.77	30.20
Stoughton-Roquemare : Mean	0.90	2.79	0.46	2.66	0.54	1.63	0.25	1.70	0.29	3.46
Stoughton-Roquemare : Median	0.87	2.61	0.44	2.52	0.51	1.56	0.23	1.63	0.28	1.80
Stoughton-Roquemare : Std. Dev	0.36	1.22	0.21	1.26	0.27	0.80	0.13	0.87	0.15	5.31
Stoughton-Roquemare : 25 percentile	0.69	2.05	0.34	1.87	0.37	1.08	0.16	1.09	0.18	0.25
Stoughton-Roquemare : 75 percentile	1.13	3.57	0.57	3.20	0.66	2.00	0.31	2.08	0.38	3.90
Stoughton-Roquemare : 90 percentile	1.32	4.52	0.78	4.69	0.97	2.87	0.44	2.98	0.51	10.98
Kidd-Munro : Minimum	0.15	0.32	0.06	0.32	0.06	0.20	0.03	0.19	0.04	0.25
Kidd-Munro : Maximum	4.11	15.80	3.12	20.40	4.20	11.60	1.71	10.40	1.78	18.40
Kidd-Munro : Mean	1.35	3.74	0.62	3.58	0.72	2.11	0.32	2.18	0.37	1.83
Kidd-Munro : Median	1.23	3.47	0.56	3.02	0.60	1.75	0.26	1.79	0.31	0.25
Kidd-Munro : Standard Deviation	0.76	2.33	0.43	2.67	0.55	1.58	0.24	1.56	0.25	2.61
Kidd-Munro : 25 percentile	0.85	2.49	0.41	2.26	0.45	1.32	0.20	1.33	0.23	0.25
Kidd-Munro : 75 percentile	1.67	4.15	0.68	4.10	0.83	2.46	0.37	2.53	0.46	2.50
Kidd-Munro : 90 percentile	2.22	5.21	0.87	5.26	1.07	3.12	0.49	3.50	0.61	4.98
Blake River : Minimum	0.21	0.92	0.17	1.05	0.21	0.59	0.09	0.54	0.09	0.25
Blake River : Maximum	3.13	25.00	5.37	37.20	8.86	27.00	4.07	25.10	4.06	8.40
Blake River : Mean	1.13	3.83	0.63	3.71	0.77	2.26	0.34	2.27	0.38	1.52
Blake River : Median	1.09	3.31	0.53	2.95	0.59	1.69	0.25	1.69	0.28	0.25
Blake River : Standard Deviation	0.44	3.12	0.65	4.44	1.05	3.18	0.48	3.00	0.49	1.91
Blake River : 25 percentile	0.87	2.75	0.43	2.43	0.48	1.37	0.21	1.37	0.23	0.25
Blake River : 75 percentile	1.32	3.87	0.59	3.45	0.72	2.06	0.32	2.23	0.38	2.05
Blake River : 90 percentile	1.68	5.63	0.92	5.22	1.09	3.19	0.49	3.25	0.53	4.38
Tisdale : Minimum	0.30	0.98	0.16	0.87	0.18	0.55	0.09	0.57	0.10	0.25
Tisdale : Maximum	4.91	16.90	1.85	8.52	1.60	4.71	0.74	5.08	0.87	23.80
Tisdale : Mean	1.13	3.46	0.52	2.95	0.59	1.71	0.25	1.76	0.30	1.40
Tisdale : Median	1.10	3.37	0.50	2.83	0.55	1.59	0.23	1.60	0.28	0.25
Tisdale : Standard Deviation	0.45	1.47	0.19	1.03	0.20	0.58	0.09	0.61	0.10	2.34
Tisdale : 25 percentile	0.91	2.69	0.40	2.33	0.46	1.36	0.20	1.42	0.25	0.25
Tisdale : 75 percentile	1.31	3.92	0.58	3.30	0.66	1.90	0.29	1.99	0.34	1.70
Tisdale : 90 percentile	1.48	4.60	0.70	3.93	0.79	2.36	0.35	2.38	0.42	2.96
Porcupine : Minimum	0.45	1.87	0.29	1.59	0.28	0.87	0.13	0.83	0.13	0.25
Porcupine : Maximum	1.99	6.82	0.96	5.39	1.05	2.99	0.41	2.87	0.47	4.00
Porcupine : Mean	1.07	3.24	0.48	2.75	0.54	1.57	0.23	1.58	0.27	0.78
Porcupine : Median	1.06	3.26	0.47	2.69	0.52	1.54	0.23	1.56	0.26	0.25
Porcupine : Standard Deviation	0.27	0.75	0.11	0.64	0.13	0.38	0.06	0.38	0.06	0.79
Porcupine : 25 percentile	0.95	2.90	0.41	2.33	0.46	1.32	0.19	1.35	0.23	0.25

Appendix A6. Principal component scores for PC1 - 4 for every black shale sample. Samples are ordered from highest to lowest PC1 score.

Sample #	PC1	PC2	PC3	PC4	Sample #	PC1	PC2	PC3	PC4
4095	13.47	-4.69	-12.31	5.19	4479	5.70	0.96	1.34	-1.33
4049	10.51	-8.81	-14.12	6.52	7408	5.68	0.31	1.86	0.18
4377	10.17	-3.57	-4.03	1.04	4077	5.68	0.59	0.05	-2.04
4087	9.75	-5.54	-11.28	4.61	7462	5.68	0.96	2.74	-1.68
8580	8.96	1.19	-1.68	-2.53	4475	5.66	1.72	2.50	-1.13
4147	8.33	-2.72	-9.19	-0.06	4456	5.65	-0.03	1.83	-1.04
4146	8.01	-5.86	-12.12	4.76	8578	5.65	0.76	0.48	-1.77
8568	7.96	-1.01	-2.46	1.52	4438	5.63	0.11	1.21	-0.58
7467	7.96	-2.66	1.48	-0.32	4499	5.62	-0.65	1.42	-0.57
4496	7.93	-1.30	1.63	-1.24	4091	5.60	-2.52	-2.44	1.21
7403	7.88	-1.25	1.44	-0.88	4062	5.57	-0.67	1.26	0.87
4047	7.88	-1.57	-5.12	4.67	4493	5.57	-1.59	2.86	-0.25
4191	7.88	-3.51	-6.62	4.54	4076	5.55	0.97	1.85	-1.44
7410	7.64	-1.31	1.47	-0.51	7409	5.54	-0.86	1.89	-1.43
4498	7.64	-1.96	0.77	-1.63	4073	5.52	2.64	-1.06	1.88
4495	7.58	-1.25	0.97	-1.08	8529	5.51	1.80	1.93	0.56
4341	7.32	-2.04	2.26	-1.82	7476	5.49	0.40	0.34	0.58
7463	7.32	0.27	1.03	-0.67	8584	5.48	0.00	0.75	-0.54
4339	7.22	1.49	1.48	-0.36	7402	5.46	-1.13	1.58	-1.35
4448	7.21	1.91	1.49	-1.78	4489	5.42	-1.78	0.84	1.61
7421	7.21	0.59	1.16	-1.79	7460	5.41	-2.34	-5.24	2.19
4096	7.10	-4.17	-9.52	2.66	4019	5.40	1.20	1.07	-1.99
4331	7.09	-1.32	1.01	-1.76	4068	5.40	1.31	2.26	-1.80
4480	7.01	0.08	1.35	-1.44	7485	5.35	-2.48	1.36	0.02
4492	6.97	-0.79	0.64	-1.57	7471	5.33	-0.40	-4.02	-1.69
7492	6.95	0.07	1.45	-1.18	4043	5.30	3.59	0.05	0.13
4120	6.81	-2.59	-8.35	4.11	4343	5.29	-0.41	2.03	-2.54
7404	6.77	-1.11	1.23	-0.87	8582	5.26	-0.02	-7.06	0.65
4383	6.77	-2.03	-1.68	2.68	7452	5.20	1.21	1.76	-0.63
8501	6.74	-0.22	-2.25	1.67	4008	5.19	0.15	-1.31	0.75
4491	6.54	-4.10	2.53	-2.46	7486	5.18	0.21	2.15	-1.52
7420	6.41	0.97	1.59	-1.39	7453	5.18	1.03	2.08	-1.24
4500	6.33	-1.30	1.82	-0.21	8538	5.17	0.49	2.33	-1.45
4166	6.32	-1.78	0.24	1.19	7418	5.07	2.18	1.27	-1.59
7407	6.30	-1.07	2.52	-1.10	8536	5.01	0.79	2.33	0.58
4347	6.29	-2.07	0.94	-2.82	4143	5.00	-0.09	-1.66	-1.50
4022	6.27	-2.81	-2.92	2.47	7488	4.99	2.65	1.03	-2.13
4078	6.22	0.45	0.48	-2.20	4348	4.96	1.38	0.34	-1.52
4478	6.22	1.21	1.13	-1.20	4158	4.96	2.68	-0.33	-0.43
8556	6.17	-2.04	2.44	1.34	7417	4.94	2.27	1.93	-0.97
4404	6.09	-0.44	2.04	-2.19	4488	4.93	1.27	1.38	-1.15
4344	6.08	-2.90	2.61	-1.45	4367	4.92	-2.14	1.70	-0.07
7498	6.06	0.87	1.36	-1.58	4381	4.89	2.24	0.80	1.00
8520	5.96	0.90	1.76	1.12	4006	4.89	-2.43	2.05	1.44
4030	5.96	-10.11	2.38	1.59	7483	4.88	0.72	1.42	-0.05
4483	5.90	1.09	1.50	-1.34	4482	4.87	1.70	0.91	-1.26
7416	5.87	1.85	1.04	-1.33	4452	4.85	0.97	2.26	-1.09
8590	5.86	0.92	-0.95	-2.59	8591	4.84	1.60	1.65	-0.87
7401	5.79	-1.17	1.57	-0.84	8537	4.83	1.48	1.81	1.11
4333	5.79	-0.83	1.65	-1.26	7441	4.77	-1.93	1.64	-0.37
8527	5.77	-0.01	2.56	-0.37	8565	4.71	-0.21	2.21	0.07
4400	5.76	0.10	2.52	-0.72	8569	4.68	-1.48	-6.59	2.56
8539	5.76	0.97	1.80	-0.74	4398	4.66	-2.57	-1.58	3.25

Sample #	PC1	PC2	PC3	PC4	Sample #	PC1	PC2	PC3	PC4
7459	4.61	-2.78	0.97	-1.50	4346	3.45	2.51	0.93	-1.44
4437	4.61	0.64	2.69	0.38	8522	3.43	2.31	3.02	0.64
4067	4.61	1.13	0.89	-1.59	7433	3.36	1.13	3.68	-0.18
4412	4.54	-2.20	2.13	-0.35	4168	3.34	0.68	0.63	1.72
4090	4.54	0.50	1.97	-0.68	4052	3.24	2.82	-0.55	-0.07
4342	4.50	1.53	3.01	-0.19	8519	3.15	1.61	2.12	-0.02
7468	4.46	-2.20	1.51	0.25	8502	3.13	1.23	-0.78	-1.21
8532	4.36	1.22	1.67	0.72	7478	3.04	2.95	-0.81	-0.68
4471	4.36	1.80	1.88	-0.57	4382	3.04	0.05	1.52	-0.10
4384	4.36	0.49	-1.85	1.43	4031	3.04	-1.21	1.55	1.25
4487	4.35	1.83	1.67	-1.12	8572	3.02	1.58	-3.84	0.90
4072	4.34	-8.44	3.13	3.92	7411	3.02	0.56	2.55	-0.06
4476	4.31	0.84	2.17	-0.66	4374	3.01	-0.19	0.09	2.79
8586	4.30	2.28	1.82	-0.43	4451	3.01	0.44	-1.07	2.02
8560	4.27	-0.62	-0.77	0.96	4104	2.99	3.43	1.97	-1.15
4378	4.25	-6.66	-0.53	-1.42	4138	2.93	1.78	1.92	-0.43
4357	4.24	-0.53	1.34	-0.85	4450	2.93	1.19	-2.13	2.18
4340	4.23	1.12	2.06	-0.51	8525	2.92	1.69	2.62	1.03
4140	4.22	-0.63	-3.20	3.34	7429	2.90	2.69	2.00	-1.26
4330	4.21	1.84	1.21	0.39	4481	2.89	-0.23	0.50	1.39
8579	4.20	2.57	1.01	-0.60	04138D	2.87	1.62	1.69	-0.50
4199	4.13	0.57	2.50	-0.91	8530	2.85	2.83	2.32	0.21
8581	4.12	0.88	-0.62	1.07	7449	2.84	1.60	2.57	-0.32
4169	4.11	-9.65	6.32	2.88	4028	2.80	1.87	-0.90	-1.84
4178	4.09	1.69	0.25	-0.57	4150	2.78	-0.08	-4.20	1.60
8570	4.06	-8.49	2.14	3.51	4070	2.74	4.06	-0.49	1.92
7430	4.06	1.00	2.63	-0.75	8571	2.73	2.12	-0.20	0.52
8524	4.05	1.27	2.59	0.39	7479	2.72	1.92	-0.94	-0.54
7477	3.99	1.38	-0.43	-1.51	7431	2.70	3.28	1.31	-0.37
4083	3.99	-2.95	3.26	1.55	7432	2.67	2.08	1.32	-1.06
4345	3.98	0.92	2.35	-0.43	4403	2.61	1.47	0.20	-2.05
4010	3.98	3.30	2.51	-0.39	8526	2.58	0.54	2.84	0.78
7412	3.88	-0.94	1.04	-0.64	4196	2.56	-0.65	-2.67	-4.29
4465	3.86	-2.39	-1.29	0.16	4075	2.54	2.10	1.18	0.64
7495	3.86	0.64	2.31	0.11	4118	2.52	2.98	0.83	0.70
4100	3.85	1.25	-0.93	2.76	4175	2.52	2.64	-0.21	-1.84
7458	3.76	-1.44	-0.01	-1.28	4159	2.49	2.44	-0.52	-0.79
4054	3.73	3.69	-0.74	-0.61	8583	2.49	3.21	-0.12	-0.24
4380	3.71	0.39	-1.52	0.89	8523	2.47	2.78	1.49	-0.11
4005	3.70	3.26	1.82	-0.40	4116	2.41	-2.40	-3.53	3.55
4061	3.69	-0.87	3.07	-1.39	4356	2.41	0.75	3.06	-0.79
8521	3.64	1.94	2.85	0.98	4023	2.40	-10.24	5.49	2.14
4184	3.63	-5.12	-0.82	-0.70	4162	2.37	-0.07	-2.57	-0.37
8528	3.63	1.05	2.81	0.32	8531	2.30	3.28	2.09	0.41
4007	3.62	-10.42	4.78	1.86	7448	2.28	1.98	2.15	0.52
04180B	3.62	0.72	-2.25	0.19	7447	2.25	1.33	2.74	0.43
7469	3.59	0.72	-1.96	2.95	4447	2.21	2.80	1.64	0.17
4185	3.58	-0.25	0.01	0.33	4057	2.00	2.04	0.50	0.35
7435	3.53	-2.03	1.93	-0.15	7466	1.91	-9.75	-2.16	-4.52
4325	3.53	1.67	-1.55	-1.30	7451	1.91	3.46	2.99	0.08
4156	3.52	-1.79	2.10	0.44	7474	1.91	3.09	-0.17	-0.51
8589	3.47	0.21	1.55	-0.24	4334	1.89	1.96	0.61	-0.36
7442	3.47	-2.34	2.15	0.27	7437	1.84	3.06	1.22	-0.28

Sample #	PC1	PC2	PC3	PC4	Sample #	PC1	PC2	PC3	PC4
4011	1.79	-4.23	6.27	4.72	4406	0.40	2.86	-1.59	-0.18
4157	1.79	0.56	-1.21	-1.74	8563	0.38	2.64	-0.26	0.75
4405	1.74	-4.83	2.09	-0.40	4197	0.36	-0.92	-2.06	-3.99
4020	1.71	1.28	2.93	-0.82	4027	0.34	2.51	0.79	-0.53
4372	1.63	-0.33	-1.74	0.88	04193B	0.29	0.69	-1.84	-2.54
4180	1.62	0.10	-1.23	1.10	4012	0.22	0.00	-1.61	0.05
7475	1.60	2.19	0.84	0.56	4119	0.22	1.48	-0.42	-1.36
4085	1.58	2.10	0.94	-0.23	7450	0.20	4.07	3.26	1.91
7482	1.56	-2.32	-4.32	-2.81	8558	0.19	0.44	0.78	0.39
4326	1.55	1.05	0.36	-0.06	4003	0.18	-3.82	1.85	1.27
7423	1.55	2.11	-4.61	-0.13	4081	0.15	2.22	-0.54	-1.77
8533	1.53	2.67	2.72	0.21	04164B	0.15	1.74	2.16	1.59
4130	1.41	3.95	0.01	-0.82	4320	0.14	-0.10	-4.56	2.24
7446	1.40	2.52	2.13	0.50	4379	0.13	3.07	-0.15	1.07
4387	1.39	-0.08	-2.31	0.86	4350	0.11	2.99	1.62	-0.47
4129	1.30	0.79	-0.40	-0.80	04171B	0.09	1.06	-3.21	1.93
04405D	1.28	-4.61	2.32	-0.33	7439	0.06	3.42	-2.11	-0.94
8546	1.27	-5.34	-5.17	-3.03	4136	0.04	2.12	-0.10	-0.64
7487	1.23	1.42	1.16	1.51	7405	0.03	-1.91	-0.83	0.84
4018	1.21	-1.58	-1.39	0.07	04320B	-0.01	1.71	-1.55	2.74
7472	1.20	1.53	-1.11	0.65	8543	-0.01	-7.77	-1.58	-5.06
07413D	1.15	2.86	-1.83	0.04	8588	-0.01	3.79	-2.69	-0.43
04112B	1.13	1.85	0.35	-0.28	7438	-0.02	3.09	-1.32	-0.91
7470	1.12	2.15	1.05	0.68	4361	-0.03	0.69	-0.07	2.47
4353	1.05	2.31	1.59	-0.21	4141	-0.04	-7.88	-1.31	-3.50
4171	1.03	2.51	-1.49	2.05	4034	-0.07	-1.47	-4.48	3.21
4058	1.02	1.64	1.93	2.35	8566	-0.09	-6.38	7.10	3.45
4174	1.01	-1.74	1.20	2.01	4399	-0.10	0.60	0.21	1.67
4172	0.99	-2.05	1.44	-1.09	4170	-0.10	-6.35	2.29	3.71
8515	0.97	-8.50	-2.96	-3.50	4192	-0.15	3.17	-1.55	-1.33
8577	0.96	-2.44	-6.31	2.77	04329A	-0.19	3.12	2.17	-0.47
4115	0.96	-1.56	-1.03	-1.94	7414	-0.21	1.96	-1.12	0.72
4421	0.96	3.65	0.28	-0.79	7464	-0.26	-8.55	2.36	-3.16
7480	0.92	3.06	0.27	-0.97	4151	-0.31	0.11	0.85	0.59
4132	0.91	3.99	-0.54	-0.85	4015	-0.33	-1.95	-1.65	-1.96
4200	0.88	0.98	0.39	-0.79	7500	-0.35	-4.64	3.08	-2.74
4375	0.85	-0.42	-3.73	-1.44	4105	-0.36	-0.09	-0.92	-2.39
4358	0.82	4.23	0.31	-1.78	04198A	-0.36	1.04	2.93	-0.83
4064	0.80	-1.04	0.60	1.64	4457	-0.41	4.64	-1.65	-0.92
4060	0.79	2.05	1.61	-0.90	4324	-0.45	1.15	-0.59	-0.59
4477	0.79	3.72	-0.05	0.25	7456	-0.46	4.25	1.58	-0.71
4160	0.72	2.59	-0.08	-0.78	4355	-0.48	0.38	3.40	-0.23
4039	0.69	4.50	0.21	0.89	4371	-0.50	3.67	-1.60	-0.35
4195	0.64	0.49	-2.66	-2.10	4126	-0.50	-0.78	-1.18	2.33
4368	0.63	-0.21	-4.63	4.41	8576	-0.51	-2.73	-5.61	2.12
4182	0.62	-2.10	-0.04	2.53	7422	-0.58	2.36	-3.28	-0.69
4173	0.60	-5.00	-0.92	-3.66	4386	-0.59	-4.18	-4.00	0.37
7413	0.59	2.94	-1.92	-0.07	4453	-0.60	1.95	-2.93	0.71
7461	0.59	-0.62	1.27	0.85	7436	-0.64	2.71	1.17	-1.18
8573	0.56	3.02	-0.13	-0.85	4366	-0.66	-6.88	6.21	5.53
4071	0.50	-7.77	6.44	2.03	4059	-0.67	2.52	1.54	0.32
7406	0.49	1.99	-1.07	0.74	4053	-0.69	4.01	1.91	-1.90
4164	0.48	2.34	2.82	1.00	4112	-0.71	1.81	0.58	1.27

Sample #	PC1	PC2	PC3	PC4	Sample #	PC1	PC2	PC3	PC4
7454	-0.74	-0.04	-0.97	0.61	4369	-2.15	3.30	-0.71	-0.69
8585	-0.74	3.16	-1.08	-1.05	04198B	-2.16	0.59	2.82	-1.15
4446	-0.75	3.65	-0.44	-0.15	4125	-2.18	2.73	-0.55	2.40
04389A	-0.78	3.33	0.44	1.12	4021	-2.28	-1.05	-0.40	1.81
4154	-0.79	2.98	-0.54	-1.14	4004	-2.29	0.60	-1.34	1.68
4106	-0.80	1.41	1.29	1.11	4388	-2.29	-0.37	-1.74	0.18
4124	-0.81	2.24	1.01	1.64	7425	-2.31	3.57	-1.04	0.07
8534	-0.82	4.21	-1.17	-1.00	8559	-2.32	3.23	-0.18	0.63
7428	-0.83	4.57	-0.20	-0.70	8513	-2.33	-7.52	-5.25	-3.74
4327	-0.86	3.17	-2.66	-1.03	4014	-2.40	-3.04	-1.90	-1.08
4016	-0.86	3.41	0.64	-1.06	4411	-2.40	4.36	-0.22	-0.98
4466	-0.88	0.87	-1.65	0.09	4152	-2.42	0.81	0.23	-0.21
4165	-0.88	3.16	-2.40	0.48	04117B	-2.44	2.82	-0.76	-1.86
4117	-0.89	2.06	-3.99	-0.44	4122	-2.47	1.43	-2.05	-0.08
7496	-0.91	-1.93	-0.30	-3.73	4153	-2.47	1.51	-1.13	1.10
4110	-0.91	3.80	1.45	-1.22	4079	-2.53	0.26	-0.08	0.61
8557	-0.96	-1.82	2.71	1.31	7490	-2.53	0.97	-0.11	1.76
8535	-0.97	4.36	0.44	-0.60	8548	-2.57	-7.16	-3.45	-4.69
4363	-0.98	3.37	-2.13	-0.84	4040	-2.57	-2.92	-3.35	-2.56
8542	-1.07	-2.70	-1.93	0.22	8506	-2.57	3.32	-1.81	-0.72
8600	-1.08	-4.29	-0.54	0.22	4179	-2.58	1.26	-0.86	-0.19
8504	-1.12	2.66	-0.09	0.11	7427	-2.64	3.86	-0.21	0.04
4032	-1.13	-5.03	5.03	2.73	4017	-2.68	2.26	1.41	1.30
8507	-1.15	1.91	-0.05	2.58	4082	-2.73	0.65	0.50	0.04
4048	-1.15	0.81	-1.25	0.17	4051	-2.73	-7.95	-2.31	-1.60
4133	-1.17	-2.58	-2.06	-3.35	4449	-2.80	-0.28	-0.54	-1.21
4434	-1.21	2.90	-0.68	-0.53	04389B	-2.90	2.86	2.61	1.15
8503	-1.23	0.91	-0.75	0.74	4459	-3.01	4.07	-3.04	0.39
4454	-1.23	2.47	-1.37	1.34	4194	-3.03	2.54	0.50	-0.80
4097	-1.28	2.56	-0.15	1.27	4410	-3.05	-1.92	3.05	1.34
4193	-1.29	1.89	-2.03	-3.04	8575	-3.06	1.49	-1.41	0.84
4145	-1.30	-0.66	-2.13	2.09	7445	-3.18	1.64	0.51	2.50
4094	-1.32	-6.01	-1.06	1.74	4181	-3.19	-4.35	-1.04	-2.35
4463	-1.33	-0.85	-3.37	-0.88	8567	-3.26	0.78	-0.66	0.77
4074	-1.33	-1.38	3.17	0.19	4161	-3.27	-1.13	2.53	0.05
4323	-1.36	-1.07	-1.16	2.19	4332	-3.29	-9.16	3.20	0.83
8544	-1.37	-9.16	-1.27	-4.85	7434	-3.30	5.93	-0.41	-1.12
4025	-1.41	2.31	0.04	2.67	4445	-3.32	4.14	-2.70	-0.40
4376	-1.43	2.89	-1.05	-1.00	7424	-3.34	0.68	0.60	3.54
4108	-1.52	-5.37	-0.18	0.30	4393	-3.39	2.41	-0.11	2.23
4065	-1.57	0.29	-2.61	-0.38	4037	-3.42	-1.82	1.33	1.35
8601	-1.63	-5.03	-2.14	-6.00	4155	-3.43	3.52	0.32	-1.13
4395	-1.68	2.30	-3.45	0.39	4462	-3.52	2.07	0.53	1.03
4013	-1.69	-4.41	7.23	0.73	4312	-3.53	-0.82	-4.44	1.75
4099	-1.71	-2.06	-1.32	0.28	4167	-3.60	-1.06	0.73	1.27
4464	-1.76	2.41	-1.04	-0.69	4045	-3.60	0.24	-2.51	0.21
4461	-1.76	3.17	-1.36	-0.41	4414	-3.62	3.68	-0.28	-0.40
4402	-1.81	-0.21	0.20	1.43	4370	-3.62	0.03	-0.85	0.89
04376B	-1.82	3.71	-0.78	-1.13	4474	-3.66	-1.95	4.53	-2.86
04360B	-1.85	2.06	-2.56	1.41	4391	-3.69	-1.70	-1.28	-1.00
4360	-1.87	2.24	-2.65	1.15	4417	-3.82	0.92	-1.03	1.97
4460	-1.87	3.41	-0.94	-0.91	4409	-3.82	4.79	-1.44	-0.73
4401	-1.91	2.36	-1.40	0.93	4046	-3.87	3.31	-1.06	0.53
04192B	-1.95	4.15	-1.65	-2.14	4069	-3.89	-11.29	7.96	0.16
4190	-1.96	0.42	-2.19	-0.86	7443	-3.90	3.97	1.22	1.83
4392	-1.98	4.24	-0.94	-0.68	8561	-3.94	0.87	2.63	1.06
4364	-1.99	1.39	-4.06	0.04	4103	-3.94	-7.96	4.94	0.10
4183	-2.10	1.78	4.53	0.88	4134	-3.97	-0.78	0.84	1.58

Sample #	PC1	PC2	PC3	PC4	Sample #	PC1	PC2	PC3	PC4
4441	-3.99	4.31	-0.46	-0.21	4044	-5.66	1.84	0.00	2.30
4418	-4.00	4.14	-0.39	0.43	4336	-5.66	-6.81	3.18	5.14
4426	-4.02	1.86	-0.88	-0.71	4316	-5.66	-0.57	-1.16	-0.89
8555	-4.02	-3.22	1.39	0.26	4109	-5.70	0.01	-1.74	0.37
4114	-4.06	-0.44	-0.93	-0.99	4055	-5.82	0.72	0.03	1.57
4470	-4.06	1.36	-1.55	-0.85	4315	-5.85	0.77	-3.63	-0.77
7491	-4.06	-2.10	-0.48	2.18	4187	-5.85	-1.41	1.07	0.40
4188	-4.11	1.77	2.90	-0.21	8604	-5.93	-1.88	-1.10	-1.60
7440	-4.17	3.29	-2.34	-0.62	4002	-6.03	4.10	2.11	2.02
4311	-4.18	-1.47	-2.91	2.42	4359	-6.19	3.82	-1.75	-1.19
4335	-4.18	-8.53	2.81	2.53	4362	-6.20	0.20	4.16	3.50
4396	-4.22	1.82	-0.09	1.15	4026	-6.23	-1.86	1.69	-0.28
8562	-4.27	-0.23	-0.03	-1.10	4137	-6.35	-3.90	0.66	-3.29
04111B	-4.28	2.37	-0.92	1.32	4036	-6.45	1.90	-0.33	-0.45
4123	-4.30	-0.04	-1.14	1.30	4029	-6.49	1.33	1.53	1.56
4163	-4.32	-1.01	0.31	2.27	8516	-6.53	-8.87	-3.10	-4.14
04307A	-4.33	-4.77	-4.89	-0.75	8549	-6.54	-3.10	-2.93	-2.52
4413	-4.37	2.99	-1.48	0.40	04373B	-6.59	2.90	-2.78	-2.46
7481	-4.38	2.09	-3.07	0.13	4128	-6.64	-5.45	1.46	2.98
4303	-4.38	-0.85	-2.91	2.85	4319	-6.70	4.59	-1.21	-0.30
4189	-4.38	-0.95	4.81	0.65	4308	-6.72	-0.04	0.11	0.48
4135	-4.41	1.50	-1.21	0.71	4107	-6.80	0.62	0.67	1.03
4416	-4.42	2.61	-1.87	0.01	4084	-6.82	0.69	-1.82	1.40
4390	-4.42	0.00	-1.61	0.02	8550	-6.88	-5.28	-2.19	-3.71
8602	-4.43	-5.88	-0.55	-3.65	8599	-6.88	-3.27	0.38	-1.26
04316B	-4.45	-0.66	-1.62	-1.18	4102	-6.91	3.48	-0.61	-0.01
4397	-4.46	0.29	-1.51	1.29	4056	-6.93	-0.59	1.37	1.69
4435	-4.46	1.59	-1.62	0.01	8508	-7.04	1.86	-0.54	2.13
8605	-4.55	-7.13	-0.83	-1.96	4458	-7.04	3.22	-1.15	-0.79
8553	-4.63	-4.09	3.66	-3.11	08574D	-7.12	-1.50	0.85	-2.05
4038	-4.64	-1.46	0.01	1.65	4373	-7.18	2.57	-2.01	-2.43
8551	-4.70	-6.39	-0.53	-2.01	4131	-7.18	0.85	-1.27	1.50
4408	-4.76	1.64	-1.97	2.22	8574	-7.18	-1.64	0.63	-2.09
4042	-4.80	2.45	1.86	2.51	04309B	-7.24	-0.41	-1.36	-0.91
4473	-4.81	-1.63	0.94	-3.26	4177	-7.24	-1.48	3.03	1.92
4035	-4.81	1.57	-1.73	0.44	8554	-7.29	-5.06	-3.36	-2.66
4469	-4.82	2.55	-1.99	0.70	8510	-7.31	-3.54	-2.24	-3.88
7444	-4.83	3.89	-0.56	0.30	8547	-7.39	-3.70	-3.76	-3.27
7465	-4.86	-6.70	3.92	-0.56	7455	-7.41	1.45	0.33	0.07
8545	-4.91	-2.82	-3.64	-3.09	4314	-7.41	0.45	-1.59	-0.98
4098	-4.95	1.88	-0.90	0.40	4092	-7.54	1.09	1.60	1.46
4101	-4.98	1.88	-0.60	1.49	4186	-7.71	1.21	-0.72	0.79
4176	-4.99	0.17	2.25	1.27	8540	-7.78	-2.13	-3.26	-2.05
4385	-5.01	3.28	-1.70	-1.09	8511	-7.81	-3.24	-3.44	-2.65
4041	-5.07	-6.82	0.96	1.06	8517	-7.81	-7.08	-1.71	-3.40
04319B	-5.07	4.08	-2.05	-0.41	4024	-7.88	2.59	-1.72	1.21
7489	-5.08	-1.84	0.62	-0.45	4309	-7.95	-0.22	-1.32	-1.12
4127	-5.11	-2.66	-1.35	-1.93	4080	-7.95	1.57	1.95	1.96
4050	-5.11	1.76	-1.99	1.82	8552	-8.11	-3.25	-3.00	-2.88
8512	-5.15	-5.39	-0.36	-1.79	8541	-8.18	-4.19	-2.12	-2.96
8505	-5.20	4.12	2.54	1.28	8587	-8.32	1.11	0.91	2.06
4144	-5.34	-4.20	-0.63	-2.23	4033	-8.33	-6.59	1.78	-2.14
4139	-5.41	2.50	1.46	-0.30	8564	-8.35	-1.42	3.17	4.78
4394	-5.43	1.24	1.82	1.42	8592	-8.43	-2.77	-0.60	-2.98
4111	-5.46	2.12	0.02	1.26	8509	-8.45	-0.66	-2.94	-2.13
4490	-5.59	0.27	-0.23	1.32	4148	-8.46	1.04	0.07	0.71
8606	-5.60	-2.51	0.40	-3.17	8514	-8.50	-0.67	-2.31	-2.70
4365	-5.65	3.66	-1.44	1.00	4063	-8.62	-1.85	7.13	2.33

Sample #	PC1	PC2	PC3	PC4
4066	-9.03	0.04	5.07	3.36
4001	-9.14	-3.27	1.53	2.67
4113	-9.15	2.52	-1.42	0.51
8518	-9.17	-0.21	-2.53	-1.18
4338	-9.19	-6.51	3.72	4.17
4121	-9.33	-1.14	4.03	0.38
4093	-9.47	-1.37	1.40	0.93
8595	-9.83	-1.35	0.71	-2.95
04177B	-10.11	0.01	5.08	1.99
4301	-10.20	0.61	3.16	1.22
4142	-10.45	0.98	2.65	1.85
4337	-10.78	-5.47	3.99	4.49
4086	-12.81	2.38	3.34	1.41

Appendix A7. PCA loadings for PC1 - 4 for individual elements. Elements are ordered by highest to lowest PC1 loading.

Element	PC1	PC2	PC3	PC4
Sm	0.190	-0.039	-0.104	-0.045
Hf	0.186	0.036	-0.086	-0.016
Al	0.186	0.035	0.113	-0.092
Nd	0.184	0.043	-0.099	-0.073
Zr	0.184	0.043	-0.077	-0.023
Nb	0.178	0.030	-0.119	-0.009
Gd	0.178	-0.135	-0.108	0.023
Pr	0.176	0.065	-0.107	-0.089
Ga	0.176	0.029	0.113	-0.086
Ta	0.171	0.048	-0.149	-0.041
Ce	0.169	0.087	-0.108	-0.093
Ti	0.164	-0.025	0.177	-0.062
La	0.162	0.099	-0.096	-0.087
Tb	0.156	-0.186	-0.123	0.059
Dy	0.144	-0.206	-0.132	0.067
P	0.140	0.035	0.123	-0.086
Be	0.137	0.056	0.094	-0.029
Y	0.133	-0.206	-0.137	0.105
Ho	0.133	-0.219	-0.136	0.081
Th	0.128	0.131	-0.128	-0.212
Er	0.127	-0.223	-0.144	0.082
Eu	0.119	-0.086	-0.066	-0.076
U	0.118	0.118	-0.115	-0.223
Tm	0.118	-0.229	-0.147	0.081
Yb	0.114	-0.228	-0.154	0.072
K	0.110	0.224	0.027	0.115
Cs	0.109	0.191	0.093	0.080
Rb	0.108	0.227	0.035	0.107
Sr	0.108	0.037	0.152	0.015
Ba	0.107	0.215	0.028	0.102
V	0.103	-0.074	0.262	-0.141
Lu	0.103	-0.231	-0.162	0.056
Sc	0.097	-0.125	0.214	-0.170
Na	0.094	0.059	0.037	-0.133

Element	PC1	PC2	PC3	PC4
Si	0.091	0.018	0.144	0.056
Mg	0.072	-0.190	0.188	-0.103
B	0.071	0.146	0.057	0.163
F	0.066	-0.093	0.175	0.025
Tl	0.054	0.213	-0.048	-0.007
Cr	0.036	-0.054	0.248	-0.272
Ge	0.034	-0.036	0.109	-0.085
Mn	0.024	-0.198	0.206	0.138
W	0.002	0.038	0.099	0.150
Ca	-0.032	-0.175	0.154	0.156
Fe	-0.034	-0.216	0.136	-0.018
In	-0.047	-0.071	0.042	-0.058
C_in_CO2_	-0.054	-0.060	0.126	0.282
Br	-0.066	0.013	0.003	0.095
Ni	-0.072	-0.107	0.120	-0.306
As	-0.085	0.058	0.001	0.070
Ag	-0.090	0.006	-0.096	-0.146
Sb	-0.096	0.082	-0.013	0.172
Sn	-0.096	0.045	-0.166	-0.044
Co	-0.102	-0.169	0.099	-0.215
Bi	-0.102	0.025	-0.128	-0.230
Mo	-0.105	-0.040	-0.141	-0.243
Se	-0.105	-0.063	-0.070	-0.087
Au	-0.110	0.002	-0.026	0.081
Cu	-0.117	-0.065	-0.035	-0.224
Pb	-0.119	0.039	-0.094	-0.126
Zn	-0.127	-0.004	-0.088	-0.057
Cd	-0.140	-0.044	-0.072	-0.056
Non_carb._C_	-0.142	0.027	-0.156	-0.054
Hg_	-0.148	0.010	-0.134	0.013
LOI	-0.149	-0.093	-0.016	0.002
Total S	-0.155	-0.012	-0.108	0.048

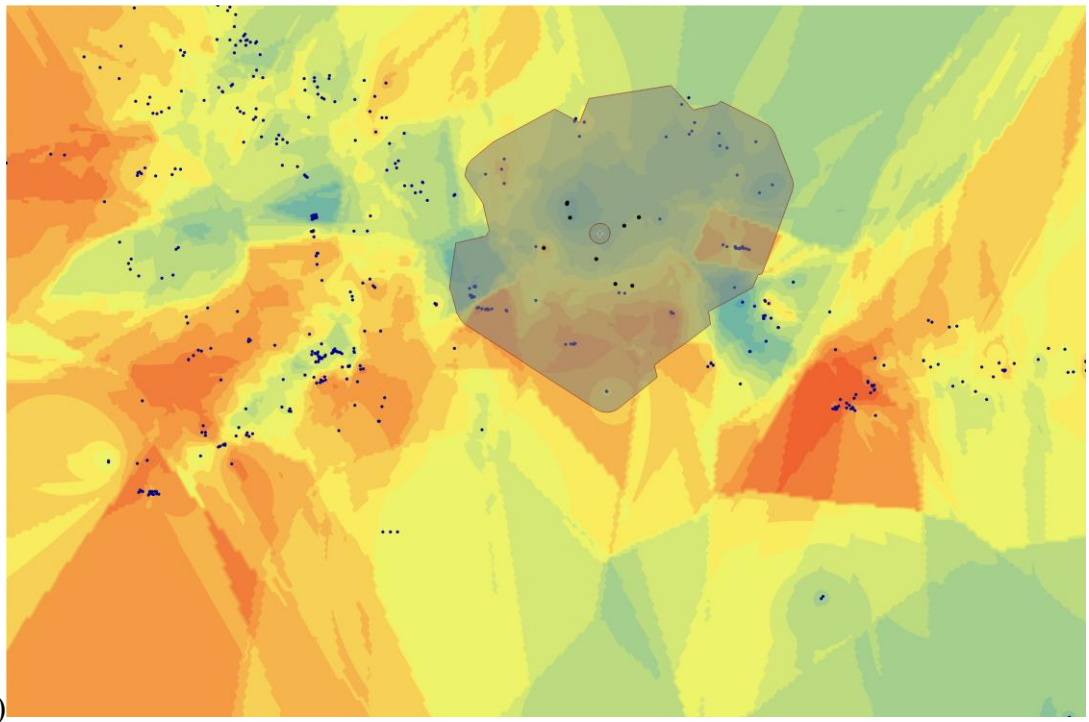
Appendix A8. Eigenvalues and Variance for each Principal Component adding up to 100% cumulative variance.

	Eigenvalues	Individual Variance (%)	Cumulative Variance (%)
PC1	21.75	32.95	32.95
PC2	8.92	13.52	46.46
PC3	6.44	9.76	56.23
PC4	3.20	4.85	61.08
PC5	3.00	4.54	65.62
PC6	2.19	3.32	68.94
PC7	2.01	3.05	71.99
PC8	1.43	2.17	74.15
PC9	1.32	2.00	76.16
PC10	1.23	1.86	78.02
PC11	1.08	1.64	79.65
PC12	1.04	1.57	81.23
PC13	0.97	1.48	82.70
PC14	0.87	1.32	84.02
PC15	0.76	1.15	85.18
PC16	0.76	1.15	86.32
PC17	0.61	0.92	87.24
PC18	0.59	0.89	88.13
PC19	0.56	0.85	88.99
PC20	0.51	0.78	89.76
PC21	0.50	0.75	90.51
PC22	0.46	0.70	91.22
PC23	0.45	0.69	91.90
PC24	0.42	0.63	92.53
PC25	0.39	0.59	93.12
PC26	0.36	0.54	93.66
PC27	0.33	0.50	94.16
PC28	0.31	0.47	94.64
PC29	0.30	0.46	95.10
PC30	0.28	0.42	95.52
PC31	0.27	0.41	95.93
PC32	0.25	0.38	96.31
PC33	0.24	0.36	96.67
PC34	0.22	0.33	97.00
PC35	0.20	0.31	97.31
PC36	0.19	0.29	97.60
PC37	0.18	0.27	97.87
PC38	0.17	0.26	98.14
PC39	0.15	0.22	98.36
PC40	0.12	0.18	98.54

	Eigenvalues	Individual Variance (%)	Cumulative Variance (%)
PC41	0.11	0.17	98.72
PC42	0.10	0.16	98.87
PC43	0.10	0.15	99.02
PC44	0.09	0.14	99.16
PC45	0.09	0.13	99.29
PC46	0.08	0.12	99.41
PC47	0.07	0.11	99.52
PC48	0.06	0.09	99.61
PC49	0.04	0.07	99.67
PC50	0.04	0.06	99.73
PC51	0.04	0.06	99.79
PC52	0.03	0.04	99.84
PC53	0.02	0.04	99.87
PC54	0.02	0.03	99.91
PC55	0.02	0.02	99.93
PC56	0.01	0.02	99.95
PC57	0.01	0.01	99.96
PC58	0.01	0.01	99.97
PC59	0.00	0.01	99.98
PC60	0.00	0.01	99.98
PC61	0.00	0.00	99.99
PC62	0.00	0.00	99.99
PC63	0.00	0.00	99.99
PC64	0.00	0.00	100.00
PC65	0.00	0.00	100.00
PC66	0.00	0.00	100.00

Appendix A9. Complementary figures for Empirical Bayesian Kriging in Chapter 5.

(A)



(B)

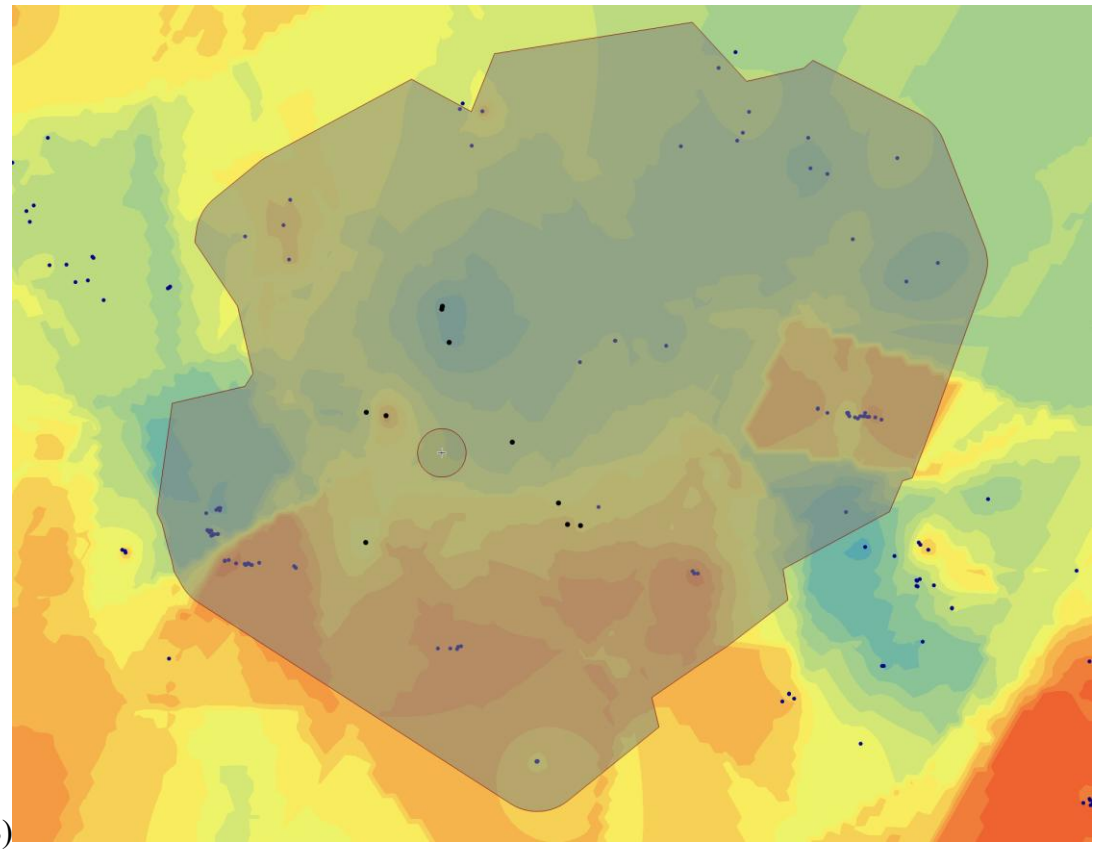


Figure 1.1 (A) Preliminary EBK interpolation map for Principal Component 1 (PC1), showing sample distribution, the color-coded continuous surface raster and one of the spatial subset polygons used to generate local semivariograms. (B) Within each subset polygon, selecting a specific location triggers the model to identify the ten nearest data points, which are then used to estimate PC1 values at unsampled locations through localized interpolation.

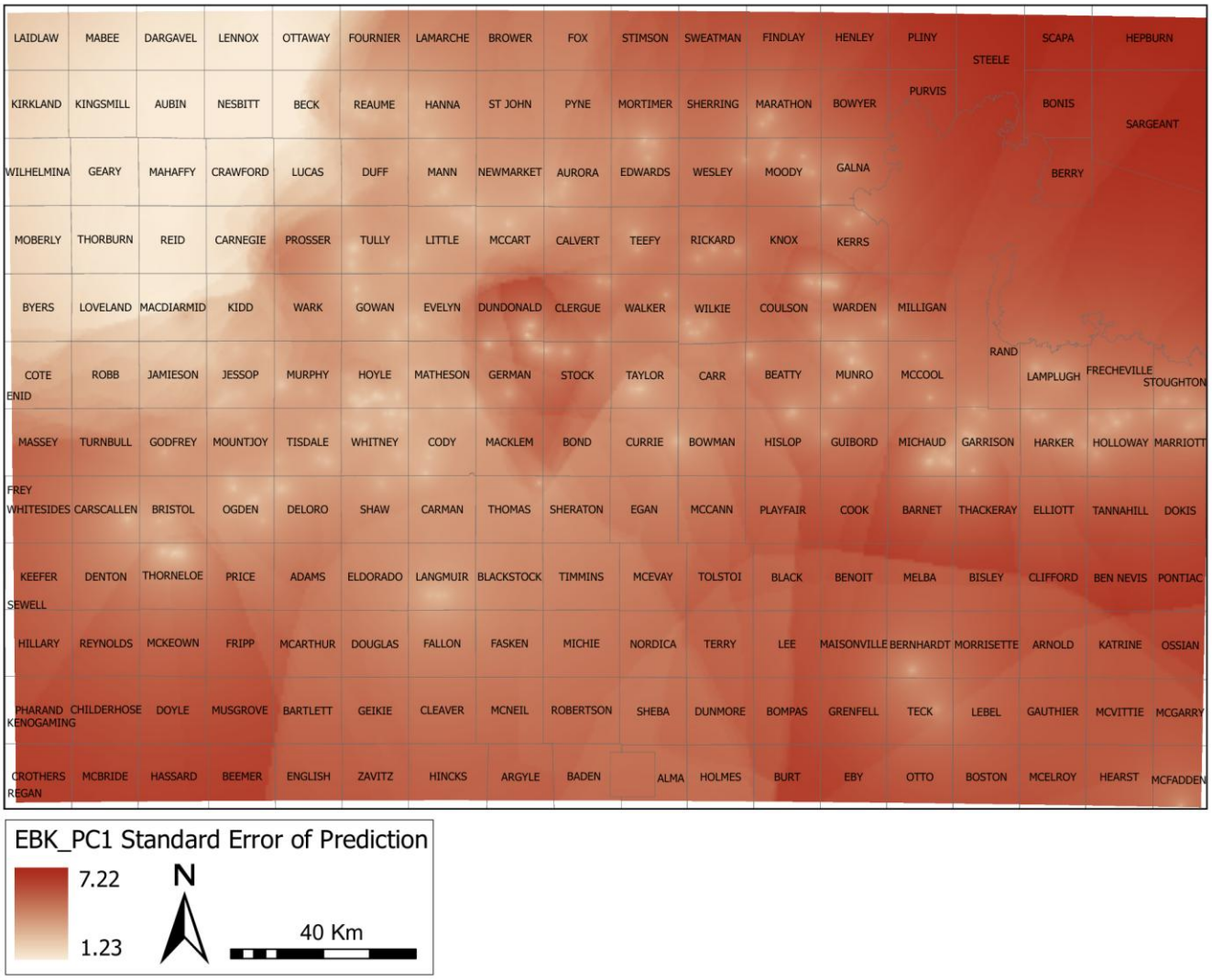


Figure 1.2. Standard Error of Prediction from Empirical Bayesian Kriging raster derived from PC1 (REE-bearing heavy mineral component). The map provides a measure of uncertainty based on the number of samples used to make a prediction. Darker red regions correspond to more error and lighter regions correspond to less error, reflecting how well the sampled data can make a prediction at an unsampled point. The values for standard error of prediction are unitless.

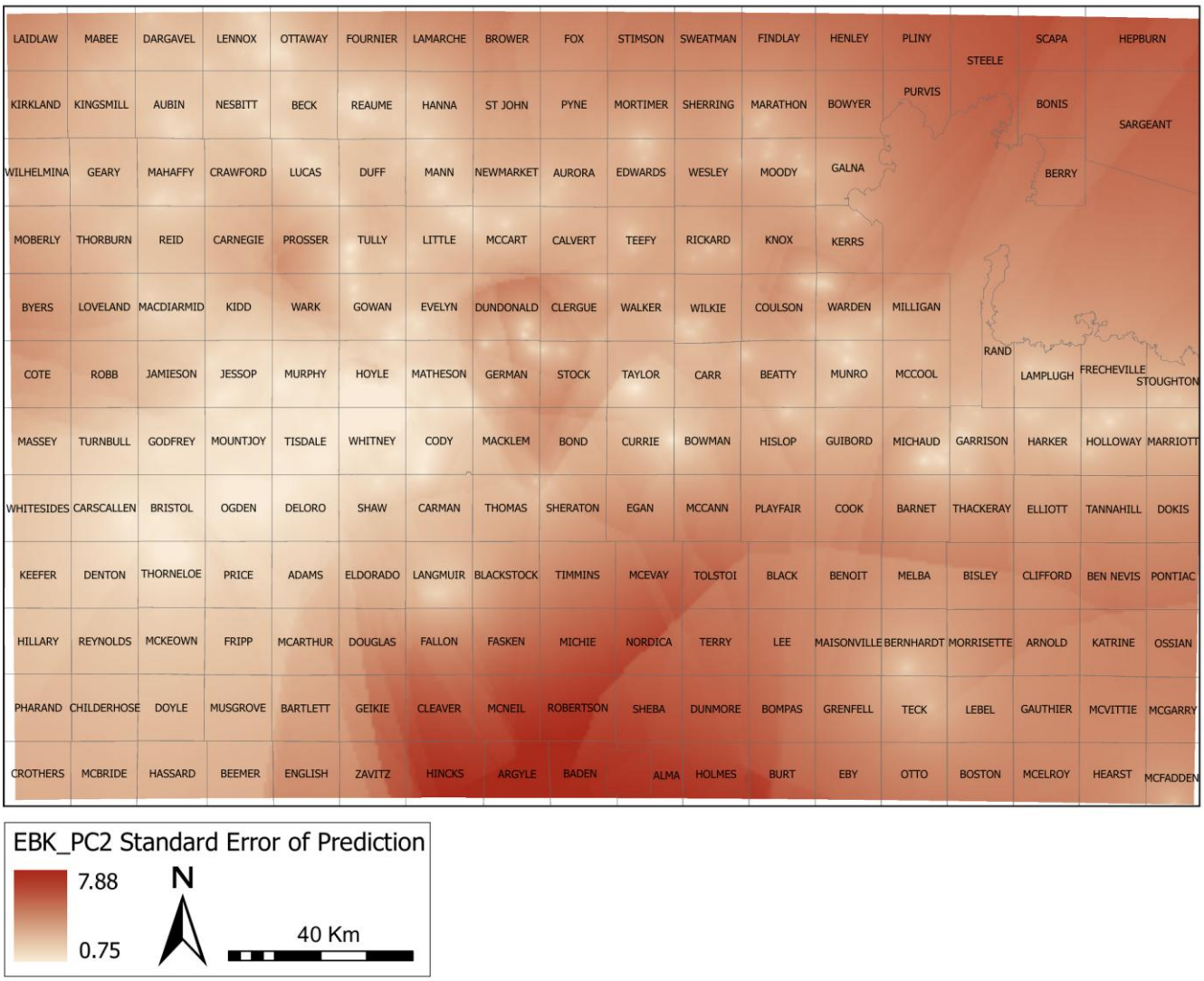


Figure 1.3. Standard Error of Prediction from Empirical Bayesian Kriging raster derived from PC2 (Muscovite component). The map provides a measure of uncertainty based on the number of samples used to make a prediction. Darker red regions correspond to more error and lighter regions correspond to less error, reflecting how well the sampled data can make a prediction at an unsampled point. The values for standard error of prediction are unitless.

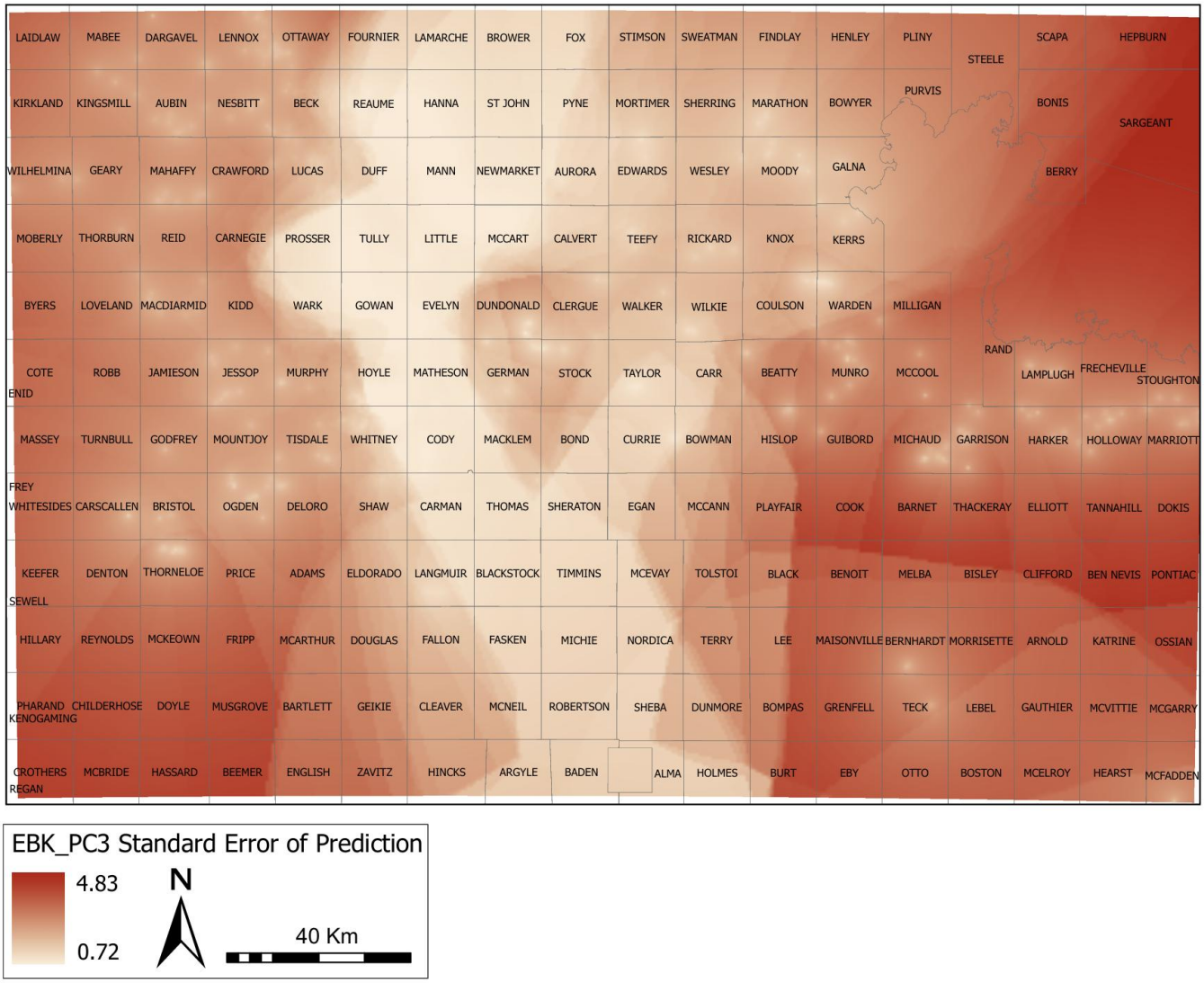


Figure 1.4. Standard Error of Prediction from Empirical Bayesian Kriging raster derived from PC3 (Mafic volcanic-derived component). The map provides a measure of uncertainty based on the number of samples used to make a prediction. Darker red regions correspond to more error and lighter regions correspond to less error, reflecting how well the sampled data can make a prediction at an unsampled point. The values for standard error of prediction are unitless.

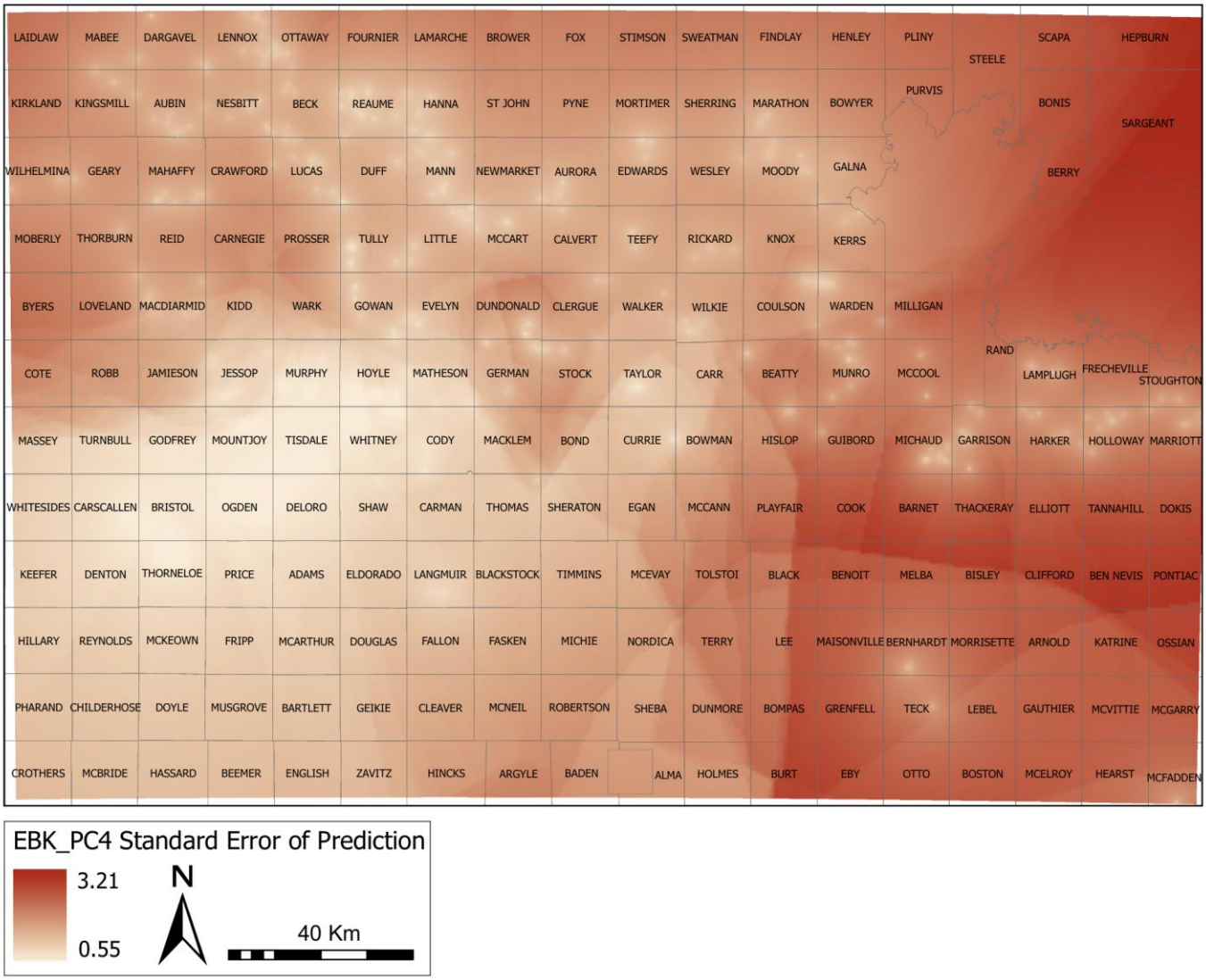


Figure 1.5. Standard Error of Prediction from Empirical Bayesian Kriging raster derived from PC4 (Carbonate and accessory mineral component). The map provides a measure of uncertainty based on the number of samples used to make a prediction. Darker red regions correspond to more error and lighter regions correspond to less error, reflecting how well the sampled data can make a prediction at an unsampled point. The values for standard error of prediction are unitless.

Appendix A10. Python Code for shale lithotype, associated mineralization style, and lithostratigraphic assemblage Random Forest classifiers, adapted from Fassbender et al. (2023). Code includes descriptions of instructions and notes above and after various lines represented by "#" *followed by italicized text*.

1. Shale Lithotype Classifier Code

```
import pandas as pd
import numpy as np
from sklearn.model_selection import train_test_split
from sklearn.ensemble import RandomForestClassifier
from sklearn.tree import DecisionTreeClassifier, plot_tree
from sklearn.metrics import (
confusion_matrix, classification_report, roc_auc_score, roc_curve, auc, accuracy_score)
from sklearn.preprocessing import label_binarize
import matplotlib.pyplot as plt
import seaborn as sns
from imblearn.over_sampling import SMOTE


# Load data
df =
pd.read_csv("C:/Rhian/Excel_&_ioGAS_data/Revised_geochem_overview_Nov_12.csv"
)


EOI = [col for col in df.columns if '_ppm' in col]
df = df.dropna(subset=EOI)
trans = df[EOI]
X = trans
y = df['Ti/Zr_Source_Rock']
feature_names = X.columns  # Get feature names
np.array(feature_names)
X_train, X_test, y_train, y_test = train_test_split(X, y, random_state=42, test_size=0.2,
stratify=y)


min_samples = y_train.value_counts().min()
n_neighbors = min(min_samples - 1, 2)  # Ensure n_neighbors is <= min_samples - 1
```

Appendix A10. Python Code for shale lithotype, associated mineralization style, and lithostratigraphic assemblage Random Forest classifiers, adapted from Fassbender et al. (2023).

```
smote = SMOTE(random_state=42, k_neighbors=n_neighbors)
X_train_smote, y_train_smote = smote.fit_resample(X_train, y_train)


# Train a decision tree classifier
model = DecisionTreeClassifier(random_state=42)
model.fit(X_train_smote, y_train_smote)
DecisionTreeClassifier?i
DecisionTreeClassifier(random_state=42)


# Train a Random Forest Classifier
rf_classifier = RandomForestClassifier(oob_score=True, random_state=42,
    n_estimators=500)
rf_classifier.fit(X_train_smote, y_train_smote)


y_pred = rf_classifier.predict(X_test)
y_pred_proba = rf_classifier.predict_proba(X_test)


# Evaluate the model
print(confusion_matrix(y_test, y_pred))
accuracy = accuracy_score(y_test, y_pred)
print(f"Random Forest Model Accuracy: {accuracy:.2f}")

# Show OOB Score
print(f"OOB Score: {rf_classifier.oob_score_:.4f}")
print(f"OOB Error Estimate: {oob_error:.4f}")
    a. [[56  1  0]
    b. [ 6 40  2]
    c. [ 0  1  7]]
Random Forest Model Accuracy: 0.91
OOB Score: 0.9272
OOB Error Estimate: 0.0728
```

2. Associated Mineralization Style Classifier Code

```
3. import pandas as pd
4. import numpy as np
5. from sklearn.model_selection import train_test_split
```

Appendix A10. Python Code for shale lithotype, associated mineralization style, and lithostratigraphic assemblage Random Forest classifiers, adapted from Fassbender et al. (2023).

```
from sklearn.ensemble import RandomForestClassifier
from sklearn.tree import DecisionTreeClassifier, plot_tree
from sklearn.metrics import (
confusion_matrix, classification_report, roc_auc_score, roc_curve, auc, accuracy_score)
from sklearn.preprocessing import label_binarize
import matplotlib.pyplot as plt
import seaborn as sns
from imblearn.over_sampling import SMOTE


# Load data
df =
pd.read_csv("C:/Rhian/Excel_&_ioGAS_data/Revised_geochem_overview_Nov_12.csv"
)


EOI = [col for col in df.columns if '_ppm' in col]
df = df.dropna(subset=EOI)
trans = df[EOI]
X = trans
y = df['Commodity']
feature_names = X.columns  # Get feature names
np.array(feature_names)
X_train, X_test, y_train, y_test = train_test_split(X, y, random_state=42, test_size=0.2,
stratify=y)


min_samples = y_train.value_counts().min()
n_neighbors = min(min_samples - 1, 2)  # Ensure n_neighbors is <= min_samples - 1


smote = SMOTE(random_state=42, k_neighbors=n_neighbors)
X_train_smote, y_train_smote = smote.fit_resample(X_train, y_train)

# Train a decision tree classifier
model = DecisionTreeClassifier(random_state=42)
model.fit(X_train_smote, y_train_smote)
DecisionTreeClassifier?i
DecisionTreeClassifier(random_state=42)

# Train a Random Forest Classifier
rf_classifier = RandomForestClassifier(oob_score=True, random_state=42,
n_estimators=500)
```

Appendix A10. Python Code for shale lithotype, associated mineralization style, and lithostratigraphic assemblage Random Forest classifiers, adapted from Fassbender et al. (2023).

```
35. rf_classifier.fit(X_train_smote, y_train_smote)


36. y_pred = rf_classifier.predict(X_test)
37. y_pred_proba = rf_classifier.predict_proba(X_test)


38. # Evaluate the model
39. print(confusion_matrix(y_test, y_pred))
40. accuracy = accuracy_score(y_test, y_pred)
41. print(f"Random Forest Model Accuracy: {accuracy:.2f}")

42. # Show OOB Score
43. print(f"OOB Score: {rf_classifier.oob_score_:.4f}")
44. print(f"OOB Error Estimate: {oob_error:.4f}")
        a. [[49  5]
        b. [19 40]]
45. Random Forest Model Accuracy: 0.79
46. OOB Score: 0.8072
47. OOB Error Estimate: 0.1928
```

48. Lithostratigraphic Assemblage Classifier Code

```
49. import pandas as pd
50. import numpy as np
51. from sklearn.model_selection import train_test_split
52. from sklearn.ensemble import RandomForestClassifier
53. from sklearn.tree import DecisionTreeClassifier, plot_tree
54. from sklearn.metrics import (
55. confusion_matrix, classification_report, roc_auc_score, roc_curve, auc, accuracy_score)
56. from sklearn.preprocessing import label_binarize
57. import matplotlib.pyplot as plt
58. import seaborn as sns
59. from imblearn.over_sampling import SMOTE


60. # Load data
61. df =
    pd.read_csv("C:/Rhian/Excel_&_ioGAS_data/Revised_geochem_overview_Nov_12.csv"
    )
```

Appendix A10. Python Code for shale lithotype, associated mineralization style, and lithostratigraphic assemblage Random Forest classifiers, adapted from Fassbender et al. (2023).

```
EOI = [col for col in df.columns if '_ppm' in col]
df = df.dropna(subset=EOI)
trans = df[EOI]
X = trans.copy()
y = df['Assemblage_corrected'].copy()


# Drop rows where either features or target are NaN
mask = X.notna().all(axis=1) & y.notna()
X = X[mask]
y = y[mask]


# Verify no NaNs remain
print("NaNs in features:", X.isna().sum().sum())
print("NaNs in target:", y.isna().sum())
feature_names = X.columns
print("Features:", np.array(feature_names))


# Split data
X_train, X_test, y_train, y_test = train_test_split(
X, y, random_state=42, test_size=0.2, stratify=y)


# Check minimum samples in any class
min_samples = y_train.value_counts().min()
print(f"Minimum samples in any class after filtering: {min_samples}")


# Adjust n_neighbors for SMOTE
n_neighbors = min(min_samples - 1, 2)


# Balance training data
smote = SMOTE(random_state=42, k_neighbors=n_neighbors)
X_train_smote, y_train_smote = smote.fit_resample(X_train, y_train)
print("Number of samples before SMOTE:", X_train.shape[0])
print("Number of samples after SMOTE:", X_train_smote.shape[0])
NaNs in features: 0
NaNs in target: 0
```

Appendix A10. Python Code for shale lithotype, associated mineralization style, and lithostratigraphic assemblage Random Forest classifiers, adapted from Fassbender et al. (2023).

```
Features: ['Si_ppm' 'Al_ppm' 'Fe_ppm' 'Mn_ppm' 'Mg_ppm' 'Ca_ppm' 'Na_ppm' 'K_ppm'
'Ti_ppm' 'P_ppm' 'LOI_ppm' 'Au_ppm' 'Ag_ppm' 'As_ppm' 'Ba_ppm' 'Be_ppm'
'Bi_ppm' 'Br_ppm' 'Cd_ppm' 'Co_ppm' 'Cr_ppm' 'Cs_ppm' 'Cu_ppm' 'Ga_ppm'
'Ge_ppm' 'Hf_ppm' 'Hg_ppm' 'In_ppm' 'Mo_ppm' 'Nb_ppm' 'Ni_ppm' 'Pb_ppm'
'Rb_ppm' 'S_ppm' 'Sb_ppm' 'Sc_ppm' 'Se_ppm' 'Sn_ppm' 'Sr_ppm' 'Ta_ppm'
'Th_ppm' 'Tl_ppm' 'U_ppm' 'V_ppm' 'W_ppm' 'Y_ppm' 'Zn_ppm' 'Zr_ppm'
'La_ppm' 'Ce_ppm' 'Pr_ppm' 'Nd_ppm' 'Sm_ppm' 'Eu_ppm' 'Gd_ppm' 'Tb_ppm'
'Dy_ppm' 'Ho_ppm' 'Er_ppm' 'Tm_ppm' 'Yb_ppm' 'Lu_ppm' 'C-Total_ppm'
'Total S_ppm' 'CO2_ppm' 'C_in_CO2_ppm' 'Non_carb._C_ppm' 'F_ppm' 'B_ppm'
'Hg_ppm.1']
Minimum samples in any class after filtering: 3
Number of samples before SMOTE: 450
Number of samples after SMOTE: 966


# Train a decision tree classifier
model = DecisionTreeClassifier(random_state=42)
model.fit(X_train_smote, y_train_smote)
DecisionTreeClassifier?i
DecisionTreeClassifier(random_state=42)


# Train a Random Forest Classifier
rf_classifier = RandomForestClassifier(oob_score=True, random_state=42,
n_estimators=500)
rf_classifier.fit(X_train_smote, y_train_smote)


y_pred = rf_classifier.predict(X_test)
y_pred_proba = rf_classifier.predict_proba(X_test)


# Evaluate the model
print(confusion_matrix(y_test, y_pred))
accuracy = accuracy_score(y_test, y_pred)
print(f"Random Forest Model Accuracy: {accuracy:.2f}")

#Show OOB Score
print(f"OOB Score: {rf_classifier.oob_score_:.4f}")
oob_accuracy = rf_classifier.oob_score_
oob_error = 1 - oob_accuracy
print(f"OOB Error Estimate: {oob_error:.4f}")

```

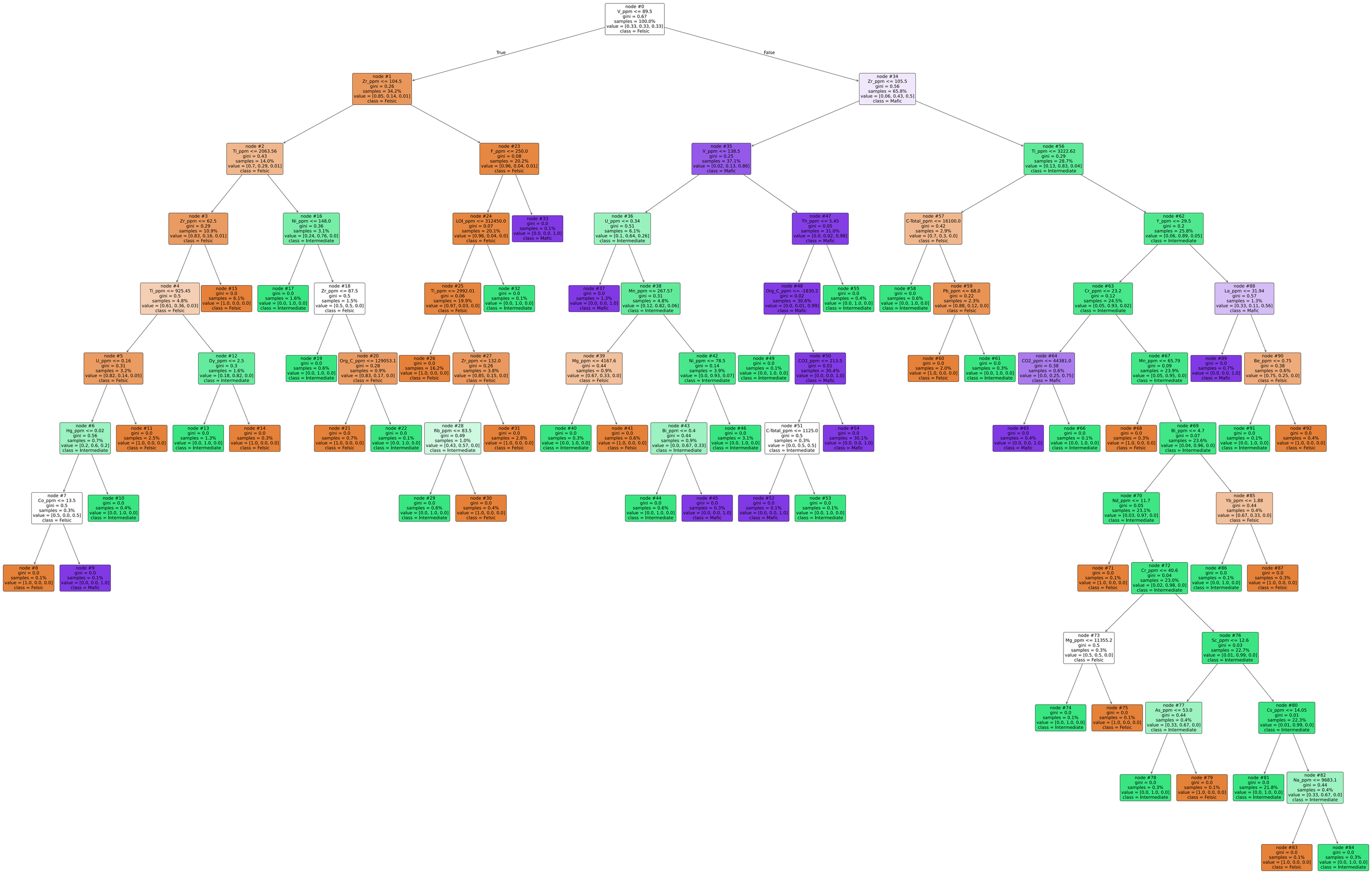
Appendix A10. Python Code for shale lithotype, associated mineralization style, and lithostratigraphic assemblage Random Forest classifiers, adapted from Fassbender et al. (2023).

a. [[5 1 4 0 3 3]
b. [0 4 1 1 2 0]
c. [2 3 19 0 3 0]
d. [0 0 1 7 0 4]
e. [2 3 2 0 7 1]
f. [1 0 5 0 2 27]]

124. Random Forest Model Accuracy: 0.61

125. OOB Score: 0.8592
126. OOB Error Estimate: 0.1408

Appendix A11. Example decision tree component of Random Forest Classifier for shale lithotype



Appendix A12. Example decision tree component of Random Forest Classifier for associated mineralization style

